

JGRG28

The 28th Workshop on General Relativity and Gravitation in Japan – JGRG28

Tachikawa Memorial Hall, Rikkyo University

5-9 November 2018

Volume II



Proceedings of the 28th Workshop on General Relativity and Gravitation in Japan

November 5th–9th 2018

**Tachikawa Memorial Hall, Rikkyo University,
3-34-1 Nishi-Ikebukuro, Toshima, Tokyo, Japan**

Volume II

Oral Presentations: Day 3, 4, 5

Contents

Wednesday 7th November	5
Invited lecture 9:00–9:45 [Chair: Hideyuki Tagoshi]	5
Jonathan Gair, “Science with the Laser Interferometer Space Antenna” (40+10 min.) [JGRG28 (2018) 110701]	5
Session S3A1 9:45–10:15 [Chair: Hideyuki Tagoshi]	26
Jiro Murata, “Laboratory Tests of Newtonian Gravity as tests of Inverse Square Law” (10+5 min.) [JGRG28 (2018) 110702]	26
Session S3A2 11:15–12:15 [Chair: Kenichi Oohara]	36
Yasutaka Koga, “Rotating accretion flows in D dimensions - sonic points, critical points and photon spheres -” (10+5 min.) [JGRG28 (2018) 110704]	36
Toshiaki Ono, “Gravitomagnetic bending angle of light in stationary axisymmetric spacetimes” (10+5 min.) [JGRG28 (2018) 110705] . . .	45
Tatsuya Ogawa, “Charge Screened Boson Stars” (10+5 min.) [JGRG28 (2018) 110706]	56
Session S3P1 14:00–15:30 [Chair: Masahide Yamaguchi]	68
Akira Matsumura, “Quantum discrimination for the Universe” (10+5 min.) [JGRG28 (2018) 110708]	68
Anupam Mazumdar, “Testing Quantum Gravity via entanglement” (10+5 min.) [JGRG28 (2018) 110709]	77
Shinpei Kobayashi, “Algebraic construction of solutions in noncom- mutative gravity and squeezed coherent state” (10+5 min.) [JGRG28 (2018) 110710]	89
Yota Watanabe, “Anisotropy problem in Horava-Lifshitz gravity” (10+5 min.) [JGRG28 (2018) 110711]	99
Tomotaka Kitamura, “Matter Scattering and Unitarity in Horava-Lifshitz Gravity” (10+5 min.) [JGRG28 (2018) 110712]	105
Satoshi Akagi, “Massive spin-two theory in arbitrary background” (10+5 min.) [JGRG28 (2018) 110713]	117
Session S3P2 16:30–18:15 [Chair: Masaru Shibata]	138
Shuntaro Mizuno, “Blue-tilted Primordial Gravitational Waves from Massive Gravity” (10+5 min.) [JGRG28 (2018) 110714]	138
Shi Pi, “Gravitational Waves Induced by non-Gaussian Scalar Pertur- bations” (10+5 min.) [JGRG28 (2018) 110715]	148
Yuki Niiyama, “Energy density of tensor perturbations in Einstein- Weyl gravity and its application to primordial gravitational waves” (10+5 min.) [JGRG28 (2018) 110717]	173
Wednesday 8th November	188

Invited lecture 9:00–9:45 [Chair: Tomohiro Harada]	188
Bernard John Carr, “PRIMORDIAL BLACK HOLES: LINKING MICRO-PHYSICS AND MACROPHYSICS” (40+10 min.) [JGRG28 (2018) 110801]	188
Session S4A1 9:45–10:15 [Chair: Tomohiro Harada]	229
Kazumasa Okabayashi, “Collisional Penrose process of spinning particles” (10+5 min.) [JGRG28 (2018) 110802]	229
Session S4A2 10:45–12:00 [Chair: Kenichi Nakao]	242
Takayuki Ohgami, “Exploring GR Effects of Super-Massive BH at Galactic Center 2: on the detail of fitting theory with observational data” (10+5 min.) [JGRG28 (2018) 110805]	242
Filip Ficek, “Planar domain walls in Kerr spacetime” (10+5 min.) [JGRG28 (2018) 110806]	249
Masashi Kimura, “Stability analysis of black holes by the S-deformation method for coupled systems” (10+5 min.) [JGRG28 (2018) 110808] .	263
Invited lecture 14:00–14:45 [Chair: Sugumi Kanno]	274
Vincent Vennin, “Stochastic Inflation and Primordial Black Holes” (40+10 min.) [JGRG28 (2018) 110810]	274
Session S4P1 14:45–15:45 [Chair: Sugumi Kanno]	285
Yuichiro Tada, “Stochastic formalism and curvature perturbations” (10+5 min.) [JGRG28 (2018) 110811]	285
Session S4P2 16:45–18:30 [Chair: Hideki Ishihara]	292
Kohei Fujikura, “Phase Transitions in Twin Higgs Models” (10+5 min.) [JGRG28 (2018) 110815]	292
Yi-Peng Wu, “Higgs as heavy-lifted physics during inflation” (10+5 min.) [JGRG28 (2018) 110816]	300
Minxi He, “Reheating in the Mixed Higgs- R^2 Model” (10+5 min.) [JGRG28 (2018) 110817]	313
Keisuke Inomata, “Power spectra of CMB circular polarizations induced by primordial perturbations” (10+5 min.) [JGRG28 (2018) 110818] .	329
Hiroyuki Kitamoto, “Schwinger Effect in Inflaton-Driven Electric Field” (10+5 min.) [JGRG28 (2018) 110821]	340
Wednesday 9th November	347
Invited lecture 9:00–9:45 [Chair: Shinji Mukohyama]	347
Alexei A. Starobinsky, “Looking for quantum-gravitational corrections to $R + R^2$ inflation” (40+10 min.) [JGRG28 (2018) 110901]	347
Invited lecture 9:45–10:30 [Chair: Shinji Mukohyama]	364
Jean-Philippe Uzan, “Astrophysical Stochastic Gravitational Wave Background” (40+10 min.) [JGRG28 (2018) 110902]	364

Session S5A 10:45–12:00 [Chair: Hideki Asada]	386
Atsushi Nishizawa, “Test of the equivalence principle at cosmological distance with gravitational waves” (10+5 min.) [JGRG28 (2018) 110903]	386
Yuki Watanabe, “Probing the Starobinsky R2 inflation with CMB precision cosmology” (10+5 min.) [JGRG28 (2018) 110904]	393
Chulmoon Yoo, “PBH abundance from random Gaussian curvature perturbations and a local density threshold” (10+5 min.) [JGRG28 (2018) 110905]	409
Marcus Christian Werner, “New developments in optical geometry” (10+5 min.) [JGRG28 (2018) 110908]	426

Wednesday 7th November
Invited lecture 9:00–9:45
[Chair: Hideyuki Tagoshi]

Jonathan Gair

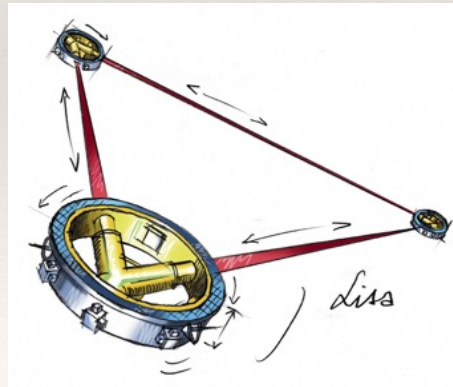
School of Mathematics, University of Edinburgh

“Science with the Laser Interferometer Space Antenna”
(40+10 min.)

[JGRG28 (2018) 110701]

Science with the Laser Interferometer Space Antenna

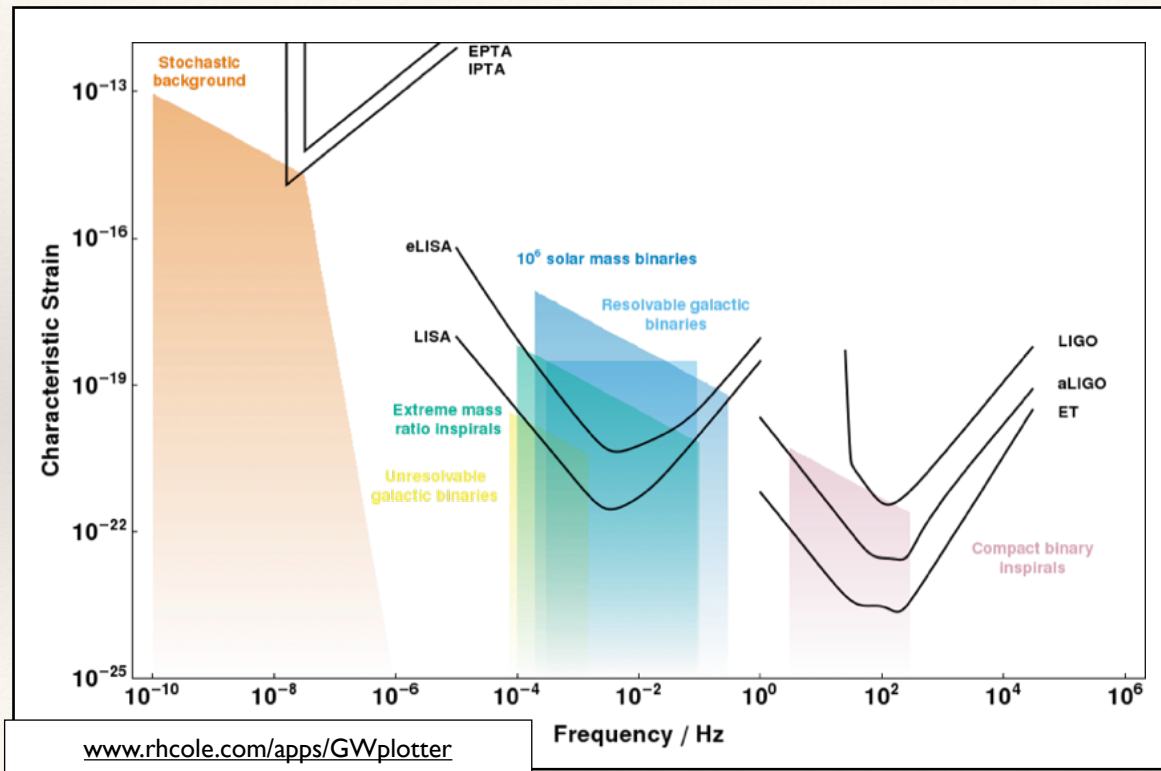
Jonathan Gair, School of Mathematics, University of Edinburgh
Japanese General Relativity Meeting, Rikkyu University, November 7th 2018



Talk Outline

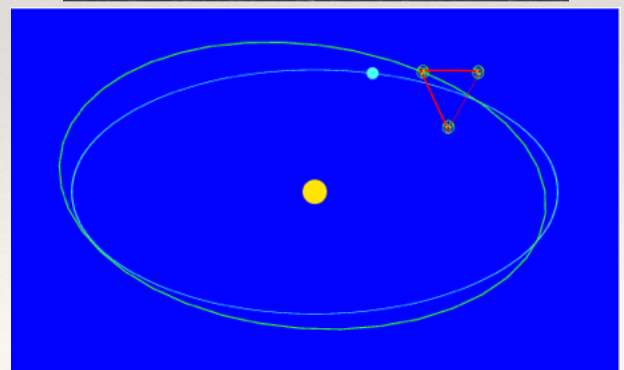
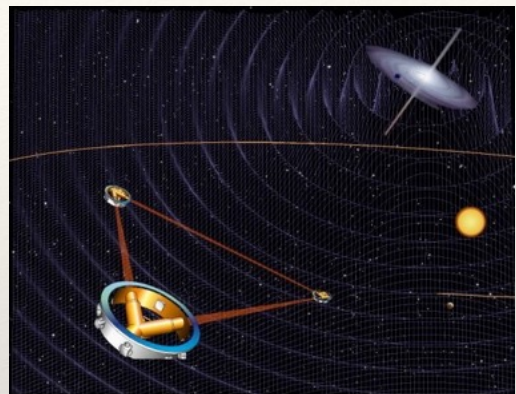
- ❖ The Laser Interferometer Space Antenna - current status
- ❖ Sources for LISA
- ❖ LISA science objectives
- ❖ The LISA Consortium
- ❖ Preparing for LISA data analysis and science delivery

Why space-based detectors?



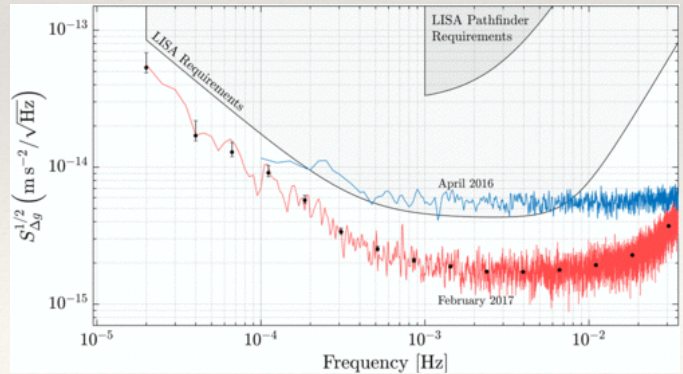
The Laser Interferometer Space Antenna

- ❖ Long history. Original design (1998)
 - Operating in millihertz band.
 - Three satellites, 5 million km apart, in heliocentric, Earth-trailing orbit. 6 laser links.
 - Joint NASA/ESA project.
 - Technology demonstrator mission, LISA Pathfinder, approved. Launched 2015.
- ❖ NASA dropped out in 2011. New ESA-only mission, termed eLISA, eventually selected for L3 (2034).

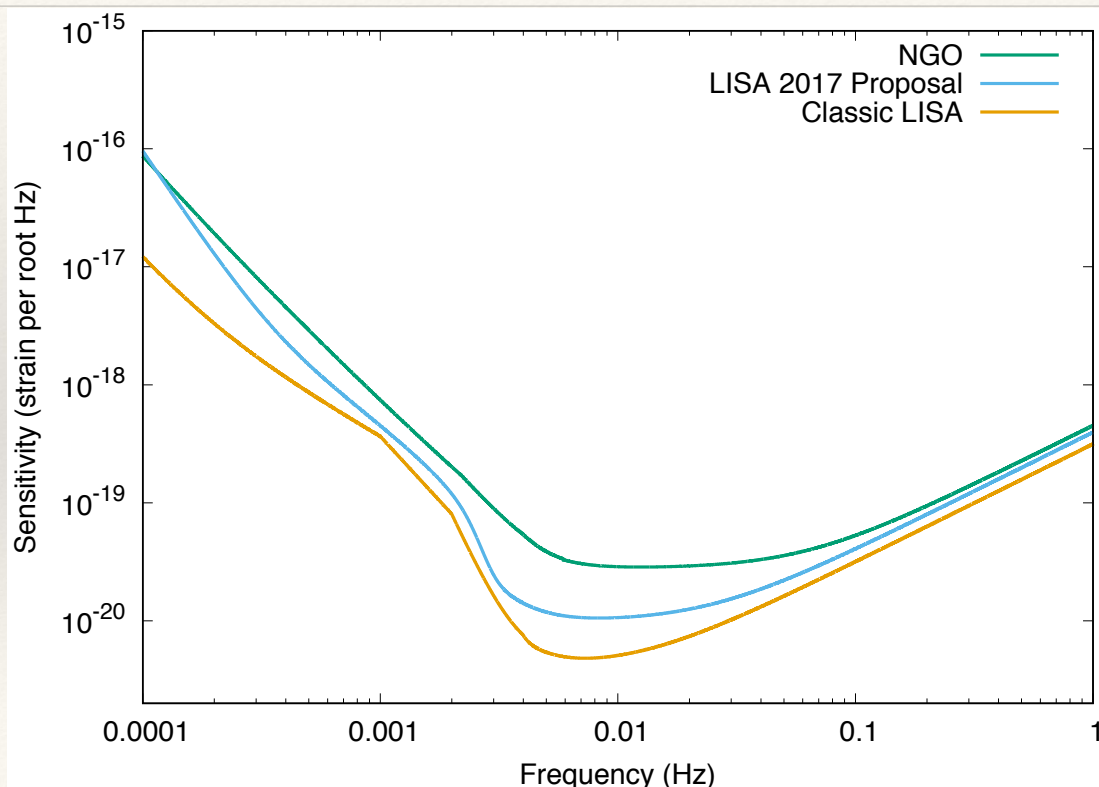


LISA Status

- ❖ LISA now reinvigorated and timetable accelerated
 - LISA Pathfinder spectacularly demonstrated the technology.
 - Detection of GW150914+ renewed interest in gravitational waves.
 - mission now in phase A, adoption in 2022-2024;
 - mission launch: by 2034.
- ❖ Mid-decadal review expressed strong support for NASA re-involvement, at probe-class level (~\$400m).
- ❖ Design: 2.5Gm arms, 6-link geometry.



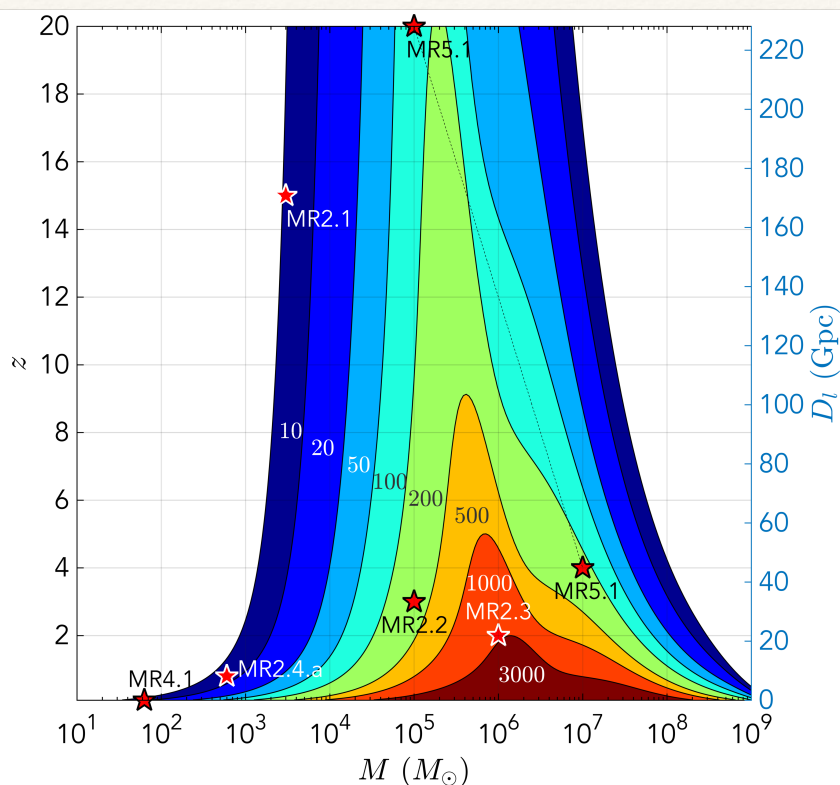
LISA Sensitivity



Sources: massive black hole mergers

- ❖ Expected to occur following mergers of the host galaxies. LISA can observe gravitational waves from these with very high signal-to-noise ratio.

Sources: massive black hole mergers



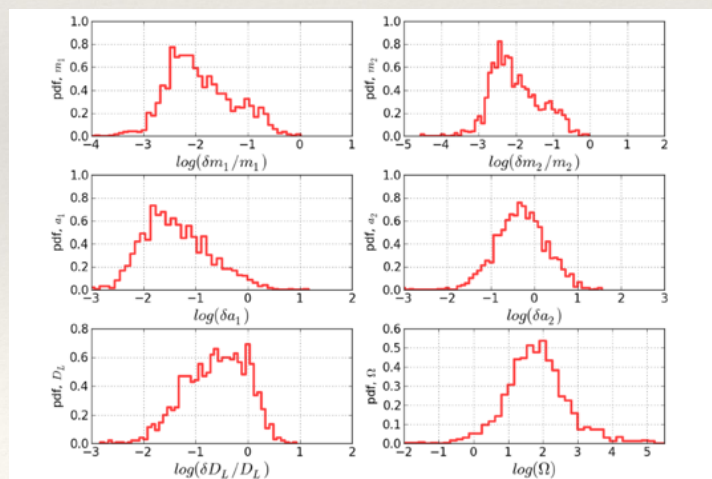
Sources: massive black hole mergers

- ❖ Expected to occur following mergers of the host galaxies. LISA can observe gravitational waves from these with very high signal-to-noise ratio.
- ❖ Expected event rate depends on assumptions about black hole population (Klein+, 2016)
 - Light pop-III seed model: baseline configuration expected to see ~350 events.
 - Heavy seed model, no delay in binary formation: ~550 events.
 - Heavy seed model, with delays: ~50 events.
- ❖ Baseline configuration would see 150/300/4 events at $z > 7$ under the different models.
 - NGO-like detector (1 Gm/4-link) would see ~15/185/3 events.
 - Classic LISA-like detector (5 Gm/6-link) would see ~400/350/4 events.

Sources: massive black hole mergers

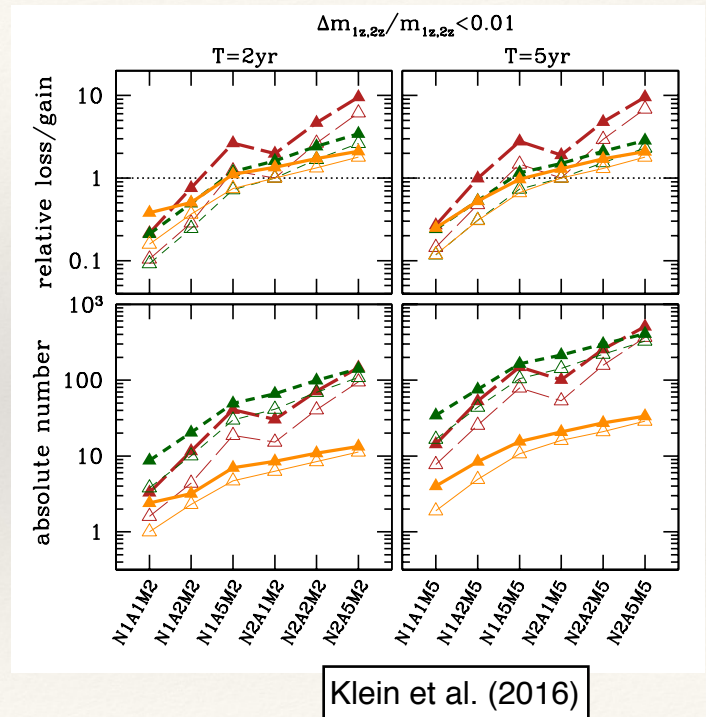
- ❖ LISA will measure the parameters of black hole mergers to high precision. Typical errors are

$$\Delta m_1/m_1, \Delta m_2/m_2 \sim 10^{-3} - 10^{-2}, \Delta a_1 \sim 10^{-2}$$
$$\Delta a_2 \sim 10^{-1}, \Delta \Omega \sim 30 \text{deg}^2, \Delta D_L/D_L \sim \text{few} \times 10^{-1}$$



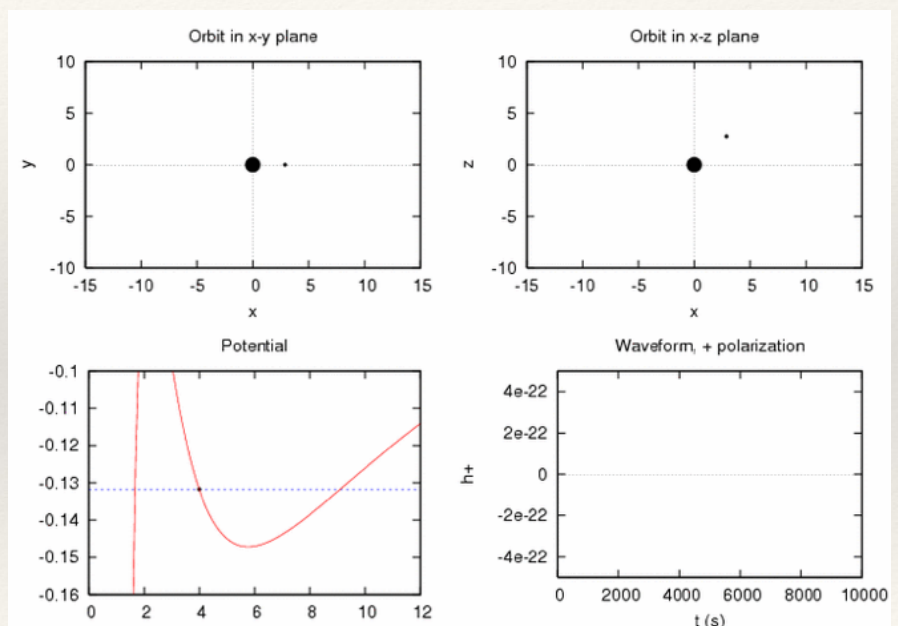
Sources: massive black hole mergers

- ❖ In two years, LISA could determine
 - both redshifted masses to 1% for $\sim 70/100/10$ systems;
 - the spin of the primary to 1% for $\sim 30/50/2$ systems;
 - sky location to 10 deg^2 and distance to 10% for $\sim 7/23/4$ systems.



Sources: extreme-mass-ratio inspirals

- ❖ The inspiral of a compact object into a massive black hole in the centre of a galaxy.
- ❖ Form as a result of scattering in dense galacto-centric stellar clusters.
- ❖ Orbits are expected to be both eccentric and inclined - rich waveform structure.



Sources: extreme-mass-ratio inspirals

- There are large astrophysical uncertainties, but expect to see between a few tens and a few hundreds of events.

Model	Mass function	MBH spin	Cusp erosion	$M-\sigma$ relation	N_p	CO mass [M_\odot]	Total	EMRI rate [yr^{-1}] Detected (AKK)	Detected (AKS)
M1	Barausse12	a98	yes	Gultekin09	10	10	1600	294	189
M2	Barausse12	a98	yes	KormendyHo13	10	10	1400	220	146
M3	Barausse12	a98	yes	GrahamScott13	10	10	2770	809	440
M4	Barausse12	a98	yes	Gultekin09	10	30	520 (620)	260	221
M5	Gair10	a98	no	Gultekin09	10	10	140	47	15
M6	Barausse12	a98	no	Gultekin09	10	10	2080	479	261
M7	Barausse12	a98	yes	Gultekin09	0	10	15800	2712	1765
M8	Barausse12	a98	yes	Gultekin09	100	10	180	35	24
M9	Barausse12	aflat	yes	Gultekin09	10	10	1530	217	177
M10	Barausse12	a0	yes	Gultekin09	10	10	1520	188	188
M11	Gair10	a0	no	Gultekin09	100	10	13	1	1
M12	Barausse12	a98	no	Gultekin09	0	10	20000	4219	2279

EMRI parameter estimation

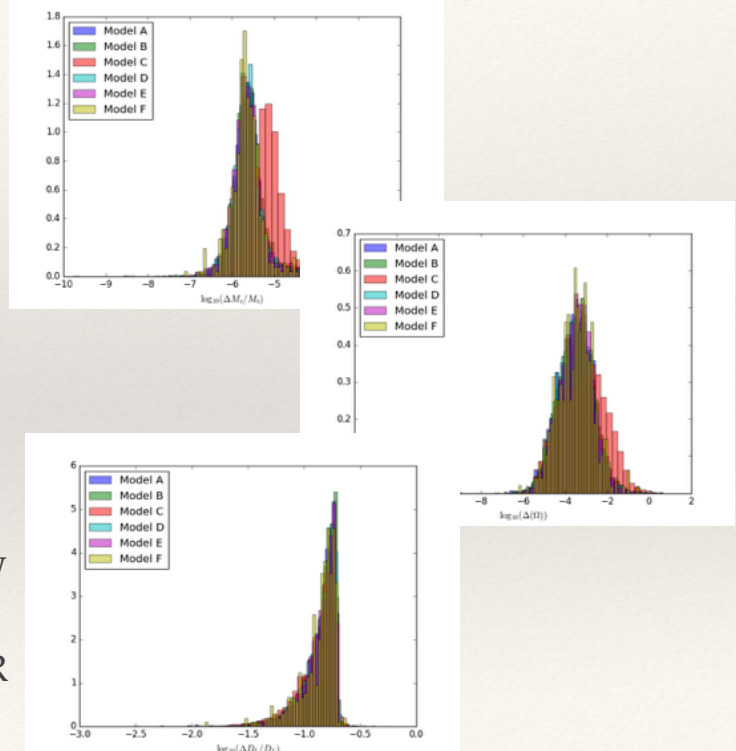
- Each EMRI observation will yield very precise parameter estimates

$$\frac{\Delta M_z}{M_z}, \frac{\Delta \mu_z}{\mu_z}, \Delta \chi, \Delta e_{\text{pl}} \sim 10^{-6} - 10^{-4}$$

$$\Delta \Omega \sim 10^{-5} - 10^{-3}$$

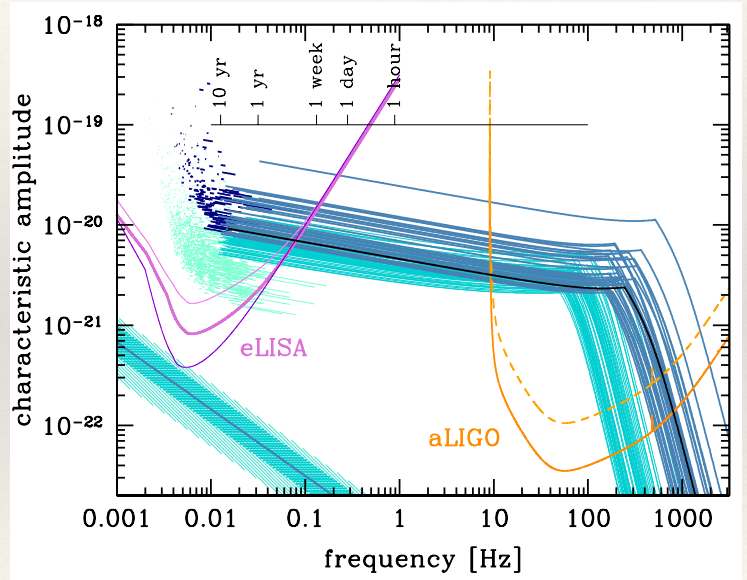
$$\frac{\Delta D_L}{D_L} \sim 0.05 - 0.2$$

- Precision arises from tracking GW phase over $O(10^5)$ cycles. Achievable even at threshold SNR of ~ 20 .



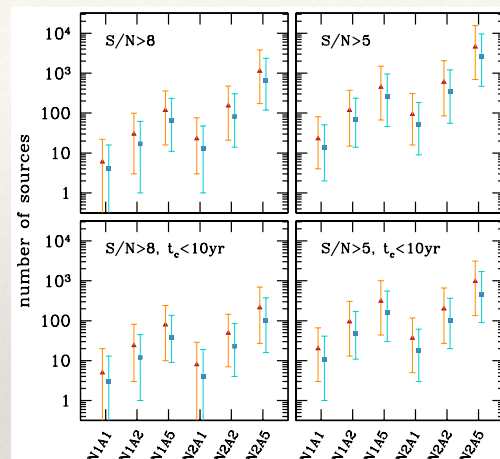
Stellar-origin black hole binaries

- ❖ GW150914 would have been observable by LISA ~5 years before being observed by LIGO, with $S/N \sim 10$ in a 5yr observation. (Sesana 2016)
- ❖ LISA provides sky location to ~0.few square degrees and time of coalescence to ~few s.
- ❖ Number of events could be high (several hundred) but there are significant uncertainties.



Stellar-origin black hole binaries

- ❖ GW150914 would have been observable by LISA ~5 years before being observed by LIGO, with $S/N \sim 10$ in a 5yr observation. (Sesana 2016)
- ❖ LISA provides sky location to ~0.few square degrees and time of coalescence to ~few s.
- ❖ Number of events could be high (several hundred) but there are significant uncertainties.

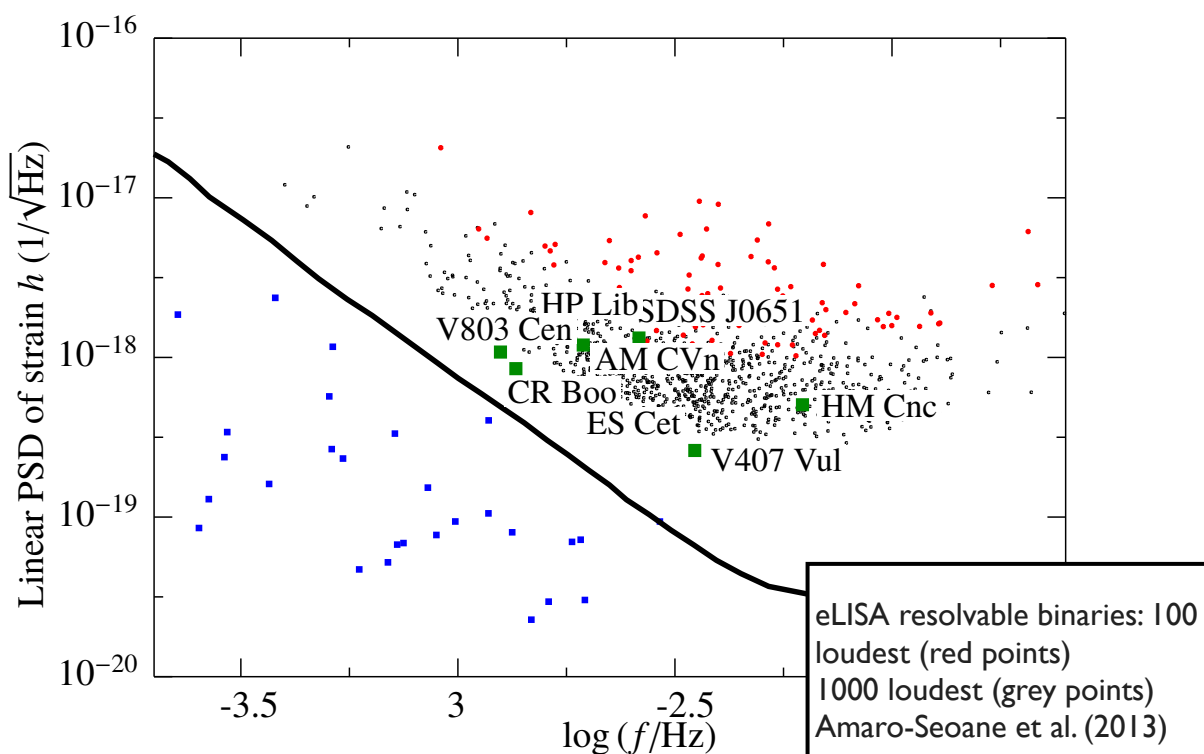


Mass distribution	$R/(\text{Gpc}^{-3}\text{yr}^{-1})$		
	PyCBC	GstLAL	Combined
Event based			
GW150914	$3.2^{+8.3}_{-2.7}$	$3.6^{+9.1}_{-3.0}$	$3.4^{+8.6}_{-2.8}$
LVT151012	$9.2^{+30.3}_{-8.5}$	$9.2^{+31.4}_{-8.5}$	$9.4^{+30.4}_{-8.7}$
GW151226	35^{+92}_{-29}	37^{+94}_{-31}	37^{+92}_{-31}
All	53^{+100}_{-40}	56^{+105}_{-42}	55^{+99}_{-41}
Astrophysical			
Flat in log mass	31^{+43}_{-21}	30^{+43}_{-21}	30^{+43}_{-21}
Power Law (-2.35)	100^{+136}_{-69}	95^{+138}_{-67}	99^{+138}_{-70}

Other sources

- ❖ Compact binaries in the Milky Way
 - Binaries of stellar remnants (white dwarfs or neutron stars) with orbital periods of ~ 1 hour.
 - Known (verification) and unknown sources.
 - Signals almost monochromatic.

Other sources



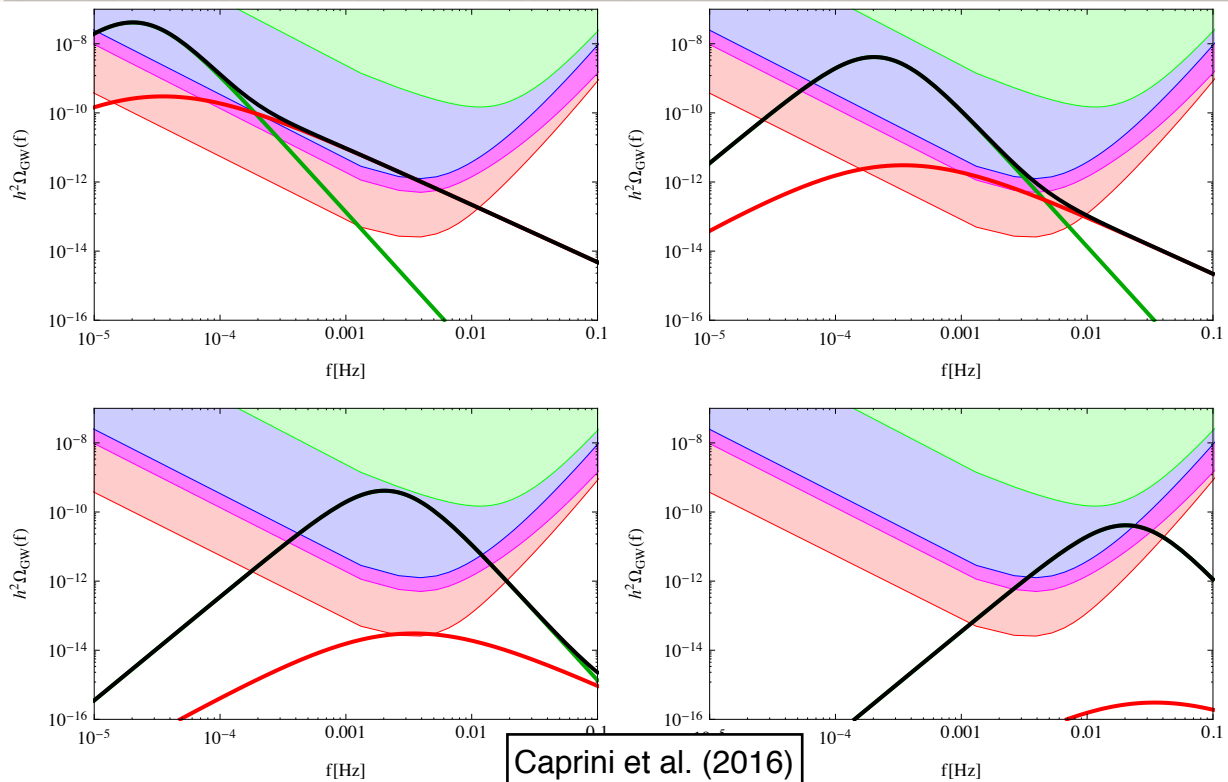
Other sources

- ❖ Compact binaries in the Milky Way
 - Binaries of stellar remnants (white dwarfs or neutron stars) with orbital periods of ~ 1 hour.
 - Known (verification) and unknown sources.
 - Signals almost monochromatic.
 - LISA expected to detect ~ 15000 binaries with $S/N > 7$.
 - LISA should determine 2D/3D location for 4500/1250 sources, measure df/dt for 3000 and d^2f/dt^2 for ~ 3 .

Other sources

- ❖ Compact binaries in the Milky Way
 - Binaries of stellar remnants (white dwarfs or neutron stars) with orbital periods of ~ 1 hour.
 - Known (verification) and unknown sources.
 - Signals almost monochromatic.
 - LISA expected to detect ~ 15000 binaries with $S/N > 7$.
 - LISA should determine 2D/3D location for 4500/1250 sources, measure df/dt for 3000 and d^2f/dt^2 for ~ 3 .
- ❖ Cosmological sources
 - Processes occurring at the TeV scale in the early Universe could generate a mHz stochastic gravitational wave background.
 - Cosmic string networks could produce both individual burst events and a stochastic background.

Other sources



LISA science objectives

- ❖ LISA science objectives cover topics in astrophysics, cosmology and fundamental physics.
- ❖ *Astrophysics: compact binaries in the Milky Way*
 - **SI1.1:** Elucidate the formation and evolution of GBs by measuring their period, spatial and mass distributions.
 - **SI1.2:** Enable joint gravitational and electromagnetic observations of GBs to study the interplay between gravitational radiation and tidal dissipation in interacting stellar systems.

LISA science objectives

❖ *Astrophysics: black holes*

- SI2.1: Search for seed black holes at cosmic dawn.
- SI2.2: Study the growth mechanism of MBHs from the epoch of the earliest quasars.
- SI2.3: Observation of EM counterparts to unveil the astrophysical environment around merging binaries.
- SI2.4: Test the existence of Intermediate Mass Black Hole Binaries (IMBHBs).
- SI3.1: Study the immediate environment of Milky Way like MBHs at low redshift.
- SI4.1: Study the close environment of SOBHs by enabling multi-band and multi-messenger observations at the time of coalescence.
- SI4.2: Disentangle SOBH binary formation channels.

LISA science objectives

❖ *Fundamental Physics*

- SI5.1 Use ring-down characteristics observed in MBHB coalescences to test whether the post-merger objects are the black holes predicted by GR.
- SI5.2 Use EMRIs to explore the multipolar structure of MBHs.
- SI5.3 Testing for the presence of beyond-GR emission channels.
- SI5.4 Test the propagation properties of GWs.
- SI5.5 Test the presence of massive fields around massive black holes with masses $> 10^3 M_{\odot}$.

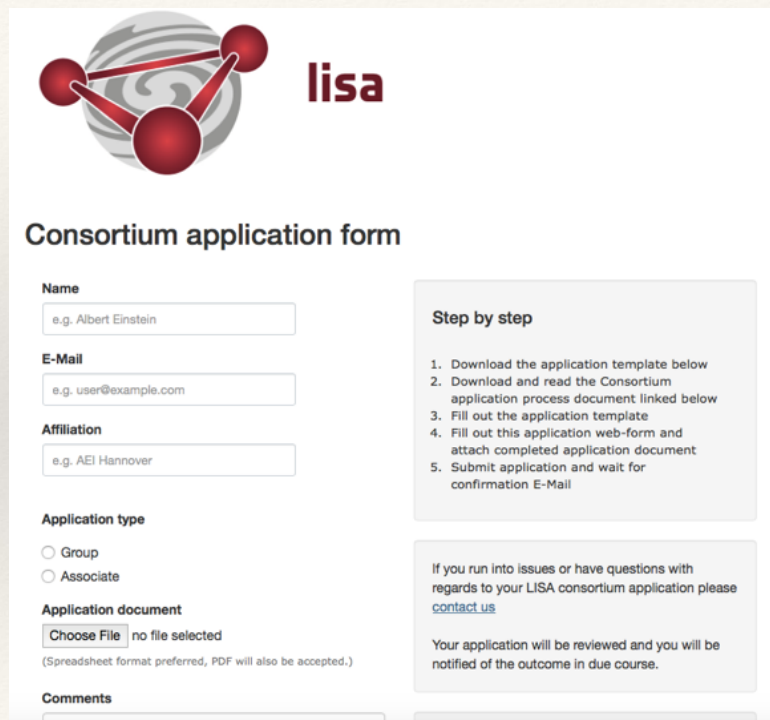
LISA science objectives

❖ *Cosmology*

- **SI6.1:** Measure the dimensionless Hubble parameter by means of GW observations only.
- **SI6.2:** Constrain cosmological parameters through joint GW and EM observations.
- **SI7.1:** Characterise the astrophysical stochastic GW background.
- **SI7.2 :** Measure, or set upper limits on, the spectral shape of the cosmological stochastic GW background.
- **SI8.1:** Search for cusps and kinks of cosmic strings.
- **SI8.2:** Search for unmodelled sources.

The LISA Consortium

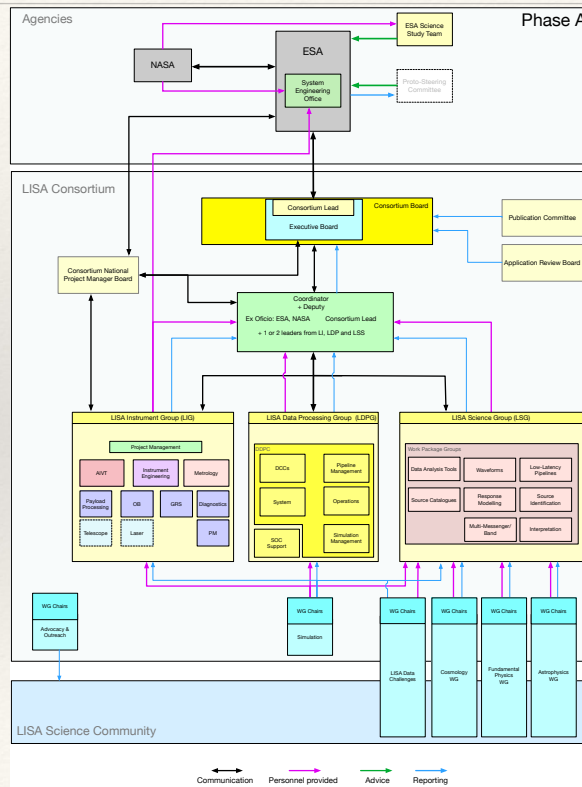
- ❖ The LISA Consortium is the community of scientists who will develop the tools to exploit LISA science.
- ❖ The Consortium was recently rebooted with a round of applications for membership.
 - *associate members:* interested in LISA science;
 - *full members:* commit to deliver something to the Consortium.
- ❖ Have accepted ~425 full and ~550 associate members.



The screenshot shows the 'Consortium application form' for LISA. It features the LISA logo (a stylized red and grey sphere with three red spheres connected by lines) and the text 'lisa'. The form includes fields for Name (e.g., Albert Einstein), E-Mail (e.g., user@example.com), Affiliation (e.g., AEI Hannover), Application type (Group or Associate), Application document (Choose File, no file selected), and Comments. A 'Step by step' guide is provided on the right, listing five steps: 1. Download the application template below, 2. Download and read the Consortium application process document linked below, 3. Fill out the application template, 4. Fill out this application web-form and attach completed application document, 5. Submit application and wait for confirmation E-Mail. A note at the bottom right states: 'If you run into issues or have questions with regards to your LISA consortium application please [contact us](#). Your application will be reviewed and you will be notified of the outcome in due course.'

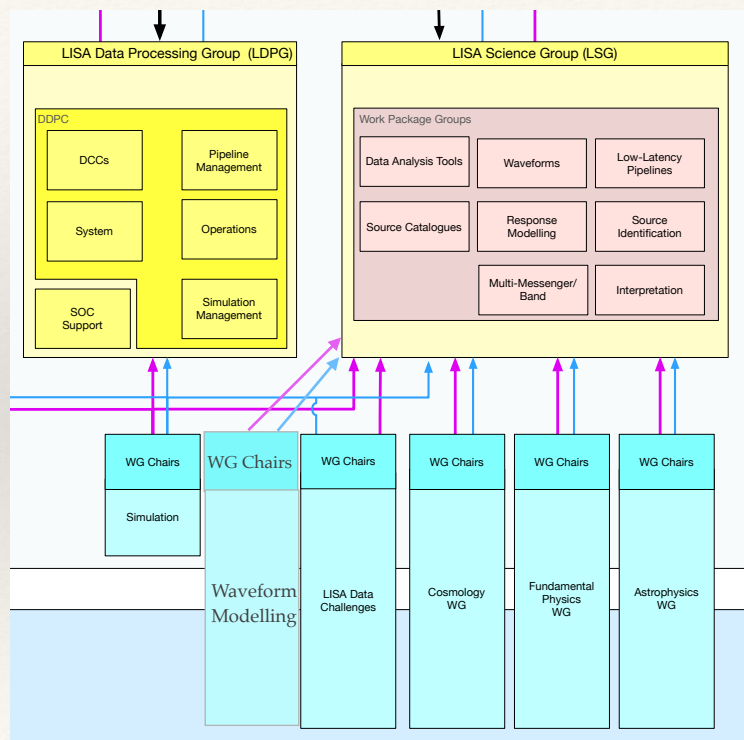
<https://signup.lisamission.org>

Consortium structure



Consortium structure

- ❖ The groups connected to the delivery of science by the LISA Consortium are in the bottom right.



LISA Science Group

- ❖ Help **define key-science objectives** for the LISA consortium; deliver work required to achieve these goals and ensure it is completed on time.
- ❖ Interface with science working groups to ensure objectives are up to date.
- ❖ Prioritise work according to project needs and work package dependencies.
- ❖ Work packages under the LSG will focus on **identification** and **delivery** of LISA consortium **science objectives**, and **develop data analysis methods** and **prototypes** that are needed to deliver this science.
- ❖ **Implementation** in LISA data processing infrastructure will be done in conjunction with the **LISA Data Processing Group**.

LISA Data Processing Group

- ❖ The LISA Data Processing Group will oversee provision of ground segment infrastructure, frameworks for data analysis and production pipelines.
- ❖ Define standards and platforms. Responsible for data management, including public data and catalogue releases.
- ❖ Ensure Data Processing Centre(s) are established with appropriate capacity.
- ❖ Interface with ESA Science Operation Centre (SOC). Manage operational software for producing calibrated TDI data, that will be run in the SOC.
- ❖ Implement production versions of pipelines developed within the LSG.

LISA Science Group Organisation

- ❖ LISA Science group structured around a data analysis description put together in September 2017. For each Science Investigation, the work needed was identified and divided into sub-elements.
- ❖ Example: **SI6.1: Measure the dimensionless Hubble parameter by means of GW observations alone; SI6.2: Constrain cosmological parameters through joint GW and EM observations.**
- ❖ Consortium must deliver GW observations, alerts and cosmological parameter estimate., which requires
 - ❖ Low-latency pipelines to trigger alerts.
 - ❖ Mechanism for sending alerts.
 - ❖ MoUs with EM partners for joint analysis (SI 6.2) or host catalogues (SI 6.1).
 - ❖ Mechanism to trigger protected periods.

LISA Science Group

- ❖ Work package description available in the document LISA-LCST-SGS-WPD-001, available on the consortium website. Work grouped into a number of themes.
- ❖ Document will evolve over time and will always reflect current plans for science delivery.
- ❖ Applicants referenced the WPs when applying for membership. Currently have ~200 members in the LISA Science Group, and ~60 committed FTEs.

WP Group	Description	Members	FTEs
1	Waveform modelling	61	15.178
2	Data analysis tools	7	0.975
4	Low-latency pipelines	12	2.125
5	Global and individual source identification	55	11.722
6	Source catalogues	3	0.375
7	Multi-messenger, multi-band	31	4.197
8	Interpretation, key-science projects	89	20.662
Unspecified		10	2.38
Total		195 (distinct)	57.6

LISA Science working groups

- ❖ Three science working groups have replaced the previous consortium working groups, one focussed on each major area:
 - ❖ **Astrophysics**
 - ❖ **Cosmology**
 - ❖ **Fundamental Physics**
- ❖ These will form a bridge between the LISA Consortium and the wider scientific community and provide an environment for discussion and promotion of LISA science.
- ❖ There are also **LISA Data Challenge**, **Waveform** and **Simulation** working groups, which form a similar role for more technical areas.

LISA Data Challenge working group

- ❖ The LDC group was established to resume activities begun by the LISA Mock Data Challenges. Biweekly telecons on Friday at 16:00 CET.
- ❖ Activity within work package group 5 (Global and individual source identification) will initially be driven by the Data Challenges. Data sets will be constructed to address specific questions posed by the Science Group.

LDC Challenge 1 Meetings Contact Admin Login Sign up

LISA Data Challenge 1: *Radler*

We are glad to announce the release of datasets for the first "new" LISA Data Challenge, codenamed **Radler**. The purpose of this first challenge is to tackle the main LISA sources separately, under an idealized instrument-noise model. Our aim is to introduce new researchers to LISA data analysis, to rehabilitate existing analysis codes developed during the [original Mock LISA Data Challenges](#) (2005–2011), and to establish LDC process and standards.

Radler includes **six subchallenges**, described below. This challenge will not be blind (source parameters are available), but you are welcome to try the analysis without referring to the answer. Furthermore, versions of the datasets without instrument noise are included in the release. LDC working-group members will be preparing their own analysis using their algorithms of choice, and invite you to join them (to do so, [e-mail us](#) so we can pair you appropriately). Of course, you may organize to work on your own, or with your collaborators.

For usage tracking purposes, we request that you set up a login for this website before downloading the datasets. Please **submit your results by December 31, 2018**, using the submission interface and format that will appear shortly on this page. Please plan to include a description of your methods (or a link to a methods paper) with your submission. We would also greatly appreciate it if you were to share your code (e.g., on GitHub, or on our GitLab).

While we did our best to check the datasets for correctness, small problems or inconsistencies may have escaped us. The best way to validate the data is to analyze it, so [let us know](#) of any problems!

[Log in to download](#)

[LDC-1 documentation](#)

[Log in to get LDC-1 code](#)

[Ask for help](#)

<https://lisa-ldc.lal.in2p3.fr/ldc>

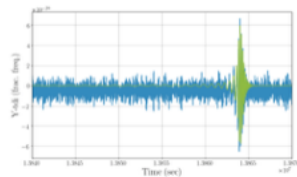
LISA Data Challenge 1

For usage tracking purposes, we request that you set up a login for this website before downloading the datasets. Please **submit your results by December 31, 2018**, using the submission interface and format that will appear shortly on this page. Please plan to include a description of your methods (or a link to a methods paper) with your submission. We would also greatly appreciate it if you were to share your code (e.g., on GitHub, or on our GitLab).

While we did our best to check the datasets for correctness, small problems or inconsistencies may have escaped us. The best way to validate the data is to analyze it, so [let us know](#) of any problems!

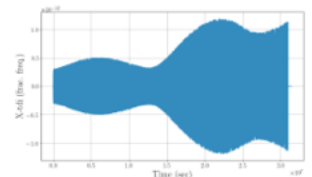
LDC1-1. A single GW signal from a merging massive-black-hole binary.

LIGO and Virgo have done it, so let's get LISA on the right path! MBHBs are represented with a frequency-domain inspiral-merger-ringdown phenomenological model (IMRPhenomD). The black holes are spinning, with spin vectors parallel to the orbital angular momentum. The release includes datasets for two methods (frequency- and time-domain) of applying the LISA response to the GWs.



LDC1-2. A single GW signal from an extreme-mass-ratio inspiral.

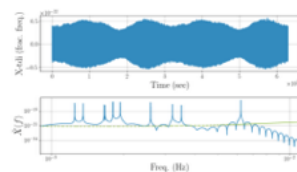
EMRIs are modeled with the "classic" *Analytic Kludge* waveforms, which will be updated in future challenges, so make your code flexible! The signal is produced in the time domain and the response is applied using LISACode. The signal is of moderate strength, but the source parameters are drawn from relatively wide priors. This should make for a good challenge!



LISA Data Challenge 1

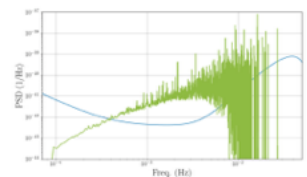
LDC1-3. Superimposed GW signals from several verification Galactic white-dwarf binaries.

We assume circular orbits and purely gravitational interactions. The phase of the signal includes frequency and first derivative. This one should be easy!



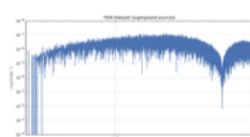
LDC1-4. A GW signal from a population of Galactic white-dwarf binaries.

Here's the classic cocktail-party problem: 26 million signals, produced with a "fast response" code. Parameters of all binaries are available in a large HDF5 file.



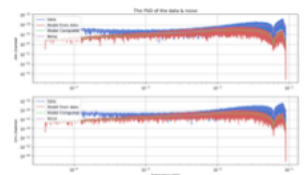
LDC1-5. A GW signal from a population of stellar-origin (stellar-mass) black-hole binaries.

LIGO and Virgo's gift to LISA. The population follows Salpeter's mass function, with an overall rate based on recent LIGO-VIRGO estimates. Waveform and LISA response are computed in the frequency domain.



LDC1-6. An isotropic stochastic GW signal of primordial origin.

Statistics are Gaussian, but the spectral shape is shrouded in mystery, with parameters chosen for us by the LISA Consortium Cosmology Working Group. The signal is generated using LISACode as a choir of elementary sources uniformly distributed across the sky. To make things easier for you, instrumental noise is Gaussian, uncorrelated, and of the same level in each LISA link.



Japanese involvement in LISA

- ❖ Associate members may come from any country, and do not need to commit any time to LISA work.
- ❖ The science and technical working groups — **astrophysics, fundamental physics, cosmology, waveforms, data challenge** and **simulation** — are open to both associate and full members.
- ❖ Full membership is restricted to countries that have an agreement with ESA.
- ❖ One Japanese group (Izumi) has already joined as full members, and are likely to provide some instrumentation. JAXA is drafting a letter of interest to ESA, so the arrangement is likely to be formalised soon.

LISA Science Group Core Team

- ❖ LISA Science Group Core Team
 - ❖ Chairs: Jonathan Gair, Michele Vallisneri
 - ❖ WP group 1 (**waveform modelling**): Leor Barack, Harald Pfeifer
 - ❖ WP group 2 (**data analysis tools**): Stas Babak, Ian Harry
 - ❖ WP group 4 (**low-latency pipelines**): Tyson Littenberg, Laurentiu-Ioan Caramete
 - ❖ WP group 5 (**global and individual source identification**): Neil Cornish, Curt Cutler
 - ❖ WP group 6 (**source catalogues**): Enrico Barausse, Curt Cutler
 - ❖ WP group 7 (**multi-messenger, multi-band**): John Baker, Zoltan Haiman, Elena Rossi
 - ❖ WP group 8 (**interpretation, key science**): Emanuele Berti, Vitor Cardoso, Alberto Sesana

LISA Science working groups

- ❖ LISA Science working group chairs
 - ❖ **Astrophysics:** Gijs Nelemans, Shane Larson, Lucio Meier, Marta Volonteri;
 - ❖ **Cosmology:** Robert Caldwell, Chiara Caprini, Germano Nardini;
 - ❖ **Fundamental Physics:** Thomas Hertog, Philippe Jetzer, Nico Yunes
- ❖ LISA technical working group chairs
 - ❖ **Data Challenge:** Stas Babak, Michele Vallisneri;
 - ❖ **Waveforms:** Maarten van de Meent, Deirdre Shoemaker, Niels Warburton, Helvi Witek;
 - ❖ **Simulation:** Luigi Ferraioli, Joseph Martino, Daniele Vetrugno.

Summary

- ❖ LISA is on course to launch in 2034 and is expected to detect a range of sources
 - Massive black hole mergers;
 - Extreme-mass-ratio inspirals;
 - Stellar-origin BH binaries, galactic binaries, cosmological sources.
- ❖ These observations will facilitate a wide range of science investigations in **astrophysics, cosmology and fundamental physics**.
- ❖ Work on LISA is being organised within the LISA Consortium.
- ❖ Science exploitation and data analysis development will be done by the **LISA Science Group** (key science definition and prototype pipelines) and the **LISA Data Processing Group** (production pipelines and infrastructure), with support from the **science, simulation and data challenge** working groups.
- ❖ We very much hope that Japanese groups will participate in this endeavour and help to deliver the great science.

Session S3A1 9:45–10:15

[Chair: Hideyuki Tagoshi]

Jiro Murata

Department of Physics, Rikkyo University

**“Laboratory Tests of Newtonian Gravity as tests of Inverse
Square Law”**

(10+5 min.)

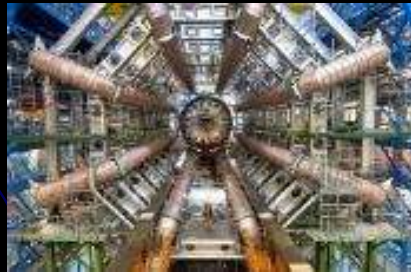
[JGRG28 (2018) 110702]

FAQ on Experimental Gravity

Q: Where is the minimum scale, at which gravity is tested?

Expected answer: 100 micron

My answer: the LHC scale ($10^{-20}m$)

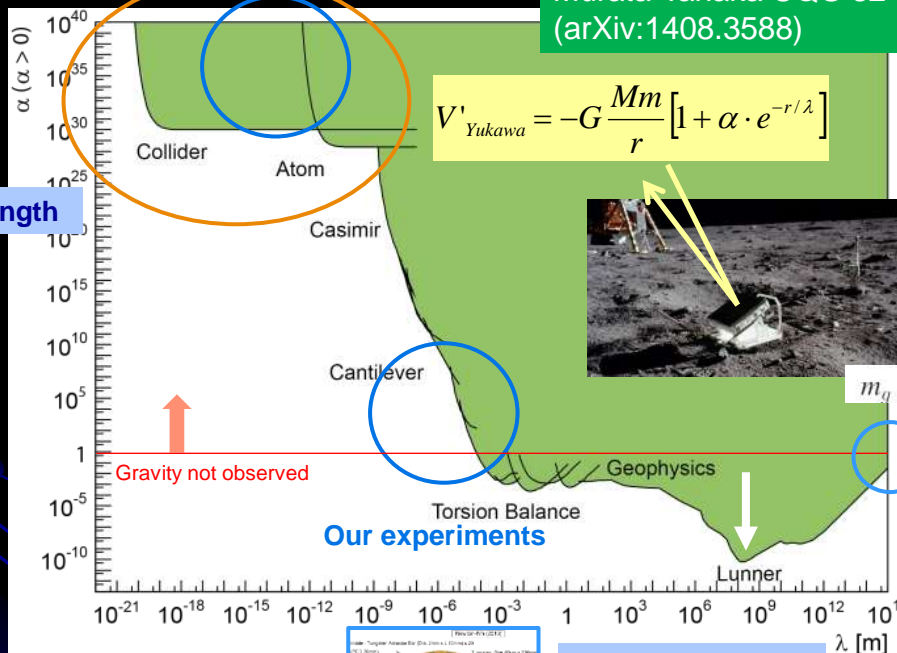


Experimental Constraints on Gravitational Inverse Square Law

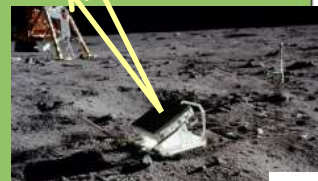
Our analysis

Murata-Tanaka CQG 32 (2015) 033001
(arXiv:1408.3588)

Coupling Strength



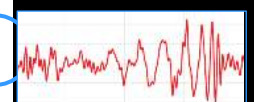
$$V'_{Yukawa} = -G \frac{Mm}{r} [1 + \alpha \cdot e^{-r/\lambda}]$$



Apollo-11

$$\lambda_g > 10^{13} \text{ km}$$

$$m_g < 1.2 \times 10^{-22} \text{ eV}/c^2$$



Gravitational Wave (LIGO)

$$\lambda_g \neq r$$

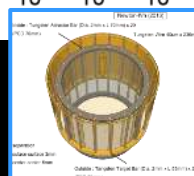
Our experiments

Interaction Range

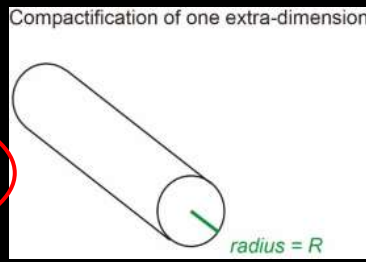
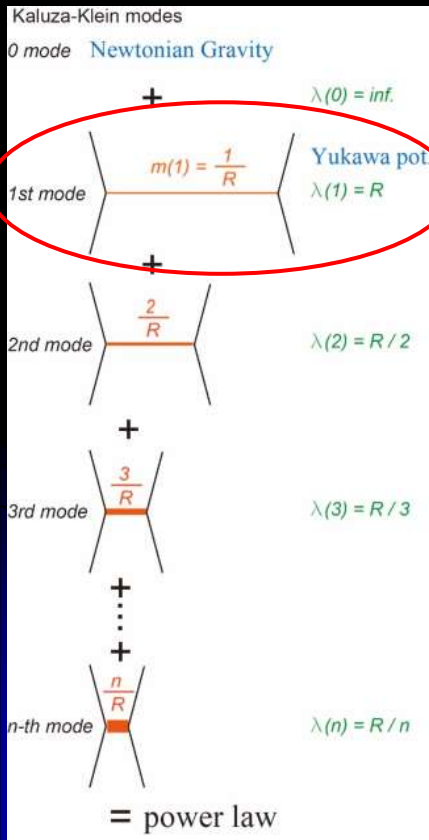
Distance (r) dep. of graviton mass

Earth – Binary Stars distance ($10^{25}m$)
& (at the Rs Schwarzschild radii 210km)

Yukawa parametrization
Boson exchange / 1st KK excitation



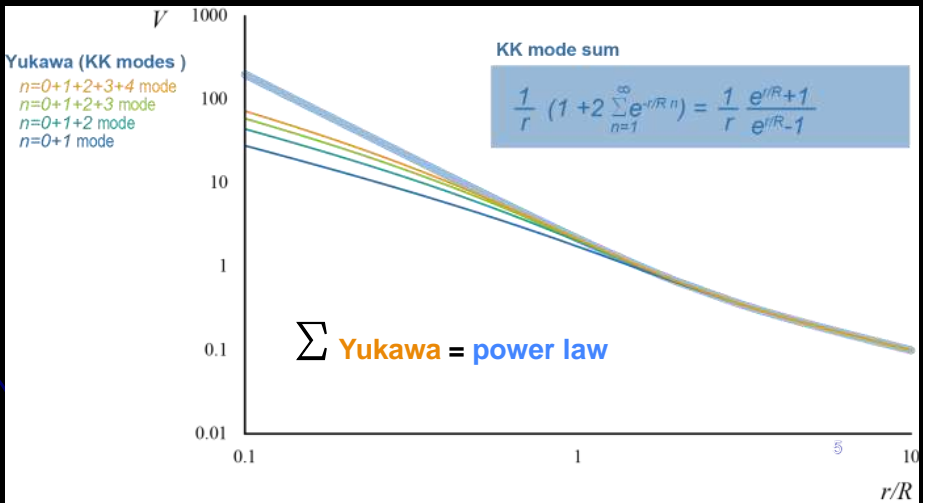
Extra Dimension : Power Law type



Compactification of extradimension

Quantification of extradimensional momentum

seen as discrete graviton "mass" in 4d world



ATLAS PRL 110, 011802 (2013) Searching graviton emission

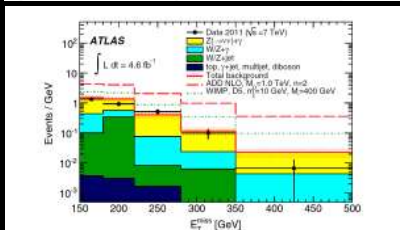
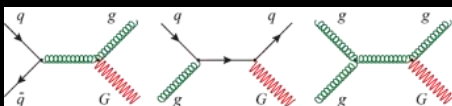


FIG. 1 (color online). The measured E_T^{miss} distribution (black dots) compared to the SM (solid lines), SM + ADD (dashed lines), and SM + WIMP (dotted lines) predictions, for two particular ADD and WIMP scenarios.

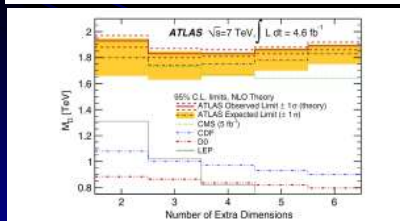
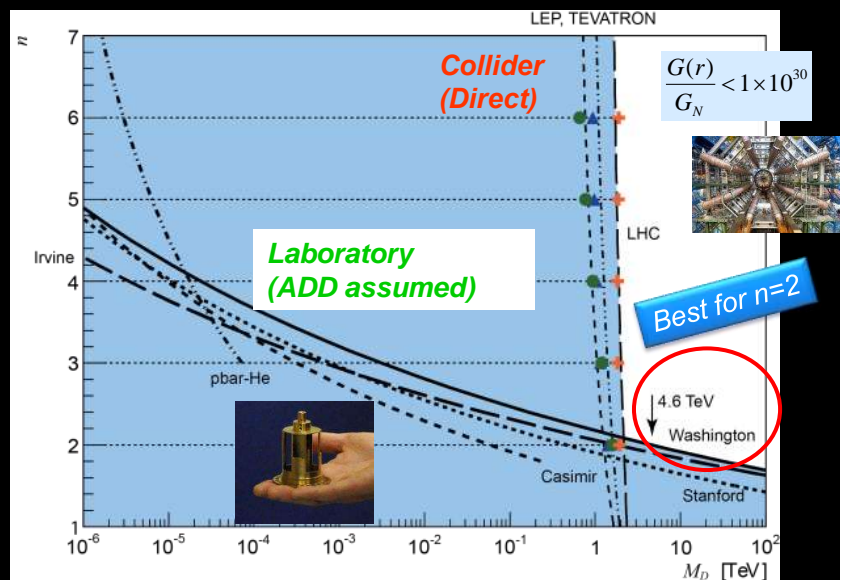


FIG. 2 (color online). Observed (solid lines) and expected (dash-dotted lines) 95% C.L. limits on M_D as a function of the number of extra spatial dimensions n in the ADD model. The results are compared with previous results [1,3,6] (other lines). In [6], weights are applied that suppress the region with $\xi > M_D$.

Murata-Tanaka CQG 32 (2015) 033001 (arXiv:1408.3588)

of Extra Dim.



$$\lambda = \frac{(M_{pl} / \sqrt{8\pi})^{2/n} \hbar}{M_D^{1+2/n} c}$$

H.D. Planck mass

ADD interpretation

$$M_{pl}^2 = M_D^{2+n} \lambda^n (c/\hbar)^n$$

Short Range : Data > Power Law Parametrization > (ADD) > MD
 Collider : Data > MD > (ADD) > Power Law Parametrization > alpha-lambda

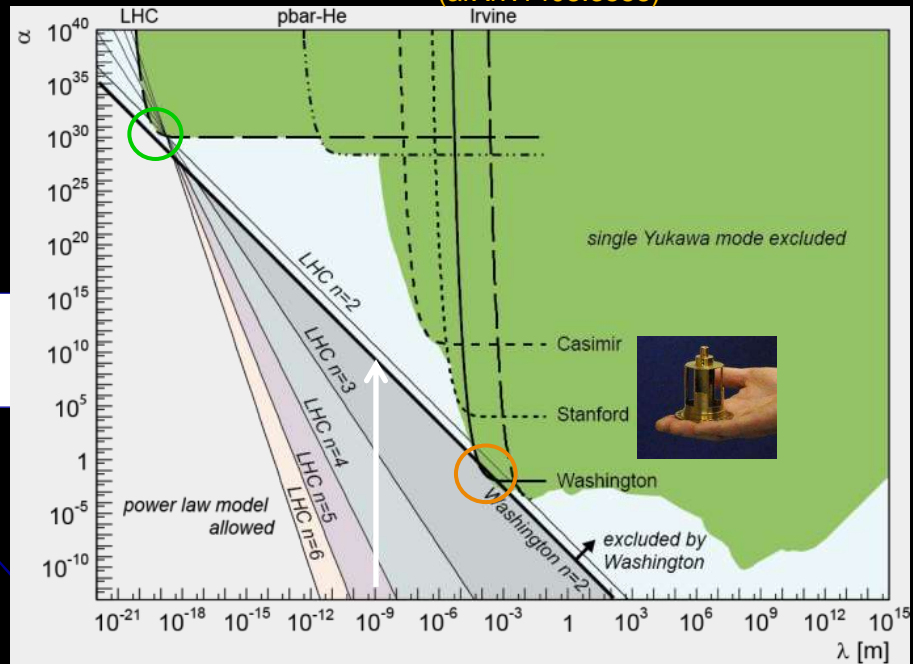
Interpretation (translation) of the ADD line (power law) in the alpha-lambda plot (Yukawa)

Murata-Tanaka CQG 32 (2015) 033001 (arXiv:1408.3588)



$$\alpha'(\lambda) = \frac{(1+n) \left(\frac{\lambda}{r}\right)^n}{(1+\frac{r}{\lambda})e^{-r/\lambda}}$$

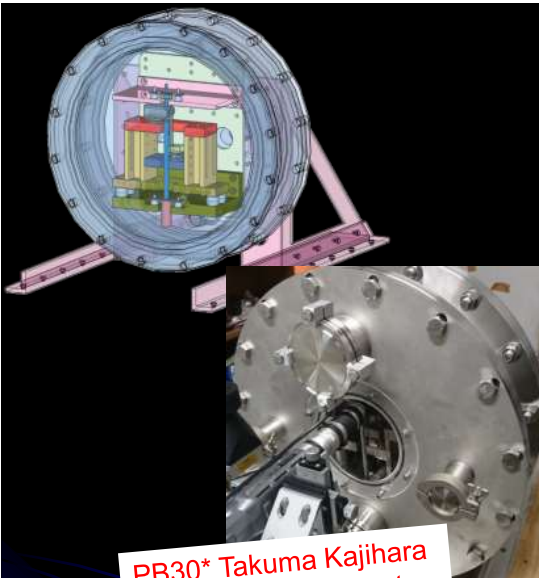
Corrected alpha:
Physics = power law
Parametrization = Yukawa



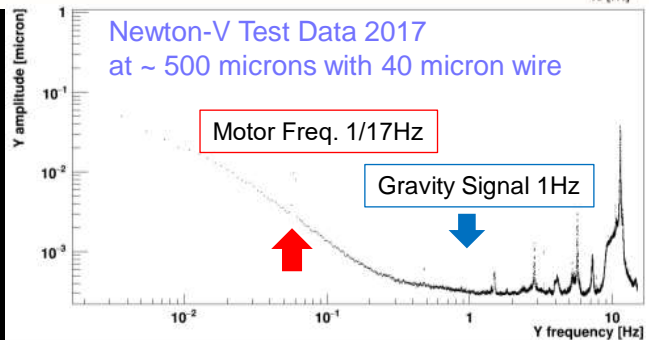
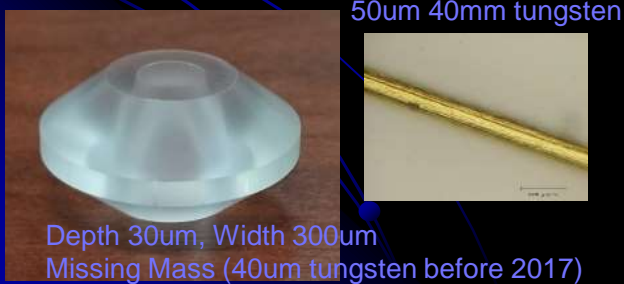
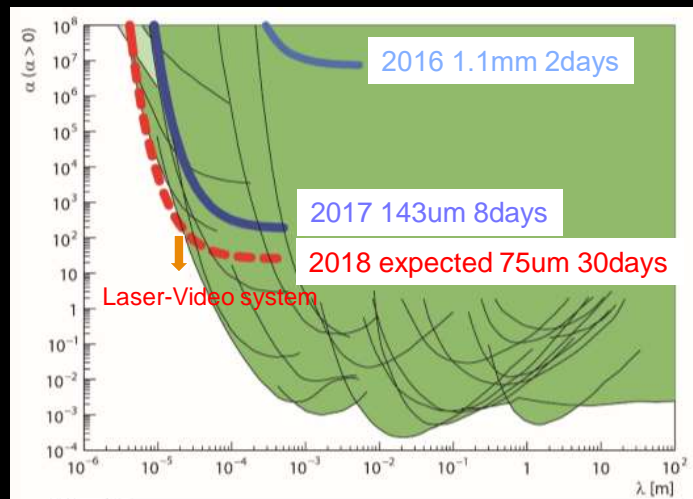
LHC is the only sensitive tool for n > 2

mm is the best place for n = 2

Newton-V status



PB30* Takuma Kajihara
Newton-V experiment:



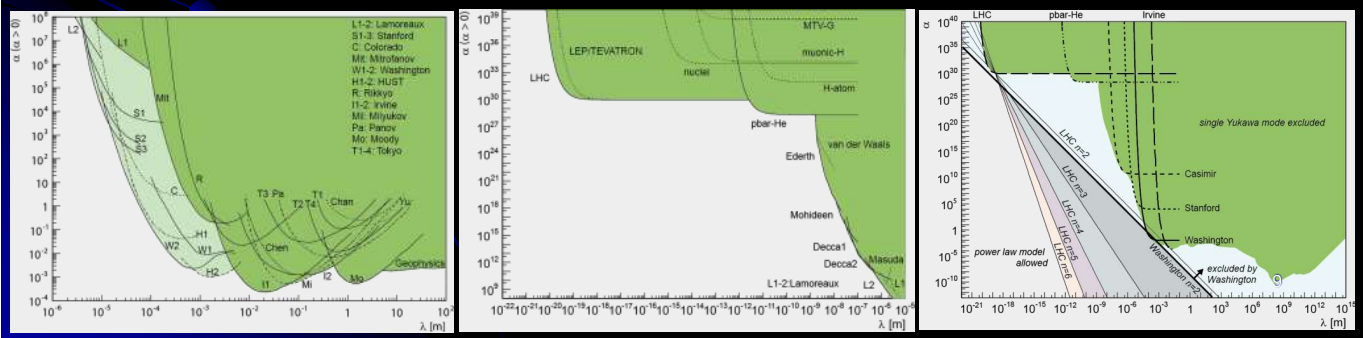


Topical Review

A review of short-range gravity experiments in the LHC era

Jiro Murata and Saki Tanaka

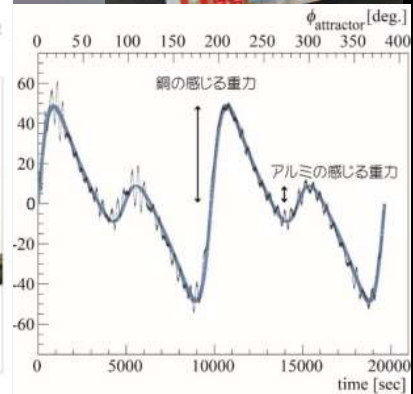
Department of Physics, Rikkyo University, 3-34-1 Nishi-Ikebukuro, Tokyo 171-8501, Japan



Test of Weak Equivalence Principle at the shortest scale



Ninomiya-Murata, Class. Quantum Grav. 34 (2017) 185005



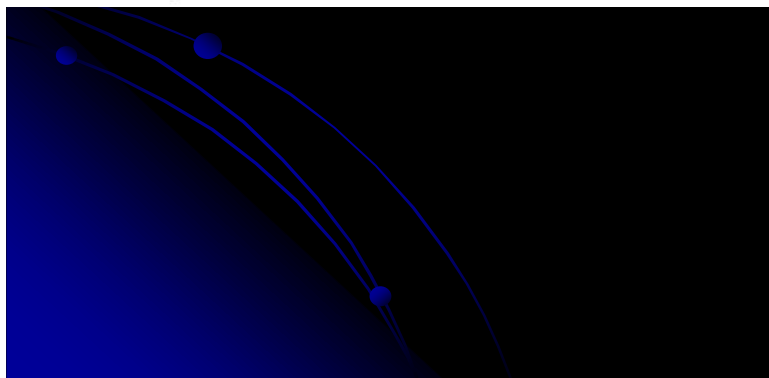
Equivalence Principle ~ Lorentz Invariance ~ Quantum Gravity



Short-range test of the universality of gravitational constant G at the millimeter scale using a digital image sensor

K Ninomiya¹, T Akiyama, M Hata, M Hatori, T Iguri, Y Ikeda, S Inaba, H Kawamura, R Kishi, H Murakami, Y Nakaya, H Nishio, N Ogawa, J Onishi, S Saiba, T Sakuta, S Tanaka, R Tanuma, Y Totsuka, R Tsutsui, K Watanabe and J Murata

Department of Physics, Rikkyo University, 3-34-1 Nishi-Ikebukuro, Tokyo 171-8501 Japan



WEP Violation Parameter

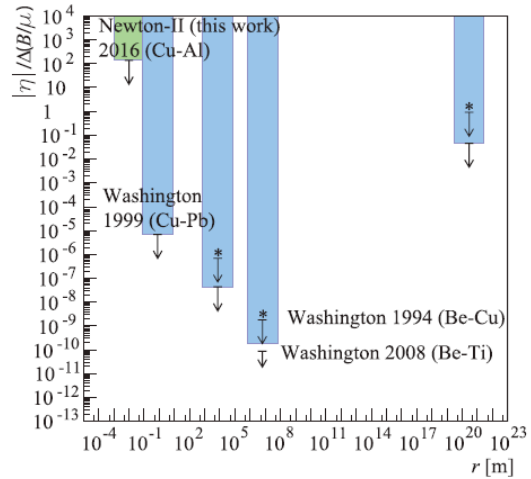


Figure 7. Constraints on the 'reduced' WEP violation parameter $\eta/\Delta(B/\mu)$, plotted as a function of measuring distance. The result of this study is shown as Newton-II 2016. References are same as figure 6.

Butsuri: Membership Journal of the Physical Society of Japan, 2018 Nov



日本物理学会誌 解説: 11月号

High Energy News 2014

重力逆二乗則の実験検証



村田 次郎
立教大学理学部
jmu@itikkyo.ac.jp

万有引力の法則は近代科学の出発点に位置する物理学の定石であり、一般相対論による修正が必要となる種々な状況を除いて、現在でも観測と一致し続ける高精度である。一方、重力の逆二乗則は高精度で検証されているのは惑星スケールであり、太陽系の外側あるいは近距離の検証状況は異質である。例えば地球と月の距離では検証精度は 10^{-11} にも達するが、センチメートル距離では 10^{-4} に悪化する。さらに 10 μm では精度が 100% を超えるに超える。つまり重力の存在自身が検証精度を阻害している。10 μm 以下の世界で観測したことがない。一方プランク長は $l_p = \sqrt{\hbar G/c^3} \sim 1.6 \times 10^{-35}$ m であり、万有引力定数 G を用いてこの寸法よりも小さな距離を算出している。これは、この距離まで万有引力定数が一定であること、すなわち逆二乗則が成立し続けることを保証したもので、実験で検証されている領域からの実測に 10 桁以上にもはる大差を有する結果であることに注意が必要である。...

スケール別では現在観測されている「閉鎖」になる。と自然に理解できる魅力的なアイデアである。その特徴的な特徴は 10 mm 程度で 4 乗に切り替わる、というものである。実験ですべての手が腐せるような領域に大発見が待ちかまわされているかもしれない。工夫を凝らした実験が多く行われることとなった。筆者もその一人であり、加速実験の検出器位置較正技術を用いた実験を進めた。筆者らの実験室実験では、小物体にはたらく重力の強さを検証する。この予定の面白い点は、重力の強まりにより加速実験でも検証が可能という点である。実際、実験型加速装置である LHC においても検証が行われてきた。予備から既に 30 年が経過し、結果として 0.1 mm での検証は実験で否定された。だが、まだまだ 10 μm 以下では可能性は残されている。...

重力の逆二乗則は以前より検証のブームが繰り返され、精度が向上してきた。それらの検証を踏まえて、実験検証は山川の (7) スケールへ移される。しかし大きな実験は検証には必要であるから、両者の比較が難しい。この実験は重力も重力もつのがわかりにくい。とりわけ LHC での重力現象の探索は定量的には感度をもちが実験室実験との階層が異なる点では定量的には不明確である。実験室実験と LHC の結果を同じ (7) スケール空間で比較することによって、重力の強まりに対しては LHC と mm スケールの実験の結果を比較し、他の領域に比べて最も強い感度をもちつことが明らかになった。この実験は次元の適合性、同じ性質による実験室実験との互換性 23 μm が最も強い。実験室実験の大きさの上限となつていく。

■ 研究紹介

余剰次元探索を目指した近距離重力実験

立教大学理学部
村田 次郎
jmu@itikkyo.ac.jp

田中 佐季, 二宮 一史, 村上 遥菜
2014年2月12日

高エネルギーニュース Vol.32 No. 4 (233) 2014

高エネルギーニュース HIGH ENERGY NEWS



Volume 32 Number 4 January/February/March 2014



ガリレオ
GALILEO X

サイエンスやテクノロジーに関わる新しい動向を注目の研究を、「深く・わかりやすく・面白く」伝える30分の科学ドキュメンタリー

BS Fuji Galileo-X, Nov 2013



NHK BS Cosmic Front, Nov 2014



Gravity Laboratory Tour

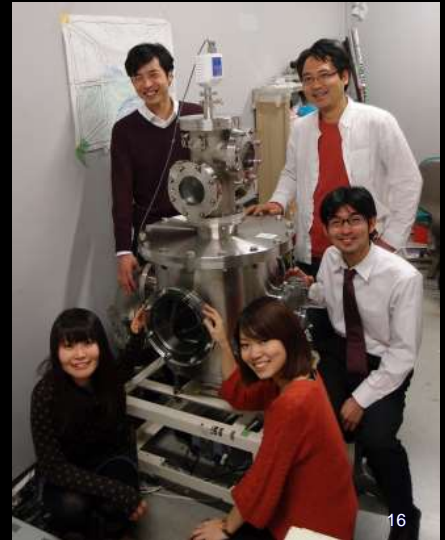
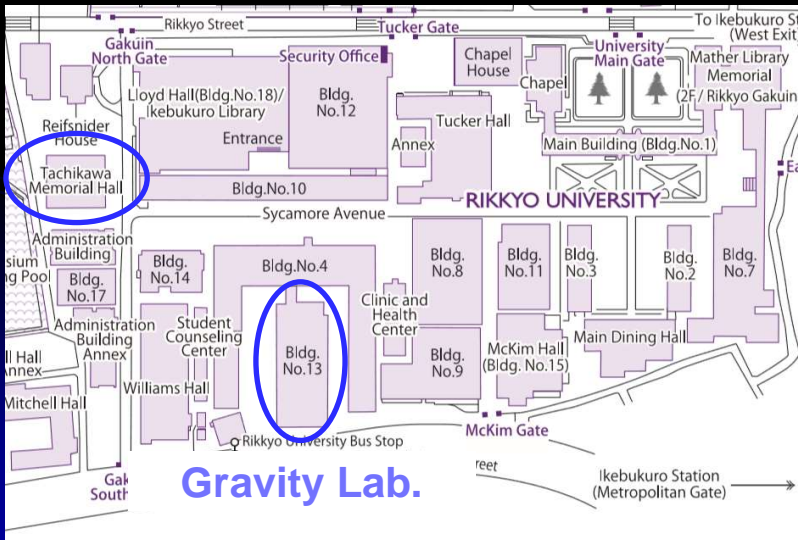
Please try to catch me!

Pre-Scheduled Tour : This afternoon

1:30PM and 3:40PM

(During Lunch or Coffee)

meet us at the 1st floor ENTRANCE





Discussion

Theoretical suggestions for future experiments are welcome!

Session S3A2 11:15–12:15

[Chair: Kenichi Oohara]

Yasutaka Koga

Rikkyo University

**“Rotating accretion flows in D dimensions - sonic points,
critical points and photon spheres -”**

(10+5 min.)

[JGRG28 (2018) 110704]

Rotating accretion flows in D dimensions

- sonic points, critical points and photon spheres -

Yasutaka Koga

Rikkyo University, Japan

November 5-9, 2018

Collaborator: Tomohiro Harada

JGRG @ Tokyo, Japan

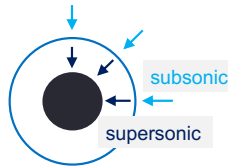
Y. Koga & T. Harada, PRD98, 024018 (2018), arXiv:1803.06486.

Outline

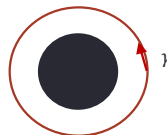
- 1 Introduction
- 2 Rotational accretion problem in D dimensions
- 3 Proof of **SP/PS correspondence**
- 4 Summary

1. Introduction

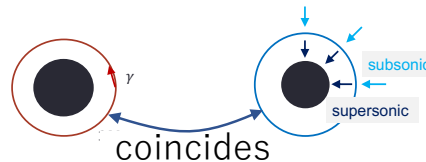
- Sonic point (SP): an accretion flow transit from subsonic to supersonic state.



- Photon sphere (PS): a sphere on which circular null geodesics exist.

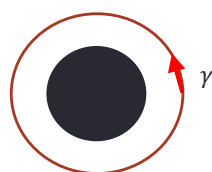


- **SP/PS correspondence**: for **radiation fluid** accretion, the radius of SP coincides with PS.

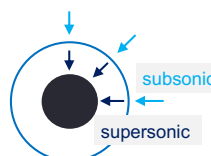


SP/PS correpondence

- Michel accretion (1972)
 - Spherical flow in Schwarzschild spacetime
 - SP at $r_s = 3M$ for radiation fluid
 - → **SP coincides to photon sphere** ($r_{ph} = 3M$ in Sch.)
- Physical reasons?
 - Just a coincidence?
 - Due to the microscopic construction of radiation fluid? (radiation fluid = system of photons)



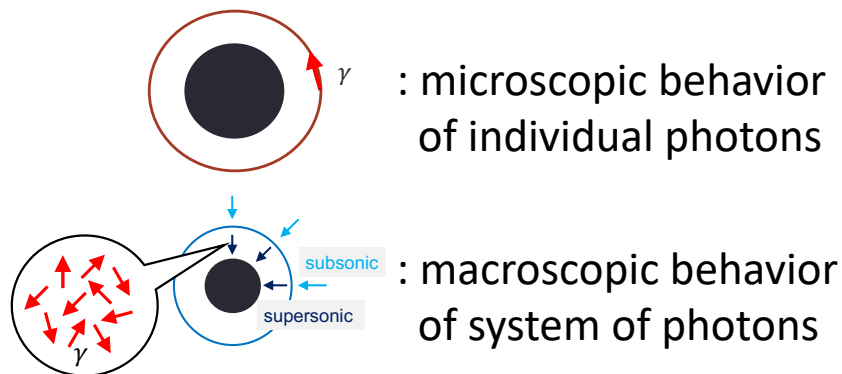
: microscopic behavior of individual photons



: macroscopic behavior of system of photons

SP/PS correspondence

- Michel accretion (1972)
 - Spherical flow in Schwarzschild spacetime
 - SP at $r_s = 3M$ for radiation fluid
 - → **SP coincides to photon sphere** ($r_{ph} = 3M$ in Sch.)
- Physical reasons?
 - Just a coincidence?
 - Due to the microscopic construction of radiation fluid? (radiation fluid = system of photons)



SP/PS correspondence

- SP/PS correspondence in more general cases
 - Koga & Harada (2016): spherical flow in **arbitrary** static spherically symmetric spacetime of **arbitrary dimensions**
 - Koga & Harada (2018): **axially symmetric flow** in arbitrary static spherically symmetric spacetime of arbitrary dimensions

⇒ **SP/PS correspondence is NOT just a coincidence.**

2. Rotational accretion problem in D dims

- Situation:
 - Stationary **axially symmetric** accretion flow **on an equatorial plane** in general static spherically symmetric spacetime in D dims.

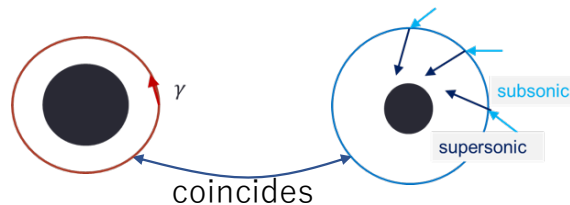
- Metric:

$$ds^2 = -f(r)dt^2 + g(r)dr^2 + r^2 d\Omega_{D-2}^2 \quad (1)$$

- SP/PS correspondence (result) :

Theorem (SP/PS correspondence)

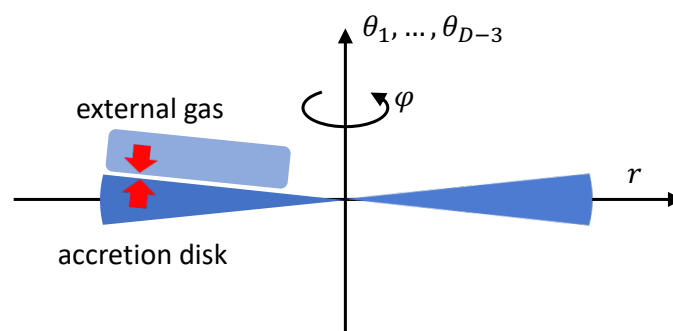
For our accretion model, for any stationary and **axially symmetric** physical transonic accretion flow of **radiation fluid**, its **sonic point is located at (one of) the unstable photon sphere(s)**.



Accretion model

[c.f. Abraham et al. (2006)]

- Rotational accretion (disk) model :
 - 1 Disk lies on the equatorial plane.
(all the polar angles $\theta_1, \dots, \theta_{D-3} = \pi/2$)
 - 2 Symmetry:
 - Stationarity & rotational symmetry along ∂_t & ∂_ϕ .
 - Reflection symmetry respective to the equatorial plane.
 - 3 Uniform distribution in θ_i -direction.
 - 4 Geometrically thin.
 - 5 Vertical pressure supported by external rarefied gas.



Formulation

- Basic equations :
 - $dh = Tds + n^{-1}dp$ (h : enthalpy)
 - $\nabla_a(nu^a) = 0$ (n : number density)
 - $\nabla_b T^{ab} = 0$, $T^{ab} := nh u^a u^b + pg^{ab}$
- Constants of integration:
 - Number flux: $j_n(r, n) =: \mu$
 - Energy flux: $j_\epsilon(r, n)$
 - Angular momentum flux: $j_\phi(r, n)$
- Energy square per particle $F := j_\epsilon^2/j_n^2$:

$$F(r, n) = h^2(n) \left[f(r) + \frac{\mu^2}{r^{2(D-2)}n^2} \right] \frac{1}{1 - \omega^2 f(r)r^{-2}}, \quad \omega := \frac{j_\phi}{j_\epsilon} \quad (2)$$

Our accretion problem

The solution of the accretion flow is the **orbit** $n = n(r)$ on (r, n) satisfying **Mater equation** $F(r, n) = \text{const.}$ with the parameters μ and ω .

Formulation

- Basic equations :
 - $dh = Tds + n^{-1}dp$ (h : enthalpy)
 - $\nabla_a(nu^a) = 0$ (n : number density)
 - $\nabla_b T^{ab} = 0$, $T^{ab} := nh u^a u^b + pg^{ab}$
- Constants of integration:
 - Number flux: $j_n(r, n) =: \mu$
 - Energy flux: $j_\epsilon(r, n)$
 - Angular momentum flux: $j_\phi(r, n)$
- Energy square per particle $F := j_\epsilon^2/j_n^2$:

$$F(r, n) = h^2(n) \left[f(r) + \frac{\mu^2}{r^{2(D-2)}n^2} \right] \frac{1}{1 - \omega^2 f(r)r^{-2}}, \quad \omega := \frac{j_\phi}{j_\epsilon} \quad (2)$$

Our accretion problem

The solution of the accretion flow is the **orbit** $n = n(r)$ on (r, n) satisfying **Mater equation** $F(r, n) = \text{const.}$ with the parameters μ and ω .

Dynamical system analysis & Critical point

[c.f. Chaverra & Sarbach (2015)]

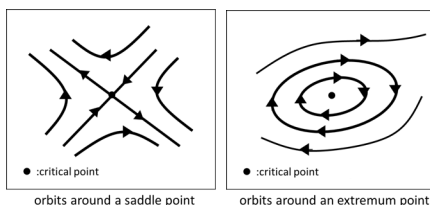
- Equation $F(r, n) = \text{const.}$ can be recasted in the system of a Hamiltonian flow of $F(r, n)$:

$$\frac{d}{d\lambda} \begin{pmatrix} r \\ n \end{pmatrix} = \begin{pmatrix} \partial_n \\ -\partial_r \end{pmatrix} F(r, n) \quad (3)$$

- Critical point (r_c, n_c)** : $\partial_r F(r_c, n_c) = \partial_n F(r_c, n_c) = 0$
- Linearization around CP :

$$\frac{d}{d\lambda} \begin{pmatrix} r - r_c \\ n - n_c \end{pmatrix} = \begin{pmatrix} \partial_r \partial_n F & \partial_n^2 F \\ -\partial_r^2 F & -\partial_r \partial_n F \end{pmatrix} \begin{pmatrix} r - r_c \\ n - n_c \end{pmatrix} \quad (4)$$

- Classification of CP : **saddle point / extremum point**



Navigation icons: back, forward, search, etc.

Sonic point & Critical point

- Sonic point
 - Sonic point (r_s, n_s)** of flow $n = n(r)$:

$$\left. \frac{v_s^2}{v^2} \right|_{(r_s, n(r_s))} = 1, \quad n_s = n(r_s) \quad (5)$$

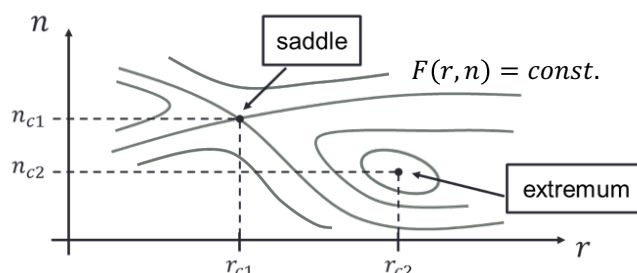
, v_s : sound speed, v : 3-velocity in co-rotating frame.

- Relation to CP :

Lemma

A sonic point of physical (= with finite density gradient) transonic flow corresponds to a **critical point of saddle-type**.

$$\left. \frac{v_s^2}{v^2} \right|_{(r_c, n_c)} = 1,$$



Navigation icons: back, forward, search, etc.

3. Proof of SP/PS correspondence

- Critical point of **radiation flow** :
 - EOS of radiation implies $v_s^2 = 1/(D - 1)$.
 - Radius r_c : $(fr^{-2})' = 0$
 - Saddle (extremum) point: $(fr^{-2})''|_{r_c} < 0$ (> 0)
- Photon sphere [c.f. Koga & Harada (2016)]:
 - Radius r_{ph} : $(fr^{-2})' = 0$
 - Unstable (stable) circular orbit: $(fr^{-2})''|_{r_c} < 0$ (> 0)
- One-to-one correspondence btw CP & PS

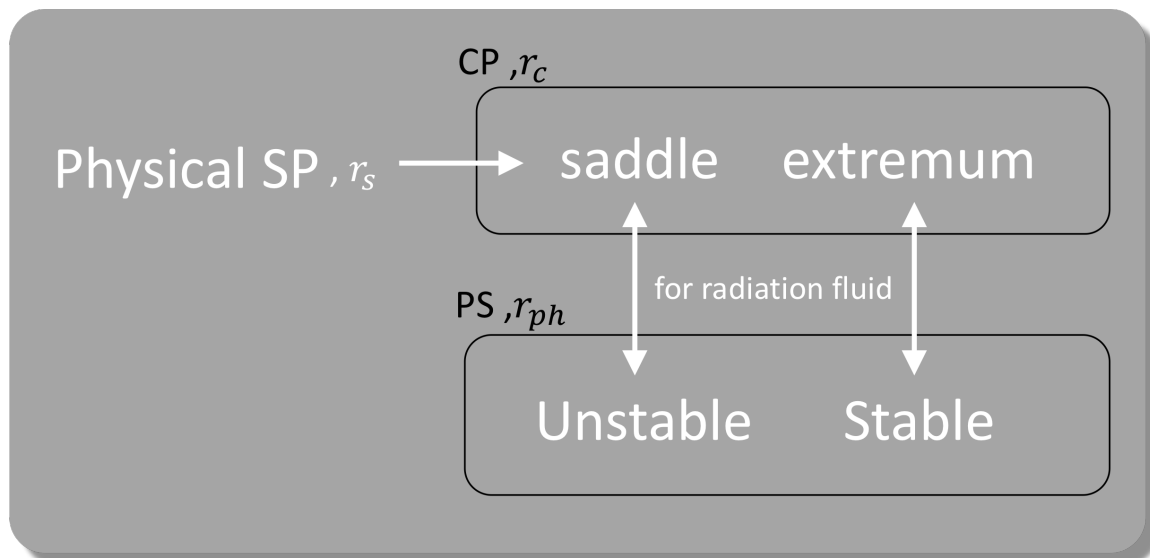
Lemma

CP of radiation flow & PS have one-to-one correspondence:

$$\begin{aligned} \text{Saddle point} &\Leftrightarrow \text{Unstable photon sphere} \\ \text{Extremum point} &\Leftrightarrow \text{Stable photon sphere} \end{aligned}$$

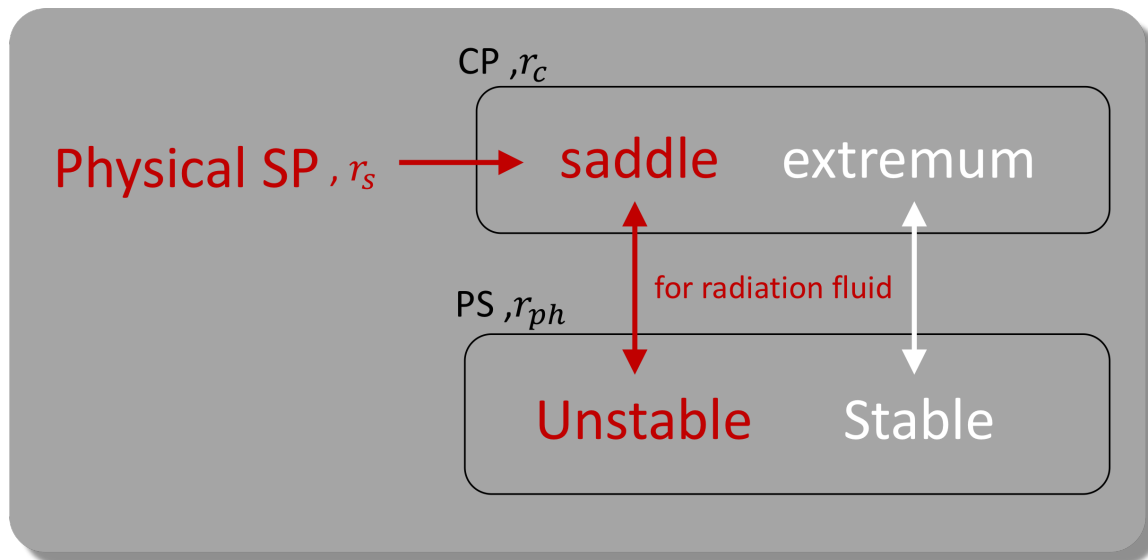
3. Proof of SP/PS correspondence

- Sketch of the proof :



3. Proof of SP/PS correspondence

- Sketch of the proof :



Physical SP is on the unstable PS. \square

4. Summary

- Accretion problem:
 - Rotational flow in spherically symmetric spacetime of D-dim.
 - Dynamical system analysis.
- SP/PS correspondence:

Theorem (SP/PS correspondence)

For our accretion model, for any stationary and **axially symmetric** physical transonic accretion flow of **radiation fluid**, its **sonic point is located at (one of) the unstable photon sphere(s)**.

- Discussions
 - The physical reason?
 - In other cases? e.g. spacetime of different symmetries (in progress)

Toshiaki Ono

Hirosaki University

**“Gravitomagnetic bending angle of light in stationary
axisymmetric spacetimes”**

(10+5 min.)

[JGRG28 (2018) 110705]

Gravitomagnetic bending angle of light in stationary axisymmetric spacetimes

Hirosaki Univ. (Japan)

Toshiaki Ono, Asahi Ishihara, Hideki Asada

Phys. Rev. D **96**, 104037 (2017)

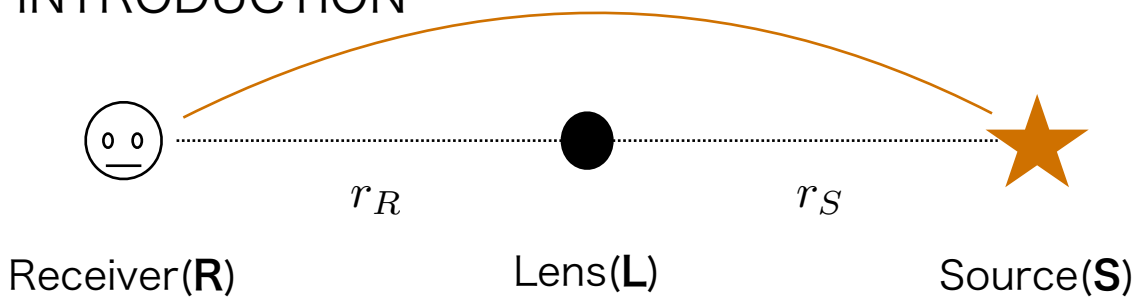
Phys. Rev. D **98**, 044047 (2018)

7 November 2018 JGRG28 @ Rikkyo University

Outline

- INTRODUCTION
- EXTENSION TO AXISYMMETRIC SPACETIMES
- Kerr black hole and rotating Teo wormhole
- CONCLUSION

INTRODUCTION



bending angle of light in Schwarzschild spacetime

$$\alpha = \frac{4GM}{c^2 b}$$

Usually, distance r_R and r_S

$$r_R, r_S \rightarrow \infty$$

However observer and source are located at finite distance from lens object.

INTRODUCTION

Gibbons and Werner (2008)

- They used the **Gauss-Bonnet theorem** to a spatial domain described by the optical metric, for which a light ray is described as a spatial curve.
- Light ray deflected by a **static, spherically symmetric massive body**
- Light ray deflection is **small**

INTRODUCTION

Werner [Gen. Rel. Grav. **44**, 3047 (2012)]

- He proposed an extension of the Gibbons-Werner approach for calculating the deflection of light in a **Kerr black hole**.
- He used the **Nazim's osculating Riemannian construction method** via the Randers-Finsler metric.

However

- **Source and receiver** are located at an **asymptotic Minkowskian region**

INTRODUCTION

Our works : [Phys. Rev. D **96**, 104037 (2017)]

[Phys. Rev. D **98**, 044047 (2018)]

- We discuss a possible extension of the method of calculating the bending angle of light to **stationary, axisymmetric and asymptotically flat spacetimes**.
- By using **generalized optical metric method**.
- Taking account of the **finite distance from a lens object to a light source and a receiver** by using the Gauss-Bonnet theorem.

EXTENSION TO AXISYMMETRIC SPACETIMES

We consider the light rays on the equatorial plane in **stationary, axisymmetric and asymptotically flat spacetime** by using the Gauss-Bonnet theorem in differential geometry.

The line element for this spacetime
(The Weyl-Lewis-Papapetrou form)

$$\begin{aligned} ds^2 &= g_{\mu\nu} dx^\mu dx^\nu \\ &= -A(r, \theta) dt^2 - 2H(r, \theta) dt d\phi \\ &\quad + B(r, \theta) dr^2 + C(r, \theta) d\theta^2 + D(r, \theta) d\phi^2 . \end{aligned}$$

where we used the polar coordinates.

$$\text{Assume } \left. \frac{\partial g_{\mu\nu}}{\partial \theta} \right|_{\theta=\pi/2} = 0$$

EXTENSION TO AXISYMMETRIC SPACETIMES

The null condition $ds^2 = 0$ is solved for dt as

$$\begin{aligned} dt &= \sqrt{\gamma_{ij} dx^i dx^j} + \beta_i dx^i , \\ dl^2 &\equiv \gamma_{ij} dx^i dx^j \equiv \frac{B(r, \theta)}{A(r, \theta)} dr^2 + \frac{C(r, \theta)}{A(r, \theta)} d\theta^2 + \frac{A(r, \theta)D(r, \theta) + H^2(r, \theta)}{A^2(r, \theta)} d\phi^2 , \\ \beta_i dx^i &\equiv -\frac{H(r, \theta)}{A(r, \theta)} d\phi . \end{aligned}$$

Generalized optical metric γ_{ij} defines the arc length (l) along the spatial curve.

l is an affine parameter along the light ray

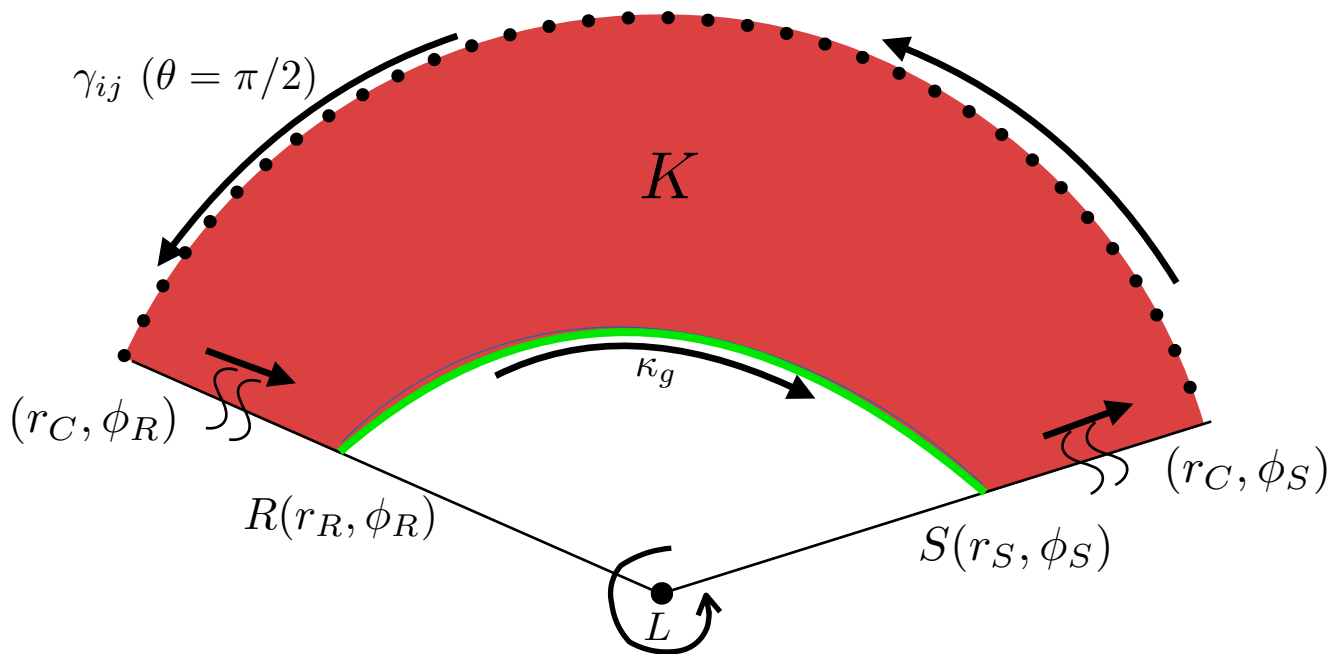
[H. Asada and M. Kasai, Prog. Theor. Phys. 104, 95 (2000)].

β_i causes difference from a static, spherically symmetric case.

EXTENSION TO AXISYMMETRIC SPACETIMES

Gauss-bonnet theorem (regular surface)

$$\int \int_T K dS + \sum_{a=1}^N \int_{\partial T_a} \kappa_g dl + \sum_{a=1}^N \theta_a = 2\pi$$



EXTENSION TO AXISYMMETRIC SPACETIMES

Gaussian curvature (For a two-dimensional surface)

$$K = \frac{R_{r\phi r\phi}}{\det \gamma_{ij}^{(2)}}$$

$$= \frac{1}{\sqrt{\det \gamma_{ij}^{(2)}}} \left[\frac{\partial}{\partial \phi} \left(\frac{\sqrt{\det \gamma_{ij}^{(2)}}}{\gamma_{rr}^{(2)}} \Gamma^{\phi}_{rr} \right) - \frac{\partial}{\partial r} \left(\frac{\sqrt{\det \gamma_{ij}^{(2)}}}{\gamma_{rr}^{(2)}} \Gamma^{\phi}_{r\phi} \right) \right]$$

$\gamma_{ij}^{(2)}$ denotes the two-dimensional metric in the equatorial plane

EXTENSION TO AXISYMMETRIC SPACETIMES

geodesic curvature can be defined in the tensor form as

$$\kappa_g = \varepsilon_{ijk} N^i a^j e^k$$

e^i : unit tangential vector along the spatial curve

N^i : unit normal vector for the surface

a^i : acceleration vector along the spatial curve

These vectors for the light ray

$$e^i = \frac{A(r)[H(r) + bA(r)]}{A(r)D(r) + H^2(r)} \left(\frac{dr}{d\phi}, 0, 1 \right), \quad a^i = \gamma^{ij} (\beta_{k|j} - \beta_{j|k}) e^k,$$

$$N^i = \left(0, \frac{1}{\sqrt{\gamma_{\theta\theta}}}, 0 \right)$$

EXTENSION TO AXISYMMETRIC SPACETIMES

In electromagnetism

variational principle

$$\delta S = -mc^2 \delta \int_{t_1}^{t_2} \sqrt{1 - v^2/c^2} dt - q \delta \int_{t_1}^{t_2} [\phi(t, x, y, z) - \underline{\vec{v} \cdot \vec{A}(t, x, y, z)}] dt$$

$$\text{Lorentz force} \propto \text{rot} \vec{A}$$

In our work, since $dt = \sqrt{\gamma_{ij} dx^i dx^j} + \beta_i dx^i$,

$$\delta S = \delta \int_{t_1}^{t_2} \left[\sqrt{\gamma_{ij} e^i e^j} + \underline{\beta_i e^i} \right] dt$$

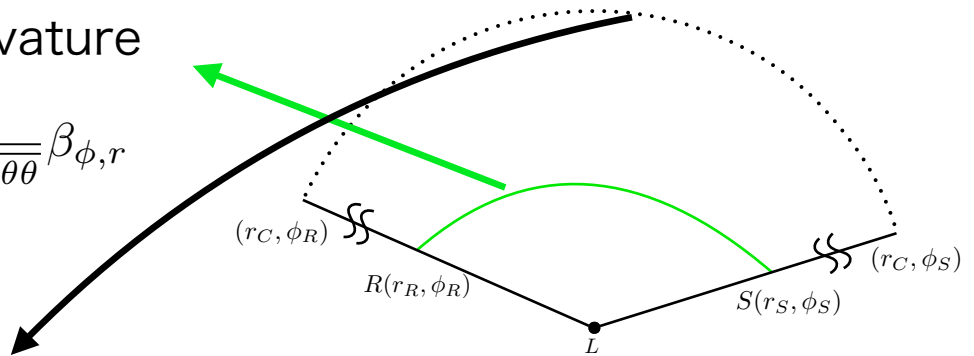
$$e^i|_k e^k = a^i, \quad a^i \equiv \gamma^{ij} (\beta_{k|j} - \beta_{j|k}) e^k$$

EXTENSION TO AXISYMMETRIC SPACETIMES

$$\gamma_{ij} (\theta = \pi/2)$$

geodesic curvature

$$\kappa_g = -\frac{1}{\sqrt{\gamma\gamma^{\theta\theta}}} \beta_{\phi,r}$$



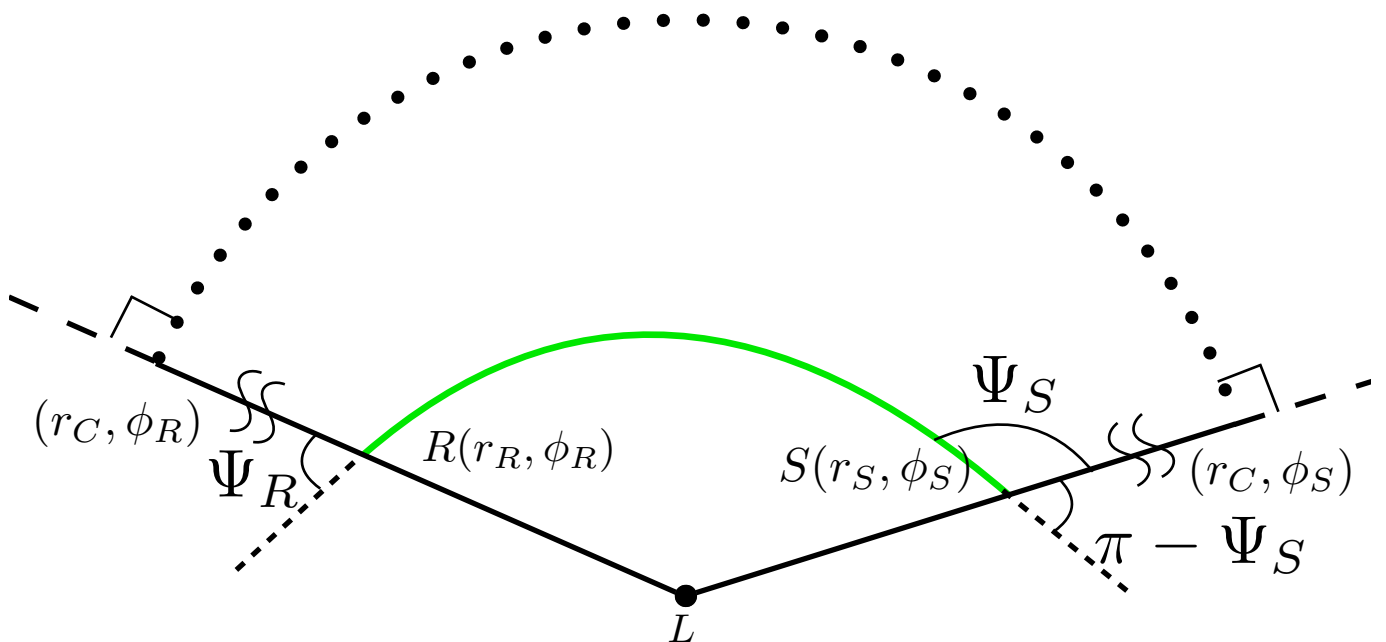
geodesic curvature

For the asymptotically flat spacetime, $\kappa_g = \frac{1}{r_C}$ and $dl \rightarrow r_C d\phi$. Hence

$$\int_S^R \kappa_g dl = \int_{\phi_S}^{\phi_R} d\phi = \phi_{RS}.$$

EXTENSION TO AXISYMMETRIC SPACETIMES

$$\gamma_{ij} (\theta = \pi/2)$$



EXTENSION TO AXISYMMETRIC SPACETIMES

Gauss-bonnet theorem (regular surface)

$$\int \int_T K dS + \sum_{a=1}^N \int_{\partial T_a} \kappa_g dl + \sum_{a=1}^N \theta_a = 2\pi \quad ,$$

$$\int \int_{R \square S} K dS + \int_R^S \kappa_g dl + \phi_{RS} + \Psi_R - \Psi_S = 2\pi .$$

We define deflection angle of light as

$$\alpha \equiv \Psi_R - \Psi_S + \phi_{RS} .$$

By using Gauss-bonnet theorem, it is rewritten as

$$\alpha = - \int \int_{R \square S} K dS - \int_R^S \kappa_g dl .$$

This form show α is **coordinate-invariant**.

Kerr spacetime and rotating Teo wormhole

The Boyer-Lindquist form of the Kerr metric is

$$ds^2 = - \left(1 - \frac{2Mr}{\Sigma} \right) dt^2 - \frac{4aMr \sin^2 \theta}{\Sigma} dt d\phi \\ + \frac{\Sigma}{\Delta} dr^2 + \Sigma d\theta^2 + \left(r^2 + a^2 + \frac{2a^2 Mr \sin^2 \theta}{\Sigma} \right) \sin^2 \theta d\phi^2 ,$$

where we denote

$$\Sigma \equiv r^2 + a^2 \cos^2 \theta ,$$

$$\Delta \equiv r^2 - 2Mr + a^2 .$$

Gaussian curvature and geodesic curvature

$$K = -\frac{2M}{r^3} + O\left(\frac{M^2}{r^4}, \frac{a^2 M}{r^5}\right) \quad , \quad \kappa_g = -\frac{2aM}{r^3} + O\left(\frac{aM^2}{r^4}\right) .$$

Kerr spacetime and rotating Teo wormhole

prograde motion of light

$$\begin{aligned}\alpha_{prog} &= - \iint_{\infty \square \infty} K dS - \int_R^S \kappa_g dl \\ &= \frac{2M}{b} \left(\sqrt{1 - b^2 u_S^2} + \sqrt{1 - b^2 u_R^2} \right) - \frac{2aM}{b^2} \left(\sqrt{1 - b^2 u_S^2} + \sqrt{1 - b^2 u_R^2} \right) + O \left(\frac{M^2}{b^2}, \frac{aM^2}{b^3} \right)\end{aligned}$$

retrograde case

$$\alpha_{retro} = \frac{2M}{b} \left(\sqrt{1 - b^2 u_S^2} + \sqrt{1 - b^2 u_R^2} \right) + \frac{2aM}{b^2} \left(\sqrt{1 - b^2 u_S^2} + \sqrt{1 - b^2 u_R^2} \right) + O \left(\frac{M^2}{b^2}, \frac{aM^2}{b^3} \right)$$

where $u \equiv 1/r$.

We take the limit as $u_R \rightarrow 0$, $u_S \rightarrow 0$

$$\begin{aligned}\alpha_{prog} &\rightarrow \frac{4M}{b} - \frac{4aM}{b^2} + O \left(\frac{M^2}{b^2} \right), \\ \alpha_{retro} &\rightarrow \frac{4M}{b} + \frac{4aM}{b^2} + O \left(\frac{M^2}{b^2} \right).\end{aligned}$$

[R. Epstein et al.,
PRD 22, 2947 (1980)].

Kerr spacetime and rotating Teo wormhole

Rotating Teo wormhole metric

[E. Teo, Phys. Rev. D 58, 024014 (1998).]

$$ds^2 = - N^2 dt^2 + \frac{dr^2}{1 - \frac{b_0}{r}} + r^2 H^2 [d\theta^2 + \sin^2 \theta (d\phi - \omega dt)^2]$$

where

$$N = H = 1 + \frac{d(4a \cos \theta)^2}{r}, \quad \omega = \frac{2a}{r^3}.$$

Gaussian curvature and geodesic curvature

$$K = -\frac{b_0}{2r^3} - \frac{56a^2}{r^6} + O \left(\frac{a^2 b_0}{r^7}, \frac{a^4}{r^{10}} \right), \quad \kappa_g = -\frac{2a}{r^3} + O \left(\frac{a^3}{r^7}, \frac{a^3 b_0}{r^8} \right).$$

Kerr spacetime and rotating Teo wormhole

prograde motion of light

$$\begin{aligned}\alpha_{prog} &= - \iint_{R \square_S} K dS - \int_R^S \kappa_g dl \\ &= \frac{b_0}{2b} \left(\sqrt{1 - b^2 u_S^2} + \sqrt{1 - b^2 u_R^2} \right) - \frac{2a}{b^2} \left(\sqrt{1 - b^2 u_S^2} + \sqrt{1 - b^2 u_R^2} \right) + O \left(\frac{b_0^2}{b^2}, \frac{ab_0}{b^3} \right)\end{aligned}$$

retrograde case

$$\alpha_{retro} = \frac{b_0}{2b} \left(\sqrt{1 - b^2 u_S^2} + \sqrt{1 - b^2 u_R^2} \right) + \frac{2a}{b^2} \left(\sqrt{1 - b^2 u_S^2} + \sqrt{1 - b^2 u_R^2} \right) + O \left(\frac{b_0^2}{b^2}, \frac{ab_0}{b^3} \right)$$

We take the limit as $u_R \rightarrow 0$, $u_S \rightarrow 0$

$$\begin{aligned}\alpha_{prog} &\rightarrow \frac{b_0}{b} - \frac{4a}{b^2} + O \left(\frac{b_0^2}{b^2}, \frac{ab_0}{b^3} \right), \\ \alpha_{retro} &\rightarrow \frac{b_0}{b} + \frac{4a}{b^2} + O \left(\frac{b_0^2}{b^2}, \frac{ab_0}{b^3} \right).\end{aligned}$$

K. Jusufi and A. Ovgun,
Phys. Rev. D 97, 024042 (2018).

CONCLUSION

- By using the **Gauss-Bonnet theorem**, we formulated the method of calculating the bending angle of light to **stationary, axisymmetric and asymptotically flat spacetimes**, especially by taking account of **the finite distance from a lens object to a light source and a receiver**.
- Bending angle of light α is **coordinate-invariant**.
- We considered **Kerr black hole** and **rotating Teo wormhole** in order to examine how the bending angle of light is computed by the our method.
- Recently, we discuss a possible extension of our method to an asymptotically nonflat spacetime.
[T. Ono et, al., arXiv]

Tatsuya Ogawa

Department of Mathematics and Physics, Graduate School of Science, Osaka
City University

“Charge Screened Boson Stars”

(10+5 min.)

[JGRG28 (2018) 110706]

Charge Screened Boson Stars

Tatsuya Ogawa

and Hideki Ishihara

Department of Mathematics and Physics,
Graduate School of Science, Osaka City University



November 7th, 2018 @Rikkyo University

• 1/16

Localized Bosonic Objects

- Classical solutions in field theories
- Bound state of bosonic particles

Attraction force:

- Gravity

Boson star : M. Colpi, et.al, (1986)

- Interaction between boson fields

Non-topological soliton

- ✓ A complex scalar field and a real scalar field
: R. Friedberg, T.D. Lee, & A. Sirlin, (1976)
- ✓ A complex scalar field with nontrivial self coupling
: S. Coleman, (1985) Q-balls

• 2/16

Basic equations

Action of our model

$$S = \int \sqrt{-g} d^4x \left\{ \begin{aligned} & - g^{\mu\nu} (D_\mu \psi)^* (D_\nu \psi) - g^{\mu\nu} (D_\mu \phi)^* (D_\nu \phi) \\ & - \frac{\lambda}{4} \left(|\phi|^2 - \eta^2 \right)^2 - \mu |\phi|^2 |\psi|^2 - \frac{1}{4} F_{\mu\nu} F^{\mu\nu} \end{aligned} \right\}$$
$$D_\mu = \nabla_\mu - ieA_\mu$$

We found the existence of the non topological soliton solutions.

We add the Einstein gravity term
and show the existence of the boson star solutions
by using numerical analysis.

•

• 3/16

Basic equations

Action of our model

$$S = \int \sqrt{-g} d^4x \left\{ \begin{aligned} & \frac{R}{16\pi G} - g^{\mu\nu} (D_\mu \psi)^* (D_\nu \psi) - g^{\mu\nu} (D_\mu \phi)^* (D_\nu \phi) \\ & - \frac{\lambda}{4} \left(|\phi|^2 - \eta^2 \right)^2 - \mu |\phi|^2 |\psi|^2 - \frac{1}{4} F_{\mu\nu} F^{\mu\nu} \end{aligned} \right\}$$
$$D_\mu = \nabla_\mu - ieA_\mu$$

•

• 4/16

Basic equations

Action of our model

$$S = \int \sqrt{-g} d^4x \left\{ \frac{R}{16\pi G} - g^{\mu\nu} (D_\mu \psi)^* (D_\nu \psi) - g^{\mu\nu} (D_\mu \phi)^* (D_\nu \phi) - \frac{\lambda}{4} (|\phi|^2 - \eta^2)^2 - \mu |\phi|^2 |\psi|^2 - \frac{1}{4} F_{\mu\nu} F^{\mu\nu} \right\}$$

Field equations

$$g^{\mu\nu} D_\mu D_\nu \psi - \mu |\psi|^2 \phi = 0, \quad D_\mu = \nabla_\mu - ieA_\mu$$

$$g^{\mu\nu} D_\mu D_\nu \phi - \frac{\lambda}{2} (|\phi|^2 - \eta^2) - \mu |\psi|^2 \phi = 0,$$

$$\nabla_\mu F^{\mu\nu} = j_\psi^\nu + j_\phi^\nu,$$

$$G_{\mu\nu} = 8\pi G T_{\mu\nu}$$

$$j_\phi^\mu = ie \{ \phi^* (D^\mu \phi) - (D^\mu \phi)^* \phi \},$$

$$j_\psi^\mu = ie \{ \psi^* (D^\mu \psi) - (D^\mu \psi)^* \psi \}$$

$$\nabla_\mu j_\phi^\mu = 0, \quad \nabla_\mu j_\psi^\mu = 0$$

• 5/16

Basic equations

Static spherically symmetric spacetime ansatz

$$ds^2 = -\sigma(r)^2 \left(1 - \frac{2m(r)}{r} \right) dt^2 + \left(1 - \frac{2m(r)}{r} \right)^{-1} dr^2 + r^2 d\theta^2 + r^2 \sin^2 \theta d\varphi^2$$

Stationary spherically symmetric matter fields ansatz

$$\phi(t, r) = e^{-i\omega t} \tilde{\phi}(r), \quad \psi(t, r) = e^{-i\omega' t} \tilde{\psi}(r), \quad A_\mu(r) = (A_t(r), 0, 0, 0)$$

$$\Omega := \omega - \omega'$$

• 6/16

Basic equations

Variables : $\tilde{\phi}(r), \tilde{\psi}(r), \tilde{A}_t(r), m(r), \sigma(r)$

Parameters : $e, \mu, \lambda, \eta, \Omega$

EOM of the complex scalar fields

$$\tilde{\psi}'' + \left\{ \frac{2}{r} \left(1 + \frac{m - rm'}{r - 2m} \right) + \frac{\sigma'}{\sigma} \right\} \tilde{\psi}' + \left(1 - \frac{2m}{r} \right) \left[\frac{(e\tilde{A}_t - \Omega)^2 \tilde{\psi}}{\sigma^2(1 - 2m/r)} - \mu \tilde{\phi}^2 \tilde{\psi} \right] = 0,$$

$$\tilde{\phi}'' + \left\{ \frac{2}{r} \left(1 + \frac{m - rm'}{r - 2m} \right) + \frac{\sigma'}{\sigma} \right\} \tilde{\phi}' + \left(1 - \frac{2m}{r} \right) \left[\frac{e^2 \tilde{\phi} \tilde{A}_t^2}{\sigma^2(1 - 2m/r)} - \frac{\lambda}{2} \tilde{\phi} (\tilde{\phi}^2 - 1) - \mu \tilde{\phi} \tilde{\psi}^2 \right] = 0,$$

Maxwell equation

$$\tilde{A}_t'' + \left(\frac{2}{r} - \frac{\sigma'}{\sigma} \right) \tilde{A}_t' + \left(1 - \frac{2m}{r} \right) \left[-2e^2 \tilde{\phi}^2 \tilde{A}_t - 2e^2 \tilde{\psi}^2 \tilde{A}_t + 2e\Omega \tilde{\psi}^2 \right] = 0,$$

$$\left(\begin{array}{l} \tilde{A}_t(r) := A_t(r) + \frac{\omega}{e}, \\ \Omega := \omega - \omega' \end{array} \right)$$

Einstein equations

$$\frac{2m'}{r^2} - 8\pi G\eta^2 \left[\frac{e^2 \tilde{\phi}^2 \tilde{A}_t^2}{\sigma^2(1 - 2m/r)} + \frac{(e\tilde{A}_t - \Omega)^2 \tilde{\psi}^2}{\sigma^2(1 - 2m/r)} + \left(1 - \frac{2m}{r} \right) \left\{ (\tilde{\phi}')^2 + (\tilde{\psi}')^2 \right\} + \frac{\lambda}{4} (\tilde{\phi}^2 - 1)^2 + \mu \tilde{\phi}^2 \tilde{\psi}^2 + \frac{(\tilde{A}_t')^2}{2\sigma^2} \right] = 0,$$

$$\frac{(r - 2m)\sigma'}{r^2\sigma} - 8\pi G\eta^2 \left[\frac{e^2 \tilde{\phi}^2 \tilde{A}_t^2}{\sigma^2(1 - 2m/r)} + \frac{(e\tilde{A}_t - \Omega)^2 \tilde{\psi}^2}{\sigma^2(1 - 2m/r)} + \left(1 - \frac{2m}{r} \right) \left\{ (\tilde{\phi}')^2 + (\tilde{\psi}')^2 \right\} \right] = 0$$

• 7/16

Boundary conditions

Potential of the Higgs field

$$V(\tilde{\phi}) = \frac{\lambda}{4} (\tilde{\phi}^2 - \eta^2)^2$$

Metric ansatz

$$ds^2 = -\sigma(r)^2 \left(1 - \frac{2m(r)}{r} \right) dt^2 + \left(1 - \frac{2m(r)}{r} \right)^{-1} dr^2 + r^2 d\theta^2 + r^2 \sin^2 \theta d\varphi^2$$



$r \rightarrow 0$: Regularity at the origin

$$\frac{d\tilde{\psi}}{dr} = 0, \quad \frac{d\tilde{\phi}}{dr} = 0, \quad \frac{d\tilde{A}_t}{dr} = 0, \quad m = 0, \quad \frac{d\sigma}{dr} = 0$$

$r \rightarrow \infty$: Fields approach to vacuum and Schwarzschild solution

$$\tilde{\psi} = 0, \quad \tilde{\phi} = \eta, \quad \tilde{A}_t = 0, \quad m = m_\infty = \text{const.}, \quad \sigma = 1$$

• 8/16

Numerical solutions ($G\eta^2 = 1$, $\mu = 1$)

$r \rightarrow 0$: Regularity at the origin

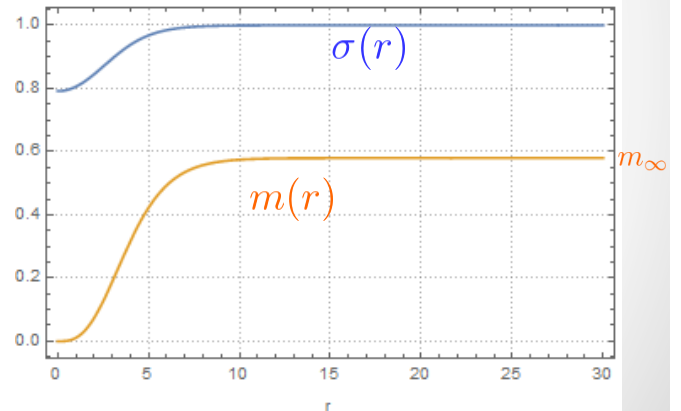
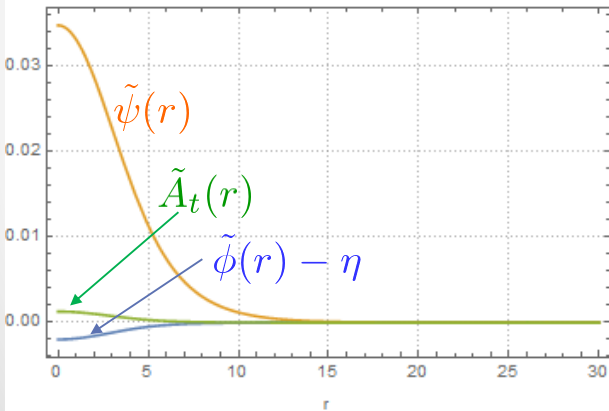
$$\Omega := \omega - \omega'$$

$$\frac{d\tilde{\psi}}{dr} = 0, \quad \frac{d\tilde{\phi}}{dr} = 0, \quad \frac{d\tilde{A}_t}{dr} = 0, \quad m = 0, \quad \frac{d\sigma}{dr} = 0$$

$$\Omega = 0.9$$

$r \rightarrow \infty$: Fields approach to vacuum and Schwarzschild solution

$$\tilde{\psi} = 0, \quad \tilde{\phi} = 1, \quad \tilde{A}_t = 0, \quad m = m_\infty = \text{const.}, \quad \sigma = 1$$

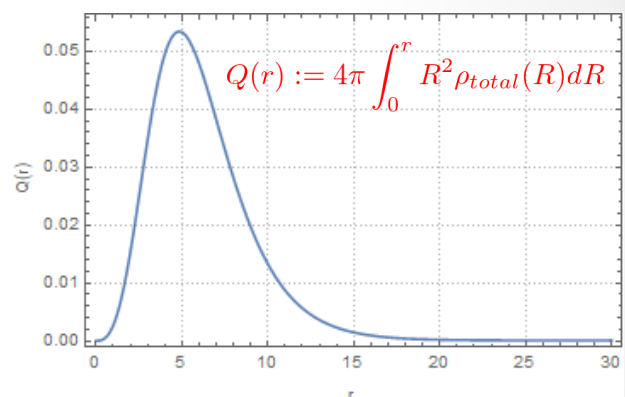
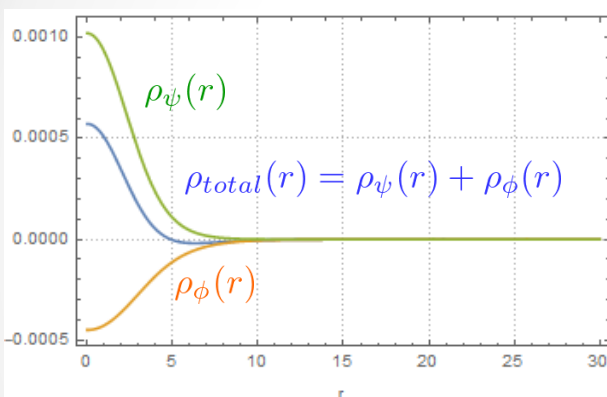


$$ds^2 = -\sigma(r)^2 \left(1 - \frac{2m(r)}{r}\right) dt^2 + \left(1 - \frac{2m(r)}{r}\right)^{-1} dr^2 + r^2 d\theta^2 + r^2 \sin^2 \theta d\varphi^2$$

• 9/16

Charge of the boson star

$$\rho_\phi(r) = \frac{-2e^2 \tilde{\phi}^2 \tilde{A}_t}{\sigma(1 - 2m/r)}, \quad \rho_\psi(r) = \frac{-2e^2 \tilde{\psi}^2 \tilde{A}_t + 2e\Omega \tilde{\psi}^2}{\sigma(1 - 2m/r)}$$



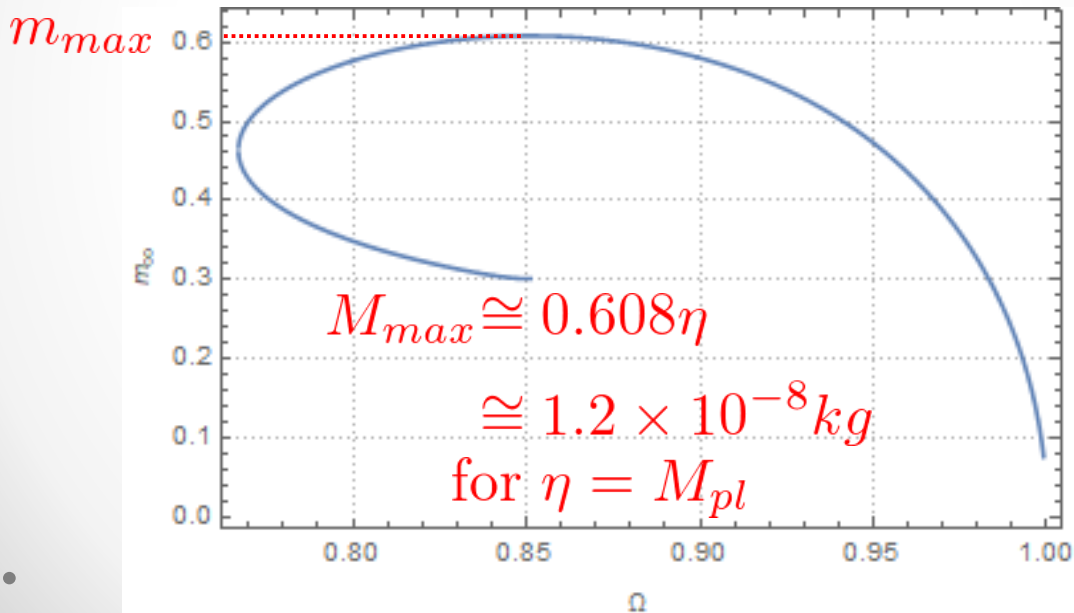
The charge distribution of ψ is screened by the counter charge distribution of ϕ .

• 10/16

Mass of the boson star ($G\eta^2 = 1$, $\mu = 1$)

Mass of boson stars

$$M := m_\infty \eta$$



• 11/16

Variation of $G\eta^2$

Einstein equations

$$\frac{2m'}{r^2} - 8\pi G\eta^2 \left[\frac{e^2 \tilde{\phi}^2 \tilde{A}_t^2}{\sigma^2(1-2m/r)} + \frac{(e\tilde{A}_t - \Omega)^2 \tilde{\psi}^2}{\sigma^2(1-2m/r)} + \left(1 - \frac{2m}{r}\right) \{(\tilde{\phi}')^2 + (\tilde{\psi}')^2\} + \frac{\lambda}{4}(\tilde{\phi}^2 - 1)^2 + \mu \tilde{\phi}^2 \tilde{\psi}^2 + \frac{(\tilde{A}_t')^2}{2\sigma^2} \right] = 0,$$

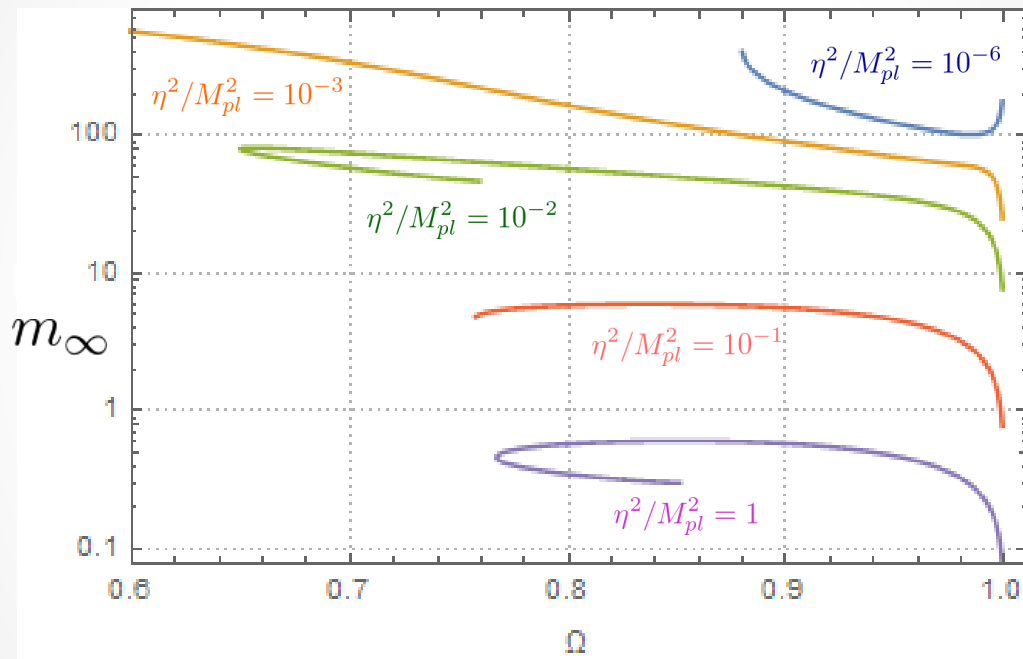
$$\frac{(r-2m)\sigma'}{r^2\sigma} - 8\pi G\eta^2 \left[\frac{e^2 \tilde{\phi}^2 \tilde{A}_t^2}{\sigma^2(1-2m/r)} + \frac{(e\tilde{A}_t - \Omega)^2 \tilde{\psi}^2}{\sigma^2(1-2m/r)} + \left(1 - \frac{2m}{r}\right) \{(\tilde{\phi}')^2 + (\tilde{\psi}')^2\} \right] = 0$$

$$G\eta^2 = \eta^2 / M_{pl}^2$$

We change breaking scale

• 12/16

Variation of $G\eta^2$

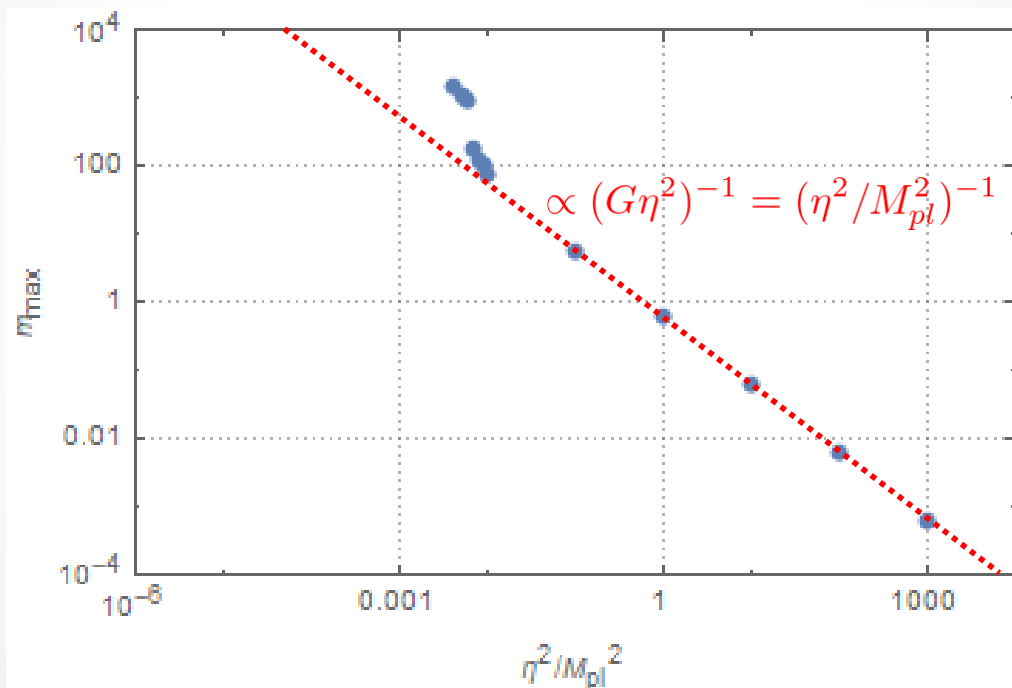


As breaking scale decreases, upper bound of the mass increases.

Upper bound of the mass

$$M_{max} = m_{max}\eta$$

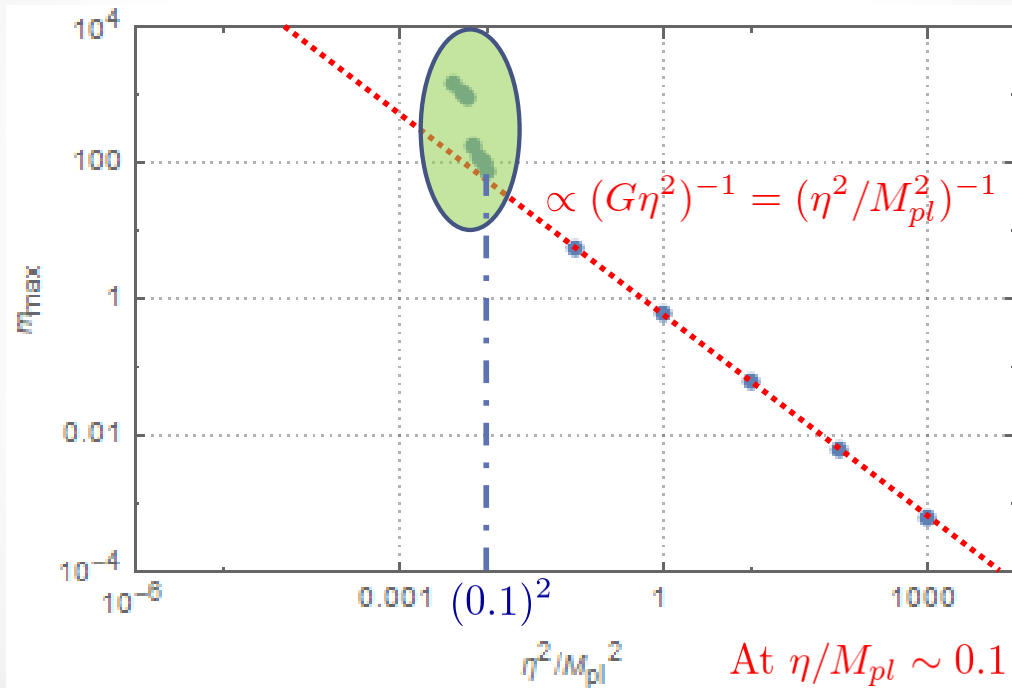
$$m_{max} := \max m_{\infty}$$



Upper bound of the mass

$$M_{max} = m_{max}\eta$$

$$m_{max} := \max m_{\infty}$$



- $m_{max} \propto (\eta/M_{pl})^{-2}$ for $\eta/M_{pl} \leq 0.1$

the line breaks.

15/16

Conclusion

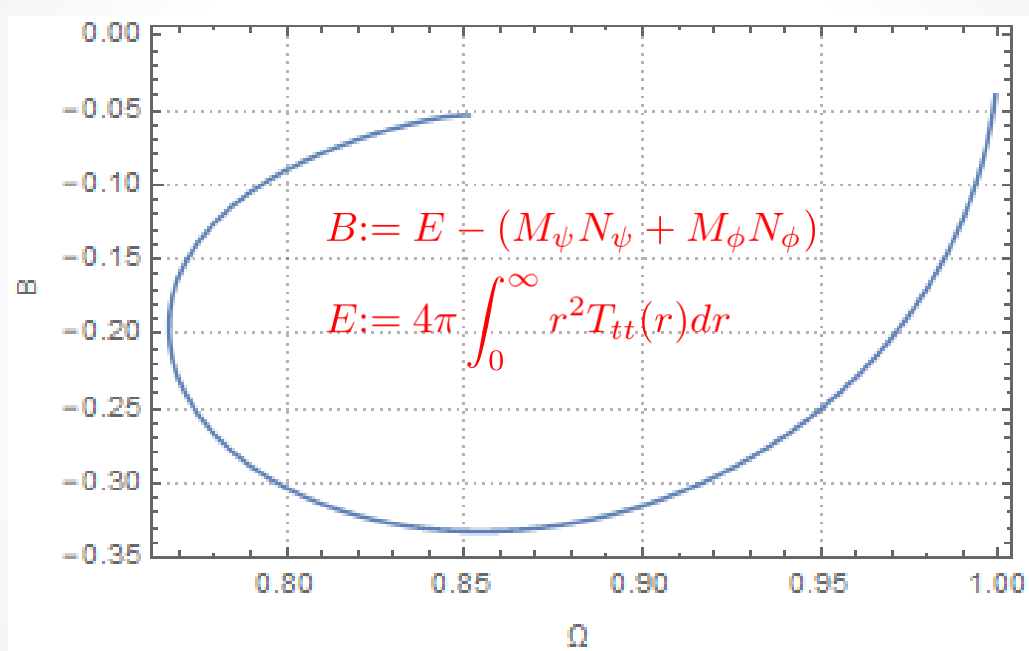
- We constructed the boson star solutions by using the gravitating gauged Friedberg-Lee-Sirlin model:
 - massless complex scalar field, U(1) gauge field, complex Higgs scalar field with the Mexican hat potential, and gravitational field.
- The charge distribution of the complex scalar field is screened by the counter charge of the Higgs scalar field.
- Maximum mass of the boson stars appear in the case of SSB η/M_{pl} is high..
- As η/M_{pl} decreases, the maximum mass of the boson stars increases.
- $\eta/M_{pl} \leq \eta_{cr}/M_{pl} \sim 0.1$, m_{max} increases rapidly as η/M_{pl} decreases .

Future work

- Stability by the perturbation.
- ➤ Does the large N solutions collapse to black hole?

16/16

Binding energy of the boson star

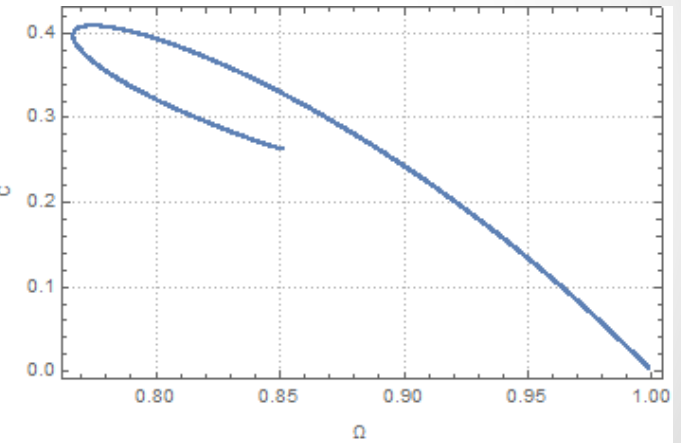
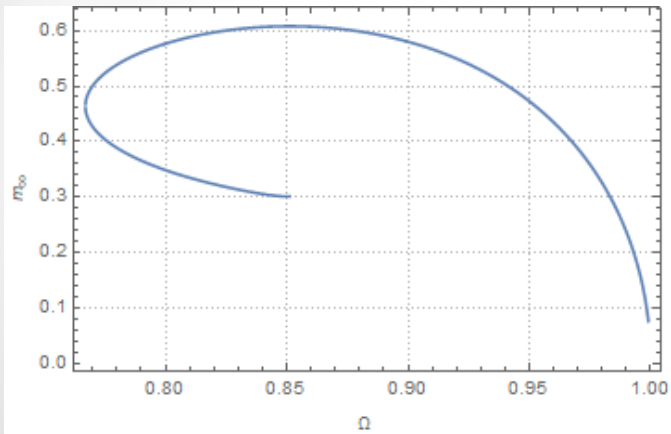


In this case, the binding energy of the boson stars are always negative.

Compactness of the boson star ($G\eta^2 = 1$, $\mu = 1$)

Compactness and radius of the boson stars

$$c := \frac{2GM}{R} \quad R := \frac{4\pi}{|Q_\psi| + |Q_\phi|} \int_0^\infty \sqrt{-gr^3} \{|\rho_\psi(r)| + |\rho_\phi(r)|\} dr$$



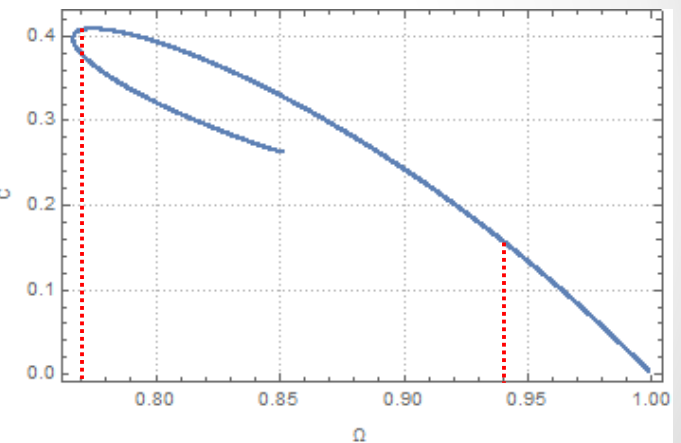
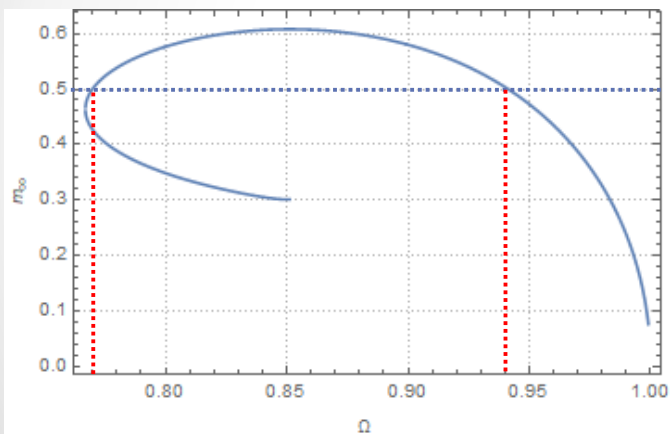
•

• 19/18

Compactness of the boson star ($G\eta^2 = 1$, $\mu = 1$)

Compactness and radius of the boson stars

$$c := \frac{2GM}{R} \quad R := \frac{4\pi}{|Q_\psi| + |Q_\phi|} \int_0^\infty \sqrt{-gr^3} \{|\rho_\psi(r)| + |\rho_\phi(r)|\} dr$$



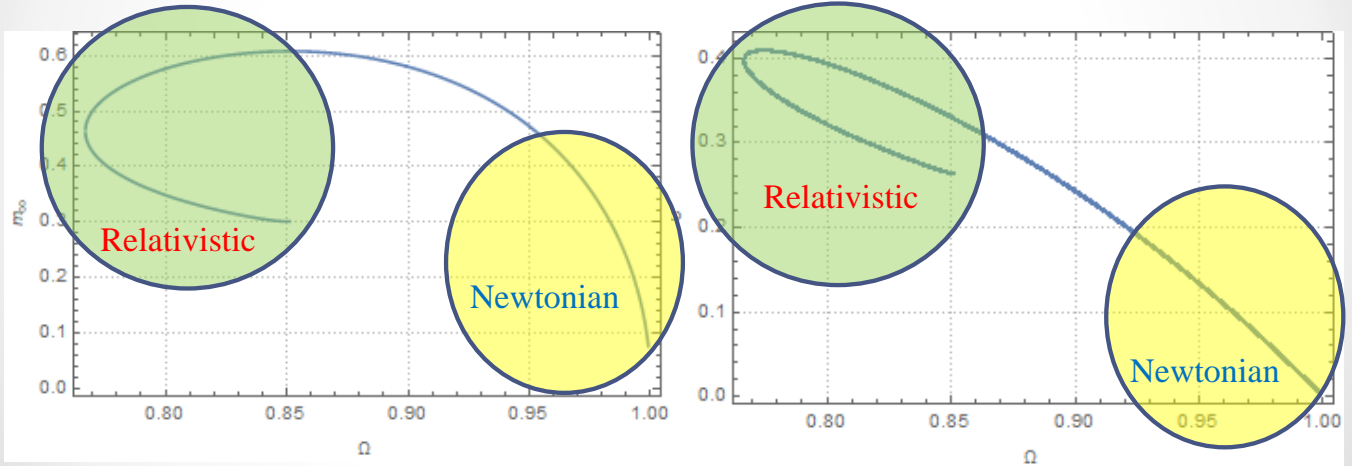
•

• 20/18

Compactness of the boson star ($G\eta^2 = 1$, $\mu = 1$)

Compactness and radius of the boson stars

$$c := \frac{2GM}{R} \quad R := \frac{4\pi}{|Q_\psi| + |Q_\phi|} \int_0^\infty \sqrt{-gr^3} \{|\rho_\psi(r)| + |\rho_\phi(r)|\} dr$$



The green region is more relativistic than the yellow region.

Session S3P1 14:00–15:30

[Chair: Masahide Yamaguchi]

Akira Matsumura

Nagoya University

“Quantum discrimination for the Universe”

(10+5 min.)

[JGRG28 (2018) 110708]

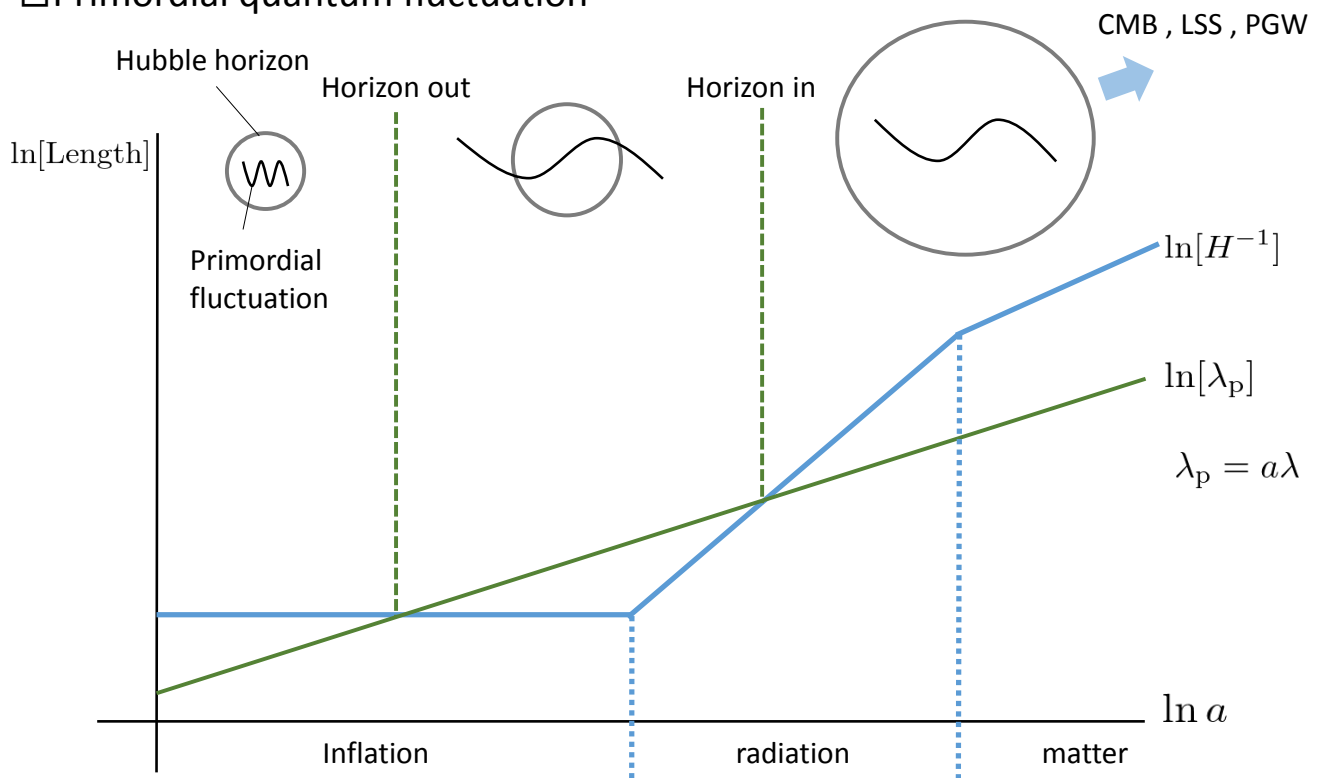
Quantum discrimination for the universe

Akira Matsumura (Nagoya Univ.)
Collaborator : Yasusada Nambu (Nagoya Univ.)

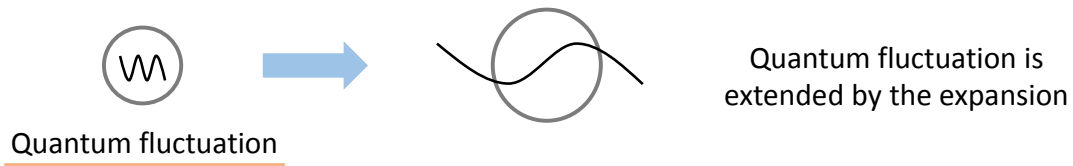
JGRG28@Rikkyo Univ.

Introduction and Motivation

□ Primordial quantum fluctuation



□ Pair creation and standing wave

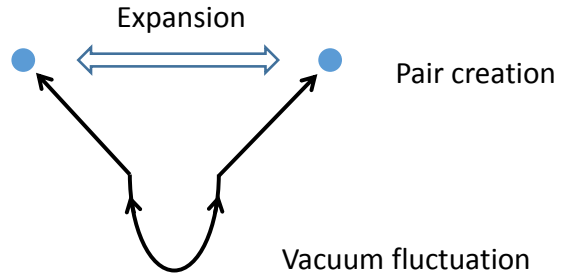


The property of the quantum fluctuation

Particle creation of k and $-k$ mode
Squeezed vacuum



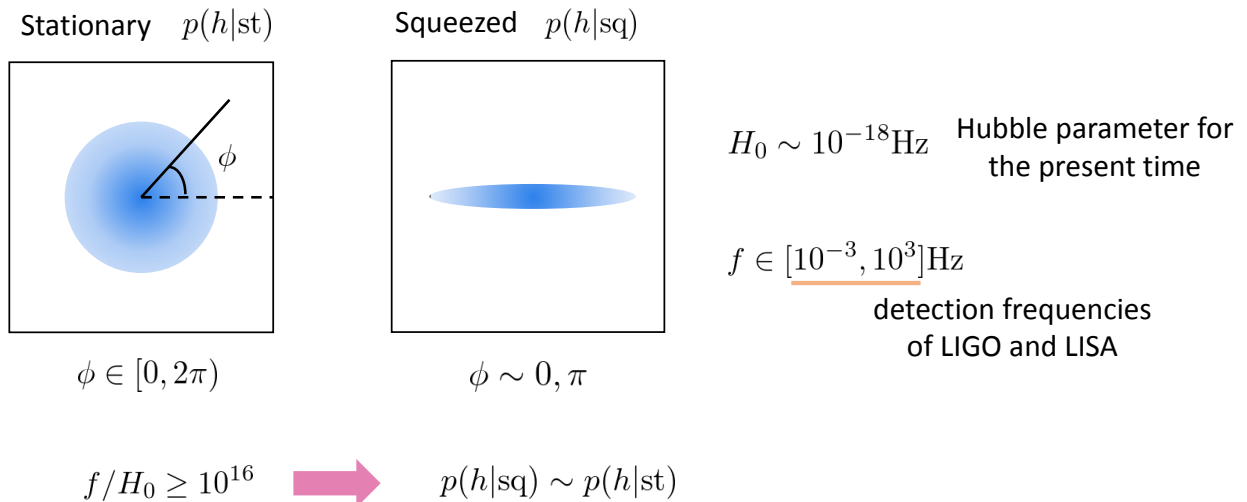
Superposition of k and $-k$ mode
Standing wave



This squeezing can be evidence of the primordial quantum fluctuation

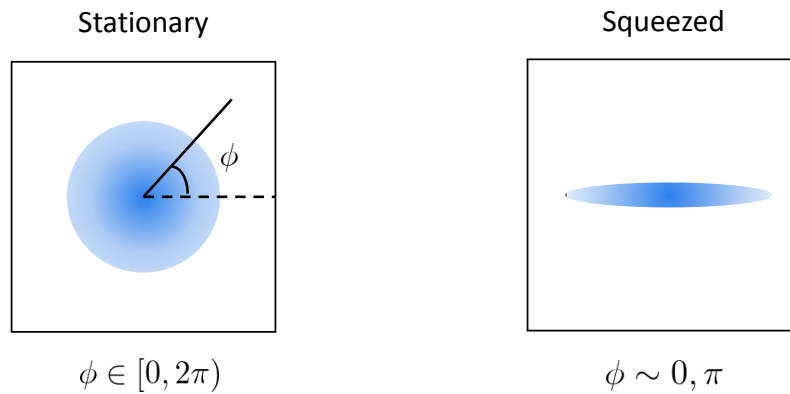
□ The squeezing cannot be detected by LIGO and LISA

B. Allen, et al. PRD 61, 024024 (1999)



These two Gaussian distributions of PGW cannot be distinguished statistically each other by LIGO and LISA

□ How can we discriminate between the stationary and squeezed state?



In the present time, it is difficult to discriminate

➔ If we do observations of the past universe, like CMB or GW map, is it possible to discriminate each other?

We want to discuss the theoretical limitation of statistical discrimination of the two distributions
Quantum discrimination problem

Massless scalar field in the expanding universe

□ Massless scalar field in the inflation and radiation era

We need to get the squeezed distribution and define the stationary one

Friedmann spacetime

$$ds^2 = a^2(\eta)(-d\eta^2 + d\mathbf{x}^2) \quad a(\eta) = \begin{cases} -\frac{1}{H_{\text{dS}}(\eta - 2\eta_r)} & (-\infty < \eta \leq \eta_r) \\ \frac{\eta}{H_{\text{dS}}\eta_r^2} & (\eta_r < \eta) \end{cases}$$

Massless scalar field (fluctuation) $\varphi(x, t)$

Equation of motion

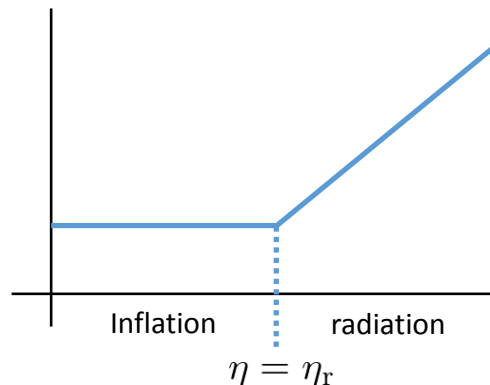
$$\ddot{q} - \nabla^2 q - \frac{\ddot{a}}{a}q = 0$$

$$q = a\varphi$$

$$\partial_\eta = \dots$$

Mode equation

$$\ddot{f}_k + \left(k^2 - \frac{\ddot{a}}{a}\right)f_k = 0$$



□ Quantization and pair creation

$$\hat{q}(\mathbf{x}, \eta) = \begin{cases} \int \frac{d^3k}{(2\pi)^{3/2}} (\hat{a}_{\mathbf{k}} f_{\mathbf{k}} + \hat{a}_{-\mathbf{k}}^\dagger f_{\mathbf{k}}^*) e^{i\mathbf{k}\cdot\mathbf{x}} & (-\infty < \eta \leq \eta_r) \\ \int \frac{d^3k}{(2\pi)^{3/2}} (\hat{b}_{\mathbf{k}} u_{\mathbf{k}} + \hat{b}_{-\mathbf{k}}^\dagger u_{\mathbf{k}}^*) e^{i\mathbf{k}\cdot\mathbf{x}} & (\eta_r < \eta) \end{cases} \quad \hat{b}_{\mathbf{k}} = \alpha_{\mathbf{k}} \hat{a}_{\mathbf{k}} + \beta_{\mathbf{k}}^* \hat{a}_{-\mathbf{k}}^\dagger$$

Mode function of the Bunch-Davies vacuum $f_{\mathbf{k}}(\eta) = \frac{1}{\sqrt{2k}} \left(1 - \frac{i}{k(\eta - 2\eta_r)}\right) e^{-ik(\eta - 2\eta_r)}$

Mode function in the radiation era $u_{\mathbf{k}}(\eta) = \frac{1}{\sqrt{2k}} e^{-ik\eta}$

Bogolyubov coefficients $\alpha_{\mathbf{k}} = \left(1 + \frac{i}{k\eta_r} - \frac{1}{2k^2\eta_r^2}\right) e^{2ik\eta_r} \quad \beta_{\mathbf{k}} = \frac{1}{2k^2\eta_r^2}$

$$|0_{\text{BD}}\rangle_{\text{a}} = N \bigotimes_{\mathbf{k} \in \mathbb{R}^{3+}} \left[\sum_{n=0}^{\infty} \left(\frac{\beta_{\mathbf{k}}^*}{\alpha_{\mathbf{k}}}\right)^n |n_{\mathbf{k}}, n_{-\mathbf{k}}\rangle_{\text{b}} \right]$$

Pair creation of \mathbf{k} and $-\mathbf{k}$ mode
squeezed distribution

□ Definition of the stationary distribution

Squeezed distribution $|0_{\text{BD}}\rangle_{\text{a}} = N \bigotimes_{\mathbf{k} \in \mathbb{R}^{3+}} \left[\sum_{n=0}^{\infty} \left(\frac{\beta_{\mathbf{k}}^*}{\alpha_{\mathbf{k}}}\right)^n |n_{\mathbf{k}}, n_{-\mathbf{k}}\rangle_{\text{b}} \right] \quad \hat{b}_{\mathbf{k}} = \alpha_{\mathbf{k}} \hat{a}_{\mathbf{k}} + \beta_{\mathbf{k}}^* \hat{a}_{-\mathbf{k}}^\dagger$

Definition of the stationary Gaussian distribution

$$\text{Tr}[\hat{b}_{\mathbf{k}} \hat{b}_{\mathbf{k}'} \rho_{\text{st}}] = 0 \quad \text{Tr}[\hat{b}_{\mathbf{k}}^\dagger \hat{b}_{\mathbf{k}'} \rho_{\text{st}}] = \langle 0_{\text{BD}} | \hat{b}_{\mathbf{k}}^\dagger \hat{b}_{\mathbf{k}'} | 0_{\text{BD}} \rangle$$

phase independent distribution



Corresponding density operator

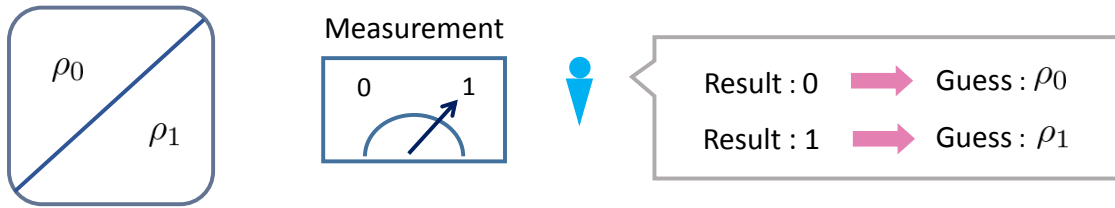
$$\rho_{\text{st}} = \bigotimes_{\mathbf{k} \in \mathbb{R}^3} \rho_{\mathbf{k}} \quad \rho_{\mathbf{k}} = |N_{\mathbf{k}}|^2 \sum_{n=0}^{\infty} \left| \frac{\beta_{\mathbf{k}}}{\alpha_{\mathbf{k}}} \right|^{2n} |n_{\mathbf{k}}\rangle \langle n_{\mathbf{k}}|$$

We consider the quantum state discrimination between $|0_{\text{BD}}\rangle$ and ρ_{st}

Quantum state discrimination

State discrimination for a single sample

System : ρ_0 or ρ_1



Failure probability of the guess probability that we mistake ρ_1 as ρ_0 or ρ_0 as ρ_1

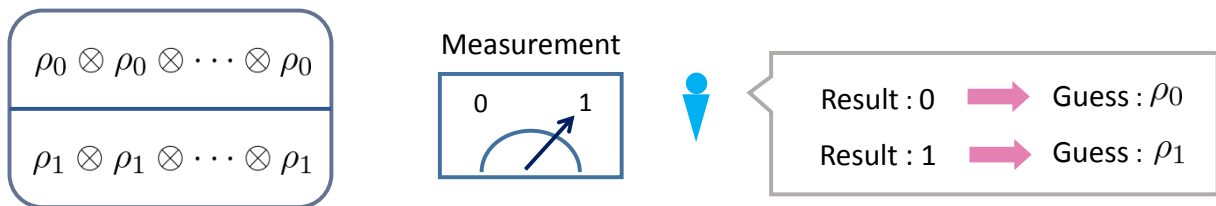
$$p_f = \frac{1}{2} \text{Tr}[\hat{E}_0 \rho_1] + \frac{1}{2} \text{Tr}[\hat{E}_1 \rho_0] \quad \hat{E}_0 + \hat{E}_1 = \hat{I} \quad \hat{E}_i : \text{projection operator}$$

prior probability

$\min_{\hat{E}_i} p_f$ characterizes the error of the statistical discrimination

State discrimination for N sample sizes

N partite system : $\rho_0^{\otimes N}$ or $\rho_1^{\otimes N}$



Failure probability of the guess

$$p_f = \frac{1}{2} \text{Tr}[\hat{E}_0^{(N)} \rho_1^{\otimes N}] + \frac{1}{2} \text{Tr}[\hat{E}_1^{(N)} \rho_0^{\otimes N}] \quad \text{we treat N partite system as a single system}$$

$\hat{E}_i^{(N)}$: projection operator for N partite system

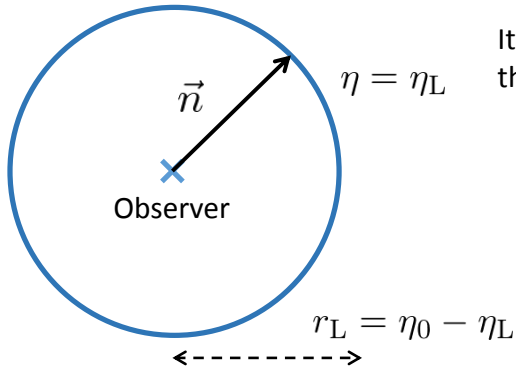
Quantum Chernoff bound

$$\frac{1}{2} \left(1 - \sqrt{1 - \left[\inf_{0 \leq s \leq 1} Q_s \right]^N} \right) \leq \min_{\hat{E}_i^{(N)}} p_f \leq \frac{1}{2} \left[\inf_{0 \leq s \leq 1} Q_s \right]^N \quad Q_s = \text{Tr}[\rho_0^{1-s} \rho_1^s] \quad 0 \leq Q_s \leq 1$$

For large N sample sizes, the failure probability can be sufficiently small

Our assumptions for the setting of observation

□ Observables on a two-dimensional sphere



It is assumed that we know the distribution on a two-dimensional sphere

for example, the last scattering surface

$$\hat{q}_L(\vec{n}) = \hat{q}(r_L, \vec{n}, \eta_L) \quad \hat{p}_L(\vec{n}) = \hat{p}(r_L, \vec{n}, \eta_L)$$

$$p = \dot{q} - \frac{\dot{a}}{a} q$$

As observables, because of focusing on Gaussian distributions

$$\left\{ \begin{aligned} C_l^{qq} &= \frac{1}{4\pi} \int_{\vec{n}_1, \vec{n}_2} P_l(\vec{n}_1 \cdot \vec{n}_2) \langle \hat{q}_L(\vec{n}_1) \hat{q}_L(\vec{n}_2) \rangle \Big|_{|\mathbf{k}| \leq \Lambda} && P_l(\vec{n}_1 \cdot \vec{n}_2): \text{Legendre function} \\ C_l^{qp} &= \frac{1}{8\pi} \int_{\vec{n}_1, \vec{n}_2} P_l(\vec{n}_1 \cdot \vec{n}_2) \langle \hat{q}_L(\vec{n}_1) \hat{p}_L(\vec{n}_2) + \hat{p}_L(\vec{n}_2) \hat{q}_L(\vec{n}_1) \rangle \Big|_{|\mathbf{k}| \leq \Lambda} && \text{UV cutoff, thickness of the sphere} \\ C_l^{pp} &= \frac{1}{4\pi} \int_{\vec{n}_1, \vec{n}_2} P_l(\vec{n}_1 \cdot \vec{n}_2) \langle \hat{p}_L(\vec{n}_1) \hat{p}_L(\vec{n}_2) \rangle \Big|_{|\mathbf{k}| \leq \Lambda} && \text{we assume the knowledge of these correlations to get the theoretical limitation} \end{aligned} \right.$$

□ Quantum Chernoff bound and Cosmic variance for our observational assumptions

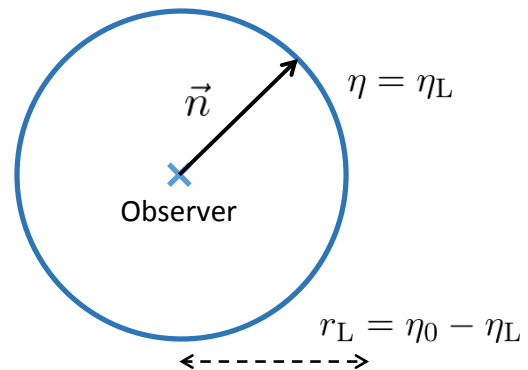
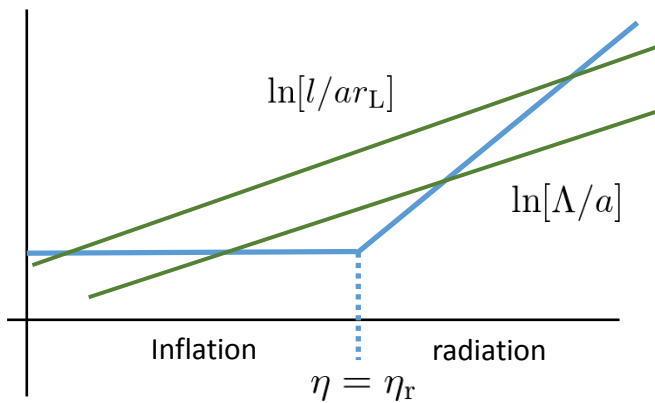
Squeezed and stationary

$$|0_{BD}\rangle \quad \rho_{st}$$



Each covariance matrix

$$V_{l,BD} \quad V_{l,st} \quad V_l = \begin{bmatrix} C_l^{qq} & C_l^{qp} \\ C_l^{qp} & C_l^{pp} \end{bmatrix}$$



Quantum Chernoff distance

$$Q_s \sim \sqrt{\frac{|V_{l,BD}|^{1-s} |V_{l,st}|^s}{|(1-s)V_{l,BD} + sV_{l,st}|}}$$

$$\Lambda \eta_r \ll 1 \quad \text{Long wave length}$$

$$\frac{1}{2} \left(1 - \sqrt{1 - \left[\inf_{0 \leq s \leq 1} Q_s \right]^N} \right) \leq \min_{\hat{E}_i^{(N)}} p_f \leq \frac{1}{2} \left[\inf_{0 \leq s \leq 1} Q_s \right]^N$$

Sample sizes $N \leq 2l + 1$ Cosmic variance

Evaluation of the quantum Chernoff bound

□ Example : discrimination efficiency on the last scattering surface for $N=1$

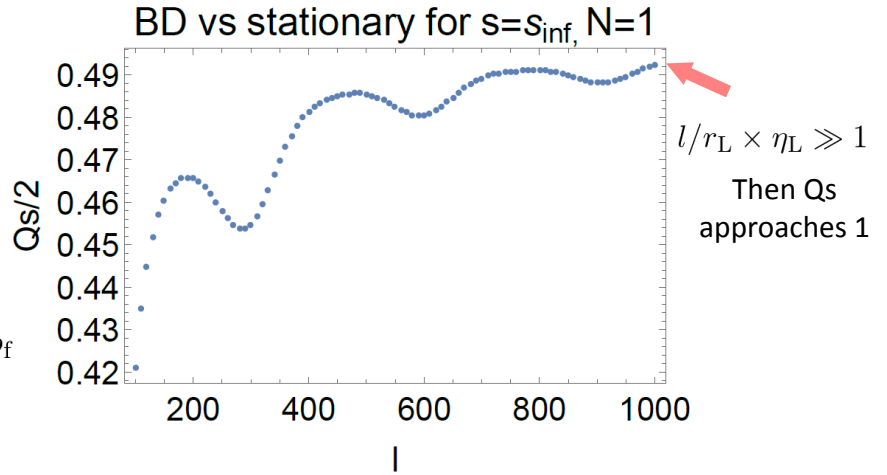
$$\left\{ \begin{array}{l} 1 + Z_{\text{end}} = \frac{(\eta_0 + \eta_{\text{eq}})^2}{4\eta_r\eta_{\text{eq}}} \approx 10^{27} \quad H_0 \sim 10^{-18}\text{Hz} \sim 10^{-43}\text{GeV} \quad H_{\text{dS}} \sim 10^{14}\text{GeV} \quad N \sim 70 \\ 1 + Z_{\text{eq}} = \frac{(\eta_0 + \eta_{\text{eq}})^2}{4\eta_{\text{eq}}^2} \approx 10^4 \quad 1 + Z_L = \left(\frac{\eta_0 + \eta_{\text{eq}}}{\eta_L + \eta_{\text{eq}}}\right)^2 \approx 10^3 \end{array} \right.$$

➡ $\eta_0/\eta_r \sim 10^{25} \quad \eta_L/\eta_r \sim 10^{23} \quad r_L/\eta_r \sim 10^{25} \quad r_L = \eta_0 - \eta_L$

$$\Lambda = l_{\text{max}}/r_L \quad l_{\text{max}} = 10^4$$

$$\min_{\hat{E}_i^{(N)}} p_f \leq \frac{1}{2} \left[\inf_{0 \leq s \leq 1} Q_s \right]^N \quad \underline{N=1}$$

$$\frac{1}{2} \left(1 - \sqrt{1 - \left[\inf_{0 \leq s \leq 1} Q_s \right]^N} \right) \leq \min_{\hat{E}_i^{(N)}} p_f$$



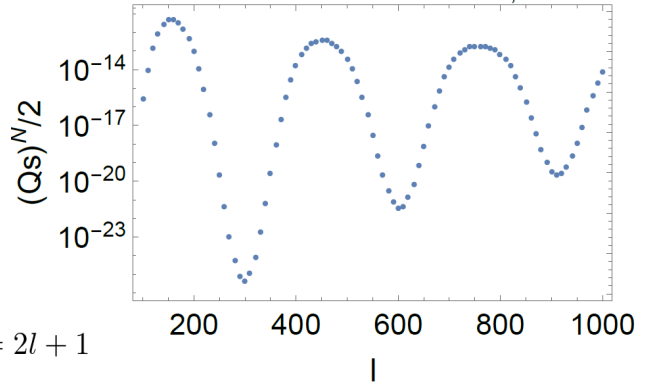
□ The case $N=2l+1$ and asymptotic approximation

$$\eta_0/\eta_r \sim 10^{25} \quad \eta_L/\eta_r \sim 10^{23} \quad r_L/\eta_r \sim 10^{25}$$

$$\Lambda = l_{\text{max}}/r_L \quad l_{\text{max}} = 10^4$$

$$\min_{\hat{E}_i^{(N)}} p_f \leq \frac{1}{2} \left[\inf_{0 \leq s \leq 1} Q_s \right]^N \quad \underline{N=2l+1}$$

BD vs stationary for $s=s_{\text{inf}}, N=2l+1$



For $l_{\text{max}}/l \gg 1 \quad l \gg 1 \quad l/r_L \times \eta_L \gg 1 \quad N=2l+1$

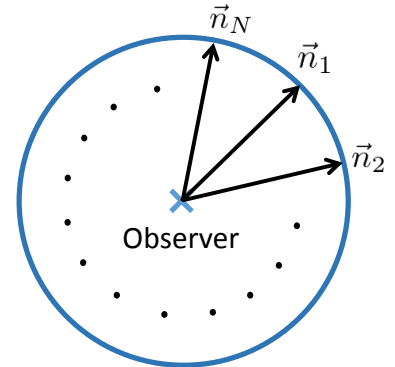
$$\left[\inf_{0 \leq s \leq 1} Q_s \right]^{2l+1} \sim \exp\left[-c \frac{r_L}{\eta_L}\right] \quad c \sim 0.3$$

For $l/r_L \times \eta_L = \frac{k_L}{H_L} \gg 1 \quad k_L = \frac{l}{a(\eta_L)r_L}$

$r_L/\eta_L = R_L H_L \ll 1$ ➡ Discrimination error cannot be ignored

$r_L/\eta_L = R_L H_L \gg 1$ ➡ Discrimination error can be small

$$R_L = a(\eta_L)r_L$$



Summary

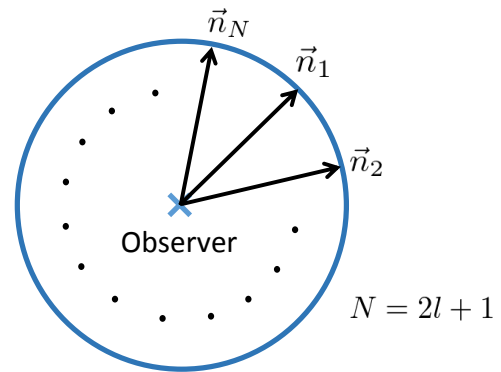
□ We consider quantum discrimination between the Bunch-Davies vacuum and the stationary distribution.

□ To get the theoretical limitation of the statistical discrimination, we assume the knowledge of qq, qp and pp correlations on a two-dimensional sphere (e.g. Last Scattering Surface).

□ For a single direction observation with a short wave length, even if we know the qq, qp and pp correlations, the efficiency of the discrimination becomes bad, similar to the previous work B. Allen, et al (1999).

□ However, if we can carry out the quantum measurement for $2l+1$ directions, then the discrimination efficiency can be improved for the observation of a short wave length.

$$\min_{\hat{E}_i^{(N)}} p_f \leq \frac{1}{2} \left[\inf_{0 \leq s \leq 1} Q_s \right]^N \quad \left[\inf_{0 \leq s \leq 1} Q_s \right]^{2l+1} \sim \exp \left[-c \frac{r_L}{\eta_L} \right]$$



Anupam Mazumdar

University of Groningen

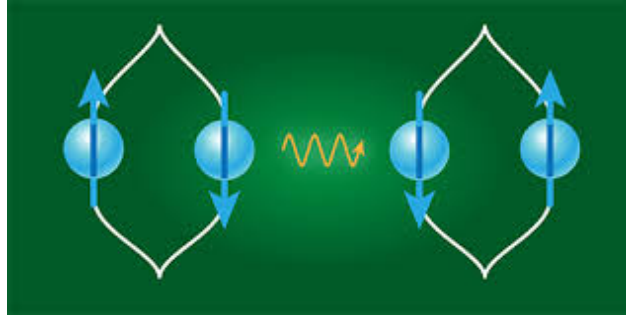
“Testing Quantum Gravity via entanglement”
(10+5 min.)

[JGRG28 (2018) 110709]

Testing Quantum Gravity via Entanglement

Anupam Mazumdar

Van Swinderen Institute, University of Groningen



Thanks to **JSPS** for the invitation & thanks to all of you for hosting me:

TiTech, Yukawa Inst./Kyoto, IPMU, KEK, Universities of Kobe, Nagoya, Tokyo & Waseda,

Part-1

Summary

Ghost free and non-singular construction of gravity & Towards Conformally flat solutions in the UV

Construction of Scale Free/Conformally Flat Theory of Classical & Quantum Gravity in the UV, which is Perturbatively Unitary

$$S = \int d^4x \sqrt{-g} \left[\frac{R}{16\pi G} + R \mathcal{F}_1 \left(\frac{\square}{M^2} \right) R + R_{\mu\nu} \mathcal{F}_2 \left(\frac{\square}{M^2} \right) R^{\mu\nu} + R_{\mu\nu\lambda\sigma} \mathcal{F}_3 \left(\frac{\square}{M^2} \right) R^{\mu\nu\lambda\sigma} \right]$$

Einstein-Hilbert
Recovers IR

UV modifications, and non-local
gravitational interactions

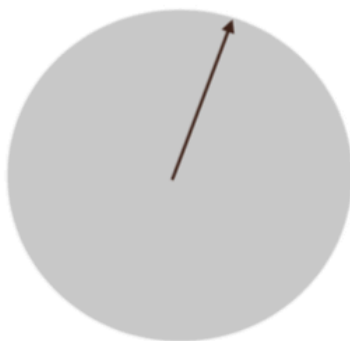
Known as IDG (infinite derivative gravity)

Salient features

- * Dynamical degrees of freedom remains the same from UV \leftrightarrow IR, but no Ghosts
- * Unitarity constraints the form factors \mathcal{F} 's around a given background
- * Non-singular Static & Rotating, No-Horizon, compact objects as planets, as heavy as billion solar masses can be formed: Testable features at LIGO/VIRGO/KAGRA
- * Non-locality plays an important role in smearing blackhole singularity and emergence of a new scale in the IR

Non local Squishy Stars

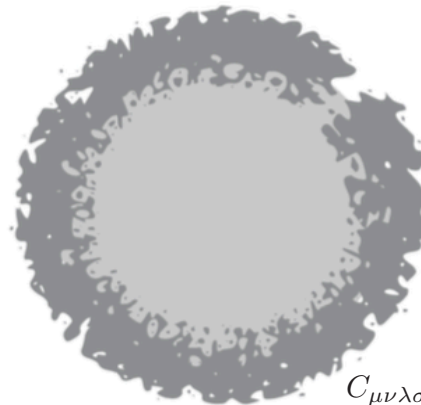
$$r_{sch} = 2Gm$$



$$C_{\mu\nu\lambda\sigma} \rightarrow \infty \text{ as } r \rightarrow 0$$

Schwarzschild's blackhole

$$r_{NL} \sim 2M_s^{-1} > r_{sch}$$



$$C_{\mu\nu\lambda\sigma} \rightarrow 0 \text{ as } r \rightarrow 0$$

Non-local, compact object
in infinite derivative gravity

Biswas+Gerwick+Koivisto+AM, PRL, 2011 [1110.5249]
Biswas+Koshelev+AM, PRD, 2017, [1606.01250]

Construction of ghost free conditions

Koshelev+Marto+AM, PRD, 2018 [1803.00309]

Buoninfante+Koshelev+Lambiase+Marto+AM, JCAP, 2018 [1804.01895]

Non-singular, Non-perturbative solutions

Buoninfante+Cornell+Harmesen+Koshelev+Lambiase+Marto+AM, PRD, 2018 [1807.08896]

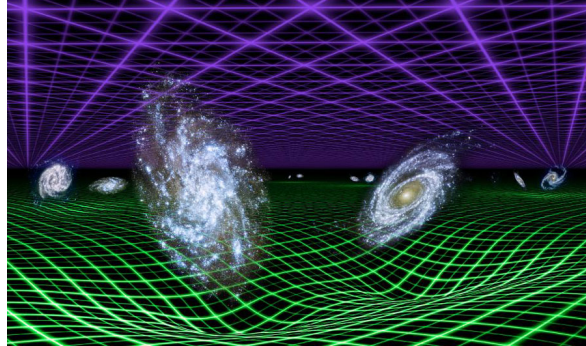
Non-singular, ROTATING, Non-perturbative solutions

AM+Stettinger [1811.00885]

Unitarity for AdS (3) massless +massive gravity

Part-2

Entangling matter via graviton

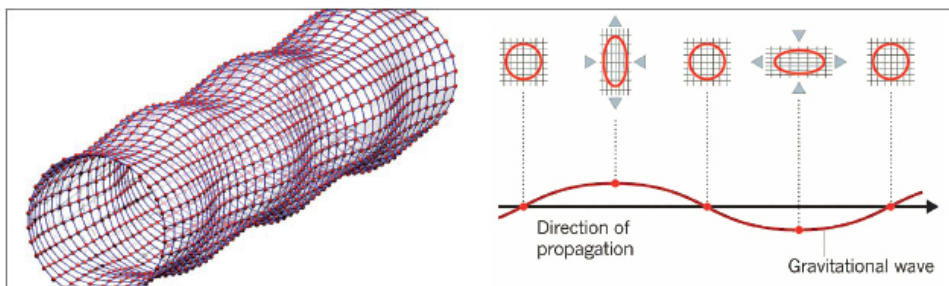


How do we know whether gravity is classical or Quantum ?

Could you devise a TEST?

Bose+AM+Morley+Ulbricht+Toros+Paternostro+Geraci+Barker+Kim+Milburn
Phys. Rev. Lett. (2017) [1707.06050]

Real versus virtual Graviton



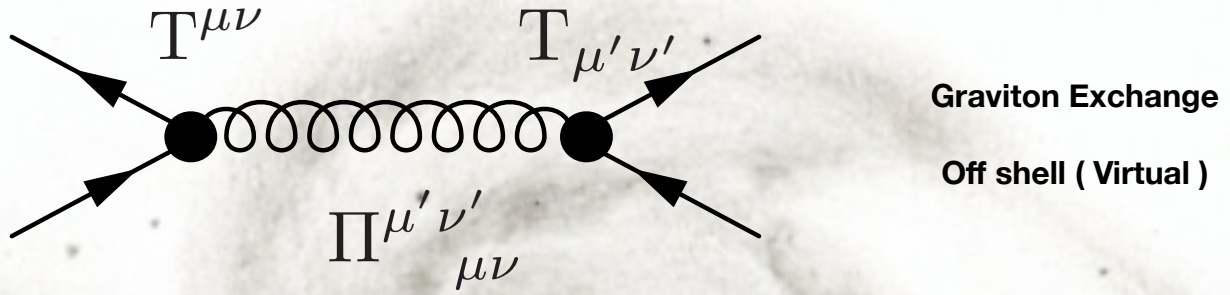
Gravitational wave

On shell

Follows classical “equations of motion”



Virtual Graviton as a Quantum Mediator



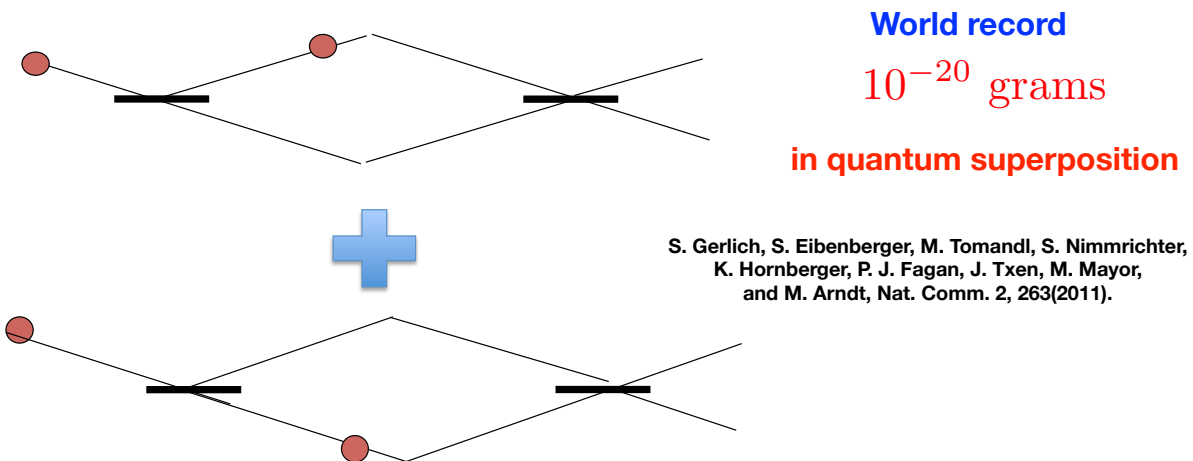
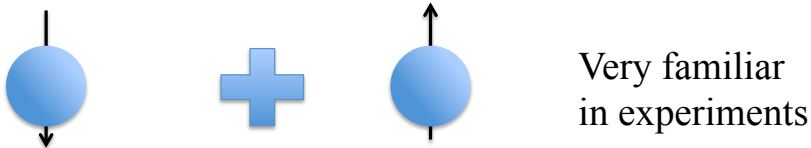
$$\Pi(k^2) \sim \frac{P^{(2)}}{k^2} - \frac{P^{(0)}}{2k^2} \qquad V \sim \frac{1}{r}$$

Graviton propagator in terms of spin projection operators in 4d, Minkowski space time

Biswas+Koivisto+AM, 1302.0532

World Record in Quantum Superposition

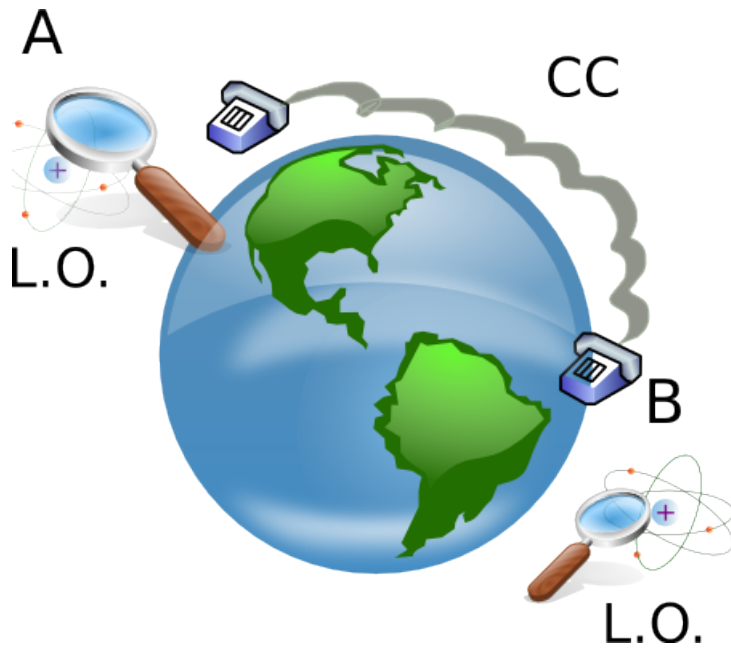
The Superposition Principle **Underpins** Quantum Mechanics



S. Gerlich, S. Eibenberger, M. Tomandl, S. Nimmrichter, K. Hornberger, P. J. Fagan, J. Txen, M. Mayor, and M. Arndt, Nat. Comm. 2, 263(2011).

If you *decohere* (kill superpositions) nonclassical features of quantum mechanics go away. Even old quantum mechanics: the right difference between energy levels obtained only through a superposition of localized states.

Local Operations & Classical Communication



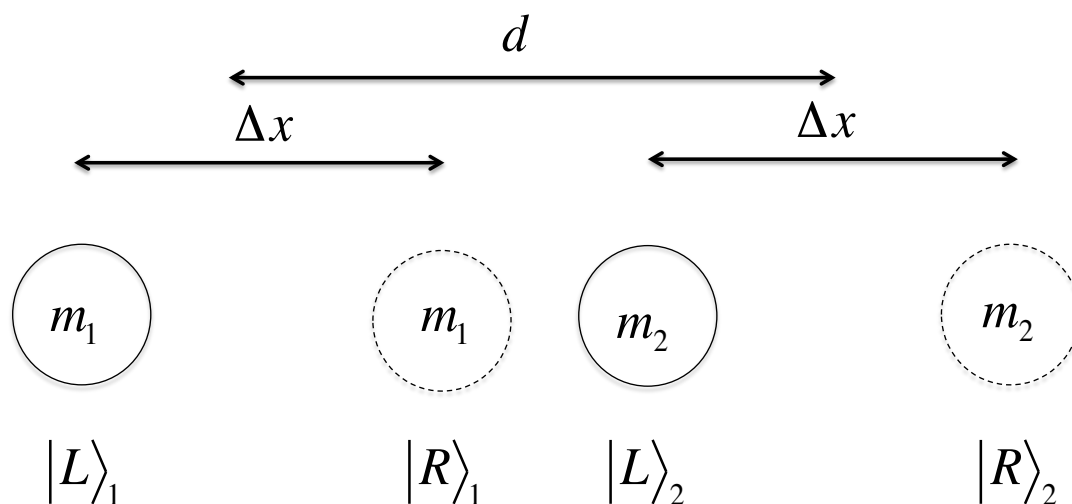
Cannot create entanglement

Nielsen, PRL (1999)

**Separable state remains Separable
(Cannot create entanglement)**

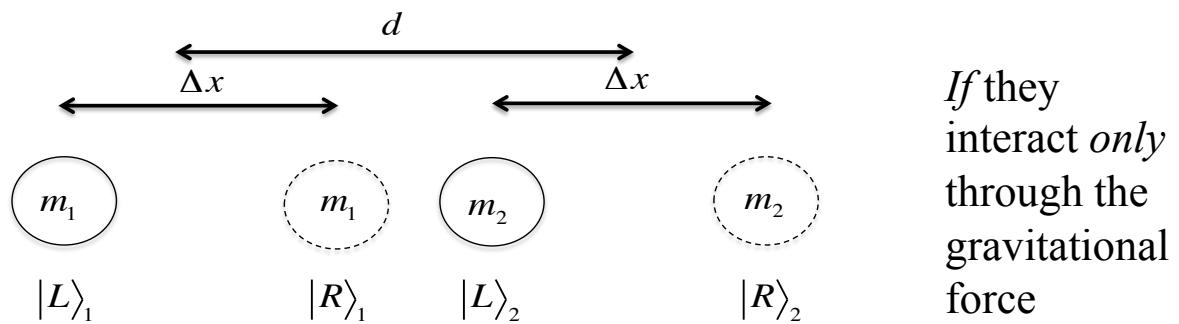
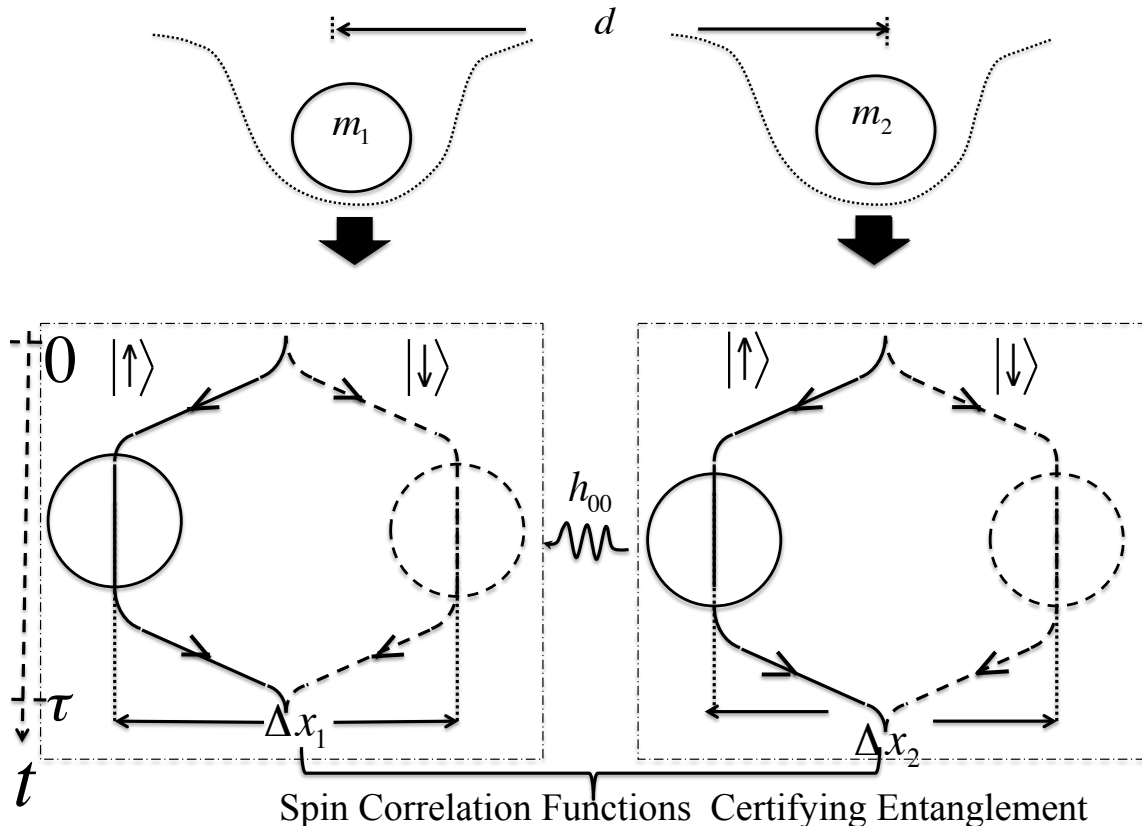
2 Masses & Virtual Graviton

A Schematic of two matter-wave interferometers near each other



Consider two neutral test masses *held* in a superposition, each exactly as a path encoded qubit (states $|L\rangle$ and $|R\rangle$), near each other.

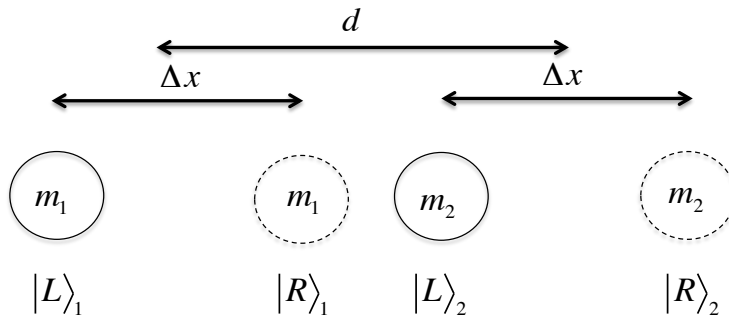
Evolving the Quantum Phase



$$\begin{aligned}
 |\Psi(t=0)\rangle_{12} &= \frac{1}{\sqrt{2}}(|L\rangle_1 + |R\rangle_1) \frac{1}{\sqrt{2}}(|L\rangle_2 + |R\rangle_2) \\
 &= \frac{1}{2}(|L\rangle_1|L\rangle_2 + |L\rangle_1|R\rangle_2 + |R\rangle_1|L\rangle_2 + |R\rangle_1|R\rangle_2) \\
 \rightarrow |\Psi(t=\tau)\rangle_{12} &= \frac{1}{2}(e^{i\phi_{LL}}|L\rangle_1|L\rangle_2 + e^{i\phi_{LR}}|L\rangle_1|R\rangle_2 \\
 &\quad + e^{i\phi_{RL}}|R\rangle_1|L\rangle_2 + e^{i\phi_{RR}}|R\rangle_1|R\rangle_2),
 \end{aligned}$$

where

$$\begin{aligned}
 \phi_{RL} &\sim \frac{Gm_1m_2\tau}{\hbar(d-\Delta x)}, \phi_{LR} \sim \frac{Gm_1m_2\tau}{\hbar(d+\Delta x)}, \\
 \phi_{LL} = \phi_{RR} &\sim \frac{Gm_1m_2\tau}{\hbar d}
 \end{aligned}$$



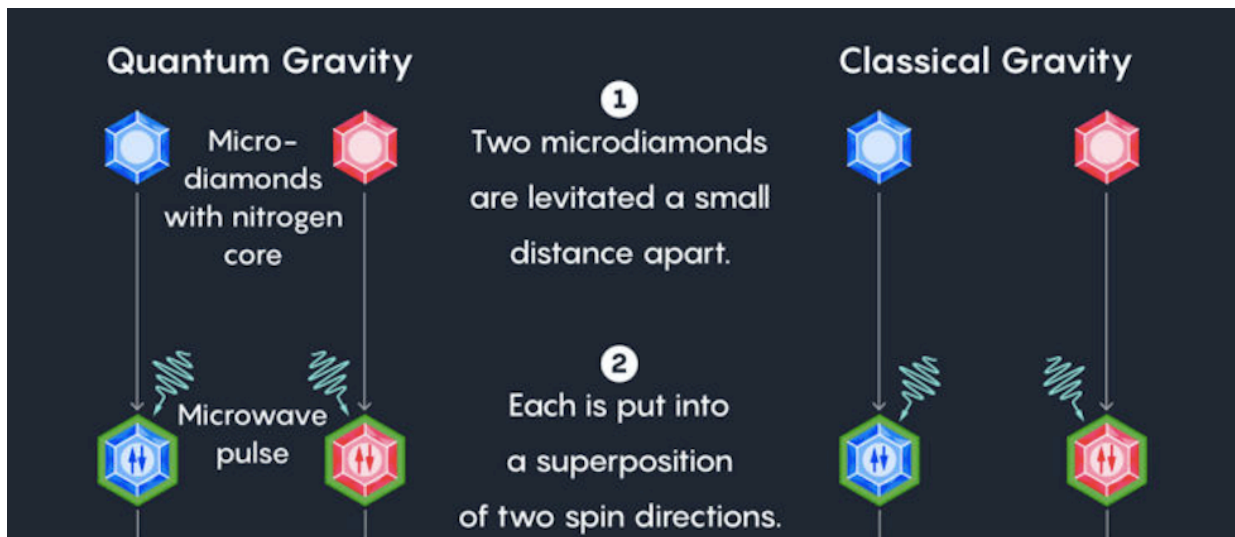
If they interact *only* through the gravitational force

$$\begin{aligned}
 |\Psi(t = \tau)\rangle_{12} &= \frac{1}{2} (e^{i\phi_{LL}} |L\rangle_1 |L\rangle_2 + e^{i\phi_{LR}} |L\rangle_1 |R\rangle_2 \\
 &\quad + e^{i\phi_{RL}} |R\rangle_1 |L\rangle_2 + e^{i\phi_{RR}} |R\rangle_1 |R\rangle_2) \\
 &= \frac{e^{i\phi_{RR}}}{\sqrt{2}} \left\{ |L\rangle_1 \frac{1}{\sqrt{2}} (|L\rangle_2 + e^{i\Delta\phi_{LR}} |R\rangle_2) \right. \\
 &\quad \left. + |R\rangle_1 \frac{1}{\sqrt{2}} (e^{i\Delta\phi_{RL}} |L\rangle_2 + |R\rangle_2) \right\}
 \end{aligned}$$

The above state is maximally entangled when $\Delta\phi_{LR} + \Delta\phi_{RL} \sim \pi$.

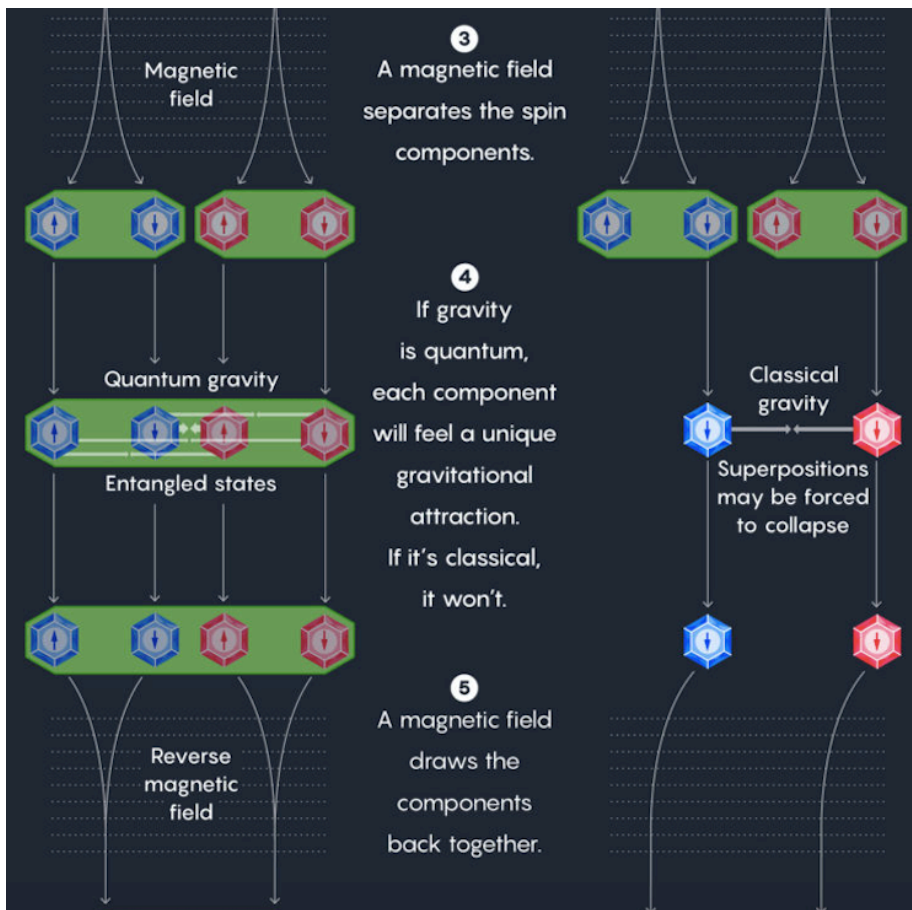
Witnessing Quantum Gravity

A newly proposed experiment could confirm that gravity is a quantum force. It involves two microdiamonds, each placed in a quantum “superposition” of two possible locations. If gravity is quantum, the gravitational attraction between the diamonds will entangle their states. If it’s not, the diamonds won’t become entangled.



Step 1: SG splitting:

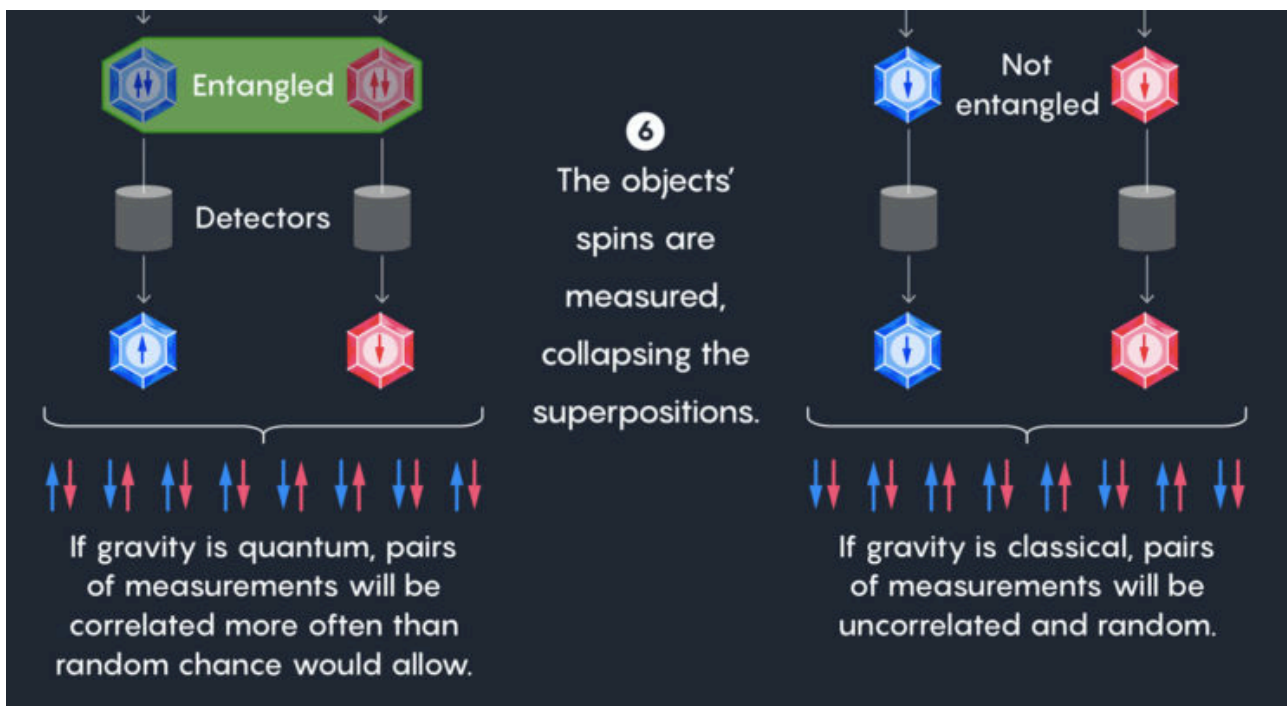
$$|C\rangle_j \frac{1}{\sqrt{2}} (|\uparrow\rangle_j + |\downarrow\rangle_j) \rightarrow \frac{1}{\sqrt{2}} (|L, \uparrow\rangle_j + |R, \downarrow\rangle_j)$$



Step 2: Gravitational interaction induced phase accumulation on the joint states of masses 1 & 2 (mapped to nuclear spins)

Step 3: SG recombination: $|L, \uparrow\rangle_j \rightarrow |C, \uparrow\rangle_j$, $|R, \downarrow\rangle_j \rightarrow |C, \downarrow\rangle_j$

Measuring Spin Correlation



Step 4: Witness spin entangled state:

$$\begin{aligned}
 |\Psi(t = t_{\text{End}})\rangle_{12} &= \frac{1}{\sqrt{2}} \{ |\uparrow\rangle_1 \frac{1}{\sqrt{2}} (|\uparrow\rangle_2 + e^{i\Delta\phi_{LR}} |\downarrow\rangle_2) \\
 &\quad + |\downarrow\rangle_1 \frac{1}{\sqrt{2}} (e^{i\Delta\phi_{RL}} |\uparrow\rangle_2 + |\downarrow\rangle_2) \} |C\rangle_1 |C\rangle_2
 \end{aligned}$$

through the correlations:

$$\mathcal{W} = |\langle \sigma_x^{(1)} \otimes \sigma_z^{(2)} \rangle - \langle \sigma_y^{(1)} \otimes \sigma_z^{(2)} \rangle|$$

we have

$$\Delta\phi_{RL} \sim \frac{Gm_1m_2\tau}{\hbar(d - \Delta x)} \gg \Delta\phi_{LR}, \Delta\phi_{LL}, \Delta\phi_{RR}$$

For mass $\sim 10^{-14}$ kg (microspheres), separation at closest approach of the masses ~ 200 microns (to prevent Casimir interaction), **time ~ 1 seconds**, gives:

Scale of superposition ~ 100 microns, **Delta phi_{RL} ~ 1**

Planck's Constant fights Newton's Constant!

Protocol

Spin Entanglement Witness:

Step 1: SG splitting:

$$|C\rangle_j \frac{1}{\sqrt{2}}(|\uparrow\rangle_j + |\downarrow\rangle_j) \rightarrow \frac{1}{\sqrt{2}}(|L, \uparrow\rangle_j + |R, \downarrow\rangle_j)$$

Step 2: Gravitational interaction induced phase accumulation on the joint states of masses 1 & 2 (*mapped to nuclear spins*)

Step 3: SG recombination: $|L, \uparrow\rangle_j \rightarrow |C, \uparrow\rangle_j$, $|R, \downarrow\rangle_j \rightarrow |C, \downarrow\rangle_j$

Step 4: Witness spin entangled state:

$$|\Psi(t = t_{\text{End}})\rangle_{12} = \frac{1}{\sqrt{2}}\left\{|\uparrow\rangle_1 \frac{1}{\sqrt{2}}(|\uparrow\rangle_2 + e^{i\Delta\phi_{LR}}|\downarrow\rangle_2) + |\downarrow\rangle_1 \frac{1}{\sqrt{2}}(e^{i\Delta\phi_{RL}}|\uparrow\rangle_2 + |\downarrow\rangle_2)\right\}|C\rangle_1|C\rangle_2$$

through the correlations:

$$\mathcal{W} = |\langle\sigma_x^{(1)} \otimes \sigma_z^{(2)}\rangle - \langle\sigma_y^{(1)} \otimes \sigma_z^{(2)}\rangle|$$

Conclusion

Alice, Bob and Eve

**We are
all
entangled
:
Gravity is
QUANTUM !**

Now we can test it !



Bose+AM+Morley+Ulbricht+Toros+Paternostro+Geraci+Barker+Kim+Milburn, PRL (2017) [1707.06050]

Many atom/laser optics groups are thinking seriously about our proposal, inspite of experimental challenges. There is a proposal to test it at IBM Quantum Computer...

Extra Slides

How can we increase the scale of the superposition?

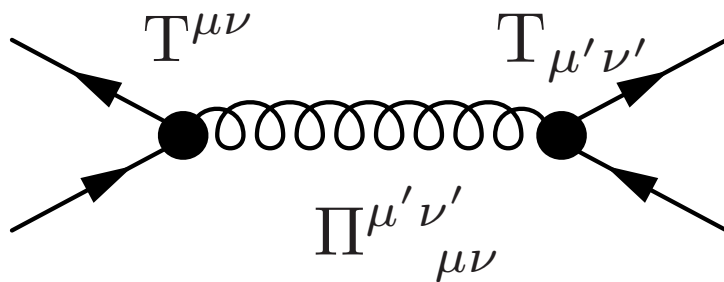
Free particle in an inhomogeneous magnetic field (acceleration $+a$ or $-a$)

$$\begin{aligned}
 x_\sigma(t, j) &= x_j(0) \pm \frac{1}{2}at^2 \\
 &= \frac{a\tau}{4}\left(t - \frac{\tau}{4}\right) \mp \frac{1}{2}a\left(t - \frac{\tau}{4}\right)^2 \\
 &= \frac{1}{2}a\left(\frac{\tau}{4}\right)^2 \mp \frac{a\tau}{4}\left(t - \frac{3\tau}{4}\right) \pm \frac{1}{2}a\left(t - \frac{3\tau}{4}\right)^2
 \end{aligned}$$

Gravity is Quantum

Graviton must obey the quantum superposition principle

Graviton as a mediator ought to be off shell



Virtual communication
or Quantum
communication via
off shell mediator

Local coupling

Local coupling

Graviton can entangle 2 masses

Shinpei Kobayashi

Tokyo Gakugei University

**“Algebraic construction of solutions in noncommutative gravity
and squeezed coherent state”**

(10+5 min.)

[JGRG28 (2018) 110710]

ALGEBRAIC CONSTRUCTION OF SOLUTIONS IN NONCOMMUTATIVE GRAVITY AND SQUEEZED COHERENT STATE

SHINPEI KOBAYASHI (TOKYO GAKUGEI UNIVERSITY)

AND

TSUGUHIKO ASAKAWA (MAEBASHI INST. OF TECH.)

JGRG28 @ Rikkyo University, November 5–9, 2018

QUANTUM GRAVITY AND NONCOMMUTATIVITY

- quantum gravity: some candidates
 - string theory, causal dynamical triangulation, ...
- noncommutativity appears: $[x, y] = i\theta$ ← Moyal plane
 - string length, D2-brane with flux and more
- minimal length and noncommutativity indicate:
 - discretized spacetime (Ueda-SK [PA7])
 - dimensional flow (Takagi-SK-Sano [PB8])
 - **nontrivial solutions** ← algebraic calculation is powerful

OPERATOR ALGEBRA & FUNCTIONS WITH DEFORMED PRODUCT

- Operators on the Moyal plane

→ all fields can be seen as operators based on

$$[\hat{x}, \hat{y}] = i\theta \iff [\hat{z}, \hat{\bar{z}}] = 1 \quad \left(\hat{z} = \frac{\hat{x} + i\hat{y}}{\sqrt{2\theta}}, \hat{\bar{z}} = \frac{\hat{x} - i\hat{y}}{\sqrt{2\theta}} \right)$$

- Functions with deformed product (e.g., Wick-Voros product)

$$(f \star g)(z, \bar{z}) = \exp\left(\frac{\partial}{\partial \bar{z}'} \frac{\partial}{\partial z''}\right) f(z', \bar{z}') g(z'', \bar{z}'') \Big|_{z'=z''=z}$$



$$[z, \bar{z}]_\star = z \star \bar{z} - \bar{z} \star z = 1$$

HOW TO USE OPERATORS: ANALOGY TO QUANTUM MECHANICS

QM

$$[x, p] = i\hbar \quad [a, a^\dagger] = 1$$

$$\hat{a} = \frac{\hat{x} + i\hat{p}}{\sqrt{2\hbar}} \quad \hat{a}^\dagger = \frac{\hat{x} - i\hat{p}}{\sqrt{2\hbar}} \quad \hat{N} = \hat{a}^\dagger \hat{a} = \frac{\hat{x}^2 + \hat{p}^2}{2\hbar}$$

← number

→ $\hat{N} |n\rangle = n |n\rangle$ any operator is written as $\hat{O} = \sum_{m,n} C_{mn} |m\rangle \langle n|$

NCG

$$[x, y] = i\theta \quad [z, z^\dagger] = 1$$

$$\hat{z} = \frac{\hat{x} + i\hat{y}}{\sqrt{2\theta}} \quad \hat{z}^\dagger = \frac{\hat{x} - i\hat{y}}{\sqrt{2\theta}} \quad \hat{N} = \hat{z}^\dagger \hat{z} = \frac{\hat{x}^2 + \hat{y}^2}{2\theta}$$

← radius

all circularly symmetric operators
in NC gravity are written as

$$\hat{O} = \sum_n C_n \frac{|n\rangle \langle n|}{\uparrow}$$

projection operator

MAP FROM OPERATOR TO FUNCTION: WEYL-WIGNER CORRESPONDENCE

operator

function

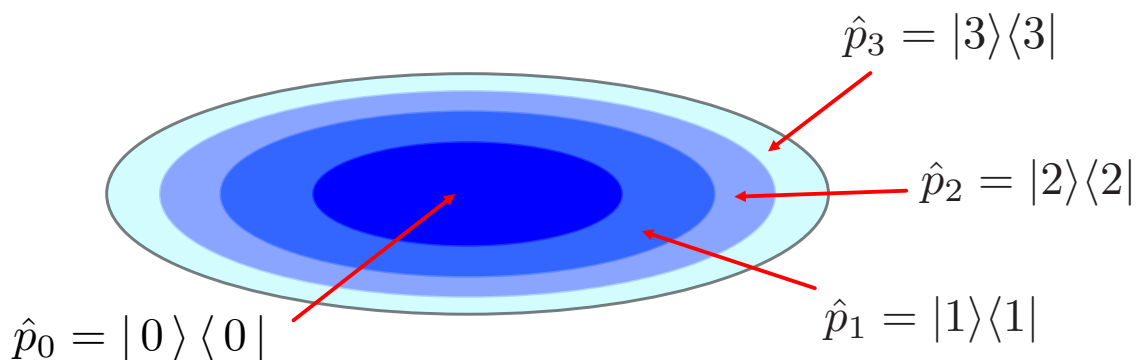
$$\hat{f} \longleftrightarrow f(z, \bar{z}) = \langle z | \hat{f} | z \rangle$$

e.g., projection operator \rightarrow generalized Gaussian function

$$|n\rangle\langle n| \longleftrightarrow f = \frac{1}{2\pi\theta(2\theta)^{n/2}} r^{2n} e^{-r^2/2\theta}$$

(\rightarrow BH with scalar & Gaussian source (Sadohara-SK [PB6]))

FROM QM TO NC GRAVITY: “NUMBER” STATE = CONCENTRIC CUTTING OF MOYAL PLANE



$\hat{p}_n \equiv |n\rangle\langle n|$: projection operator

radius $R \sim \sqrt{2N\theta}$ Each annulus has the area $2\pi\theta$

TWO GENERALIZATIONS: TRANSLATION AND SQUEEZING

- many nontrivial solutions in NC gravity [Asakawa-SK 2010]
← circularly symmetric with centers at the origin
- **two generalizations**
 - translation
→ coherent state
 - squeezing
→ squeezed state
& time-dependent harmonic oscillator

COHERENT STATES AND TRANSLATION OF SOLUTIONS

- coherent state
 $a|\alpha\rangle = \alpha|\alpha\rangle$: eigenstate of annihilation operator
- displacement operator
 $|\alpha\rangle = e^{\alpha\hat{a}^\dagger - \alpha^*\hat{a}}|0\rangle \equiv D(\alpha)|0\rangle$
 $D(\alpha)\hat{a}D(\alpha)^\dagger = \hat{a} - \alpha$: displacement in complex plane
- wave function (e.g., ground state)
$$\varphi(\alpha; x) \propto \exp \left\{ -\frac{m\omega}{2\hbar} \left(x - \sqrt{\frac{2\hbar}{m\omega}} \operatorname{Re}(\alpha) \right)^2 + i\sqrt{\frac{2m\omega}{\hbar}} \operatorname{Im}(\alpha)x \right\}$$

DISPLACED PROJECTION OPERATOR AND TRANSLATION OF SOLUTIONS

- translation in complex plane (QM)

$$\langle x_\alpha \rangle \sim \text{Re}(\alpha), \quad \langle p_\alpha \rangle \sim \text{Im}(\alpha)$$

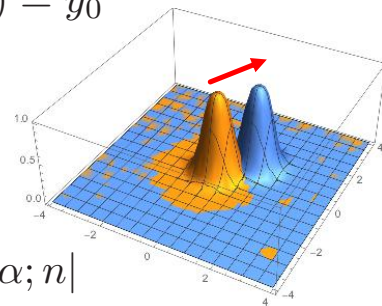
- translation in xy -plane (NC gravity)

$$\langle x_\alpha \rangle \sim \text{Re}(\alpha) = x_0, \quad \langle y_\alpha \rangle \sim \text{Im}(\alpha) = y_0$$

$$\left(\alpha = \frac{z}{\sqrt{2\theta}} = \frac{x_0 + iy_0}{\sqrt{2\theta}} \right)$$

- displaced projection operator:

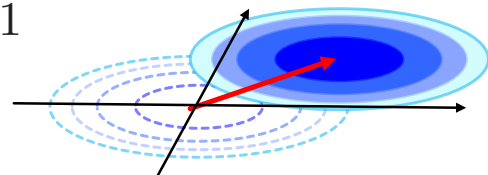
$$\hat{p}_n(\alpha) = D(\alpha)|n\rangle\langle n|D(\alpha)^\dagger = |\alpha; n\rangle\langle\alpha; n|$$



FEATURES OF DISPLACED PROJECTION OPERATOR

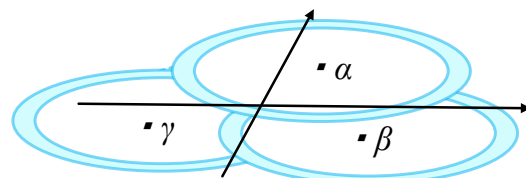
- orthogonal: $\hat{p}_m(\alpha)\hat{p}_n(\alpha) = \delta_{mn}\hat{p}_n(\alpha)$

- completeness for n : $\sum_{n=0}^{\infty} \hat{p}_n(\alpha) = 1$



- overcomplete for α : $\frac{1}{\pi} \int d^2\alpha \hat{p}_n(\alpha) = 1$

→ multi BH sln?



APPLICATION: SOLUTIONS OF NC GRAVITY

- noncommutative gravity with large- θ

$$S = -\frac{\Lambda}{\kappa^2} \int d^3x \sqrt{-g_\star} = -\frac{\Lambda}{\kappa^2} \int d^3x \frac{1}{3!} \epsilon_{abc} \epsilon^{\mu\nu\rho} E_\mu^a \star E_\nu^b \star E_\rho^c$$

- diagonal solution using projection operator

$$E_i^i = \hat{p}_i(\alpha) = |\alpha; i\rangle \langle \alpha; i| \quad (i = 0, 1, 2)$$

- diagonal solution using Clifford algebra with arbitrary size

$$E_0^0 = \gamma^3, \quad E_1^1 = \gamma^1, \quad E_2^2 = \gamma^2 \quad \{ \gamma^i \}: \text{Gamma matrices}$$

$$\longrightarrow ds^2 = C e^{-\frac{(x-x_0)^2 + (y-y_0)^2}{2\theta}} \eta_{\mu\nu} dx^\mu dx^\nu$$

SQUEEZED STATES AND SQUEEZING OF SOLUTIONS

- squeezed state

$$\hat{b}|\zeta\rangle = \zeta|\zeta\rangle \quad \hat{b} = \mu\hat{a} + \nu\hat{a}^\dagger \quad (|\mu|^2 - |\nu|^2 = 1)$$

- squeezing operator

$$|\zeta\rangle = e^{\frac{\zeta}{2}(\hat{a}^2 - \hat{a}^{\dagger 2})}|0\rangle \equiv S(\zeta)|0\rangle$$

$$S(\zeta)\hat{a}S(\zeta)^\dagger = \hat{a} \cosh \zeta - \hat{a}^\dagger \sinh \zeta$$

$$= \hat{x}e^{-\zeta} + i\hat{p}e^\zeta \quad \leftarrow \text{squeezed}$$

$$\langle x \rangle \sim x e^{-\zeta}, \quad \langle p \rangle \sim p e^\zeta$$

↑ ↑
squeezing parameter

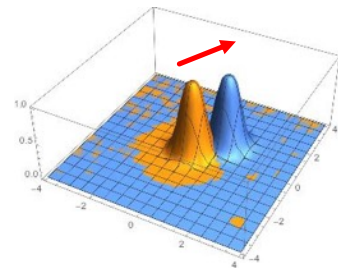
DISPLACEMENT OPERATOR AND ISOMETRY

- unitary transformation by displacement operator

$$\hat{p}_n(\alpha) = D(\alpha)|n\rangle\langle n|D(\alpha)^\dagger = |\alpha, n\rangle\langle\alpha, n|$$

$$\varphi_n(\alpha; x) = \langle x|\alpha; n\rangle = \langle x|D(\alpha)|n\rangle$$

- translation symmetry
= isometry of the Moyal plane



- There is Weyl-Wigner correspondence
→ function counterpart exists: translated Gaussian function

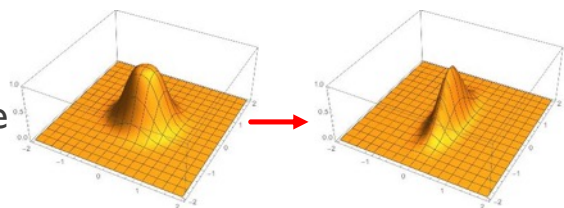
SQUEEZING OPERATOR AND ISOMETRY

- unitary transformation by squeezing operator

$$\hat{p}_n(0, \zeta) \equiv S(\zeta)D(0)|n\rangle\langle n|D(0)^\dagger S(\zeta)^\dagger = |0, \zeta; n\rangle\langle 0, \zeta; n|$$

$$\varphi_n(0, \zeta; x) = \langle x|S(\zeta)D(0)|n\rangle$$

- squeezing
≠ isometry of the Moyal plane



- Is there Weyl-Wigner correspondence?
squeezed function \Leftrightarrow ?

TIME-DEPENDENT “HARMONIC OSCILLATOR”

- general, quadratic, time-dependent Hamiltonian of HO

$$\hat{H}(\hat{x}, \hat{p}, t) \quad [\text{Choi-Gweon (2004)}]$$

$$= A(t)\hat{x}^2 + B(t)(\hat{x}\hat{p} + \hat{p}\hat{x}) + C(t)\hat{p}^2 + D(t)\hat{x} + E(t)\hat{p} + F(t)$$

- time-dependent creation and annihilation operators

$$\hat{a} = \sqrt{\frac{1}{\theta k^{1/2}}} \left\{ \left[\frac{\sqrt{k}}{2\rho} + i \frac{2B\rho - \dot{\rho}}{2A} \right] (\hat{x} - x_p(t)) + i\rho(\hat{y} - y_p(t)) \right\}$$

$$\hat{a}^\dagger = \sqrt{\frac{1}{\theta k^{1/2}}} \left\{ \left[\frac{\sqrt{k}}{2\rho} - i \frac{2B\rho - \dot{\rho}}{2A} \right] (\hat{x} - x_p(t)) - i\rho(\hat{y} - y_p(t)) \right\}$$

They satisfy time-independent commutation relation:

$$[\hat{a}, \hat{a}^\dagger] = 1$$

LEWIS-RIESENFELD METHOD: SOLVING TIME-DEPENDENT HO

- time-dependent Schroedinger equation: $i\hbar \frac{\partial}{\partial t} \psi = \hat{H} \psi$

- invariant operator $\hat{I} : \frac{d\hat{I}}{dt} = \frac{\partial \hat{I}}{\partial t} + \frac{1}{i\hbar} [\hat{I}, \hat{H}] = 0$

- eigenvalue problem:
$$\begin{cases} \hat{I} \phi_n(x, p, t) = \lambda_n \phi_n(x, p, t) \\ \psi(x, p, t) = e^{i\epsilon(t)} \phi(x, p, t) \\ \hbar \dot{\epsilon} = \langle \phi_n(t) | \left(i\hbar \frac{\partial}{\partial t} - \hat{H} \right) | \phi_n(t) \rangle \end{cases}$$

- time-dependent solution can be obtained

→ e.g., Caldirola-Kanai oscillator $\hat{H} = A e^{\gamma t} \hat{x}^2 + B e^{-\gamma t} \hat{p}^2$

SUMMARY

- A gravity theory based on noncommutative geometry
- Product of functions is deformed
→ algebraic method using operators is useful
- Extension to more general solutions
 - translation of functions \Leftrightarrow coherent state
 - squeezing of functions $\not\leftrightarrow$ squeezed state
 - \Leftrightarrow time-dependent HO with
 - ? appropriate identification
- future work: quantum diffeo and function counterpart?
→ check with spherical D2-brane and fuzzy sphere

Yota Watanabe

Kavli IPMU, University of Tokyo

“Anisotropy problem in Horava-Lifshitz gravity”

(10+5 min.)

[JGRG28 (2018) 110711]

Anisotropy problem in Hořava-Lifshitz gravity

Yota Watanabe (Kavli IPMU, U Tokyo)

JGRG28@Rikkyo, 7 Nov 2018

Ongoing work

based on discussion
with S. Mukohyama

Outline

- Hořava-Lifshitz gravity
- As an alternative to inflation
- Kinetic eq. from action
- Kinetic eq. for Lifshitz scalar

Hořava-Lifshitz gravity (HL)

Hořava 0901.3775

➤ GR: non-renormalizable

HL: a candidate of quantum gravity

achieved by Lorentz breaking $(t \rightarrow b^3 t, \vec{x} \rightarrow b\vec{x}) @ E \gtrsim M$

Propagator $\sim \frac{1}{\omega^2 - k^6/M^4}$: more convergent

Renormalizability has been shown
in minimal setup $N = N(t)$

Barvinsky, Blas,
Herrero-Valea, Sibiryakov,
Steinwachs 1512.02250

➤ Foliation-preserving diffeo.

$$t \rightarrow t'(t), \vec{x} \rightarrow \vec{x}'(t, \vec{x})$$

- No local Hamiltonian constraint
- 2+1 DoF: scalar graviton behaves as dark matter

Mukohyama 0905.3563

HL as an alternative to inflation

➤ HL has some properties of inflation

- Scale-invariant perturbation
- Solves Horizon problem
- Solves Flatness problem

Mukohyama 0904.2190

Bramberger, Coates, Magueijo,
Mukohyama, Namba, YW 1706.06809

➤ Isotropy problem

Vector perturbation around flat FLRW in GR

$$(\text{Vorticity}) \propto a^{-\frac{1}{2}(1-9w)}$$

w : EOS param. of matter

Albrecht, Magueijo 9811018

Kodama, Sasaki (1984) PTP Suppl.

If $w > 1/9$, vorticity grows: isotropy problem
cf. Inflation ($w \simeq -1$) is a solution

➤ This can be used a test for an alternative to inflation

Does HL solve the isotropy problem?: Goal

This talk is 1st step

3 / 9

Vector perturbations in HL

➤ Consider the action of HL gravity & vector field A_i

- Photons are described by distribution func. $f(x^\mu, p_i)$

Need evolution eq. for f

- In ordinary cases f obeys the Boltzmann eq.

in kinetic theory derived from 1st principle

What is the Boltzmann eq. for Lifshitz vector?

4 / 9

Derivation of kinetic eq.

- Relativistic kinetic eq.

$$\left[p^\mu \partial_\mu + p^\mu p_\nu \Gamma_{\mu i}^\nu \frac{\partial}{\partial p_i} \right] f \simeq (\text{interactions, corrections})$$

- Method: use Wigner func. de Groot, van Leeuwen, van Weert (1980)

$$\tilde{f}_{\text{flat}}(x^\mu, p_i) = \int d^3r e^{-\frac{i}{\hbar} r^i p_i} \left\langle : \phi \left(x + \frac{r}{2} \right) \phi \left(x - \frac{r}{2} \right) : \right\rangle$$

- Known to systematically derive interaction, quantum correction & field-theoretic correction terms
- Formalism for curved spacetime is developed Winter (1985)

Calzetta, Habib, Hu (1988)

Fonarev 9309005

Antonsen 9701182

5 / 9

Review: for relativistic real scalar

Friedrich, Prokopec 1805.02767

based on 3+1 decomposition

- Wigner func. on curved spacetime

$$X, Y = \left\{ \phi, \frac{\Pi}{\sqrt{\gamma}} = \partial_\perp \phi \right\}$$

$$F_{XY}(x^\mu, p_i) = \sqrt{\gamma} \int d^3r e^{-\frac{i}{\hbar} r^i p_i} \left\langle : \left[e^{\frac{r^i}{2} \nabla_i^H} X(x^\mu) \right] \left[e^{-\frac{r^i}{2} \nabla_i^H} Y(x^\mu) \right] : \right\rangle$$

$$f_1^+ = \frac{1}{2\hbar} \left[\frac{\omega}{\hbar} F_{\phi\phi} + \frac{\hbar}{\omega} F_{\Pi\Pi} \right] = \left(1 + \frac{r^i}{2} \nabla_i + \frac{r^i r^j}{8} \nabla_i \nabla_j + \dots \right) X$$

$$f_1^- = \frac{i}{2\hbar} [F_{\Pi\phi} - F_{\phi\Pi}]$$

$$f_2 = \frac{1}{2\hbar} \left[\frac{\omega}{\hbar} F_{\phi\phi} - \frac{\hbar}{\omega} F_{\Pi\Pi} \right]$$

$$f_3 = \frac{i}{2\hbar} [F_{\Pi\phi} + F_{\phi\Pi}]$$

6 / 9

Review: for relativistic real scalar

Friedrich, Prokopec 1805.02767
based on 3+1 decomposition

$$T_{\perp\perp} = \frac{1}{\sqrt{\gamma}} \int \frac{d^3p}{(2\pi\hbar)^3} \omega f_1 + \mathcal{O}(\hbar^2) \quad f_1 = f_1^+ + f_1^-$$

$$T_{\perp i} = \frac{1}{\sqrt{\gamma}} \int \frac{d^3p}{(2\pi\hbar)^3} p_i f_1 + \mathcal{O}(\hbar)$$

$$T_{ij} = \frac{1}{\sqrt{\gamma}} \int \frac{d^3p}{(2\pi\hbar)^3} \frac{p_i p_j}{\omega} f_1 + \mathcal{O}(f_2) + \mathcal{O}(\hbar)$$

➡ f_1 : classical distribution func.

f_2, f_3 : field-theoretic corrections

➤ Calculate $\partial_t f$ using EOM: $\square\phi = (\text{int.})$

➡ $\left[p^\mu \partial_\mu + p^\mu p_\nu \Gamma_{\mu i}^\nu \frac{\partial}{\partial p_i} \right] f_1 \simeq (\text{interactions, corrections})$ 7/9

Kinetic eq. for Lifshitz matter

➤ Apply the method to Lifshitz matter

Final goal: Vector with $\omega^2 \simeq p^6/M^4$ (called $z = 3$)

1st step: Scalar with $\omega^2 \simeq p^4/M^2$ (called $z = 2$)

➤ EOM for $N = N(t)$

$$\square\phi + \frac{\hbar^2}{M^2} \Delta^2 \phi = 0$$

➤ New result:

Kinetic eq. for $z = 2$ Lifshitz scalar with $N = N(t)$

$$\left[p^\mu \partial_\mu + p^\mu p_\nu \Gamma_{\mu i}^\nu \frac{\partial}{\partial p_i} - \frac{4}{M^2} p^2 p^i \left(\nabla_i + {}^{(3)}\Gamma_{ij}^k p_k \frac{\partial}{\partial p_j} \right) \right] f_1 \simeq 0$$

RHS: interactions, $\mathcal{O}(\hbar)$, field-theoretic corrections 8/9

Summary & discussion

➤ HL: candidate of quantum gravity & alternative to inflation

- Alternative to inflation must solve isotropy problem in vector perturbation

Photons: described by distribution func. $f(x^\mu, p_i)$

- Derived kinetic eq. for f using Wigner func.

for $z = 2$ Lifshitz scalar as 1st step

➤ Future work

- Obtain kinetic eq. for f for $z = 3$ vector
- Obtain eq. for vector pert. combining EOM for gravity
- See whether vorticity grows or not

→ whether HL gravity can be an alternative to inflation or not

Tomotaka Kitamura

Waseda University

“Matter Scattering and Unitarity in Horava-Lifshitz Gravity”

(10+5 min.)

[JGRG28 (2018) 110712]

Matter Scattering and Unitarity in Horava-Lifshitz Gravity

The 28th Workshop on General Relativity and Gravitation in Japan

Tomotaka Kitamura

Waseda University

with
Takeo Inami
Keisuke Izumi

SungKyunKwan U
Nagoya University

Purpose

Checking

Renormalizability of Horava-Lifshitz gravity
via **Tree-Level Unitarity** of Matter scattering

1. Introduction

Tree-level Unitarity

Conjecture

C.H.Llewellyn Smith '73
J. M. Cornwall et al '73

tree unitarity \longleftrightarrow renormalizability
equivalent?

Tree unitarity in Lorentz inv. theory

an scattering amplitude does not grow as $E \rightarrow \infty$

$$\mathcal{M} \sim E^\epsilon \quad (\epsilon \leq 0) \quad \underline{E \rightarrow \infty}$$

\mathcal{M} amplitude E Energy in center of mass

if $\epsilon \leq 0$

\longrightarrow a theory has tree unitarity

this condition is modified in Lifshitz theories

Tree-level Unitarity

tree unitarity condition: Lorentz invariant theory

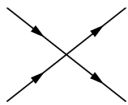
(1+d)dim 2-2 scattering

amplitude $\langle 2 | T | 2 \rangle \sim k^\beta \quad \beta \leq 3 - d$

(1+3)dim 2-2 scattering

amplitude $\langle 2 | T | 2 \rangle \sim k^\beta \quad \beta \leq 0$

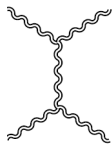
(e.g 1) ϕ^4 theory



$\mathcal{M} \sim \lambda (\sim k^0)$

tree unitarity ○

(e.g 2) Einstein gravity



$\mathcal{M} \sim k^2$

tree unitarity ✗

Tree-level Unitarity

No counterexample is known

C.H.Llewellyn Smith '73

J. M. Cornwall et al '73

Berends & Gastmans '74

tree-level unitarity ↔ renormalizability

(e.g)

Tree-level unitarity renormalizability

QED	○	○
Y-M theory	○	○
Weinberg-Salam model	○	○
4-Fermi theory	✗	✗
Einstein Gravity	✗	✗

No counter-example!

Tree-level Unitarity

No counterexample is known

C.H.Llewellyn Smith '73
J. M. Cornwall et al '73
Berends & Gastmans '74

tree-level unitarity \longleftrightarrow renormalizability

(e.g)

	Tree-level unitarity	renormalizability
QED	○	○
Y-M theory	○	○
Weinberg-Salam model	○	○
4-Fermi theory	×	×
Einstein Gravity	×	×

No counter-example!

Tree-level Unitarity

Matter scattering and Unitarity

Berends & Gastmans '74
Abe, Inami, Izumi, TK '18

tree-level unitarity \longleftrightarrow renormalizability

(e.g)

	Tree-level unitarity	renormalizability
Einstein Gravity	×	×
Matter in Einstein Gravity	×	×
Matter in $R_{\mu\nu}^2$ Gravity	○	○

No counter-example!

Tree-level Unitarity

S-Matrix Unitarity and Renormalizability in HD theory

Abe, Inami, Izumi, Noumi, TK '18

See Keisuke's Poster PB27

Even the existence of Ghost

tree-level unitarity \longleftrightarrow renormalizability

(e.g)

Non-renormalizable

$$\int d^4x \phi^2 (\square\phi)^2$$

Renormalizable

$$\lambda \int d^4x \{(\partial_\mu\phi)^2\}^2$$

Tree-level unitarity renormalizability

×

×

○

○

No counter-example!

2. Horava-Lifshitz Gravity

2. Horava-Lifshitz gravity

Lifshitz scaling

$$[x] = -1 \quad [t] = -z \quad \text{in mass dim}$$

$$\vec{x} \mapsto b\vec{x} \quad b \quad \text{arbitrary number}$$

$$t \mapsto b^z t \quad z \quad \text{dynamical critical exponent}$$

z=3 (1+3) dim

P. Hořava '09

$$S_{\text{HL}} = \int dt d^3x \sqrt{g} N \left\{ \frac{M_p}{2} \underbrace{(K_{ij} K^{ij} - \lambda K^2)}_{\text{Kinetic term}} + \underbrace{(\alpha_1 \nabla_i R_{jk} \nabla_i R^{jk} + \alpha_2 \nabla_i R \nabla^i R + \dots)}_{\text{Potential term}} \right\} \quad (i, j, k = 1, 2, 3)$$

extrinsic curvature **Potential term** **Power-counting renormalizable**

$$K_{ij} = \frac{1}{2N} (\dot{g}_{ij} - \nabla_i N_j - \nabla_j N_i) \quad [M_p, \alpha_1, \alpha_2, \dots, \alpha_n \dots] = 0$$

$$z \neq 1 \quad \rightarrow \quad \text{Lorenz symmetry}$$

Even containing Higher derivative, there no ghost

3d g_{ij} **lapse variable** N **shift vector** N_i

2. Hořava-Lifshitz gravity

Remarks:

Two important problems in Hořava gravity

1. proof of renormalizability

(non-Projectable version $N = N(\mathbf{x}, t)$)

2. restoration of Lorentz sym in IR?

(Projectable version $N = N(t)$)

(Non-Projectable version $N = N(\mathbf{x}, t)$)

Tree-level unitarity and HLGravity

Remarks:

Tree-level unitarity



tree unitarity ~ renormalization

we use the way to **check the tree unitarity** instead of loop calculation

1. don't have to introduce Faddeev-Popov ghost

2. easier and simpler than loop calculation

As first step to study the renormalizability of non-Projectable HL Gravity, we try to check the correspondence in projectable HI gravity

Horava-Lifshitz gravity

$z=3$ (1+3) dim

Projectable HL gravity

$$S_{pHL} = \frac{1}{2\kappa^2} \int dt dx^d \sqrt{\gamma} N (K_{ij}K^{ij} - \lambda K^2 - \mathcal{V}_{pHL})$$

$$\mathcal{V}_{pHL}^{d=3} = 2\Lambda - \eta R^2 + \mu_1 R^2 + \mu_2 R_{ij}R^{ij} + \nu_1 R^3 + \nu_2 R R_{ij}R^{ij} + \nu_3 R^i_j R^j_k R^k_i + \nu_4 \nabla_i R \nabla^i R + \nu_5 \nabla_i R_{jk} \nabla^i R^{jk}$$

Propagator

$$\begin{aligned} \langle h_{ij}(p)h_{kl}(-p) \rangle = & 2\kappa^2 (\delta_{ik}\delta_{jl} + \delta_{il}\delta_{jk}) \mathcal{P}_{tt}(p) - 2\kappa^2 \delta_{ij}\delta_{kl} \left[\mathcal{P}_{tt}(p) - \frac{1-\lambda}{1-3\lambda} \mathcal{P}_s(p) \right] \\ & - 2\kappa^2 (\delta_{ik}\hat{k}_j\hat{k}_l + \delta_{il}\hat{k}_j\hat{k}_k + \delta_{jk}\hat{k}_i\hat{k}_l + \delta_{jl}\hat{k}_i\hat{k}_k) [\mathcal{P}_{tt}(p) - \mathcal{P}_1(p)] \\ & + 2\kappa^2 (\delta_{ij}\hat{k}_k\hat{k}_l + \hat{k}_i\hat{k}_j\delta_{kl}) [\mathcal{P}_{tt}(p) - \mathcal{P}_s(p)] \\ & + 2\kappa^2 \hat{k}_i\hat{k}_j\hat{k}_k\hat{k}_l \left[\mathcal{P}_{tt}(p) + \frac{1-3\lambda}{1-\lambda} \mathcal{P}_s(p) - 4\mathcal{P}_1(p) + \frac{2\mathcal{P}_2(p)}{1-\lambda} \right], \end{aligned}$$

$$\mathcal{P}_{tt} = \frac{1}{\omega^2 + \nu_4 k^6},$$

$$\mathcal{P}_1 = \left[\omega^2 + \frac{k^6}{2\sigma} \right]^{-1},$$

$$\mathcal{P}_s = \left[\omega^2 + \frac{(8\nu_4 + 3\nu_5)(1-\lambda)}{1-3\lambda} k^6 \right]^{-1}$$

$$\mathcal{P}_2 = \left[\omega^2 + \frac{(1-\lambda)(1+\xi)}{\sigma} k^6 \right]^{-1}$$

Lifshitz Scalar theory

$z=1,2,3$ (1+3) dim

Projectable Lifshitz scalar theory

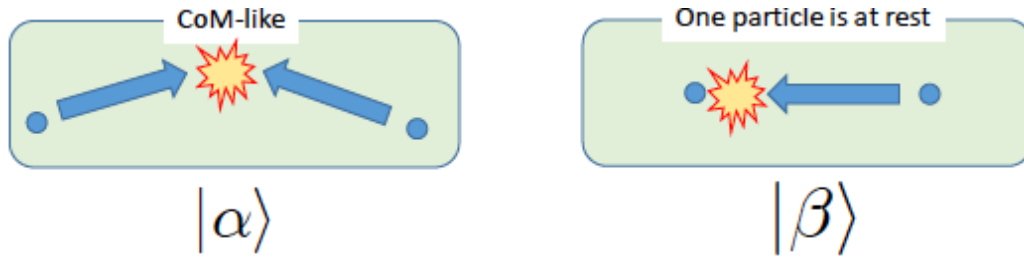
$$S_{pLS} = \frac{1}{2\kappa^2} \int dt dx^3 \sqrt{g} \frac{1}{N} \left((\partial_t \phi - N^i \partial_i \phi)^2 - \beta_1 \phi (D_i D^i) \phi - \beta_2 \phi (D_i D^i)^2 \phi - \beta_3 \phi (D_i D^i)^3 \phi \right)$$

$\phi\phi h_{ij}$ 3 point vertex

$$-(\mathbf{k}_1^2 \mathbf{k}_3^2 (\mathbf{k}_1)_l (\mathbf{k}_3)_l) + \dots$$

Tree-level Unitarity in HL gravity

Two scattering states are considered in Lifshitz-type theory



All scattering systems are able to be studied in CM system thanks to Lorentz symmetry.

Lifshitz-type theory : Lorentz symmetry is violated

all scattering process are independent

Need to study even laboratory-like system



Unitarity conditions of Lab-like system is **more strict** than CM-like system

Tree-level Unitarity in HL gravity

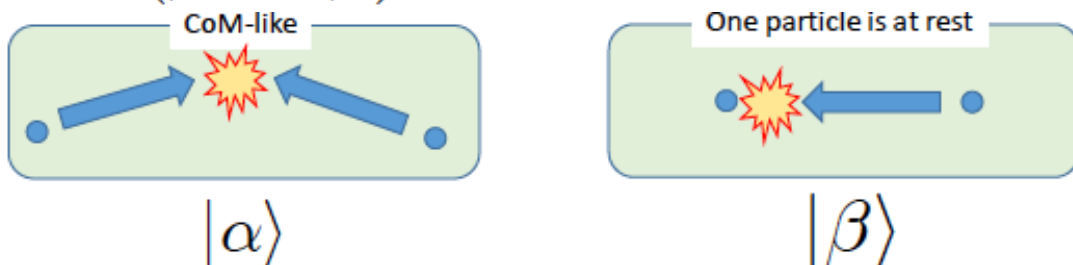
Unitarity bound for scattering amplitude

UB for scattering amplitude

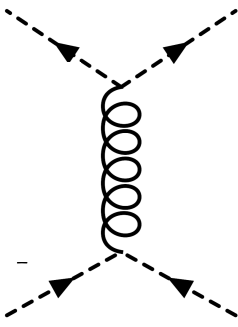
$$|\mathcal{M}(\mathbf{p}_1, \mathbf{p}_2 \rightarrow \mathbf{k}_1, \mathbf{k}_2)| = P^a \quad z=3 \quad d=3$$

$$\mathcal{M}(\alpha \rightarrow \alpha) \quad a \leq 3z - d \quad 6$$

$$\mathcal{M}(\beta \rightarrow \beta) \quad a \leq 2z - 1 \quad 5$$



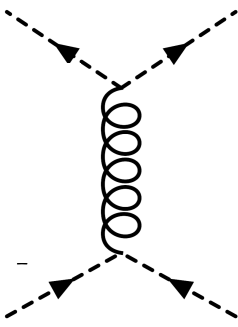
Tree-level Unitarity in HL gravity



CM -like system

$$\mathcal{M} \sim \mathbf{k}^6$$

$$\mathbf{k} \rightarrow \infty$$



Lab-like system

$$\mathcal{M} \sim \mathbf{k}^5$$

$$\mathbf{k} \rightarrow \infty$$

Summary

Even **Matter scattering** in Projectable Horava gravity

implication that the relation between renormalizability
and tree-level unitarity

Projectable Horava gravity

→

Renormalizable

Appropriate gauge fixing ○

Non-projectable Horava gravity

→

Renormalizable?

Appropriate gauge ✕

Thank you!!

Satoshi Akagi

Nagoya University

“Massive spin-two theory in arbitrary background”

(10+5 min.)

[JGRG28 (2018) 110713]

MASSIVE SPIN-TWO THEORY IN ARBITRARY BACKGROUND



SATOSHI AKAGI, NAGOYA UNIVERSITY

[ARXIV:1810.02065 [HEP-TH]]

JGRG 28

INTRODUCTION

Linear theory of massive spin-two field

- **Flat spacetime:** Fierz-Pauli (FP) model, DoF=5 in 4 dim
- **Arbitrary background:** Minimal coupled model, DoF=6=Spin2+ghost
- Nonminimal coupling terms (NCT) are necessary

INTRODUCTION

Bottom-up approach [Buchbinder et al. (2000)]

- Small curvature approximation $R/m^2 \ll 1$, Leading order

$$S_{\text{general}} = \int d^D x \sqrt{-g} \left[\frac{1}{2} g^{\mu_1 \nu_1 \mu_2 \nu_2 \mu_3 \nu_3} \nabla_{\mu_1} h_{\mu_2 \nu_2} \nabla_{\nu_3} h_{\mu_3 \nu_3} + \frac{1}{2} \{ m^2 g^{\mu_1 \nu_1 \mu_2 \nu_2} + \gamma_1 R g^{\mu_1 \nu_1 \mu_2 \nu_2} + \frac{\gamma_2}{2} (R^{\mu_1 [\nu_1} g^{\nu_2] \mu_2} - R^{\mu_2 [\nu_1} g^{\nu_2] \mu_1}) + \gamma_3 R^{\mu_1 \mu_2 \nu_1 \nu_2} \} h_{\mu_1 \nu_1} h_{\mu_2 \nu_2} + \mathcal{O}(R^2/m^2) \right]$$

- Three free parameters are allowed, Existence of completion is NOT guaranteed

Top-down approach [L. Bernard et al. (2015)]

- Linearized dRGT model = A class of the completion

$$\gamma_1 = \frac{s_2 D - 1}{2(D - 1)}, \quad \gamma_2 = -4s_2, \quad \gamma_3 = 1$$

- Only one free parameter, Existence of completion is guaranteed

Bottom-up

dRGT

INTRODUCTION

Our research

- **Purpose:** Identifying the most general class whose completion exists

Bottom-up

- **Possibility:** Leading order NCTs may be constrained by higher order conditions

- **Result:** Linear order NCTs are constrained by **fourth order condition**

$$\gamma_1, \gamma_2, \gamma_3 : \text{not constrained} \longrightarrow \gamma_1, \gamma_2 : \text{not constrained}, \gamma_3 = 1$$

Top-down

- **Possibility:** Linearized dRGT model may be extended

- **Result:** A trivial **extension of linearized dRGT** coincides with bottom-up result

$$\gamma_1 = \frac{s_2 D - 1}{2(D - 1)}, \quad \gamma_2 = -4s_2, \quad \gamma_3 = 1 \longrightarrow \gamma_1, \gamma_2 : \text{not constrained}, \gamma_3 = 1$$

- **Conclusion:** We identify the most general class of the leading order NCTs

OUTLINE

- Constraints in FP theory
- Irreducible decomposition
- Condition for ghost-freeness
- Perturbative solution
- Trivial extension
- Summary

NOTATION

Definition

- $\eta^{\mu_1\nu_1\mu_2\nu_2\cdots\mu_n\nu_n}$: Anti-symmetrization of $\eta^{\mu_1\nu_1}\eta^{\mu_2\nu_2}\cdots\eta^{\mu_n\nu_n}$ with respect to $\nu_1\nu_2\cdots\nu_n$
- $\eta^{\mu_1\nu_1\mu_2\nu_2} \equiv \eta^{\mu_1\nu_1}\eta^{\mu_2\nu_2} - \eta^{\mu_1\nu_2}\eta^{\mu_2\nu_1}$
- $\eta^{\mu_1\nu_1\mu_2\nu_2\mu_3\nu_3} \equiv \eta^{\mu_1\nu_1}\eta^{\mu_2\nu_2}\eta^{\mu_3\nu_3} + \eta^{\mu_1\nu_2}\eta^{\mu_2\nu_3}\eta^{\mu_3\nu_1} + \eta^{\mu_1\nu_3}\eta^{\mu_2\nu_1}\eta^{\mu_3\nu_2}$
 $- \eta^{\mu_1\nu_2}\eta^{\mu_2\nu_1}\eta^{\mu_3\nu_3} - \eta^{\mu_1\nu_1}\eta^{\mu_2\nu_3}\eta^{\mu_3\nu_2} - \eta^{\mu_1\nu_3}\eta^{\mu_2\nu_2}\eta^{\mu_3\nu_1}$

Fierz-Pauli theory

- $\mathcal{L}_{\text{FP}} = -\frac{1}{2}\partial_\lambda h_{\mu\nu}\partial^\lambda h^{\mu\nu} + \partial_\mu h_{\nu\lambda}\partial^\nu h^{\mu\lambda} - \partial_\mu h^{\mu\nu}\partial_\nu h + \frac{1}{2}\partial_\lambda h\partial^\lambda h - \frac{1}{2}m^2(h_{\mu\nu}h^{\mu\nu} - h^2)$
 $= \frac{1}{2}\eta^{\mu_1\nu_1\mu_2\nu_2\mu_3\nu_3}\partial_{\mu_1}h_{\mu_2\nu_2}\partial_{\nu_1}h_{\mu_3\nu_3} + \frac{m^2}{2}\eta^{\mu_1\nu_1\mu_2\nu_2}h_{\mu_1\nu_1}h_{\mu_2\nu_2}$
- As the same way, we would like to define $g^{\mu_1\nu_1\mu_2\nu_2\cdots\mu_n\nu_n}, \delta^{i_1j_1i_2j_2\cdots i_nj_n}$.

CONSTRAINTS IN FP-MODEL

Fierz–Pauli model

- EoM of the FP model in flat spacetime,

$$E^{\mu\nu} \equiv -\eta^{\mu\nu\mu_1\nu_1\mu_2\nu_2} \partial_{\mu_1} \partial_{\nu_1} h_{\mu_2\nu_2} + m^2 \eta^{\mu\nu\mu_1\nu_1} h_{\mu_1\nu_1} = 0$$

- Lorentz covariant constraints:

$$\phi_{\text{vector}}^\nu \equiv \partial_\mu E^{\mu\nu} = m^2 \eta^{\mu\nu\mu_1\nu_1} \partial_\mu h_{\mu_1\nu_1} = 0 \quad : \text{Vector constraints}$$

$$\phi_{\text{scalar}} \equiv \partial_\mu \partial_\nu E^{\mu\nu} + \frac{m^2}{D-2} \eta^{\mu\nu} E_{\mu\nu} = \frac{D-1}{D-2} m^4 h = 0 \quad : \text{Scalar constraint}$$

- In the Fourier space, these constraints reduce the number of the polarizations
- In curved background, minimal coupled model violate a scalar constraint
- We construct the model in curved background so that a scalar constraint exists

IRREDUCIBLE DECOMPOSITION

Assumption

$$S = \int d^D x \sqrt{-g} \left[\frac{1}{2} g^{\mu_1\nu_1\mu_2\nu_2\mu_3\nu_3} \nabla_{\mu_1} h_{\mu_2\nu_2} \nabla_{\nu_1} h_{\mu_3\nu_3} + \frac{1}{2} \{ m^2 g^{\mu_1\nu_1\mu_2\nu_2} + \Delta^{\mu_1\nu_1\mu_2\nu_2} \} h_{\mu_1\nu_1} h_{\mu_2\nu_2} \right]$$

- $\Delta^{\mu_1\nu_1\mu_2\nu_2}$: General covariant, First or higher order with respect to curvatures
- $\Delta^{\mu_1\nu_1\mu_2\nu_2}$ **does not contain any covariant derivatives acting on** $h_{\mu\nu}$

IRREDUCIBLE DECOMPOSITION

Irreducible decomposition

- Let us decompose $\Delta^{\mu_1\nu_1\mu_2\nu_2}$ into irreducible symmetric tensors.
- For any $\Delta^{\mu_1\nu_1\mu_2\nu_2}$, NCT can be decomposed as follows,

$$\Delta^{\mu_1\nu_1\mu_2\nu_2} h_{\mu_1\nu_1} h_{\mu_2\nu_2} = T^{\mu_1\nu_1\mu_2\nu_2} h_{\mu_1\nu_1} h_{\mu_2\nu_2} + N^{\mu_1\nu_1\mu_2\nu_2} h_{\mu_1\nu_1} h_{\mu_2\nu_2}.$$

$$T^{\mu_1\nu_1\mu_2\nu_2} \sim \begin{array}{|c|c|} \hline & \\ \hline & \\ \hline \end{array} \quad T^{\mu_1\nu_1\mu_2\nu_2} = -T^{\mu_2\nu_1\mu_1\nu_2} = -T^{\mu_1\nu_2\mu_2\nu_1} = T^{\mu_2\nu_2\mu_1\nu_1}$$

$$T^{[\mu_1\nu_1\mu_2]\nu_2} = 0 \quad : \text{ ``Mixed symmetric tensor''}$$

$$N^{\mu_1\nu_1\mu_2\nu_2} \sim \begin{array}{|c|c|c|c|} \hline & & & \\ \hline & & & \\ \hline \end{array} \quad N^{\mu_1\nu_1\mu_2\nu_2} = N^{(\mu_1\nu_1\mu_2\nu_2)} : \text{ ``Totally symmetric tensor''}$$

- We would like to proceed our calculation with using the symmetries of these tensors, without giving the specific forms, until the specific forms become necessary.

CONDITION FOR GHOST-FREENESS

EoM in curved background

$$E^{\mu\nu} \equiv \left[-g^{(\mu\nu)\mu_1\nu_1\mu_2\nu_2} \nabla_{\mu_2} \nabla_{\nu_2} + m^2 g^{(\mu\nu)(\mu_1\nu_1)} + T^{(\mu\nu)(\mu_1\nu_1)} + N^{\mu\nu\mu_1\nu_1} \right] h_{\mu_1\nu_1} = 0$$

Vector constraints

$$\nabla_{\mu} E^{\mu\nu} = \left[m^2 g^{(\mu\nu)(\mu_1\nu_1)} + S^{(\mu\nu)(\mu_1\nu_1)} + N^{\mu\nu\mu_1\nu_1} + Q^{\mu\nu\mu_1\nu_1} \right] \nabla_{\mu} h_{\mu_1\nu_1}$$

+ (terms without any derivatives of h)

$$S^{\mu\nu\mu_1\nu_1} \equiv T^{\mu\nu\mu_1\nu_1} - R^{\mu\mu_1\nu\nu_1} + \left(R^{\mu[\nu} g^{\nu_1]\mu_1} - R^{\mu_1[\nu} g^{\nu_1]\mu} \right) \sim \begin{array}{|c|c|} \hline & \\ \hline & \\ \hline \end{array}$$

$$Q^{\mu\nu\mu_1\nu_1} \equiv \frac{1}{2} \left[R^{\mu\nu} g^{\mu_1\nu_1} - g^{\mu\nu} R^{\mu_1\nu_1} + 2R^{\mu(\mu_1} g^{\nu_1)\nu} - 2R^{\nu(\mu_1} g^{\nu_1)\mu} \right]$$

- **There are contributions from kinetic terms = Problem in arbitrary background**
- For the existence of a scalar constraint, we have to restrict $S^{\mu\nu\mu_1\nu_1}$, $N^{\mu\nu\mu_1\nu_1}$

CONDITION FOR GHOST-FREENESS

Vector constraints

$$\nabla_\mu E^{\mu\nu} = \left[m^2 g^{(\mu\nu)(\mu_1\nu_1)} + S^{(\mu\nu)(\mu_1\nu_1)} + N^{\mu\nu\mu_1\nu_1} + Q^{\mu\nu\mu_1\nu_1} \right] \nabla_\mu h_{\mu_1\nu_1} \\ + (\text{terms without any derivatives of } h)$$

Condition for ghost-freeness

$\text{Det}(V_\nu^{\mu 0}) = 0$: Determinant is defined on ν^μ

$$V^{\mu\nu\mu_1\nu_1} \equiv m^2 g^{(\mu\nu)(\mu_1\nu_1)} + \bar{S}^{\mu\nu\mu_1\nu_1} + N^{\mu\nu\mu_1\nu_1} + Q^{\mu\nu\mu_1\nu_1}$$

$$\bar{S}^{\mu\nu\mu_1\nu_1} \equiv S^{(\mu\nu)(\mu_1\nu_1)} \quad : \text{Symmetric bases of the mixed tableau } \begin{array}{|c|c|} \hline & \\ \hline & \\ \hline \end{array}$$

PERTURBATIVE SOLUTION

Perturbation

- We solve the condition $\text{Det}(V_\nu^{\mu 0}) = 0$ perturbatively
- Let us expand tensors $S^{\mu\nu\mu_1\nu_1}$, $N^{\mu\nu\mu_1\nu_1}$ in powers of curvatures R/m^2 ,

$$\bar{S}^{\mu_1\nu_1\mu_2\nu_2} = \sum_{n=1}^{\infty} \frac{1}{m^{2(n-1)}} \bar{S}^{(n)\mu_1\nu_1\mu_2\nu_2} \quad N^{\mu_1\nu_1\mu_2\nu_2} = \sum_{n=1}^{\infty} \frac{1}{m^{2(n-1)}} N^{(n)\mu_1\nu_1\mu_2\nu_2}$$

- Superscript (n): n th-order terms with respect to curvature

(1) Leading order

$$0 = N^{(1)0000} + \bar{S}^{(1)0000} + Q^{0000} = N^{(1)0000} \longrightarrow N^{(1)\mu_1\nu_1\mu_2\nu_2} = 0$$

- There are no totally symmetric tensors satisfying the above condition
- There are no constraints on the mixed symmetric tensor $S^{(1)\mu_1\nu_1\mu_2\nu_2}$

$$S^{(1)\mu_1\nu_1\mu_2\nu_2} \ni Rg^{\mu_1\nu_1\mu_2\nu_2}, R^{\mu_1[\nu_1}g^{\nu_2]\mu_2} - R^{\mu_2[\nu_1}g^{\nu_2]\mu_1}, R^{\mu_1\mu_2\nu_1\nu_2}$$

PERTURBATIVE SOLUTION

(2) Second order

$$N^{(2)0000} + \frac{1}{2}g^{00\mu\nu}R_{\mu}^0R_{\nu}^0 = 0 \longrightarrow N^{(2)\mu_1\nu_1\mu_2\nu_2} = -\frac{1}{2}g^{\alpha\beta(\mu_1\nu_1}R_{\alpha}^{\mu_2}R_{\beta}^{\nu_2)}$$

- Full components of totally symmetric tensor $N^{(n)\mu_1\nu_1\mu_2\nu_2}$ are uniquely determined
- **Nonminimal coupling terms cannot be truncated at leading order**

(3) Third order

$$N^{(3)0000} + \bar{S}^{(1)0\alpha\beta 0}R_{\alpha}^0R_{\beta}^0 = 0 \longrightarrow N^{(3)\mu_1\nu_1\mu_2\nu_2} = \frac{1}{2}S^{(1)\alpha\beta(\mu_1\nu_1}R_{\alpha}^{\mu_2}R_{\beta}^{\nu_2)}$$

- We find that $N^{\mu_1\nu_1\mu_2\nu_2}$ is not independent of $S^{\mu_1\nu_1\mu_2\nu_2}$
- At this time, there are no constraints on $S^{\mu_1\nu_1\mu_2\nu_2}$

PERTURBATIVE SOLUTION

(4) Fourth order

$$N^{(4)0000} + \left(\bar{S}^{(2)0\alpha\beta 0} + N^{(2)0\alpha\beta 0}\right)R_{\alpha}^0R_{\beta}^0 + \frac{1}{8}g^{00\alpha\beta}(R^2)_{\alpha}^0(R^2)_{\beta}^0 + \frac{2}{g^{00}}R^{0\nu}\bar{S}^{(1)0}_{\nu}{}^{\rho 0}\bar{S}^{(1)0}_{\rho}{}^{\sigma 0}R_{\sigma}^0 = 0$$

- Fourth order condition contains a **noncovariant term**
- This term cannot be canceled by the other terms
- This fact means that $S^{(1)\mu_1\nu_1\mu_2\nu_2}$ **is constrained** by the condition,

$$R^{0\nu}\bar{S}^{(1)0}_{\nu}{}^{\rho 0}\bar{S}^{(1)0}_{\rho}{}^{\sigma 0}R_{\sigma}^0 = g^{00}M^{0000} \quad M^{0000} : \text{Some covariant tensor}$$

- This condition reduce the three free parameters of $S^{(1)\mu_1\nu_1\mu_2\nu_2}$ to the following two free parameters,

$$S^{(1)\mu_1\nu_1\mu_2\nu_2} = \gamma_1^{(1)}Rg^{\mu_1\nu_1\mu_2\nu_2} + \frac{\gamma_2^{(1)}}{2}\left(R^{\mu_1[\nu_1}g^{\nu_2]\mu_2} - R^{\mu_2[\nu_1}g^{\nu_2]\mu_1}\right)$$

PERTURBATIVE SOLUTION

Resulting NCT in leading order

$$S_{\text{general}} = \int d^D x \sqrt{-g} \left[\frac{1}{2} g^{\mu_1 \nu_1 \mu_2 \nu_2 \mu_3 \nu_3} \nabla_{\mu_1} h_{\mu_2 \nu_2} \nabla_{\nu_3} h_{\mu_3 \nu_3} + \frac{1}{2} \{ m^2 g^{\mu_1 \nu_1 \mu_2 \nu_2} + \gamma_1 R g^{\mu_1 \nu_1 \mu_2 \nu_2} \right. \\ \left. + \frac{\gamma_2}{2} (R^{\mu_1 [\nu_1} g^{\nu_2] \mu_2} - R^{\mu_2 [\nu_1} g^{\nu_2] \mu_1}) + \gamma_3 R^{\mu_1 \mu_2 \nu_1 \nu_2} \} h_{\mu_1 \nu_1} h_{\mu_2 \nu_2} + \mathcal{O}(R^2/m^2) \right]$$

Leading order condition

$\gamma_1, \gamma_2, \gamma_3$: not constrained

Fourth order condition

γ_1, γ_2 : not constrained, $\gamma_3 = 1$

Linearized dRGT model

$$\gamma_1 = \frac{s_2 D - 1}{2(D - 1)}, \quad \gamma_2 = -4s_2, \quad \gamma_3 = 1$$

- Compatible with fourth order condition
- However, there remains a difference by one free parameter

TRIVIAL EXTENSION

Trivial extension

- Let us consider the model obtained by the replacement $m^2 \rightarrow \mu^2(x)$: any local function

$$S' = \int d^D x \sqrt{-g} \left[\frac{1}{2} g^{\mu_1 \nu_1 \mu_2 \nu_2 \mu_3 \nu_3} \nabla_{\mu_1} h_{\mu_2 \nu_2} \nabla_{\nu_3} h_{\mu_3 \nu_3} + \frac{1}{2} \{ \mu^2(x) g^{\mu_1 \nu_1 \mu_2 \nu_2} + T^{\mu_1 \nu_1 \mu_2 \nu_2} + N^{\mu_1 \nu_1 \mu_2 \nu_2} \} h_{\mu_1 \nu_1} h_{\mu_2 \nu_2} \right]$$

- The condition for ghost-freeness

$$\text{Det}(V^{0\mu\nu 0} g_{\nu\rho}) = 0,$$

$$V^{0\mu\nu 0} = \mu^2(x) g^{(0\mu)(\nu 0)} + \bar{S}^{0\mu\nu 0} + N^{0\mu\nu 0} + Q^{0\mu\nu 0}$$

- Although a derivative of $\mu^2(x)$ appears in $\nabla_\mu E^{\mu\nu}$, it does not affect to the condition.

Once we obtain a ghost-free model with m^2 , $T^{\mu_1 \nu_1 \mu_2 \nu_2}(m^2)$, $N^{\mu_1 \nu_1 \mu_2 \nu_2}(m^2)$

➡ A model with $\mu^2(x)$, $T^{\mu_1 \nu_1 \mu_2 \nu_2}(\mu^2(x))$, $N^{\mu_1 \nu_1 \mu_2 \nu_2}(\mu^2(x))$ is also ghost-free

TRIVIAL EXTENSION

Trivial extension of linearized dRGT model

- We obtain the trivial extension by replacing $m^2 \rightarrow \mu^2(x)$

$$S'_{\text{dRGT}} \equiv \int d^D x \sqrt{-g} \left[\frac{1}{2} g^{\mu_1 \nu_1 \mu_2 \nu_2 \mu_3 \nu_3} \nabla_{\mu_1} h_{\mu_2 \nu_2} \nabla_{\nu_1} h_{\mu_3 \nu_3} + \frac{1}{2} \left\{ \mu^2(x) g^{\mu_1 \nu_1 \mu_2 \nu_2} + \frac{s_2 D - 1}{2(D-1)} R g^{\mu_1 \nu_1 \mu_2 \nu_2} - 2s_2 \left(R^{\mu_1 [\nu_1} g^{\nu_2] \mu_2} - R^{\mu_2 [\nu_1} g^{\nu_2] \mu_1} \right) + R^{\mu_1 \mu_2 \nu_1 \nu_2} \right\} h_{\mu_1 \nu_1} h_{\mu_2 \nu_2} + \mathcal{O}(R^2/\mu^2(x)) \right].$$

$$\mu^2(x) = m^2 + \alpha R + \mathcal{O}(R^2/m^2)$$

$$S'_{\text{dRGT}} = \int d^D x \sqrt{-g} \left[\frac{1}{2} g^{\mu_1 \nu_1 \mu_2 \nu_2 \mu_3 \nu_3} \nabla_{\mu_1} h_{\mu_2 \nu_2} \nabla_{\nu_1} h_{\mu_3 \nu_3} + \frac{1}{2} \left\{ m^2 g^{\mu_1 \nu_1 \mu_2 \nu_2} + \gamma'_1 R g^{\mu_1 \nu_1 \mu_2 \nu_2} + \frac{\gamma'_2}{2} \left(R^{\mu_1 [\nu_1} g^{\nu_2] \mu_2} - R^{\mu_2 [\nu_1} g^{\nu_2] \mu_1} \right) + R^{\mu_1 \mu_2 \nu_1 \nu_2} \right\} h_{\mu_1 \nu_1} h_{\mu_2 \nu_2} + \mathcal{O}(R^2/m^2) \right]$$

$$\gamma'_1 \equiv \alpha + \frac{s_2 D - 1}{2(D-1)}, \quad \gamma'_2 \equiv -4s_2$$

- γ'_1, γ'_2 are no longer related with each other \rightarrow Coincides with the Bottom-up result

SUMMARY

Summary

- In previous works, the linearized dRGT model seems a subclass of the bottom-up result based on the leading order condition.
- We obtained a constraint on the leading order NCTs from the fourth order condition.
- We found a trivial extension of the linearized dRGT model.
- We confirmed the equivalence between the bottom-up result and the top-down result.

Future works

- Confirmation of the correspondence beyond the leading order
- Derivative nonminimal coupling terms
- Spin-three extension (There is a work solving the leading order condition [M. Fukuma et al. (2016)])

THANK YOU FOR YOUR ATTENTION

INTRODUCTION

Linear theory of massive spin-two field

- **Flat spacetime:** Fierz-Pauli model, DoF=5 for D=4
- **Arbitrary background:** Minimal coupled model, DoF=6=Spin2+ghost
- Nonminimal coupling terms (NCT) are necessary

Bottom-up approach [Buchbinder et.al. (2000)]

- Small curvature approximation $R/m^2 \ll 1$

$$S_{\text{general}} = \int d^D x \sqrt{-g} \left[\frac{1}{2} g^{\mu_1 \nu_1 \mu_2 \nu_2 \mu_3 \nu_3} \nabla_{\mu_1} h_{\mu_2 \nu_2} \nabla_{\nu_3} h_{\mu_3 \nu_3} + \frac{1}{2} \left\{ m^2 g^{\mu_1 \nu_1 \mu_2 \nu_2} + \gamma_1 R g^{\mu_1 \nu_1 \mu_2 \nu_2} + \frac{\gamma_2}{2} \left(R^{\mu_1 [\nu_1} g^{\nu_2] \mu_2} - R^{\mu_2 [\nu_1} g^{\nu_2] \mu_1} \right) + \gamma_3 R^{\mu_1 \mu_2 \nu_1 \nu_2} \right\} h_{\mu_1 \nu_1} h_{\mu_2 \nu_2} + \mathcal{O}(R^2/m^2) \right]$$

- Three free parameters are allowed
- Existence of completion is NOT guaranteed

INTRODUCTION

Our research

Purpose: Identifying the most general class whose completion exists

Possibilities and results

Bottom-up: Leading order NCTs may be constrained by higher order conditions

Leading order condition

$\gamma_1, \gamma_2, \gamma_3$: not constrained

Fourth order condition

γ_1, γ_2 :not constrained, $\gamma_3 = 1$

Top-down: Linearized dRGT model may be extended

Original linearized dRGT

$\gamma_1 = \frac{s_2 D - 1}{2(D - 1)}, \gamma_2 = -4s_2, \gamma_3 = 1$

A trivial extension

γ_1, γ_2 :not constrained, $\gamma_3 = 1$

Conclusion: We identify the most general class of the leading order NCTs

CONSTRAINTS IN FP-MODEL

Fierz–Pauli model

➤ EoM of the FP model in flat spacetime,

$$E^{\mu\nu} \equiv -\eta^{\mu\nu\mu_1\nu_1\mu_2\nu_2} \partial_{\mu_1} \partial_{\nu_1} h_{\mu_2\nu_2} + m^2 \eta^{\mu\nu\mu_1\nu_1} h_{\mu_1\nu_1} = 0$$

➤ Lorentz covariant constraints:

$$(1) \phi_{\text{vector}}^{\nu} \equiv \partial_{\mu} E^{\mu\nu} = m^2 \eta^{\mu\nu\mu_1\nu_1} \partial_{\mu} h_{\mu_1\nu_1} = 0 \quad : \text{Vector constraints}$$

$$(2) \phi_{\text{scalar}} \equiv \partial_{\mu} \partial_{\nu} E^{\mu\nu} + \frac{m^2}{D-2} \eta^{\mu\nu} E_{\mu\nu} = \frac{D-1}{D-2} m^4 h = 0 \quad : \text{Scalar constraint}$$

$$(3) E_{\mu\nu} \Big|_{\substack{\phi_{\text{vector}}=0 \\ \phi_{\text{scalar}}=0}} = (\square - m^2) h_{\mu\nu} = 0$$

➤ In the Furrier space, Eq.(3) determine the dispersion relation.

➤ Eqs.(1), (2) can be regarded as constraints

➤ In the case of curved background, minimal coupled model violate a scalar constraint.

LAGRANGIAN ANALYSIS

Lagrangian analysis

- Lagrangian analysis = Method for counting DoF in lagrangian formulation
- Let us count DoF of Fierz-Pauli theory

Fierz-Pauli theory

$$E^{\mu\nu} \equiv -\eta^{\mu\nu\mu_1\nu_1\mu_2\nu_2} \partial_{\mu_1} \partial_{\nu_1} h_{\mu_2\nu_2} + m^2 \eta^{\mu\nu\mu_1\nu_1} h_{\mu_1\nu_1} = 0$$

$$E^{ij} = \delta^{ij i_1 j_1} \ddot{h}_{i_1 j_1} + (\text{terms without } \ddot{h})^{ij} = 0 \quad (\text{a})$$

$$\phi^{(1)\nu} \equiv E^{0\nu} = -\eta^{0\nu i_1 \nu_1 i_2 \nu_2} \partial_{i_1} \partial_{\nu_1} h_{i_2 \nu_2} + m^2 \eta^{0\nu i_1 \nu_1} h_{i_1 \nu_1} = 0 \quad (\text{b})$$

- Eqs.(a) contain \ddot{h}_{ij}
- Eqs.(b) do not contain any accelerations → All the Eqs do not contain $\ddot{h}_{0\mu}$
- $\ddot{h}_{0\mu}$ can be decided from time derivative of Eqs.(b)

LAGRANGIAN ANALYSIS

$$\phi^{(1)\nu} \equiv E^{0\nu} = -\eta^{0\nu i_1 \nu_1 i_2 \nu_2} \partial_{i_1} \partial_{\nu_1} h_{i_2 \nu_2} + m^2 \eta^{0\nu i_1 \nu_1} h_{i_1 \nu_1} = 0 \quad (\text{b})$$

- Requiring ``consistency condition'' of Eqs.(b):

$$\dot{\phi}^{(1)\nu} = 0. \quad (\text{c})$$

- Eqs.(b) are satisfied in initial time \Rightarrow Eqs.(b) are valid in any time
- Eqs.(b) can be regarded as ``constraints'' on initial values
- Equivalence on initial time: \approx

$$\phi^{(1)\nu} \approx 0.$$

- We continue this procedure until $\ddot{h}_{0\mu}$ appears in the equations
- Counting the numbers of constraint \rightarrow DoF can be decided
- We would like to deform consistency condition (c)

LAGRANGIAN ANALYSIS

Consistency condition of Eqs.(b)

$$0 = \dot{\phi}^{(1)\nu} \approx \partial_\mu E^{\mu\nu} = m^2 \eta^{\mu\nu\mu_1\nu_1} \partial_\mu h_{\mu_1\nu_1} \equiv \phi^{(2)\nu}. \quad (c')$$

- Eqs.(c') can also be regarded as constraints

Consistency condition of (c')

$$\dot{\phi}^{(2)i} = m^2 \ddot{h}_{0i} + (\text{terms without } \ddot{h}) = 0, \quad (d)$$

$$0 = \dot{\phi}^{(2)0} \approx \frac{D-1}{D-2} m^4 h \equiv \phi^{(3)}. \quad (e)$$

- From Eqs.(d), acceleration \ddot{h}_{0i} is decided
- On the other hand, Eq.(e) is constraint
- Consistency condition of (e) is also constraint: $\phi^{(4)} = \dot{\phi}^{(3)} \approx 0$
- Finally, we obtain two vector constraints and two scalar constraints

IRREDUCIBLE DECOMPOSITION

Reconsideration

- From Buchbinder's result, basis of linear order NCTs are given by,

$$Rg^{\mu_1\nu_1\mu_2\nu_2}, \quad R^{\mu_1[\nu_1}g^{\nu_2]\mu_2} - R^{\mu_2[\nu_1}g^{\nu_2]\mu_1}, \quad R^{\mu_1\mu_2\nu_1\nu_2} \quad (a)$$

- All of the above terms have same symmetries as,

$$T^{\mu_1\nu_1\mu_2\nu_2} = -T^{\mu_2\nu_1\mu_1\nu_2} = -T^{\mu_1\nu_2\mu_2\nu_1} = T^{\mu_2\nu_2\mu_1\nu_1}, \quad T^{[\mu_1\nu_1\mu_2]\nu_2} = 0$$

- Those are symmetries corresponding to Young tableau:

- Conversely, the terms in (a) are also the most general representation of $T^{\mu_1\nu_1\mu_2\nu_2}$ in leading order

- By only using these symmetries, we ought to show that the terms in (a) is not constrained in leading order

IRREDUCIBLE DECOMPOSITION

We consider the model with the nonderivative nonminimal coupling terms expressed by general tensor $\Delta^{\mu_1\nu_1\mu_2\nu_2}$ constructed by curvature and metric,

$$S = \int d^D x \sqrt{-g} \left[\frac{1}{2} g^{\mu_1\nu_1\mu_2\nu_2\mu_3\nu_3} \nabla_{\mu_1} h_{\mu_2\nu_2} \nabla_{\nu_1} h_{\mu_3\nu_3} + \frac{1}{2} \{ m^2 g^{\mu_1\nu_1\mu_2\nu_2} + \Delta^{\mu_1\nu_1\mu_2\nu_2} \} h_{\mu_1\nu_1} h_{\mu_2\nu_2} \right]$$

The tensor $\Delta^{\mu_1\nu_1\mu_2\nu_2}$ can be decomposed as follows,

$$\begin{aligned} \Delta^{\mu_1\nu_1\mu_2\nu_2} h_{\mu_1\nu_1} h_{\mu_2\nu_2} &= T^{\mu_1\nu_1\mu_2\nu_2} h_{\mu_1\nu_1} h_{\mu_2\nu_2} + N^{\mu_1\nu_1\mu_2\nu_2} h_{\mu_1\nu_1} h_{\mu_2\nu_2}, \\ T^{\mu_1\nu_1\mu_2\nu_2} &= \frac{1}{2} \left(\Delta^{[\mu_1|\nu_1|\mu_2]\nu_2} - \Delta^{[\mu_1|\nu_2|\mu_2]\nu_1} \right) + \frac{1}{6} \left(\Delta^{\mu_1[\nu_1\nu_2]\mu_2} - \Delta^{\mu_2[\nu_1\nu_2]\mu_1} \right) + \frac{1}{3} \Delta^{[\nu_2\nu_1][\mu_1\mu_2]}, \\ N^{\mu_1\nu_1\mu_2\nu_2} &= \Delta^{(\mu_1\nu_1\mu_2\nu_2)} \\ \Delta^{[\mu_1|\nu_1|\mu_2]\nu_2} &\equiv \frac{1}{2} \left(\Delta^{\mu_1\nu_1\mu_2\nu_2} - \Delta^{\mu_2\nu_1\mu_1\nu_2} \right) \\ \Delta^{(\mu_1\nu_1\mu_2\nu_2)} &: \text{perfect symmetrization of } \Delta^{\mu_1\nu_1\mu_2\nu_2} \end{aligned}$$

EINSTEIN MANIFOLD CASE

Einstein manifold case [Buchbinder et.al.(2000)] [Akagi, Ohara, Nojiri(2014)]

- We consider the case of Einstein manifold $R_{\mu\nu} = \frac{R}{D} g_{\mu\nu}$
- $Q^{\mu\nu\mu_1\nu_1} \equiv \frac{1}{2} \left[R^{\mu\nu} g^{\mu_1\nu_1} - g^{\mu\nu} R^{\mu_1\nu_1} + 2R^{(\mu_1} g^{\nu_1)\nu} - 2R^{\nu(\mu_1} g^{\nu_1)\mu} \right] = 0$
- In this case, the condition $\text{Det}(V^0_{\nu}{}^{\mu_0}) = 0$ is "uniquely" solved as,

$$N^{\mu_1\nu_1\mu_2\nu_2} = 0 \quad S^{\mu_1\nu_1\mu_2\nu_2} : \text{not constrained}$$

- Indeed,

$$V^{0\mu\nu 0} = m^2 g^{(0\mu)(\nu 0)} + S^{(0\mu)(\nu 0)} \implies V^{0\mu\nu 0} g_{\mu}^0 = 0$$

- There is a zero eigen vector g_{μ}^0

LEMMA

Proposition

1. $D^{\mu_1\nu_1\mu_2\nu_2}$ depends only on metric and its partial derivatives
2. $D^{\mu_1\nu_1\mu_2\nu_2}$ is general covariant
3. $D^{0000}(g_{\mu\nu}) = 0$ for any metric

For any $D^{\mu_1\nu_1\mu_2\nu_2}$ satisfying the above properties, we can show $D^{(\mu_1\nu_1\mu_2\nu_2)} = 0$

Proof

- From assumption 3, $D^{0000}(g_{\mu\nu} + \delta g_{\mu\nu}) - D^{0000}(g_{\mu\nu}) = 0$ for any $\delta g_{\mu\nu}$
- Taking $\delta g_{\mu\nu}$ as $\delta g_{\mu\nu} = \mathcal{L}_\xi g_{\mu\nu} = 2\nabla_{(\mu}\xi_{\nu)}$
- Using assumption 1 and commutativity $[\mathcal{L}_\xi, \partial_\mu] = 0$, $\mathcal{L}_\xi D^{0000} = 0$
- From assumption 2, $\mathcal{L}_\xi D^{0000} = \xi^\alpha \partial_\alpha D^{0000} - 4D^{(\rho 000)} \partial_\rho \xi^0$.
- Thus, $D^{(\rho 000)} = 0 \rightarrow$ Repeating this procedure, $D^{(\mu_1\nu_1\mu_2\nu_2)} = 0$

DRGT MODEL

The action [C. de Rham et al. (2010)]

$$S_{\text{dRGT}}[g; f] = M_g^{D-2} \int d^D x \sqrt{-g} \left[R(g) - 2m^2 \sum_{n=0}^{D-1} \beta_n e_{(n)}(\mathcal{S}) \right],$$

$$e_{(n)}(\mathcal{S}) = \frac{1}{n!} \delta_{\mu_1 \mu_2 \dots \mu_n}^{\nu_1 \nu_2 \dots \nu_n} \mathcal{S}^{\mu_1}_{\nu_1} \mathcal{S}^{\mu_2}_{\nu_2} \dots \mathcal{S}^{\mu_n}_{\nu_n}, \quad \mathcal{S}^\mu_{\nu} \equiv \sqrt{g^{-1}} f^\mu_{\nu}$$

- The potential terms have been tuned so that a ``scalar'' constraint exists.

``Scalar'' constraint [S. Akagi and T. Mori (In preparation)]

$$\Psi \equiv \nabla_\nu (\mathcal{S}^{-1\nu}_{\rho} \nabla_\mu E^{\mu\rho}) + \sum_{n=1}^{D-1} \frac{\beta_n}{(n-1)!} \theta^{\mu_1\nu_1\mu_2\nu_2\dots\mu_n\nu_n} \mathcal{S}_{\mu_2\nu_2} \dots \mathcal{S}_{\mu_n\nu_n} \left(\frac{\theta_{\mu_1\nu_1}\theta_{\rho\sigma}}{D-2} - \theta_{\rho(\mu_1}\theta_{\nu_1)\sigma} \right) E^{\rho\sigma}$$

= (terms without $\partial_\mu \partial_\nu g_{\alpha\beta}$)

$$\theta^{\mu\nu} \equiv g^{\mu\nu} - \frac{g^{0\mu} g^{0\nu}}{g^{00}} \quad : \text{Projection operator living in D-1 dim space}$$

$$\theta^{\mu_1\nu_1\mu_2\nu_2\dots\mu_n\nu_n} \equiv \delta_{\rho_1 \rho_2 \dots \rho_n}^{\mu_1 \mu_2 \dots \mu_n} \theta^{\rho_1\nu_1} \theta^{\rho_2\nu_2} \dots \theta^{\rho_n\nu_n}$$

LINEARIZATION

Complete NCT from dRGT [L. Bernard et al. (2015)]

$$E^{\mu\nu} \equiv G^{\mu\nu} + m^2 \sum_{n=0}^{D-1} \frac{\beta_n}{n!} g^{\mu\nu\mu_1\nu_1\cdots\mu_n\nu_n} \mathcal{S}_{\mu_1\nu_1} \cdots \mathcal{S}_{\mu_n\nu_n} = 0$$

- Background EoM can be solved for $f \rightarrow$ denoting as $f=f(g)$
- Substituting $f=f(g)$ into the linearized action, we obtain,

$$\begin{aligned} S_{\text{dRGT}} \left[g + \frac{\sqrt{2}}{M_g^{(D-2)/2}} h ; f(g) \right]_{\text{linear}} \\ = \int d^D x \sqrt{-g} \left[\frac{1}{2} g^{\mu_1\nu_1\mu_2\nu_2\mu_3\nu_3} \nabla_{\mu_1} h_{\mu_2\nu_2} \nabla_{\nu_1} h_{\mu_3\nu_3} + \frac{1}{2} \left\{ m^2 g^{\mu_1\nu_1\mu_2\nu_2} + \frac{s_2 D - 1}{2(D-1)} R g^{\mu_1\nu_1\mu_2\nu_2} \right. \right. \\ \left. \left. - 2s_2 \left(R^{\mu_1[\nu_1} g^{\nu_2]\mu_2} - R^{\mu_2[\nu_1} g^{\nu_2]\mu_1} \right) + R^{\mu_1\mu_2\nu_1\nu_2} \right\} h_{\mu_1\nu_1} h_{\mu_2\nu_2} + \mathcal{O}(R^2/m^2) \right] \end{aligned}$$

- This result is included in the bottom-up result by, $\gamma_1 = \frac{s_2 D - 1}{2(D-1)}, \quad \gamma_2 = -4s_2$

CONDITION FOR GHOST-FREENESS

$$\text{Det}(V^0_{\nu}{}^{\mu 0}) = 0 \quad V^{0\mu\nu 0} \equiv m^2 g^{(0\mu)(\nu 0)} + \bar{S}^{0\mu\nu 0} + N^{0\mu\nu 0} + P^{0\mu\nu 0}$$



Properties of decomposition into time+space direction

$$\theta_{\nu}^{\mu} \equiv \delta_{\nu}^{\mu} - \frac{g^{\mu 0} g_{\nu}^0}{g^{00}} \quad g^{(0\mu)(\nu 0)} = -\frac{1}{2} g^{00} \theta^{\mu\nu}$$

$$\bar{S}^{0\mu\nu 0} = \theta_{\alpha}^{\mu} \bar{S}^{0\alpha\beta 0} \theta_{\beta}^{\nu}$$

$$\hat{N}^{\mu\nu} \equiv N^{0\mu\nu 0} \quad \hat{S}^{\mu\nu} \equiv \bar{S}^{0\mu\nu 0} \quad [XY]^{\mu\nu} \equiv X^{\mu}_{\rho} Y^{\rho\nu}$$

SCALAR CONSTRAINT

$$E^{\mu\nu} = G^{\mu\nu} + m^2\beta_0 g^{\mu\nu} + m^2\beta_1 g^{\mu\nu\mu_1\nu_1} \mathcal{S}_{\mu_1\nu_1}$$

$$\nabla_\mu E^{\mu\nu} = m^2\beta_1 g^{\mu\nu\mu_1\nu_1} \nabla_\mu \mathcal{S}_{\mu_1\nu_1}.$$

$$\frac{1}{m^2\beta_1} \nabla_\nu (\mathcal{S}^{-1\nu}{}_\rho \nabla_\mu E^{\mu\rho}) + \frac{1}{D-2} g_{\mu\nu} E^{\mu\nu} = \Phi + \Psi + \frac{D}{D-2} m^2\beta_0 + \frac{D-1}{D-2} m^2\beta_1 \mathcal{S}$$

$$\Phi \equiv \frac{1}{2} \nabla_\nu (\mathcal{S}^{-1\mu\nu} \mathcal{S}^{-1\mu_1\nu_1} - \mathcal{S}^{-1\mu(\mu_1} \mathcal{S}^{-1\nu_1)\nu}) \cdot \nabla_\mu f_{\mu_1\nu_1} - \nabla_\nu \mathcal{S}^{-1[\nu}{}_\rho \cdot \nabla_\mu \mathcal{S}^{\mu]\rho}$$

$$\Psi \equiv \frac{1}{2} (\mathcal{S}^{-1\mu\nu} \mathcal{S}^{-1\mu_1\nu_1} - \mathcal{S}^{-1\mu(\mu_1} \mathcal{S}^{-1\nu_1)\nu}) \nabla_\nu \nabla_\mu f_{\mu_1\nu_1} - \frac{1}{2} R^{\mu_1\mu_2\nu_1\nu_2} \mathcal{S}_{\mu_1\nu_1}^{-1} \mathcal{S}_{\mu_2\nu_2} = (\text{terms without } \partial_\mu \partial_\nu g_{\alpha\beta})$$

COFACTOR EXPANSION

$$\text{Det}(V^{0\mu\nu 0} g_{\nu\rho}) = V^{0000} \text{Det}_\theta(V^{0\mu\nu 0} \theta_{\nu\rho}) - V^0{}_\mu{}^{00} V^0{}_\nu{}^{00} Y_\theta^{\mu\nu}(V^{0\alpha\beta 0})$$

$$\text{Det}_\theta(V^{0\mu\nu 0} \theta_{\nu\rho}) \equiv \frac{1}{(D-1)!} \theta^{\mu_2\nu_2 \dots \mu_D\nu_D} V^0{}_{\mu_2\nu_2}{}^0 \dots V^0{}_{\mu_D\nu_D}{}^0$$

$$Y_\theta^{\mu\nu}(V^{0\alpha\beta 0}) \equiv \frac{1}{(D-2)!} \theta^{\mu\nu\mu_3\nu_3 \dots \mu_D\nu_D} V^0{}_{\mu_3\nu_3}{}^0 \dots V^0{}_{\mu_D\nu_D}{}^0$$

$$\theta_\nu^\mu \equiv \delta_\nu^\mu - \frac{g^{\mu 0} g_\nu^0}{g^{00}}$$

COFACTOR EXPANSION

$$\text{Det}(V^{0\mu\nu 0} g_{\nu\rho}) = V^{0000} \text{Det}_\theta(V^{0\mu\nu 0} \theta_{\nu\rho}) - V^0_{\mu}{}^{00} V^0_{\nu}{}^{00} Y_\theta^{\mu\nu}(V^{0\alpha\beta 0})$$

$$\text{Det}_\theta(V^{0\mu\nu 0} \theta_{\nu\rho}) \equiv \frac{1}{(D-1)!} \theta^{\mu_2\nu_2 \dots \mu_D\nu_D} V^0_{\mu_2\nu_2}{}^0 \dots V^0_{\mu_D\nu_D}{}^0$$

$$Y_\theta^{\mu\nu}(V^{0\alpha\beta 0}) \equiv \frac{1}{(D-2)!} \theta^{\mu\nu\mu_3\nu_3 \dots \mu_D\nu_D} V^0_{\mu_3\nu_3}{}^0 \dots V^0_{\mu_D\nu_D}{}^0$$

$$V^{0\mu\nu 0} = -\frac{m^2}{2} g^{00} \theta^{\mu\nu} + \Delta^{\mu\nu}.$$

$$\Delta^{\mu\nu} \equiv \bar{S}^{0\mu\nu 0} + N^{0\mu\nu 0} + Q^{0\mu\nu 0}$$

$$\Delta^{00} + \sum_{n=0}^{\infty} \left(\frac{2}{m^2 g^{00}} \right)^{n+1} \Delta^0_{\nu} [\theta(\Delta\theta)^n]^{\nu\mu} \Delta^0_{\mu} := 0$$

PERTURBATIVE SOLUTION

Restriction up to fourth order

$$S = \int d^D x \sqrt{-g} \left[\frac{1}{2} g^{\mu_1\nu_1\mu_2\nu_2\mu_3\nu_3} \nabla_{\mu_1} h_{\mu_2\nu_2} \nabla_{\nu_1} h_{\mu_3\nu_3} + \frac{1}{2} \{ m^2 g^{\mu_1\nu_1\mu_2\nu_2} + T^{\mu_1\nu_1\mu_2\nu_2} + N^{\mu_1\nu_1\mu_2\nu_2} \} h_{\mu_1\nu_1} h_{\mu_2\nu_2} \right]$$

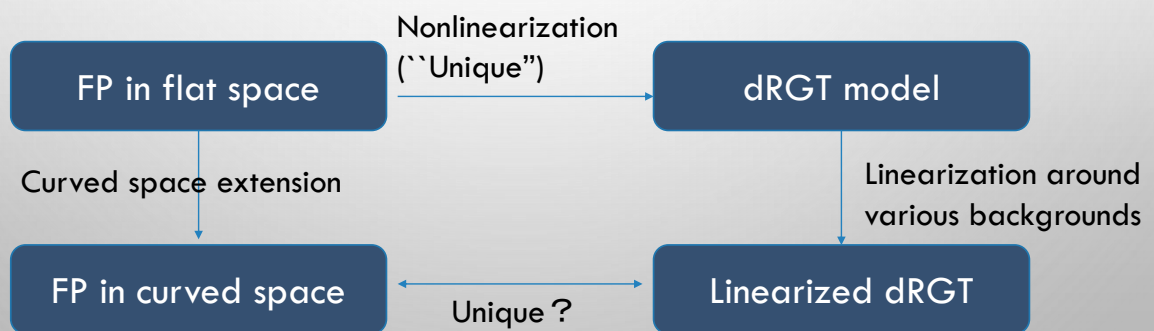
$$\begin{aligned} T^{(1)\mu_1\nu_1\mu_2\nu_2} &= S^{(1)\mu_1\nu_1\mu_2\nu_2} + R^{\mu_1\mu_2\nu_1\nu_2} - \left(R^{\mu_1[\nu_1} g^{\nu_2]\mu_2} - R^{\mu_2[\nu_1} g^{\nu_2]\mu_1} \right) \\ &= \gamma_1^{(1)} R g^{\mu_1\nu_1\mu_2\nu_2} + \frac{\gamma_2^{(1)} - 2}{2} \left(R^{\mu_1[\nu_1} g^{\nu_2]\mu_2} - R^{\mu_2[\nu_1} g^{\nu_2]\mu_1} \right) + R^{\mu_1\mu_2\nu_1\nu_2} \end{aligned}$$

$$N^{(1)\mu_1\nu_1\mu_2\nu_2} = 0$$

$$N^{(2)\mu_1\nu_1\mu_2\nu_2} = \frac{1}{2} g^{\alpha\beta(\mu_1\nu_1} R_\alpha^{\mu_2} R_\beta^{\nu_2)}$$

$$N^{(3)\mu_1\nu_1\mu_2\nu_2} = -\frac{1}{2} S^{(1)\alpha\beta(\mu_1\nu_1} R_\alpha^{\mu_2} R_\beta^{\nu_2)}$$

Extensions of FP model



SUMMARY

Relationships with other theories

- Our result: γ_1, γ_2 :not constrained, $\gamma_3 = 1$
- Linearized dRGT model: $\gamma_1 = -\frac{1}{2} \left(\frac{1}{D-1} - s \right)$, $\gamma_2 = -4s$, $\gamma_3 = 1$ → Compatible
- String theory: $\gamma_1 = 0$, $\gamma_2 = -2$, $\gamma_3 = -1$ → Incompatible
→ Derivative NCT? Background EoM?

Future works

- Higher order calculation → More on relationship with linearized dRGT
- Simplification of constraint analysis of linearized dRGT
→ Minimal model has been completed
- Derivative NCT → String theory? No-go? G-B dRGT?
- Higher spin extension

TRIVIAL EXTENSION

Trivial extension

- Let us consider the model obtained by the replacement $m^2 \rightarrow \mu^2(x)$: any local function

$$S' = \int d^D x \sqrt{-g} \left[\frac{1}{2} g^{\mu_1 \nu_1 \mu_2 \nu_2 \mu_3 \nu_3} \nabla_{\mu_1} h_{\mu_2 \nu_2} \nabla_{\nu_1} h_{\mu_3 \nu_3} + \frac{1}{2} \{ \mu^2(x) g^{\mu_1 \nu_1 \mu_2 \nu_2} + T^{\mu_1 \nu_1 \mu_2 \nu_2} + N^{\mu_1 \nu_1 \mu_2 \nu_2} \} h_{\mu_1 \nu_1} h_{\mu_2 \nu_2} \right]$$

- The condition for ghost-freeness

$$\text{Det}(V'^{0\mu\nu 0} g_{\nu\rho}) = 0,$$

$$V'^{0\mu\nu 0} = \mu^2(x) g^{(0\mu)(\nu 0)} + \bar{S}'^{0\mu\nu 0} + N'^{0\mu\nu 0} + Q^{0\mu\nu 0}$$

- Although a derivative of $\mu^2(x)$ appears in $\nabla_\mu E^{\mu\nu}$, it does not affect to the condition.
- Once we obtain a ghost-free model with mass m^2 and tensors $T^{\mu_1 \nu_1 \mu_2 \nu_2}(m^2)$, $N^{\mu_1 \nu_1 \mu_2 \nu_2}(m^2)$, the model with local mass $\mu^2(x)$ and tensors $T^{\mu_1 \nu_1 \mu_2 \nu_2}(\mu^2(x))$, $N^{\mu_1 \nu_1 \mu_2 \nu_2}(\mu^2(x))$ are also ghost-free.

INTRODUCTION

Our research

- **Possibility:** 1. Leading order NCTs may be constrained by higher order conditions
2. Linearized dRGT model may be extended
- **Result:** Linear order NCTs are constrained by fourth order condition
A trivial extension of linearized dRGT coincides with bottom-up result

Bottom-up result

Leading order condition

$\gamma_1, \gamma_2, \gamma_3$: not constrained

Fourth order condition

γ_1, γ_2 :not constrained, $\gamma_3 = 1$



Top-down result

Original linearized dRGT

$$\gamma_1 = \frac{s_2 D - 1}{2(D - 1)}, \quad \gamma_2 = -4s_2, \quad \gamma_3 = 1$$

A trivial extension

γ_1, γ_2 :not constrained, $\gamma_3 = 1$



Session S3P2 16:30–18:15

[Chair: Masaru Shibata]

Shuntaro Mizuno

Yukawa Institute for Theoretical Physics

“Blue-tilted Primordial Gravitational Waves from Massive Gravity”
(10+5 min.)

[JGRG28 (2018) 110714]

Blue-tilted primordial gravitational waves from massive gravity

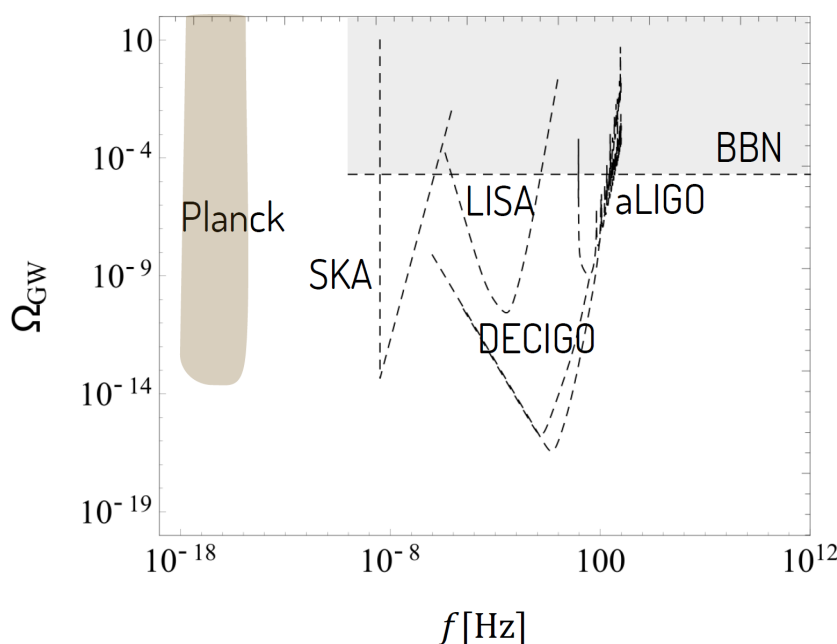
Shuntaro Mizuno (YITP, Kyoto)



with Tomohiro Fujita, Sachiko Kuroyanagi, Shinji Mukohyama

[arXiv:1808.02381\[gr-qc\]](https://arxiv.org/abs/1808.02381)

Interferometers and PGWs



Density parameter of PGWs

$$\Omega_{\text{GW}} \equiv \frac{1}{\rho_{\text{tot}}} \frac{d\rho_{\text{GW}}}{d \ln k}$$

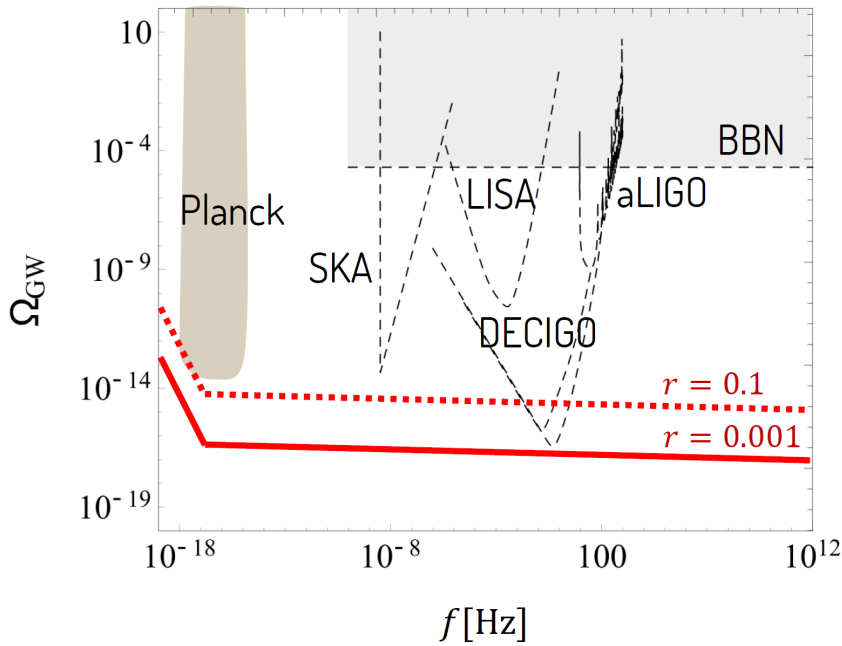
Frequency

$$f \equiv k/2\pi$$

We have already constraints on Ω_{GW} from BBN and Planck

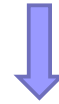
Interferometers can get information of PGWs on various scales !!

Interferometers and "Standard" PGWs



PGWs from inflation

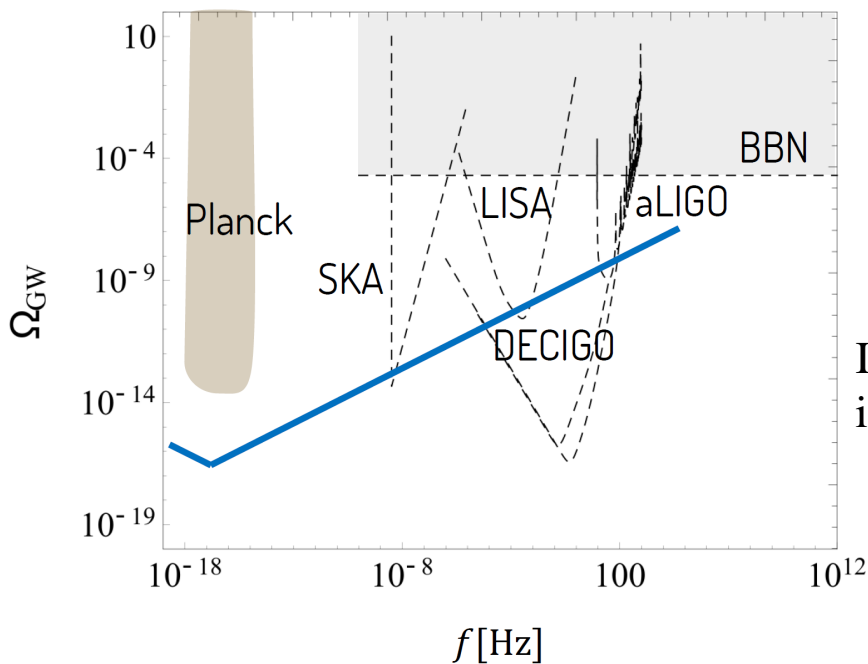
$$\mathcal{P}_{\text{GW}} = \frac{2H^2}{\pi^2 M_{\text{Pl}}^2}$$



Almost flat (Red-tilted)
PGWs spectrum

Planck constrains $\Omega_{\text{GW}} \lesssim 10^{-15}$ on interferometers' scales !!

Interferometers and Blue-tilted PGWs



Blue-tilted PGWs
are better for detection



In standard inflation,
it is difficult to realize

Can we obtain consistent and detectable blue-tilted PGWs ?

Blue-tilted PGWs from Supersolid inflation

- **Supersolid inflation** is based on effective field theory of inflation with both ~~time diffs~~ and ~~space diffs~~.

Endlich, Nicolis, Wang `12, Nicolis, Penco, Rosen `14

interpreted as (Lorentz violating) massive gravity

$$m/H \sim \text{degree of space diffs.}$$

- Because of the mass term of the graviton, we can obtain **Blue-tilted PGWs** without violating the null energy condition

Cannone, Tasinato, Wands `14

massive gravity has Higuchi ghost in de Sitter space

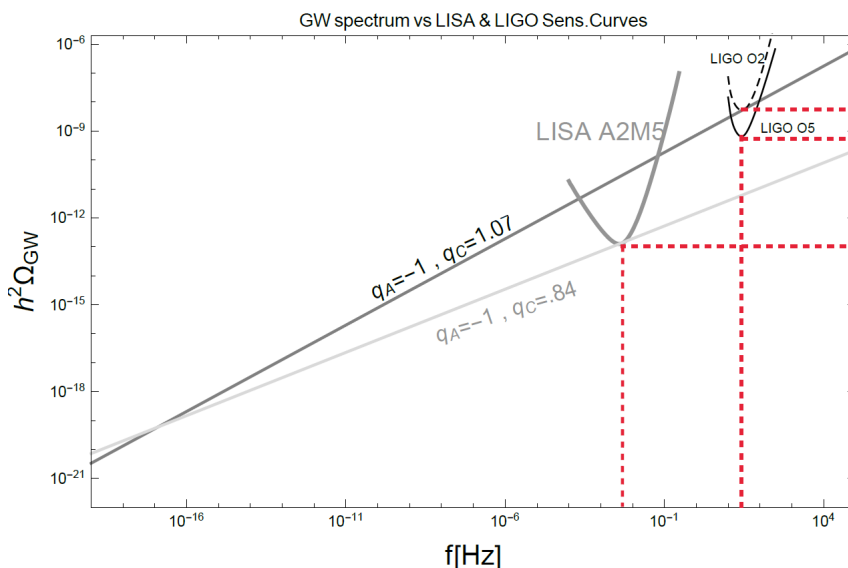
$$\text{when } 0 < m^2 < 2H^2$$

➔ In supersolid inflation, n_T can be positive but still $\mathcal{O}(\epsilon)$..

PGWs from extended supersolid inflation

Ricciardone, Tasinato `17

Extension with **nonminimal coupling** to introduce **hierarchy** between the degree of ~~time diffs~~ and ~~spatial diffs~~ .



$$n_T \simeq 3 - 2\nu$$

$$\nu \equiv \sqrt{\frac{9}{4} - \frac{m^2}{H^2}},$$

$$\frac{m}{H} = \mathcal{O}(1) \text{ is possible}$$

with small ϵ

But we still need some enhancement mechanism for detection

Minimal theory of massive gravity (MTMG)

De Felice, Mukohyama '15

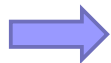
Cf. Oliosi's talk

• Properties of MTMG

Having only 2 propagating d.o.f. (No scalar and vector gravitons)

FRW background, tensor perturbations around it are same as

the nonlinear massive gravity by de Rham, Gabadaze, Tolley (dRGT)



Higuchi ghost and other ghosts are absent !!

• Construction of MTMG

- Obtaining Precursor theory by fixing vielbein in dRGT to be ADM one
- Writing down the Hamiltonian based on the canonical variables
- Imposing 2 constraints to obtain desirable d.o.f.

Set-up

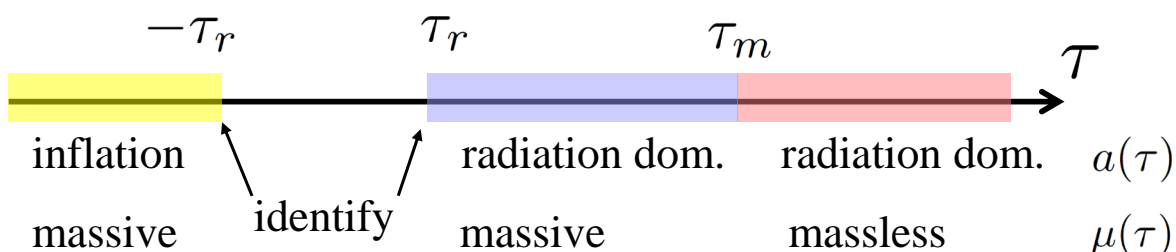
- Decomposition and quantization of h_{ij} with $g_{ij} = a^2 [e^h]_{ij}$

$$h_{ij} = \frac{2}{aM_{\text{Pl}}} \sum_{\lambda=+,\times} \int \frac{d^3k}{(2\pi)^3} e^{i\mathbf{k}\cdot\mathbf{x}} e_{ij}^\lambda [v_k^\lambda(\tau) \hat{a}_k^\lambda + \text{h.c.}],$$

- Equation of motion for the mode function

$$v_k'' + \left[k^2 + a^2 \mu^2 - \frac{a''}{a} \right] v_k = 0,$$

$$\text{with } a(\tau) = \begin{cases} -1/(H_{\text{inf}}\tau) & (\tau < -\tau_r) \\ a_r \tau / \tau_r & (\tau > \tau_r) \end{cases} \quad \mu(\tau) = \begin{cases} m & (\tau < \tau_m) \\ 0 & (\tau > \tau_m) \end{cases}$$



Evolution – inflation era

$$v_k'' + \left[k^2 - \frac{1}{\tau^2} \left(\nu^2 - \frac{1}{4} \right) \right] v_k = 0 \quad \nu \equiv \sqrt{\frac{9}{4} - \frac{m^2}{H_{\text{inf}}^2}}$$

with Bunch-Davies vacuum initial condition

$$\rightarrow v_k(\tau) = \frac{\sqrt{-\pi\tau}}{2} H_\nu^{(1)}(-k\tau) \propto \tau^{\frac{1}{2}-\nu} k^{-\nu}$$

on super horizon scales

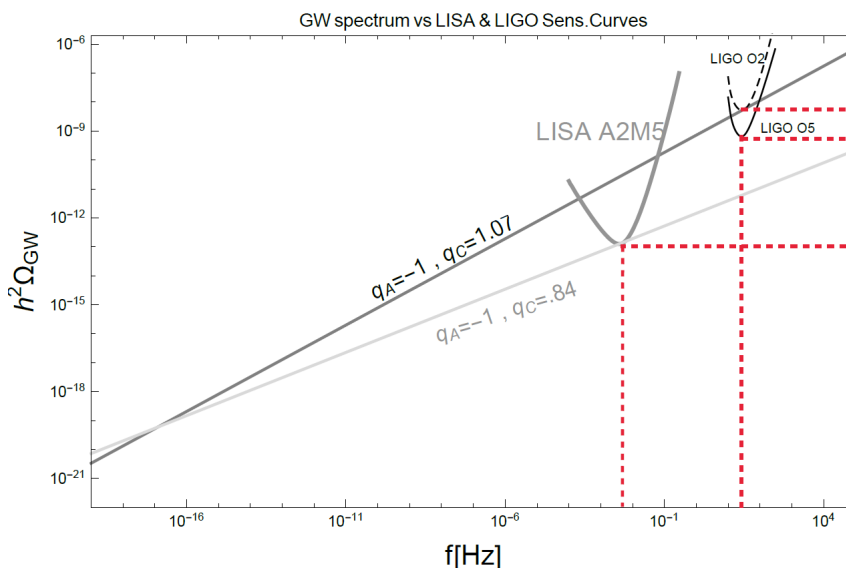
$$\rightarrow \mathcal{P}_{\text{GW}} \simeq \frac{2H_{\text{inf}}^2}{\pi^2 M_{\text{Pl}}^2} \left(\frac{k}{k_{\text{UV}}} \right)^{3-2\nu} \quad \text{for } k < k_{\text{UV}} = a(\tau_r) H_{\text{inf}}$$

Compared with the standard (massless) case,
PGWs decrease due to the graviton mass during inflation !!

PGWs from extended supersolid inflation

Ricciardone, Tasinato '17

Extension with **nonminimal coupling** to introduce **hierarchy**
between the degree of time ~~diffs~~ and spatial ~~diffs~~.



$$n_T \simeq 3 - 2\nu$$

$$\nu \equiv \sqrt{\frac{9}{4} - \frac{m^2}{H^2}},$$

$\frac{m}{H} = \mathcal{O}(1)$ is possible

with small ϵ

But we still need some enhancement mechanism for detection

Graviton energy density

- Graviton energy density

$$T_{\mu\nu}^{(\text{GW})} = \frac{M_{\text{Pl}}^2}{4} \langle \partial_\mu h_{ij} \partial_\nu h_{ij} \rangle \quad \longrightarrow \quad \rho^{(\text{GW})} \propto \frac{1}{2a^2} (h'_{ij})^2 \quad (\text{massless})$$

(analogy with scalar field) $\longrightarrow \rho^{(\text{GW})} \propto \frac{1}{2a^2} (h'_{ij})^2 + \frac{1}{2} m^2 h_{ij}^2$

- Massive phase

$$\rho_k^{\text{GW}} \propto m^2 h_k^2 \propto a^{-2} v_k^2 \propto a^{-3}$$

decays like non-relativistic matter!!

- Massless phase

$$\rho_k^{\text{GW}} \propto a^{-2} h_k'^2 \propto a^{-2} [(a^{-1} v_k)']^2 \propto a^{-4}$$

decays like relativistic matter (as usual)

Power spectrum of PGWs

$$\mathcal{P}_{\text{GW}}^{\text{massive}} \sim \frac{\tau_m}{\tau_r} (k\tau_r)^{3-2\nu} \mathcal{P}_{\text{GW}}^{\text{standard}}$$

$$\mathcal{P}_{\text{GW}} \equiv \frac{4k^3 |v_k|^2}{\pi^2 M_{\text{Pl}}^2 a^2}$$

$$\nu \equiv \sqrt{9/4 - m^2/H_{\text{inf}}^2}$$

1. Inflation

From BD-vacuum, GWs are produced and decay on super-horizon scales in same way as $\delta\phi_k$

Blue-tilt

$$\mathcal{P}_{\text{GW}} \sim (k\tau_r)^{3-2\nu}$$

2. Mass-dominant

After instant reheating, $k \ll am$ and gravitons behave as matter.

Slow decay

$$\rho_k^{\text{GW}} \propto a^{-3}$$

3. Massless

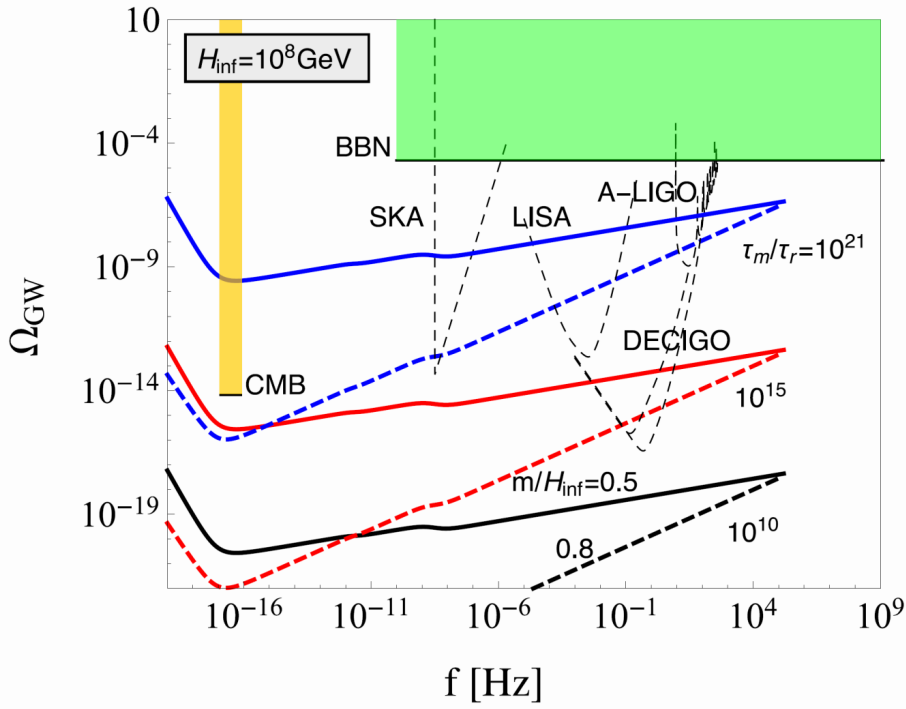
At some point in RD era, gravitons lose the mass to avoid some obs. bounds.

Detection

$$\rho_k^{\text{GW}} \propto a^{-4}$$

Theoretical prediction of Ω_{GW}

$$\Omega_{\text{GW}}(f) \simeq 10^{-15} \frac{\tau_m}{\tau_r} \left[\frac{H_{\text{inf}}}{10^{14} \text{ GeV}} \right]^{\nu + \frac{1}{2}} \left[\frac{f}{2 \times 10^8 \text{ Hz}} \right]^{3-2\nu}$$



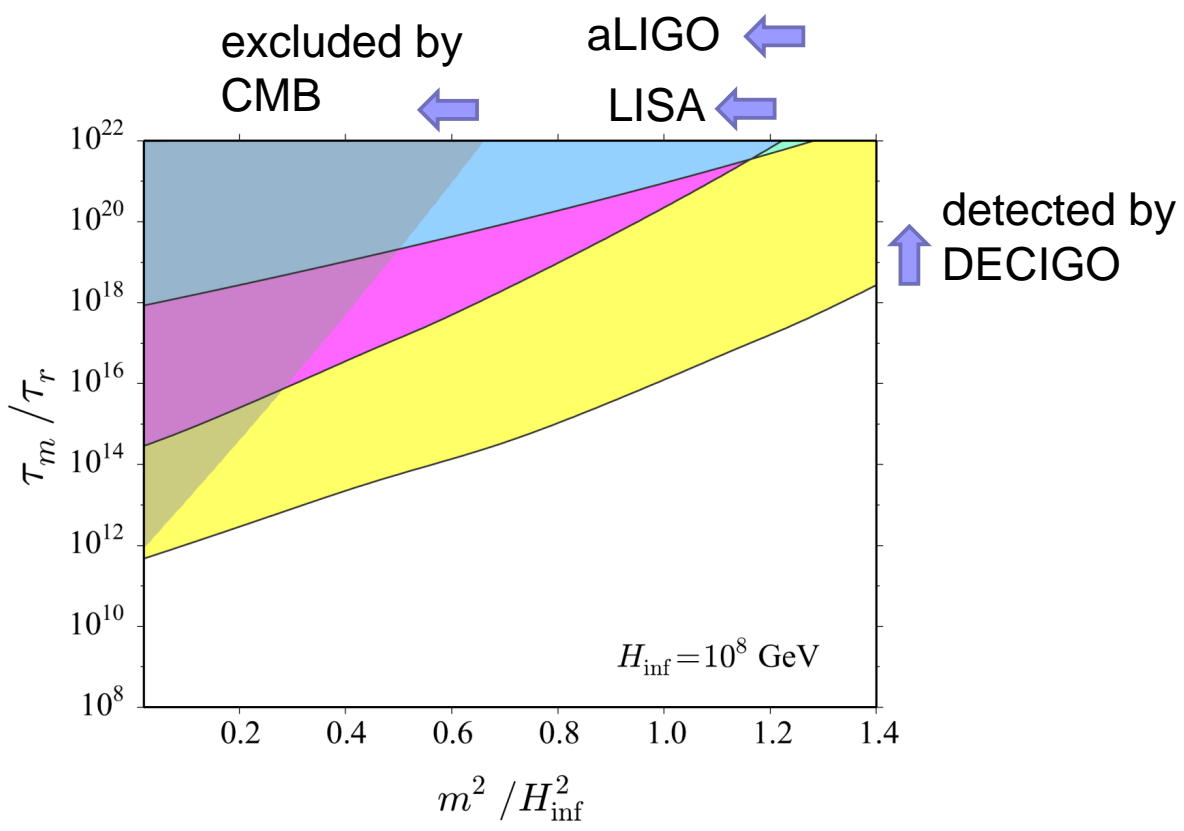
$$f \equiv \frac{k}{2\pi}$$

$$f < f_{\text{UV}}$$

\wr

$$2 \times 10^8 \left[\frac{H_{\text{inf}}}{10^{14} \text{ GeV}} \right]^{\frac{1}{2}} \text{ Hz}$$

Constraints and classifications of parameters



Conclusions

- PGWs gives information of scales different from CMB, which is very helpful to distinguish and/or constrain inflation models
- **Highly blue-tilted PGWs** can be detected by interferometers, even if their signal is not observed on the CMB scales
- There were obstacles to construct consistent theoretical model producing highly blue-tilted and detectable PGWs
- We construct **a consistent model** producing **highly blue-tilted** and **largely amplified PGWs** based on MTMG

Discussions

- Non-Gaussianity of primordial gravitational waves

Fujita, SM, Mukohyama, in preparation

- Extension of MTMG

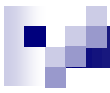
As in dRGT, μ is related with effective cosmological constant

$$\Lambda_{\text{eff}} = \frac{m_{\text{g}}^2}{2} X (c_1 X^2 + 3c_2 X + 3c_3) \quad X : \text{ratio of scale factors}$$
$$\mu^2 = \frac{m_{\text{g}}^2}{2} X \left[c_2 X + c_3 + \frac{H}{H_f} (c_1 X + c_2) \right] \quad \text{satisfying}$$
$$c_1 X^2 + 2c_2 X + c_3 = 0$$

To make c_i dynamical, one must promote them to $c_i(\phi)$

- Influence of reheating/preheating

Kuroyanagi, Lin, Sasaki, Tsujikawa, `17



Thank you very much !!

Shi Pi

Kavli Institute for the Physics and Mathematics of the Universe

**“Gravitational Waves Induced by non-Gaussian Scalar
Perturbations”**

(10+5 min.)

[JGRG28 (2018) 110715]

Gravitational Waves Induced by non-Gaussian Scalar Perturbations

Shi Pi

Kavli IPMU, University of Tokyo

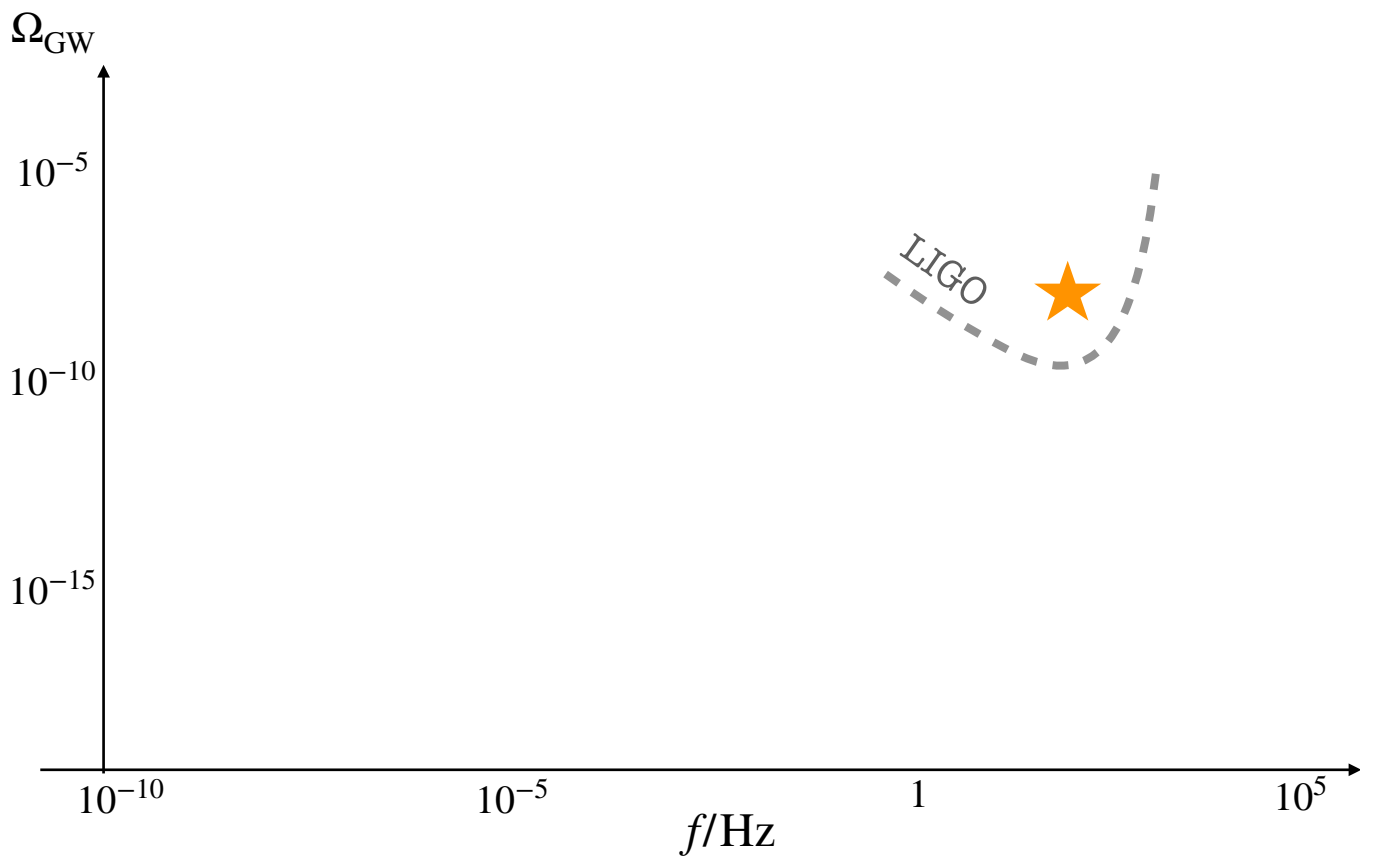
Based on arXiv:1810.11000,
with Rong-Gen Cai and Misao Sasaki

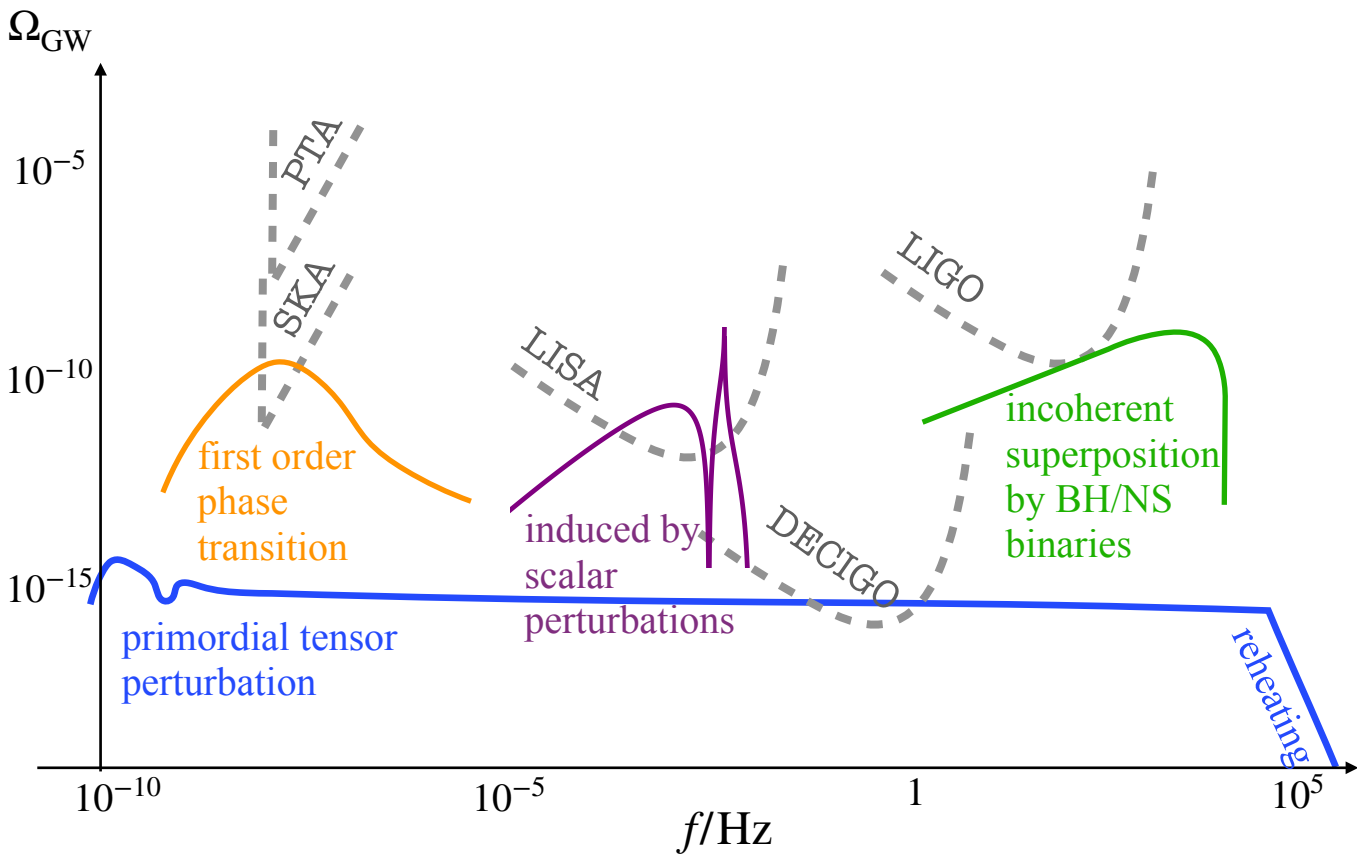
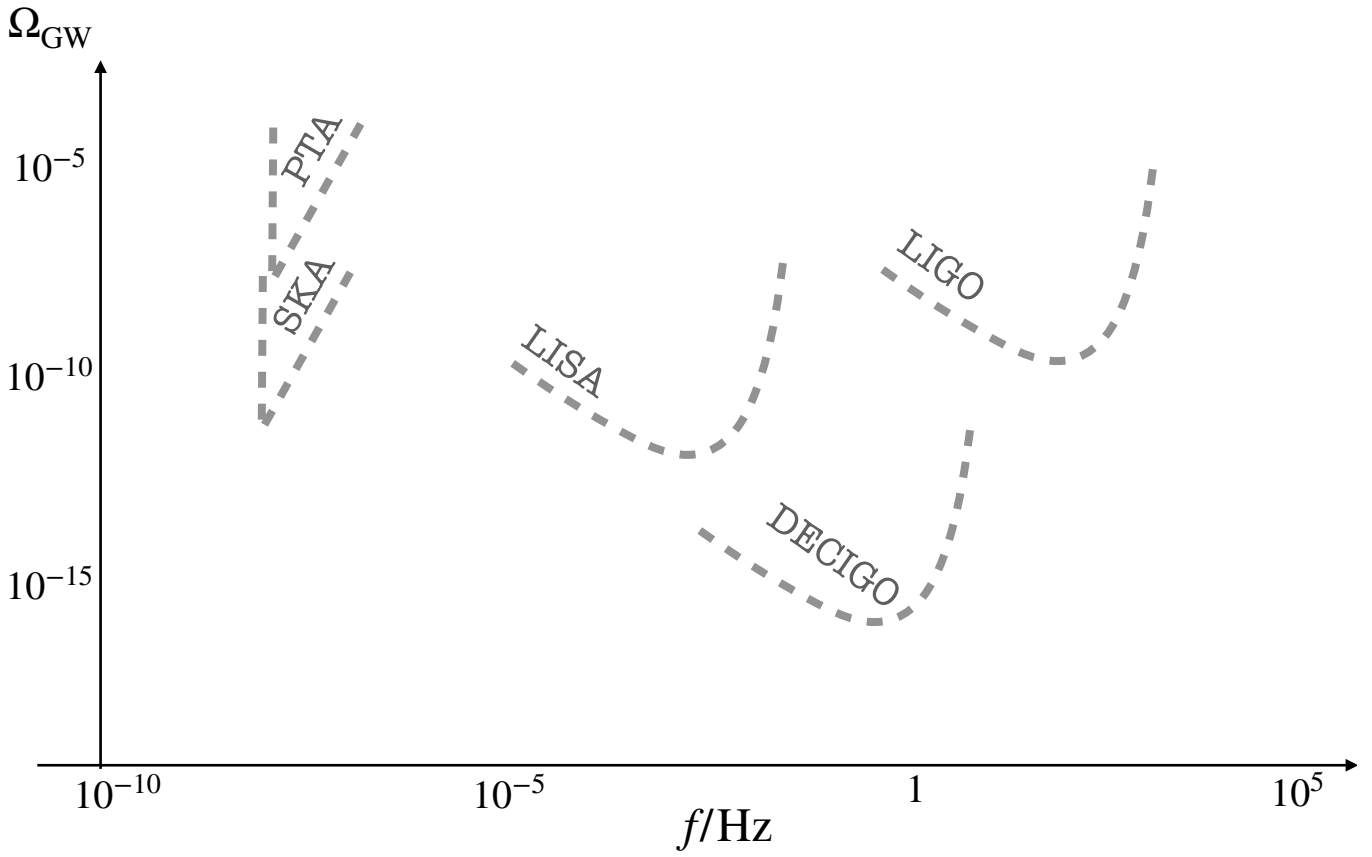
Content

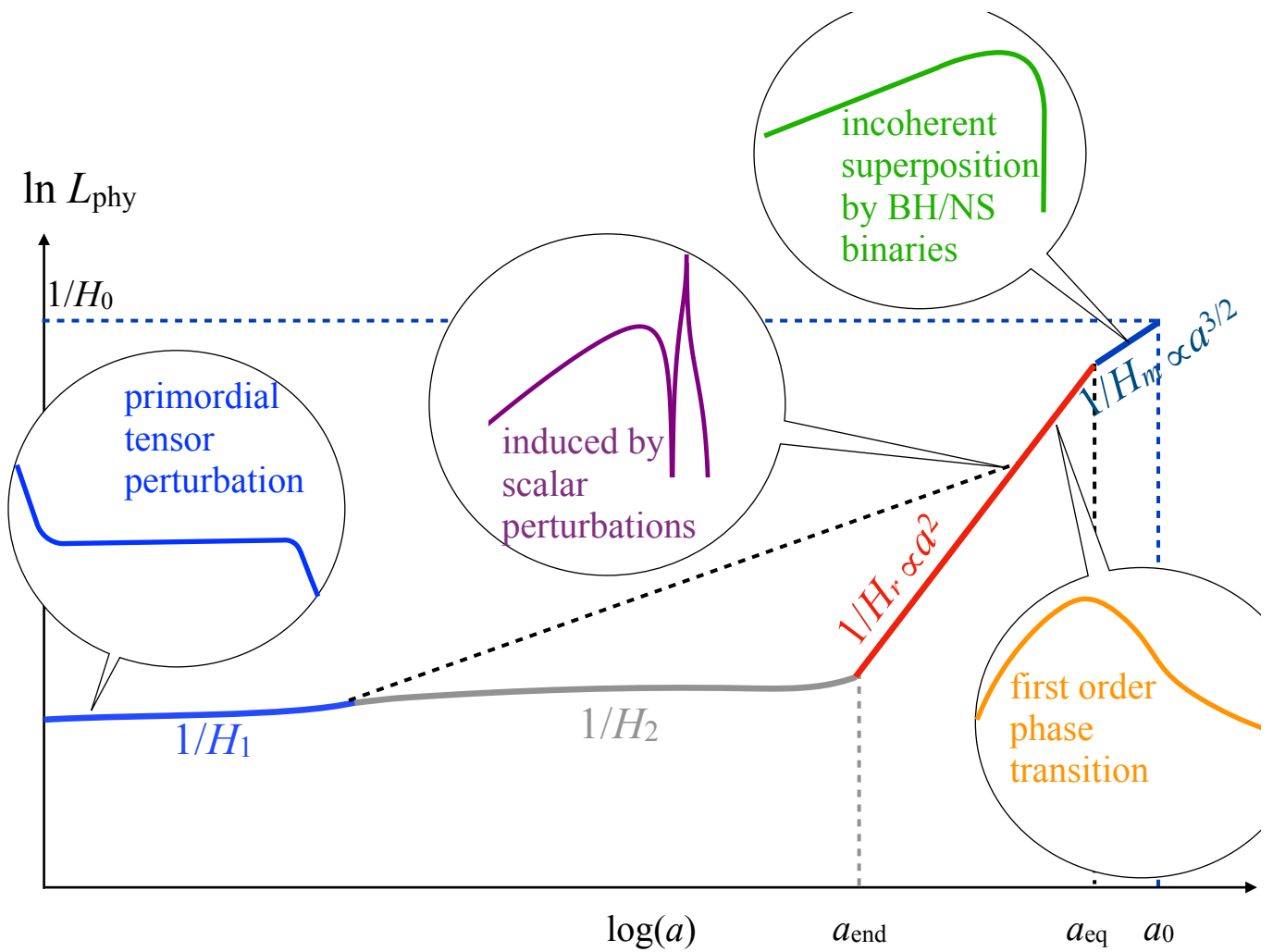
- Mechanism of SGWB
- PBH abundances
- Induced GWs: A probe for non-Gaussianity
- Conclusion

Content

- Mechanism of SGWB
- PBH abundances
- Induced GWs: A probe for non-Gaussianity
- Conclusion

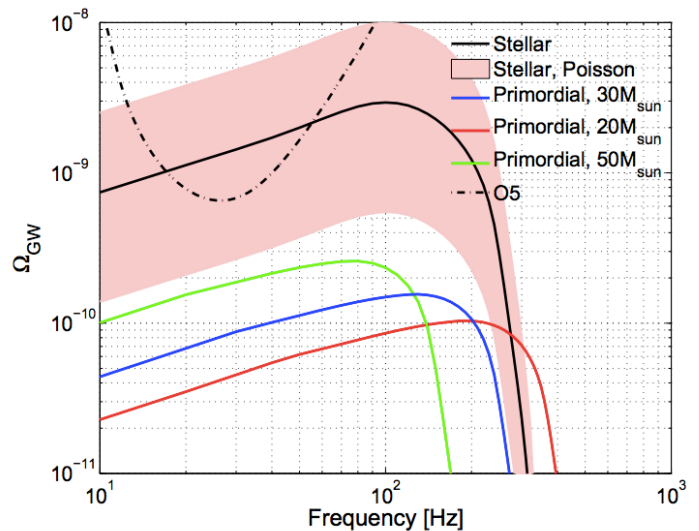






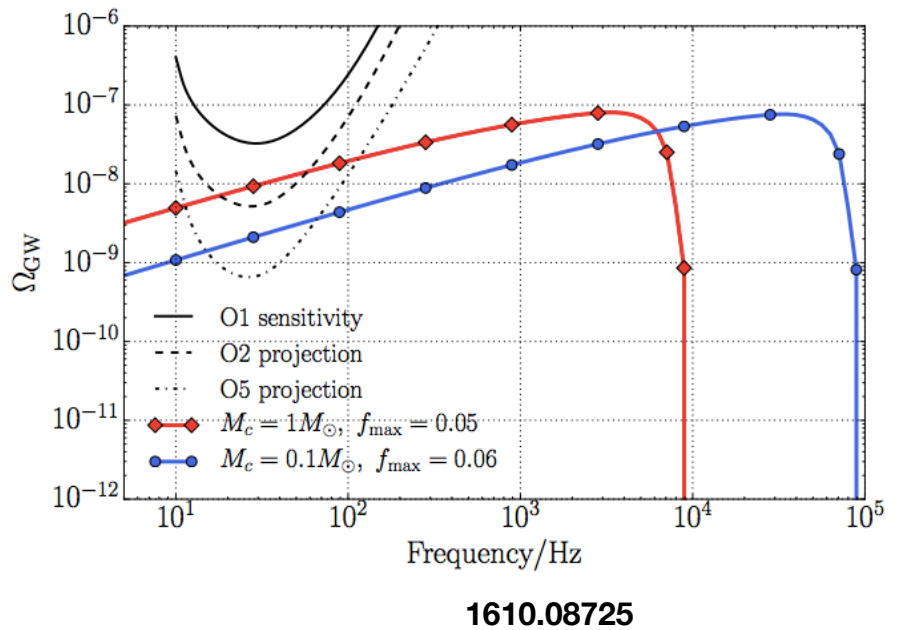
SGWB from binaries

- Origin: incoherent superposition of the GWs emitted by compact star binaries (BH, NS,...)
- Frequencies: 100 Hz (for $10M_{\odot}$)
- Amplitude: 10^{-9} Hz



SGWB from PBHB

- PBH binaries
- Frequency: 1000Hz (for $1M_{\odot}$)
- Amplitude: 10^{-9} Hz
- Can be used to constrain PBH abundances

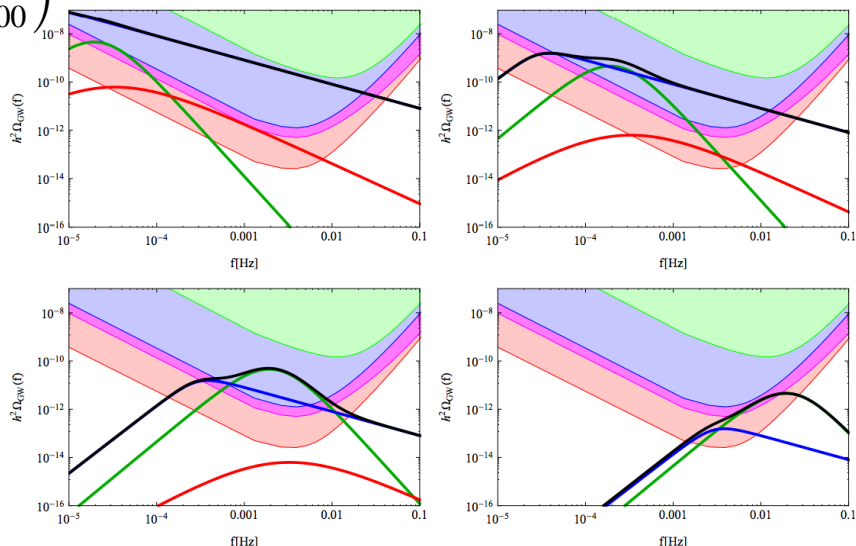


SGWB from 1OPT

$$f_{\text{peak}} \simeq 10^{-6} \text{Hz} \left(\frac{\beta}{H_*} \right) \left(\frac{T_*}{100 \text{GeV}} \right) \left(\frac{g_*}{100} \right)^{1/6}$$

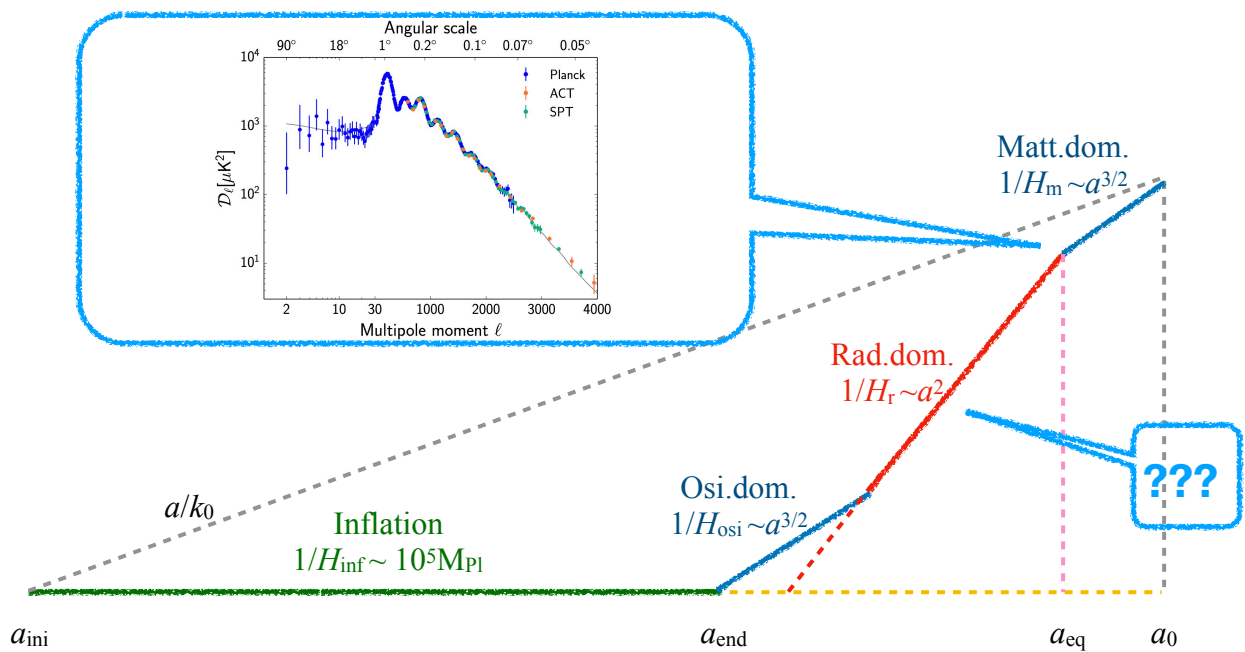
$$\Omega_{\text{peak}} h^2 \simeq 10^{-6} \left(\frac{\beta}{H_*} \right)^{-2} \left(\frac{g_*}{100} \right)^{-1/3}$$

- For $\beta/H_* \sim 100$, frequency is 10^{-4} Hz, in LISA band, but the peak is only 10^{-10} .

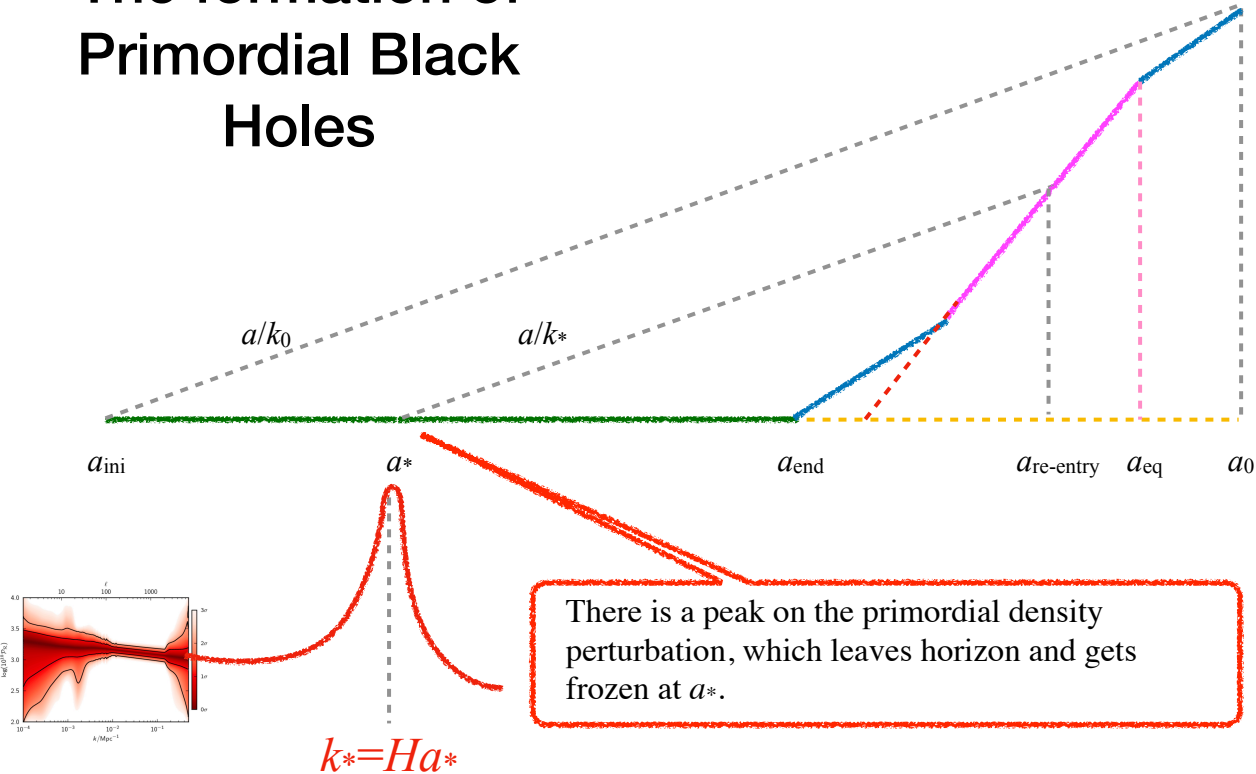


Content

- Mechanism of SGWB
- PBH abundances
- Induced GWs: A probe for non-Gaussianity
- Conclusion

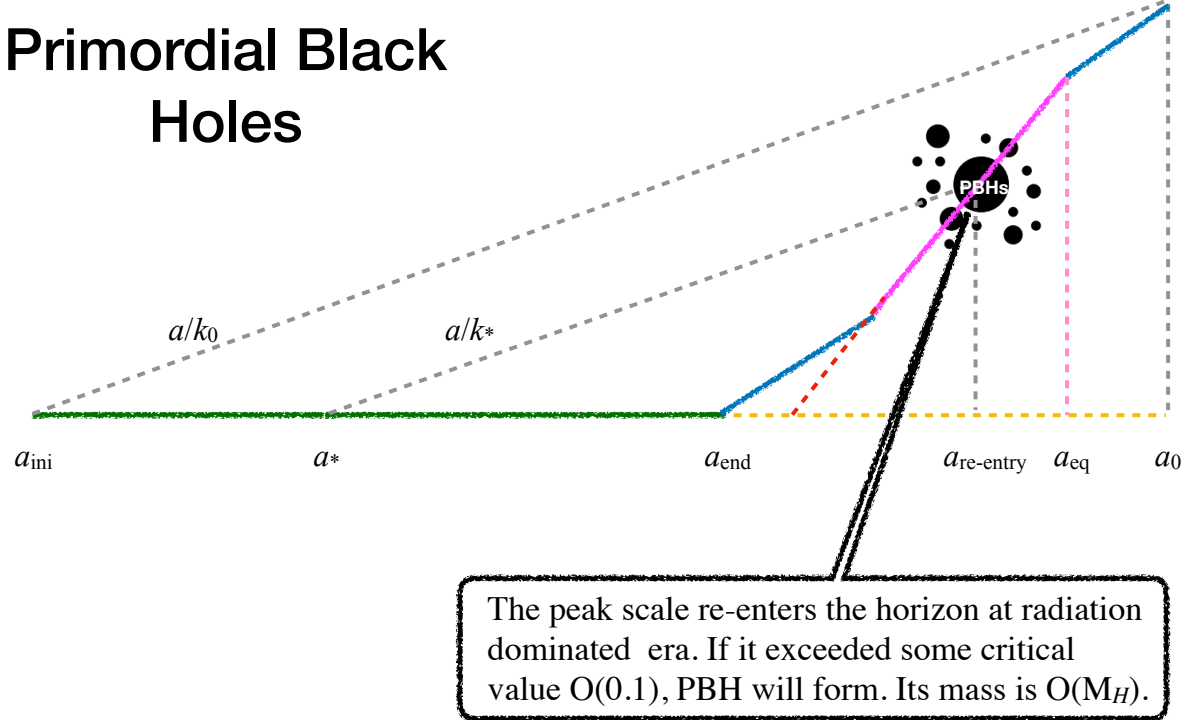


The formation of Primordial Black Holes

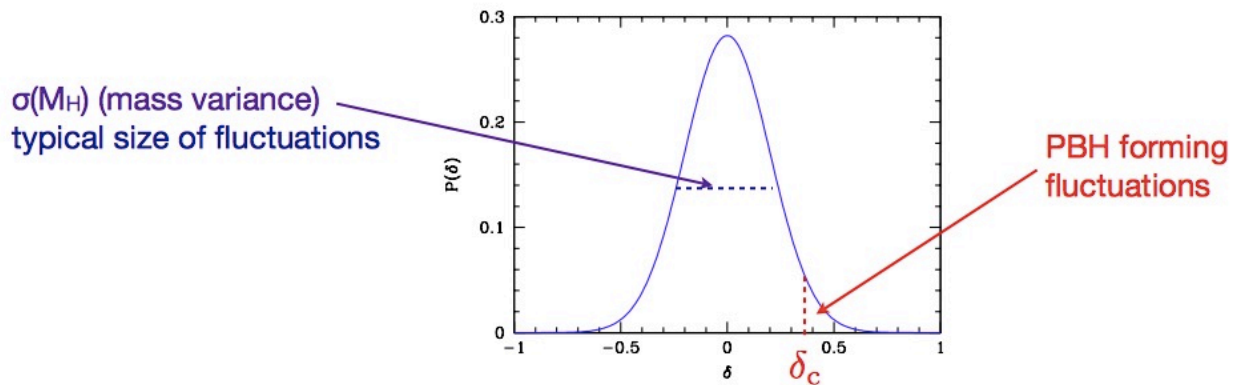


SP, Zhang, Huang & Sasaki 1712.09896

The formation of Primordial Black Holes



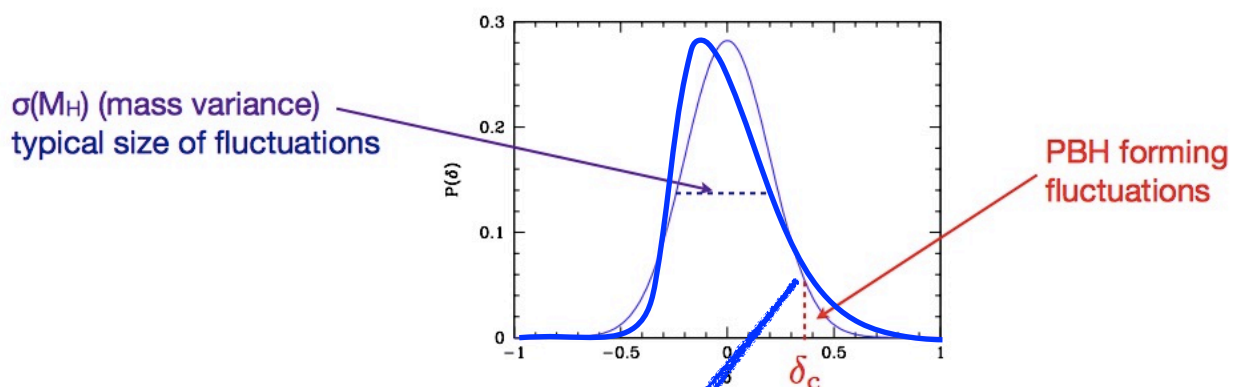
The Press-Schechter Mass Function



- When $\sigma_M \ll \delta_c$, β can be approximated by exponential:

$$\beta \approx \sqrt{\frac{2}{\pi}} \frac{\sigma_M}{\delta_c} \exp\left(-\frac{\delta_c^2}{2\sigma_M^2}\right)$$

The Press-Schechter Mass Function



Non-Gaussianity can increase ($f_{NL} > 0$) or decrease ($f_{NL} < 0$) the PBH abundances.

The Press-Schechter Mass Function

- The current PBH mass measured in critical mass is

$$\Omega_{\text{PBH}} = \beta \frac{a_{\text{eq}}}{a_{\text{re}}} = \beta \frac{a_{\text{eq}}}{a_0} \frac{a_0}{a_{\text{re}}} \simeq \beta \Omega_r (1 + z_{\text{re}}(M))$$

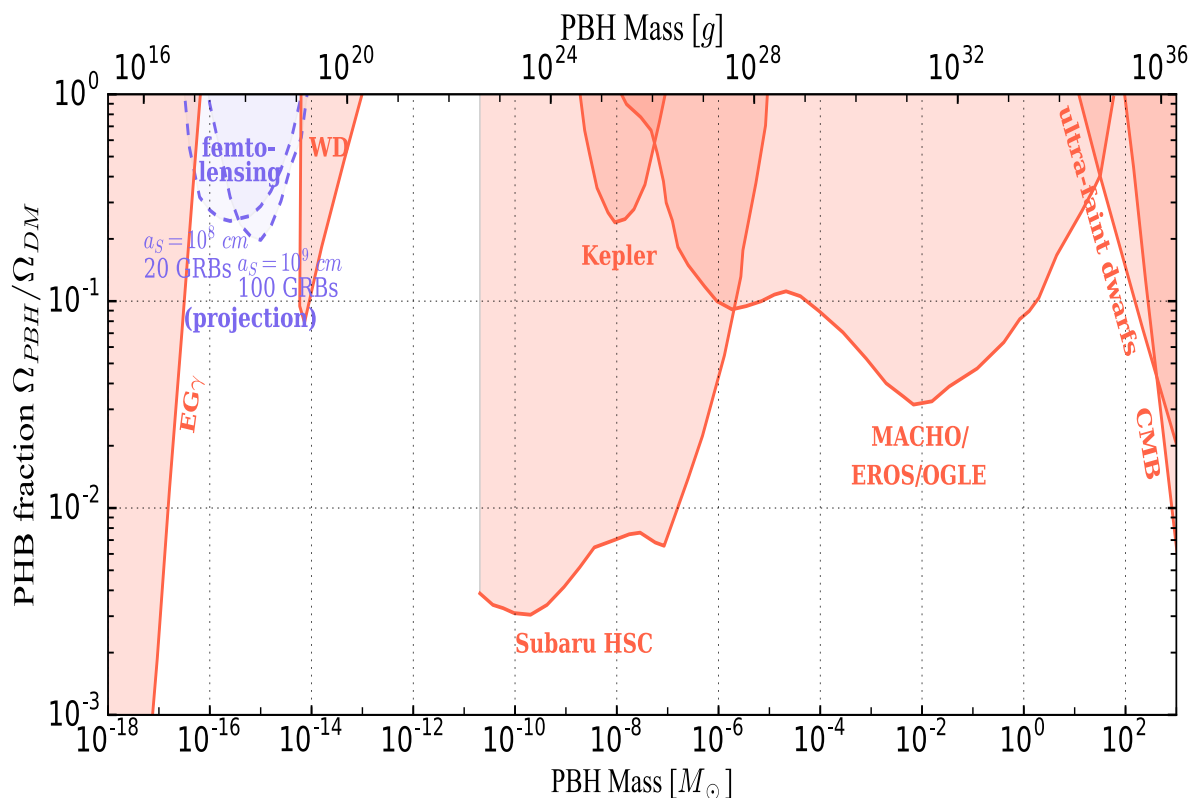
- where “eq” means equality and “re” means re-entry for the peak of the variance of the density perturbation at mass M .

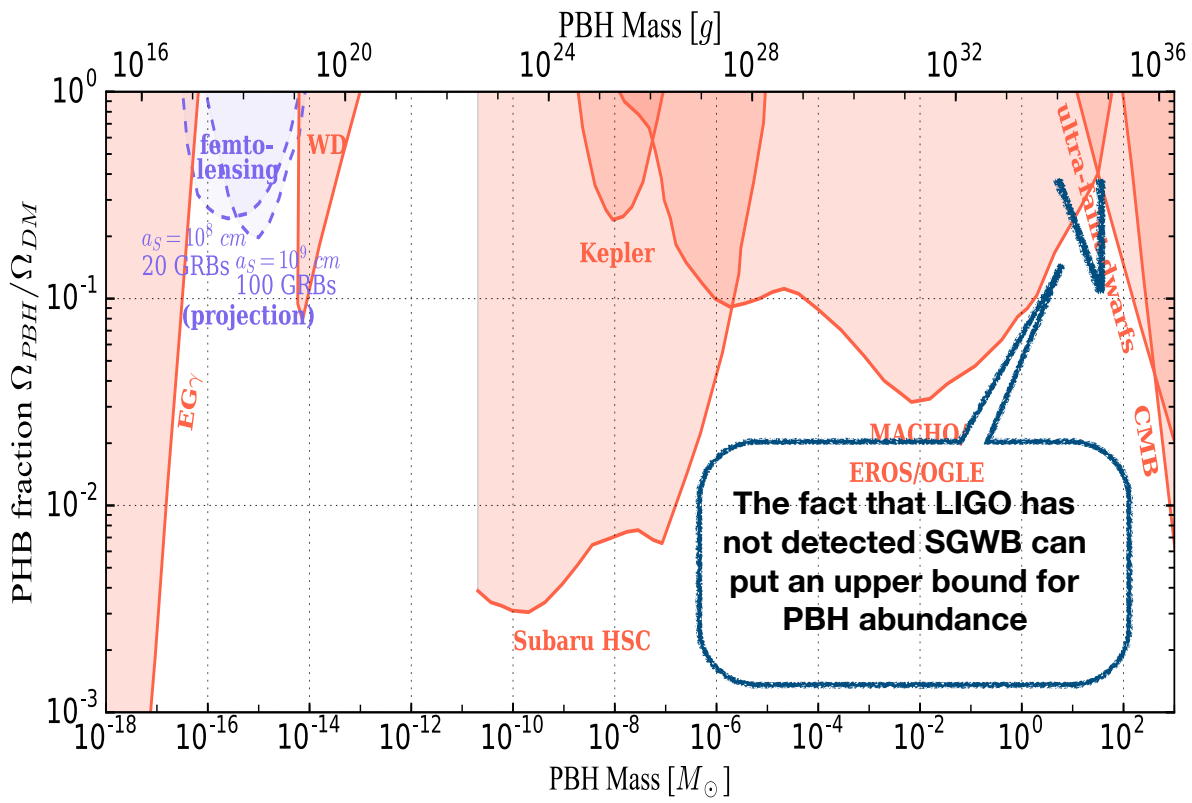
- It is easy to estimate $z(M)$ relation at horizon reentry

$$M = \frac{c^3}{GH_{\text{re}}} = \frac{c^3}{G\Omega_r^{1/2}(1+z)^2 H_0}$$

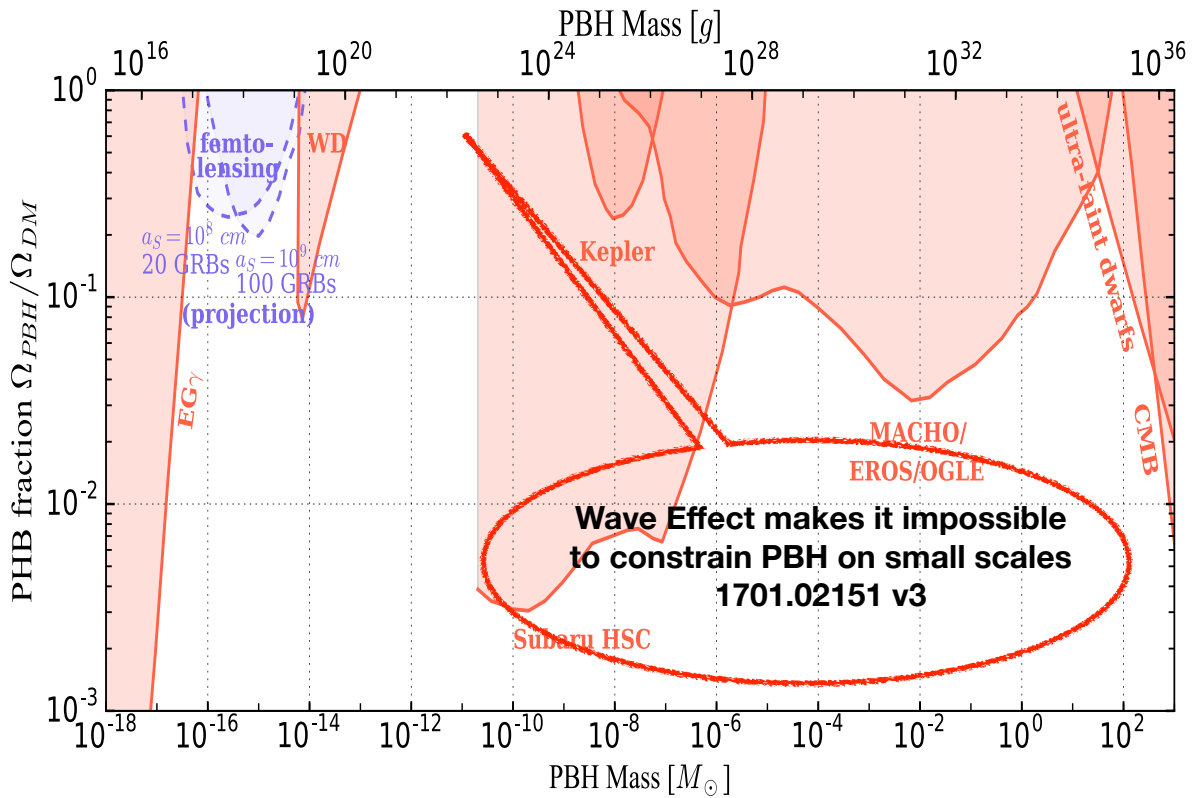
- Therefore we have

$$f \equiv \frac{\Omega_{\text{PBH}}}{\Omega_{\text{CDM}}} \approx 4.11 \times 10^8 \beta(M) \left(\frac{M}{M_\odot} \right)^{-1/2}$$

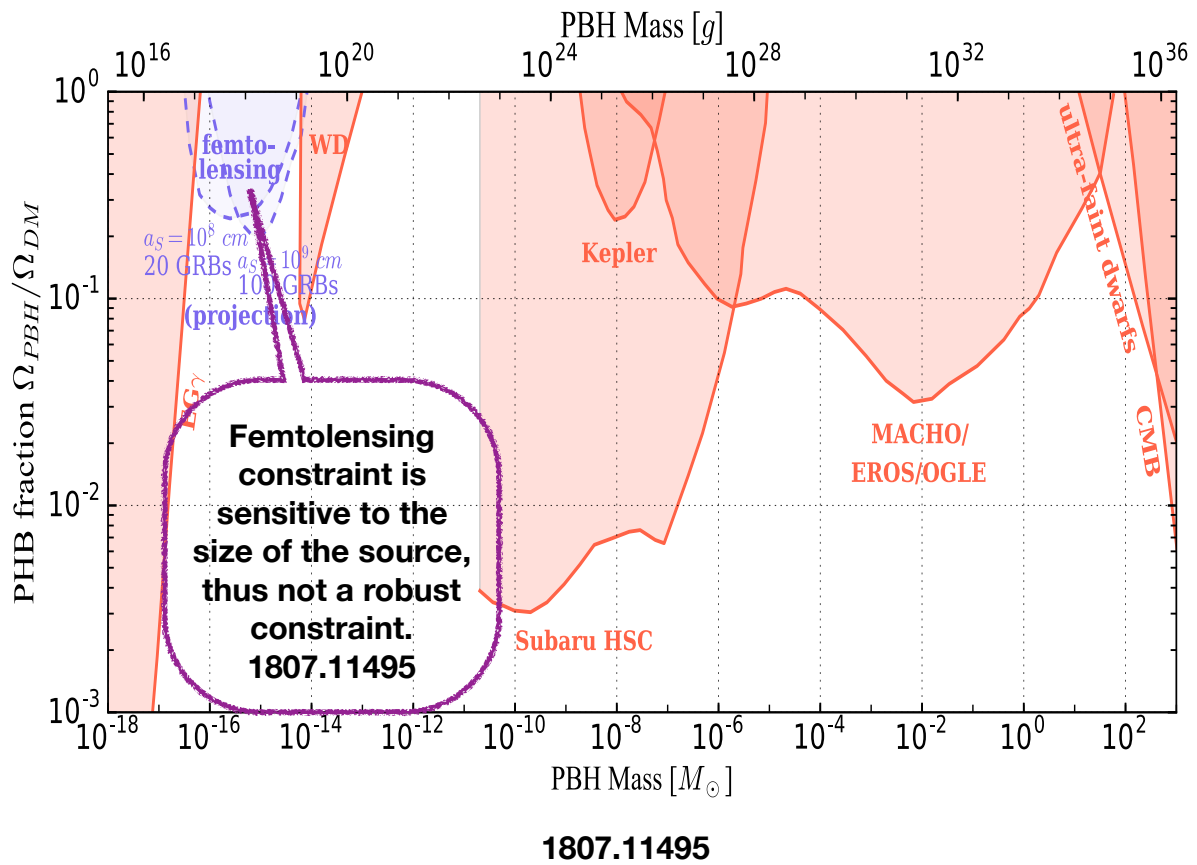




1807.11495



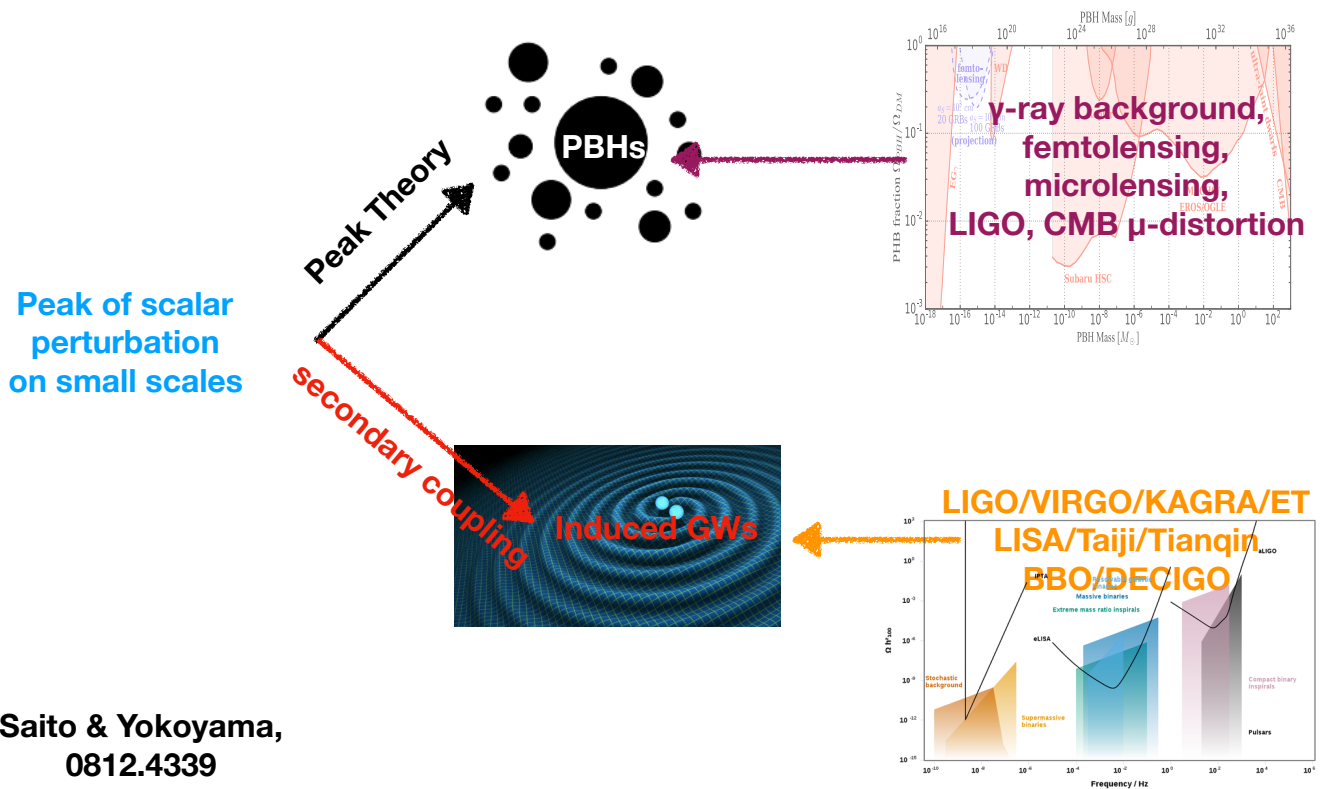
1807.11495



Content

- Mechanism of SGWB
- PBH abundances and GWs
- Induced GWs: A probe for non-Gaussianity
- Conclusion

Induced GWs



Saito & Yokoyama,
0812.4339

Induced GWs

- From the nonlinear equation of motion for the tensor perturbation

$$h''_{\mathbf{k}} + 2\mathcal{H}h'_{\mathbf{k}} + k^2 h_{\mathbf{k}} = \mathcal{S}(\mathbf{k}, \eta)$$

- where the source term is (Ananda et al. gr-qc/0612013)

$$\mathcal{S}(\mathbf{k}, \eta) = 36 \int \frac{d^3 l}{(2\pi)^{3/2}} \frac{l^2}{\sqrt{2}} \sin^2 \theta \begin{pmatrix} \cos 2\varphi \\ \sin 2\varphi \end{pmatrix} \Phi_{\mathbf{l}} \Phi_{\mathbf{k}-\mathbf{l}} \\ \times \left[j_0(ux)j_0(vx) - 2 \frac{j_1(ux)j_0(vx)}{ux} - 2 \frac{j_0(ux)j_1(vx)}{vx} + 3 \frac{j_1(ux)j_1(vx)}{uvx^2} \right].$$

- This equation can be solved by the Green function method.

Induced GWs

- The quantity we want to calculate is

$$\Omega_{\text{GW}}(k) \equiv \frac{1}{12} \left(\frac{k}{Ha} \right)^2 \frac{k^3}{\pi^2} \overline{\langle h_{\mathbf{k}}(\eta) h_{\mathbf{k}}(\eta) \rangle}.$$

- Then we know that $\Omega_{\text{GW}} \sim \langle hh \rangle \sim \langle SS \rangle \sim \langle \Phi \Phi \Phi \Phi \rangle \sim P_{\Phi}^2$.
- It is naive to believe that Φ stays Gaussian when it becomes very large on small scales.
- Therefore we want to consider the non-Gaussian scalar induced GWs (Komatsu & Spergel astro-ph/0005036)

$$\mathcal{R}(\mathbf{x}) = \mathcal{R}_g(\mathbf{x}) + F_{\text{NL}} \left[\mathcal{R}_g^2(\mathbf{x}) - \langle \mathcal{R}_g^2(\mathbf{x}) \rangle \right].$$

Induced GWs

- Then the 2pt of Φ is

$$\langle \Phi_{\mathbf{k}} \Phi_{\mathbf{p}} \rangle = (2\pi)^3 \delta^{(3)}(\mathbf{k} + \mathbf{p}) \frac{4}{9} \left(P_{\mathcal{R}}(k) + 2F_{\text{NL}}^2 \int d^3l P_{\mathcal{R}}(|\mathbf{k} - \mathbf{l}|) P_{\mathcal{R}}(l) \right).$$

- And we have to specify the power spectrum of the primordial curvature perturbation. As we mentioned, we suppose there is a narrow peak at around k^* .

$$P_{\mathcal{R}}(k) = \frac{\mathcal{A}_{\mathcal{R}}}{(2\pi)^{3/2} 2\sigma k_*^2} \exp\left(-\frac{(k - k_*)^2}{2\sigma^2}\right).$$

- Narrow means $\sigma \ll k^*$. This is for simplicity.

Induced GWs

- The result is the integral (Cai, SP & Sasaki, 1810.11000):

$$\Omega_{\text{GW}} = 6\mathcal{A}_{\mathcal{R}}^2 \frac{k^2}{2\pi\sigma^2} \left(\frac{k}{k_*}\right)^4 \int_0^\infty dv \int_{|1-v|}^{1+v} du uv \mathcal{T}(u, v)$$

$$\times \left[e^{-\frac{(vk-k_*)^2}{2\sigma^2}} + 2\mathcal{A}_{\mathcal{R}} F_{\text{NL}}^2 \frac{\sigma}{vk} \sqrt{\frac{\pi}{2}} \text{erf}\left(\frac{vk}{2\sigma}\right) \right]$$

$$\times \left[e^{-\frac{(uk-k_*)^2}{2\sigma^2}} + 2\mathcal{A}_{\mathcal{R}} F_{\text{NL}}^2 \frac{\sigma}{uk} \sqrt{\frac{\pi}{2}} \text{erf}\left(\frac{uk}{2\sigma}\right) \right].$$

$$\mathcal{T}(u, v) = \frac{1}{4} \left(\frac{4v^2 - (1 + v^2 - u^2)^2}{4uv} \right)^2 \left(\frac{u^2 + v^2 - 3}{2uv} \right)^2$$

$$\times \left\{ \left(-2 + \frac{u^2 + v^2 - 3}{2uv} \ln \left| \frac{3 - (u+v)^2}{3 - (u-v)^2} \right| \right)^2 \right.$$

$$\left. + \pi^2 \left(\frac{u^2 + v^2 - 3}{2uv} \right)^2 \Theta(u + v - \sqrt{3}) \right\}.$$

Induced GWs

- Then the result is the integral:

$$\Omega_{\text{GW}} = 6\mathcal{A}_{\mathcal{R}}^2 \frac{k^2}{2\pi\sigma^2} \left(\frac{k}{k_*}\right)^4 \int_0^\infty dv \int_{|1-v|}^{1+v} du uv \mathcal{T}(u, v)$$

$$\times \left[e^{-\frac{(vk-k_*)^2}{2\sigma^2}} + 2\mathcal{A}_{\mathcal{R}} F_{\text{NL}}^2 \frac{\sigma}{vk} \sqrt{\frac{\pi}{2}} \text{erf}\left(\frac{vk}{2\sigma}\right) \right]$$

$$\times \left[e^{-\frac{(uk-k_*)^2}{2\sigma^2}} + 2\mathcal{A}_{\mathcal{R}} F_{\text{NL}}^2 \frac{\sigma}{uk} \sqrt{\frac{\pi}{2}} \text{erf}\left(\frac{uk}{2\sigma}\right) \right].$$

$$\mathcal{T}(u, v) = \frac{1}{4} \left(\frac{4v^2 - (1 + v^2 - u^2)^2}{4uv} \right)^2 \left(\frac{u^2 + v^2 - 3}{2uv} \right)^2$$

$$\times \left\{ \left(-2 + \frac{u^2 + v^2 - 3}{2uv} \ln \left| \frac{3 - (u+v)^2}{3 - (u-v)^2} \right| \right)^2 \right.$$

$$\left. + \pi^2 \left(\frac{u^2 + v^2 - 3}{2uv} \right)^2 \Theta(u + v - \sqrt{3}) \right\}.$$

Saito & Yokoyama,
0812.4339

Kohri & Tareda,
1804.08577

Induced GWs

non-Gaussian contributions

- Then the result is the integral:

$$\Omega_{\text{GW}} = 6\mathcal{A}_{\mathcal{R}}^2 \frac{k^2}{2\pi\sigma^2} \left(\frac{k}{k_*}\right)^4 \int_0^\infty dv \int_{|1-v|}^{1+v} du uv \mathcal{T}(u, v)$$

Saito & Yokoyama,
0812.4339

$$\times \left[e^{-\frac{(vk-k_*)^2}{2\sigma^2}} + 2\mathcal{A}_{\mathcal{R}} F_{\text{NL}}^2 \frac{\sigma}{vk} \sqrt{\frac{\pi}{2}} \text{erf}\left(\frac{vk}{2\sigma}\right) \right]$$

$$\times \left[e^{-\frac{(uk-k_*)^2}{2\sigma^2}} + 2\mathcal{A}_{\mathcal{R}} F_{\text{NL}}^2 \frac{\sigma}{uk} \sqrt{\frac{\pi}{2}} \text{erf}\left(\frac{uk}{2\sigma}\right) \right]$$

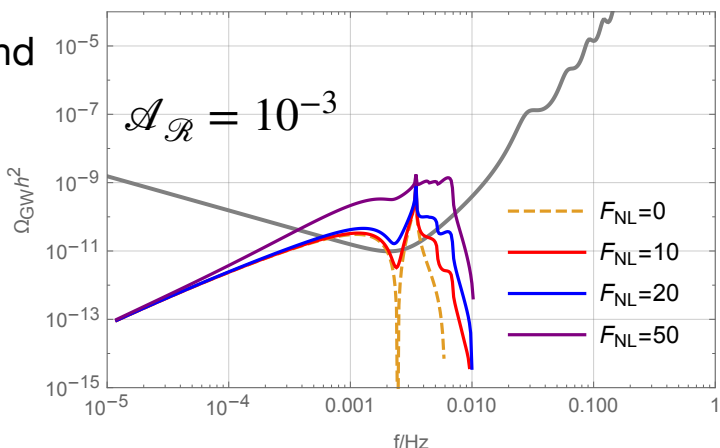
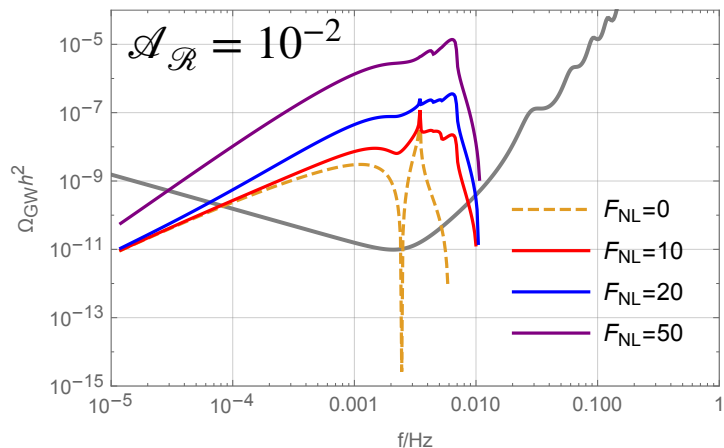
Kohri & Tareda,
1804.08577

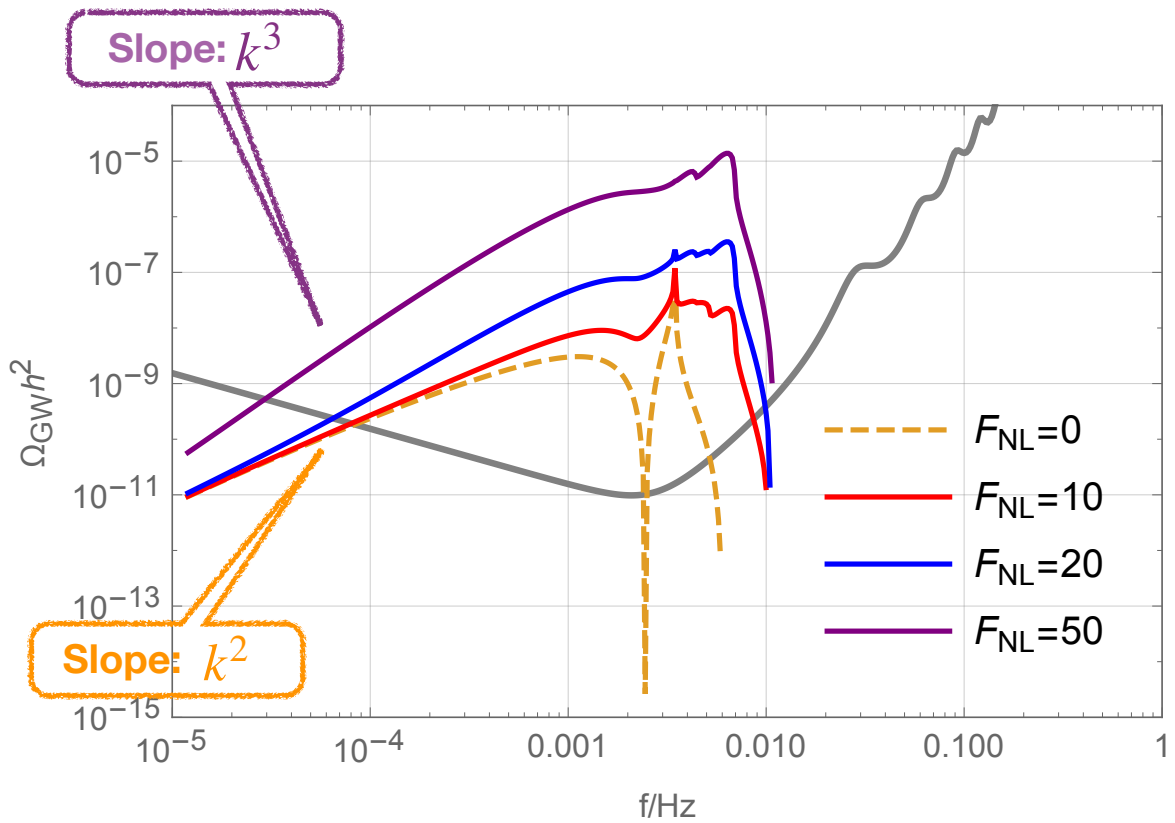
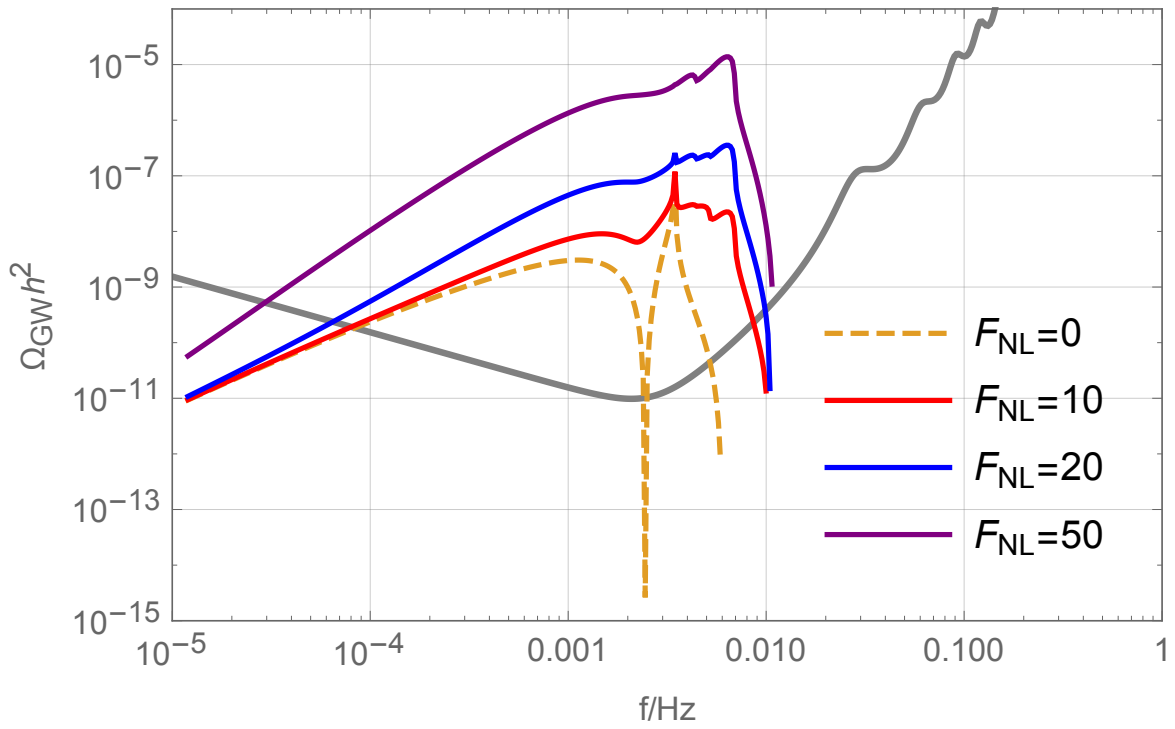
$$\mathcal{T}(u, v) = \frac{1}{4} \left(\frac{4v^2 - (1 + v^2 - u^2)^2}{4uv} \right)^2 \left(\frac{u^2 + v^2 - 3}{2uv} \right)^2$$

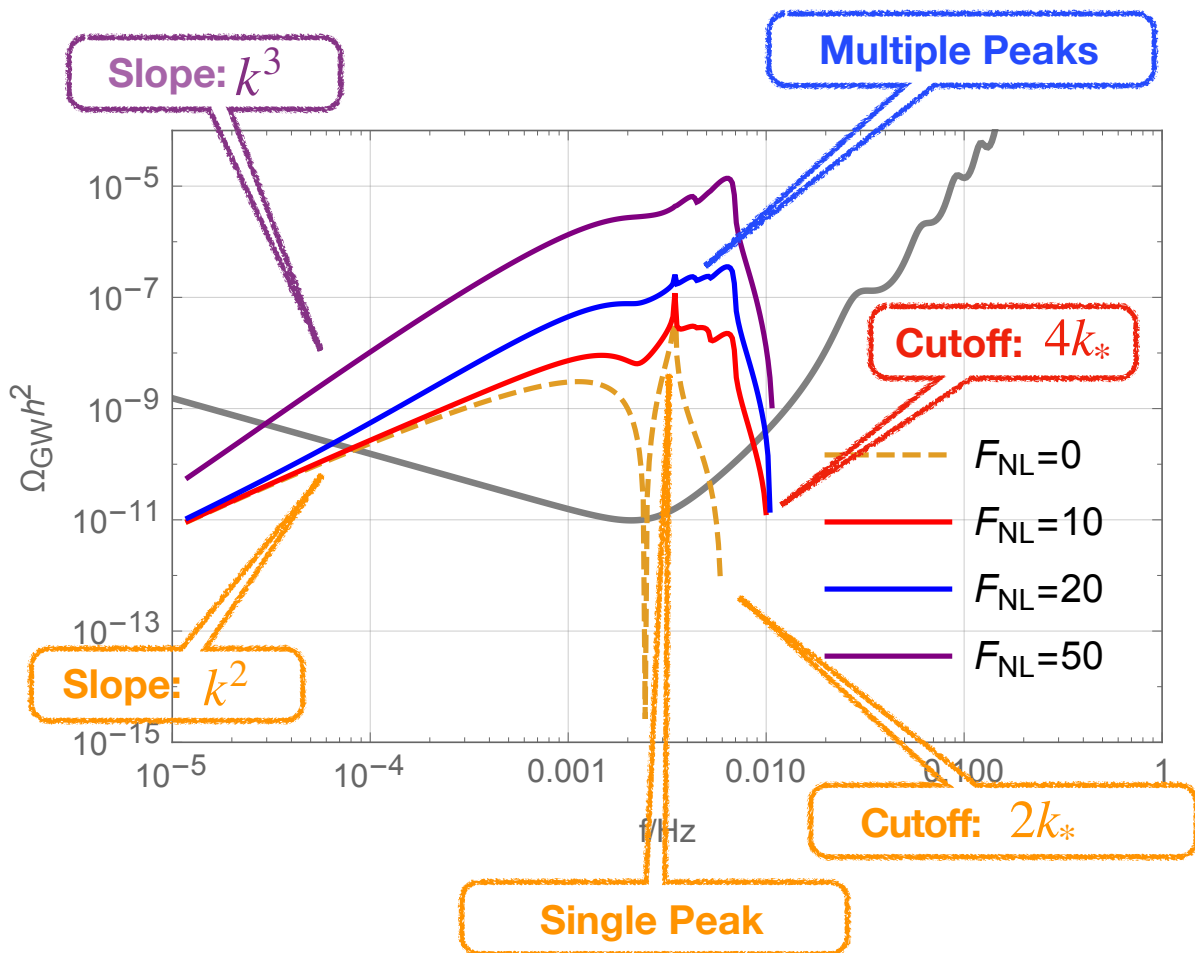
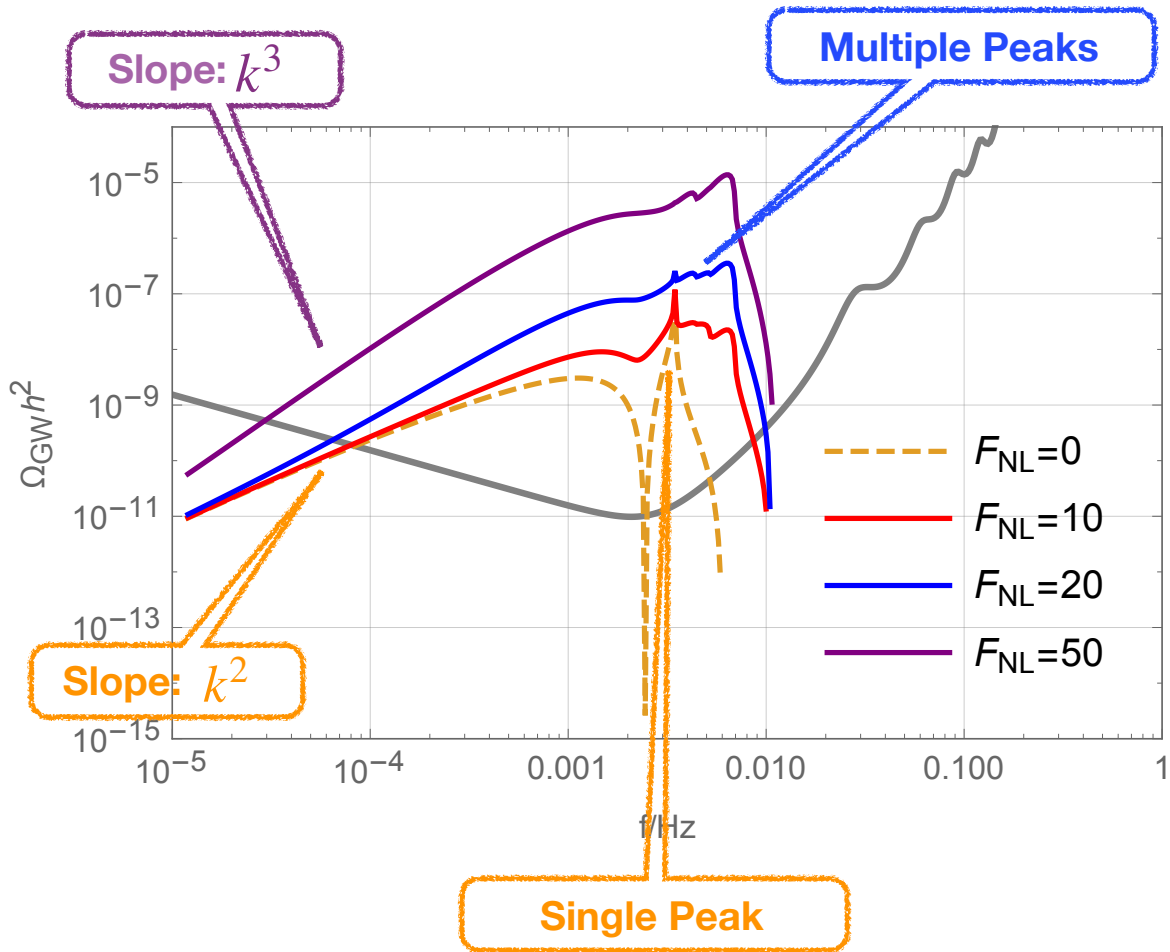
$$\times \left\{ \left(-2 + \frac{u^2 + v^2 - 3}{2uv} \ln \left| \frac{3 - (u+v)^2}{3 - (u-v)^2} \right| \right)^2 \right.$$

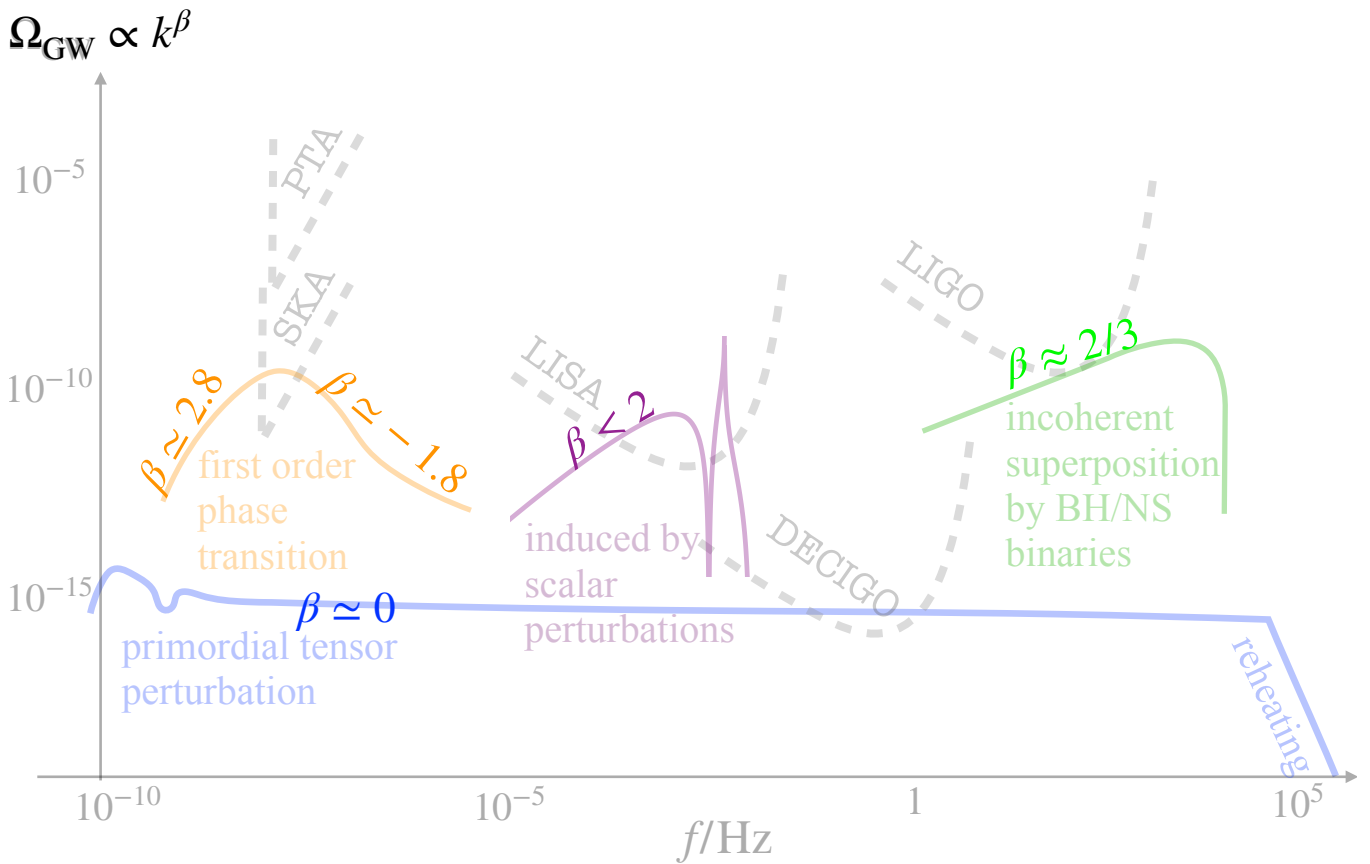
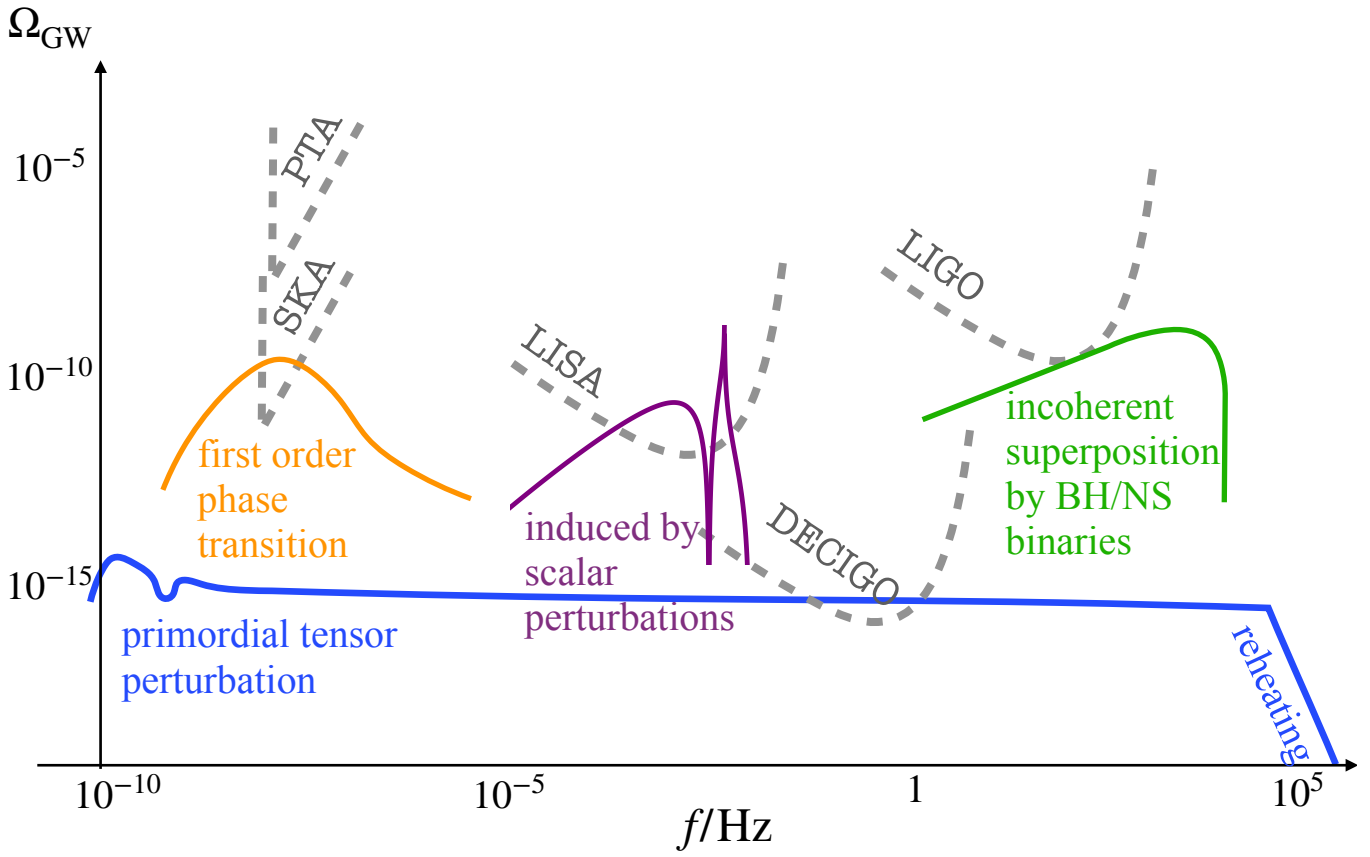
$$\left. + \pi^2 \left(\frac{u^2 + v^2 - 3}{2uv} \right)^2 \Theta(u + v - \sqrt{3}) \right\}.$$

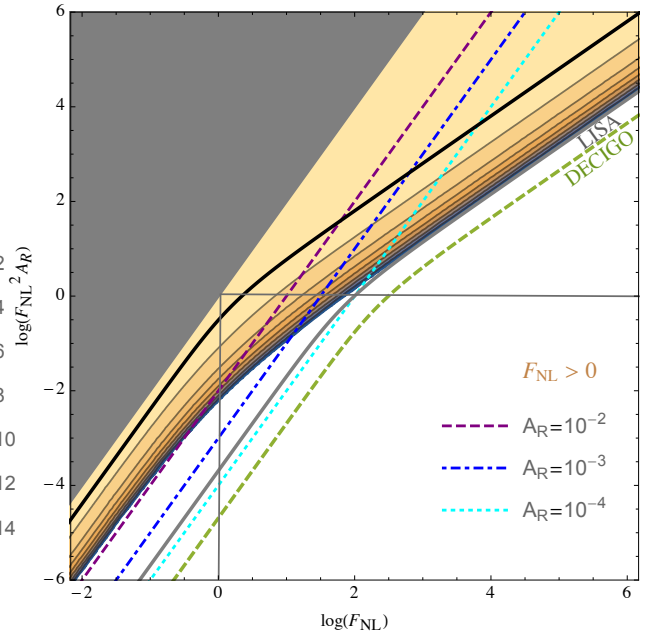
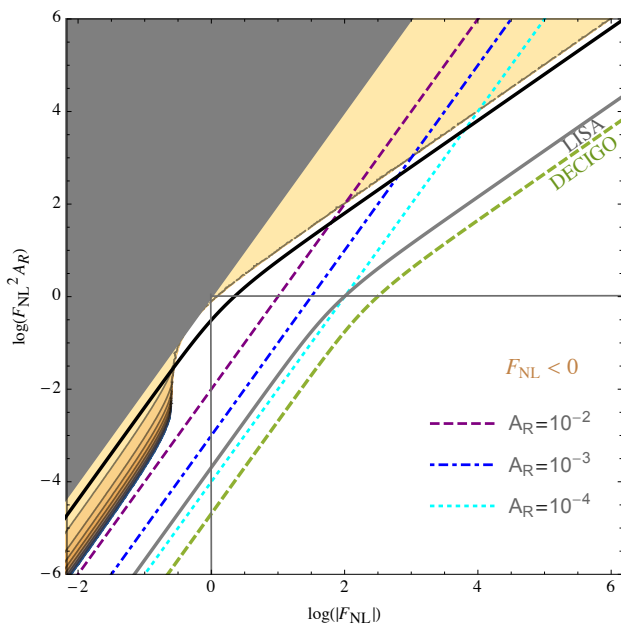
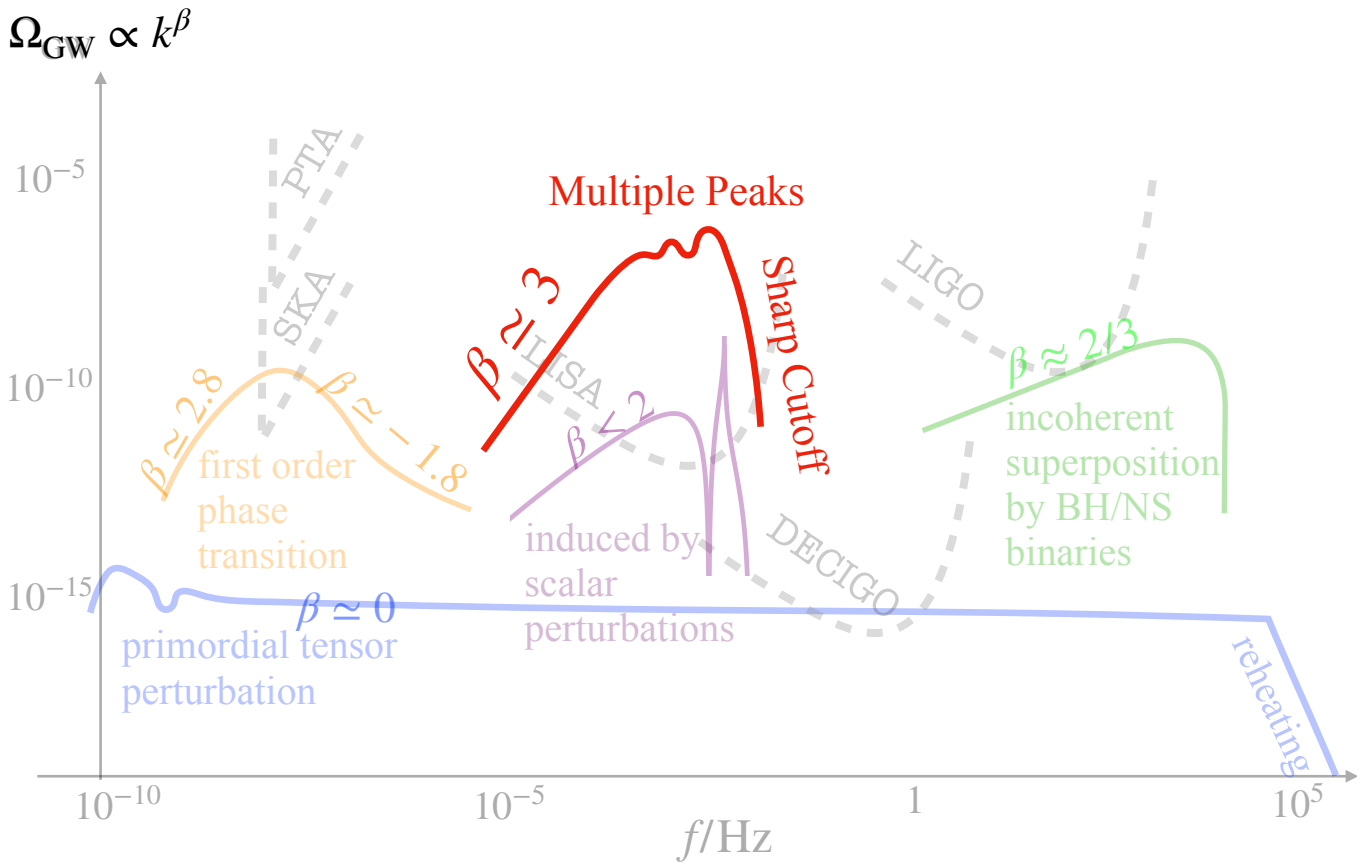
- Up: $\mathcal{A}_{\mathcal{R}} = 10^{-2}$
- Down: $\mathcal{A}_{\mathcal{R}} = 10^{-3}$
- Gray curve: LISA
- Frequency:
PBH window \leftrightarrow LISA band
- Coincidence, but fortunate for our universe.



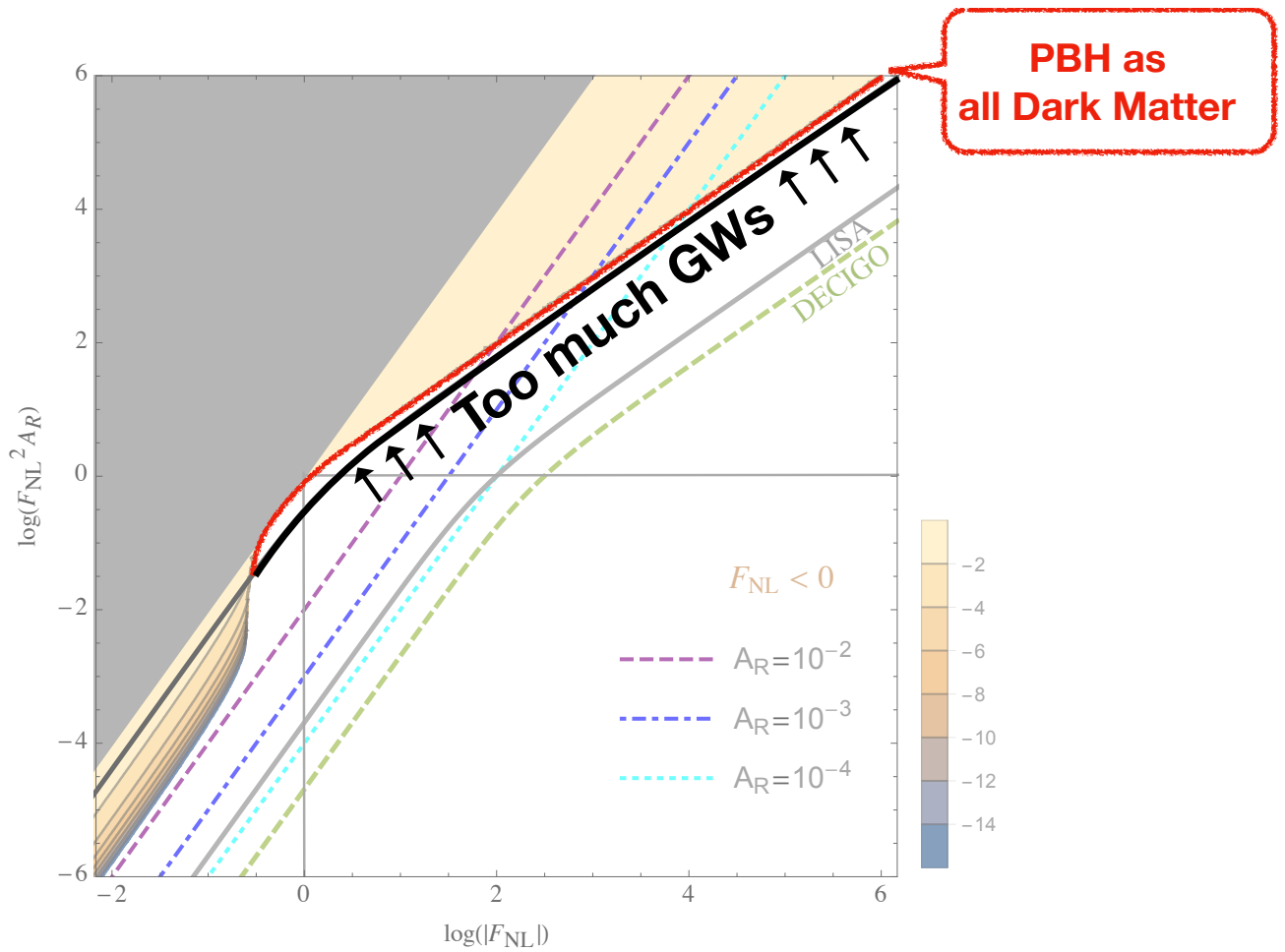
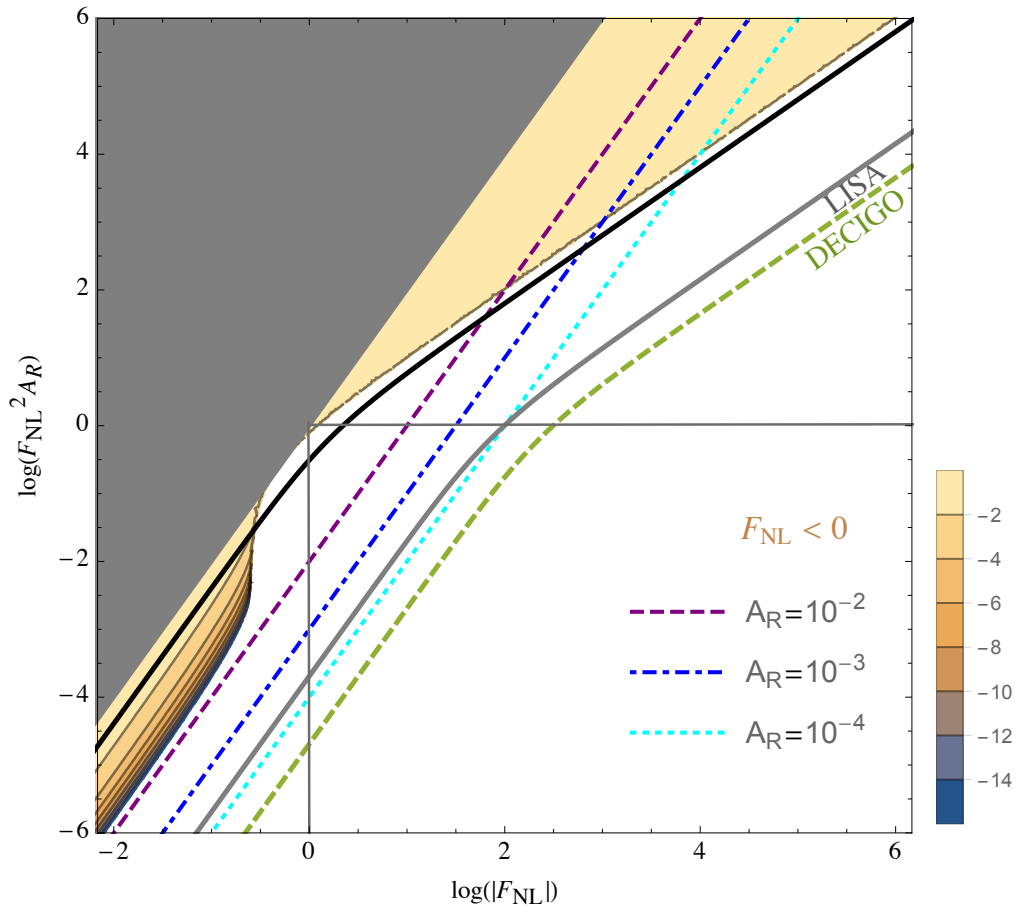


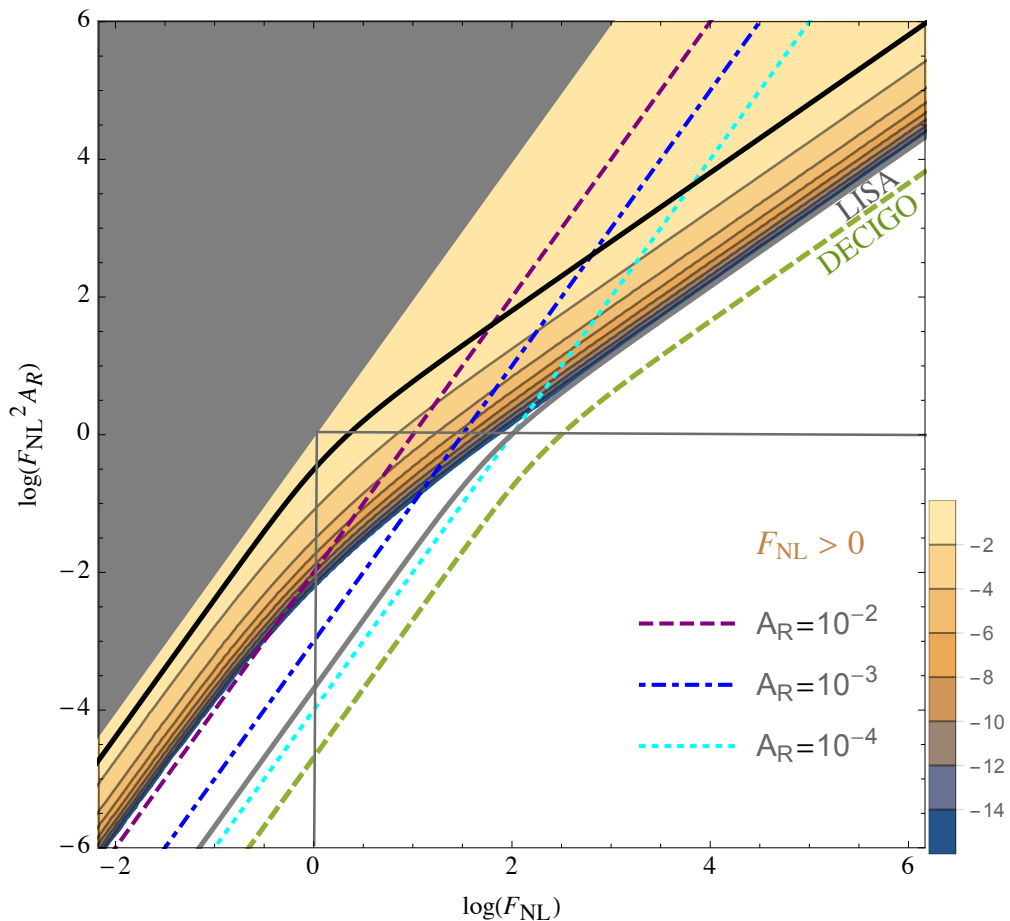
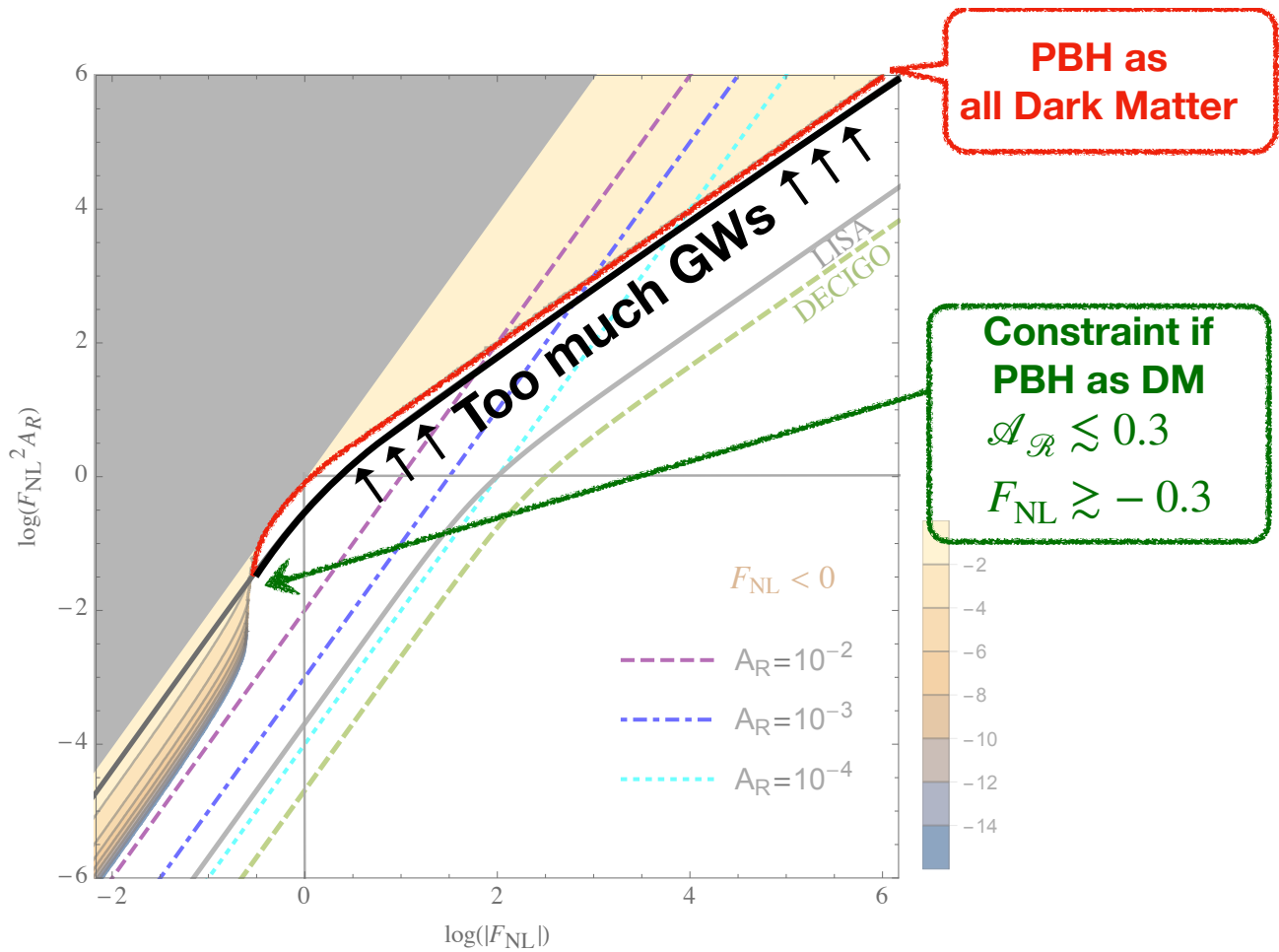


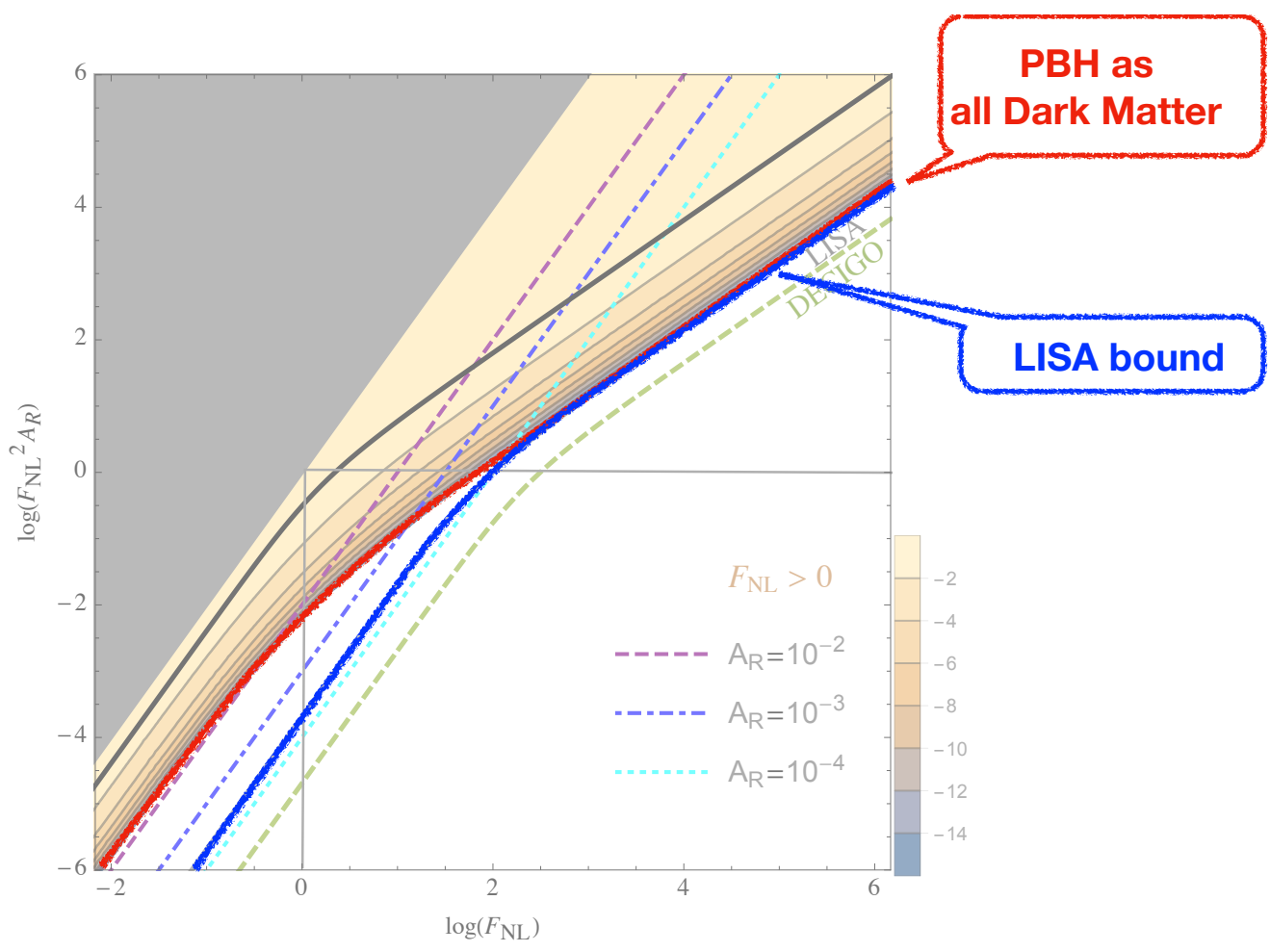
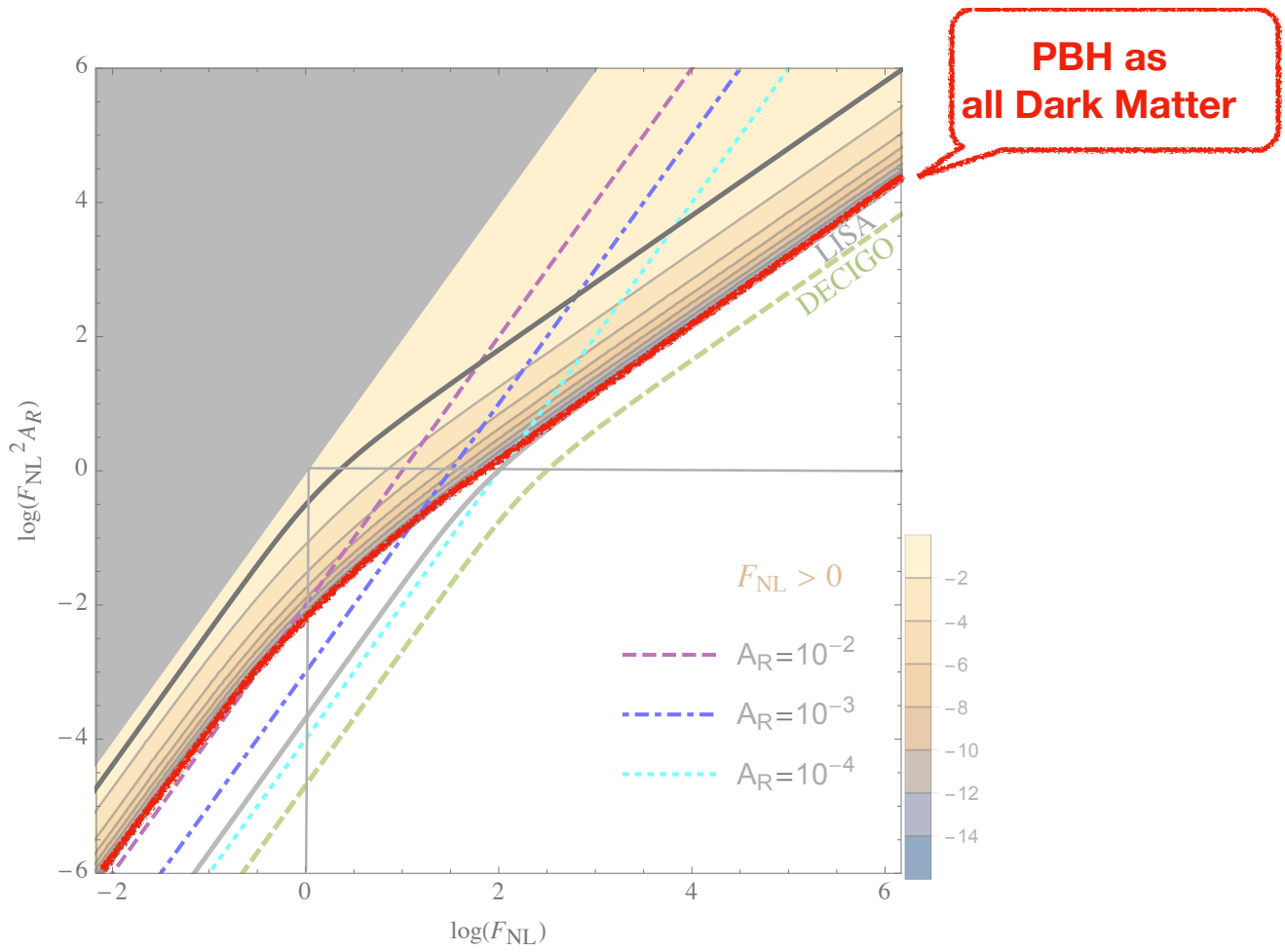


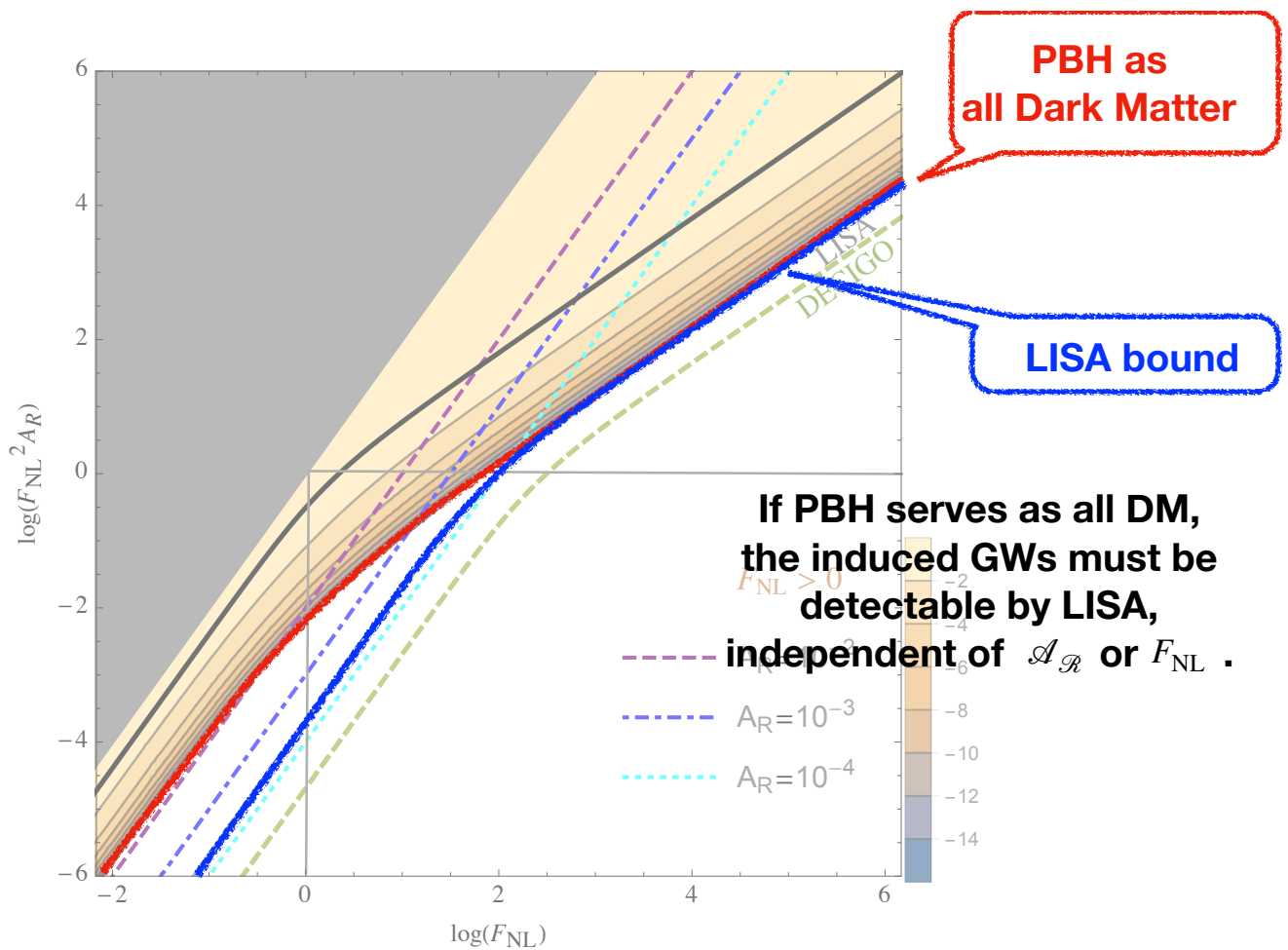


- Frequency: 0.003 Hz









Summary

- Induced GW is a very important source of SGWB.
- GWs induced by non-Gaussian scalar perturbations: k^3 -slope, multiple peaks, cutoff.
- If PBHs can serve as all the DM, induced GWs must be detectable by LISA, no matter how small \mathcal{A}_R or f_{NL} is.

Thank you!

Yuki Niiyama

Hirosaki University

**“Energy density of tensor perturbations in Einstein-Weyl
gravity and its application to primordial gravitational waves”**
(10+5 min.)

[JGRG28 (2018) 110717]

Energy density of tensor perturbation in Einstein-Weyl gravity and its application to primordial gravitational waves

Yuki Niyama (Hirosaki U.)

Collaborator

Nathalie Deruelle (Université Paris 7)

Yu Furuya, Yuuiti Sendouda (Hirosaki U.)

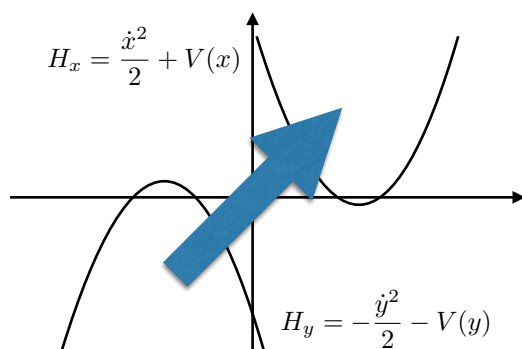
■ Introduction

1/10

- Consider Einstein-Weyl gravity whose action is

$$S[g] = \frac{1}{2\kappa} \int d^4x \sqrt{-g} \left[R - \frac{\gamma}{2} C_{\mu\nu\rho\sigma} C^{\mu\nu\rho\sigma} \right] \quad \begin{array}{l} \kappa = 8\pi G, \quad c = 1 \\ \gamma : \text{coupling constant} \end{array}$$

- A motivation to add such quadratic curvature terms is from renormalization of quantum field theory [1,2].
- There exist massless and massive spin-2 DOFs in Minkowski space, but the massive ones are ghost [3], which is thought to lead to instabilities when interacting with the other non-ghost fields [4].



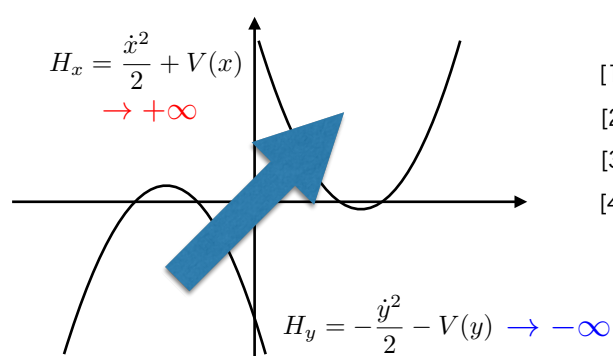
- [1] G. 't Hooft et al., Ann. Inst. Henri. Poincaré(1974)
- [2] K. S. Stelle, Phys. Rev. D16(1977)
- [3] K. S. Stelle, Gen. Rel. Grav. 9(1978)
- [4] A. Pais and G. E. Uhlenbeck, Phys. Rev. 79(1950)

■ Introduction

- Consider Einstein-Weyl gravity whose action is

$$S[g] = \frac{1}{2\kappa} \int d^4x \sqrt{-g} \left[R - \frac{\gamma}{2} C_{\mu\nu\rho\sigma} C^{\mu\nu\rho\sigma} \right] \quad \begin{array}{l} \kappa = 8\pi G, \quad c = 1 \\ \gamma : \text{coupling constant} \end{array}$$

- A motivation to add such quadratic curvature terms is from renormalization of quantum field theory [1,2].
- There exist massless and massive spin-2 DOFs in Minkowski space, but the massive ones are ghost [3], which is thought to lead to instabilities when interacting with the other non-ghost fields [4].



[1] G. 't Hooft et al., Ann. Inst. Henri. Poincaré(1974)

[2] K. S. Stelle, Phys. Rev. D16(1977)

[3] K. S. Stelle, Gen. Rel. Grav. 9(1978)

[4] A. Pais and G. E. Uhlenbeck, Phys. Rev. 79(1950)

■ Introduction

- This theory should be tested by observations, quantitatively.
- As a first step, we concentrate on the classical theory.
- The two DOFs are decoupled at linear level on Minkowski [3] and de Sitter background [5], so they are harmless on these background.
- What happens in the case that two DOFs are coupled each other has not been clarified so far on, e.g., the decelerated universe.
- In this talk, we show how the two primordial gravitational waves (PGWs), massless and massive DOFs, can contribute to the cosmic expansion as energy components.

[5] T. Clunan and M. Sasaki, Class. Quant. Grav. 27(2010)

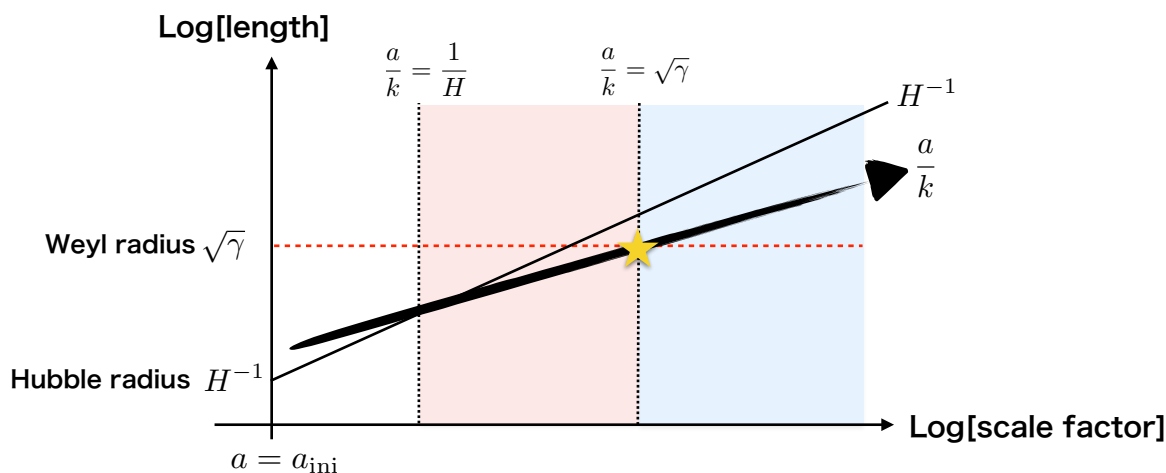
■ Setup and assumptions

- Consider the tensor perturbation h_{ij} on the flat FLRW metric:

$$ds^2 = a^2(\tau)[-d\tau^2 + (\delta_{ij} + h_{ij})dx^i dx^j]$$

$$a : \text{scale factor} \quad \mathcal{T} : \text{conformal time} \quad \delta^{ij} h_{ij} = 0 = \partial^j h_{ij}$$

- Introduce the Weyl radius, $\sqrt{\gamma}$, and assume $\sqrt{\gamma} \gg H_{\text{ini}}^{-1}$.
- The modes, with physical wavelength $\frac{a}{k}$, cross with the Weyl radius $\sqrt{\gamma}$ after entering the horizon.



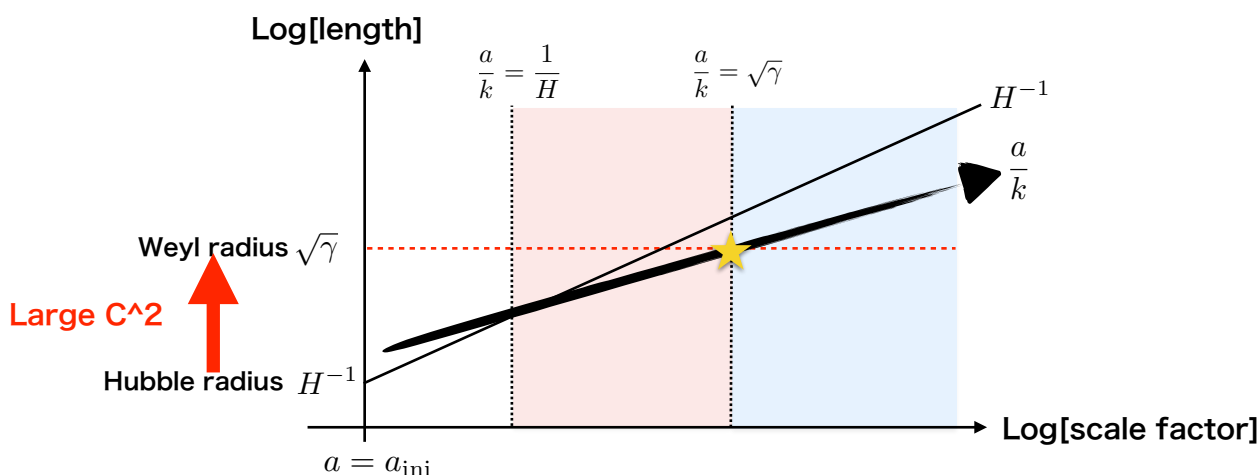
■ Setup and assumptions

- Consider the tensor perturbation h_{ij} on the flat FLRW metric:

$$ds^2 = a^2(\tau)[-d\tau^2 + (\delta_{ij} + h_{ij})dx^i dx^j]$$

$$a : \text{scale factor} \quad \mathcal{T} : \text{conformal time} \quad \delta^{ij} h_{ij} = 0 = \partial^j h_{ij}$$

- Introduce the Weyl radius, $\sqrt{\gamma}$, and assume $\sqrt{\gamma} \gg H_{\text{ini}}^{-1}$.
- The modes, with physical wavelength $\frac{a}{k}$, cross with the Weyl radius $\sqrt{\gamma}$ after entering the horizon.



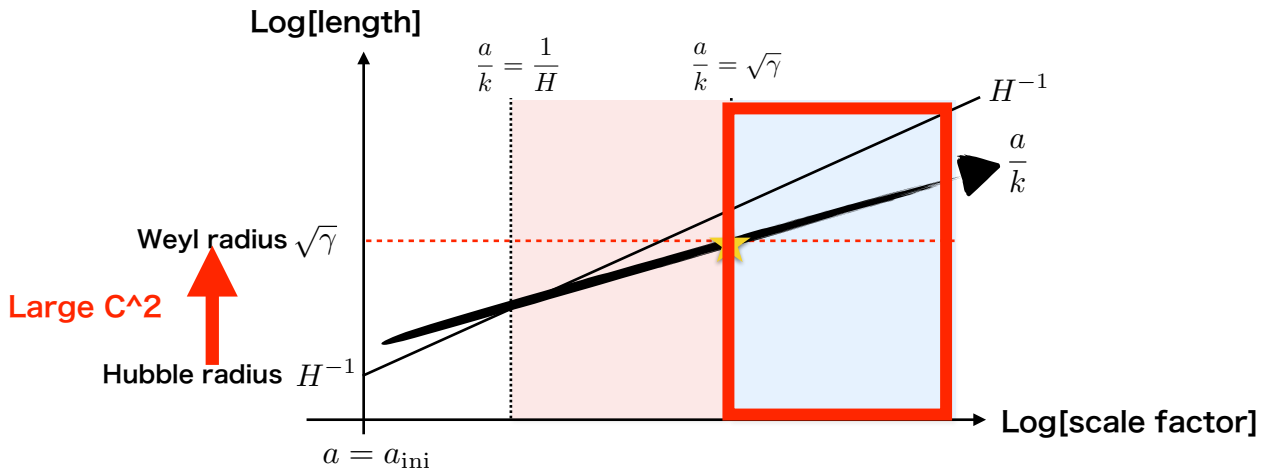
■ Setup and assumptions

- Consider the tensor perturbation h_{ij} on the flat FLRW metric:

$$ds^2 = a^2(\tau)[-d\tau^2 + (\delta_{ij} + h_{ij})dx^i dx^j]$$

$$a : \text{scale factor} \quad \tau : \text{conformal time} \quad \delta^{ij} h_{ij} = 0 = \partial^j h_{ij}$$

- Introduce the Weyl radius, $\sqrt{\gamma}$, and assume $\sqrt{\gamma} \gg H_{\text{ini}}^{-1}$.
- The modes, with physical wavelength $\frac{a}{k}$, cross with the Weyl radius $\sqrt{\gamma}$ after entering the horizon.



■ Second order action

- Consider an action equivalent to the second order action for tensor perturbation h_{ij} in Einstein-Weyl gravity:

$$8\kappa S[\phi, \psi] = \int d^4x \left[-\frac{1}{2}(\partial\phi)^2 + \frac{\ddot{a}}{a}\phi \cdot \phi + \frac{1}{2}(\partial\psi)^2 + \frac{1}{2}\left(\frac{\ddot{a}}{a} + 2\frac{\dot{a}^2}{a^2} + \frac{a^2}{\gamma}\right)\psi \cdot \psi + 2\frac{\dot{a}^2}{a^2}\phi \cdot \psi - 2\frac{\dot{a}}{a}\dot{\phi} \cdot \psi \right]$$

$$h_{ij} = \frac{1}{\sqrt{2}a}(\phi_{ij} + \psi_{ij})$$

Massless tensor field ϕ_{ij}

$$\phi_{ij} = -\frac{\sqrt{2}\gamma}{a}\square h_{ij} + \sqrt{2}ah_{ij}$$

Massive ghost tensor field ψ_{ij}

$$\psi_{ij} = \frac{\sqrt{2}\gamma}{a}\square h_{ij}$$

Second order action in E+W gravity

$$8\kappa S[h] = \int d^4x [-a^2(\partial h)^2 - \gamma(\square h)^2]$$

Note: ϕ_{ij} and ψ_{ij} are NOT metric, but ϕ_{ij}/a and ψ_{ij}/a correspond to metric.

- ϕ_{ij} and ψ_{ij} are useful to investigate the late-time behavior since the interaction gets negligible as time proceeds.

■ EOM in the radiation era: $a(\tau) \propto \tau$

- In this talk, we only consider the evolution of the modes ϕ_k and ψ_k in radiation era, $a \propto \tau$, where

$$f_{ij}(\tau, \vec{x}) = \sum_{\lambda=+, \times} \int \frac{d^3k}{(2\pi)^{3/2}} f_k(z) \epsilon_{ij}^\lambda(\vec{k}) e^{i\vec{k} \cdot \vec{x}} \quad (f \text{ is either } \phi, \psi \text{ or } h.)$$

- The System of equations is, with a time coordinate $z := k\tau \propto a$,

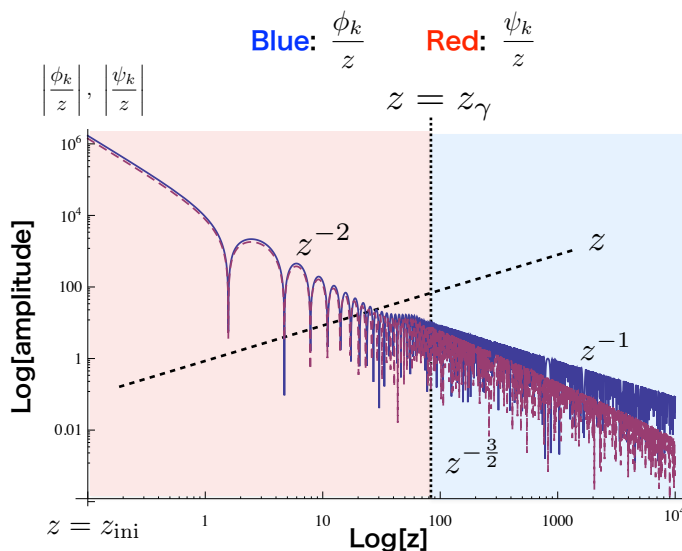
$$\phi_k'' + \phi_k = \frac{2}{z} \psi_k', \quad \psi_k'' + \left(1 + \frac{2}{z^2} + \frac{z^2}{z_\gamma^2}\right) \psi_k = \frac{2}{z} \phi_k' - \frac{2}{z^2} \phi_k,$$

where a prime denotes the derivative wrt z , and

$$\frac{z^2}{z_\gamma^2} = \frac{a^2}{\gamma k^2}, \quad \phi_k = \frac{z_\gamma^2}{z} (h_k'' + h_k) + z h_k, \quad \psi_k = -\frac{z_\gamma^2}{z} (h_k'' + h_k).$$

- z_γ is a dimension-less parameter, and $z = z_\gamma$ represents a time when the wavelength catches up with Weyl radius $\sqrt{\gamma}$.

■ Numerical solutions (Radiation era: $a \propto z$)



Boundary condition at $z = z_{\text{ini}} = 0.1$

A simple setup:

$$h_k(z_{\text{ini}}) = 1, \\ h_k'(z_{\text{ini}}) = h_k''(z_{\text{ini}}) = h_k'''(z_{\text{ini}}) = 0$$

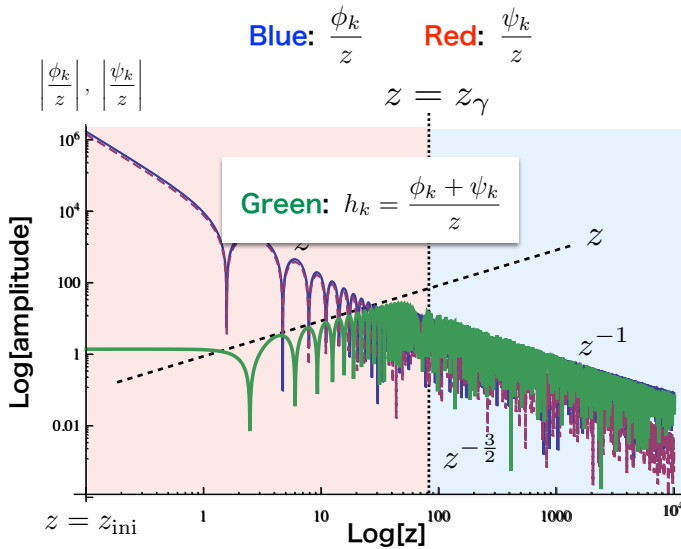
Insert them into
the derivatives below

$$\phi_k = \phi_k(h, h''), \quad \phi_k' = \phi_k(h, h', h'', h''')$$

$$\psi_k = \psi_k(h, h''), \quad \psi_k' = \psi_k(h, h', h'', h''')$$

- We can see that ϕ_k and ψ_k are decoupled after $z = z_\gamma$.
- For $z > z_\gamma$, ϕ_k/z is damped as z^{-1} , while ψ_k/z scales as $z^{-\frac{3}{2}}$.
- We further find an interesting behavior that $h_k = \frac{\phi_k + \psi_k}{z}$ grows as z at early time $z < z_\gamma$, but it will be discussed somewhere else.

Numerical solutions (Radiation era: $a \propto z$)



Boundary condition at $z = z_{ini} = 0.1$

A simple setup:

$$h_k(z_{ini}) = 1,$$

$$h'_k(z_{ini}) = h''_k(z_{ini}) = h'''_k(z_{ini}) = 0$$

↓
Insert them into
the derivatives below

$$\phi_k = \phi_k(h, h''), \quad \phi'_k = \phi_k(h, h', h'', h''')$$

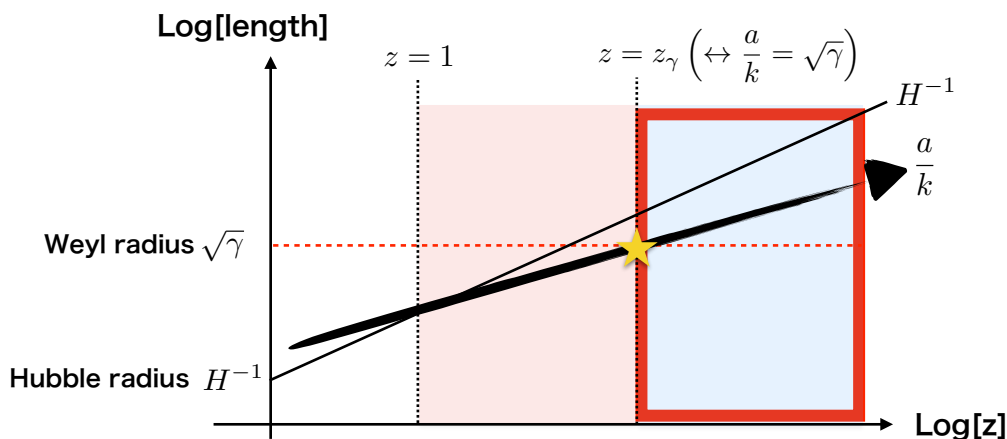
$$\psi_k = \psi_k(h, h''), \quad \psi'_k = \psi_k(h, h', h'', h''')$$

- We can see that ϕ_k and ψ_k are decoupled after $z = z_\gamma$.
- For $z > z_\gamma$, ϕ_k/z is damped as z^{-1} , while ψ_k/z scales as $z^{-\frac{3}{2}}$.
- We further find an interesting behavior that $h_k = \frac{\phi_k + \psi_k}{z}$ grows as z at early time $z < z_\gamma$, but it will be discussed somewhere else.

Behavior at the late time: $z \gg z_\gamma$

- From now on, we concentrate on understanding this behavior of tensor mode at late time, analytically.
- As $z \rightarrow \infty$, the system of equation is reduced to

$$\phi''_k + \phi_k = \frac{2}{z} \psi'_k, \quad \psi''_k + \left(1 + \frac{2}{z^2} + \frac{z^2}{z_\gamma^2}\right) \psi_k = \frac{2}{z} \phi'_k - \frac{2}{z^2} \phi_k$$

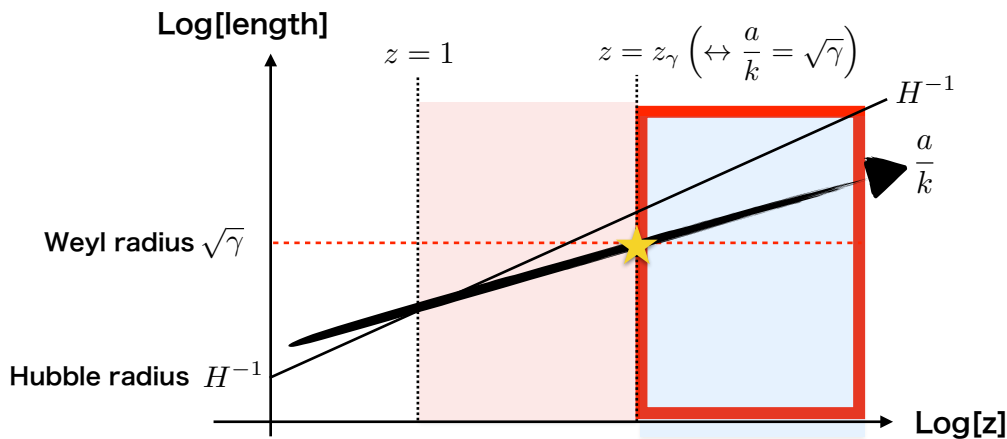


Behavior at the late time: $z \gg z_\gamma$

- From now on, we concentrate on understanding this behavior of tensor mode at late time, analytically.
- As $z \rightarrow \infty$, the system of equation is reduced to

$$\phi_k'' + \phi_k = \frac{2}{z} \psi_k', \quad \psi_k'' + \left(1 + \frac{2}{z^2} + \frac{z^2}{z_\gamma^2}\right) \psi_k = \frac{2}{z} \phi_k' + \frac{2}{z^2} \phi_k$$

The interaction between ϕ_{ij} and ψ_{ij} becomes negligible.



Behavior at the late time: $z \gg z_\gamma$

- The problem to solve is the approximated equations below:

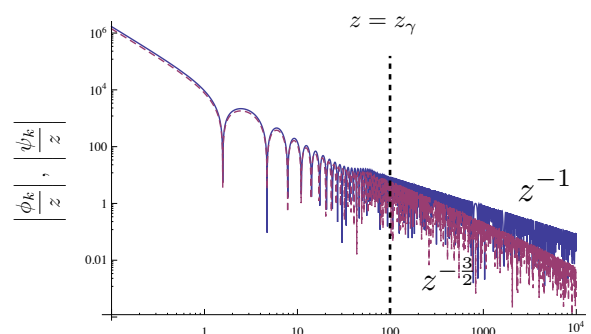
$$\phi_k'' + \phi_k \simeq 0, \quad \psi_k'' + \frac{z^2}{z_\gamma^2} \psi_k \simeq 0 \quad \text{as } z \rightarrow \infty.$$

- We then have the following solutions:

$$\frac{\phi_k}{z} \propto \frac{e^{\pm iz}}{z}, \quad \frac{\psi_k}{z} \propto \frac{D_{-\frac{1}{2}}[-(i \pm 1)z/\sqrt{z_\gamma}]}{z} \xrightarrow{z \rightarrow \infty} \frac{e^{\pm i \frac{t}{\sqrt{\gamma}}}}{z^{\frac{3}{2}}} \quad \begin{matrix} t : \text{cosmic time} \\ t = \int^\tau a(\bar{\tau}) d\bar{\tau} \end{matrix}$$

- We can see from the above solutions that ϕ_k oscillates with the conformal time τ while ψ_k with the cosmic time t .

- These solutions agree with the numerical solutions on the right or previous slide.



■ Behavior at the late time: $z \gg z_\gamma$

- The problem to solve is the approximated equations below:

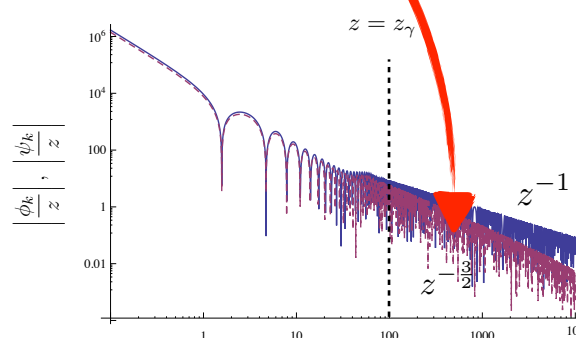
$$\phi_k'' + \phi_k \simeq 0, \quad \psi_k'' + \frac{z^2}{z_\gamma^2} \psi_k \simeq 0 \quad \text{as } z \rightarrow \infty.$$

- We then have the following solutions:

$$\frac{\phi_k}{z} \propto \frac{e^{\pm iz}}{z}, \quad \frac{\psi_k}{z} \propto \frac{D_{-\frac{1}{2}}[-(i \pm 1)z/\sqrt{z_\gamma}]}{z} \xrightarrow{z \rightarrow \infty} \frac{e^{\pm i \frac{t}{\sqrt{\gamma}}}}{z^{\frac{3}{2}}} \quad \begin{array}{l} t : \text{cosmic time} \\ t = \int^\tau a(\bar{\tau}) d\bar{\tau} \end{array}$$

- We can see from the above solutions that ϕ_k oscillates with the conformal time τ while ψ_k with the cosmic time t .

- These solutions agree with the numerical solutions on the right or previous slide.



■ Behavior at the late time: $z \gg z_\gamma$

- The problem to solve is the approximated equations below:

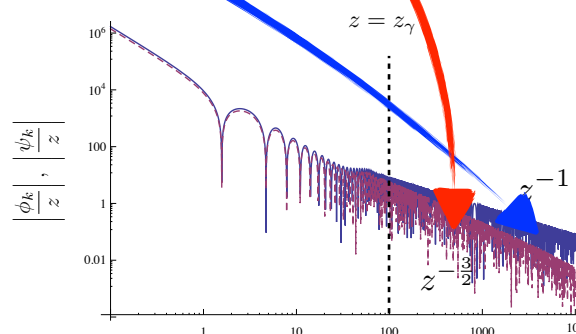
$$\phi_k'' + \phi_k \simeq 0, \quad \psi_k'' + \frac{z^2}{z_\gamma^2} \psi_k \simeq 0 \quad \text{as } z \rightarrow \infty.$$

- We then have the following solutions:

$$\frac{\phi_k}{z} \propto \frac{e^{\pm iz}}{z}, \quad \frac{\psi_k}{z} \propto \frac{D_{-\frac{1}{2}}[-(i \pm 1)z/\sqrt{z_\gamma}]}{z} \xrightarrow{z \rightarrow \infty} \frac{e^{\pm i \frac{t}{\sqrt{\gamma}}}}{z^{\frac{3}{2}}} \quad \begin{array}{l} t : \text{cosmic time} \\ t = \int^\tau a(\bar{\tau}) d\bar{\tau} \end{array}$$

- We can see from the above solutions that ϕ_k oscillates with the conformal time τ while ψ_k with the cosmic time t .

- These solutions agree with the numerical solutions on the right or previous slide.



■ Energy density of GWs

- Give a definition for energy density of GWs in Einstein-Weyl gravity from the (00) component of Noether pseudo tensor.
- The Noether pseudo for ϕ_{ij} and ψ_{ij} are

$$\begin{aligned}\Theta_{\mu}^{\nu(\phi)} &:= -\frac{1}{\sqrt{-g}} \frac{\partial L_{\phi}}{\partial(\partial_{\nu}\phi_{ij})} \partial_{\mu}\phi_{ij} + \delta^{\nu}_{\mu} \frac{L_{\phi}}{\sqrt{-g}} \\ &= \frac{1}{8\kappa a^4} \partial^{\nu}\phi \cdot \partial_{\mu}\phi + \delta^{\nu}_{\mu} \frac{L_{\phi}}{a^4}\end{aligned}\quad \begin{aligned}\Theta_{\mu}^{\nu(\psi)} &:= -\frac{1}{\sqrt{-g}} \frac{\partial L_{\psi}}{\partial(\partial_{\nu}\psi_{ij})} \partial_{\mu}\psi_{ij} + \delta^{\nu}_{\mu} \frac{L_{\psi}}{\sqrt{-g}} \\ &= -\frac{1}{8\kappa a^4} \partial^{\nu}\psi \cdot \partial_{\mu}\psi + \delta^{\nu}_{\mu} \frac{L_{\psi}}{a^4}\end{aligned}$$

where $\sqrt{-g} = a^4$, L_{ϕ} and L_{ψ} are extracted from the total Lagrangian L :

$$\begin{aligned}8\kappa L_{\phi} &= -\frac{1}{2}(\partial\phi)^2 + \frac{\ddot{a}}{2a}\phi \cdot \phi \\ L &= L_{\phi} + L_{\psi} + L_{\text{int}} \\ 8\kappa L_{\psi} &= \frac{1}{2}(\partial\psi)^2 + \frac{1}{2}\left(\frac{\ddot{a}}{a} + 2\frac{\dot{a}^2}{a^2} + \frac{a^2}{\gamma}\right)\psi \cdot \psi \\ 8\kappa L_{\text{int}} &= 2\frac{\dot{a}}{a}\psi \cdot \left(\frac{\dot{a}}{a}\phi - \dot{\phi}\right)\end{aligned}$$

■ Energy density of GWs

- Give a definition for energy density of GWs in Einstein-Weyl gravity from the (00) component of Noether pseudo tensor.
- The Noether pseudo for ϕ_{ij} and ψ_{ij} are

$$\begin{aligned}\Theta_{\mu}^{\nu(\phi)} &:= -\frac{1}{\sqrt{-g}} \frac{\partial L_{\phi}}{\partial(\partial_{\nu}\phi_{ij})} \partial_{\mu}\phi_{ij} + \delta^{\nu}_{\mu} \frac{L_{\phi}}{\sqrt{-g}} \\ &= \frac{1}{8\kappa a^4} \partial^{\nu}\phi \cdot \partial_{\mu}\phi + \delta^{\nu}_{\mu} \frac{L_{\phi}}{a^4}\end{aligned}\quad \begin{aligned}\Theta_{\mu}^{\nu(\psi)} &:= -\frac{1}{\sqrt{-g}} \frac{\partial L_{\psi}}{\partial(\partial_{\nu}\psi_{ij})} \partial_{\mu}\psi_{ij} + \delta^{\nu}_{\mu} \frac{L_{\psi}}{\sqrt{-g}} \\ &= -\frac{1}{8\kappa a^4} \partial^{\nu}\psi \cdot \partial_{\mu}\psi + \delta^{\nu}_{\mu} \frac{L_{\psi}}{a^4}\end{aligned}$$

where $\sqrt{-g} = a^4$, L_{ϕ} and L_{ψ} are extracted from the total Lagrangian L :

$$\begin{aligned}8\kappa L_{\phi} &= -\frac{1}{2}(\partial\phi)^2 + \frac{\ddot{a}}{2a}\phi \cdot \phi \\ L &= L_{\phi} + L_{\psi} + L_{\text{int}} \\ 8\kappa L_{\psi} &= \frac{1}{2}(\partial\psi)^2 + \frac{1}{2}\left(\frac{\ddot{a}}{a} + 2\frac{\dot{a}^2}{a^2} + \frac{a^2}{\gamma}\right)\psi \cdot \psi \\ 8\kappa L_{\text{int}} &= 2\frac{\dot{a}}{a}\psi \cdot \left(\frac{\dot{a}}{a}\phi - \dot{\phi}\right)\end{aligned}$$

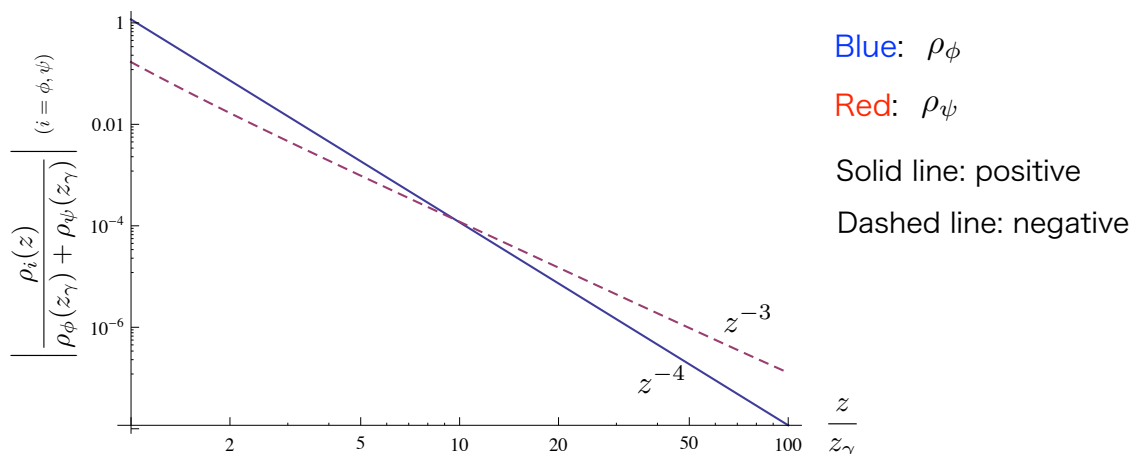
Time dependence of energy density: $z \gg z_\gamma$

- Inserting the analytical solutions at late time into the (00) component of Noether pseudo tensor, we find

$$\phi_k \propto e^{\pm iz} \quad \longrightarrow \quad \rho_\phi = \langle \Theta_{00}^{(\phi)} \rangle \propto z^{-4} \quad \text{Radiation}$$

$$\psi_k \propto \frac{e^{\pm it/\sqrt{\gamma}}}{\sqrt{z}} \quad \longrightarrow \quad \rho_\psi = \langle \Theta_{00}^{(\psi)} \rangle \propto -z^{-3} \quad \text{Negative matter}$$

- Insertion of numerical solutions into ρ_ϕ and ρ_ψ yields



Time dependence of energy density: $z \gg z_\gamma$

- Inserting the analytical solutions at the late time into the (00) component of Noether pseudo tensor, we find

$$\phi_k \propto e^{\pm iz} \quad \longrightarrow \quad \rho_\phi = \langle \Theta_{00}^{(\phi)} \rangle \propto z^{-4} \quad \text{Radiation}$$

- Inserti

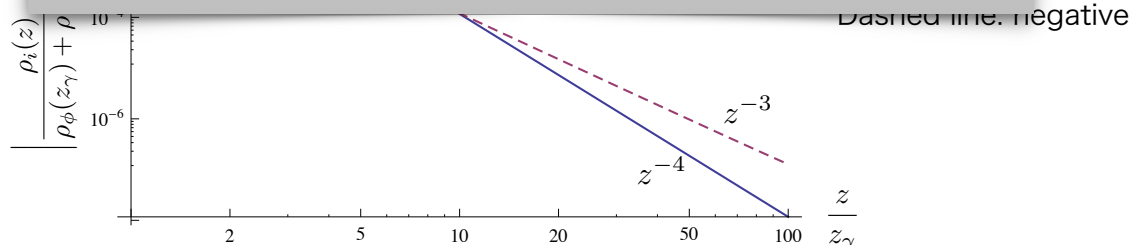
For consistency with observations, they need to satisfy

$$\left\{ \begin{array}{l} \Omega_\phi < \Omega_r \\ |\Omega_\psi| < \Omega_{DM} \quad \text{or} \quad \Omega_\psi + \Omega_{DM} \sim 0.3 \end{array} \right.$$

$$\Omega_i := \frac{1}{\rho_c} \frac{d\rho_i}{d \log k}, \quad (i = \phi, \psi), \quad \rho_c = 3H^2/\kappa$$

Ω_r : energy density of radiation

Ω_{DM} : energy density of dark matter



■ Summary

- We investigated the behavior of tensor mode at the late time.
- Two DOFs, ϕ_{ij} and ψ_{ij} , are decoupled after the wavelength catches up with the Weyl radius $\sqrt{\gamma}$.
- ϕ_{ij} behaves as radiation, while ψ_{ij} as matter with negative energy.
- The amount of their energy should be restricted by

$$\blacktriangleright \Omega_\phi < \Omega_r \quad \blacktriangleright |\Omega_\psi| < \Omega_{DM} \quad \text{or} \quad \Omega_\psi + \Omega_{DM} \sim 0.3$$

■ Future work

- To evaluate the observable, energy of GWs at the current epoch, we'd like to decide the initial condition for ϕ_{ij} and ψ_{ij} by, e.g., connecting the solution in the radiation era with the one in the inflationary era.

Inflationary era	Connected at $z = z_{\text{reh}}$	Radiation era
$h_k(z_{\text{reh}}) \simeq \sqrt{\frac{2\kappa}{k^3}} \frac{H_{\text{inf}}}{\sqrt{1 + 2\gamma H_{\text{inf}}^2}}$		$h_k(z_{\text{reh}}) = \frac{\phi_k(z_{\text{reh}}) + \psi_k(z_{\text{reh}})}{z_{\text{reh}}}$
[N. Deruelle et al., JHEP09(2012)009]		with 4 constants of integration

■ Noether pseudo tensor

- Variation of the Lagrangian density is

$$\begin{aligned}\partial_\mu L &= \frac{\partial L}{\partial \phi_{ij}} \partial_\mu \phi_{ij} + \frac{\partial L}{\partial (\partial_\nu \phi_{ij})} \partial_{\mu\nu} \phi_{ij} + \frac{\partial L}{\partial \psi_{ij}} \partial_\mu \psi_{ij} + \frac{\partial L}{\partial (\partial_\nu \psi_{ij})} \partial_{\mu\nu} \psi_{ij} + \hat{\partial}_\mu L \\ &= \mathcal{E}_\phi^{ij} \partial_\mu \phi_{ij} + \mathcal{E}_\psi^{ij} \partial_\mu \psi_{ij} + \partial_\nu \left(\frac{\partial L}{\partial (\partial_\nu \phi_{ij})} \partial_\mu \phi_{ij} + \frac{\partial L}{\partial (\partial_\nu \psi_{ij})} \partial_\mu \psi_{ij} \right) + \hat{\partial}_\mu L ,\end{aligned}$$

where L , \mathcal{E}_ϕ^{ij} , and \mathcal{E}_ψ^{ij} are

$$L = L_\phi + L_\psi + L_{\text{int}} , \quad \mathcal{E}_\psi^{ij} := \frac{\partial L}{\partial \psi_{ij}} - \partial_\nu \frac{\partial L}{\partial (\partial_\nu \psi_{ij})} , \quad \mathcal{E}_\phi^{ij} := \frac{\partial L}{\partial \phi_{ij}} - \partial_\nu \frac{\partial L}{\partial (\partial_\nu \phi_{ij})} .$$

- Moving the divergence term on RHS to LHS, we have

$$\partial_\nu (\sqrt{-g} \Theta^\nu_\mu) = \mathcal{E}_\phi^{ij} \partial_\mu \phi_{ij} + \mathcal{E}_\psi^{ij} \partial_\mu \psi_{ij} + \hat{\partial}_\mu L , \quad \Theta^\nu_\mu := \frac{1}{\sqrt{-g}} \left(\delta^\nu_\mu L - \frac{\partial L}{\partial (\partial_\nu \phi_{ij})} \partial_\mu \phi_{ij} - \frac{\partial L}{\partial (\partial_\nu \psi_{ij})} \partial_\mu \psi_{ij} \right)$$

- Finally we define the energy density for ϕ and ψ as follows:

$$\Theta^\nu_{\mu(f)} := -\frac{1}{\sqrt{-g}} \frac{\partial L_f}{\partial (\partial_\nu f_{ij})} \partial_\mu f_{ij} + \delta^\nu_\mu \frac{L_f}{\sqrt{-g}} \quad (f \text{ is either } \phi \text{ or } \psi .)$$

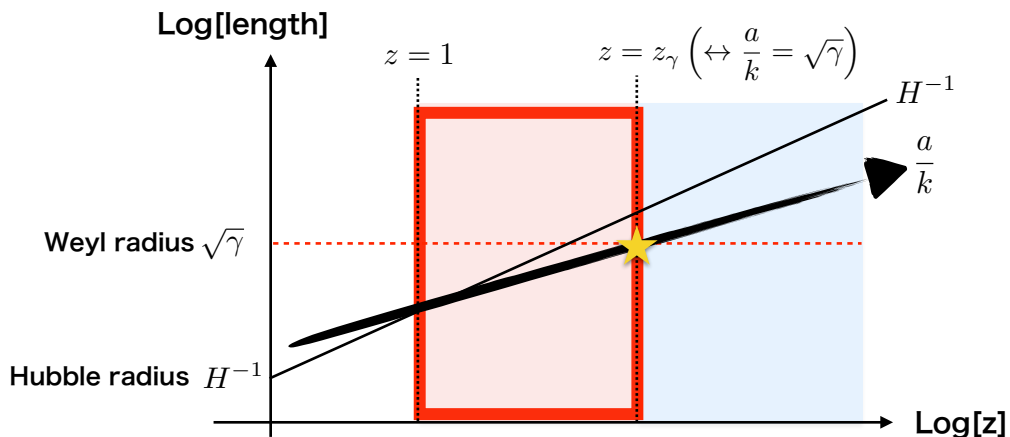
■ Behavior at the Early time: $z \ll z_\gamma$

- The variables ϕ_k and ψ_k are not convenient, so let us take the variable transformation such that

$$\phi_k = z Q_k + \frac{R_k}{z} , \quad \psi_k = -\frac{R_k}{z}$$

- Thus the EOM for new variables is

$$R_k'' + \left(1 + \frac{z^2}{z_\gamma^2} \right) R_k = -2z Q_k' , \quad Q_k'' + Q_k = \frac{R_k}{z_\gamma^2} .$$



■ Behavior at the Early time: $z \ll z_\gamma$

- Assuming that the term zQ'_k in the EOM is negligible, we have

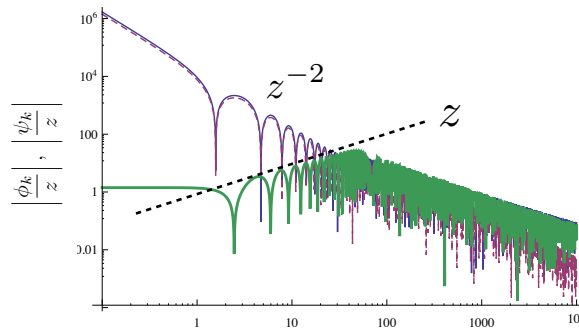
$$R_k'' + \left(1 + \frac{z^2}{z_\gamma^2}\right) R_k = \frac{R_k}{z_\gamma^2}, \quad Q_k'' + Q_k = \frac{R_k}{z_\gamma^2} \quad \text{as } z \rightarrow 0,$$

where we have used $z \ll z_\gamma$ on LHS, so its solutions are

$$R_k = C_1 e^{iz} + C_2 e^{-iz}, \quad Q_k = \frac{C_1}{2i} \frac{z}{z_\gamma^2} e^{iz} - \frac{C_2}{2i} \frac{z}{z_\gamma^2} e^{-iz} + C_3 e^{iz} + C_4 e^{-iz}.$$

- Going back to ϕ_k/z and ψ_k/z they behave as

$$\frac{\psi_k}{z} = -\frac{R_k}{z^2} = C_1 \frac{e^{iz}}{z^2} + C_2 \frac{e^{-iz}}{z^2}, \quad \frac{\phi_k}{z} = Q_k + \frac{R_k}{z^2} = C_1 \left(\frac{1}{z^2} + \frac{1}{2i} \frac{z}{z_\gamma^2}\right) e^{iz} + C_2 \left(\frac{1}{z^2} - \frac{1}{2i} \frac{z}{z_\gamma^2}\right) e^{-iz} + C_3 e^{iz} + C_4 e^{-iz}.$$



■ Behavior at the Early time: $z \ll z_\gamma$

- Assuming that the term zQ'_k in the EOM is negligible, we have

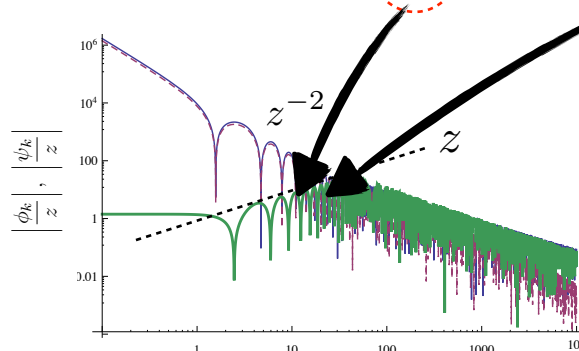
$$R_k'' + \left(1 + \frac{z^2}{z_\gamma^2}\right) R_k = \frac{R_k}{z_\gamma^2}, \quad Q_k'' + Q_k = \frac{R_k}{z_\gamma^2} \quad \text{as } z \rightarrow 0,$$

where we have used $z \ll z_\gamma$ on LHS, so its solutions are

$$R_k = C_1 e^{iz} + C_2 e^{-iz}, \quad Q_k = \frac{C_1}{2i} \frac{z}{z_\gamma^2} e^{iz} - \frac{C_2}{2i} \frac{z}{z_\gamma^2} e^{-iz} + C_3 e^{iz} + C_4 e^{-iz}.$$

- Going back to ϕ_k/z and ψ_k/z they behave as

$$\frac{\psi_k}{z} = -\frac{R_k}{z^2} = C_1 \frac{e^{iz}}{z^2} + C_2 \frac{e^{-iz}}{z^2}, \quad \frac{\phi_k}{z} = Q_k + \frac{R_k}{z^2} = C_1 \left(\frac{1}{z^2} + \frac{1}{2i} \frac{z}{z_\gamma^2}\right) e^{iz} + C_2 \left(\frac{1}{z^2} - \frac{1}{2i} \frac{z}{z_\gamma^2}\right) e^{-iz} + C_3 e^{iz} + C_4 e^{-iz}.$$

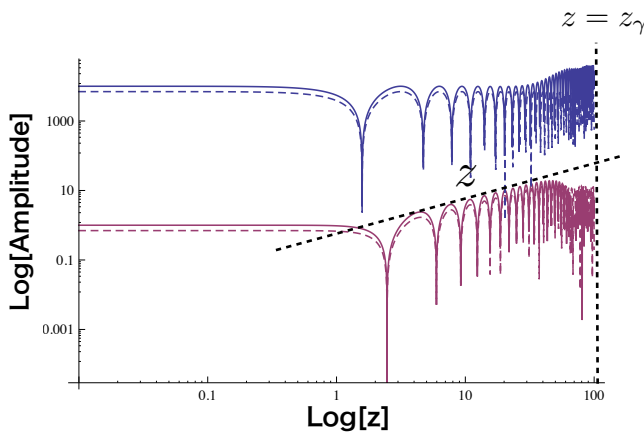


■ Behavior at the Early time: $z \ll z_\gamma$

- Discuss about the validity of neglecting zQ'_k term in the EOM for R_k .
- If the initial value for Q_k is smaller than the one for R_k , $Q_k(z_{\text{ini}}) \ll R_k(z_{\text{ini}})$, we can see from the below plot that the term zQ'_k is negligible numerically. (Inflationary setup yields $Q_k(z_{\text{ini}}) \ll R_k(z_{\text{ini}})$.)

Red: Q_k , **Blue:** R_k

Solid line: presence of zQ'_k , **Dashed line:** absence of zQ'_k .



Boundary condition at $z = z_{\text{ini}} = 0.01$

$$V = \left\{ \frac{R_k(z)}{Q_k(z)}, \frac{R'_k(z)}{Q_k(z)}, 1, \frac{Q'_k(z)}{Q_k(z)} \right\} \Big|_{z=z_{\text{ini}}}$$

$$Q_k = h_k , \quad R_k = z_\gamma^2 (h''_k + h_k)$$

Inflationary setup

$$h_k(z_{\text{ini}}) = \text{const.},$$

$$h'_k(z_{\text{ini}}) = h''_k(z_{\text{ini}}) = h'''_k(z_{\text{ini}}) = 0$$

Wednesday 8th November

Invited lecture 9:00–9:45

[Chair: Tomohiro Harada]

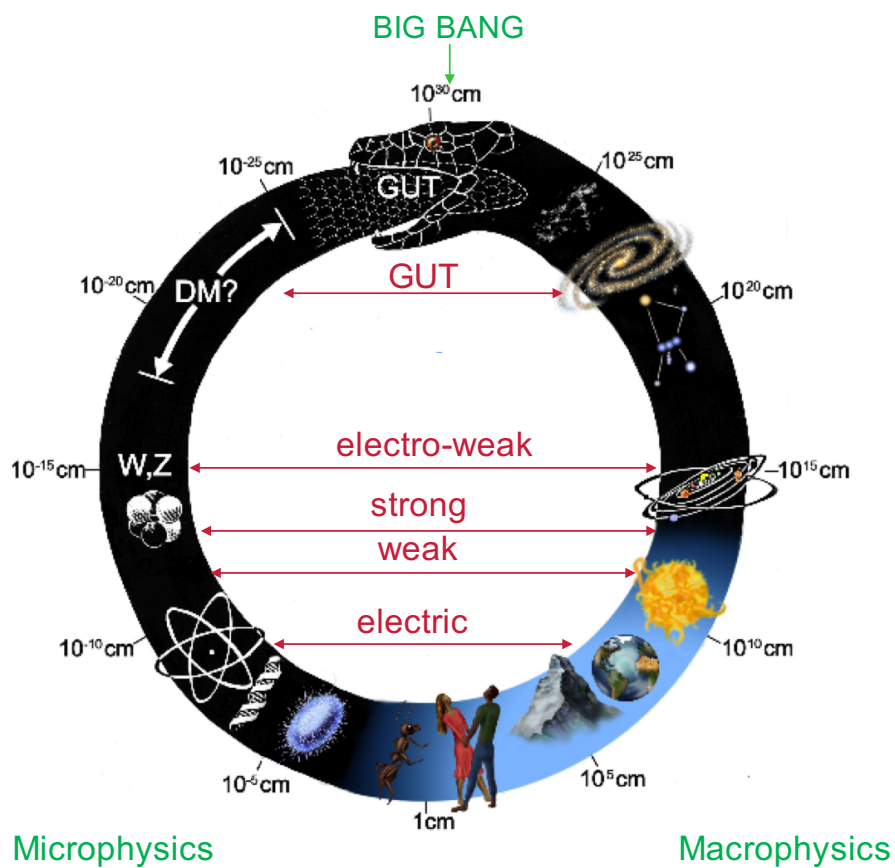
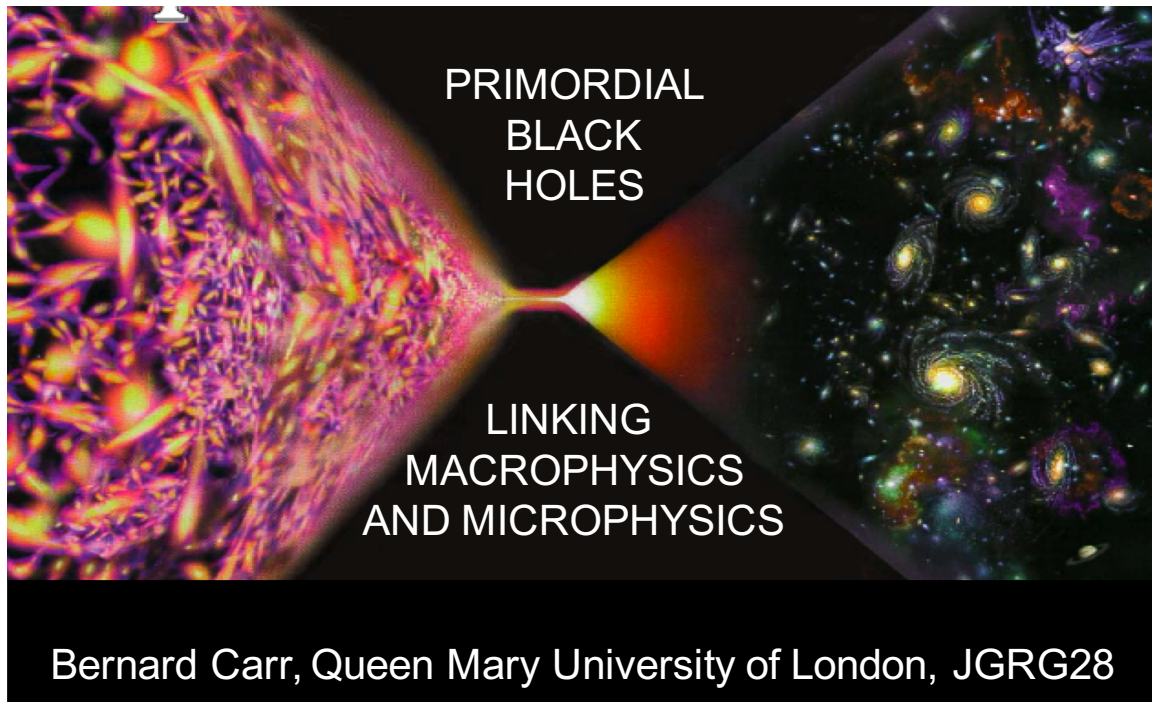
Bernard John Carr

Queen Mary University of London

**“PRIMORDIAL BLACK HOLES: LINKING MICROPHYSICS
AND MACROPHYSICS”**

(40+10 min.)

[JGRG28 (2018) 110801]



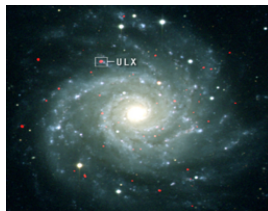
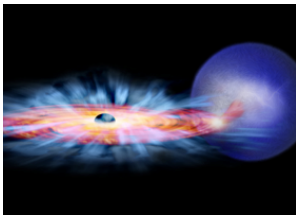
PLAN OF TALK

- Formation and evaporation of PBHs
- PBHs, dark matter and LIGO events
- PBHs and large-scale structure
- PBHs and quantum gravity

BLACK HOLE FORMATION

$$R_S = 2GM/c^2 = 3(M/M_\odot) \text{ km} \Rightarrow \rho_S = 10^{18}(M/M_\odot)^{-2} \text{ g/cm}^3$$

Stellar BH ($M \sim 10^{1-2} M_\odot$), IMBH ($M \sim 10^{3-5} M_\odot$), SMBH ($M \sim 10^{6-9} M_\odot$)



Small “primordial” BHs can only form in early Universe

cf. cosmological density $\rho \sim 1/(Gt^2) \sim 10^6(t/s)^{-2} \text{ g/cm}^3$

$$M_{\text{PBH}} \sim c^3 t / G = \begin{array}{ll} 10^{-5} \text{ g} & \text{at } 10^{-43} \text{ s} & \text{(minimum)} \\ 10^{15} \text{ g} & \text{at } 10^{-23} \text{ s} & \text{(evaporating)} \\ 10^5 M_\odot & \text{at } 1 \text{ s} & \text{(maximum)} \end{array} \Rightarrow \text{huge range}$$

Mon. Not. R. astr. Soc. (1971) **152**, 75-78.



GRAVITATIONALLY COLLAPSED OBJECTS OF VERY LOW MASS

Stephen Hawking

(Communicated by M. J. Rees)

(Received 1970 November 9)

SUMMARY

It is suggested that there may be a large number of gravitationally collapsed objects of mass 10^{-5} g upwards which were formed as a result of fluctuations in the early Universe. They could carry an electric charge of up to ± 30 electron units. Such objects would produce distinctive tracks in bubble chambers and could form atoms with orbiting electrons or protons. A mass of 10^{17} g of such objects could have accumulated at the centre of a star like the Sun. If such a star later became a neutron star there would be a steady accretion of matter by a central collapsed object which could eventually swallow up the whole star in about ten million years.

SOVIET ASTRONOMY - AJ VOL. 10, NO. 4 JANUARY-FEBRUARY, 1967

THE HYPOTHESIS OF CORES RETARDED DURING EXPANSION AND THE HOT COSMOLOGICAL MODEL

Ya. B. Zel'dovich and I. D. Novikov

Translated from *Astronomicheskii Zhurnal*, Vol. 43, No. 4,
pp. 758-760, July-August, 1966
Original article submitted March 14, 1966

The existence of bodies with dimensions less than $R_g = 2GM/c^2$ at the early stages of expansion of the cosmological model leads to a strong accretion of radiation by these bodies. If further calculations confirm that accretion is catastrophically high, the hypothesis on cores retarded during expansion [3, 4] will conflict with observational data.

BLACK HOLES IN THE EARLY UNIVERSE

B. J. Carr and S. W. Hawking

(Received 1974 February 25)

SUMMARY

The existence of galaxies today implies that the early Universe must have been inhomogeneous. Some regions might have got so compressed that they underwent gravitational collapse to produce black holes. Once formed, black holes in the early Universe would grow by accreting nearby matter. A first estimate suggests that they might grow at the same rate as the Universe during the radiation era and be of the order of 10^{15} to 10^{17} solar masses now. The observational evidence however is against the existence of such giant black holes. This motivates a more detailed study of the rate of accretion which shows that black holes will not in fact substantially increase their original mass by accretion. There could thus be primordial black holes around now with masses from 10^{-5} g upwards.



⇒ no observational evidence against them!

⇒ need to consider quantum effects

letters to nature

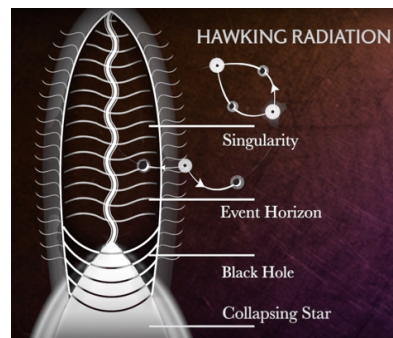
Nature 248, 30 - 31 (01 March 1974); doi:10.1038/248030a0

Black hole explosions?

S. W. HAWKING

Department of Applied Mathematics and Theoretical Physics and Institute of Astronomy University of Cambridge

QUANTUM gravitational effects are usually ignored in calculations of the formation and evolution of black holes. The justification for this is that the radius of curvature of space-time outside the event horizon is very large compared to the Planck length $(G\hbar/c^3)^{1/2} \approx 10^{-33}$ cm, the length scale on which quantum fluctuations of the metric are expected to be of order unity. This means that the energy density of particles created by the gravitational field is small compared to the space-time curvature. Even though quantum effects may be small locally, they may still, however, add up to produce a significant effect over the lifetime of the Universe $\approx 10^{17}$ s which is very long compared to the Planck time $\approx 10^{-43}$ s. The purpose of this letter is to show that this indeed may be the case: it seems that any black hole will create and emit particles such as neutrinos or photons at just the rate that one would expect if the black hole was a body with a temperature of $(\kappa/2\pi)(\hbar/2k) \approx 10^{-6} (M_{\odot}/M)K$ where κ is the surface gravity of the black hole¹. As a black hole emits this thermal radiation one would expect it to lose mass. This in turn would increase the surface gravity and so increase the rate of emission. The black hole would therefore have a finite life of the order of $10^{71} (M_{\odot}/M)^{-3}$ s. For a black hole of solar mass this is much longer than the age of the Universe. There might, however, be much smaller black holes which were formed by fluctuations in the early Universe². Any such black hole of mass less than 10^{15} g would have evaporated by now. Near the end of its life the rate of emission would be very high and about 10^{30} erg would be released in the last 0.1 s. This is a fairly small explosion by astronomical standards but it is equivalent to about 1 million 1 Mton hydrogen bombs.



PBHs are important even if they never formed!

PBH EVAPORATION

Black holes radiate thermally with temperature

$$T = \frac{hc^3}{8\pi GkM} \sim 10^{-7} \left[\frac{M}{M_0} \right]^{-1} \text{ K}$$

=> evaporate completely in time $t_{\text{evap}} \sim 10^{64} \left[\frac{M}{M_0} \right]^3 \text{ y}$

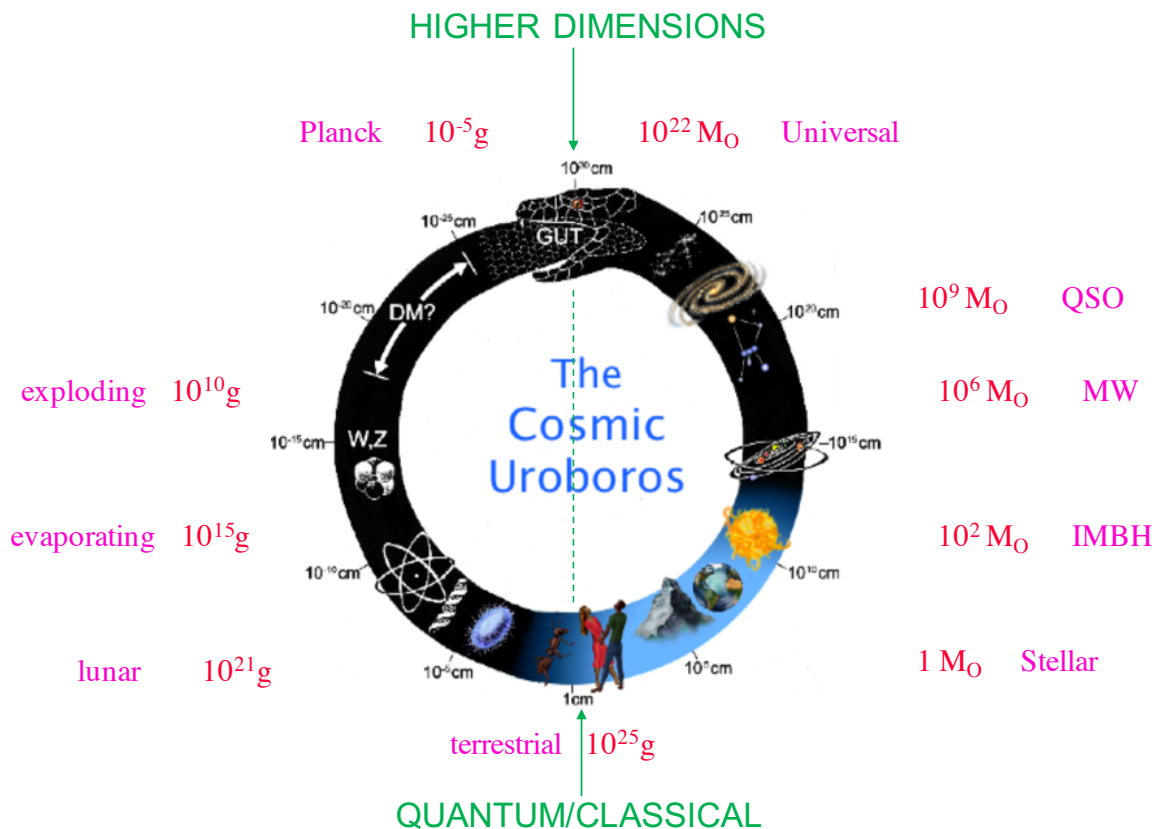
M ~ 10¹⁵g => final explosion phase today (10³⁰ ergs)

γ-ray background at 100 MeV => $\Omega_{\text{PBH}}(10^{15}\text{g}) < 10^{-8}$

=> explosions undetectable in standard particle physics model

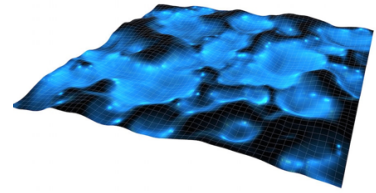
T > T_{CMB}=3K for M < 10²⁶g => “quantum” black holes

BLACK HOLES



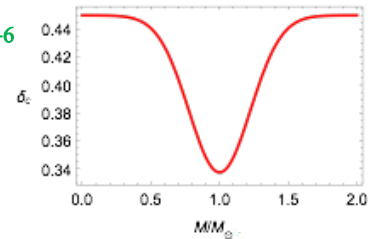
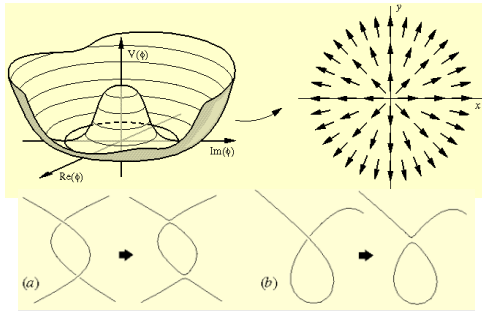
FORMATION MECHANISMS

Primordial inhomogeneities **Inflation**



Pressure reduction **Form more easily but need spherical symmetry**

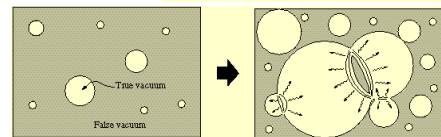
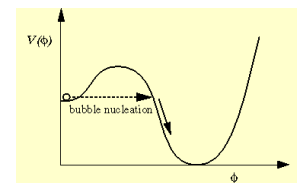
Cosmic strings **PBH constraints => $G\mu < 10^{-6}$**



Bubble collisions

Need fine-tuning of bubble formation rate

Domain walls **PBHs can be very large**



PBH FORMATION => LARGE INHOMOGENEITIES

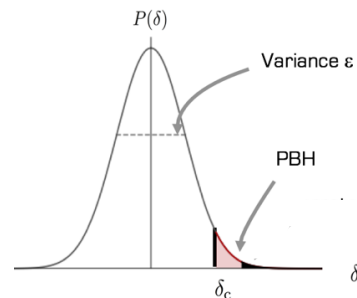
To collapse against pressure, need (Carr 1975)

$$R > \sqrt{\alpha} ct \quad \text{when } \delta \sim 1 \Rightarrow \delta_H > \alpha \quad (p = \alpha \rho c^2)$$

Gaussian fluctns with $\langle \delta_H^2 \rangle^{1/2} = \epsilon(M)$

=> fraction of PBHs

$$\beta(M) \sim \epsilon(M) \exp \left[-\frac{\alpha^2}{2\epsilon(M)^2} \right]$$



$$\epsilon(M) \text{ constant} \Rightarrow \beta(M) \text{ constant} \Rightarrow dN/dM \propto M^{-\left(\frac{1+3\alpha}{1+\alpha}\right)-1}$$

$$p=0 \Rightarrow \text{need spherical symmetry} \Rightarrow \beta(M) \sim 0.06 \epsilon(M)^6$$

(Khlopov & Polnarev 1980)

Limit on fraction of Universe collapsing

$\beta(M)$ fraction of density in PBHs of mass M at formation

General limit

$$\frac{\rho_{PBH}}{\rho_{CBR}} \approx \frac{\Omega_{PBH}}{10^{-4}} \left[\frac{R}{R_0} \right] \Rightarrow \beta \sim 10^{-6} \Omega_{PBH} \left[\frac{t}{\text{sec}} \right]^{1/2} \sim 10^{-18} \Omega_{PBH} \left[\frac{M}{10^{15} \text{ g}} \right]^{1/2}$$

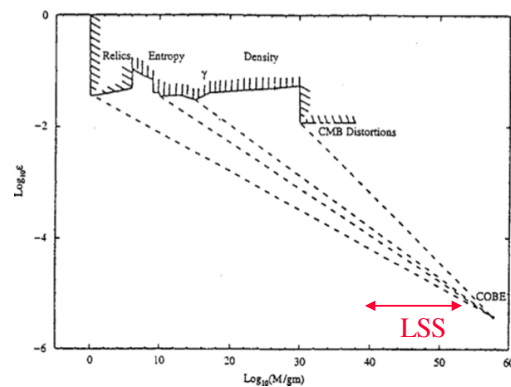
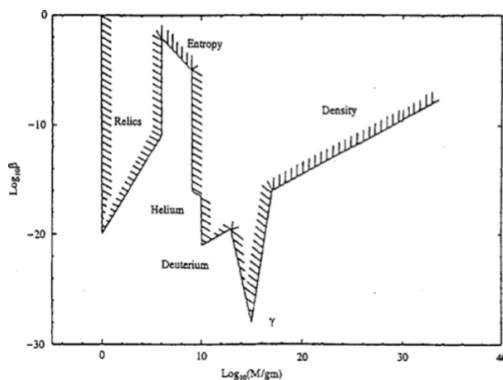
Unevaporated $M > 10^{15} \text{ g} \Rightarrow \Omega_{PBH} < 0.25$ (CDM)

Evaporating now $M \sim 10^{15} \text{ g} \Rightarrow \Omega_{PBH} < 10^{-8}$ (GRB)

Evaporated in past $M < 10^{15} \text{ g}$

\Rightarrow constraints from entropy, γ -background, BBNS

CONSTRAINTS ON $\beta(M)$ \Rightarrow CONSTRAINTS ON $\varepsilon(M)$



PBHs are unique probe of ε on small scales.

Need blue spectrum or spectral feature to produce them.

PBHS FROM NEAR-CRITICAL COLLAPSE

Critical phenomena $\Rightarrow M = k M_H (\delta - \delta_c)^\gamma$

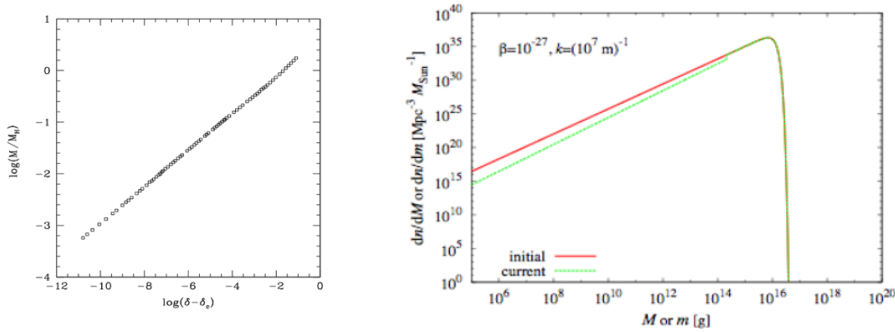
(Niemeyer & Jedamzik 1999, Shibata & Sasaki 1999)

spectrum peaks at horizon mass with extended low mass tail

$$dN/dM \propto M^{1/\gamma-1} \exp[-(M/M_f)^{1/\gamma}] \quad (\gamma = 0.35) \quad (\text{Yokoyama 1998})$$

Later calculations and peak analysis \Rightarrow

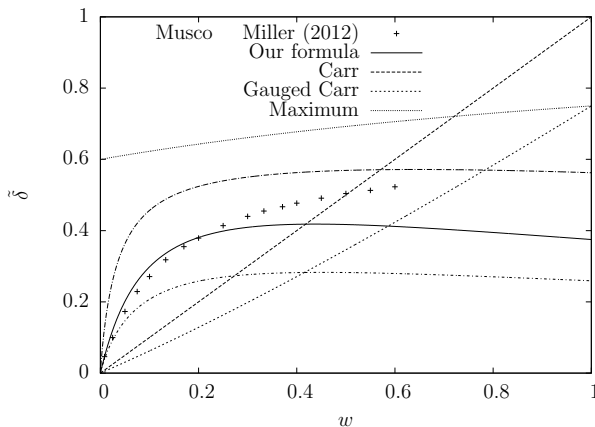
$\delta_c \sim 0.45$ and applies to $\delta - \delta_c \sim 10^{-10}$ (Musco & Miller 2013)



MORE PRECISE ESTIMATE OF δ_c

Threshold of primordial black hole formation

¹Tomohiro Harada, ²Chul-Moon Yoo, and ^{3,4}Kazunori Kohri



PRD 88 084051 (2013)

$$\delta_{Hc}^{UH} = \sin^2 \left(\frac{\pi \sqrt{w}}{1 + 3w} \right)$$

0.62 for radiation *

* For uniform-Hubble gauge but 0.4 for synchronous gauge

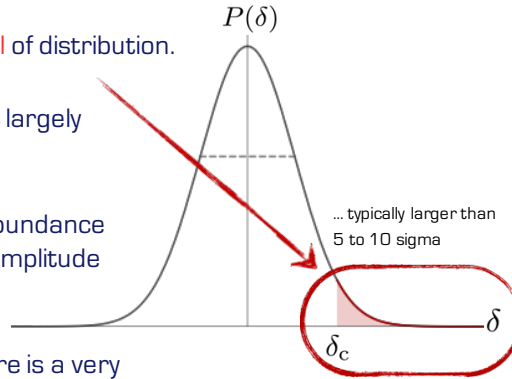
NON-GAUSSIAN EFFECTS

Expected whenever fluctuations are large

Bullock & Primack 1997, Ivanov 1998, Hidalgo 2007, Young & Byres 2013, Byrnes et al 2014

PBH production is **deep inside tail** of distribution.

- ★ This means, PBH production is largely sensitive to **non-Gaussianity**.
- ★ ... even more so, as the PBH abundance depends **exponentially** on the amplitude of the perturbations.
- ★ As shown by Byrnes et al., there is a very strong **modal coupling** between long- and short-wavelength modes.



Quantum field theory => n-point correlation function
Slow-roll correction using inflation 3-point correlator

$$P(\delta) = \frac{1}{\sqrt{2\pi}\Sigma} \left[1 - \left(\frac{\delta^3}{\Sigma^6} - \frac{3\delta}{\Sigma^4} \right) \right] \exp \left[-\frac{\delta^2}{2\Sigma^2} \right]$$

Seery & Hidalgo 2006

NON-SPHERICITY EFFECTS

On Ellipsoidal Collapse and Primordial Black-Hole Formation

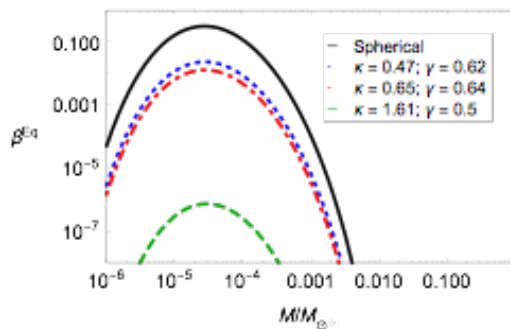
Florian Kühnel^{1,*} and Marit Sandstad^{2,†}

arXiv:1602:04815

- ★ Non-Sphericity

$$\frac{\delta_{ec}}{\delta_c} \simeq 1 + \kappa \left(\frac{\sigma^2}{\delta_c^2} \right)^\gamma$$

↖ ellipsoidal threshold
↖ spherical threshold



- ★ Simple estimate: → consider collapse of largest enclosed sphere (green curve):

$$\frac{\delta_{ec}}{\delta_c} \simeq (1 + 3e) = 1 + \frac{9}{\sqrt{10}\pi} \left(\frac{\sigma^2}{\delta_c^2} \right)^{1/2}$$

PBHS AND INFLATION

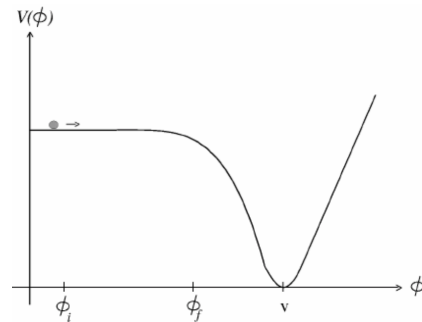
PBHs formed before reheat inflated away =>

$$M > M_{\min} = M_{\text{Pl}}(T_{\text{reheat}}/T_{\text{Pl}})^{-2} > 1 \text{ gm}$$

$$\text{CMB quadrupole} \Rightarrow T_{\text{reheat}} < 10^{16} \text{ GeV}$$

But inflation generates fluctuations

$$\frac{\delta\rho}{\rho} \sim \left[\frac{V^{3/2}}{M_{\text{Pl}}^3 V'} \right]_H$$



Can these generate PBHs?

Slow roll plus friction-domination

$$\xi = (M_{\text{Pl}} V' / V)^2 \ll 1, \quad \eta = M_{\text{Pl}} V'' / V \ll 1$$

=> nearly scale-invariant fluctuations

$$|\delta_k^2| \sim k^n, \quad \delta_H \sim M^{(1-n)/4} \text{ with } n = 1 - 3\xi + 2\eta \sim 1$$

CMB => $\delta_H \sim 10^{-5}$ => need $n > 1$ for PBHs

Observe $n < 1$ on horizon scale => need running index for PBHs.

$$\text{Planck gives } \frac{d \ln n}{dk} \approx -0.02 \pm 0.01 \text{ (wrong sign!)}$$

Need inflation model with $n > 1$ or some feature in $V(\phi)$ at large k

There are numerous other inflationary models for PBH formation.

Vincent Vennin “Stochastic inflation and PBHs”

CONSTRAINTS FOR EVAPORATING PBHS

B. Carr, K. Kohri, Y. Sendouda & J. Yokoyama PRD 81(2010) 104019

Big bang nucleosynthesis

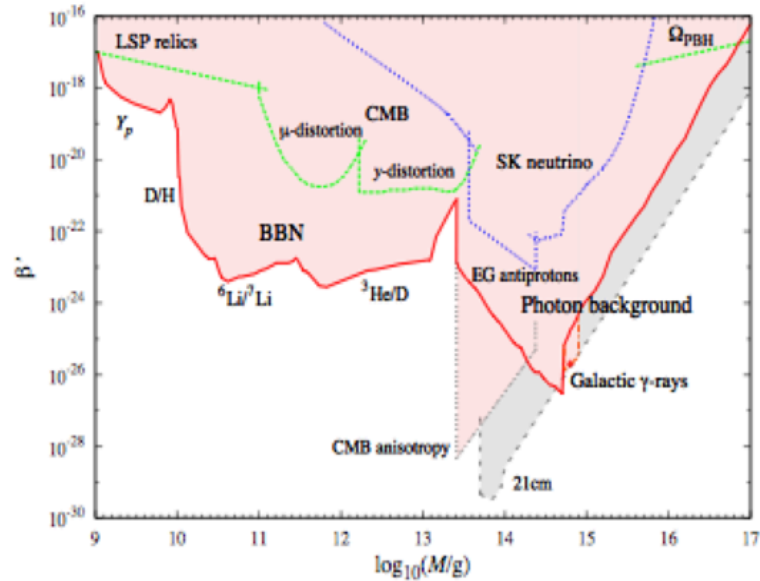
Gamma-ray background

Extragalactic cosmic rays

Neutrino relics

LSP relics

CMB distortions



CAN PBH EXPLOSIONS GENERATE \$\gamma\$-RAY BURSTS?

GRB => $dn/dt < 10^{-6} \text{ pc}^{-3}\text{y}^{-1}$ (if uniform) or $< 1 \text{ pc}^{-3}\text{y}^{-1}$ (if in halo)

Galactic \$\gamma\$-halo => $dn/dt = 0.06 \text{ pc}^{-3}\text{y}^{-1}$ Lehoucq et al (2009)

Cosmic rays => $dn/dt = 0.02 \text{ pc}^{-3}\text{y}^{-1}$ Maki et al (1996)

Observational limit depends on details of final explosive phase

Can some short (100msec) \$\gamma\$-ray bursts be PBH explosions?

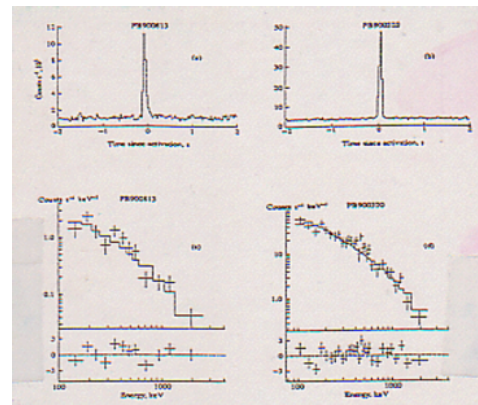
Cline et al (2003) => 42 BATSE events

Cline et al (2005) => ? KONUS events

Cline et al (2007) => 8 Swift events

Local => Euclidean dbn, V/V_{max} test

Maybe Shibasaki not so wrong!



PRIMORDIAL BLACK HOLES AS DARK MATTER

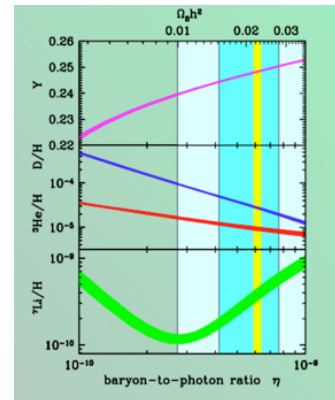
PRO

- * Black holes exist
- * No new physics needed
- * LIGO results

CON

- * Requires fine-tuning

PBH can do it!



BBNS $\Rightarrow \Omega_{\text{baryon}} = 0.05$

$\Omega_{\text{vis}} = 0.01, \Omega_{\text{dm}} = 0.25 \Rightarrow$ need baryonic and non-baryonic DM

↑ MACHOs
 ↑ WIMPs

PBHs are non-baryonic with features of both WIMPs and MACHOs

- 10¹⁷-10²⁰g PBHs excluded by femtolensing of GRBs
- 10²⁶-10³³g PBHs excluded by microlensing of LMC (2010)
- Above 10³M₀ excluded by dynamical effects

\Rightarrow windows at 10¹⁶-10¹⁷g or 10²⁰-10²⁴g or 10³³-10³⁶g for dark matter

↑ Asteroid
 ↑ Sublunar
 ↑ Intermediate Mass

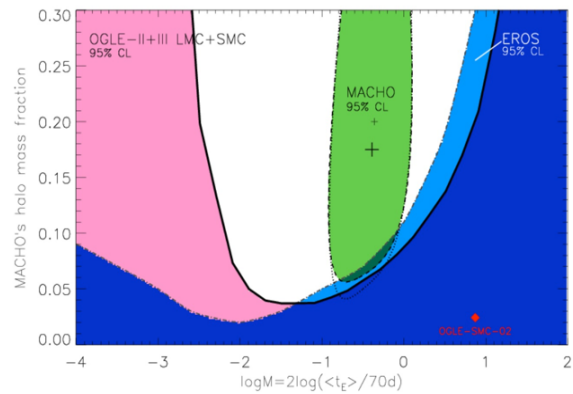
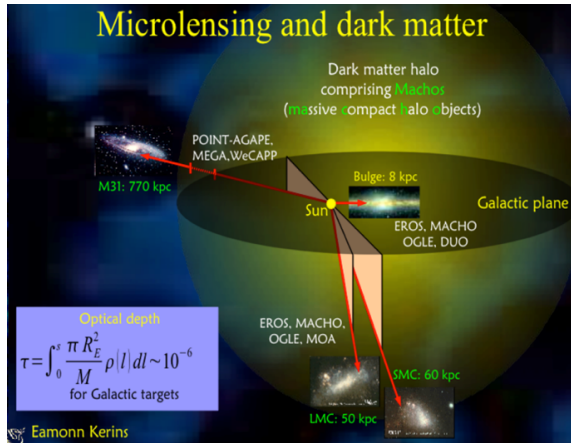


Image credit: Wyrzykowski et al., 2011, MNRAS, (astro-ph/1106.2925).

Early microlensing searches suggested MACHOs with $0.5 M_{\odot}$

=> PBH formation at QCD transition?

Pressure reduction => PBH mass function peak at $0.5 M_{\odot}$

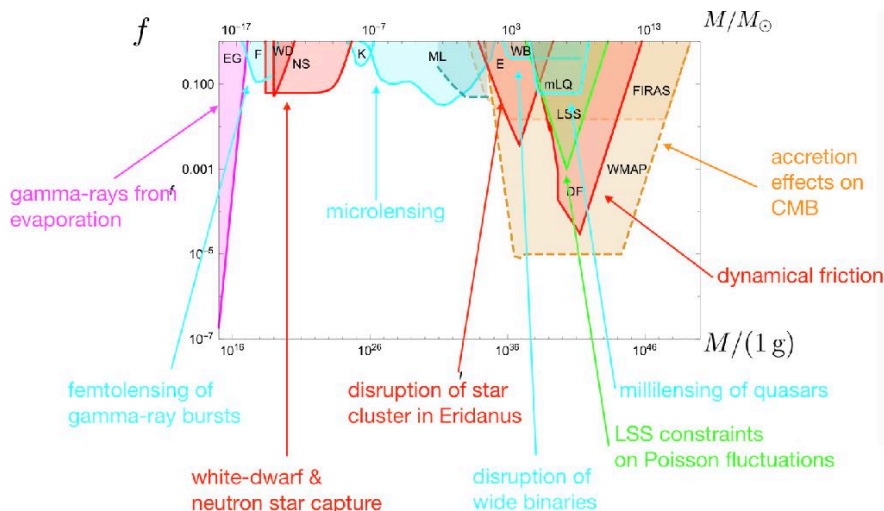
Later found that at most 20% of DM can be in these objects

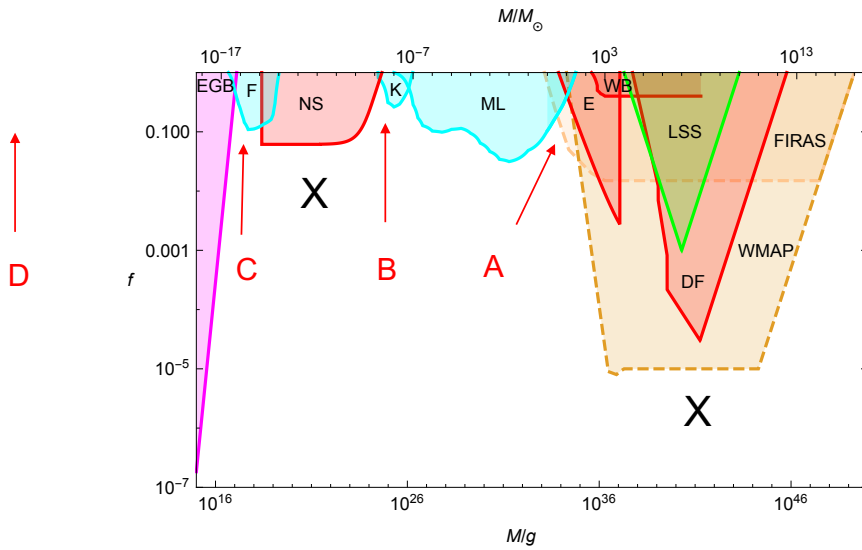
PRIMORDIAL BLACK HOLES AS DARK MATTER

Bernard Carr,^{1,*} Florian Kühnel,^{2,†} and Marit Sandstad^{3,‡}

PRD 94, 083504, arXiv:1607.06077

$$f(M) \sim (\beta / 10^{-8}) (M/M_{\odot})^{-1/2}$$





Three windows: (A) intermediate mass; (B) sublunar mass; (C) asteroid mass.

Also (D) Planck mass relics

But some of these limits are now thought to be wrong

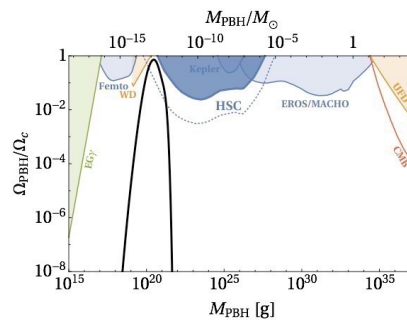
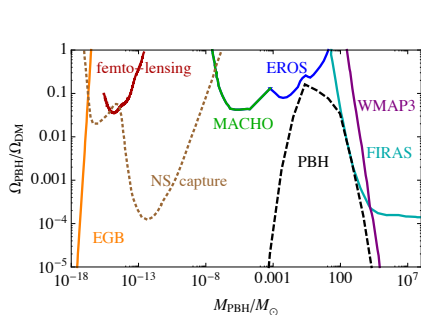
WHICH MASS WINDOW IS MOST PLAUSIBLE?

PBH dark matter @10 M_{\odot}
from hybrid inflation

Clesse & Garcia-Bellido
arXiv:1501.07565

PBH dark matter @10²⁰g
from double inflation

Inomata et al
arXiv:1701.02544

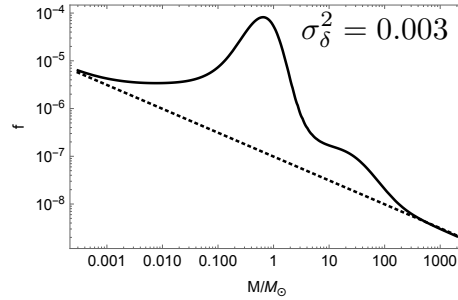
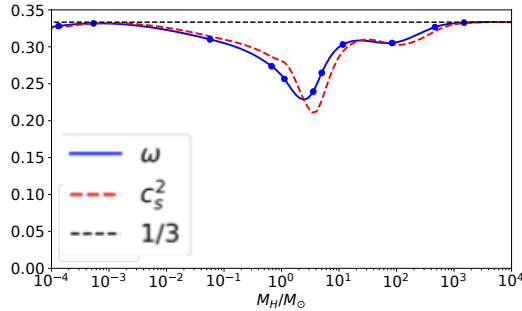


Primordial black holes with an accurate QCD equation of state

Christian T. Byrnes,^{1,*} Mark Hindmarsh,^{1,2,†} Sam Young,^{1,‡} and Michael R. S. Hawkins^{3,§}

arXiv:1801.06138

$$f(M) \propto M^{-1/2} e^{-\frac{\delta_C^2}{2\sigma_\delta^2}}$$



Explains why $M_{\text{PBH}} \sim M_C \sim 1 M_\odot$ but β must be fine-tune

Primordial black holes from inflaton and spectator field perturbations in a matter-dominated era

Bernard Carr,^{1,*} Tommi Tenkanen,^{1,†} and Ville Vaskonen^{2,‡}

Phys Rev D 96, 063507 (2017)

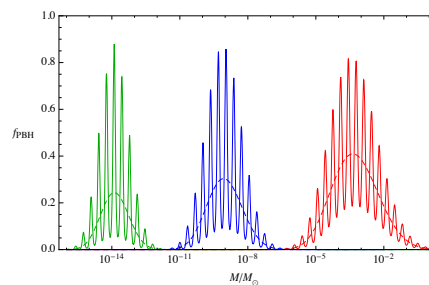
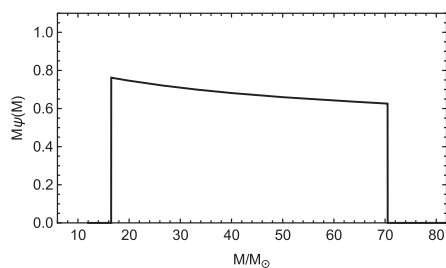
Primordial Black Hole Formation During Slow Reheating After Inflation

Bernard Carr,^{1,*} Konstantinos Dimopoulos,^{2,†} Charlotte Owen,^{2,‡} and Tommi Tenkanen^{1,§}

arXiv:1804.08639

Primordial Black Holes With Multi-Spike Mass Spectra

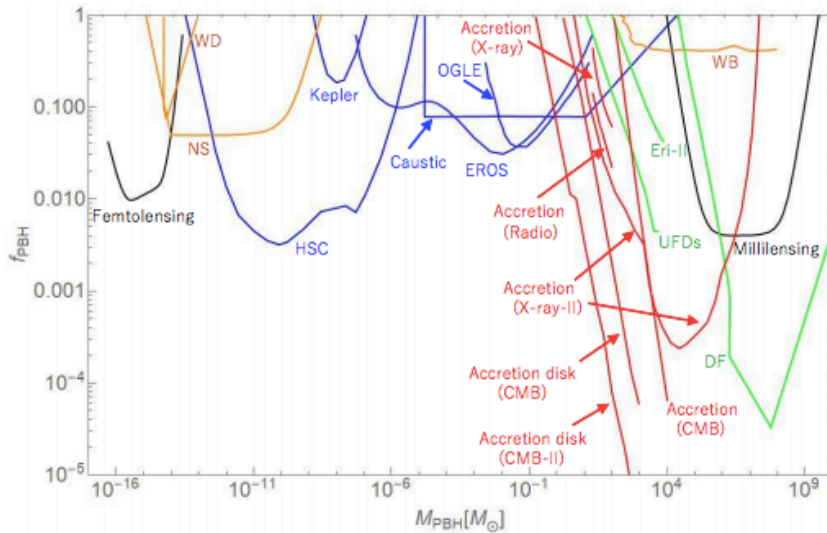
Bernard Carr^{1,*} and Florian Kühnel^{2,3,†}



Primordial Black Holes Perspectives in Gravitational Wave Astronomy

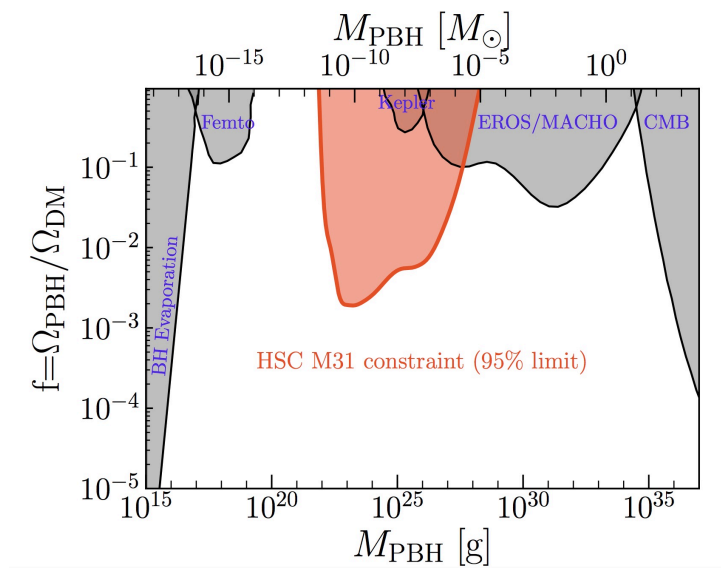
Misao Sasaki^a, Teruaki Suyama^b, Takahiro Tanaka^{c,a}, and Shuichiro Yokoyama^{d,e}

arXiv:1801.05235



Microlensing constraints on primordial black holes with the Subaru/HSC Andromeda observation

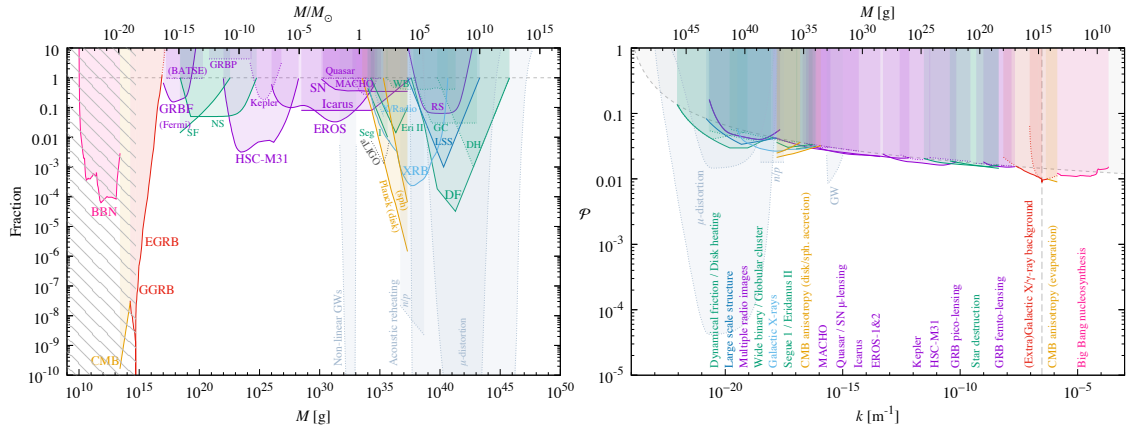
Niikura et al. arXiv:1701.02151v3



CONSTRAINTS ON PRIMORDIAL BLACK HOLES

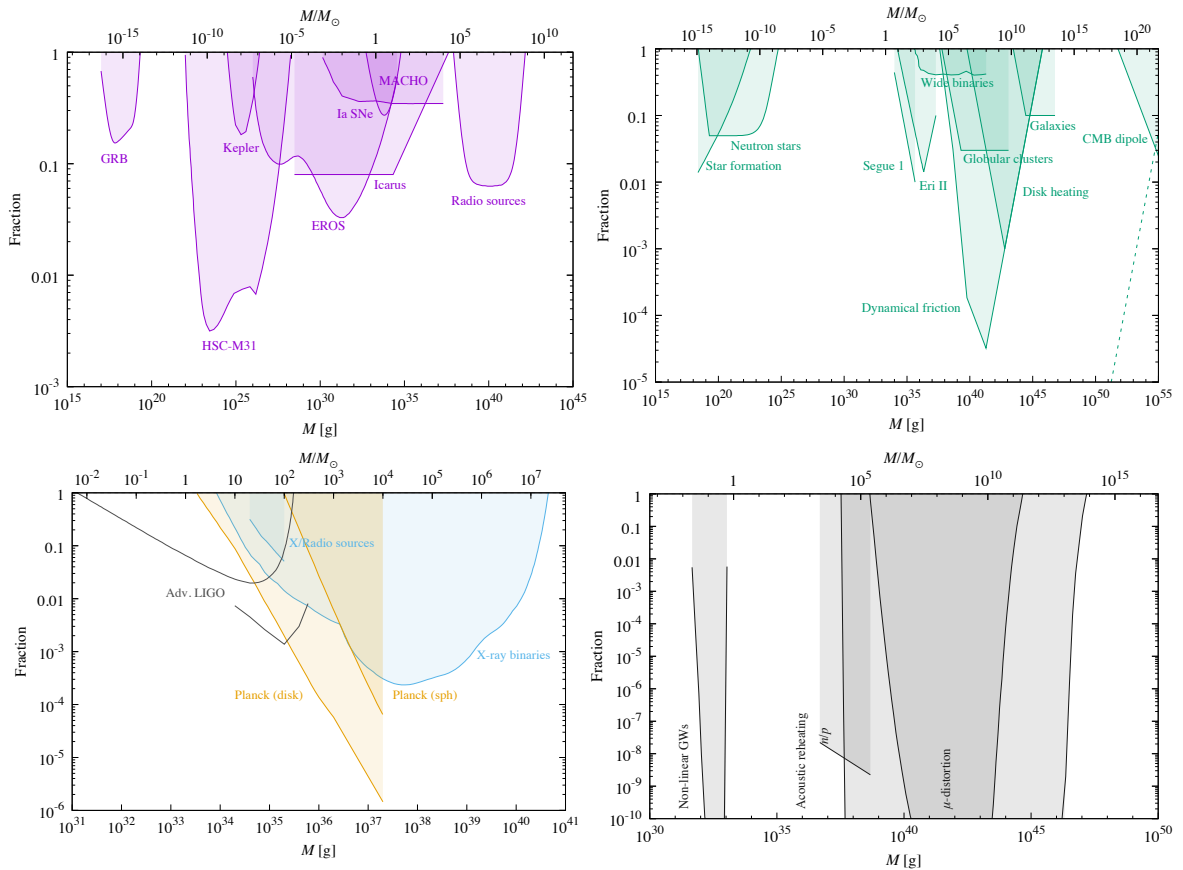
Bernard Carr,^{1,2,*} Kazunori Kohri,^{3,†} Yuuiti Sendouda,^{4,‡} and Jun'ichi Yokoyama^{2,5,§}

Progress Theoretical Physics (2018)



Each constraint comes with caveats and may improve or go away.

LENSING, DYNAMICAL, ACCRETION AND COSMOLOGICAL LIMITS



These constraints are not just nails in a coffin!



Each constraint is a potential signature

PBHs are interesting even if $f \ll 1$

CKS 2016

EXTENDED MASS FUNCTION?

Most constraints assume monochromatic PBH mass function

Can we evade standard limits with extended mass spectrum?

But this is two-edged sword!

PBHs may be dark matter even if fraction is low at each scale

PBHs giving dark matter at one scale may violate limits at others

PBH CONSTRAINTS FOR EXTENDED MASS FUNCTIONS

Carr, Raidal, Tenkanen, Vaskonen & Veermae (arXiv:1705.05567)

Possible PBH mass functions $\psi(M) \propto M \frac{dn}{dM} \Rightarrow \frac{\Omega_{\text{PBH}}}{\Omega_{\text{DM}}} = \int dM \psi(M)$

lognormal $\psi(M) = \frac{f_{\text{PBH}}}{\sqrt{2\pi}\sigma M} \exp\left(-\frac{\log^2(M/M_c)}{2\sigma^2}\right)$

2 parameters (M_c, σ)

power-law $\psi(M) \propto M^{\gamma-1} \quad (M_{\text{min}} < M < M_{\text{max}})$

critical collapse $\psi(M) \propto M^{2.85} \exp(-(M/M_f)^{2.85})$

f(M) limits themselves depend on PBH mass function

$$\int dM \frac{\psi(M)}{f_{\text{max}}(M)} \leq 1 \quad + \quad \psi(M; f_{\text{PBH}}, M_c, \sigma) \Rightarrow f_{\text{PBH}}(M_c, \sigma)$$

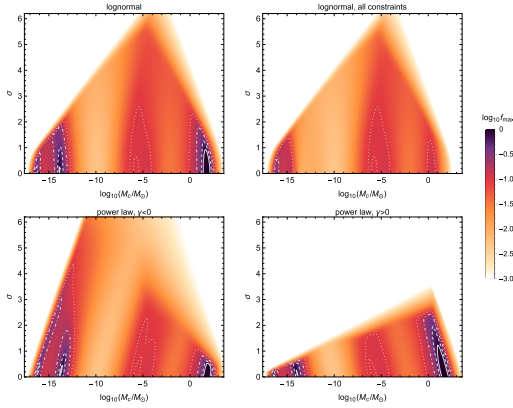
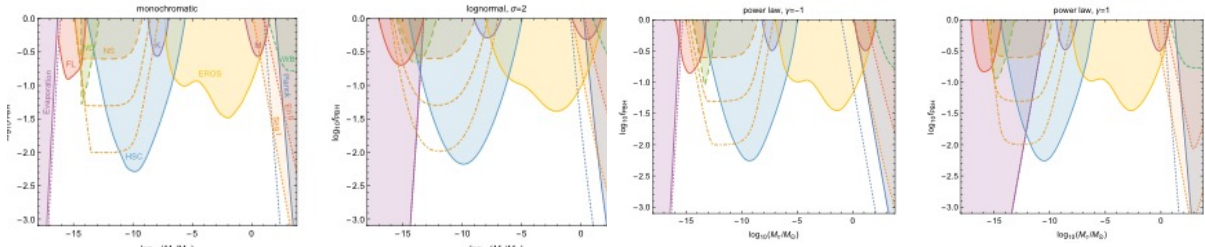


FIG. 2. Upper panels: Combined observational constraints on M_c and σ for a lognormal PBH mass function. The color coding shows the maximum allowed fraction of PBH DM. In the white region $\log_{10} f_{\text{max}} < -3$, while the solid, dashed, dot-dashed, and dotted contours correspond to $f_{\text{max}} = 1, f_{\text{max}} = 0.5, f_{\text{max}} = 0.2$, and $f_{\text{max}} = 0.1$, respectively. In the left panel only the constraints depicted by the solid lines in Fig. 1 are included, whereas the right panel includes all the constraints. Lower panels: Same as the upper left panel but for a power-law mass function with $\gamma < 0$ (left) and $\gamma > 0$ (right).

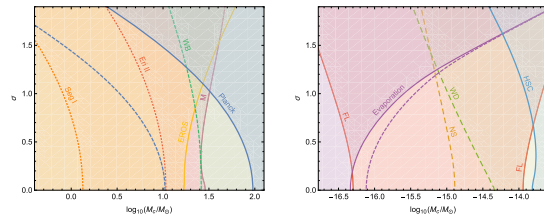


FIG. 3. Observational constraints on M_c and σ for a lognormal PBH mass function, assuming 100% PBH DM. The left panel presents a zoom into the high-mass region relevant for the LIGO events, while the right panel presents a zoom into the low-mass region. The color coding is the same as in Fig. 1.

PBHs AS GENERATORS OF COSMIC STRUCTURES

B.J. Carr & J. Silk

[arXiv:1801.00672](https://arxiv.org/abs/1801.00672)

What is maximum mass of PBH?

Could $10^6 - 10^{10} M_{\odot}$ black holes in galactic nuclei be primordial?

BBNS $\Rightarrow t < 1 \text{ s} \Rightarrow M < 10^5 M_{\odot}$ but $\beta < 10^{-6} (t/s)^{1/2}$

Supermassive PBHs could also generate cosmic structures on larger scale through 'seed' or 'Poisson' effect

Upper limit on μ distortion of CMB excludes $10^4 < M/M_{\odot} < 10^{12}$ for Gaussian fluctuations but some models evades these limits. Otherwise need accretion factor of $(M/10^4 M_{\odot})^{-1}$

CONSTRAINTS FROM CMB DISTORTIONS

PBHs \Rightarrow density fluctuations

S increase for $t < 7 \times 10^6 \text{ s} \Rightarrow$ weak BBNS limit
 \Rightarrow μ distortions for $7 \times 10^6 \text{ s} < t < 3 \times 10^9 \text{ s}$
y distortions for $3 \times 10^9 \text{ s} < t < 3 \times 10^{12} \text{ s}$

$\Rightarrow \delta(M) < \mu^{1/2} \sim 10^{-2}$ for $10^4 < M/M_{\odot} < 10^{12}$

\Rightarrow PBHs have $M < 10^5 M_{\odot}$ for Gaussian fluctuations

[Kohri, Suyama & Yokoyama PRD 90, 083514 \(2014\)](#)

But can alleviate limits if PBHs form from phase transition or from non-Gaussian fluctuations or in 'patch' model

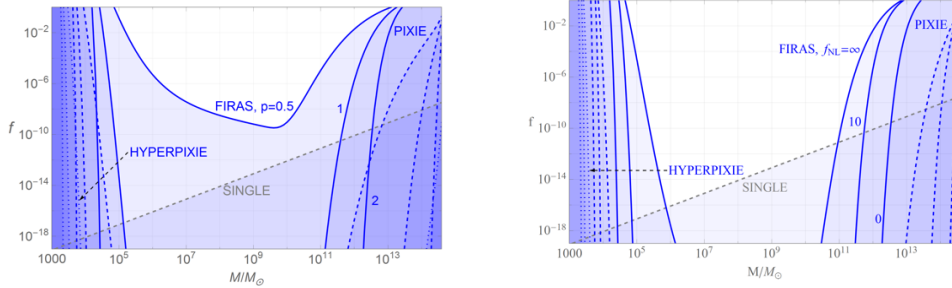
[Nakama, Suyama & Yokoyama PRD 93, 103522 \(2016\)](#)

Limits on primordial black holes from μ distortions in cosmic microwave background

Tomohiro Nakama,¹ Bernard Carr,^{2,3} and Joseph Silk^{1,4,5}

PHYSICAL REVIEW D **97**, 043525 (2018)

If primordial black holes (PBHs) form directly from inhomogeneities in the early Universe, then the number in the mass range $10^5 - 10^{12} M_\odot$ is severely constrained by upper limits to the μ distortion in the cosmic microwave background (CMB). This is because inhomogeneities on these scales will be dissipated by Silk damping in the redshift interval $5 \times 10^4 \lesssim z \lesssim 2 \times 10^6$. If the primordial fluctuations on a given mass scale have a Gaussian distribution and PBHs form on the high- σ tail, as in the simplest scenarios, then the μ constraints exclude PBHs in this mass range from playing any interesting cosmological role. Only if the fluctuations are highly non-Gaussian, or form through some mechanism unrelated to the primordial fluctuations, can this conclusion be obviated.



SEED AND POISSON FLUCTUATIONS

PBHs larger than $10^2 M_\odot$ cannot provide dark matter but can affect large-scale structure through seed effect on small scales or Poisson effect on large scales even if f small.

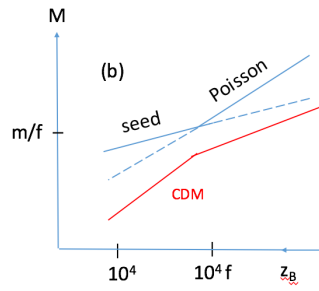
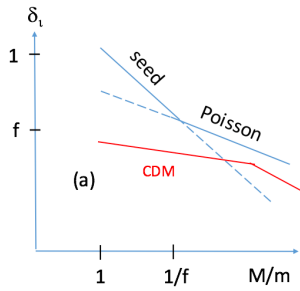
If region of mass M contains PBHs of mass m , initial fluctuation is

$$\delta_i \sim \begin{cases} m/M & \text{(seed)} \\ (fm/M)^{1/2} & \text{(Poisson)} \end{cases}$$

$f = 1 \Rightarrow$ Poisson dominates; $f \ll 1 \Rightarrow$ seed dominates for $M < m/f$. Fluctuation grows as z^{-1} from $z_{\text{eq}} \sim 10^4$, so mass binding at z_B is

$$M \approx \begin{cases} 4000 m z_B^{-1} & \text{(seed)} \\ 10^7 f m z_B^{-2} & \text{(Poisson)} \end{cases}$$

SEED VERSUS POISSON



cf. CDM fluctuations

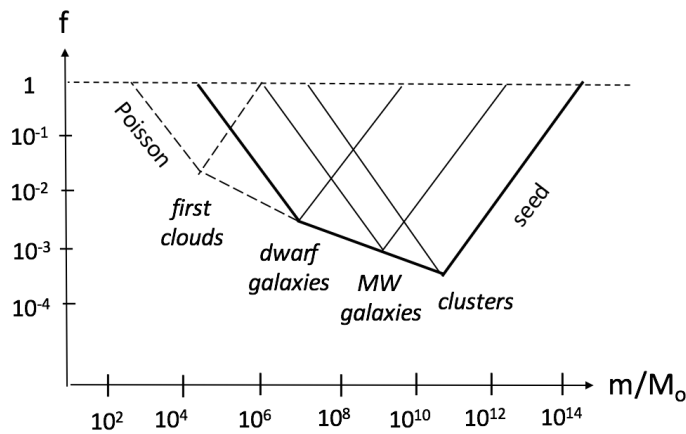
$$\delta_{eq} \propto \begin{cases} M^{-1/3} & (M < M_{eq}) \\ M^{-2/3} & (M > M_{eq}) \end{cases}$$

$$f = 1 \Rightarrow m < 10^3 M_O \Rightarrow M < 10^{11} z_B^{-2} M_O < M_{gal} \text{ (Poisson)}$$

Can constrain PBH scenarios by requiring that various cosmic structures do not form too early

Can apply to

first bound clouds ($M = 10^6 M_O$)
 dwarf galaxies ($M = 10^{10} M_O$)
 MW galaxies ($M = 10^{12} M_O$)
 clusters ($M = 10^{13} M_O$)



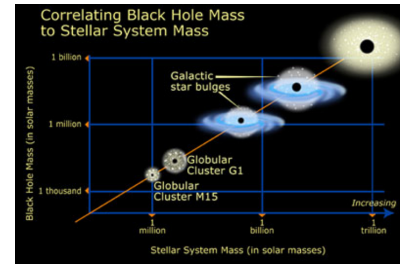
First clouds bind earlier than in standard model

Extended PBH mass function => DM and cosmic structures

SUPERMASSIVE PBHS AS SEEDS FOR GALAXIES

Seed effect $\Rightarrow M_B \sim 10^3 m (z_B/10)$
 \Rightarrow naturally explain M_{BH}/M_{bulge} relation

Effect of mergers?



Also predict mass function of galaxies (cf. Press-Schechter)

$$dN_g/dM \propto M^{-2} \exp(-M/M_*) \quad M_* \sim 10^{12} M_\odot$$

and core density profile $\rho(r) \propto r^{-9/4}$.

Bondi accretion $\Rightarrow m \approx m_i / (1 - m_i \eta t)$, $M_{eq} \sim 10^{15} M_\odot$

\Rightarrow diverges at $\tau = 1/(\eta m_i) \sim (M_{eq}/m_i)(c_{eq}/c)^3 t_{eq}$

\Rightarrow upper limit $m_i > M_{eq}(t_{eq}/t_o) \sim 10^{10} M_\odot$

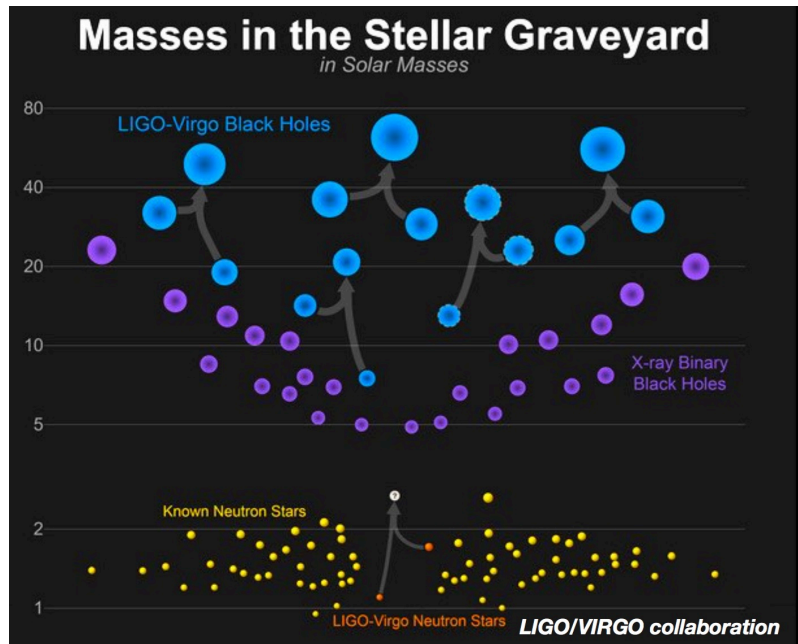
Joe Silk

What IMBH can do for dwarf galaxies
 motivation: something new may be needed
 mostly passive today but active in gas-rich past

- 1. Suppress number of luminous dwarfs
- 2. Generate cores in dwarfs by dynamical heating
- 3. Resolve the "too big to fail" problem
- 4. Create bulgeless disks
- 5. Form ultrafaint dwarfs & ultradiffuse galaxies
- 6. Reduce baryon fraction in MWG-mass galaxies
- 7. Seeds for SMBH at high z
- 8. ULXs in outskirts of galaxies: relics of dwarfs
- 9. AGN triggering of star formation in dwarfs
- 10. Early galaxy formation

Predictions: 21cm, LISA, TDEs, μ -lensing

PBHS AND LIGO



Do we need Population III or primordial BHs?

Prescience of Japanese!

GRAVITATIONAL WAVES FROM COALESCING BLACK HOLE MACHO BINARIES
Takashi Nakamura, Misao Sasaki, Takahiro Tanaka and Kip Thorne

THE ASTROPHYSICAL JOURNAL, 487:L139–L142, 1997

If MACHOs are black holes of mass $\sim 0.5 M_{\odot}$, they must have been formed in the early universe when the temperature was ~ 1 GeV. We estimate that in this case in our Galaxy's halo out to ~ 50 kpc there exist $\sim 5 \times 10^8$ black hole binaries the coalescence times of which are comparable to the age of the universe, so that the coalescence rate will be $\sim 5 \times 10^{-2}$ events yr^{-1} per galaxy. This suggests that we can expect a few events per year within 15 Mpc. The gravitational waves from such coalescing black hole MACHOs can be detected by the first generation of interferometers in the LIGO/VIRGO/TAMA/GEO network. Therefore, the existence of black hole MACHOs can be tested within the next 5 yr by gravitational waves.

POSSIBLE INDIRECT CONFIRMATION OF THE EXISTENCE OF POP III MASSIVE STARS BY GRAVITATIONAL WAVES

Tomoya Kinagawa, Kohei Inayoshi, Kenta Hotokezaka, Daisuka Nakauchi and Takashi Nakamura

MNRAS **442**, 2963–2992 (2014)

We perform population synthesis simulations for Population III (Pop III) coalescing compact binary which merges within the age of the Universe. We found that the typical mass of Pop III binary black holes (BH–BHs) is $\sim 30 M_{\odot}$ so that the inspiral chirp signal of gravitational waves can be detected up to $z = 0.28$ by KAGRA, Adv. LIGO, Adv. Virgo and GEO



Did LIGO detect dark matter?

Simeon Bird,* Ilias Cholis, Julian B. Muñoz, Yacine Ali-Haïmoud, Marc Kamionkowski, Ely D. Kovetz, Alvise Raccanelli, and Adam G. Riess¹

[arXiv:1603.00464](#)

Dark matter in 20-100 M_{\odot} binaries may provide observed rate of 2-53 $\text{Gpc}^{-1}\text{yr}^{-1}$

Primordial Black Hole Scenario for the Gravitational-Wave Event GW150914

Misao Sasaki,¹ Teruaki Suyama,² Takahiro Tanaka,^{3,1} and Shuichiro Yokoyama⁴

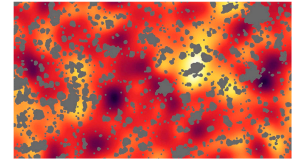
[arXiv:1603.08338](#)

Only need small f and comparable to limits from CMB distortion

LIGO gravitational wave detection, primordial black holes and the near-IR cosmic infrared background anisotropies

A. Kashlinsky¹,

[arXiv:1605.04023](#)



PBHs generate early structure => infrared background

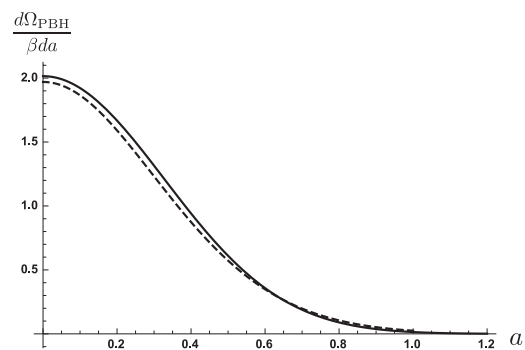
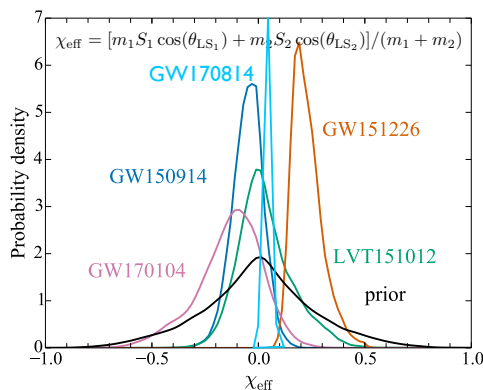
Spin Distribution of Primordial Black Holes

Takeshi Chiba¹ and Shuichiro Yokoyama²

[arXiv:1704.06573](#)

Abstract

We estimate the spin distribution of primordial black holes based on the recent study of the critical phenomena in the gravitational collapse of a rotating radiation fluid. We find that primordial black holes are mostly slowly rotating.



Gravitational Waves Induced by non-Gaussian Scalar Perturbations

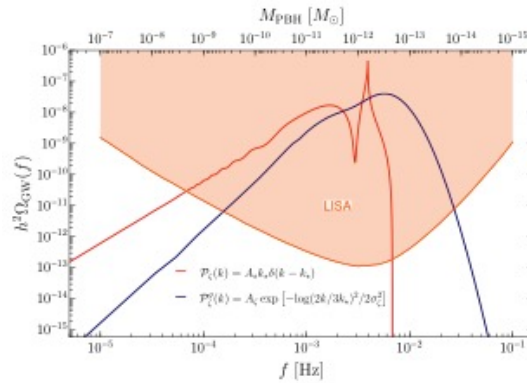
Rong-gen Cai^{a,b}, Shi Pi^c and Misao Sasaki^{c,a,d,e}

arXiv:1810.11000

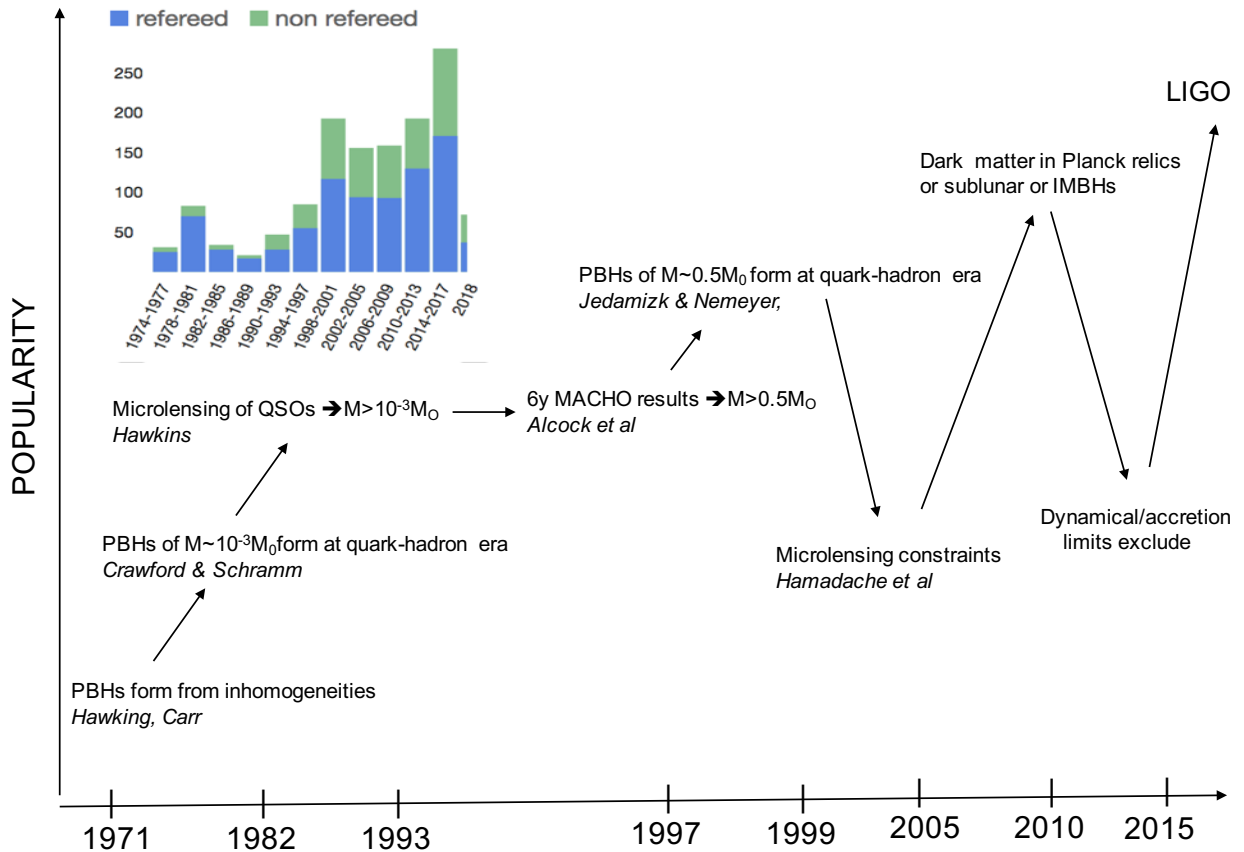
if PBHs with masses of 10^{20} g to 10^{22} g are identified as cold dark matter of the Universe, the corresponding GWs must be detectable by LISA, irrespective of the value of f_{NL} .

Testing Primordial Black Holes as Dark Matter through LISA

N. Bartolo^{a,b,c}, V. De Luca^d, G. Franciolini^d, M. Peloso^{a,b}, D. Racco^{d,e} and A. Riotto^d



arXiv:1810.12224



CONCLUSIONS

PBHs are best MACHO candidate and invoked for three roles:

Dark matter

LIGO events

Cosmic structure

These are distinct roles but with an extended mass function PBHs could possibly fulfill all three.

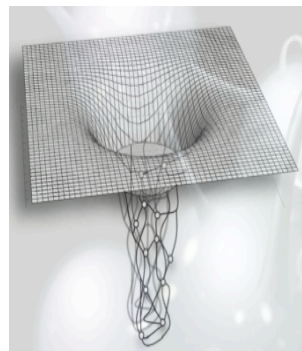
This talk is dedicated to the memory of my friend and mentor Stephen Hawking. He wrote the first paper on primordial black holes in 1971. If they play any of the roles discussed here, this may have been his most prescient and important work



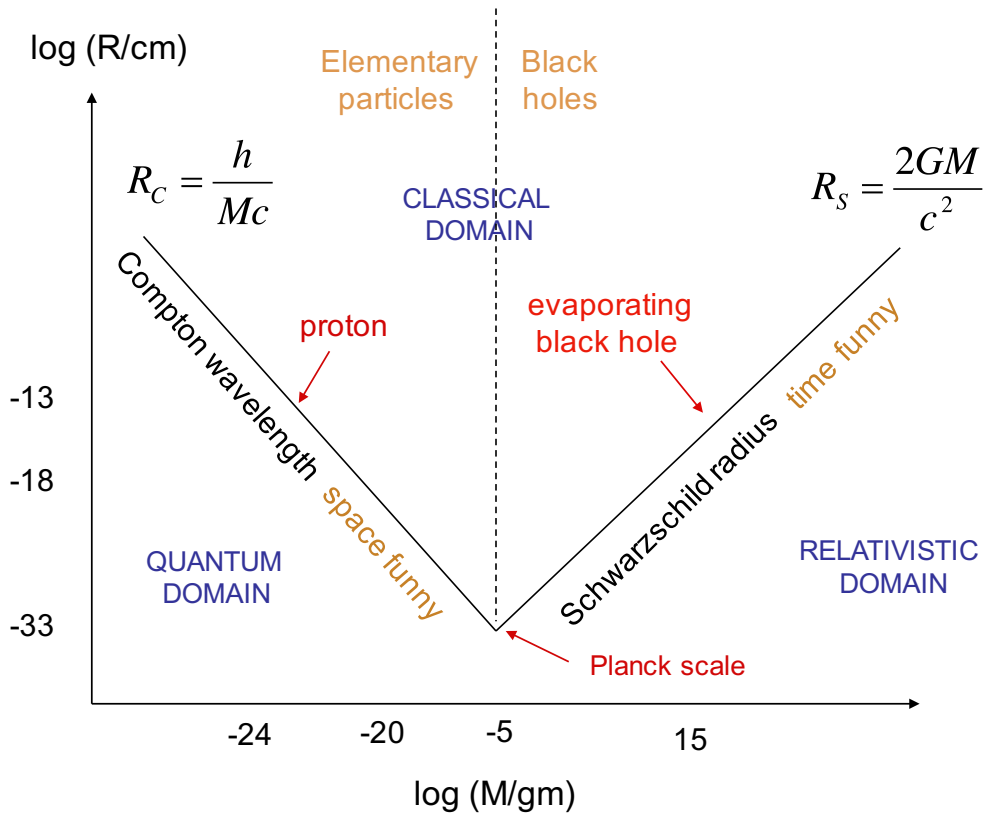
[FOLLOWING SLIDES NOT SHOWN]

PBHS, HIGHER DIMENSIONS AND QUANTUM GRAVITY

COMPTON-SCHWARZSCHILD DUALITY

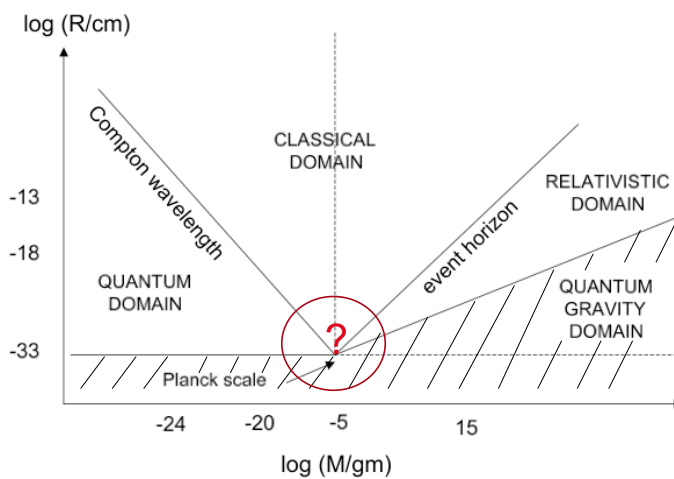


BLACK HOLE UNCERTAINTY PRINCIPLE CORRESPONDENCE



What happens where Compton and Schwarzschild intersect?

$$R_p = \sqrt{Gh/c^3} \sim 10^{-33} \text{ cm}, \quad M_p = \sqrt{hc/G} \sim 10^{-5} \text{ g},$$

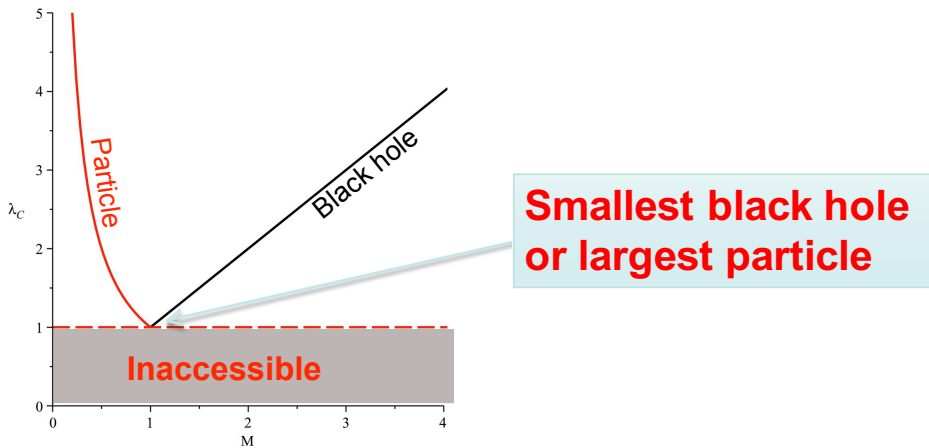


$$\rho_p = \frac{c^5}{h^2 G} \sim 10^{94} \text{ gcm}^{-3}$$

This must be an important feature of theory of quantum gravity.

Critical point or smooth minimum?

Planck Scale Criticality?

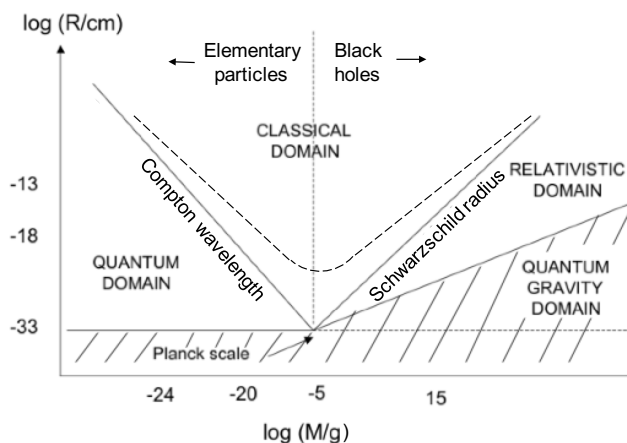


But this breaks T-duality $M \rightarrow M_P^2/M, R \rightarrow R_P^2/R$

In string theory this relates momentum-carrying string states to winding states & relates sub-Planck and super-Planck lengths

Smooth minimum?

Preserves T-duality?



Compton scale becomes Schwarzschild scale for $M \gg M_P$?

Compton irrelevant for $M \gg M_P$ since $R_C \ll R_P$?

Cannot localize on scale below R_S ?

=> BHs are intrinsically quantum (BH radiation, firewalls)

Schwarzschild scale becomes Compton scale for $M \ll M_P$?

=> link between elementary particles and sub-Planckian BHs

ARE ELEMENTARY PARTICLES SPINNING BLACK HOLES?

Sivaram & Sinha “Strong gravity, black holes and hadrons” PRD 16, 1975 (1977)

1. Both hadrons and Kerr-Newman black holes are almost entirely characterized by just three parameters: mass, charge and angular momentum.
2. Both hadrons and Kerr-Newman black holes have magnetic dipole moments, but do not have electric dipole moments.
3. Typical hadrons and Kerr-Newman black holes have gyromagnetic ratios of ≈ 2 .
4. Hadrons and Kerr-Newman black holes have similar linear relationships between angular momentum and mass squared, i.e., $J \propto M^2$.
5. When Kerr-Newman black holes interact, their surface areas may increase but can never decrease, which is potentially analogous to the increase of cross-sections found in hadron collisions.

Oldershaw “Hadrons as Kerr-Newman black holes” arXiv/0701006

COMPTON-SCHWARZSCHILD CORRESPONDENCE

Simplest expression asymptoting to Compton/Schwarzschild is

$$R_{CS} = \frac{\beta \hbar}{Mc} + \frac{2GM}{c^2}$$

$$R'_C = \frac{\beta \hbar}{Mc} \left[1 + \frac{2}{\beta} \left(\frac{M}{M_P} \right)^2 \right] \quad (M \ll M_P) \quad \text{generalised Compton wavelength}$$

$$R'_S = \frac{2GM}{c^2} \left[1 + \beta \left(\frac{M_P}{M} \right)^2 \right] \quad (M \gg M_P) \quad \text{generalised event horizon}$$

More generally consider any function $R'_C(M) \equiv R'_S(M)$ such that

$$R'_C \equiv R'_S \approx \begin{cases} h/(Mc) & (M \ll M_P) \\ 2GM/c^2 & (M \gg M_P) \end{cases}$$

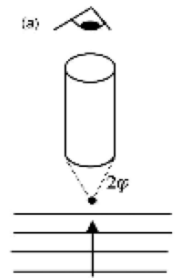
Can interpret in terms of Generalised Uncertainty Principle.

UNCERTAINTY PRINCIPLE

Photon of momentum p determines position to precision

$\Delta x > \lambda = h/p$ but imparts momentum $\Delta p \sim p$

$$\Rightarrow \Delta x > \frac{h}{(2)\Delta p} \Rightarrow R_c = \frac{h}{Mc} \quad (\text{Compton wavelength})$$



GENERALIZED UNCERTAINTY PRINCIPLE

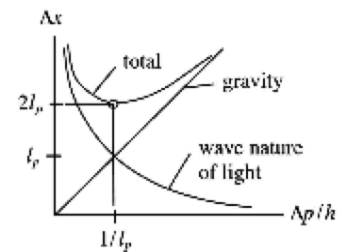
Photon of frequency ω approaching to distance R induces

\Rightarrow acceleration $a \sim Gh\omega/(cR)^2$ over time $t \sim R/c$

\Rightarrow uncertainty in momentum $\Delta p \sim p \sim h\omega/c$ and in position

$$\Delta x_g > at^2 \sim Gh\omega/c^4 \sim G\Delta p/c^3 \sim R_p^2 \Delta p/h$$

$$\Rightarrow \Delta x > \frac{h}{\Delta p} + R_p^2 \frac{\Delta p}{h} > 2R_p$$



This suggests
$$\Delta x > \frac{h}{\Delta p} + \alpha R_p^2 \frac{\Delta p}{h} = \frac{h}{\Delta p} \left[1 + \alpha \left(\frac{\Delta p}{cM_p} \right)^2 \right]$$

Putting $\Delta x \rightarrow R$ and $\Delta p \rightarrow cM$ gives

$$R > R_c' = \frac{h}{Mc} + \frac{\alpha GM}{c^2} \approx \frac{h}{Mc} \left[1 + \alpha \left(\frac{M}{M_p} \right)^2 \right] \quad (M \ll M_p)$$

\Rightarrow Generalized Compton Wavelength

DO GUP UNCERTAINTIES ADD LINEARLY?

Root-mean-square error would give

$$\Delta x > \sqrt{\left(\frac{h}{\Delta p} \right)^2 + \left(\alpha R_p^2 \frac{\Delta p}{h} \right)^2} \Rightarrow R_c' = \sqrt{\left(\frac{h}{Mc} \right)^2 + \left(\frac{\alpha GM}{c^2} \right)^2}$$

$$\Rightarrow R_s' = \sqrt{\left(\frac{2GM}{c^2} \right)^2 + \left(\frac{\beta h}{Mc} \right)^2} \approx \frac{2GM}{c^2} \left[1 + \frac{\beta^2}{8} \left(\frac{M_p}{M} \right)^4 \right]$$

“Generalized Uncertainty and Self-dual Black Holes”

Carr, Modesto & Premont-Schwarz, arXiv: 1107.0708

LOOP BLACK HOLES

Metric $ds^2 = -G(r)dt^2 + \frac{dr^2}{F(r)} + H(r)d\Omega^{(2)}$, $G(r) = \frac{(r-r_+)(r-r_-)(r+r_*)^2}{r^4 + a_0^2}$,
 $F(r) = \frac{(r-r_+)(r-r_-)r^4}{(r+r_*)^2(r^4 + a_0^2)}$,
 $H(r) = r^2 + \frac{a_0^2}{r^2}$.

where $r_+ = 2Gm/c^2$ and $a_0 = A_{\min}/8\pi = \sqrt{3}\gamma\zeta R_P^2/2$
 $r_- = 2GmP^2/c^2$
 $r_* \equiv \sqrt{r_+r_-}$

At large r $G(r) \rightarrow 1 - \frac{2M}{r}(1 - \epsilon^2)$, $F(r) \rightarrow 1 - \frac{2M}{r}$, $H(r) \rightarrow r^2$, implies $M = m(1+P)^2$ (ADM mass)

Metric has self-duality with dual radius $\bar{r} = r = \sqrt{a_0}$

=> another asymptotic infinity ($r=0$) with BH mass M_P^2/m

Physical radial coordinate $R = \sqrt{H(r)} = \sqrt{r^2 + \frac{a_0^2}{r^2}}$

$$\Rightarrow R_s = \sqrt{\left(\frac{2Gm}{c^2}\right)^2 + \left(\frac{c^2 a_0}{2Gm}\right)^2} \approx \frac{2Gm}{c^2} \quad (m > M_P)$$

$$\beta \frac{\sqrt{3}\gamma\zeta}{4} \frac{h}{mc} \quad (m < M_P)$$

This removes singularity and corresponds to the quadratic GEH.

Suggests GR origin for quantum effects!

Sub-Planckian black holes are hidden within wormholes

Sub-Planckian Black Holes and the GUP

B. Carr, J. Mureika, P. Nicolini, JHEP 07 (2015) 52, arXiv:1504.07637

Can black holes exist *below* the Planck mass?

Include GUP in GR by emphasizing **duality** in the black hole mass

$$M \longrightarrow M \left(1 + \frac{\beta}{2} \frac{M_{\text{Pl}}^2}{M^2} \right)$$

Metric is:

$$ds^2 = F(r)dt^2 - F(r)^{-1}dr^2 - r^2d\Omega^2$$

$$F(r) = 1 - \frac{2}{M_{\text{Pl}}^2} \frac{M}{r} \left(1 + \frac{\beta}{2} \frac{M_{\text{Pl}}^2}{M^2} \right)$$

Planck mass is now critical point for which...

$$M \gg M_{\text{Pl}} \implies F(r) \sim 1 - \frac{M}{r}$$

$$M \ll M_{\text{Pl}} \implies F(r) \sim 1 - \frac{1}{Mr}$$

Black Hole Characteristics: Horizon

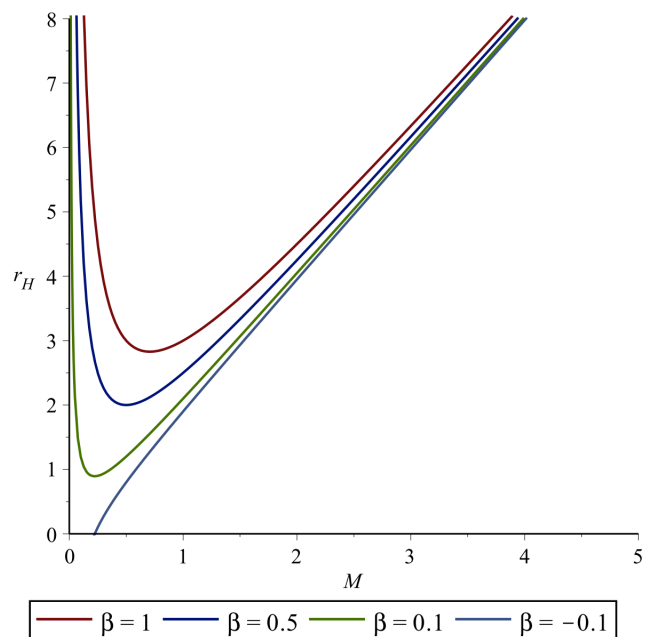
$$F(r_H) = 0$$

$$r_H = \frac{2}{M_{\text{Pl}}^2} \left(\frac{M^2 + \frac{\beta}{2} M_{\text{Pl}}^2}{M} \right)$$

$$M \gg M_{\text{Pl}} \implies r_H \approx \frac{2M}{M_{\text{Pl}}^2}$$

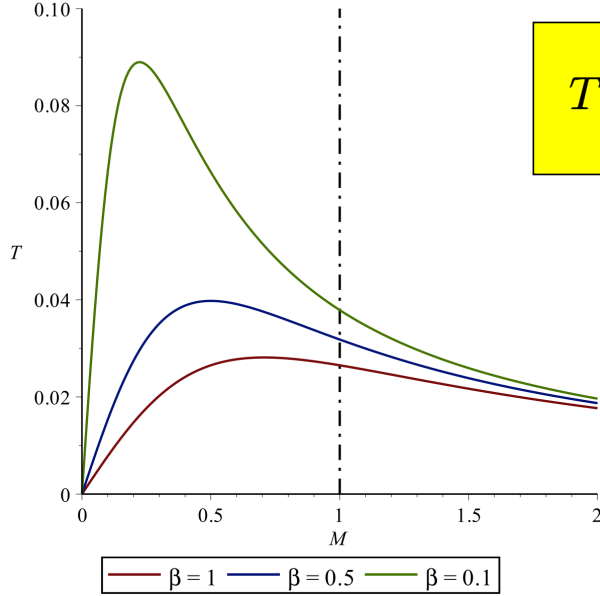
$$M \sim M_{\text{Pl}} \implies r_H \approx \frac{2 + \beta}{M_{\text{Pl}}}$$

$$M \ll M_{\text{Pl}} \implies r_H \approx \frac{\beta}{M}$$



Black Hole Temperature

From surface gravity: $T = \frac{\kappa}{2\pi}$, $\kappa = \frac{1}{2} \frac{dF}{dr} (r = r_H)$



$$T = \frac{M_{\text{Pl}}^2}{8\pi M(1 + \beta M_{\text{Pl}}^2/2M^2)}$$

$$M \gg M_{\text{Pl}} \implies T \approx \frac{M_{\text{Pl}}^2}{8\pi M}$$

$$M \sim M_{\text{Pl}} \implies T \sim \frac{M_{\text{Pl}}}{8\pi(1 + \beta/2)}$$

$$M \ll M_{\text{Pl}} \implies T \approx \frac{M}{4\pi\beta}$$

A Duality Between Curvature and Torsion

Swanand Khanapurkar^{*†} and Tejinder P. Singh[†]

[arXiv: 1804.00167](https://arxiv.org/abs/1804.00167)

ABSTRACT

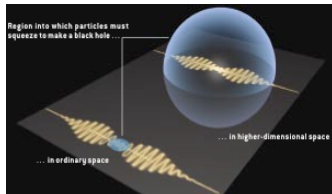
Compton wavelength and Schwarzschild radius are considered here as limiting cases of a unified length scale. Using this length, it is shown that the Dirac equation and the Einstein equations for a point mass are limiting cases of an underlying theory which includes torsion. We show that in this underlying theory the gravitational interaction between small masses is weaker than in Newtonian gravity. We explain as to why the Kerr-Newman black hole and the electron both have the same non-classical gyromagnetic ratio. We propose a duality between curvature and torsion and show that general relativity and teleparallel gravity are respectively the large mass and small mass limit of the ECSK theory. We demonstrate that small scale effects of torsion can be tested with current technology.

BLACK HOLES IN HIGHER DIMENSIONS

M-theory => extra compactified dimensions (n)

Standard model => $V_n \sim M_P^{-n}$, $M_D \sim M_P$,

Large extra dimensions => $V_n \gg M_P^{-n}$, $M_D \ll M_P$

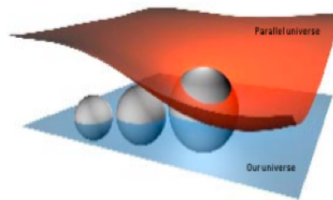
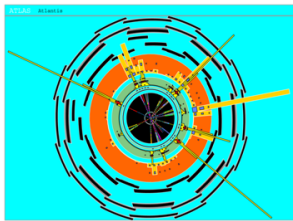


TeV quantum gravity?

Schwarzschild radius $r_S = M_P^{-1} (M_{BH}/M_P)^{1/(1+n)}$

Temperature $T_{BH} = (n+1)/r_S$ < 4D case

Lifetime $\tau_{BH} = M_P^{-1} (M_{BH}/M_P)^{(n+3)/(1+n)}$ > 4D case



BLACK HOLES AND HIGHER DIMENSIONS

Assume $D=3+n$ dimensions for $R < R_E$

Gauss law

$$F_{grav} = \frac{G_D m_1 m_2}{R^{2+n}} \quad (R < R_E)$$

$$F_{grav} = \frac{G m_1 m_2}{R^2} \quad (R > R_E)$$

$$G = \left(\frac{G_D}{R_E^n} \right)$$

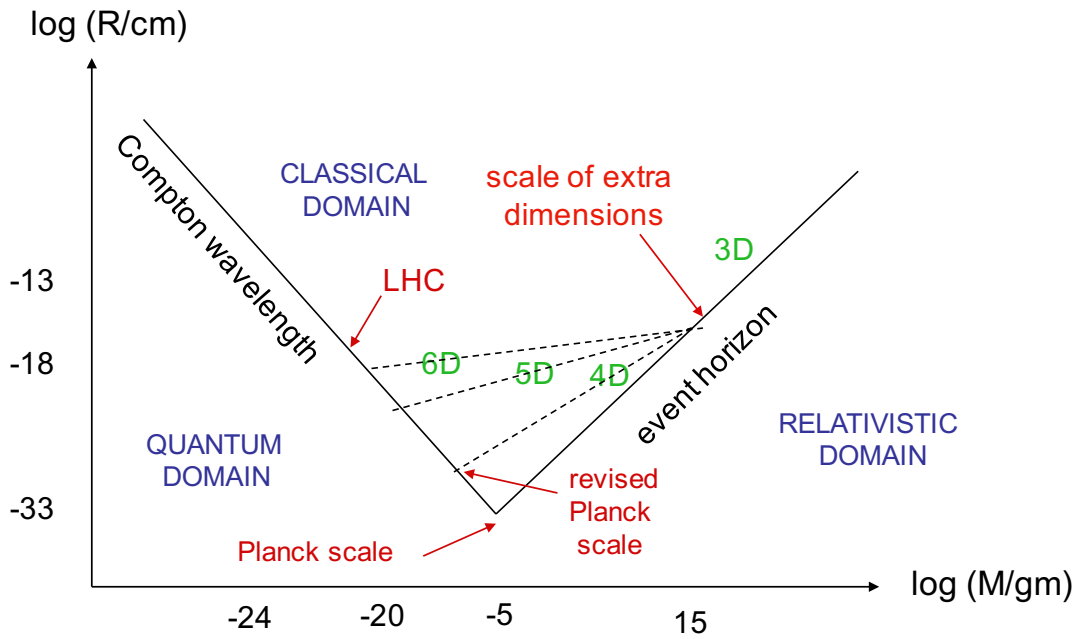
3D black hole smaller than R_E for $M < M'_E \equiv c^2 R_E / G$

$$R_S = R_E \left(\frac{M}{M'_E} \right)^{1/(1+n)} \quad \text{for } M_P < M < M'_E \equiv c^2 R_E / G.$$

This intersects standard Compton boundary at new Planck scales

$$R'_P \sim (R_P^2 R_E^n)^{1/(2+n)}, \quad M'_P \sim (M_P^2 M_E^n)^{1/(2+n)}$$

All extra dimensions with scale R_E



For hierarchy of compactification scales:

$$R_i = \alpha_i R_P \quad \alpha_1 \geq \alpha_2 \geq \dots \geq \alpha_n \geq 1,$$

we can define average compactification scale

$$\langle R_E \rangle = \left(\prod_{i=1}^n R_i \right)^{1/n} = R_P \left(\prod_{i=1}^n \alpha_i \right)^{1/n}$$

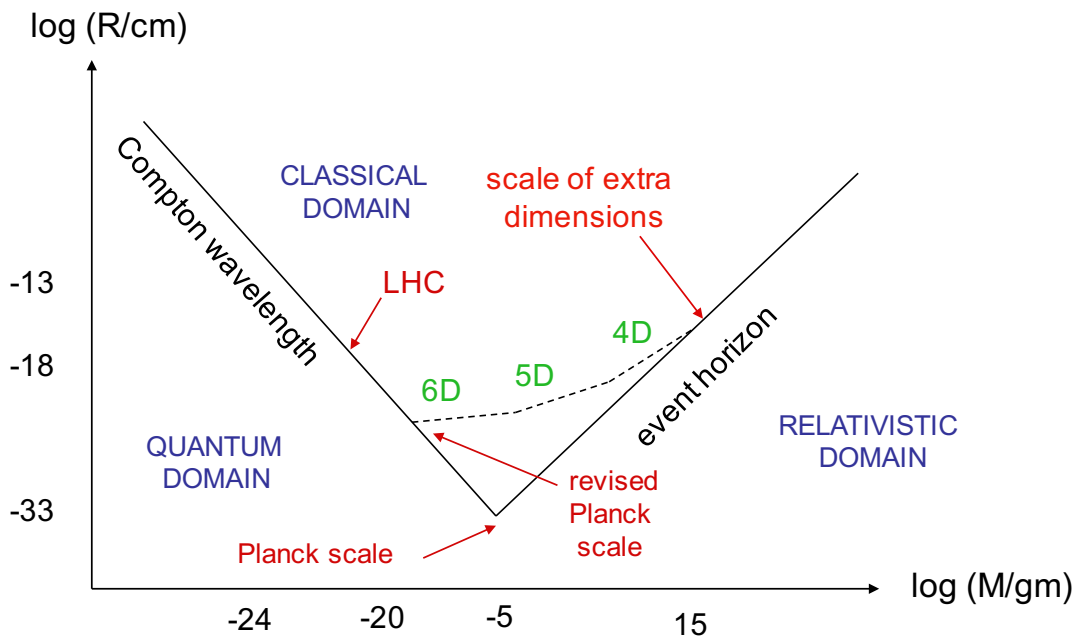
For $R_{k+1} \lesssim R \lesssim R_k$ Schwarzschild radius becomes

$$R_S = R_{*(k)} \left(\frac{M}{M_P} \right)^{1/(1+k)}, \quad R_{*(k)} = \left(R_P \prod_{i=1}^{k \leq n} R_i \right)^{1/(1+k)}.$$

This intersects standard Compton boundary at

$$R'_P \sim (R_P^2 \langle R_E \rangle^n)^{1/(2+n)} \quad M'_P \sim (M_P^2 \langle M_E \rangle^n)^{1/(2+n)}$$

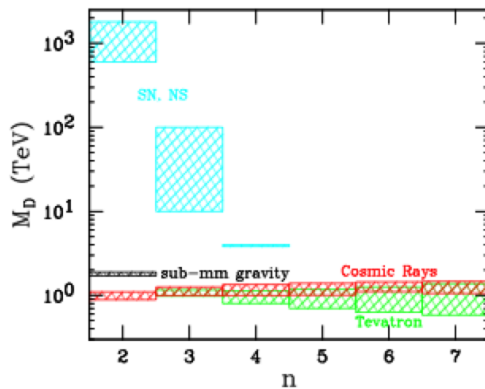
Hierarchy of compactified dimensions



DETECTABLE AT LHC?

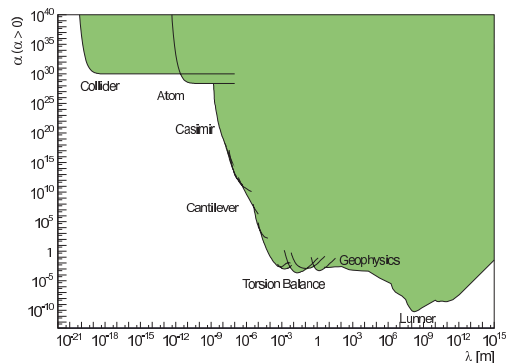
$$M_D \sim \text{TeV} \Rightarrow R_C \sim 10^{(32/n)-17} \text{ cm} \sim \begin{matrix} 10^{16} \text{ cm} & (n=1) & \text{excluded} \\ 10^{-1} \text{ cm} & (n=2) \\ 10^{-6} \text{ cm} & (n=3) \\ 10^{-13} \text{ cm} & (n=7) \end{matrix}$$

No evidence from LHC so far



Yukawa correction

$$V = \frac{G_D m_1 m_2}{r} \left[1 + \alpha \exp\left(-\frac{r}{\lambda}\right) \right]$$



Murata & Tanaka 2015

“Does Compton–Schwarzschild duality in higher dimensions exclude TeV quantum gravity?”

Matthew Lake and Bernard Carr

IJMPD 28 (2019) 1930001

COMPTON WAVELENGTH IN 3D

Cross-section for photon-electron scattering $R_C = h/(Mc)$

Reduced wavelength appears in KG or Dirac equations $\hbar/(Mc)$

de Broglie $E = \hbar\omega$, $\vec{p} = \hbar\vec{k}$. \Rightarrow pair-production for $R < R_C$

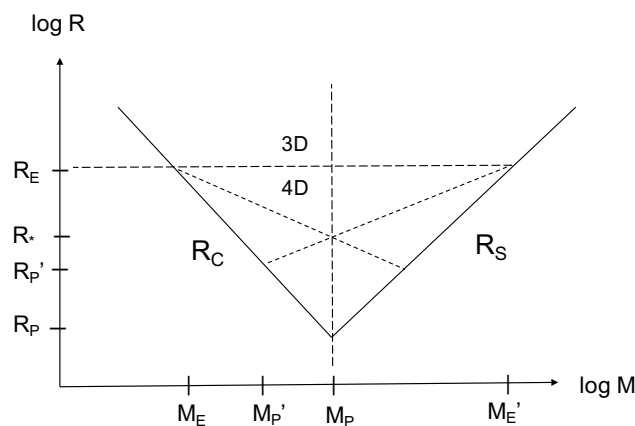
COMPTON WAVELENGTH IN (3+n) SPATIAL DIMENSIONS

To preserve duality, effective Compton wavelength must become

$$R_C = R_E \left(\frac{M}{M_E} \right)^{-1/(1+n)} \quad \text{for } M > M_E \equiv \hbar/(cR_E) = M_P^2/M'_E$$

Then revised Planck length is $R_* \sim (R_P R_E^n)^{1/(1+n)} \gg R'_P$

but Planck mass is unchanged \Rightarrow no TeV quantum gravity!



BUT IS THIS TRUE?

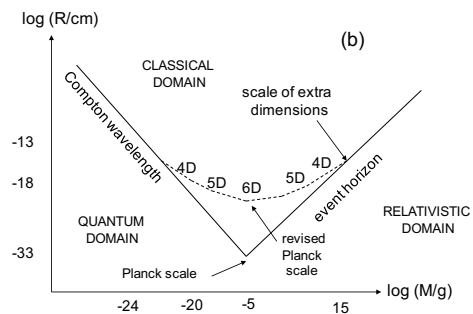
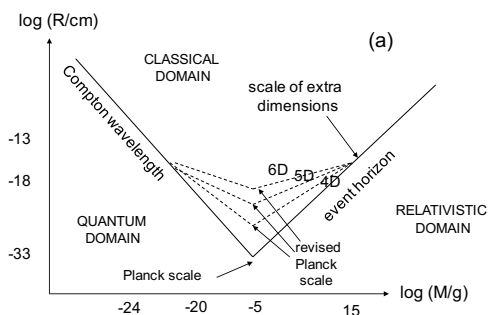
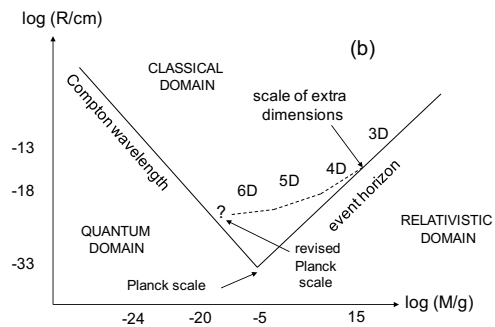
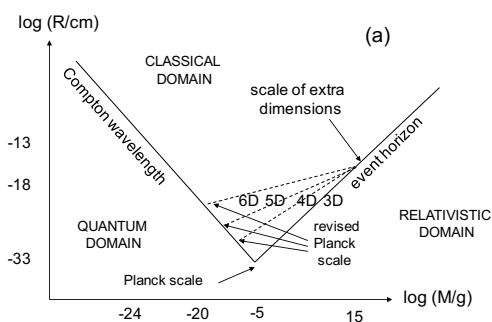
If $(3+n)D$ wave function is spherically symmetric in all dim'

$$\Rightarrow R_C \sim M^{-1} \text{ (as in 3D case)}$$

If $(3+n)D$ wave function is quasi-spherical (i.e. spherically symmetric in large dimensions but pancaked in extra dim')

$$\Rightarrow R_C \sim M^{-1/(1+n)}$$

This preserves duality between R_C and R_S



REFERENCES

B. Carr, L. Modesto & I. Premont-Schwarz, Generalized Uncertainty Principle and Self-Dual Black Holes, arXiv: 1107.0708 [gr-qc] (2011).

B. Carr, Black Holes, Generalized Uncertainty Principle and Higher Dimensions, Mod. Phys. Lett. A 28, 134001 (2013).

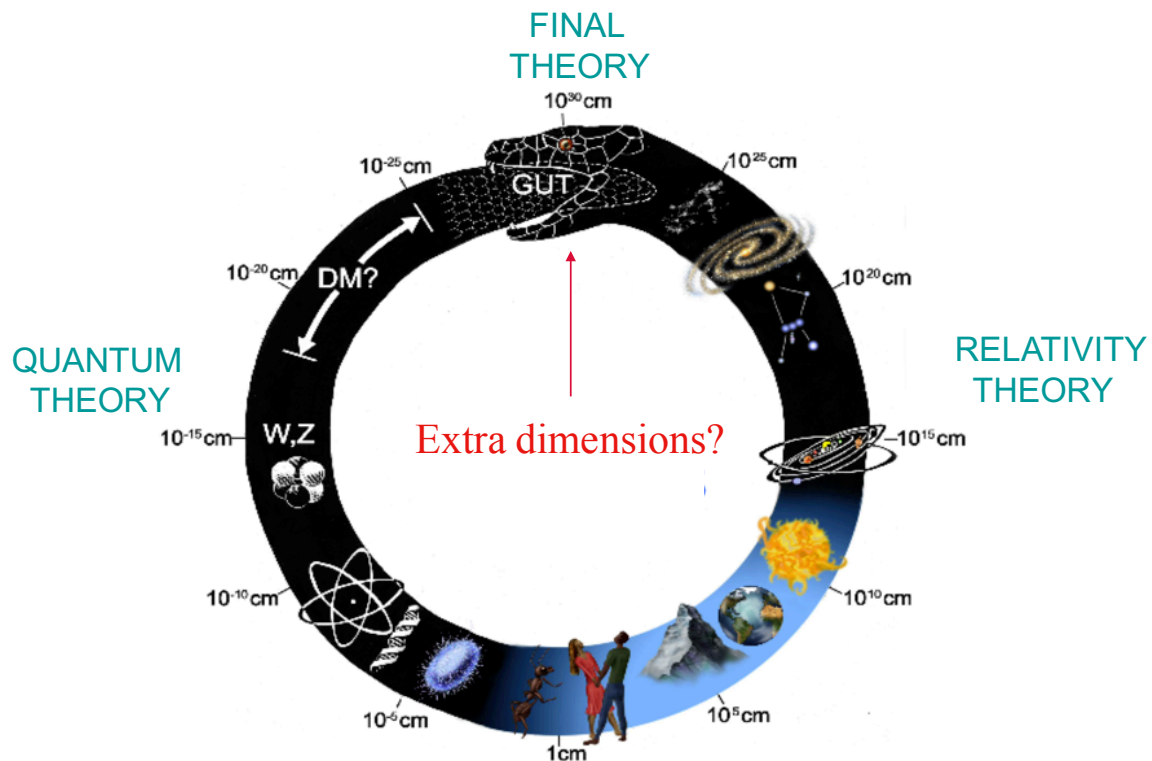
B. Carr, Black Hole Uncertainty Principle Correspondence, Proc KSM 2013 (2015); arXiv:1402.1427.

B. Carr, J. Mureika, P. Nicolini, Sub-Planckian black holes and Generalized Uncertainty Principle, JHEP 07, 52 (2015).

M. Lake and B. Carr, Compton-Schwarzschild correspondence from extended de Broglie relations, JHEP 1511, 105 (2015)

M. Lake and B. Carr, Does Compton-Schwarzschild duality in higher dimensions exclude TeV quantum gravity? IJMPD 28, 1930001(2018).

B. Carr, Quantum Black Hole as the Link between Microphysics and Macrophysics, Proc KSM 2015 (2018); arXiv:1703.08655.



PBHs may play a crucial role in the marriage of QT and GR

Session S4A1 9:45–10:15

[Chair: Tomohiro Harada]

Kazumasa Okabayashi

Department of Physics, Waseda University.

“Collisional Penrose process of spinning particles”

(10+5 min.)

[JGRG28 (2018) 110802]

Collisional Penrose process of spinning particles

Kazumasa Okabayashi(Waseda Uni.)

with Kei-ichi Maeda(Waseda Uni.)

and Hirotada Okawa(YITP)

Based on PhysRevD.98.064027

(arXiv:1804.07264)

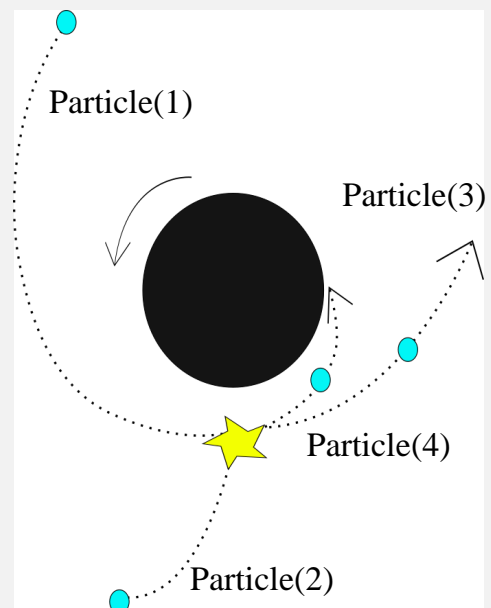
Introduction

- In 2009, it is showed that the center of mass energy diverges when two particles (1),(2) collide near the horizon of an extreme Kerr BH. (BSW process) (Banados, Silk and West '09)

$$E_{cm} \equiv -(P_1^\mu + P_2^\mu)(P_{1\mu} + P_{2\mu}) \rightarrow \infty$$

(at the horizon of an extreme BH)

- Due to the red shift, it is not trivial that the energy at infinity (of a resulting particle (3)) also diverges.



Introduction

- The observable energy efficiency at infinity

$$\eta \equiv \frac{E_3}{E_1 + E_2} \quad \text{The ratio of the resulting energy to the sum of initially energy}$$

Elastic collision of the same mass particles

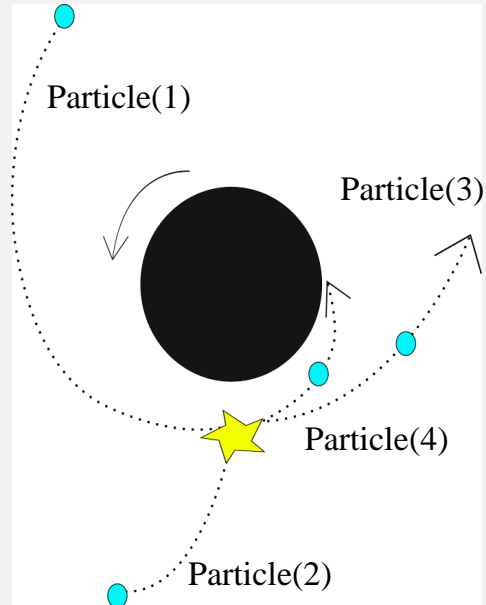
→ 6.32 (Leiderschneider & Piran '16)

Compton scattering (a photon & a massive particle)

→ 13.92 (Schnittman '14) → Maximum efficiency

(c.f. Ogasawara, Harada & Miyamoto '16, Leiderschneider & Piran '16, Zaslavskii '16)

- The above works do not include the case that particles are spinning. This case is also physically reasonable.



- We studied the effect of spin to the energy efficiency.

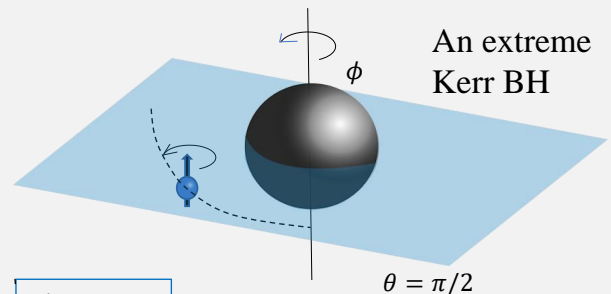
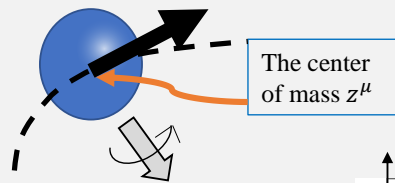
Spinning particle

- E.O.M

$$\frac{Dp^\mu}{d\tau} = -\frac{1}{2}R^\mu{}_{\nu\rho\sigma}v^\nu S^{\rho\sigma}$$

$$\frac{DS^{\mu\nu}}{d\tau} = p^\mu v^\nu - p^\nu v^\mu$$

$$S^{\mu\nu}p_\nu = 0$$



$$S^{\mu\nu}S_{\mu\nu} = 2\mu^2 s^2$$

- The Momentum and the four velocity

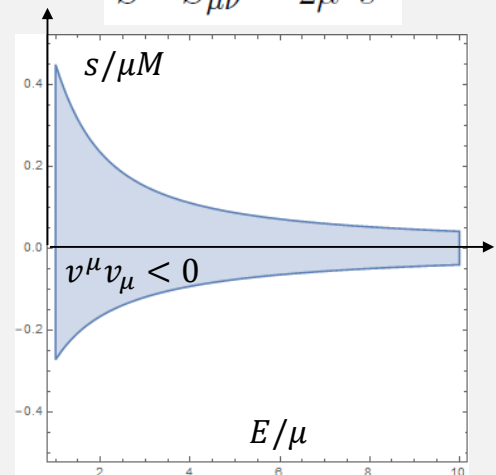
$$p^\mu = \mu v^\mu + v_\nu \frac{DS^{\mu\nu}}{d\tau}$$

$$v^\mu = \frac{dz^\mu}{d\tau}$$

$$\mu^2 = -p^\mu p_\mu$$



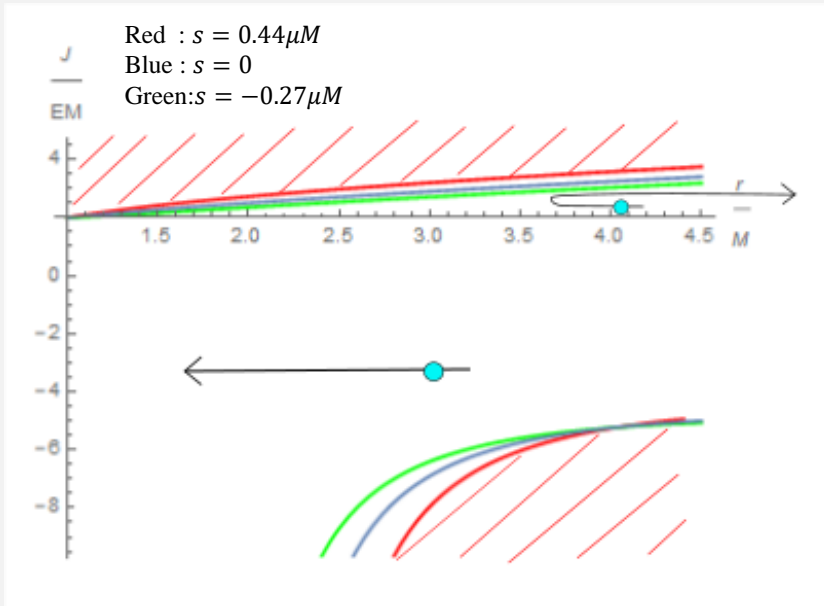
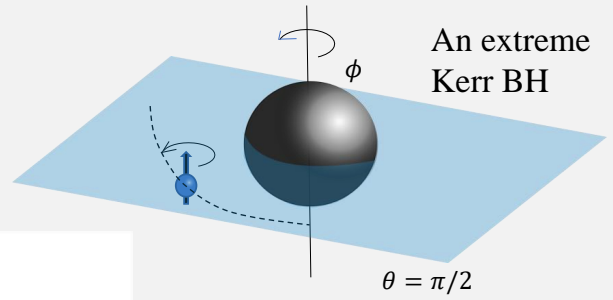
The signature $v^\mu v_\mu$ is non trivial



The relation between E and s for a particle to reach the horizon with satisfying $v^\mu v_\mu < 0$.

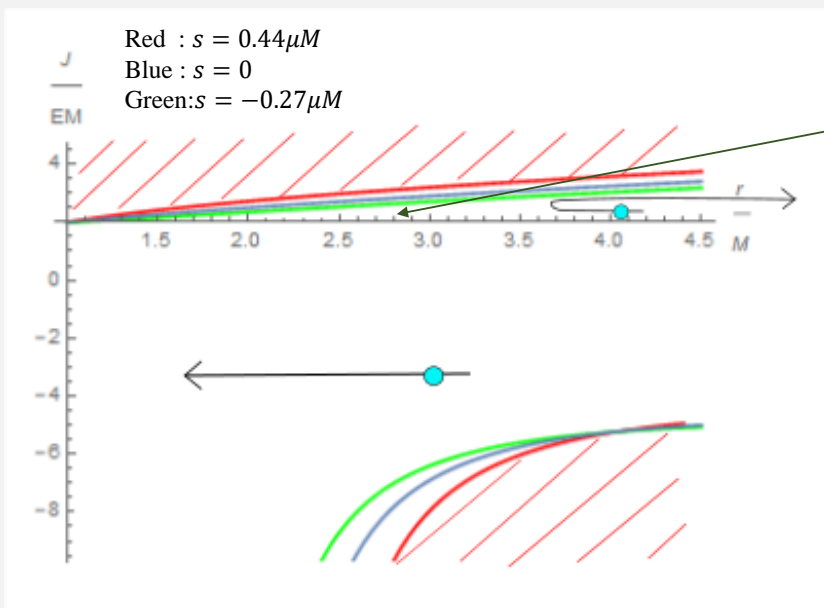
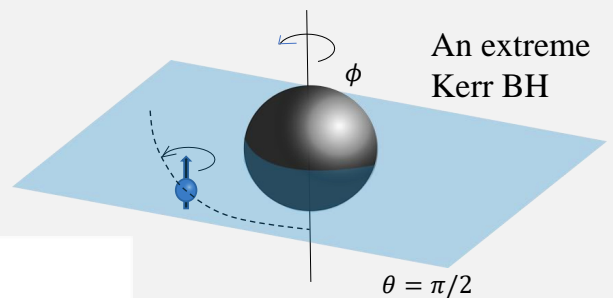
Spinning particle

- The radial motion



Spinning particle

- The radial motion

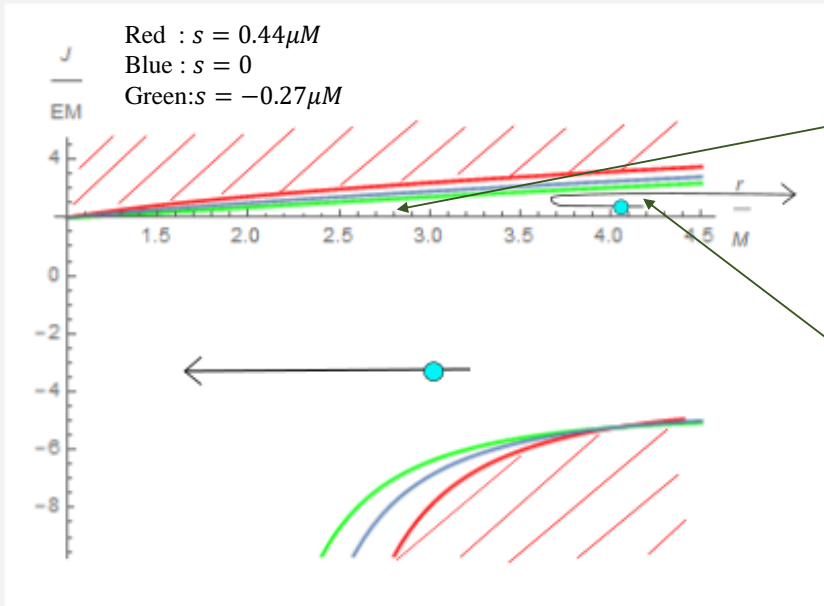
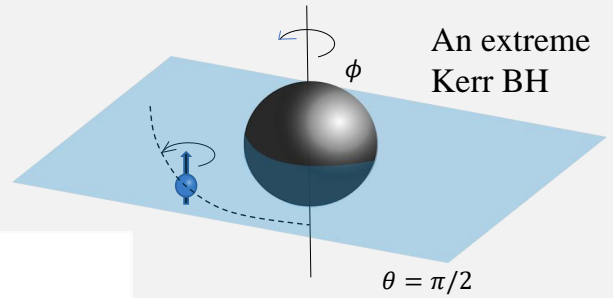


This value is the max angular momentum with which the particle can reach the horizon. This particle is called critical.

$$J = 2EM$$

Spinning particle

- The radial motion



This value is the max angular momentum with which the particle can reach the horizon. This particle is called critical.

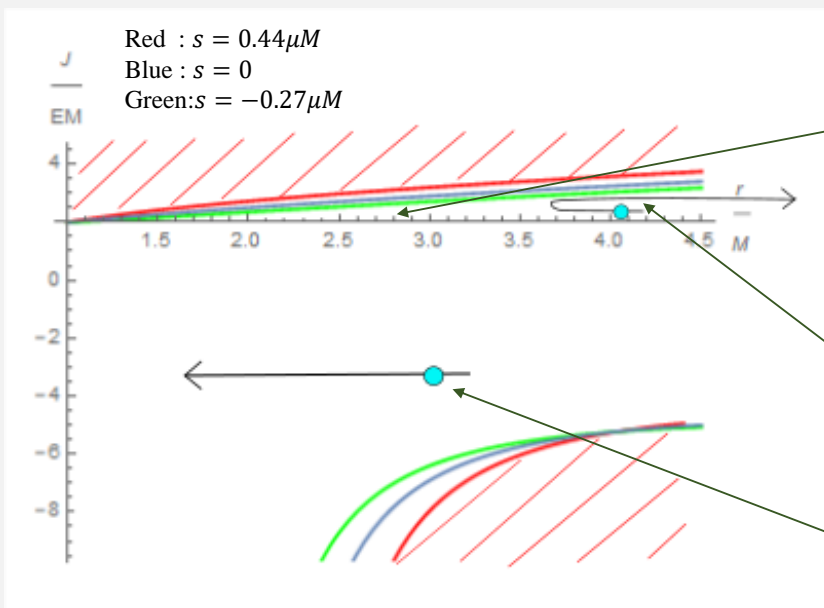
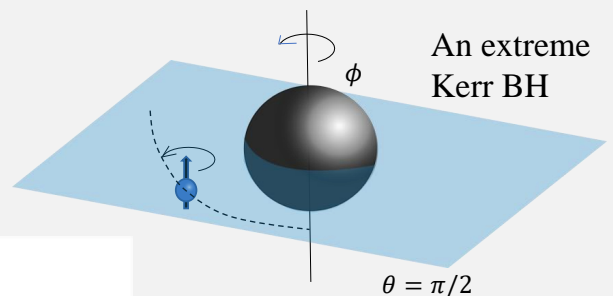
$$J = 2EM$$

A particle greater than critical is called super-critical.

$$J > 2EM$$

Spinning particle

- The radial motion



This value is the max angular momentum with which the particle can reach the horizon. This particle is called critical.

$$J = 2EM$$

A particle greater than critical is called super-critical.

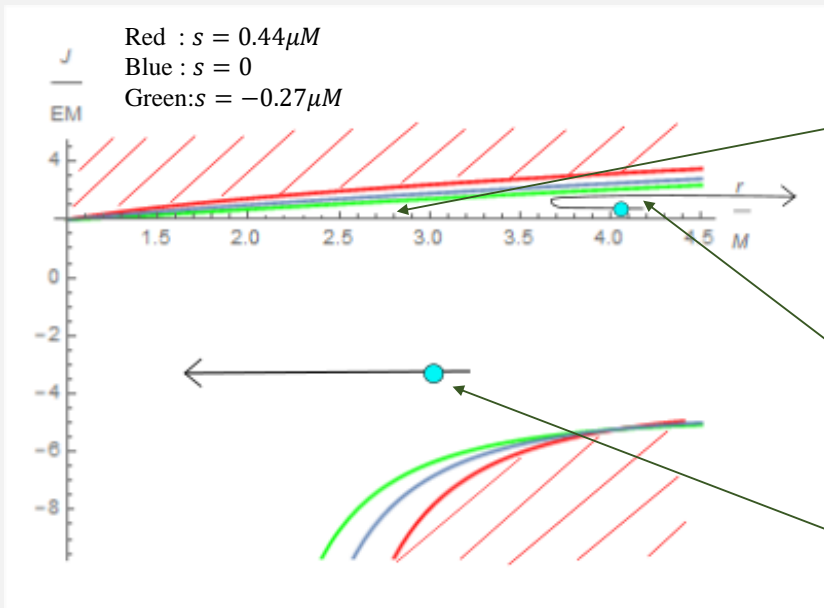
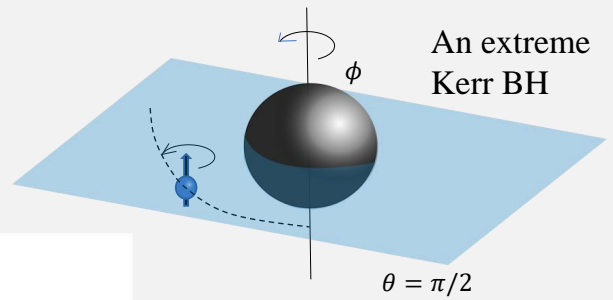
$$J > 2EM$$

sub-critical

$$J < 2EM$$

Spinning particle

- The radial motion



This value is the max angular momentum with which the particle can reach the horizon. This particle is called critical.

$$J = 2EM$$

A particle greater than critical is called super-critical.

$$J > 2EM$$

sub-critical

$$J < 2EM$$

(1): critical (2): sub-critical.

We choose the property of the spinning particle as with the spinless case.

Collisional Penrose Process

- Conservation laws

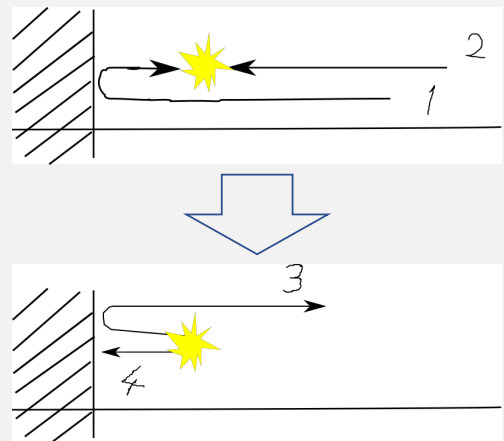
$$E_1 + E_2 = E_3 + E_4$$

$$J_1 + J_2 = J_3 + J_4$$

$$P_1^r + P_2^r = P_3^r + P_4^r$$

$$S_1 + S_2 = S_3 + S_4$$

- The collision near the horizon: $r_c = \frac{M}{1-\epsilon}$



Head-on collision

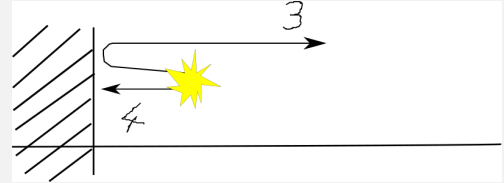
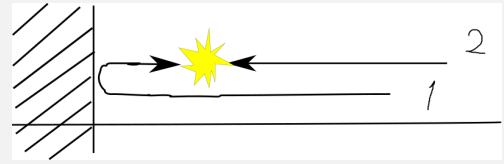
Collisional Penrose Process

- Conservation laws

$$\begin{aligned}
 E_1 + E_2 &= E_3 + E_4 \\
 J_1 + J_2 &= J_3 + J_4 \\
 P_1^r + P_2^r &= P_3^r + P_4^r \\
 S_1 + S_2 &= S_3 + S_4
 \end{aligned}$$

- The collision near the horizon: $r_c = \frac{M}{1-\epsilon}$

$$J_1 = 2E_1M, \quad J_2 = 2E_2M(1 + \zeta) \quad (\zeta < 0)$$



Head-on collision

Collisional Penrose Process

- Conservation laws

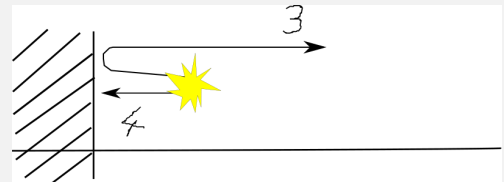
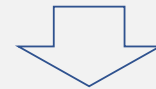
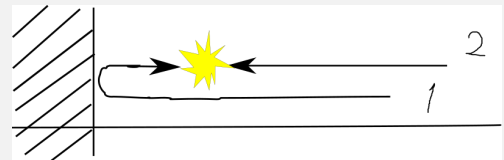
$$\begin{aligned}
 E_1 + E_2 &= E_3 + E_4 \\
 J_1 + J_2 &= J_3 + J_4 \\
 P_1^r + P_2^r &= P_3^r + P_4^r \\
 S_1 + S_2 &= S_3 + S_4
 \end{aligned}$$

- The collision near the horizon: $r_c = \frac{M}{1-\epsilon}$

$$J_1 = 2E_1M, \quad J_2 = 2E_2M(1 + \zeta) \quad (\zeta < 0)$$

$$J_3 = 2E_3M(1 + \alpha_3\epsilon + \beta_3\epsilon^2)$$

$$S_3 = S_1, \quad S_4 = S_2$$

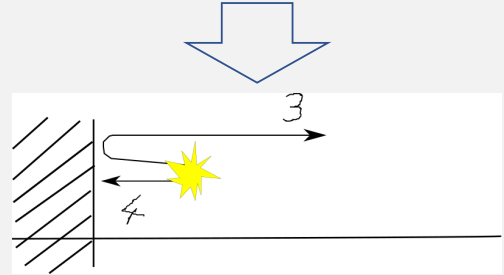
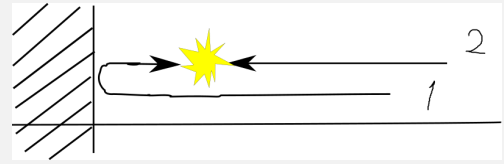


Head-on collision

Collisional Penrose Process

- Conservation laws

$$\begin{aligned}
 E_1 + E_2 &= E_3 + E_4 \\
 J_1 + J_2 &= J_3 + J_4 \\
 P_1^r + P_2^r &= P_3^r + P_4^r \\
 s_1 + s_2 &= s_3 + s_4
 \end{aligned}$$



Head-on collision

The collision near the horizon: $r_c = \frac{M}{1-\epsilon}$

$$J_1 = 2E_1M, \quad J_2 = 2E_2M(1 + \zeta) \quad (\zeta < 0)$$

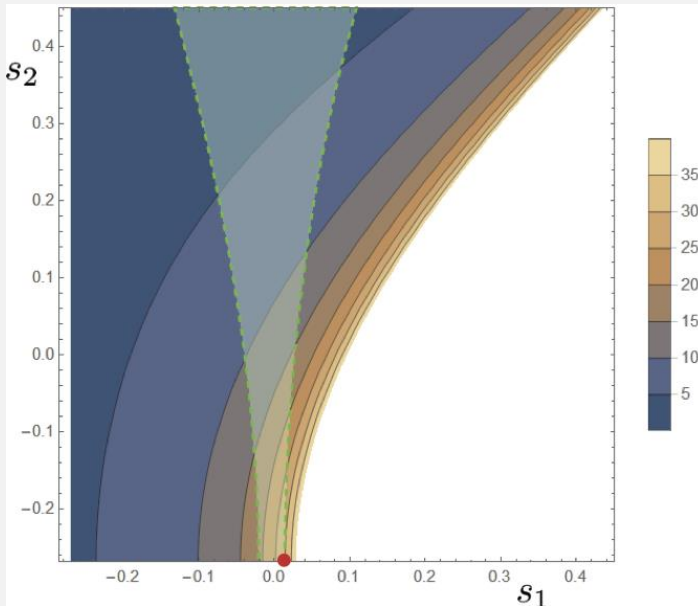
$$J_3 = 2E_3M(1 + \alpha_3\epsilon + \beta_3\epsilon^2)$$

$$s_3 = s_1, \quad s_4 = s_2$$

- Expand the radial momentum about ϵ and check the conservation law order by order.
- Solve in terms of E_2 and E_3
- Analyze the energy efficiency: $\eta = \frac{E_3}{E_1 + E_2}$

The elastic scattering (the same masses)

The effect of spin in the case of $E_1 = \mu, \alpha_3 = +0$



The contour map of E_3 in terms of s_1 and s_2 . In the green region the timelike condition of the particle (3) is satisfied. E_3 can reach the maximum at the red point: $(s_1, s_2) = (0.013, -0.27)$

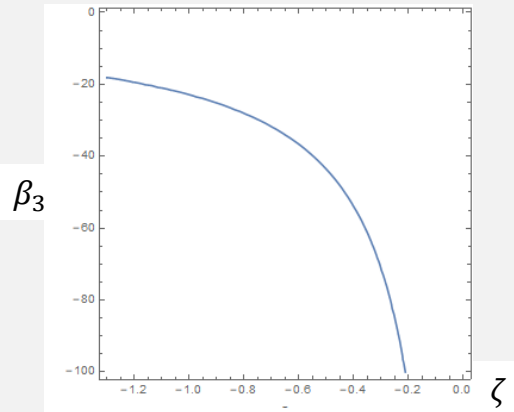
$$E_{3,max} = 30.016\mu$$

$$J_3 = 2E_3M(1 + \alpha_3\epsilon + \beta_3\epsilon^2)$$

$$J_1 = 2E_1M, \quad J_2 = 2E_2M(1 + \zeta)$$

$$\begin{aligned}
 E_3 &= E_3(E_1, s_1, s_2, \alpha_3), \\
 E_2 &= E_2(E_1, s_1, s_2, \alpha_3, \beta_3, \zeta).
 \end{aligned}$$

It has to be analyzed whether $E_2 = \mu$ is possible or not since the particle (2) has the restriction $E_2 \geq \mu$,

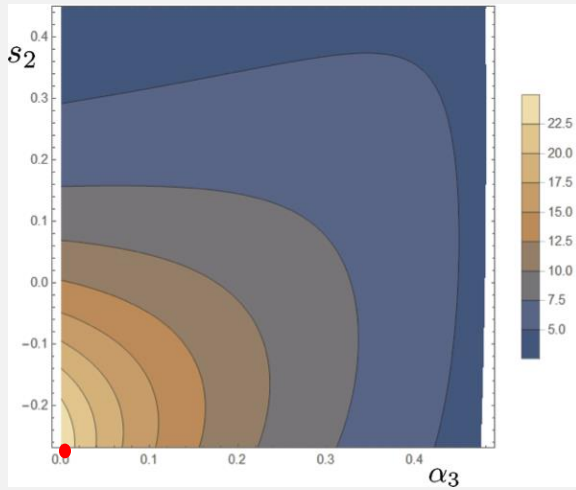


The relation giving $E_2 = \mu$ in terms of ζ and β_3

$$\text{Maximum efficiency: } 15.01$$

The “Compton” scattering (the scattering of a massless particle (1) and a massive particle (2))

The contour map of E_3/E_1 in terms of s_2 and α_3 .
The timelike condition is trivial for a spinless particle.



E_3/E_1 can also reach the maximum at the red point: $(s_2, \alpha_3) = (-0.27, +0)$

$$E_{3,max} = 26.85 E_1$$

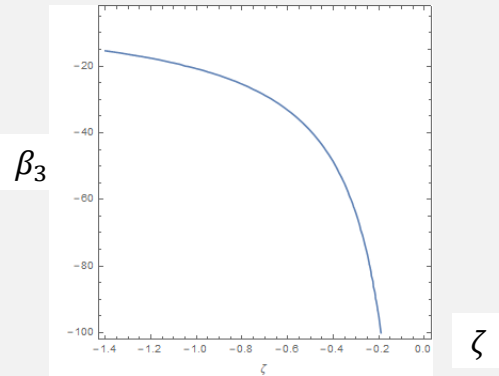
$$J_3 = 2E_3 M (1 + \alpha_3 \epsilon + \beta_3 \epsilon^2)$$

$$J_1 = 2E_1 M, J_2 = 2E_2 M (1 + \zeta)$$

$$E_3/E_1 = E_3(s_2, \alpha_3),$$

$$E_2 = E_2(E_1, s_2, \alpha_3, \beta_3, \zeta).$$

The parameters giving $E_2 = \mu$



The relation giving $E_2 = \mu$ in terms of ζ and β_3 in the case of $E_1 = 10^2 \mu$.

The maximum efficiency:
 $26.85 (E_1 \rightarrow \infty)$.

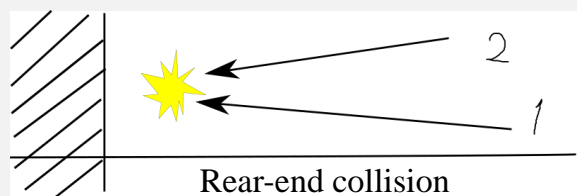
Conclusion and discussion

- The maximum efficiency in the elastic collision of the same mass spinning particles: 15.01
(the spinless case: 6.32)
- The maximum efficiency in the “Compton” scattering: 26.85
(the spinless case: 13.93)

we can obtain about twice as large efficiency as the spinless case when the spin of the particle (2) is negative. (chosen as antiparallel to the BH).

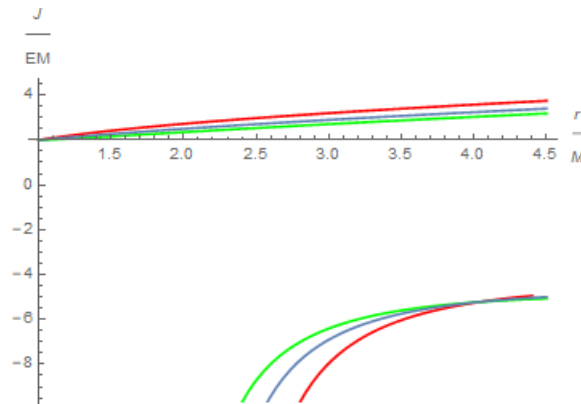
- In the case of the rear-end collision, the efficiency is not good as the head-on collision case.

- ❑ The case where particle (2) is also near critical
- ❑ The case of non-extreme BH
- ❑ About the super Penrose process



Negative β_3 when α_3 is zero

To bounce back, $\alpha_3\epsilon + \beta_3\epsilon^2 > 0$ is needed; hence, the particle 3 cannot come back to infinity when α_3 is exactly zero and β_3 is negative.



Like (ϵ, δ) -definition of limit, we can choose ϵ as much smaller than any small α_3 . Therefore, the particle 3 can bounce back when β_3 is negative and in the sense of $\alpha_3 \rightarrow +0, \alpha_3 = 0$.

The elastic scattering (the same masses)

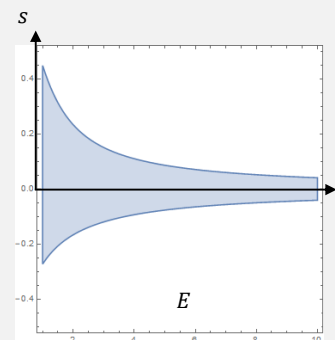
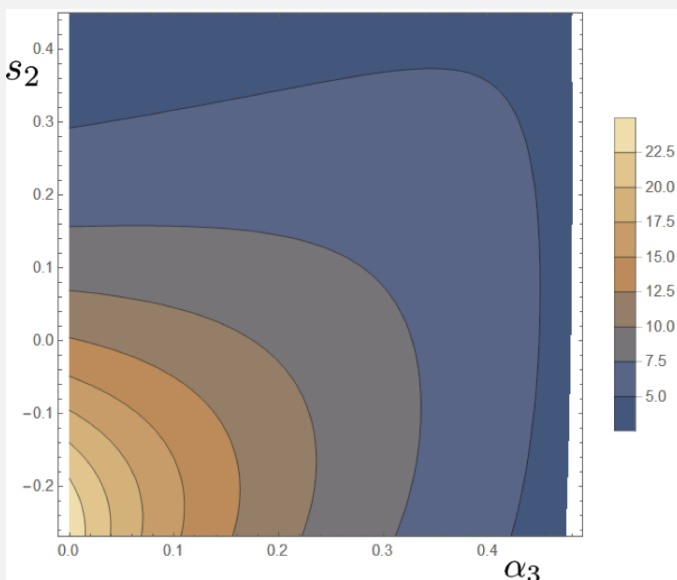
From the timelike condition we find that s_1 and s_3 must be small. Hence, we first set s_1 and s_3 is set to zero.

$$J_3 = 2E_3M(1 + \alpha_3\epsilon + \beta_3\epsilon^2)$$

$$J_1 = 2E_1M, J_2 = 2E_2M(1 + \zeta)$$

$$E_3 = E_3(E_1, s_1, s_2, \alpha_3),$$

$$E_2 = E_2(E_1, s_1, s_2, \alpha_3, \beta_3, \zeta).$$

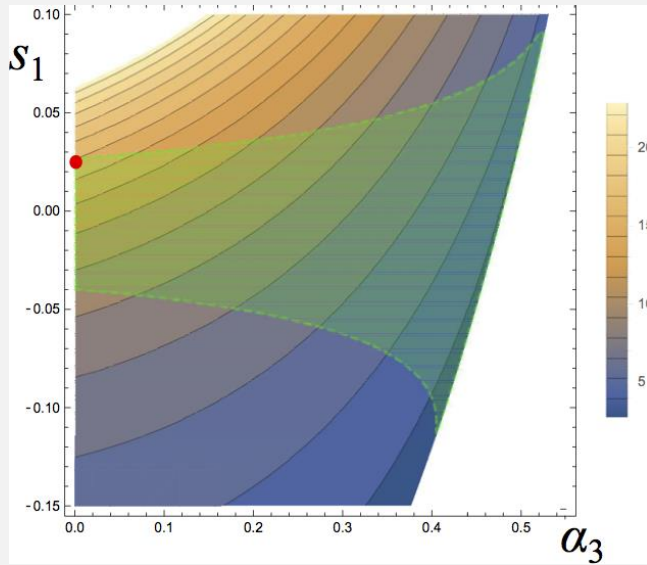


From the left graph, we find $\alpha_3 = +0$ gives the largest efficiency. Hence next we set $\alpha_3 = +0$ and analyze the maximal efficiency.

The contour map of E_3 in terms of α_3 and s_2 when s_1 and s_3 is set to zero.

The inverse “Compton” scattering (the scattering of a massive particle (1) and a massless particle (2))

The effect of spin in the case of $E_1 = \mu, \alpha_3 = +0$



The contour map of E_3 in terms of s_1 and s_2 .
In the green region the timelike condition of the
particle (3) is satisfied.

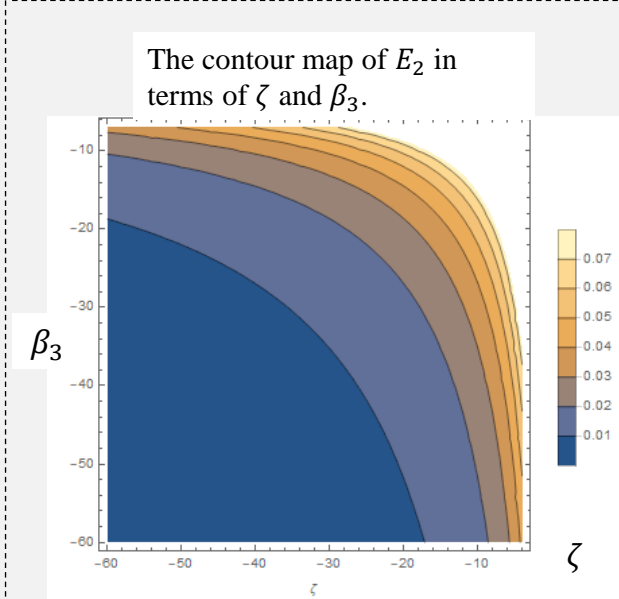
$$E_{3,max} = 15.64\mu$$

$$J_3 = 2E_3M(1 + \alpha_3\epsilon + \beta_3\epsilon^2)$$

$$J_1 = 2E_1M, J_2 = 2E_2M(1 + \zeta)$$

$$E_3 = E_3(E_1, s_1, \alpha_3),$$

$$E_2 = E_2(E_1, s_1, \alpha_3, \beta_3, \zeta).$$



$E_2 = 0$ is possible when $\beta_3\zeta \rightarrow \infty$.

Maximum efficiency: 15.64

How to describe a spinning particle

- Timelike condition

$$p^\mu = \mu v^\mu + v_\nu \frac{DS^{\mu\nu}}{d\tau}$$

$$u^\mu = \frac{p^\mu}{\mu} \quad u^\mu v_\mu = -1$$

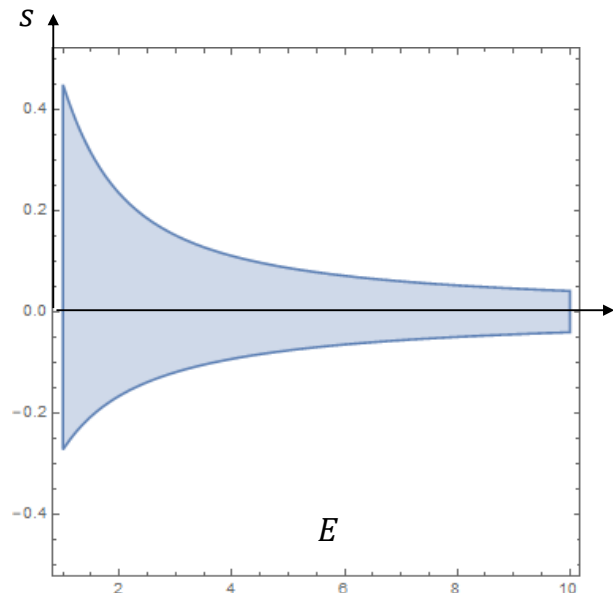
In the case of the spin-less case, the time-like condition is trivial but in this case this condition nontrivial because momentum is not parallel to 4 velocity.

$$v^\mu v_\mu < 0 \quad \longrightarrow$$

This graph is obtained by
 $a \rightarrow M$ (Extreme Kerr),
 $r \rightarrow M$ (to evaluate at the horizon)

$$\text{For } E = \mu,$$

$$-0.270 < s < 0.449$$



Momentum of a spinning particle

Momentums of a particle can be written by E, J as below;

$$u^{(0)} = \frac{(r^3 + (1+s)r + s)E - (r+s)J}{\mu r^2 \sqrt{\Delta} (1 - \frac{s^2}{r^3})}$$

$$\Delta = (r-1)^2$$

$$\Sigma = r^2$$

$$u^{(3)} = \frac{-(1+s)E + J}{\mu r (1 - \frac{s^2}{r^3})}$$

$$u^{(1)} =$$

$$\frac{\sigma \sqrt{r^2 [(r^3 + (1+s)r + s)E - (r+s)J]^2 - (r-1)^2 [(r^3 - s^2)^2 + r^4 (J - (1+s)E)^2]}}{(r-1)(r^3 - s^2)}$$

$$e_{\mu}^{(a)} = \begin{pmatrix} \sqrt{\frac{\Delta}{\Sigma}} & 0 & 0 & -a\sqrt{\frac{\Delta}{\Sigma}} \sin^2 \theta \\ 0 & \sqrt{\frac{\Sigma}{\Delta}} & 0 & 0 \\ 0 & 0 & \sqrt{\Sigma} & 0 \\ -\frac{a}{\sqrt{\Sigma}} \sin \theta & 0 & 0 & \frac{(r^2 + a^2)}{\sqrt{\Sigma}} \sin \theta \end{pmatrix}$$

Radial momentum conservation at 1st order

The elastic scattering
(the same masses)

$$\sigma_3 \frac{f(s_1, E_3, \alpha_3)}{1 - s_1^2} = \sigma_1 \frac{f(s_1, E_1, 0)}{1 - s_1^2} + \frac{[E_1(2 + s_2) - E_3 g_1(s_2, \alpha_3)]}{1 - s_2^2}$$

$$f(s, E, \alpha) := \sqrt{E^2 [3 - 2\alpha(1+s)][1 + 2s - 2\alpha(1+s)] - (1 - s^2)^2},$$

$$g_1(s, \alpha) := 2 + s - 2\alpha(1+s),$$

We get a quadratic equation of E_3 : $\mathcal{A}E_3^2 - 2\mathcal{B}E_3 + \mathcal{C} = 0$

$$E_3 = \frac{\mathcal{B} + \sqrt{\mathcal{B}^2 - \mathcal{A}\mathcal{C}}}{\mathcal{A}}$$

$$\mathcal{A} = -[3 - 2\alpha_3(1 + s_1)][1 + 2s_1 - 2\alpha_3(1 + s_1)] + \frac{(1 - s_1^2)^2}{(1 - s_2^2)^2} g_1^2(s_2, \alpha_3)$$

$$\mathcal{B} = g_1(s_2, \alpha_3) \frac{(1 - s_1^2)}{(1 - s_2^2)} \left[(2 + s_2) \frac{(1 - s_1^2)}{(1 - s_2^2)} E_1 + \sigma_1 f(s_1, E_1, 0) \right]$$

$$\mathcal{C} = E_1 \left[\left(\frac{3(1 + 2s_1)(1 - s_2^2)^2 + (1 - s_1^2)^2 (2 + s_2)^2}{(1 - s_2^2)^2} \right) E_1 + 2\sigma_1 \frac{(1 - s_1^2)(2 + s_2)}{(1 - s_2^2)} f(s_1, E_1, 0) \right]$$

Radial momentum conservation at 2nd order

The elastic scattering
(the same masses)

$$\mathcal{P}E_2 = (1 - s_2)^3(E_1 - E_3)^2, \quad \text{Linear equation of } E_2$$

Since this fixes the value of E_2 ,
we obtain the efficiency by

$$\eta \equiv \frac{E_3}{E_1 + E_2}$$

This efficiency is obtained
when α_3, β_3 , and ζ are given.

$$\begin{aligned} \mathcal{P} &:= 2(E_3 - E_1)(1 - s_2)^3 + 4\zeta \left[\frac{(1 - s_2^2)^2}{(1 - s_1^2)^2} \mathcal{Q} + 2(1 + s_2)E_3[\alpha_3(2 + s_2) - \beta_3(1 - s_2^2)] - s_2(2 + s_2)^2(E_3 - E_1) \right] \\ \mathcal{Q} &:= \sigma_1 \frac{E_1^2 h(s_1)}{f(s_1, E_1, 0)} - \sigma_3 \left[\frac{E_3^2}{f(s_1, E_3, \alpha_3)} \times \left(h(s_1) - 2(1 + s_1)^2(2 + s_1)g_2(s_1, \alpha_3) + 2\beta_3(1 + s_1)(1 - s_1^2)g_1(s_1, \alpha_3) \right) \right] \\ f(s, E, \alpha) &:= \sqrt{E^2[3 - 2\alpha(1 + s)][1 + 2s - 2\alpha(1 + s)] - (1 - s^2)^2} \\ g_1(s, \alpha) &:= 2 + s - 2\alpha(1 + s), \\ g_2(s, \alpha) &:= \alpha(2 + s - 2\alpha), \\ h(s) &:= 1 + 7s + 9s^2 + 11s^3 - s^4 \end{aligned}$$

Session S4A2 10:45–12:00

[Chair: Kenichi Nakao]

Takayuki Ohgami

Daido Univ.

**“Exploring GR Effects of Super-Massive BH at Galactic Center
2: on the detail of fitting theory with observational data”**

(10+5 min.)

[JGRG28 (2018) 110805]

Exploring GR Effects of Super-Massive BH at Galactic Center 2: on the detail of fitting theory with observational data

Takayuki Ohgami (Daido Univ.) / 大神隆幸 (大同大学)
member

H. Saida (Daido Univ.) / 齋田浩見 (大同大学)

S. Nishiyama (Miyagi U. Edu) / 西山正吾 (宮城教育大学)

Y. Takamori (Wakayama NCT) / 孝森洋介 (和歌山高専)

M. Takahashi (Aichi U. Edu) / 高橋真聡 (愛知教育大学)

+Some Collaborators in Obs. and Instr.

JGRG28@Rikkyo Univ., Tokyo

Nov. 8, 2018

1. What we want to do

1. Fitting with data and Parameter search (Newton, GR)

2. Simulation and obtaining RV curve ($c z_{\text{Newton}}(t)$, $c z_{\text{GR}}(t)$)

3. Calculate GR effect $c \Delta z := c z_{\text{GR}}(t) - c z_{\text{Newton}}(t)$

4. Comparison between $c \Delta z$ and data

Saida-san has talked about Step 2, 3 and 4.
I will talk about detail of Step 1.

2. fitting method : χ^2 -fitting

- Method

χ^2 - fitting of theory with obs. data

Newton Gravity
General Relativity

Astro. data : Keck + VLT
Spect. data : Subaru + Keck + VLT

- fitting parameters (19 parameters)

- M_{SgrA^*} : Mass of Sgr A*
 - R_{SgrA^*} : Distance to Sgr A*
 - $\vec{x}_{\text{apo}}, \vec{v}_{\text{apo}}$: S2's initial conditions
 - \vec{v}_{E} : Our velocity
 - $(X, Y)_{\text{Keck}}$: Astro. ref. point for Keck
 - $(\dot{X}, \dot{Y})_{\text{Keck}}$: Velocity of ref. point for Keck
 - $(X, Y)_{\text{VLT}}$: Astro. ref. point for VLT
 - $(\dot{X}, \dot{Y})_{\text{VLT}}$: Velocity of ref. point for VLT
- $(X, Y) = (\text{RA}, \text{Dec})$

- Fitting and Test of a Model using Obs. Data

- ▶ Hypotheses

- Measurement of each obs. data z_i is individually a stochastic process obeying $P(Z; \mu_i, \sigma_i)$.
- Mean μ_i of each obs. data z_i is modeled with L parameters, $\mu_i = f_i(A_1, \dots, A_L)$.

Step1 : Find the best-fit values of A_i .

Step2 : Test the goodness of fitting.

Step3 : If good, then estimate the error of fitting.

3. Best-fit parameter

Best-fit values $A_1^{(\text{best})}, \dots, A_L^{(\text{best})}$ correspond to the minimum of χ^2

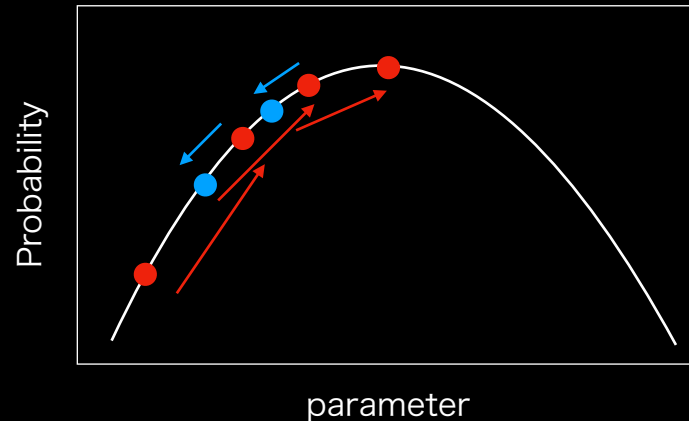
$$\chi_{\min}^2 = \sum_{i=1}^N \left[\frac{z_i - f_i(A_1^{(\text{best})}, \dots, A_L^{(\text{best})})}{\sigma_i} \right]^2$$

- χ_{\min}^2 is a stochastic variable, because z_i 's are the stochastic variables.
- The probability distribution of χ_{\min}^2 is χ^2 -distribution of $N-L$ degrees of freedom.

Two approaches to find χ_{\min}^2

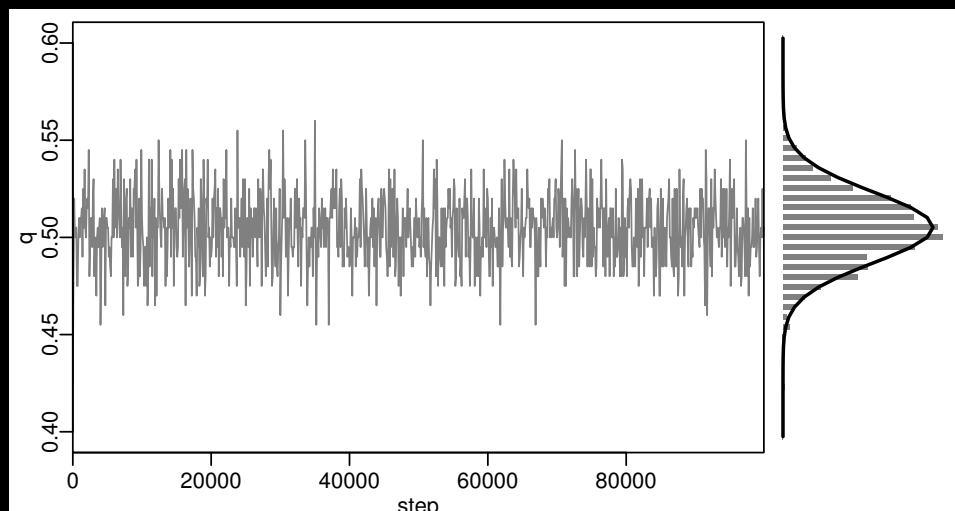
- Maximum Likelihood Estimation (MLE)
 - Just find χ_{\min}^2
 - Merit : Short calculation times
 - Demerit : Cannot obtain the error (Need an extra estimation)
- Bayesian inference ← Our next approach
 - Compute probability distribution of parameters A_i .
 - Merit : Introduction of a prior Prob. Dist. from previous result.
Prob. Dist. we want = Likelihood \times prior Prob. Dist.
 - Demerit : very long time

- Markov Chain Monte Carlo method (MCMC)
 - One of the Monte Carlo method
 - Random Walk following Markov process (Markov Chain)
 - Change the parameter values following probability (Likelihood).
 - Next step tends to go to high likelihood value. (Metropolis method)



- How to obtain the Likelihood?
 - Now, we use χ^2 -fitting.
 - p-value (cumulative probability) of $\chi^2 = \text{Likelihood}$

- Histogram by MCMC
 - Taking many step of Markov chain, we can obtain the histogram showing prob. dis. of parameters.
 - Estimate mean, deviation, ... form this histogram.



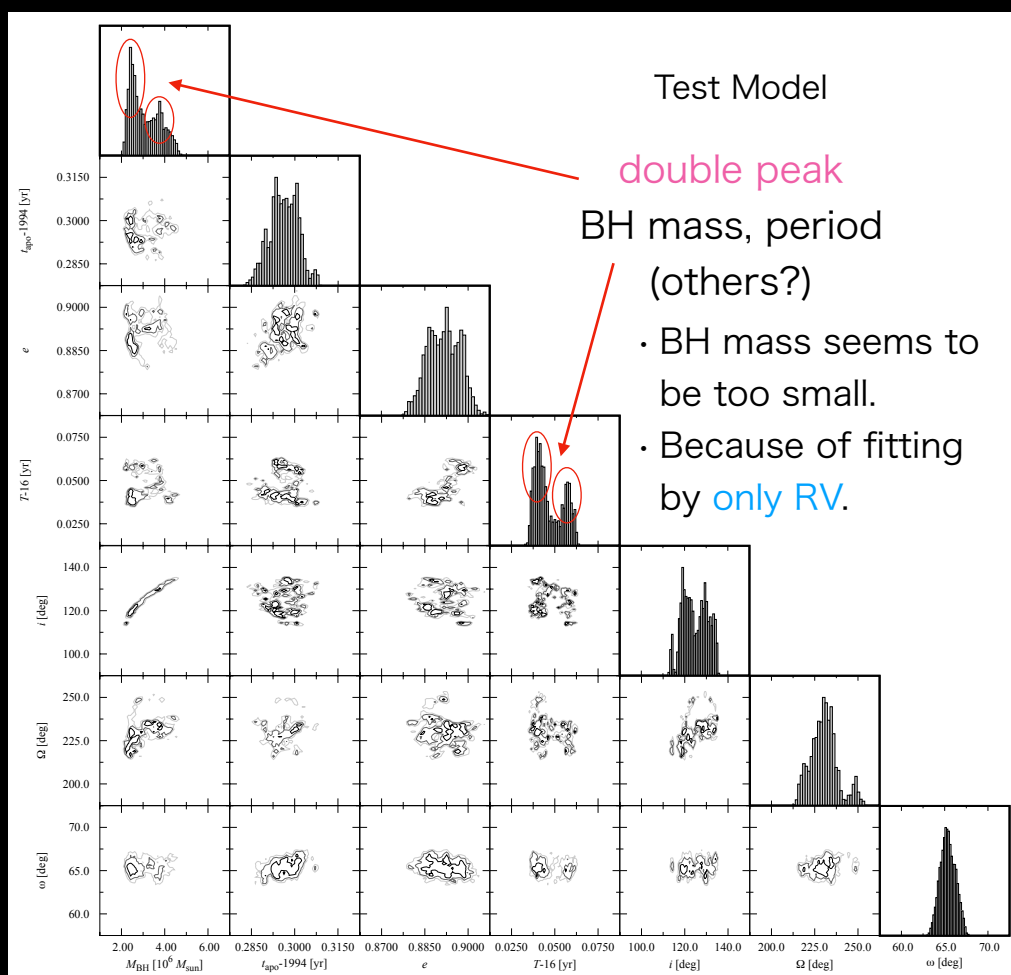
4. Fitting Examples

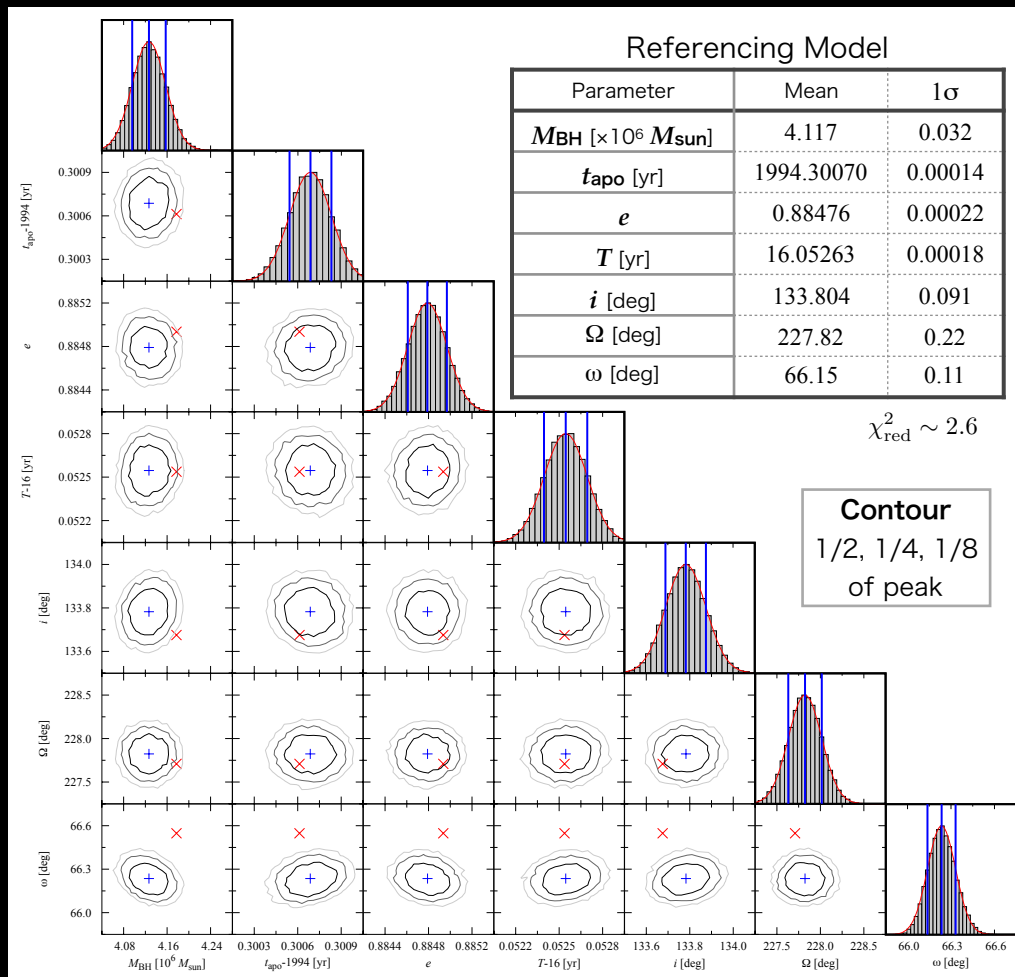
- Setting
 - Theory : Newton Gravity
 - Fitting data : only RV data (Subaru + Keck + VLT)
 - Fitting params. : M_{SgrA^*} , \vec{x}_{apo} , \vec{v}_{apo}

Here, we can convert \vec{x}_{apo} , \vec{v}_{apo} to

t_{apo}	: Date at apocenter	i	: inclination
e	: Eccentricity	Ω	: Longitude of the Ascending Node
T	: Period	ω	: Argument of Perigee

- Prior Prob. Dist. :
 - ▶ Uniform \rightarrow Test Model
 - ▶ Normal Dist. following result of GRAVITY+(2018) \rightarrow Referencing Model





5. Summary

- I explained detail of our fitting theory with observational data (χ^2 - fitting, MCMC).
 - The plan using MCMC is not complete yet. (in progress)
- Test fitting by MCMC (only Newton Grav.)
 - If we fit with only RV data, does NOT work.
 - RV data is not enough statistically.
 - It is necessary to fit with both datas (Astro. and RV).

Filip Ficek

Jagiellonian University

“Planar domain walls in Kerr spacetime”

(10+5 min.)

[JGRG28 (2018) 110806]

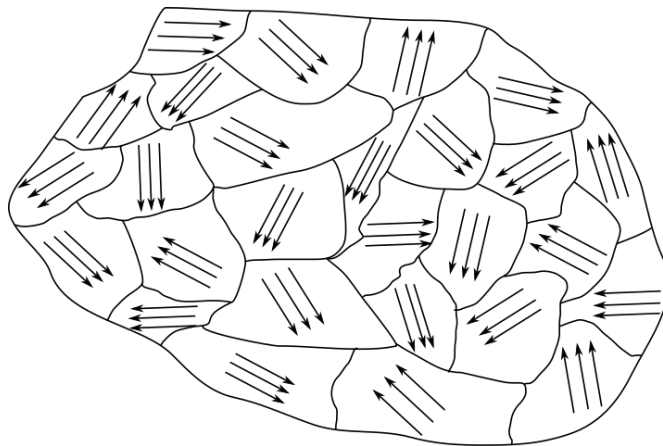
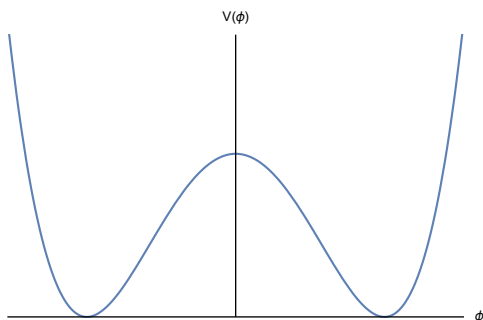
Planar domain walls in Kerr spacetime

Filip Ficek
Jagiellonian University
Cracow, Poland

Plan

- Domain walls
- Searching for domain wall transits
- Details of the simulation
- Results
- Summary

Domain walls



PHYSICAL REVIEW D **67**, 025017 (2003)

Thick domain walls around a black hole

Yoshiyuki Morisawa,^{1,*} Daisuke Ida,^{2,†} Akihiro Ishibashi,^{3,‡} and Ken-ichi Nakao^{1,§}

¹*Department of Physics, Osaka City University, Osaka 558-8585, Japan*

²*Department of Physics, Tokyo Institute of Technology, Tokyo 152-8551, Japan*

³*Yukawa Institute for Theoretical Physics, Kyoto University, Kyoto 606-8502, Japan*

and Enrico Fermi Institute, University of Chicago, Chicago, Illinois 60637

(Received 20 September 2002; published 28 January 2003)

We discuss the gravitationally interacting system of a thick domain wall and a black hole. We numerically solve the scalar field equation in the Schwarzschild spacetime and obtain a sequence of static axisymmetric solutions representing thick domain walls. We find that, for the walls near the horizon, the Nambu-Goto approximation is no longer valid.

PHYSICAL REVIEW D **73**, 125017 (2006)

Black holes escaping from domain walls

Antonino Flachi,^{1,*} Oriol Pujolàs,^{1,2,†} Misao Sasaki,^{1,‡} and Takahiro Tanaka^{3,§}

¹*Yukawa Institute for Theoretical Physics, Kyoto University, Kyoto 606-8503, Japan*

²*Center for Cosmology and Particle Physics, Department of Physics, New York University,*

4 Washington Place, New York, New York 10003 US, USA

³*Department of Physics, Kyoto University, Kyoto 606-8502, Japan*

(Received 14 February 2006; published 20 June 2006)

Previous studies concerning the interaction of branes and black holes suggested that a small black hole intersecting a brane may escape via a mechanism of reconnection. Here we consider this problem by studying the interaction of a small black hole and a domain wall composed of a scalar field and simulate the evolution of this system when the black hole acquires an initial recoil velocity. We test and confirm previous results, however, unlike the cases previously studied, in the more general set-up considered here, we are able to follow the evolution of the system also during the separation, and completely illustrate how the escape of the black hole takes place.

The Global Network of Optical Magnetometers for Exotic physics (GNOME): A novel scheme to search for physics beyond the Standard Model

Szymon Pustelny^{1,2,*}, Derek F. Jackson Kimball³, Chris Pankow⁴, Micah P. Ledbetter^{2,**}, Przemysław Włodarczyk⁵, Piotr Wcisło^{1,6}, Maxim Pospelov^{7,8}, Joshua R. Smith⁹, Jocelyn Read⁹, Wojciech Gawlik¹, and Dmitry Budker^{2,10}

Received 18 March 2013, revised 10 July 2013, accepted 22 July 2013
Published online 21 August 2013

nature
physics

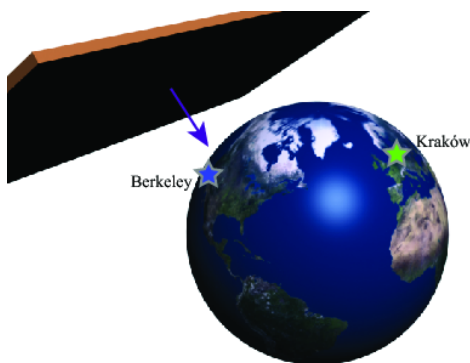
LETTERS

PUBLISHED ONLINE: 17 NOVEMBER 2014 | DOI: 10.1038/NPHYS3137

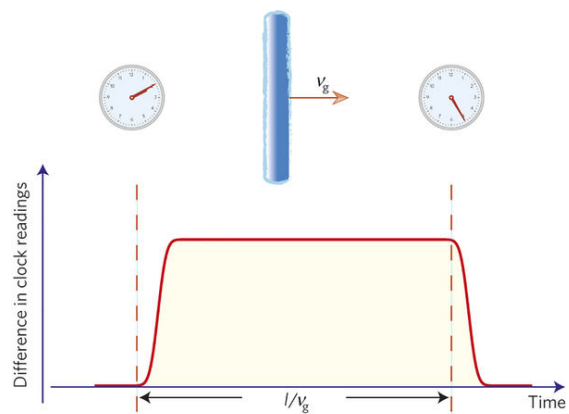
Hunting for topological dark matter with atomic clocks

A. Derevianko^{1*} and M. Pospelov^{2,3}

Terrestrial experiments

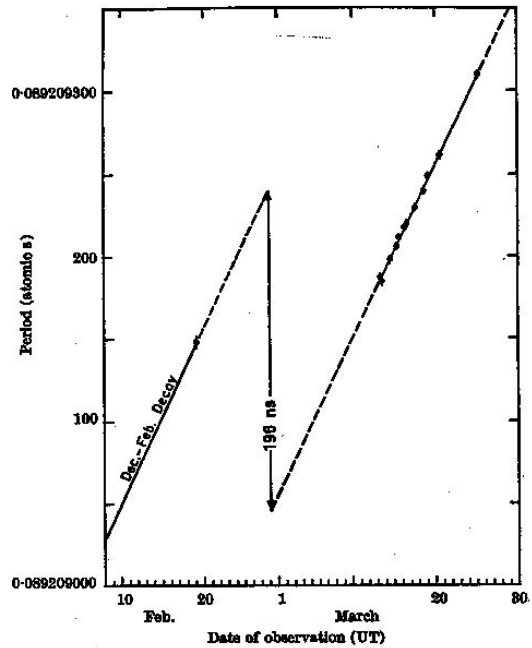
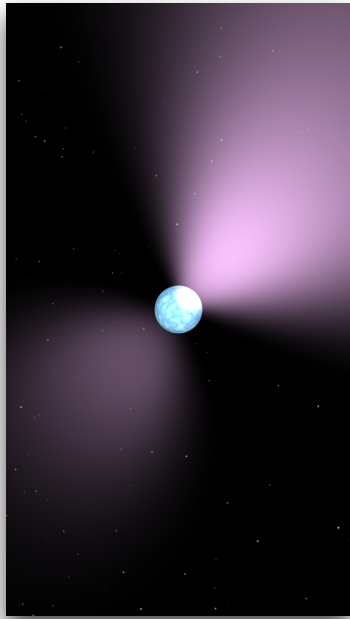


Global Network of Optical Magnetometers for Exotic Physics



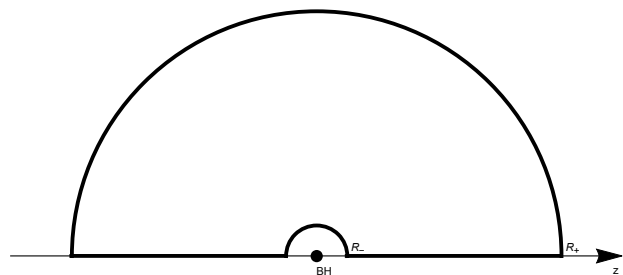
GPS.DM

Astrophysical effects

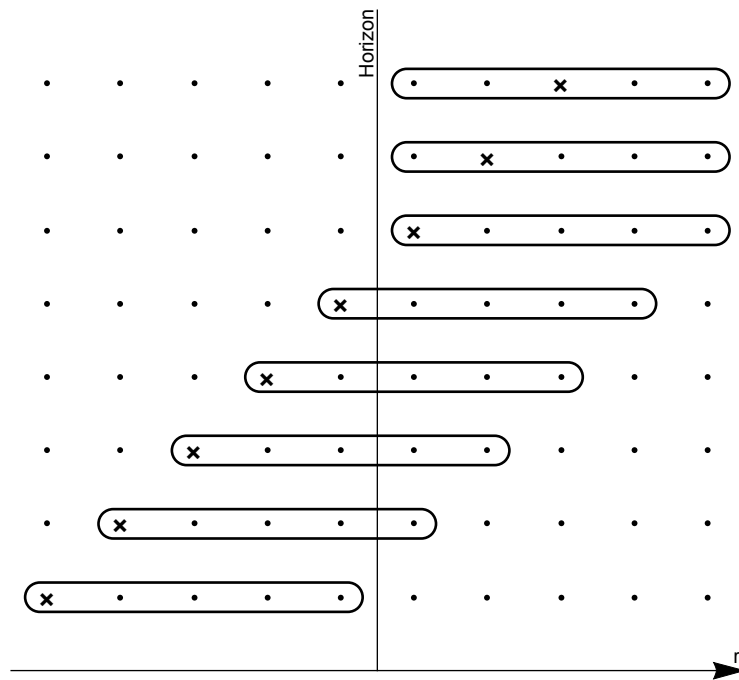


Details of the simulation

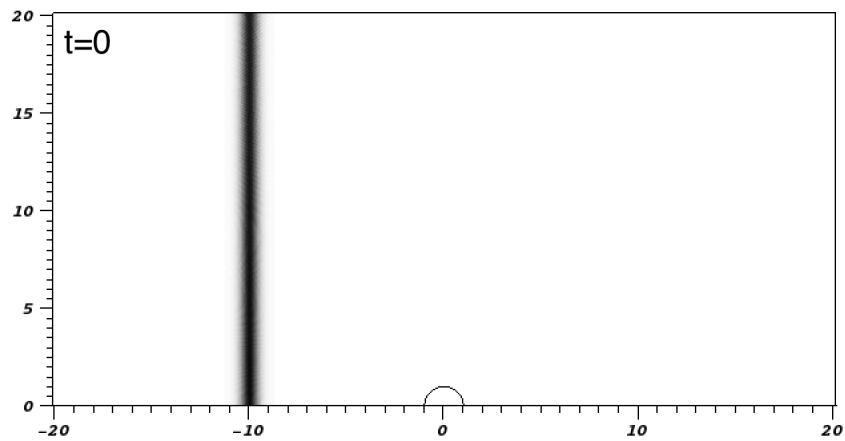
- ϕ^4 model
- Black hole with either angular momentum or charge
- Initially planar domain wall
- Axial symmetry (2D simulation)
- Crank-Nicholson method
- Kerr-Schild-type coordinates
- Minkowski solution as a boundary condition at the outer boundary
- Inner boundary of the domain below the outer horizon (no boundary conditions)
- Causality under the horizon imposed during the discretisation



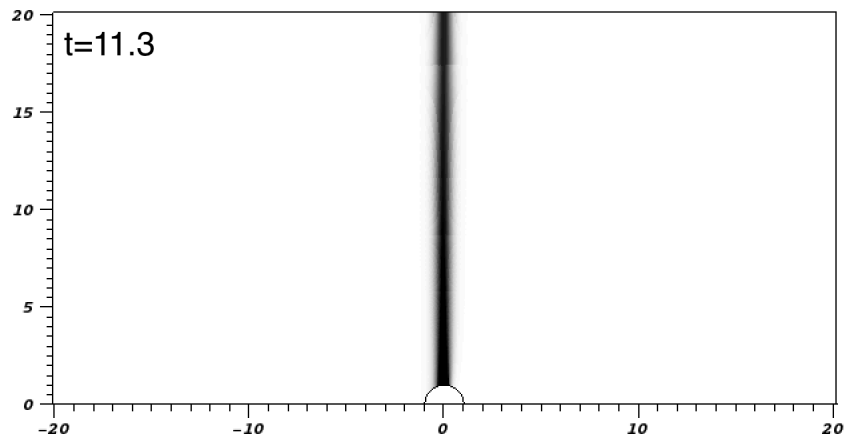
Details of the simulation



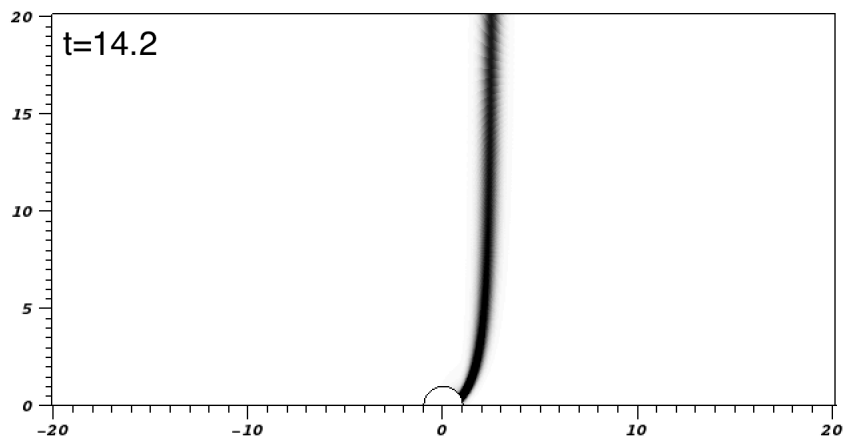
Results



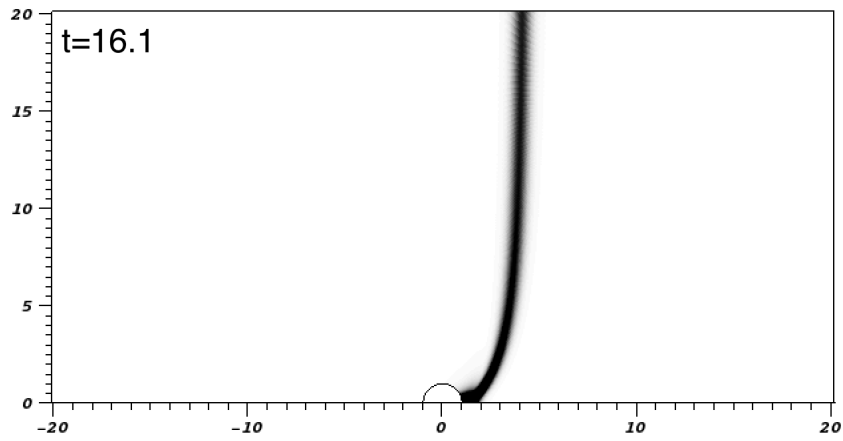
Results



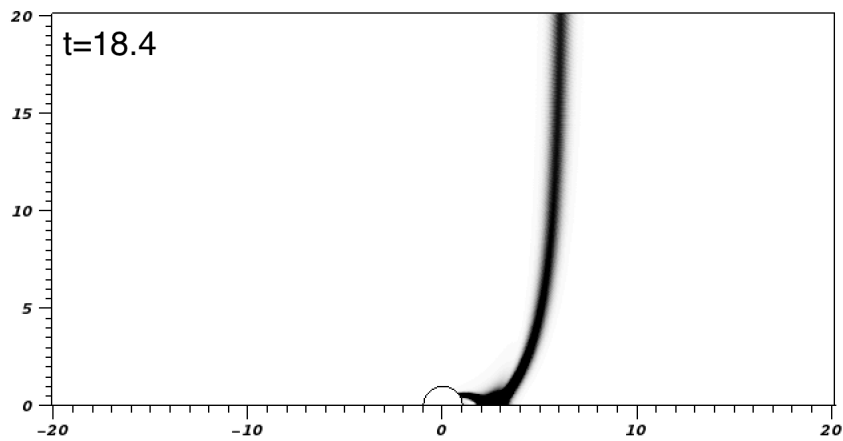
Results



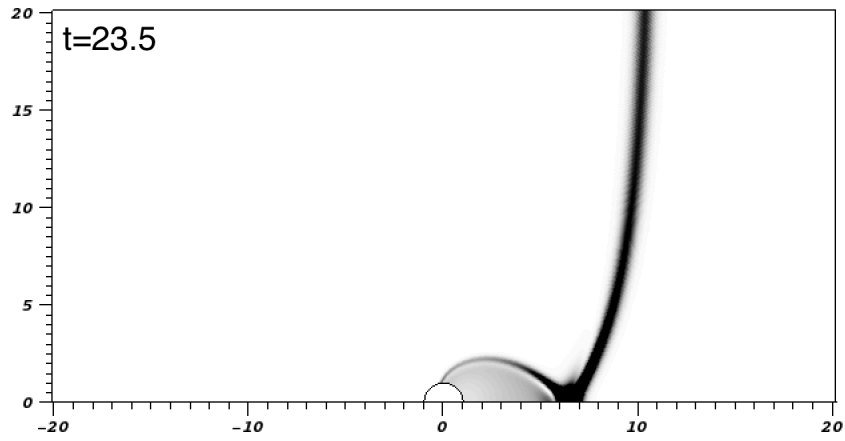
Results



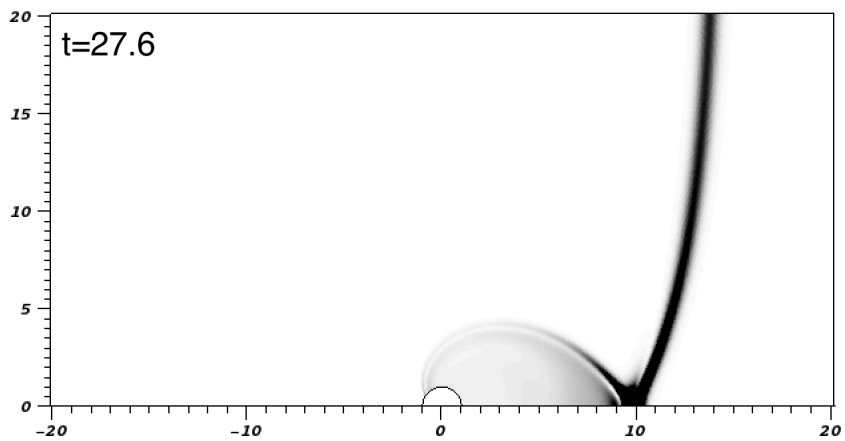
Results



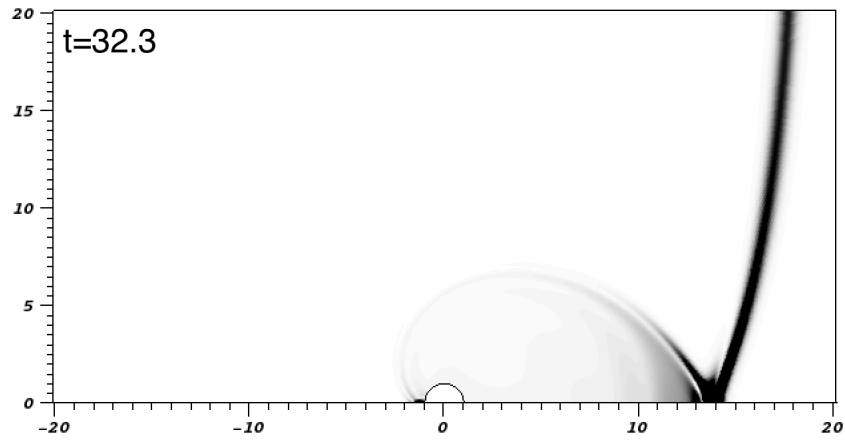
Results



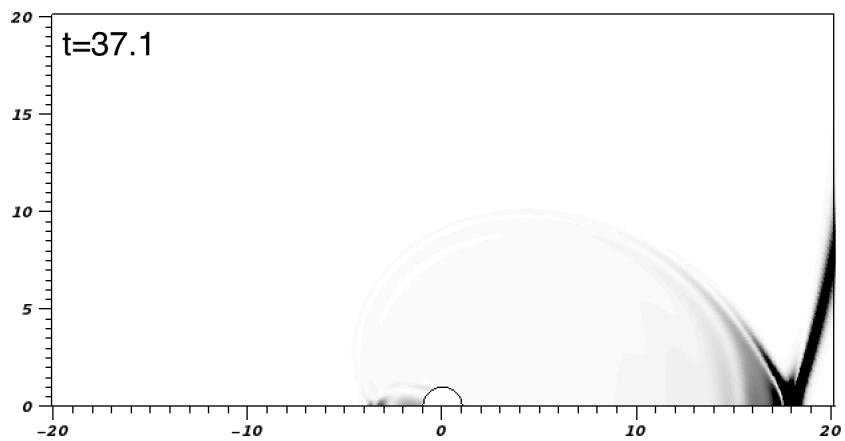
Results



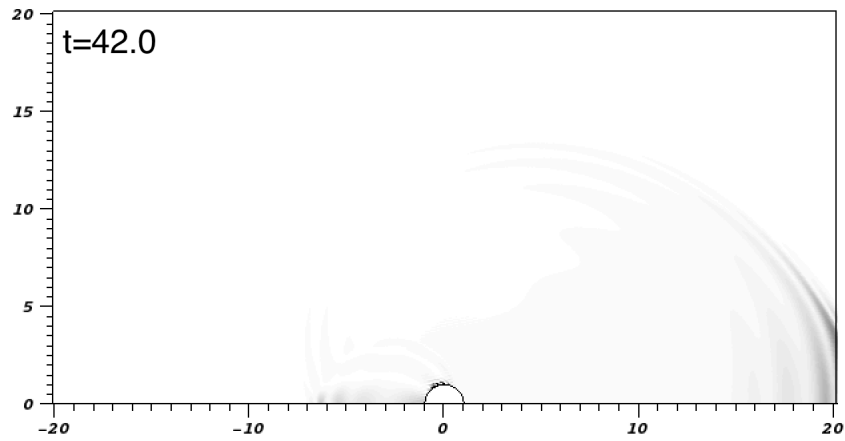
Results



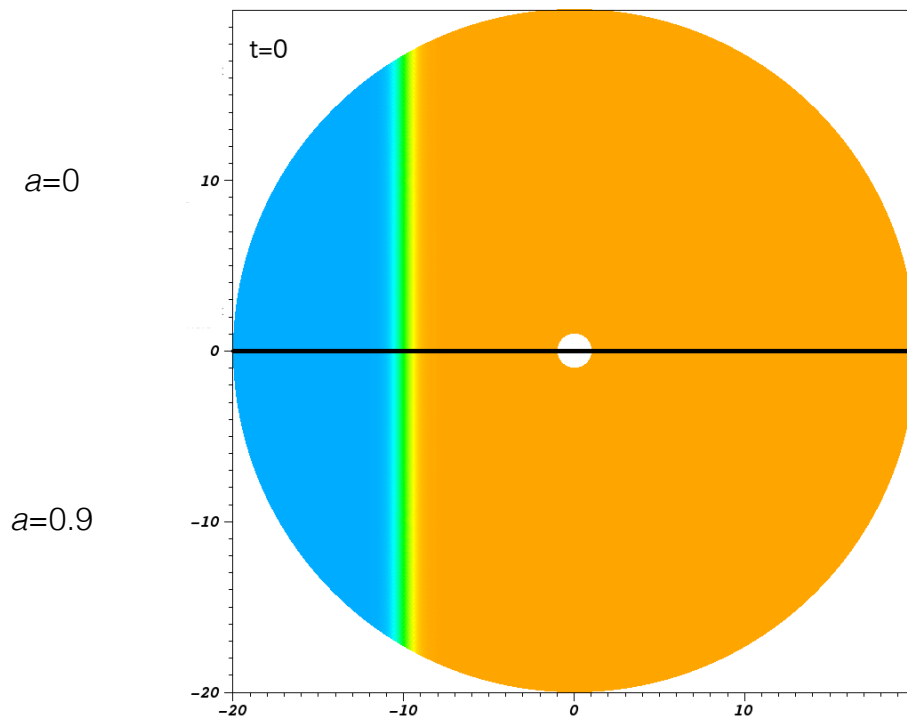
Results



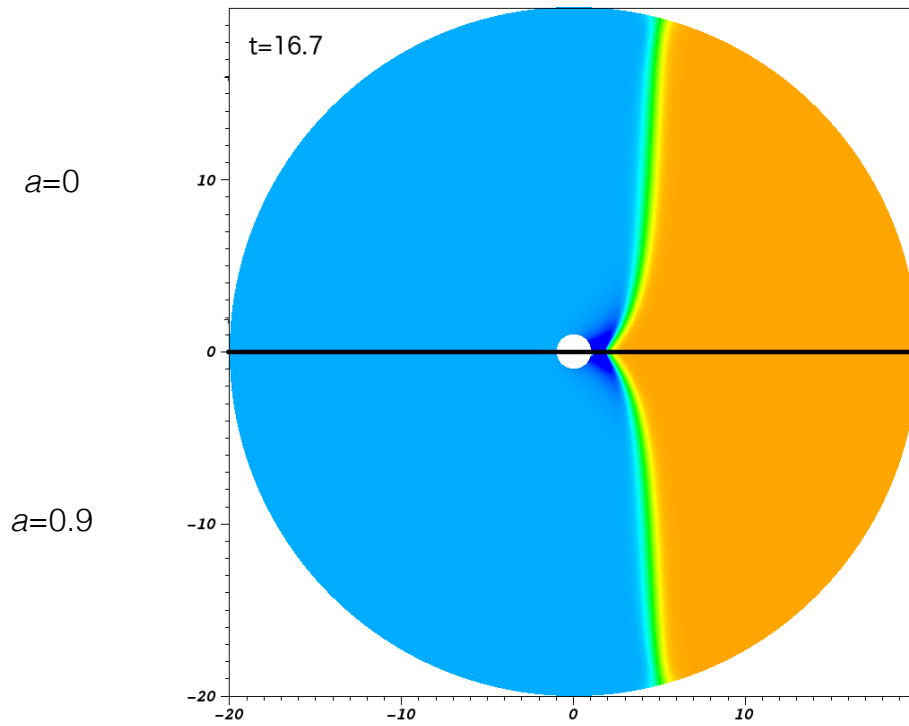
Results



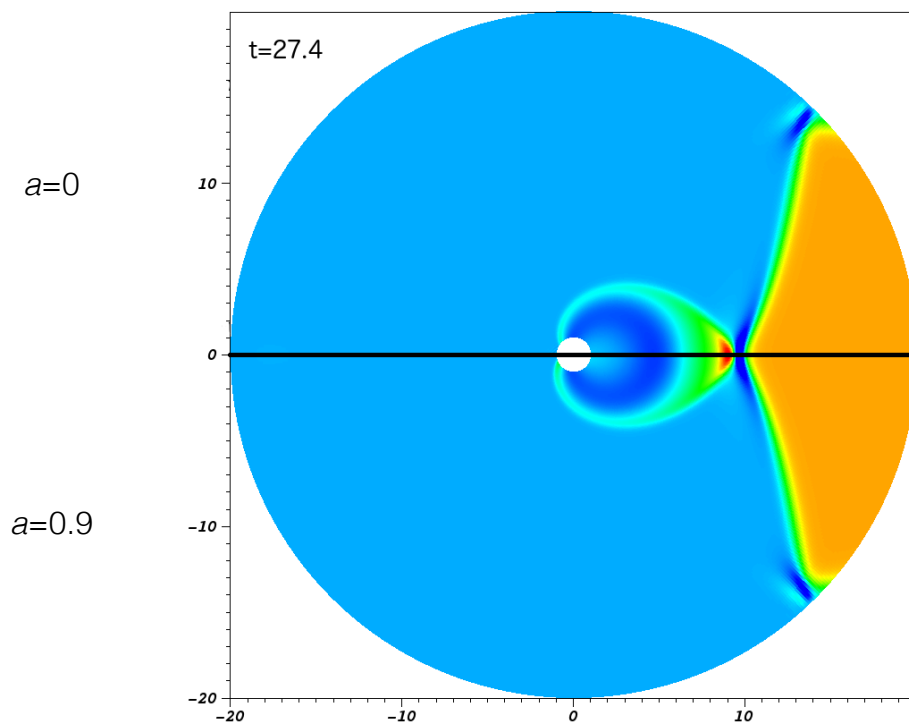
Results



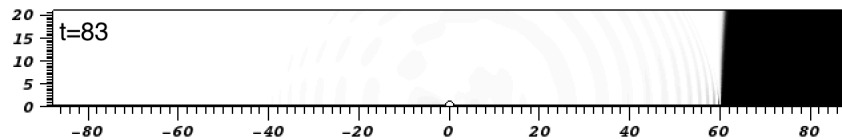
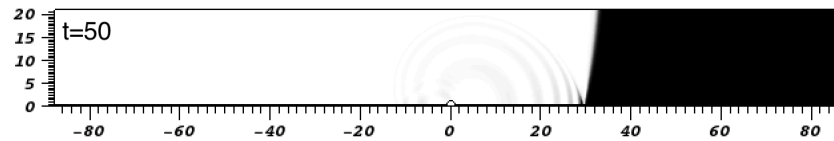
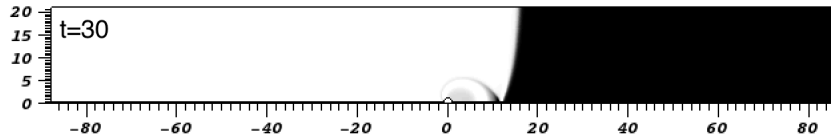
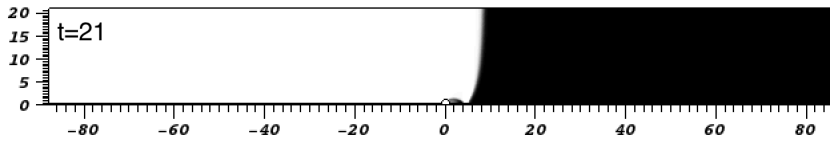
Results



Results



Results



Summary

- Domain wall transits are an active area of research.
- There exist observational campaigns, both terrestrial and astrophysical.
- Domain walls seem to be stable under the black hole transits
- Angular momentum of the black hole have a little impact on the results

Thank you for your attention

- F. Ficek, P. Mach, *Planar domain walls in black hole spacetimes*, Phys. Rev. D **97**, 044012 (2018)
- S. Pustelny et. al. *The Global Network of Optical Magnetometers for Exotic physics (GNOME): A novel scheme to search for physics beyond the Standard Model*, Annalen der Physik **525**, 659 (2013)
- A. Derevianko, M. Pospelov, *Hunting for topological dark matter with atomic clocks*, Nature Physics **10**, 933 (2014)
- Y.V. Stadnik, V.V. Flambaum, *Searching for Topological Defect Dark Matter via Nongravitational Signatures*, PRL **113**, 151301 (2014)
- V. Radhakrishnan, R. N. Manchester, *Detection of a Change of State in the Pulsar PSR 0833-45*, Nature **222**, 228 (1969)
- Y. Morisawa, D. Ida, A. Ishibashi, K. Nakao, *Thick domain walls around a black hole*, Phys. Rev. D **69**, 084018 (2004)
- A. Flachi et. al. *Black holes escaping from domain walls*, Phys. Rev. D **73**, 125

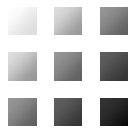
Masashi Kimura

Instituto Superior Tecnico, Universidade de Lisboa

**“Stability analysis of black holes by the S-deformation method
for coupled systems”**

(10+5 min.)

[JGRG28 (2018) 110808]



Stability analysis of BHs by the S-deformation method for coupled systems

MK, CQG **34**, 235007 (2017)

MK & T.Tanaka, CQG **35**, 195008 (2018)

MK & T.Tanaka, arXiv:1809.00795

Masashi Kimura
(IST, Univ. of Lisbon)

w/ Takahiro Tanaka (Kyoto Univ.)

8th Nov 2018

Linear (mode) stability of BH

Linear gravitational perturbation on a highly symmetric BH usually reduces to

$$\left[-\frac{\partial^2}{\partial t^2} + \frac{\partial^2}{\partial x^2} - V(x) \right] \tilde{\Phi} = 0$$

$$\tilde{\Phi}(t, x) = e^{-i\omega t} \Phi(x)$$

$$\left[-\frac{d^2}{dx^2} + V \right] \Phi = \omega^2 \Phi$$

unstable mode $\rightarrow \omega^2 < 0$ mode

(negative energy bound state)

To prove (mode) stability, we need to show the non-existence of $\omega^2 < 0$ mode

$$\left[-\frac{d^2}{dx^2} + V \right] \Phi = \omega^2 \Phi$$

$$\implies \left[\bar{\Phi} \frac{d\Phi}{dx} \right]_{-\infty}^{\infty} + \int dx \left[\left| \frac{d\Phi}{dx} \right|^2 + V |\Phi|^2 \right] = \omega^2 \int dx |\Phi|^2$$

$V \geq 0$ implies non-existence of $\omega^2 < 0$ mode

Sometimes, V contains negative regions

2/18

S-deformation [Kodama and Ishibashi 2003]

$$-\frac{d}{dx} \left[\bar{\Phi} \frac{d\Phi}{dx} + S |\Phi|^2 \right] + \left| \frac{d\Phi}{dx} + S \Phi \right|^2 + \left(V + \frac{dS}{dx} - S^2 \right) |\Phi|^2 = \omega^2 |\Phi|^2$$

For continuous S

$$-\left[\bar{\Phi} \frac{d\Phi}{dx} + S |\Phi|^2 \right]_{-\infty}^{\infty} + \int dx \left[\left| \frac{d\Phi}{dx} + S \Phi \right|^2 + \left(V + \frac{dS}{dx} - S^2 \right) |\Phi|^2 \right] = \omega^2 \int dx |\Phi|^2$$

We can say $\omega^2 \geq 0$ if $V + \frac{dS}{dx} - S^2 \geq 0$

In general, it is hard to find an appropriate S analytically

In that case, numerical approach

(e.g. solving PDE) was used so far 3/18

Today's talk

We propose a simple method for finding an appropriate S-deformation

Also, extend this method to coupled systems

4/18

Very easy method

[Kimura 2017]

[Kimura & Tanaka2018]

Just solve $V + \frac{dS}{dx} - S^2 = 0$ numerically

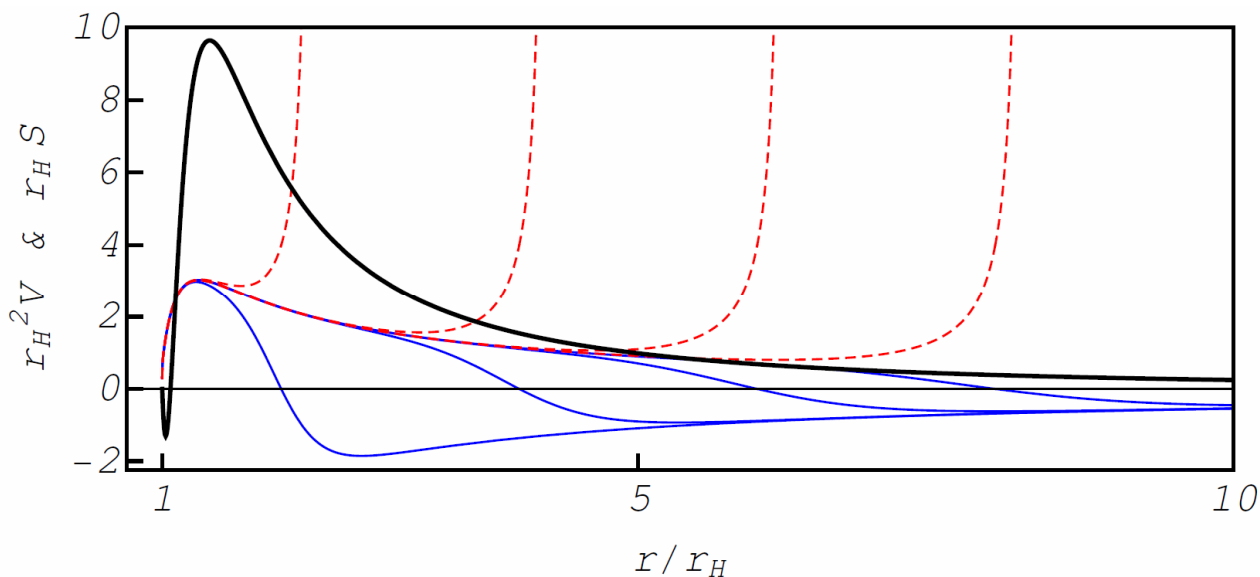
The existence of global regular solution is non-trivial

Regular S usually can be obtained from the initial condition $S = 0$ at $V > 0$ region

5/18



10 Dim Schwarzschild BH

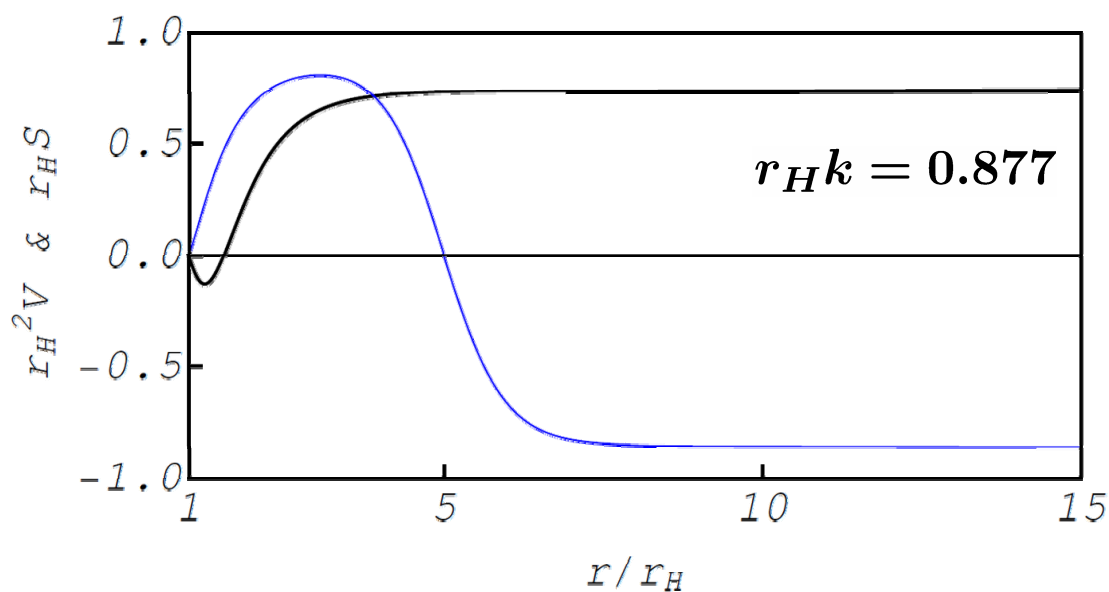


We can find regular S without fine-tuning

6/18



5D Black string



(If $r_H k < r_H k_{cr} \simeq 0.876$ there exists an
 unstable mode [Gregory and Laflamme, 1993])

7/18

Relation with Schrödinger Eq.

$V + \frac{dS}{dx} - S^2 = 0$ is the Riccati equation

$$\frac{1}{\phi} \frac{d\phi}{dx} := -S \quad \rightarrow \quad -\frac{d^2\phi}{dx^2} + V\phi = 0$$

Schrödinger Eq. with zero energy

A solution which does not have any zero corresponds to a regular S

8/18

Nodal theorem

A theorem in the Sturm–Liouville theory

$$\left[-\frac{d^2}{dx^2} + V \right] \Phi = E\Phi$$

If we solve the Schrödinger Eq. with the boundary condition $\Phi = 0, d\Phi/dx = 1$ at a sufficiently large distance, the number of zeros coincides with the number of the negative energy bound states.

There should exist a regular S for stable spacetime

9/18

Under some assumption, we can show that S constructed from a sol. with decaying boundary condition is regular if the spacetime is stable.

Proposition. *There exists a regular S -deformation for stable spacetimes*

10/18

Extension to multiple degrees of freedom

If there exist two or more physical degrees of freedom, and they are coupled, master Eqs sometimes become

$$\left[-\frac{d^2}{dx^2} + V \right] \Phi = \omega^2 \Phi$$

V : $n \times n$ Hermitian matrix

Φ : n components vector

We assume the coupling term $\mathcal{L} \sim \Phi^\dagger V \Phi$

11/18

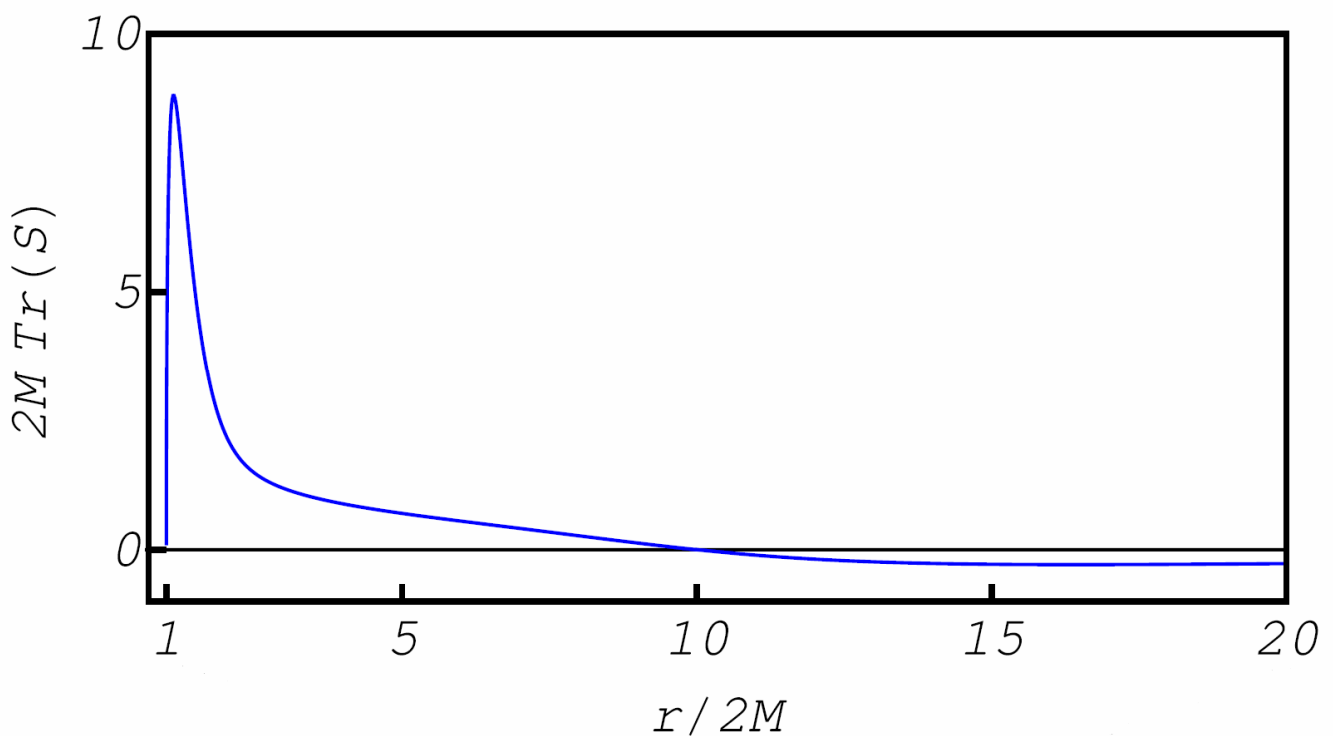
Schwarzschild BH in dCS

We solve $V + \frac{dS}{dx} - S^2 = 0$ numerically

with the initial condition

$S = 0$ at a large distance

14/18



$$\ell = 2, \beta M^4 = 1/10$$

$$V + \frac{dS}{dx} - S^2 = 0$$

(S is bounded if $\text{Tr}(S)$ is bounded) 15/18

Remarks for general case

The nodal theorem for coupled systems suggest the existence of regular S
(we can explicitly show the existence of regular S for rapidly decaying potential)

If $V > 0$ in asymptotic region,
 $S = 0$ at large x is a candidate for an appropriate initial condition

Merit of S -deformation method

- We do not need to care about boundary condition at infinity very much, we can solve equation from finite point
- Any fine-tuning is not needed
- It is clear that the existence of regular S is the sufficient condition for stability (proof of nodal theorem is very difficult)
- Easy to show the non-existence of zero mode (by showing two different S)

Summary

We proposed a simple method for finding S-deformation by solving $V + \frac{dS}{dx} - S^2 = 0$

This is a good test for stability of BH

If stable, this method should work

We can guess the threshold of the parameter where unstable mode appears

Invited lecture 14:00–14:45

[Chair: Sugumi Kanno]

Vincent Vennin

APC Paris

“Stochastic Inflation and Primordial Black Holes”

(40+10 min.)

[JGRG28 (2018) 110810]



Stochastic Inflation and Primordial Black Holes

Vincent Vennin

JGRG28

Tokyo, 8th November 2018

Outline

- Quantum State of Cosmological Perturbations
- The Stochastic- δN Inflation Formalism
- Primordial Black Holes

14:00 – 14:45

Invited Talk 7 (Chair: S. Kanno)

Vincent Vennin *APC Paris*
Stochastic Inflation and Primordial Black Holes

14:45 – 15:45

Session 4P1

[T61*] Yuichiro Tada *Nagoya University*
Stochastic formalism and curvature perturbations

[T62*] Junsei Tokuda *Kyoto University*

On the contribution of infrared secular effects to primordial fluctuations via quantum interference

Outline

- Quantum State of Cosmological Perturbations
- The Stochastic- δN Inflation Formalism
- Primordial Black Holes

Based on:

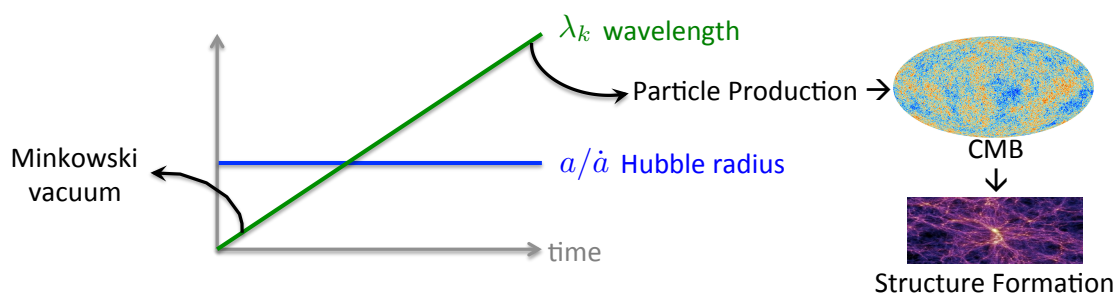
- VV and A. Starobinsky, 1506.04732 (EPJC)
- H. Assadullahi, H. Firouzjahi, M. Noorbala, VV, D. Wands, 1604.04502 (JCAP)
- VV, H. Assadullahi, H. Firouzjahi, M. Noorbala, D. Wands, 1604.06017 (PRL)
- C. Pattison, VV, H. Assadullahi, D. Wands, 1705.05746 (JCAP)

Cosmological Perturbations in Inflation

- Inflation is a high energy phase of accelerated expansion in the early Universe

$$ds^2 = -dt^2 + a^2(t)dx^2 \quad \text{with} \quad \ddot{a} > 0$$

- Quantum vacuum fluctuations are stretched to cosmological scales



Quantum fluctuations sourcing the background

Cosmological Perturbations in Inflation

- One scalar degree of freedom: $v \propto \zeta$ (curvature perturbation) $\propto \delta T/T$ (CMB T° fluctuation)

- $|\Psi\rangle = \bigotimes_{\mathbf{k} \in \mathbb{R}^{3+}} |\Psi_{\mathbf{k}}\rangle$ with $|\Psi_{\mathbf{k}}\rangle = \frac{1}{\cosh r_k} \sum_{n=0}^{\infty} e^{2in\varphi_k} (-1)^n \tanh^n r_k |n_{\mathbf{k}}, n_{-\mathbf{k}}\rangle$

Two-mode squeezed state (Gaussian state)

- Wigner function $W(v_{\mathbf{k}}, p_{\mathbf{k}}) = \int \frac{dx}{2\pi^2} \Psi^*(v_{\mathbf{k}} - \frac{x}{2}) e^{-ip_{\mathbf{k}}x} \Psi(v_{\mathbf{k}} + \frac{x}{2})$

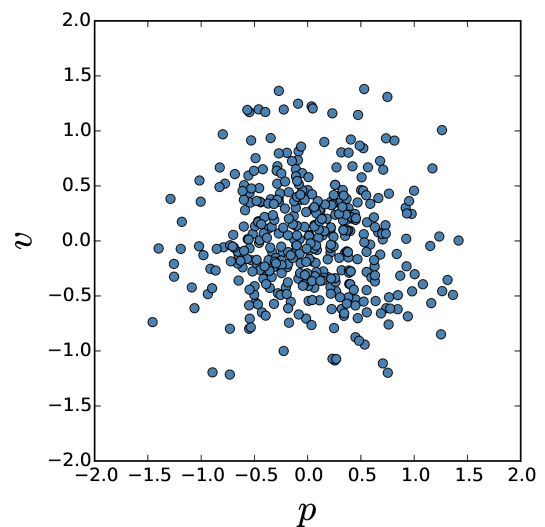
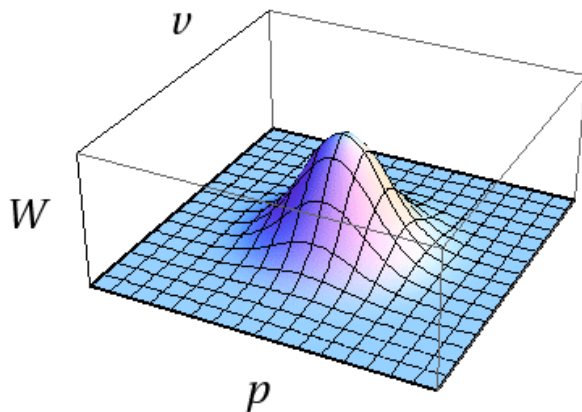
- Evolution Equation $\frac{\partial}{\partial t} W(v, p, t) = -\{W(v, p, t), H(v, p, t)\}_{\text{Poisson Bracket}}$

For quadratic Hamiltonians

2/15

Quantum State of Cosmological Perturbations

$$\frac{\partial}{\partial t} W(v, p, t) = -\{W(v, p, t), H(v, p, t)\}_{\text{Poisson Bracket}}$$



Cosmological Perturbations in Inflation

• One scalar degree of freedom: $v \propto \zeta$ (curvature perturbation) $\propto \delta T/T$ (CMB T° fluctuation)

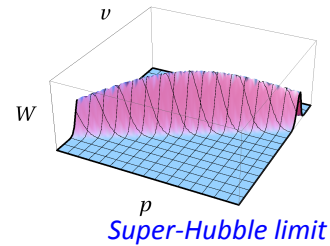
• Evolution Equation $\frac{\partial}{\partial t} W(v, p, t) = - \{W(v, p, t), H(v, p, t)\}_{\text{Poisson Bracket}}$
For quadratic Hamiltonians

• Quantum Mean Value and Stochastic Average

$$\langle \hat{O}(\hat{v}, \hat{p}) \rangle_{\text{quant}} \stackrel{?}{=} \int W(v, p) \mathcal{O}(v, p) dv dp$$

Lesgourgues, Polarski, Starobinsky (1997)
 J. Martin, VV (2016)

- True for $\mathcal{O}(\hat{v})$ and $\mathcal{O}(\hat{p})$
- True for Hermitian, quadratic $\mathcal{O}(\hat{v}, \hat{p})$
- True for proper $\mathcal{O}(\hat{v}, \hat{p})$ in the super-Hubble limit



Example: $\hat{O} = v_{\mathbf{k}} v_{\mathbf{k}}^\dagger p_{\mathbf{k}} p_{\mathbf{k}}^\dagger + p_{\mathbf{k}} p_{\mathbf{k}}^\dagger v_{\mathbf{k}} v_{\mathbf{k}}^\dagger \longrightarrow \langle \hat{O} \rangle_{\text{quant}} = \langle \hat{O} \rangle_{\text{stoch}} + 1/4$
 $\searrow e^{2(N - N_{\text{Hubble crossing}})}$

4/15

Stochastic Formalism

Starobinsky, 1986

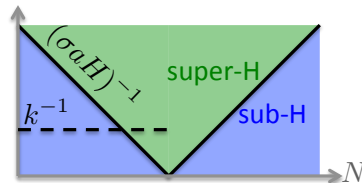
coarse-grained field:

$$\hat{\phi}_{\text{coarse grained}} = \int_{k < \sigma a H(N)} d^3 \mathbf{k} \left[\phi_{\mathbf{k}}(N) e^{-i\mathbf{k} \cdot \mathbf{x}} \hat{a}_{\mathbf{k}} + \phi_{\mathbf{k}}^*(N) e^{i\mathbf{k} \cdot \mathbf{x}} \hat{a}_{\mathbf{k}}^\dagger \right]$$

at leading order in slow roll:

$$\frac{d}{dN} \phi_{\text{cg}} = - \frac{V'(\phi_{\text{cg}})}{3H^2(\phi_{\text{cg}})} + \frac{H(\phi_{\text{cg}})}{2\pi} \xi(N)$$

Modes smaller than the coarse-graining scale are constantly escaping the Hubble radius and **source the coarse-grained sector.**



\longrightarrow Quantum backreaction on super-Hubble scales

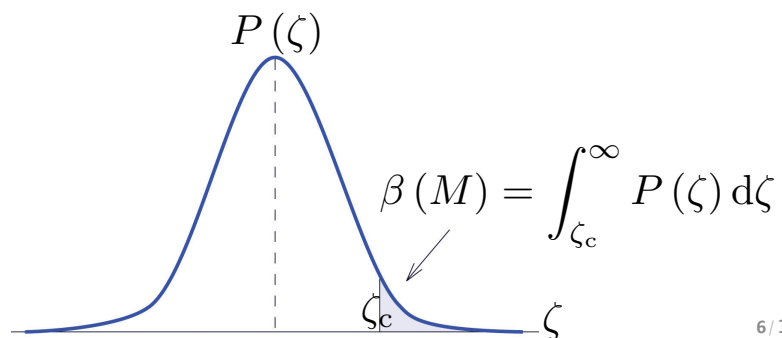
Primordial Black Holes from Inflation

- Primordial density perturbations when modes re-enter the Hubble radius after inflation

$$\left. \frac{\delta\rho}{\rho} \right|_{k=aH} \sim \zeta$$

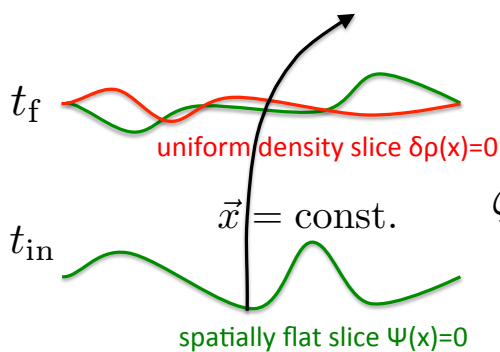
- Rare fluctuations exceeding critical value $\zeta > \zeta_c \sim 1$ collapse to form black holes

- Mass fraction $\beta(M) < 10^{-8}$



6/15

The Stochastic- δN Formalism



Enqvist, Nurmi, Podolsky, Rigopoulos (2008)
 Fujita, Kasawaki, Tada, Takesako (2014)
 VV, Starobinsky (2015)
 VV, Assadullahi, Firouzjahi, Noorbala, Wands (2017)

$$\zeta(t, x) = N(t, x) - N_0(t) \equiv \delta N$$

- number of e-fold is a stochastic variable $\mathcal{N}(\phi)$

$$\zeta_{\text{coarse grained}} = \mathcal{N} - \langle \mathcal{N} \rangle$$

- Moments obey an iterative relation (Vennin and Starobinsky 2015)

$$\langle \mathcal{N}^n \rangle'' - \frac{v'}{v^2} \langle \mathcal{N}^n \rangle' = -\frac{n}{v M_{\text{Pl}}^2} \langle \mathcal{N}^{n-1} \rangle$$

Power Spectrum

$$\mathcal{P}_\zeta(\phi_*) = 2 \left\{ \int_{\phi_*}^{\bar{\phi}} \frac{dx}{M_{\text{Pl}}} \frac{1}{v(x)} \exp \left[\frac{1}{v(x)} - \frac{1}{v(\phi_*)} \right] \right\}^{-1} \times \int_{\phi_*}^{\bar{\phi}} \frac{dx}{M_{\text{Pl}}} \left\{ \int_x^{\bar{\phi}} \frac{dy}{M_{\text{Pl}}} \frac{1}{v(y)} \exp \left[\frac{1}{v(y)} - \frac{1}{v(x)} \right] \right\}^2 \exp \left[\frac{1}{v(x)} - \frac{1}{v(\phi_*)} \right]$$

Saddle Point Approximation

$$\left| 2v - \frac{v''v^2}{v'^2} \right| \ll 1$$

$$\mathcal{P}_\zeta(\phi_*) \simeq \frac{2}{M_{\text{Pl}}^2} \frac{v^3(\phi_*)}{v'^2(\phi_*)} \left[1 + 5v(\phi_*) - 4 \frac{v^2(\phi_*) v''(\phi_*)}{v'^2(\phi_*)} + \dots \right]$$

Classical result

First order correction

$$f_{\text{NL}} = \frac{5}{24} M_{\text{Pl}}^2 \left[6 \frac{v'^2}{v^2} - 4 \frac{v''}{v} + v \left(11 \frac{v'^2}{v^2} - 158 \frac{v''}{v} - 9 \frac{v'''}{v'} + 118 \frac{v''^2}{v'^2} \right) + \dots \right]$$

November 2018

JGRG 28

8 / 15

Full PDF required for PBHs!

- Define characteristic function (includes all the moments)

$$\chi_{\mathcal{N}}(t, \phi) = \langle e^{it\mathcal{N}}(\phi) \rangle = \int e^{it\mathcal{N}(\phi)} P(\mathcal{N}, \phi) d\mathcal{N}$$

- Obeys partial differential equation

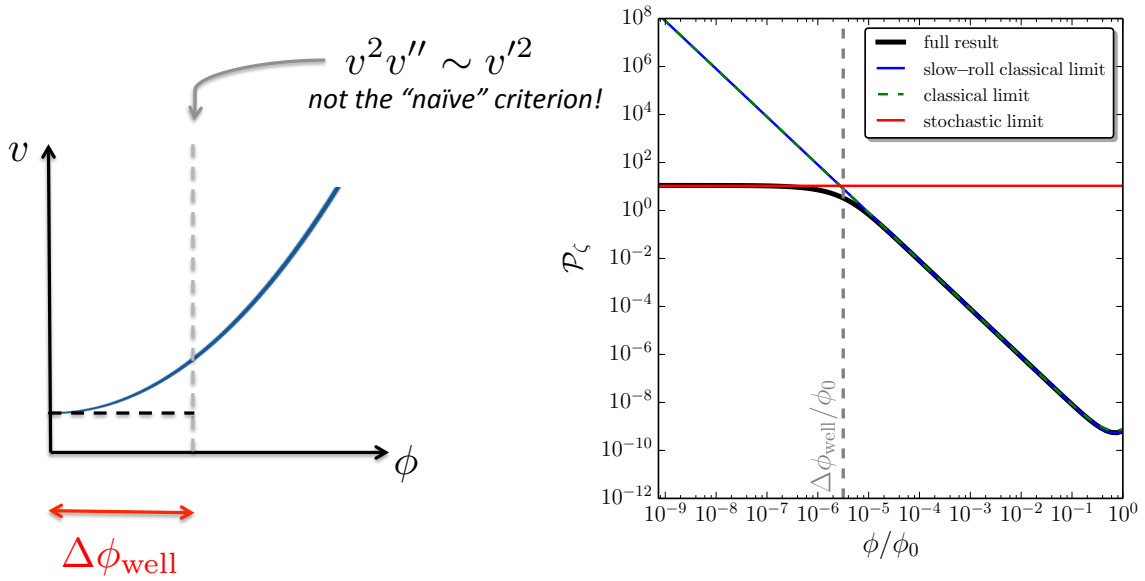
$$\left(\frac{\partial^2}{\partial \phi^2} - \frac{v'}{v^2} \frac{\partial}{\partial \phi} + \frac{it}{v M_{\text{Pl}}^2} \right) \chi_{\mathcal{N}}(t, \phi) = 0$$

- Inverse Fourier transform gives full probability distribution

$$P(\mathcal{N}, \phi) = \frac{1}{2\pi} \int_{-\infty}^{\infty} e^{-it\mathcal{N}} \chi_{\mathcal{N}}(t, \phi) dt$$

9 / 15

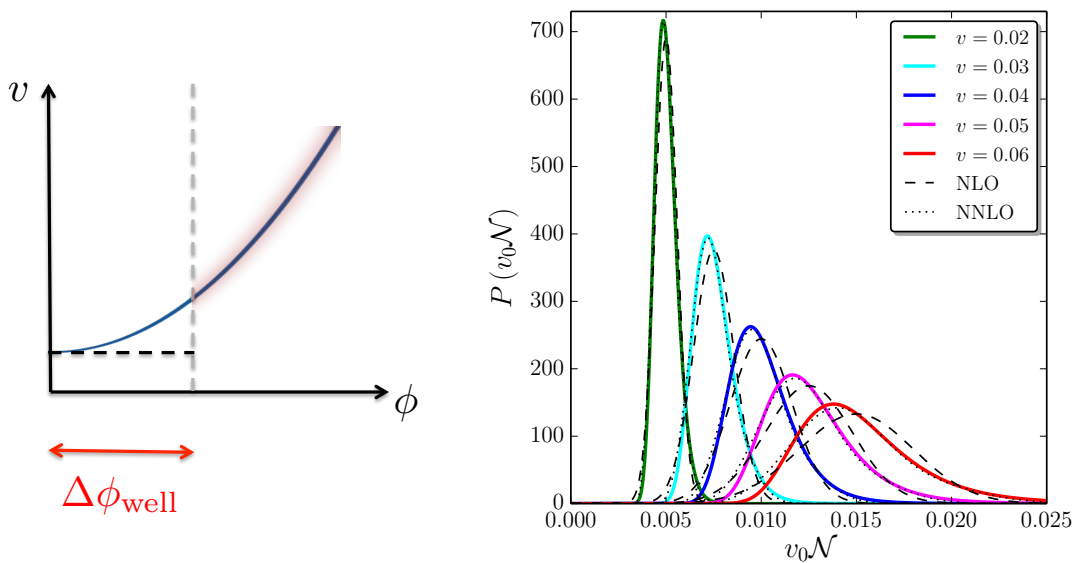
Example: $v(\phi) = v_0 \left[1 + \left(\frac{\phi}{\phi_0} \right)^p \right]$



10/15

Example: $v(\phi) = v_0 \left[1 + \left(\frac{\phi}{\phi_0} \right)^p \right]$

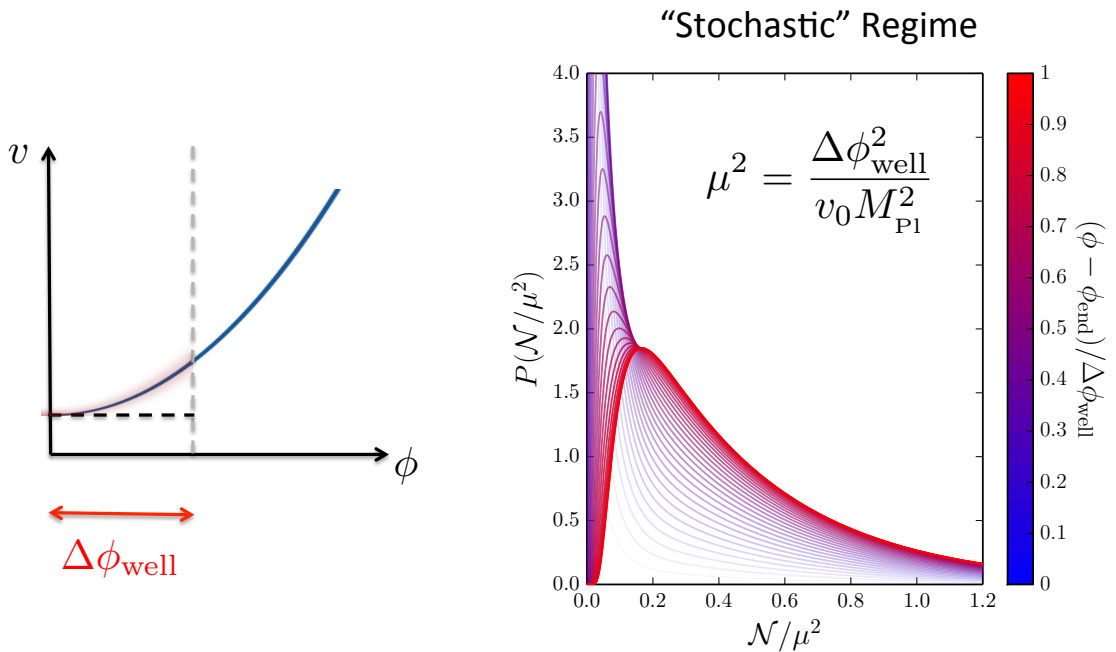
"Classical" Regime



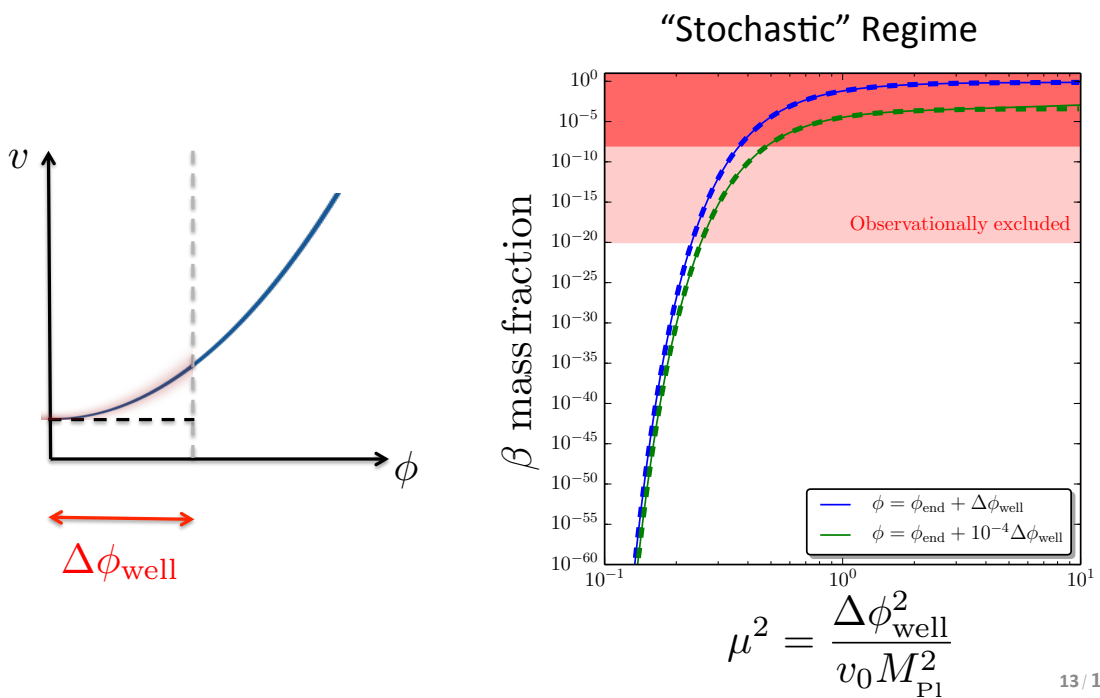
Is the Gaussian approximation sufficient?

11/15

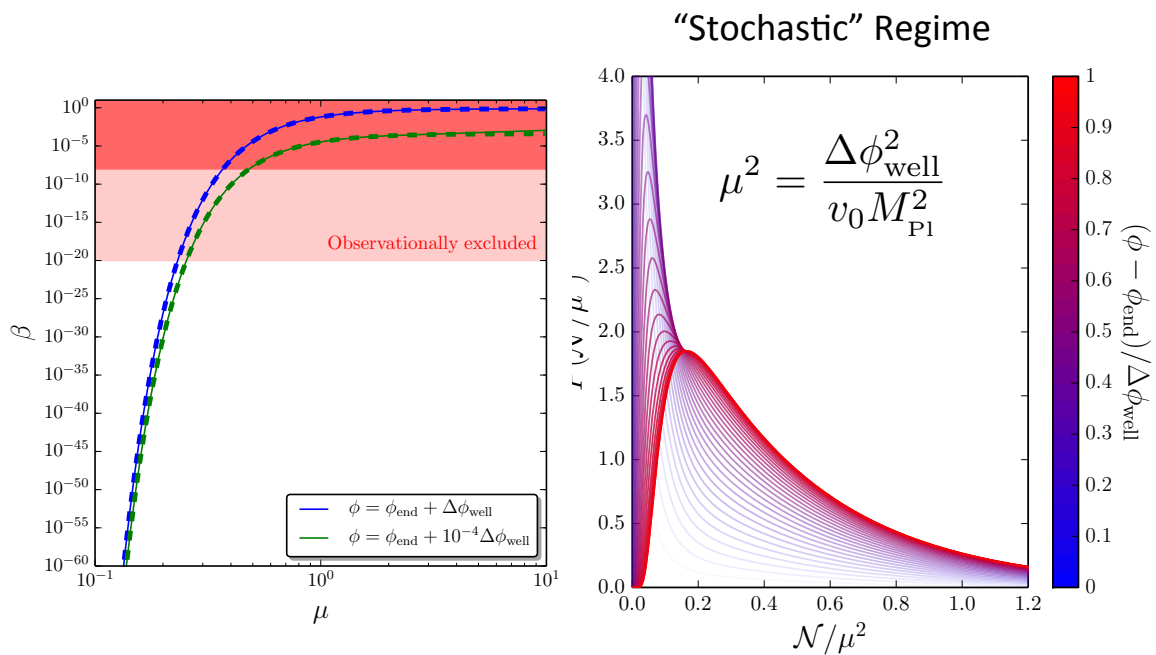
Example: $v(\phi) = v_0 \left[1 + \left(\frac{\phi}{\phi_0} \right)^p \right]$



Example: $v(\phi) = v_0 \left[1 + \left(\frac{\phi}{\phi_0} \right)^p \right]$



$$\text{Example: } v(\phi) = v_0 \left[1 + \left(\frac{\phi}{\phi_0} \right)^p \right]$$



14/15

Conclusions

- **Stochastic- $\delta\mathcal{N}$** needed to calculate primordial density perturbations beyond perturbative approach
- In the classical regime, **Gaussian approximation may fail!**
- **Primordial Black Hole bounds require $\mathcal{N} < 1$ in quantum diffusion regime**
- Extension to **multi-field?**
- Transient **slow-roll violation** (inflection point models)?

Thank you for your attention!

Session S4P1 14:45–15:45

[Chair: Sugumi Kanno]

Yuichiro Tada

Nagoya U.

“Stochastic formalism and curvature perturbations”

(10+5 min.)

[JGRG28 (2018) 110811]



Stochastic Formalism & Curvature Perturbations

Yuichiro Tada (C-lab. Nagoya U.)

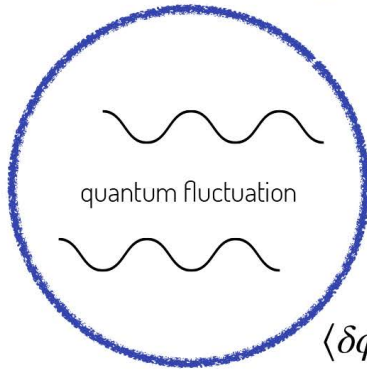
Pinol, Renaux-Petel, Vennin, Fujita, Tokuda
arXiv: 1806.10126 and in preparation

Key Question

- Curv. PTB beyond 1st order?
- Resummation eff.?
- Intuitive understanding of curv. PTB?

scalar PTB

horizon: R_H



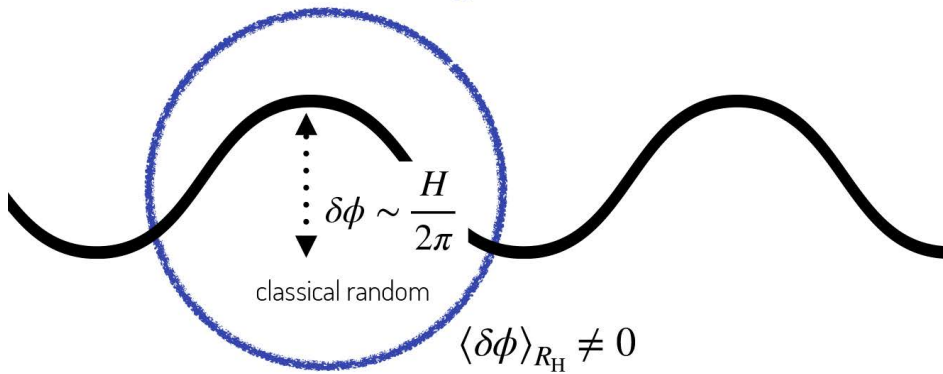
$$\langle \delta\phi \rangle_{R_H} = 0$$

slow-roll EoM

$$\frac{d\phi_0}{dN} = -\frac{V'}{3H^2}$$

scalar PTB

horizon: R_H

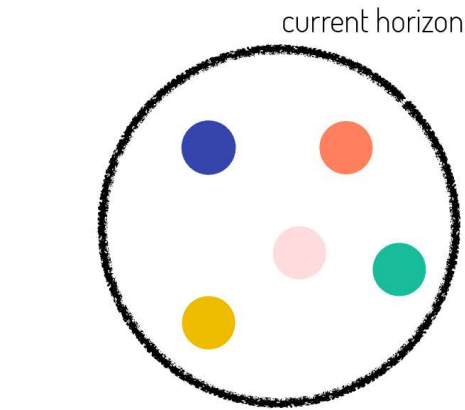


$$\langle \delta\phi \rangle_{R_H} \neq 0$$

slow-roll **stochastic** EoM Starobinsky 1986

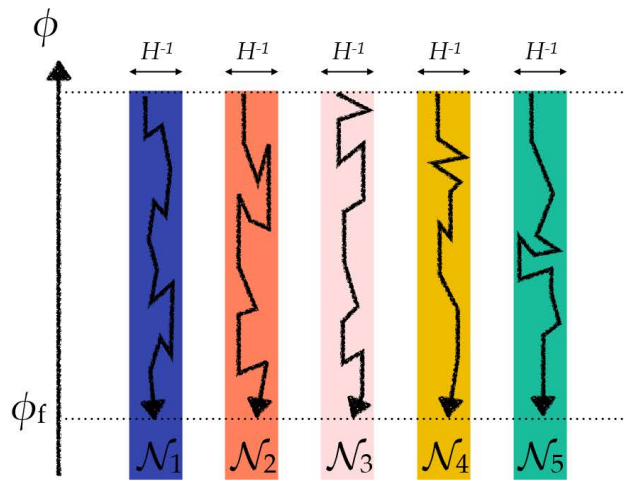
$$\frac{d\phi_{IR}}{dN} = -\frac{V'}{3H^2} + \frac{H}{2\pi}\xi, \quad \langle \xi(N)\xi(N') \rangle = \delta(N - N')$$

scalar PTB



slow-roll **stochastic** EoM Starobinsky 1986

$$\frac{d\phi_{\text{IR}}}{dN} = -\frac{V'}{3H^2} + \frac{H}{2\pi}\xi$$



δN formalism Starobinsky 1985

$$a = a_0 e^{\mathcal{N}}$$

$$\delta \mathcal{N} = \mathcal{N} - \langle \mathcal{N} \rangle : \text{curv. PTB } \zeta$$

Stochastic Form.

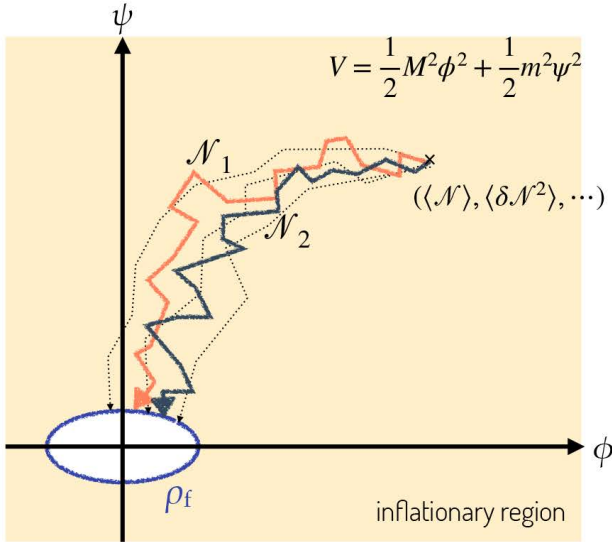
- ✓ intuition in x -space
- ✓ all resummation eff.
- ✓ all info. about ζ stat.

✗ classical approx.

✗ unclear k -dependence

Stochastic- $\delta\mathcal{N}$

Fujita, Kawasaki, YT, Takesako 2013
Fujita, Kawasaki, YT 2014



$$\begin{aligned} \langle \delta \mathcal{N}^2 \rangle &= \langle \zeta^2(\mathbf{x}) \rangle \\ &= \int \frac{d^3 k}{(2\pi)^3} P_\zeta(\mathbf{k}) e^{i\mathbf{k}\cdot\mathbf{0}} \\ &= \int_{\log k_f - \langle \mathcal{N} \rangle}^{\log k_f} d \log k \mathcal{P}_\zeta(k) \quad \left(\mathcal{P}_\zeta = \frac{k^3}{2\pi^2} P_\zeta \right) \end{aligned}$$



$$\mathcal{P}_\zeta(k) = \left. \frac{d\langle \delta \mathcal{N}^2 \rangle}{d\langle \mathcal{N} \rangle} \right|_{k=k_f e^{-\langle \mathcal{N} \rangle}}$$

Vennin's PDE

Vennin & Starobinsky 2015

e.g. $V = \frac{1}{2} M^2 \phi^2 + \frac{1}{2} m^2 \psi^2$

Fokker-Planck eq.

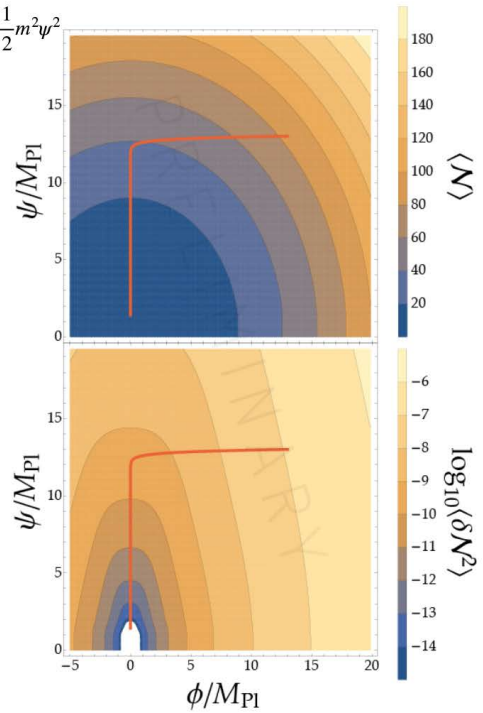
$$\begin{aligned} \partial_N P &= -\partial_I (D^I P) + \frac{1}{2} \partial_I \partial_J (D^{IJ} P) \\ \text{e.g. } D^I &= -M_{\text{Pl}}^2 \frac{V^I}{V}, \quad D^{IJ} = \left(\frac{H}{2\pi} \right)^2 G^{IJ} \end{aligned}$$



Vennin's PDE

$$\begin{cases} \left(D^I \partial_I + \frac{1}{2} D^{IJ} \partial_I \partial_J \right) \mathcal{M}_n = -n \mathcal{M}_{n-1} \\ \left(D^I \partial_I + \frac{1}{2} D^{IJ} \partial_I \partial_J \right) \mathcal{E}_2 = -D^{IJ} (\partial_I \mathcal{M}_1) (\partial_J \mathcal{M}_1) \end{cases}$$

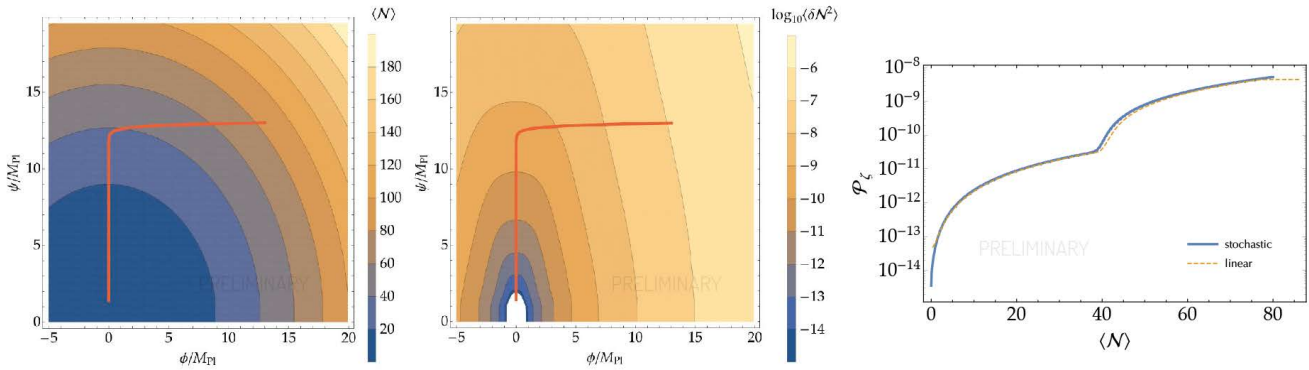
$\mathcal{M}_n(\phi) = \langle \mathcal{N}^n \rangle(\phi), \quad \mathcal{E}_2(\phi) = \langle \delta \mathcal{N}^2 \rangle(\phi)$



StocDeltaN.cpp

- double mass-term

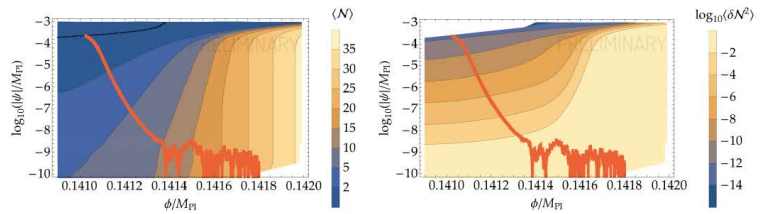
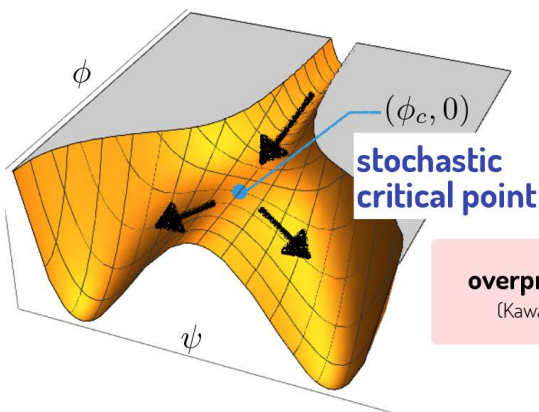
$$V = \frac{1}{2}M^2\phi^2 + \frac{1}{2}m^2\psi^2, \quad M = 9m = 10^{-5}M_{\text{Pl}}$$



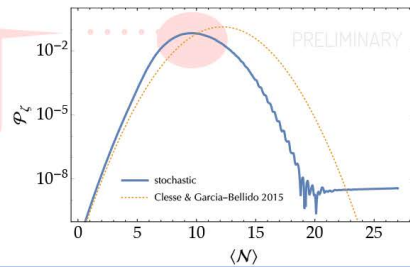
StocDeltaN.cpp

- hybrid inflation

$$V = \Lambda^4 \left[\left(1 - \frac{\psi^2}{M^2} \right)^2 + 2 \frac{\phi^2 \psi^2}{\phi_c^2 M^2} + \frac{\phi - \phi_c}{\mu_1} - \frac{(\phi - \phi_c)^2}{\mu_2^2} \right]$$



overproduce PBHs
(Kawasaki, YT 2015)



Conclusions

- Stochastic + δN \rightarrow non-pert. algorithm
- StocDeltaN : automatic num. code
 - visit my GitHub page (NekomammaT/StocDeltaN_dist)!

Session S4P2 16:45–18:30

[Chair: Hideki Ishihara]

Kohei Fujikura

Tokyo Institute of Technology

“Phase Transitions in Twin Higgs Models”

(10+5 min.)

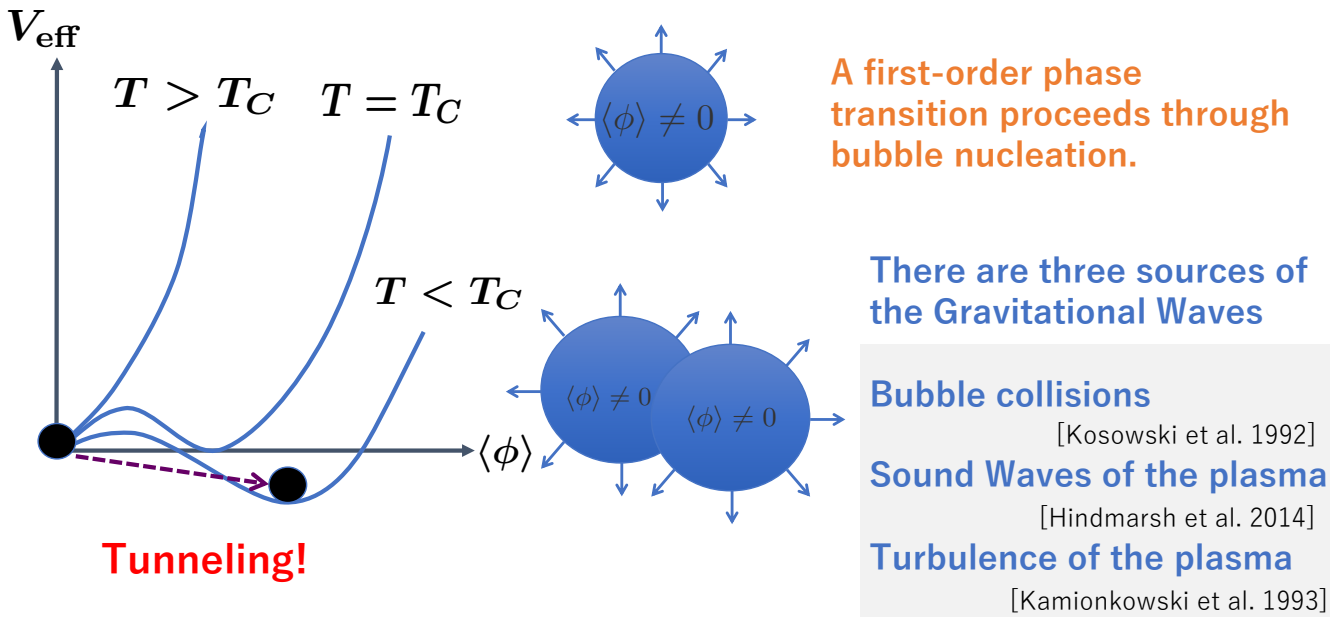
[JGRG28 (2018) 110815]

Phase Transitions in Twin Higgs Models

Kohei Fujikura (Titech)
In collaboration with
Kohei Kamada (RESCEU)
Yuichiro Nakai (Rutgers.U)
Masahide Yamaguchi (Titech)

Based on arXiv:1810.00574

First-order Phase Transitions



Motivation

Twin Higgs models

BSM physics

Constraints from
Collider searches

Figure

Constraints from
observation of GW

Figure

Hierarchy Problem

Electroweak phase transition in SM is not first order with $m_h \simeq 125\text{GeV}$

However, SM has a problem.

$$\delta m_h^2 = \text{---} \text{---} \text{---} + \text{---} \text{---} \text{---} + \text{---} \text{---} \text{---}$$
$$= -\frac{3y_t^2}{4\pi^2}\Lambda^2 + \frac{9g_2^2}{32\pi^2}\Lambda^2 + \frac{\lambda}{4\pi^2}\Lambda^2$$

Λ : cut-off scale

$\delta m_h^2 \gg m_h^2 \simeq 125^2\text{GeV}^2$ Fine-tuning is needed!

It is natural to consider Beyond Standard Model (BSM) physics.

Twin Higgs Models

[Chacko et al. 2005]

Twin Higgs provides excellent solution to the (Little) Hierarchy Problem.

SM Higgs is considered as pseudo-Nambu-Goldstone Boson.

$$\mathcal{H} = \begin{pmatrix} \Phi_1 \\ \Phi_2 \\ \Phi_3 \\ \Phi_4 \end{pmatrix} \quad V(\Phi) = \lambda \left(|\mathcal{H}|^2 - \frac{f^2}{2} \right)^2$$

\mathcal{H} : belongs to the (global) U(4) Fundamental Representation

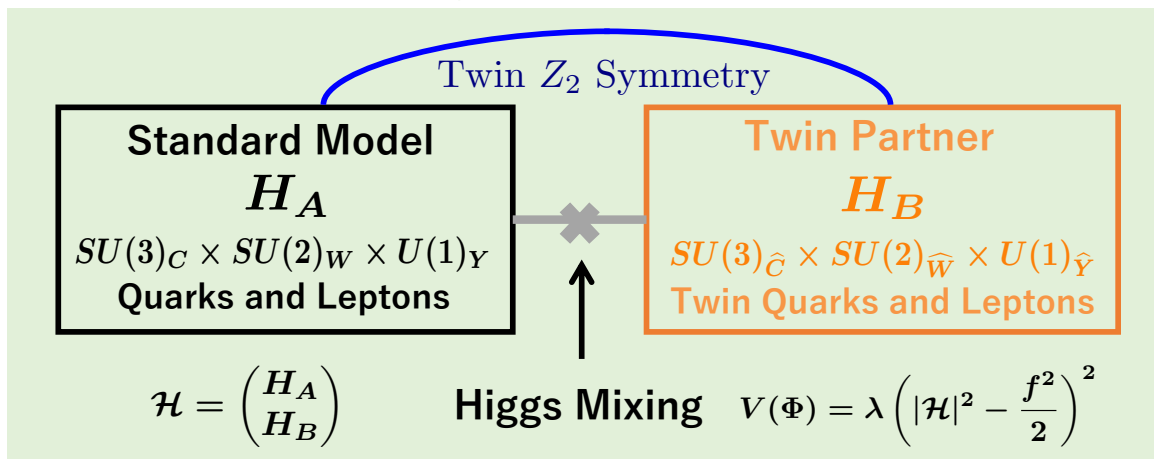
$\langle \Phi_4 \rangle = \frac{f}{\sqrt{2}} \Rightarrow$ U(4) symmetry is spontaneously broken to U(3) symmetry.

$$\dim(U(4)/U(3)) = 16 - 9 = 7$$

7 Nambu-Goldstone modes arise
(4 of them are identified with SM-like Higgs)

Matter contents

copy of SM sector



$V_{\text{eff}} \supset \left(-\frac{3y_t^2}{8\pi^2} + \frac{9g_2^2}{64\pi^2} \right) (|H_A|^2 + |H_B|^2) \Lambda^2$ respects the global U(4) symmetry.

pNGB (SM-like Higgs) is insensitive to the mass correction.

Higgs potential

General Higgs potential

$$V = \lambda \left(|H_A|^2 + |H_B|^2 - \frac{f^2}{2} \right)^2 + \sigma_1 f^2 |H_A|^2 + \kappa_1 (|H_A|^4 + |H_B|^4) + \rho_1 |H_A|^4$$

<p>Spontaneous symmetry breaking $U(4) \rightarrow U(3)$</p> <p>This term must be dominant compared to (explicit) $U(4)$ breaking term.</p> <p>$\lambda \gg \sigma_1, \kappa_1, \rho_1$</p>	<p>Soft twin Z_2 breaking</p> <p>To satisfy $2v_A < f$</p>	<p>Twin Z_2 preserving but (explicit) $U(4)$ breaking term.</p> <p>This term is naturally generated by Coleman-Weinberg (CW) potential.</p>	<p>Twin Z_2 and $U(4)$ symmetries breaking term.</p>
<p>These quartic terms generate the SM-like Higgs mass</p>			

A structure of Higgs potential in SUSY twin Higgs models is too complicated.

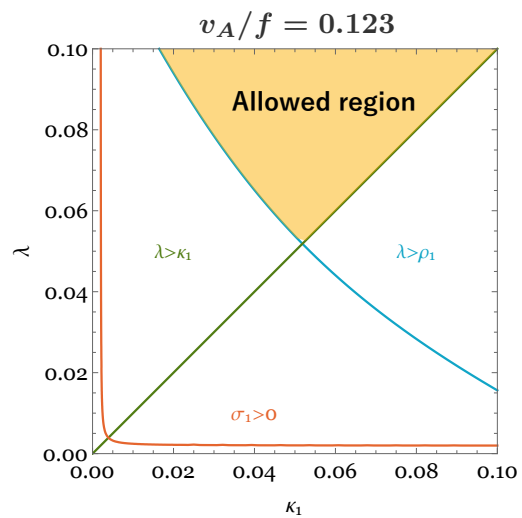
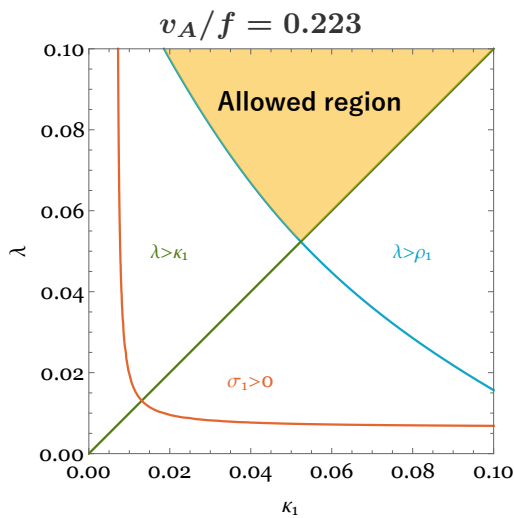
We take the decoupling limit to consider the general features of twin Higgs models.

Electroweak symmetry breaking(EWSB)

To realize correct EWSB, following conditions must be satisfied.

$$\langle H_A \rangle = v_A \simeq 246\text{GeV}, \quad m_h \simeq 125\text{GeV}$$

Yellow regions satisfy the two conditions and $\lambda > \kappa_1, \rho_1$.



Phase Transition(s) in Twin Higgs Models

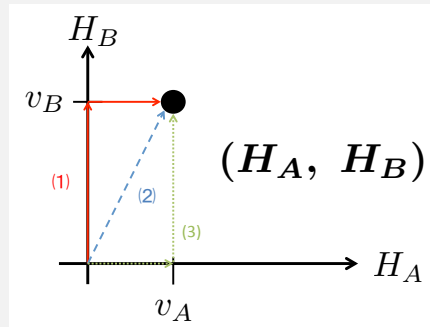
There are two spontaneous symmetry breakings
(twin EW symmetry and EW symmetry)

$$(1) (0, 0) \Rightarrow (0, v_B) \Rightarrow (v_A, v_B)$$

$$(2) (0, 0) \Rightarrow (v_A, v_B)$$

$$(3) (0, 0) \Rightarrow (v_A, 0) \Rightarrow (v_A, v_B)$$

We consider the case (1) and analyze the two phase transitions.



In this talk, I focus on the phase transition associated with twin EW symmetry breaking.

$$H_A = \begin{pmatrix} 0 \\ 0 \end{pmatrix}, H_B = \begin{pmatrix} 0 \\ \frac{\phi_B}{\sqrt{2}} \end{pmatrix}$$

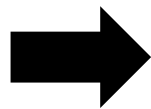
+

Twin Top quark
 $SU(2)_{\widehat{W}}$ gauge fields thermal loops
Twin stop (SUSY partner of twin top)

Overview of calculation method

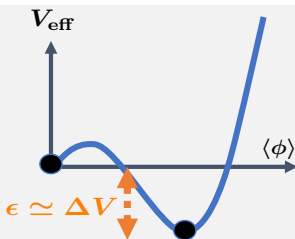
Fix a model

$$\mathcal{L}(\phi, \psi, A_\mu^a, \dots)$$



Quantum and Thermal effects

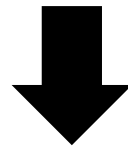
$$V_{\text{CW}}(\phi) \text{ and } V_{\text{Thermal}}(\phi)$$



$$\alpha \sim \frac{\epsilon}{\rho_{\text{rad}}} \quad \Gamma \simeq \Gamma_0 e^{\beta t}$$

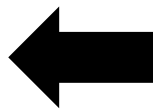
Γ : Bubble nucleation rate per unit time per unit volume

Solve bounce eq.



GW spectrum

$$\square h_{\mu\nu} = 16\pi G T_{\mu\nu}$$



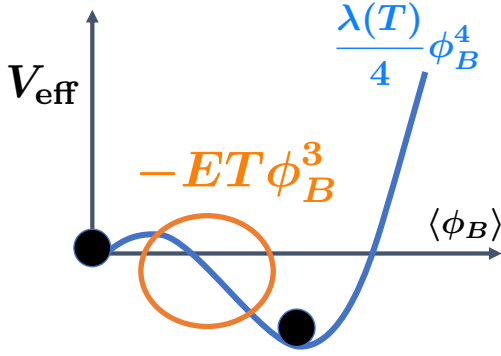
Bubble and fluid dynamics

Latent heat density: α

Duration of phase transition: β

etc..

Effective potential and GW



$$V_{\text{eff}} = \frac{M^2(T)}{2} \phi_B^2 - ET\phi_B^3 + \frac{\lambda + \kappa}{4} \phi_B^4$$

Potential barrier is generated by bosonic thermal loop.

$$E \simeq \frac{3}{32\pi} \hat{g}_2^3 + \frac{\sqrt{2}}{6\pi} \hat{y}_t^3 \quad \text{SU(2) gauge coupling: } \hat{g}_2 \simeq g_2$$

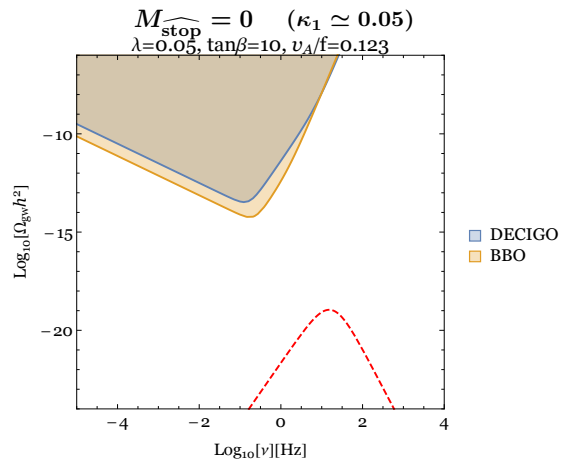
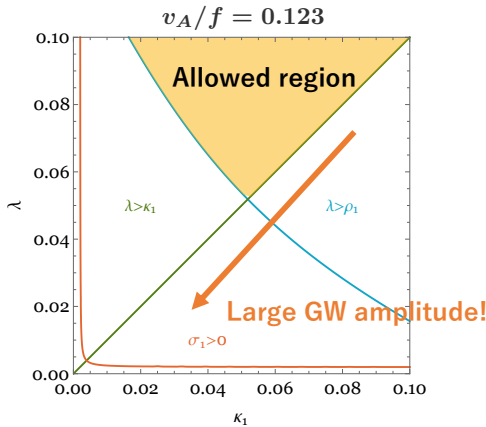
$$\text{top Yukawa coupling: } \hat{y}_t \simeq y_t$$

$$M^2(T) \simeq aT^2 - \lambda f^2 \quad (a : \text{const.})$$

We (numerically) calculate the bounce eq. and found the following statement.

small	$\lambda + \kappa$	Large latent heat density and long-duration	large	Ω_{GW}
large	$\lambda + \kappa$	Small latent heat density and short-duration	small	Ω_{GW}

GW amplitude



λ, κ bounded below to realize the SM-like Higgs mass.

$$\lambda \gtrsim 0.05 \quad \kappa \gtrsim 0.05$$

Maximal GW amplitude

T_n [GeV]	$\phi_B(T_n)/T_n$	α	$\beta/H(T_n)$
682	1	7×10^{-3}	7×10^4

GW amplitude cannot be detected by DECIGO and BBO...

Summary

GWs from first-order phase transitions are tested by future experiments such as DECIGO and BBO.

We calculate the GW amplitude from a first-order phase transition associated with twin EW symmetry breaking in twin Higgs models with the light twin stop effect.

Twin Higgs models cannot provide detectable GW amplitude by DECIGO and BBO with light twin stop in the linear realization and decoupling limit.

Yi-Peng Wu

RESCEU, the University of Tokyo

“Higgs as heavy-lifted physics during inflation”
(10+5 min.)

[JGRG28 (2018) 110816]



Higgs as heavy-lifted physics during inflation

Yi-Peng Wu

in progress

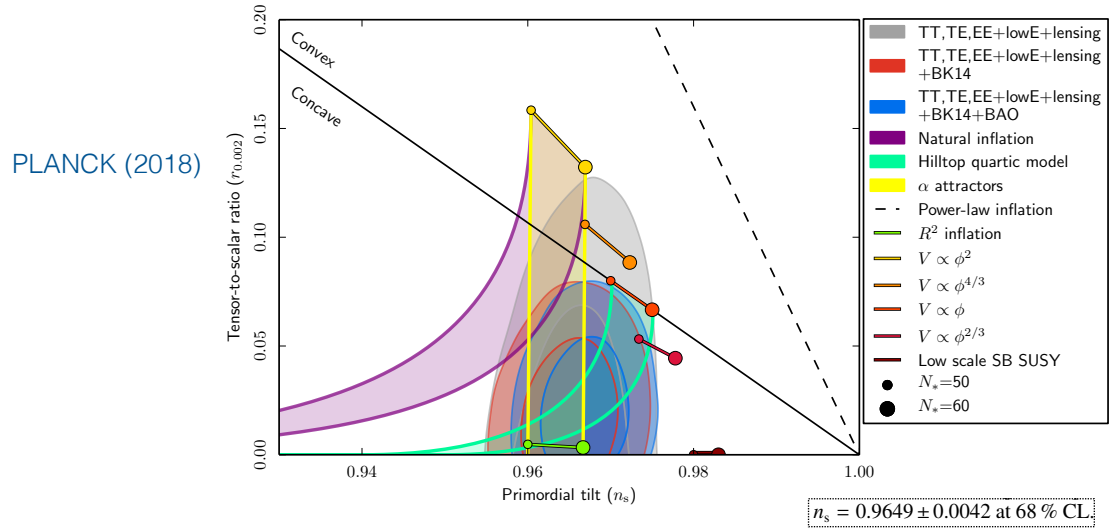
RESearch Center for the Early Universe (RESCEU)

The University of Tokyo

November 8th (2018)

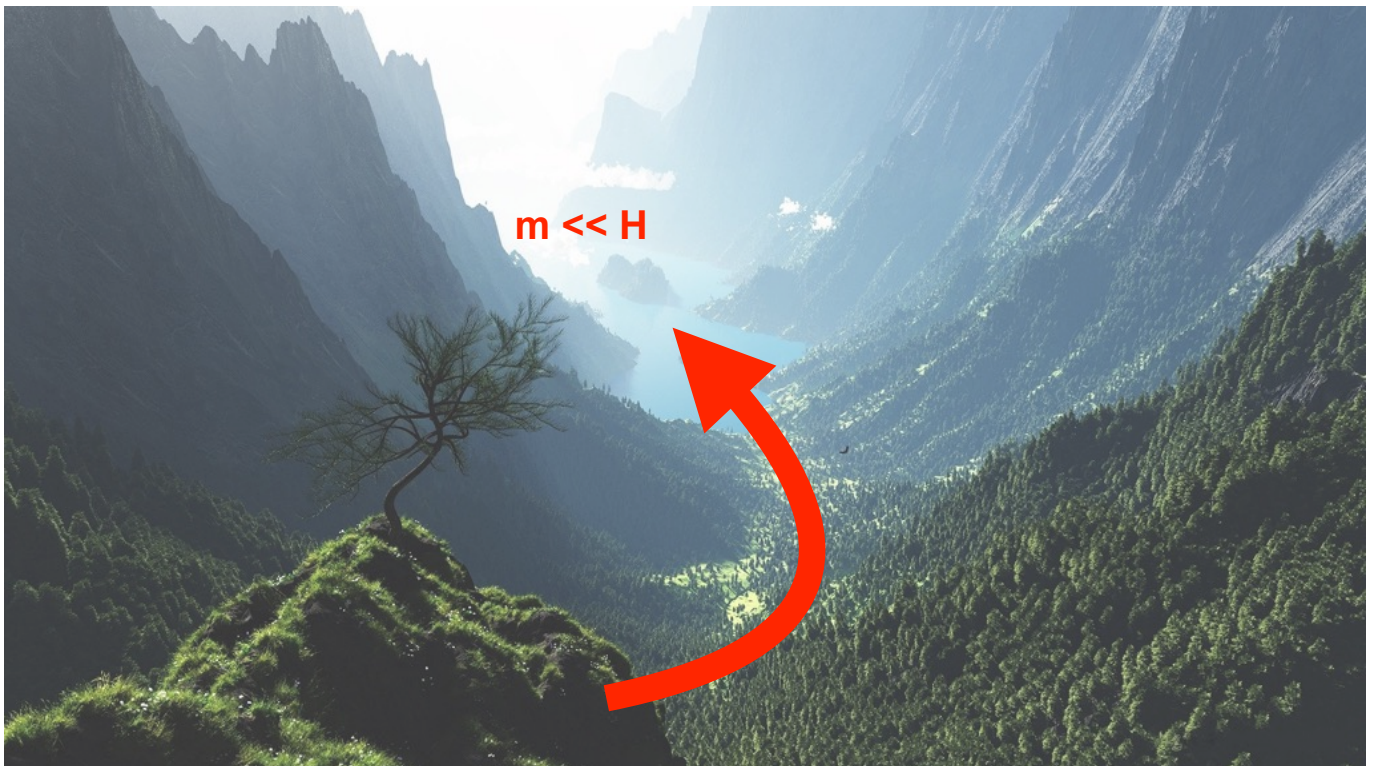
Heavy particles during inflation

Standard single-field inflation with Einstein gravity

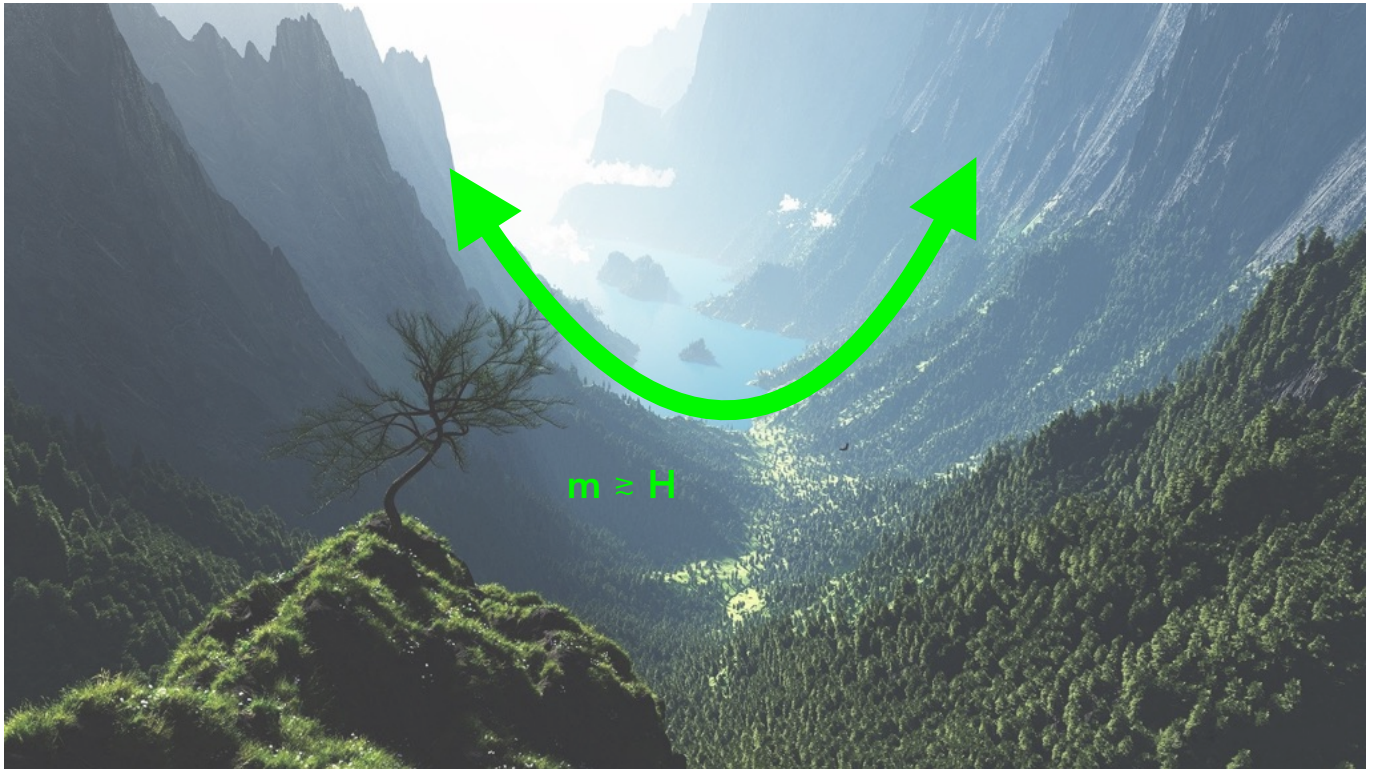


➤ No evidence beyond slow-roll (nor feature in the potential).

UV completion of single-field inflation



UV completion of single-field inflation



The origin of heavy particles

- © SUSY breaking / SUGRA ?

Baumann & Green [1109.0292]

Yamaguchi [1101.2488]



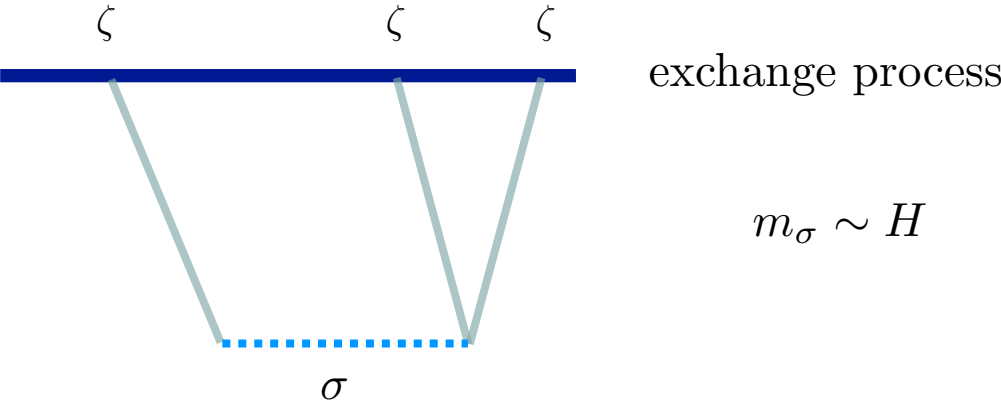
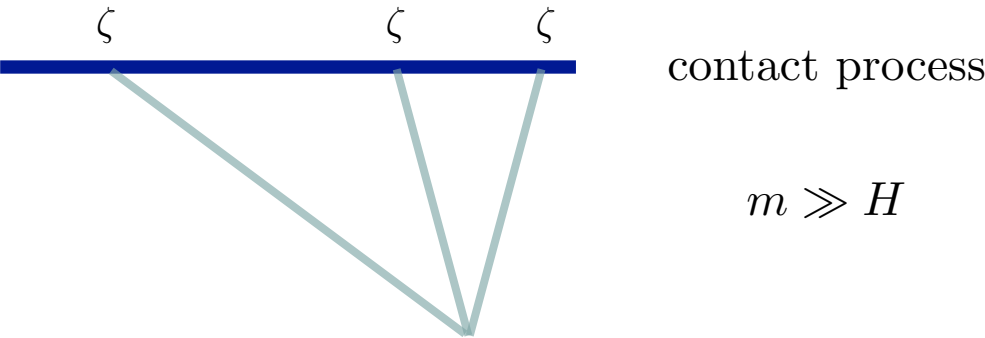
- © heavy-lifted SM particles ?

Chen, Wang & Xianyu [1610.06597]

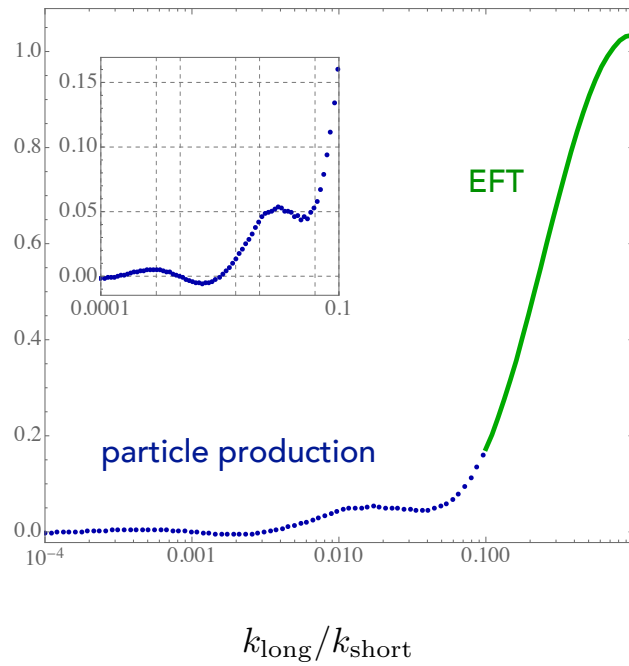
Kumar & Sundrum [1711.03988]



Heavy particle production



The simplest non-Gaussian observable $\langle \zeta^3 \rangle$



wave interference

The source

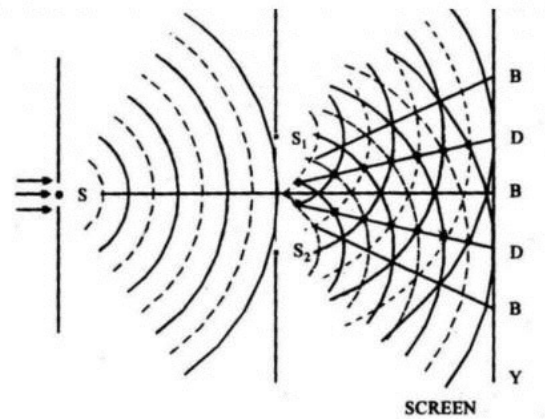
$$\Psi_1(\vec{r}, t) = A_1(\vec{r})e^{-i[\omega t - \alpha_1(\vec{r})]}$$

$$\Psi_2(\vec{r}, t) = A_2(\vec{r})e^{-i[\omega t - \alpha_2(\vec{r})]}$$

The intensity

$$I(\vec{r}) = \int dt \Psi \Psi^*$$

$$\sim A_1^2 + A_2^2 + 2A_1A_2 \cos[\alpha_1 - \alpha_2]$$



credit: physics@TutorVista.com

$$\Psi = \Psi_1 + \Psi_2$$

cosmological quantum interference

Two sources in de Sitter space

$$\zeta(k, \eta) \sim \hat{O}(\mathbf{k}) \eta^{3/2} \quad \text{analytic waves}$$

$$\sigma(k, \eta) \sim \hat{O}^+(\mathbf{k}) \eta^{\Delta^+} + \hat{O}^-(\mathbf{k}) \eta^{\Delta^-} \quad \text{analytic + non-analytic waves}$$

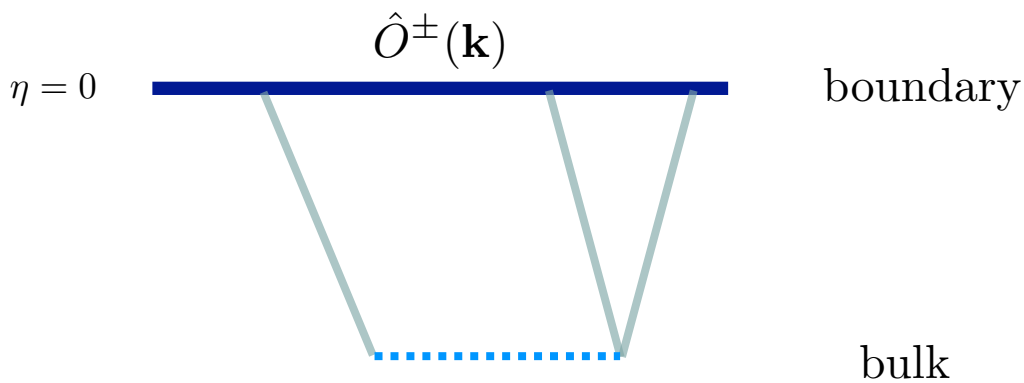
fixed by isometries of dS: $\Delta^\pm = \frac{3}{2} \pm i \sqrt{\frac{m_\sigma^2}{H^2} - \frac{9}{4}}$

non-analytic effects

The correlation function

$$\langle \hat{Q}[\zeta, \dot{\zeta}, \sigma, \dot{\sigma}] \rangle = (\text{non-oscillatory}) + (\text{oscillatory})$$

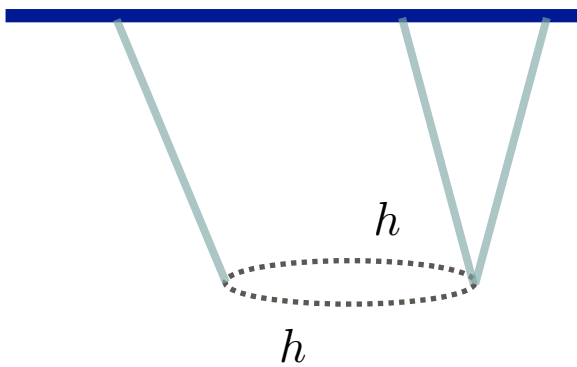
Arkani-Hamed et. al [arXiv:last week]



The bulk time evolution is encoded in boundary correlators.

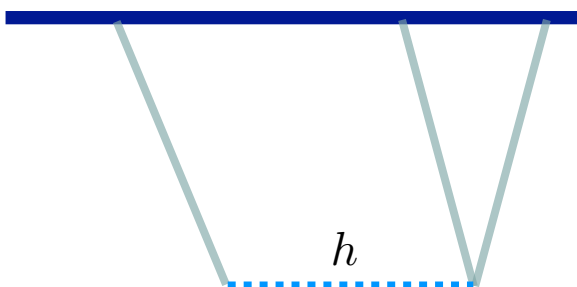
$$\frac{\langle \zeta^3 \rangle}{\langle \zeta^2 \rangle_S \langle \zeta^2 \rangle_L} \sim \sum_i w_i \left(\frac{k_L}{k_S} \right)^{\Delta_i}$$

Heavy-lifting mechanism



Chen, Wang & Xianyu [1610.06597]

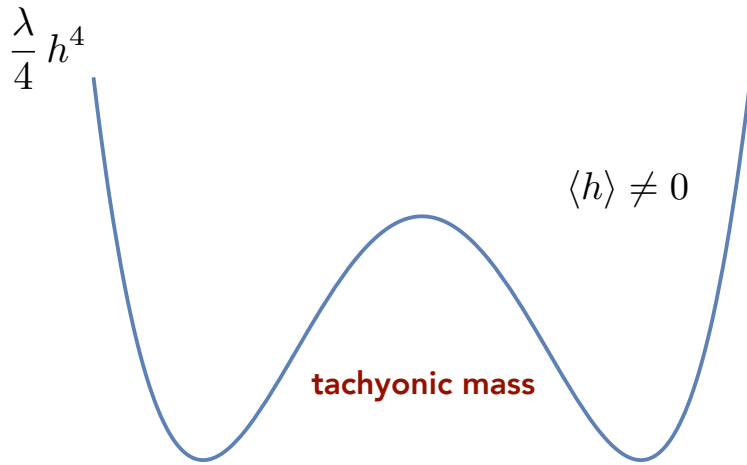
Chen, Wang & Xianyu [1612.08122]



Kumar & Sundrum [1711.03988]

\Rightarrow larger f_{NL}

Spontaneous symmetry breaking during inflation



Kumar & Sundrum [1711.03988]

see also Minxi He's talk

$$-\xi R h^2$$

$$-F(\phi, \partial_\mu \phi) h^2$$

Heavy-lifting from EFT

Kumar & Sundrum [1711.03988]

(weak-coupling)

$$\mathcal{L}_{\text{int}}^{\text{inf-gauge}} = \frac{c_1}{\Lambda} \partial_\mu \phi (\mathcal{H}^\dagger D^\mu \mathcal{H}) + \frac{c_2}{\Lambda^2} (\partial\phi)^2 \mathcal{H}^\dagger \mathcal{H} + \frac{c_3}{\Lambda^4} (\partial\phi)^2 |D\mathcal{H}|^2 + \frac{c_4}{\Lambda^4} (\partial\phi)^2 Z_{\mu\nu}^2 + \frac{c_5}{\Lambda^5} (\partial\phi)^2 \partial_\mu \phi (\mathcal{H}^\dagger D^\mu \mathcal{H}) + \dots$$

conclusion for non-Gaussianity

	Goldstone EFT with $\Lambda \sim 5H$	Goldstone EFT with $\Lambda \sim 10H$	Slow-roll Models with $\Lambda \sim 60H$
F			
h	1 – 10	0.1 – 1	0.01 – 0.1
Z	0.1 – 1	0.01 – 0.1	0.001 – 0.01

Heavy-lifting from broken symmetry

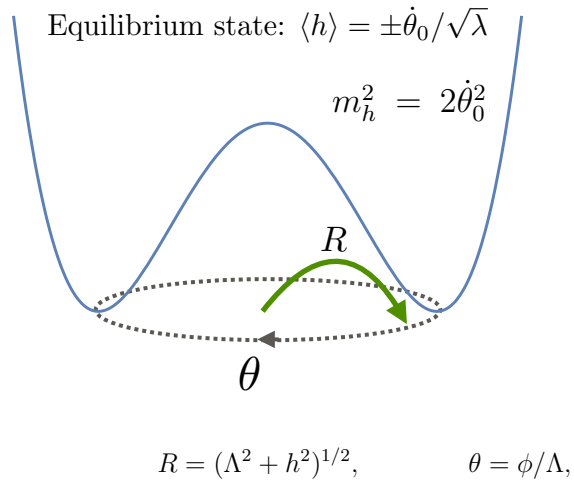
this work

(can be strongly coupled)

$$\Phi'_H = \Phi_H e^{i\phi/\Lambda}$$

$$\Phi_H = \frac{1}{\sqrt{2}} \begin{pmatrix} 0 \\ h \end{pmatrix}$$

$$|\partial_\mu \Phi'_H|^2 \rightarrow |\partial_\mu \Phi_H|^2 + \frac{\Phi_H^\dagger \Phi_H}{\Lambda^2} (\partial\phi)^2 + \dots$$



Heavy-lifting from broken symmetry

this work

(can be strongly coupled)

non-flat field space

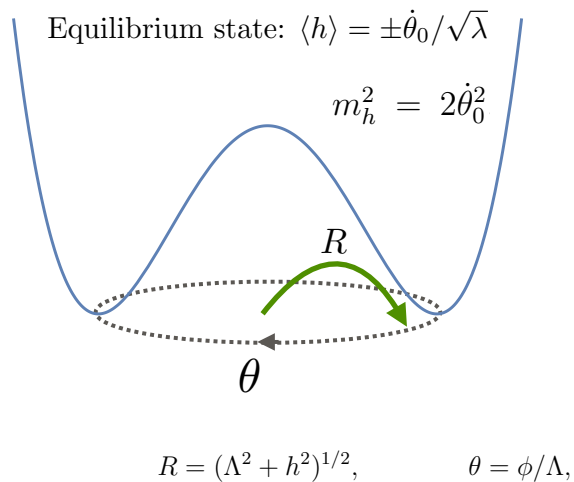
$$\mathcal{L} \supset -\frac{1}{2} \left(1 + \frac{h^2}{\Lambda^2} \right) (\partial_\mu \phi)^2 - \frac{1}{2} (\partial_\mu h)^2$$

weak – coupling : $h^2/\Lambda^2 \ll 1$

strong – coupling : $h^2/\Lambda^2 \gg 1$

quadratic coupling

$$\delta \mathcal{L}_2 = \mu \delta h (R \delta \dot{\theta})$$

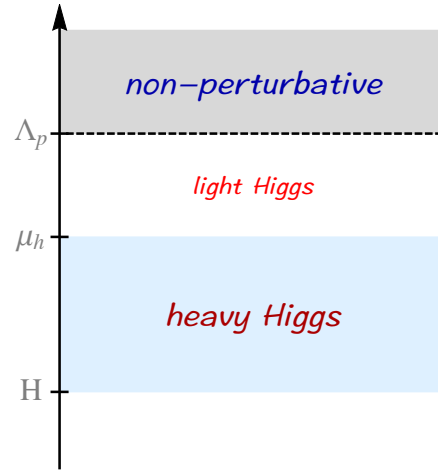


Energy scales in this talk:

scale of heavy Higgs

$$\mu_h \equiv (m_h^2 + \mu^2)^{1/2} = m_h/c_h$$

(energy)

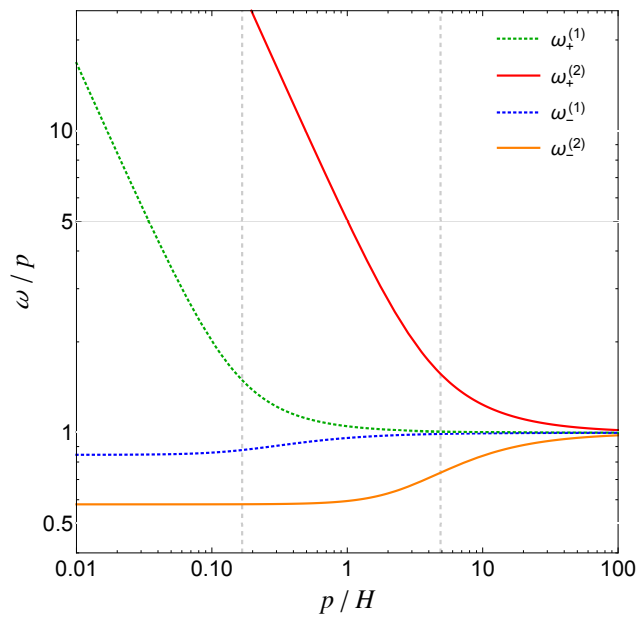


➤ strong-coupling does not necessarily violate perturbativity.

dispersion relations

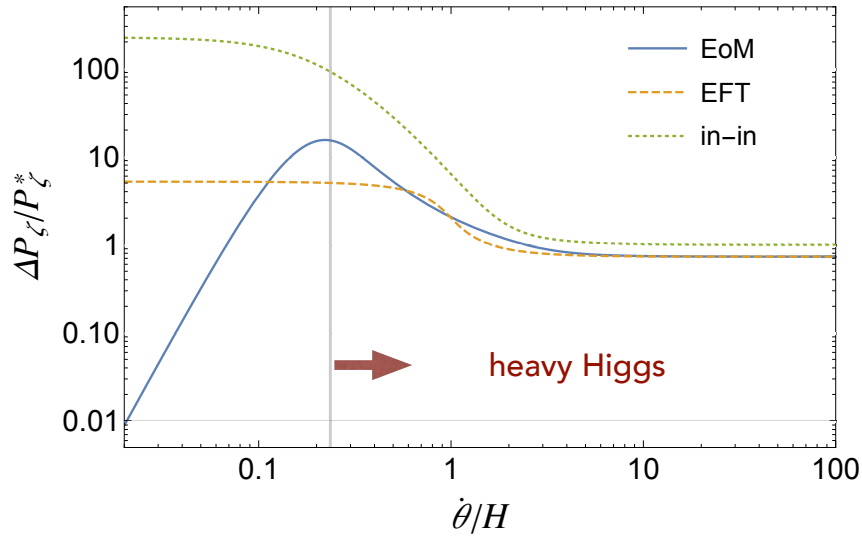
(1) $\mu_h < H$

(2) $\mu_h > H$



Power spectrum

ΔP_ζ : Higgs contribution to power spectrum



two-field inflation

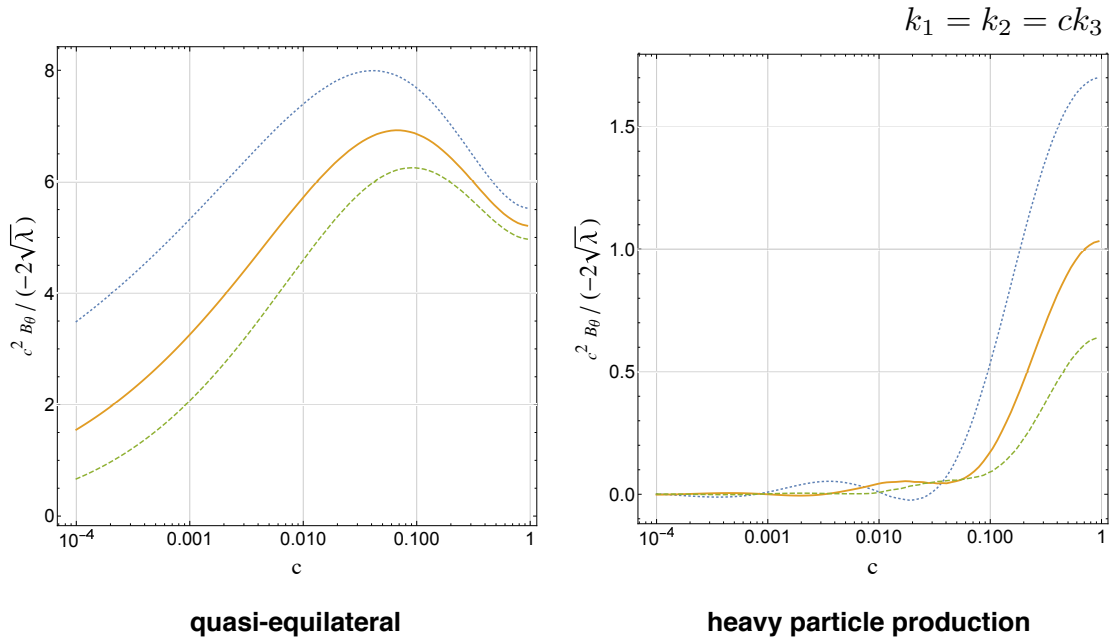
$$c_h^2 \rightarrow 1$$



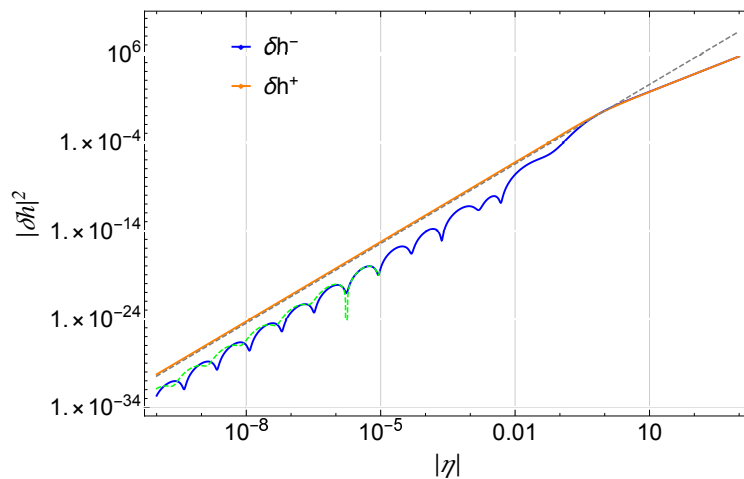
quasi-single field inflation

$$c_h^2 \rightarrow 1/3$$

Bispectrum (beyond single-field inflation)



Heavy Higgs production



$$\delta h \sim \sum_i \hat{O}_i \eta^{\Delta_i}$$

See also An et. al [1706.09971]
for three-point functions

the non-analytic scaling with strong-coupling:

$$L_h \rightarrow \sqrt{\frac{\mu_h^2}{H^2} - \frac{9}{4}} = \sqrt{\frac{m_h^2}{H^2 c_h^2} - \frac{9}{4}}$$

REMARKS

and outlook

$$L_h \rightarrow \sqrt{\frac{\mu_h^2}{H^2} - \frac{9}{4}} = \sqrt{\frac{m_h^2}{H^2 c_h^2} - \frac{9}{4}}$$

- SM particles can turn into heavy degrees of freedom during inflation, due to lifting mechanism (important background signals for the cosmological collider physics).
- Spontaneous symmetry breaking during inflation makes SM particle production more efficient (larger non-Gaussianity signals).
- In this work, we numerically confirm the non-analytic scaling of heavy particle production in the strong-coupling regime (enhanced oscillatory feature).
- Challenge: SM signals or new physics?

Minxi He

RESCEU, UTokyo

“Reheating in the Mixed Higgs- R^2 Model”
(10+5 min.)

[JGRG28 (2018) 110817]



Reheating in the Mixed Higgs- R^2 Model

SPEAKER: Minxi He

COLLABORATORS: Ryusuke Jinno, Kohei Kamada, Seong Chan Park,
Alexei A. Starobinsky, Jun'ichi Yokoyama

JGRG28@Rikkyo University

Contents

- Inflation in the Mixed Higgs- R^2 model
- Spikes in preheating
- Preheating in the Mixed Higgs- R^2 model
- Future Work and Outlook

JGRG28@Rikkyo University

Inflation in the Mixed Higgs- R^2 Model

$$S = \int d^4x \sqrt{-\hat{g}} \left[\frac{M_p^2}{2} \hat{R} + \frac{M_p^2}{12M^2} \hat{R}^2 + \frac{1}{2} \xi \chi^2 \hat{R} - \frac{1}{2} \hat{g}^{\mu\nu} \hat{\nabla}_\mu \chi \hat{\nabla}_\nu \chi - \frac{\lambda}{4} \chi^4 \right]$$

Starobinsky model

Higgs inflation

A. A. Starobinsky, Phys. Lett. B 91, 99 (1980)
 J.L. Cervantes-Cota and H. Dehnen, Nucl. Phys. B 442 (1995) 391
 F. L. Bezrukov, M. E. Shaposhnikov, Phys.Lett. B659:703-706,2008
 A.O. Barvinsky, A. Yu. Kamenshchik and A.A. Starobinsky, JCAP 11 (2008) 021
 Y. Ema, Phys. Lett. B770:403-411, 2017
 Y-C. Wang, T. Wang, Phys. Rev. D96(12):123506, 2017
MH, A. A. Starobinsky, J. Yokoyama, JCAP, 1805(05):064, 2018

JGRG28@Rikkyo University

Inflation in the Mixed Higgs- R^2 Model

$$S = \int d^4x \sqrt{-g} \left[\frac{M_p^2}{2} R - \frac{1}{2} g^{\mu\nu} \nabla_\mu \psi \nabla_\nu \psi - \frac{1}{2} e^{-\sqrt{\frac{2}{3}} \frac{\psi}{M_p}} g^{\mu\nu} \nabla_\mu \chi \nabla_\nu \chi - U(\psi, \chi) \right]$$

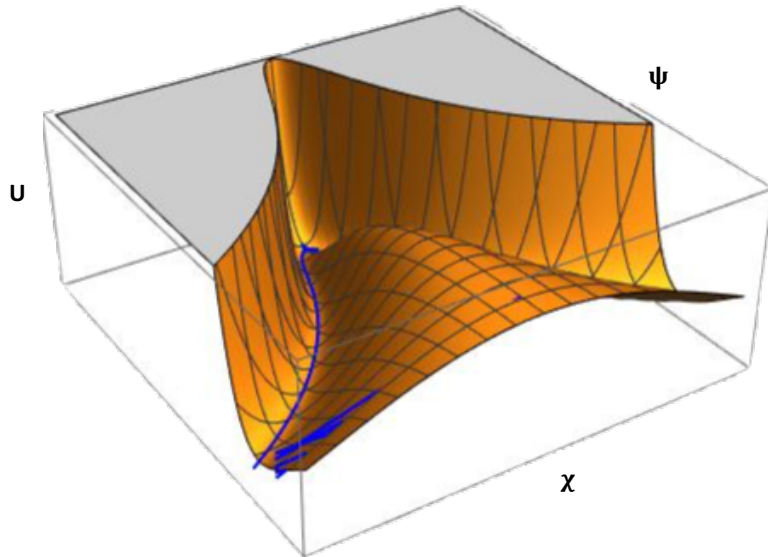
scalonon

Curved field space

$$U(\psi, \chi) \equiv \frac{\lambda}{4} \chi^4 e^{-2\sqrt{\frac{2}{3}} \frac{\psi}{M_p}} + \frac{3}{4} M_p^2 M^2 e^{-2\sqrt{\frac{2}{3}} \frac{\psi}{M_p}} \left(e^{\sqrt{\frac{2}{3}} \frac{\psi}{M_p}} - 1 - \frac{1}{M_p^2} \xi \chi^2 \right)^2$$

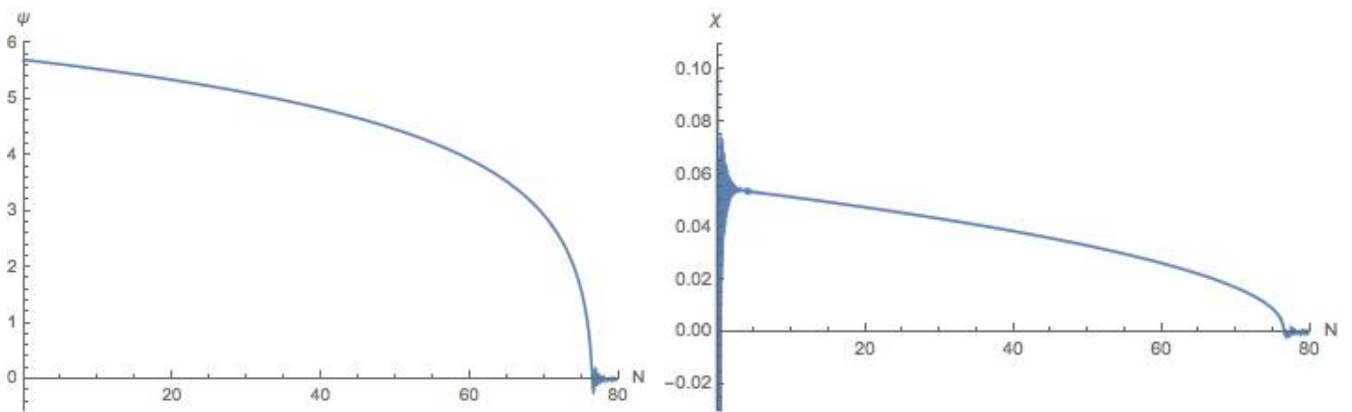
MH, A. A. Starobinsky, J. Yokoyama, JCAP, 1805(05):064, 2018

JGRG28@Rikkyo University



MH, A. A. Starobinsky, J. Yokoyama, JCAP, 1805(05):064, 2018

JGRG28@Rikkyo University



JGRG28@Rikkyo University

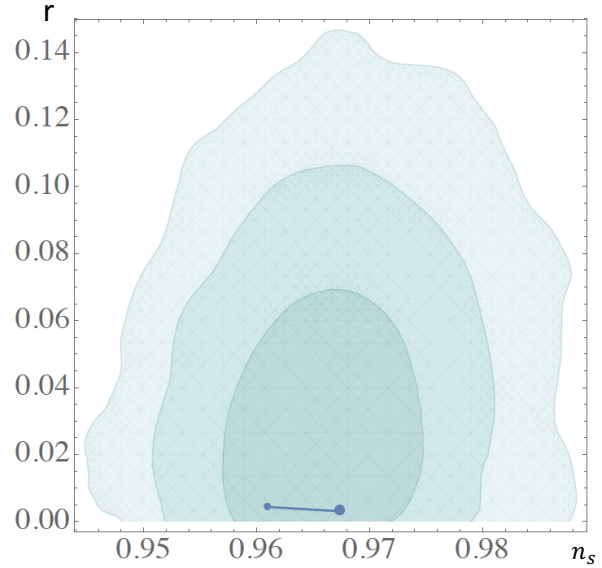
Low energy effective single field theory

A. Achucarro et al, JCAP 1101:030,2011
 A. Achucarro et al, Phys. Rev. D 86, 121301(R) (2012)

$$S_{\text{eff}} = \frac{1}{2} \int a^3 \frac{\dot{\phi}_0^2}{H^2} \left[\frac{\mathcal{R}^2}{c_s^2(k)} - \frac{k^2 \mathcal{R}^2}{a^2} \right]$$

$$c_s^{-2} = 1 + \frac{4\dot{\theta}^2}{\frac{k^2}{a^2} + U_{NN} + \epsilon H^2 R - \dot{\theta}^2}$$

Fix $\lambda = 0.01$, $c_s \approx 1$;
 Amplitude of curvature
 perturbations $\sim 2 \times 10^{-9}$.



MH, A. A. Starobinsky, J. Yokoyama, JCAP, 1805(05):064, 2018

JGRG28@Rikkyo University

Effective Starobinsky model

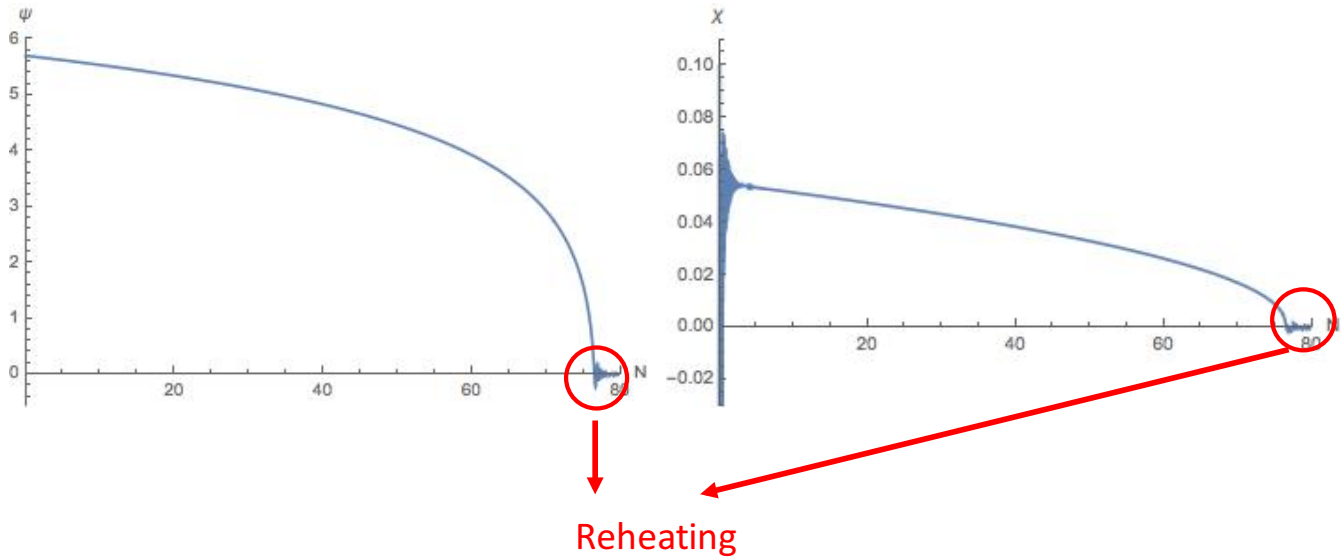
$$S_J = \int d^4x \sqrt{-\hat{g}} \left[\frac{M_p^2}{2} \hat{R} + \frac{M_p^2}{12M_{\text{eff}}^2} \hat{R}^2 \right]$$

$$M_{\text{eff}}^2 \equiv \frac{M^2}{1 + \frac{3\xi^2 M^2}{\lambda M_p^2}}$$

Higgs inflation: $\xi \rightarrow \xi_c \sim 4441$

MH, A. A. Starobinsky, J. Yokoyama, JCAP, 1805(05):064, 2018

JGRG28@Rikkyo University



JGRG28@Rikkyo University

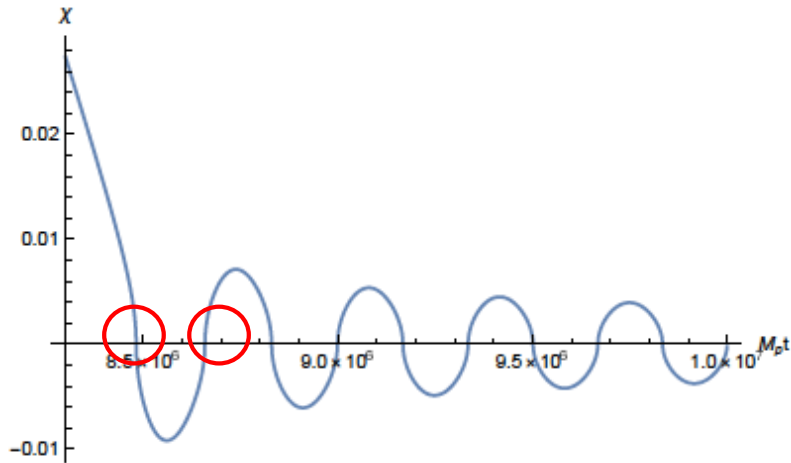
Spikes in Preheating

$$S_{\text{single-J}} = \int d^4x \sqrt{-g_J} \left[\frac{M_P^2}{2} R_J + \frac{1}{2} \xi \chi^2 R_J - \frac{1}{2} (\nabla \chi)_J^2 - \frac{\lambda}{4} \chi^4 \right]$$

$$\ddot{\chi} + 3H_J \dot{\chi} + \lambda \chi^3 - \xi \left(6\dot{H}_J + 12H_J^2 \right) \chi = 0$$

Effective mass of the Higgs field

Spikes in Preheating



Y. Ema et al, JCAP 1702(02):045, 2017

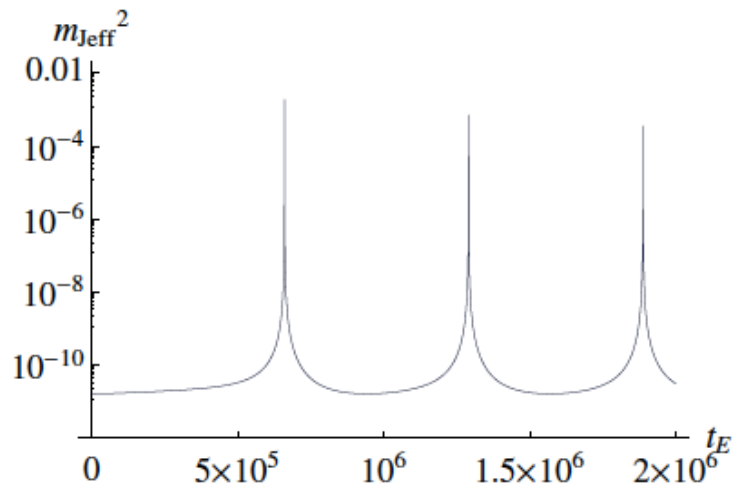
JGRG28@Rikkyo University

Spikes in Preheating

$$m \propto \sqrt{\lambda}$$

$$\Delta t \propto \sqrt{\lambda}^{-1}$$

ξ -independent



Y. Ema et al, JCAP 1702(02):045, 2017

JGRG28@Rikkyo University

Spikes in Preheating

$$S = \int d^4x \sqrt{-g_J} \left[\left(\frac{M_{\text{P}}^2}{2} + \xi |\phi_J|^2 \right) R_J - \frac{1}{4} F_{\mu\nu} F^{\mu\nu} - (D_\mu \phi_J)^\dagger (D^\mu \phi_J) - V_J(|\phi_J|^2) \right]$$

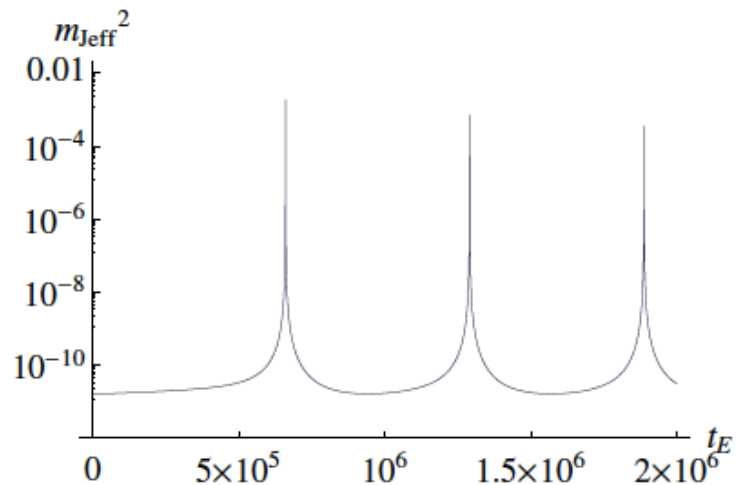
$$m_{A_L}^2 \sim \frac{k^2}{k^2 + m_A^2} \frac{m_{\text{Jeff}}^2}{\Omega^2}$$

Y. Ema et al, JCAP 1702(02):045, 2017

JGRG28@Rikkyo University

Spikes in Preheating

Unphysical? $\Lambda \sim M_p / \xi$
Small number density?



Y. Ema et al, JCAP 1702(02):045, 2017

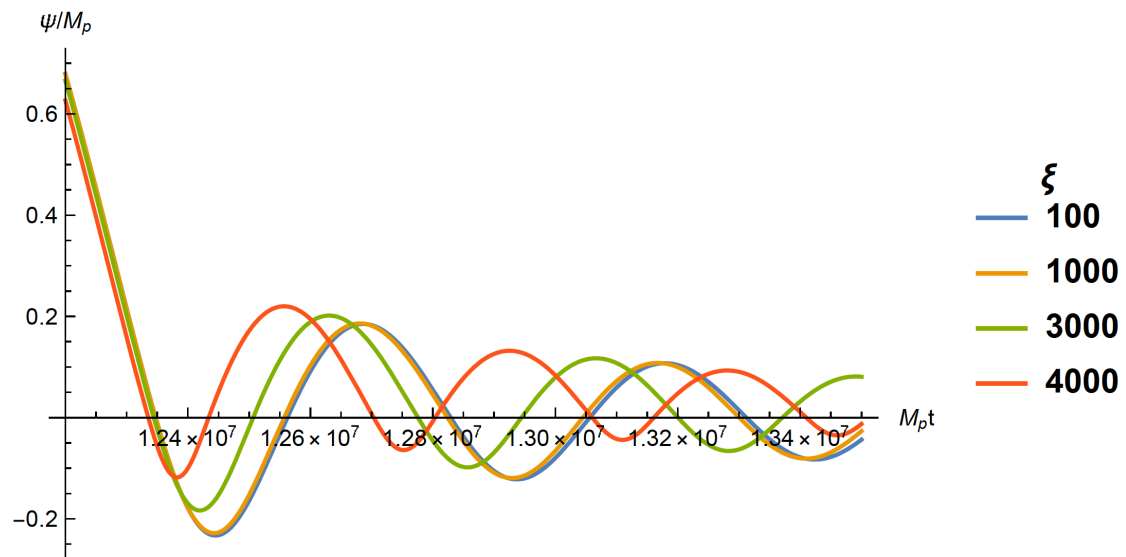
JGRG28@Rikkyo University

Preheating in the Mixed Higgs- R^2 Model

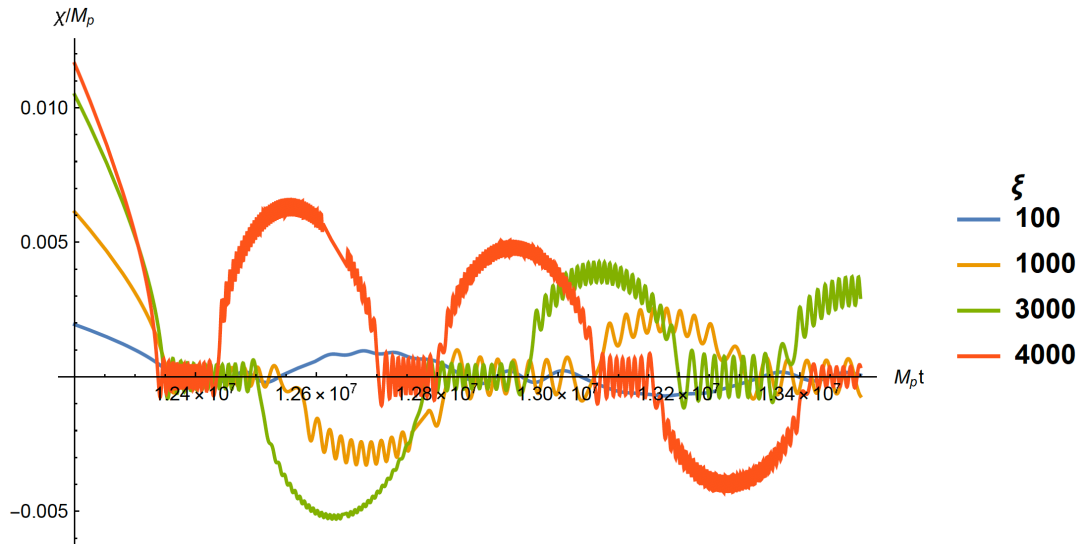
Cutoff scale $\Lambda \rightarrow M_p$

D. Gorbunov and A. Tokareva, arXiv:1807.02392 [hep-ph]

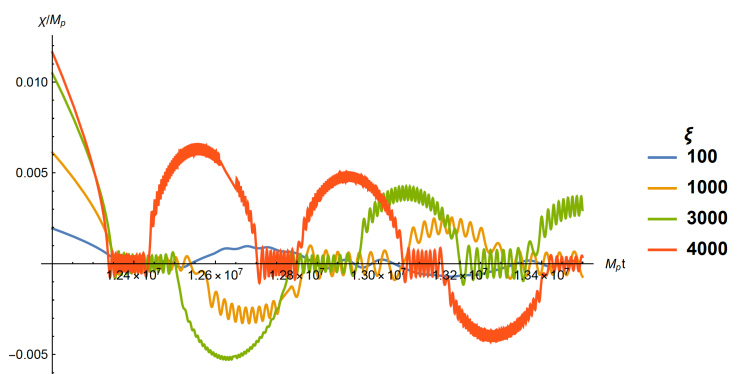
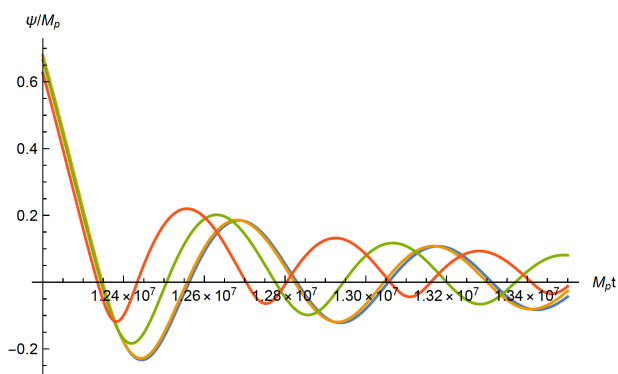
JGRG28@Rikkyo University



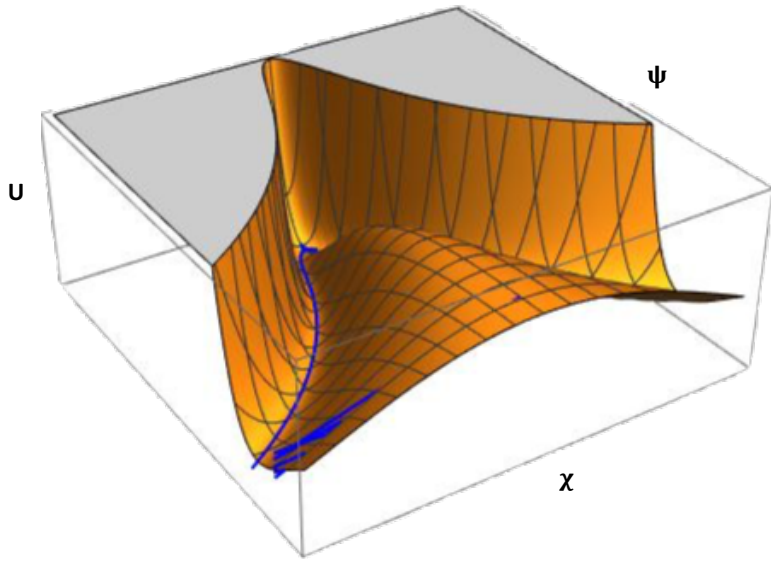
JGRG28@Rikkyo University



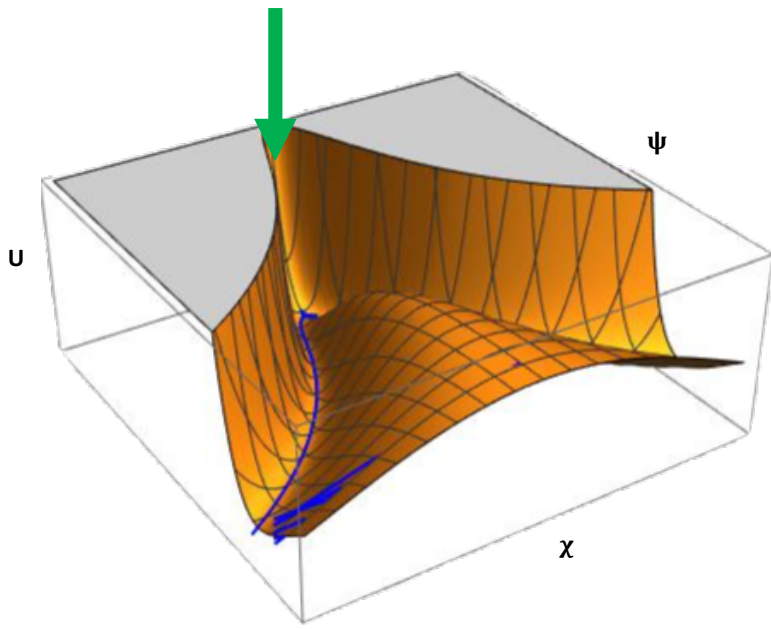
JGRG28@Rikkyo University



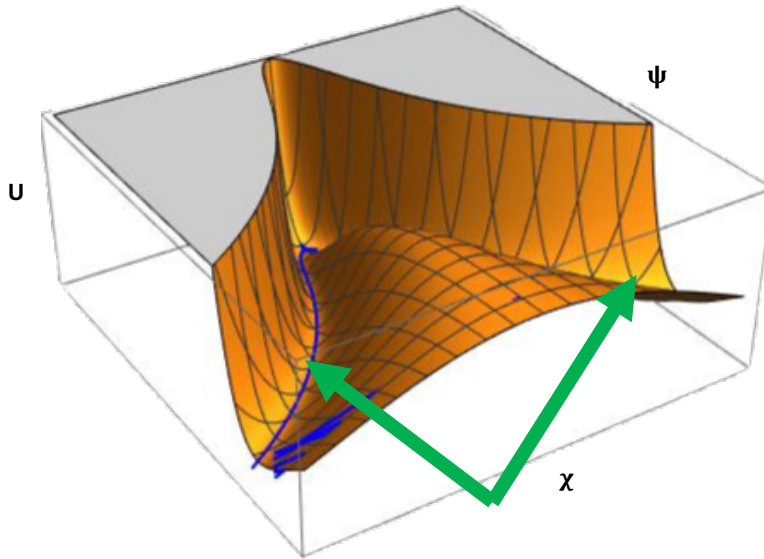
JGRG28@Rikkyo University



JGRG28@Rikkyo University

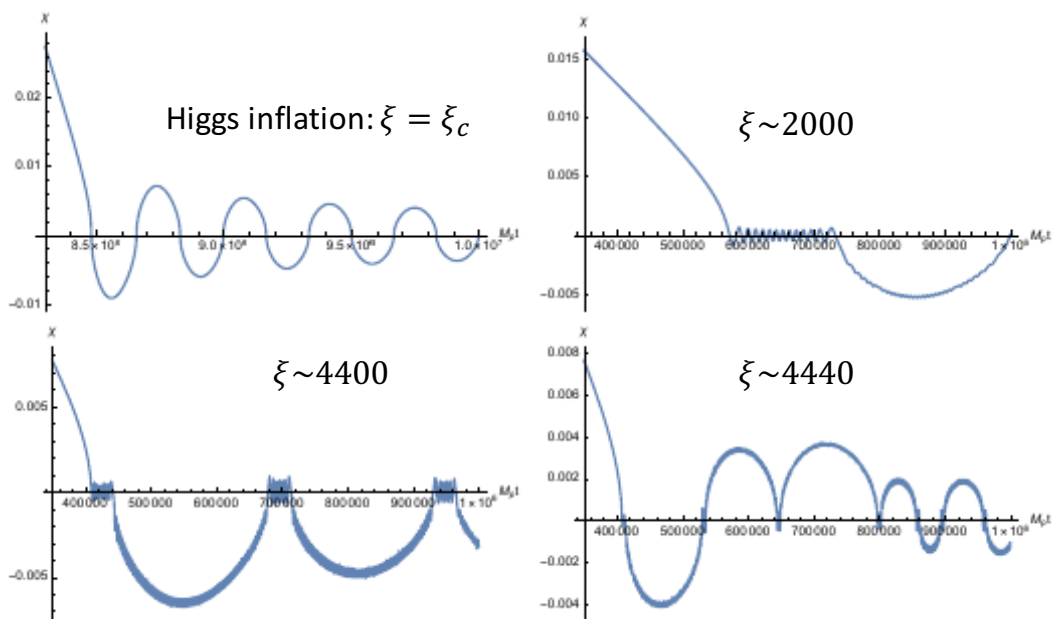


JGRG28@Rikkyo University

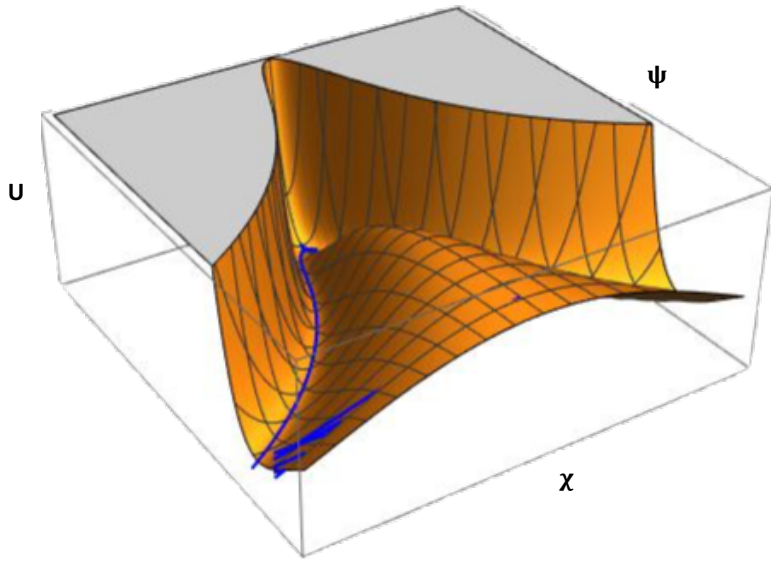


JGRG28@Rikkyo University

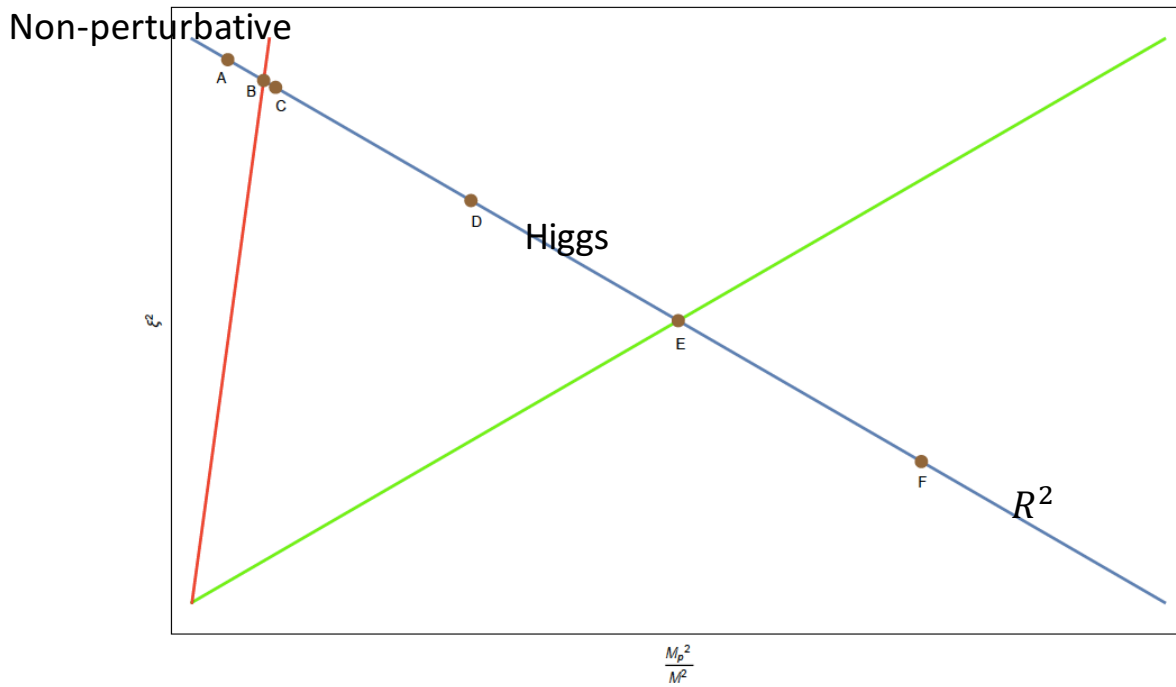
The behavior of the Higgs field



JGRG28@Rikkyo University

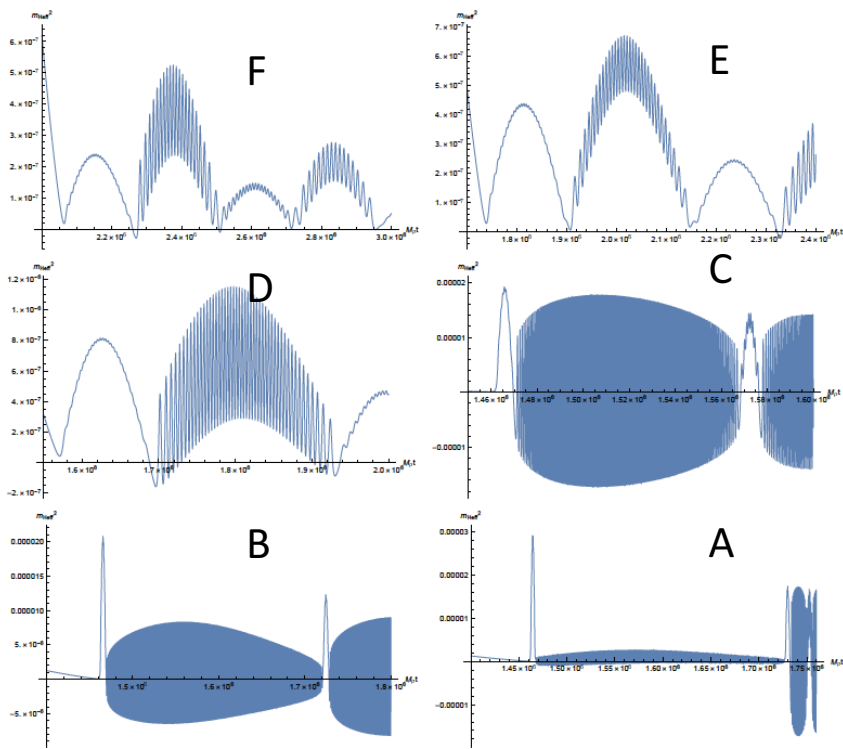


JGRG28@Rikkyo University



Y. Ema et al, JCAP 1702(02):045, 2017

JGRG28@Rikkyo University



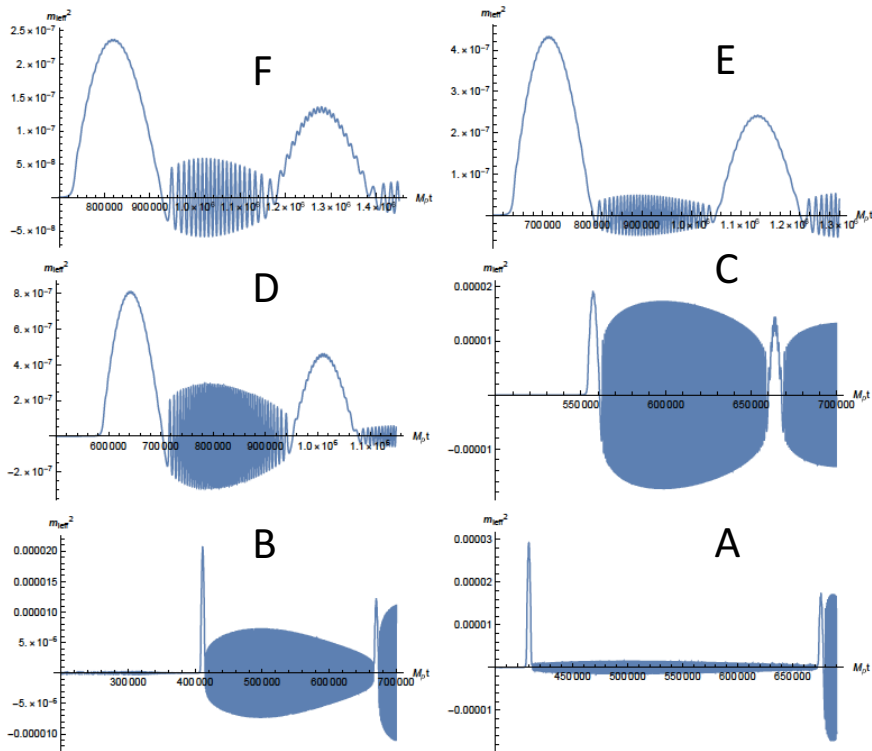
The effective mass squared of the Higgs field in Jordan frame

JGRG28@Rikkyo University

$$\chi = h e^{i\theta}$$

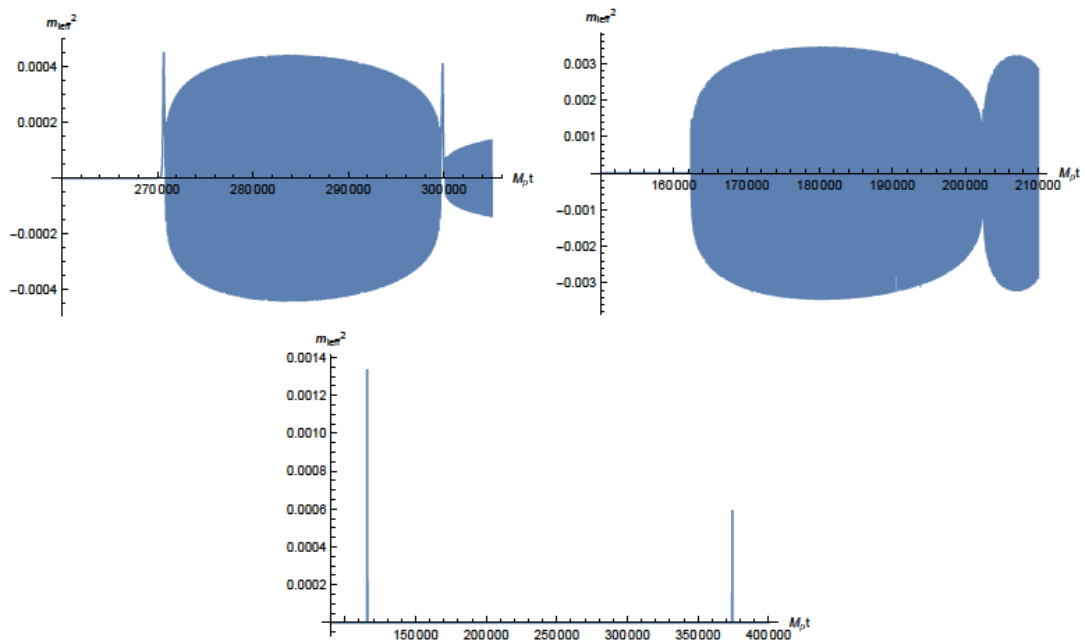
$$\theta_c \equiv a^{3/2} e^{-\sqrt{\frac{1}{6}} \frac{\psi}{M_P}} h \theta$$

JGRG28@Rikkyo University



The effective mass squared of the imaginary part of the Higgs field in Jordan frame

JGRG28@Rikkyo University



JGRG28@Rikkyo University

Future Work and Outlook

- The distribution of the height of the spikes in the parameter space
- Calculate the height of the spikes analytically to find out the nature of them
- Number density of the produced gauge bosons
- The reheating process after preheating

JGRG28@Rikkyo University



Reheating in the Mixed Higgs- R^2 Model



Thank you!

SPEAKER: Minxi He

COLLABORATORS: Ryusuke Jinno, Kohei Kamada, Seong Chan Park,
Alexei A. Starobinsky, Jun'ichi Yokoyama

JGRG28@Rikkyo University

Keisuke Inomata

ICRR, The University of Tokyo

**“Power spectra of CMB circular polarizations induced by
primordial perturbations”**
(10+5 min.)

[JGRG28 (2018) 110818]

Power spectra of CMB circular polarizations induced by primordial perturbations

Institute for Cosmic Ray Research (ICRR),
The University of Tokyo

Keisuke Inomata

Collaborator: Marc Kamionkowski (Johns Hopkins University)
(cf. arXiv:1804.06412)

2/20

What we focus on

The state of CMB radiation can be described with Stokes parameters.

$$\langle E_i^* E_j \rangle = \frac{1}{2} \begin{pmatrix} \mathcal{I} + \mathcal{Q} & \mathcal{U} - i\mathcal{V} \\ \mathcal{U} + i\mathcal{V} & \mathcal{I} - \mathcal{Q} \end{pmatrix}$$

\mathcal{I} : related to temperature perturbations of CMB

\mathcal{Q}, \mathcal{U} : related to E-mode, B-mode polarizations of CMB

\mathcal{V} : describes circular polarizations of CMB

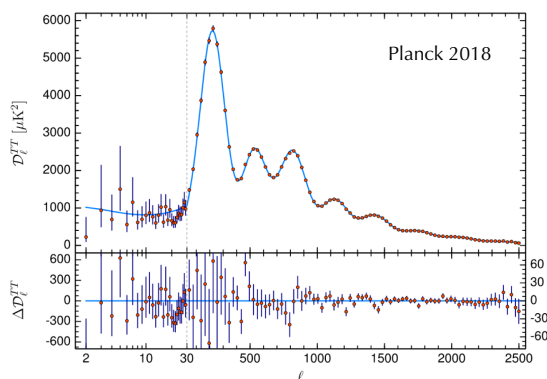
← We focus on this!

Outline

- Introduction
- Calculation of Φ_{ab}
- Power spectra of circular polarization
- Summary

CMB and Cosmology

CMB anisotropies have determined and constrained the cosmological parameters.



However

The Planck mission has already reached cosmic variance in temperature perturbations.

Therefore

It is important to discuss other quantities.

distortion, CMB Polarization

Polarizations and Stokes parameters

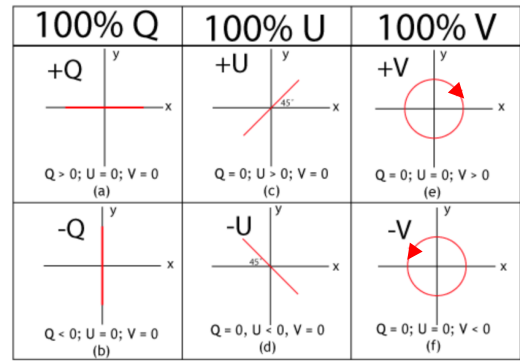
The state of radiations can be described with Stokes parameters.

$$\langle E_i^* E_j \rangle = \frac{1}{2} \begin{pmatrix} \mathcal{I} + \mathcal{Q} & \mathcal{U} - i\mathcal{V} \\ \mathcal{U} + i\mathcal{V} & \mathcal{I} - \mathcal{Q} \end{pmatrix}$$

Time ave. ↗

Concrete example (plane wave)

$$\begin{aligned} E_x &= E_x^0 e^{i(\omega t - \epsilon_1)} \\ E_y &= E_y^0 e^{i(\omega t - \epsilon_2)} \end{aligned} \quad \rightarrow \quad \begin{aligned} \mathcal{I} &= (E_x^0)^2 + (E_y^0)^2 \\ \mathcal{Q} &= (E_x^0)^2 - (E_y^0)^2 \\ \mathcal{U} &= 2E_x^0 E_y^0 \cos[\epsilon_1 - \epsilon_2] \\ \mathcal{V} &= 2E_x^0 E_y^0 \sin[\epsilon_1 - \epsilon_2] \end{aligned}$$



Wikipedia

Polarizations in CMB

$$\langle E_i^* E_j \rangle = \frac{1}{2} \begin{pmatrix} \mathcal{I} + \mathcal{Q} & \mathcal{U} - i\mathcal{V} \\ \mathcal{U} + i\mathcal{V} & \mathcal{I} - \mathcal{Q} \end{pmatrix} \quad \begin{array}{l} \mathcal{I} : \text{related to temperature perturbations} \\ \mathcal{Q}, \mathcal{U} : \text{related to E-mode, B-mode polarizations} \\ \mathcal{V} : \text{describes circular polarizations} \end{array}$$

Thomson scattering can produce only linear polarizations.
There is no circular polarization at the last scattering surface (LSS).

However,

circular polarizations can be produced from the linear polarizations through the Faraday conversion.



Faraday conversion 1

Faraday conversion occurs due to the anisotropic refraction (birefringence).

General refraction tensor:

$$n_{ij} = \begin{pmatrix} n_I + n_Q & n_U + in_V \\ n_U - in_V & n_I - n_Q \end{pmatrix}$$

Difference of refraction indexes
= Difference of phase velocities

Example

$$\delta\mathcal{V} = \mathcal{U} \frac{2\omega}{c} n_Q \delta r \quad Q = 0, \mathcal{U} \neq 0$$



100% Q	100% U	100% V
<p>+Q</p> <p>$n_I + n_Q$</p> <p>Q > 0; U = 0; V = 0 (a)</p>	<p>+U</p> <p>$n_I + n_U$</p> <p>Q = 0; U > 0; V = 0 (c)</p>	<p>+V</p> <p>$n_I + n_V$</p> <p>Q = 0; U = 0; V > 0 (e)</p>
<p>-Q</p> <p>$n_I - n_Q$</p> <p>Q < 0; U = 0; V = 0 (b)</p>	<p>-U</p> <p>$n_I - n_U$</p> <p>Q = 0; U < 0; V = 0 (d)</p>	<p>-V</p> <p>$n_I - n_V$</p> <p>Q = 0; U = 0; V < 0 (f)</p>

Wikipedia

Faraday conversion 2

Generally speaking, the induced circular polarization can be described as



$$V(\hat{n}) = \phi_Q(\hat{n})U(\hat{n}) - \phi_U(\hat{n})Q(\hat{n})$$

$$\phi_{Q,U}(\hat{n}) = \frac{2}{c} \int_0^{X_{LSS}} \frac{d\chi}{1+z} \omega(\chi) n_{Q,U}(\hat{n}\chi)$$

$$Q \equiv \frac{Q}{\bar{I}}, U \equiv \frac{U}{\bar{I}}, V \equiv \frac{V}{\bar{I}},$$

\bar{I} : Averaged intensity
 \hat{n} : The direction from which photons come

For later convenience, we define P_{ab} and Φ_{ab} as

$$P_{ab}(\hat{n}) = \frac{1}{\sqrt{2}} \begin{pmatrix} Q(\hat{n}) & U(\hat{n}) \\ U(\hat{n}) & -Q(\hat{n}) \end{pmatrix},$$

$$\Phi_{ab}(\hat{n}) = \frac{1}{\sqrt{2}} \begin{pmatrix} \phi_Q(\hat{n}) & \phi_U(\hat{n}) \\ \phi_U(\hat{n}) & -\phi_Q(\hat{n}) \end{pmatrix}.$$



Then we can rewrite V as $V(\hat{n}) = \epsilon_{ac} P^{ab}(\hat{n}) \Phi_b^c(\hat{n})$.

Outline

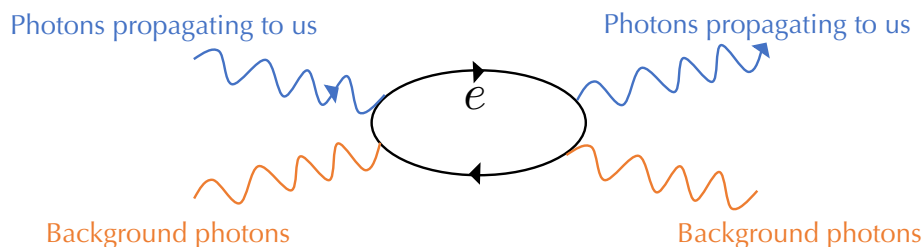
- Introduction
- Calculation of Φ_{ab}
- Power spectra of circular polarization
- Summary

Source of anisotropic refraction

We focus on the source coming from primordial scalar, vector, tensor perturbations.

The dominant source comes from photon-photon scattering.

(Montero-Camacho, Hirata, 2018)



The perturbations of background radiation leads to the anisotropic refraction.

Induced by primordial perturbations

Anisotropic refraction index

The refraction index: (Montero-Camacho, Hirata, 2018)

$$n_Q(\mathbf{x}) \equiv \frac{1}{2}(n_{xx} - n_{yy})(\mathbf{x}) \simeq 48\sqrt{\frac{\pi}{5}} A_e \mu_0 a_{\text{rad}} T_{\text{CMB}}^4 \text{Re } a_{2,-2}^E(\mathbf{x})$$

$$n_U(\mathbf{x}) \equiv n_{xy}(\mathbf{x}) \simeq 48\sqrt{\frac{\pi}{5}} A_e \mu_0 a_{\text{rad}} T_{\text{CMB}}^4 \text{Im } a_{2,-2}^E(\mathbf{x})$$

Induced by primordial perturbations

$$Q(\hat{\mathbf{p}}, \mathbf{x}) = \frac{1}{2} \sum_{l,m} (a_{2,lm}(\mathbf{x}) {}_2Y_{lm}(\hat{\mathbf{p}}) + a_{-2,lm}(\mathbf{x}) {}_{-2}Y_{lm}(\hat{\mathbf{p}})), \quad A_e = \frac{2}{45\mu_0} \frac{\alpha^2 \lambda_e^3}{m_e c^2}$$

$$U(\hat{\mathbf{p}}, \mathbf{x}) = \frac{1}{2i} \sum_{l,m} (a_{2,lm}(\mathbf{x}) {}_2Y_{lm}(\hat{\mathbf{p}}) - a_{-2,lm}(\mathbf{x}) {}_{-2}Y_{lm}(\hat{\mathbf{p}})),$$

$$a_{lm}^E(\mathbf{x}) = -\frac{1}{2}(a_{2,lm}(\mathbf{x}) + a_{-2,lm}(\mathbf{x})) \quad \hat{\mathbf{p}} : \text{Photon momentum direction}$$

What we derive in this work

To get V, we need to calculate

$$P_{ab}(\hat{\mathbf{n}}) = \frac{1}{\sqrt{2}} \begin{pmatrix} Q(\hat{\mathbf{n}}) & U(\hat{\mathbf{n}}) \\ U(\hat{\mathbf{n}}) & -Q(\hat{\mathbf{n}}) \end{pmatrix},$$

$$\Phi_{ab}(\hat{\mathbf{n}}) = \frac{1}{\sqrt{2}} \begin{pmatrix} \phi_Q(\hat{\mathbf{n}}) & \phi_U(\hat{\mathbf{n}}) \\ \phi_U(\hat{\mathbf{n}}) & -\phi_Q(\hat{\mathbf{n}}) \end{pmatrix}.$$

$$\phi_{Q,U}(\hat{\mathbf{n}}) = \frac{2}{c} \int_0^{\chi_{\text{LSS}}} \frac{d\chi}{1+z} \omega(\chi) n_{Q,U}(\hat{\mathbf{n}}\chi)$$

$$n_Q(\mathbf{x}) \equiv \frac{1}{2}(n_{xx} - n_{yy})(\mathbf{x}) \simeq 48\sqrt{\frac{\pi}{5}} A_e \mu_0 a_{\text{rad}} T_{\text{CMB}}^4 \text{Re } a_{2,-2}^E(\mathbf{x})$$

$$n_U(\mathbf{x}) \equiv n_{xy}(\mathbf{x}) \simeq 48\sqrt{\frac{\pi}{5}} A_e \mu_0 a_{\text{rad}} T_{\text{CMB}}^4 \text{Im } a_{2,-2}^E(\mathbf{x})$$

Concretely speaking, we calculate $P_{lm}^{E/B}$ and $\Phi_{lm}^{E/B}$, which are defined as

$$P_{ab}(\hat{\mathbf{n}}) = \sum_{lm} (P_{lm}^E Y_{(lm)ab}^{TE}(\hat{\mathbf{n}}) + P_{lm}^B Y_{(lm)ab}^{TB}(\hat{\mathbf{n}})),$$

$$\Phi_{ab}(\hat{\mathbf{n}}) = \sum_{lm} (\Phi_{lm}^E Y_{(lm)ab}^{TE}(\hat{\mathbf{n}}) + \Phi_{lm}^B Y_{(lm)ab}^{TB}(\hat{\mathbf{n}})).$$

$$Y_{lm}^{TE} \equiv \frac{\sqrt{2}}{4} \begin{pmatrix} +2Y_{lm} +2Y_{lm} & -i(+2Y_{lm} -2Y_{lm}) \\ -i(+2Y_{lm} -2Y_{lm}) & -(+2Y_{lm} +2Y_{lm}) \end{pmatrix}$$

$$Y_{lm}^{TB} \equiv \frac{\sqrt{2}}{4} \begin{pmatrix} i(+2Y_{lm} -2Y_{lm}) & +2Y_{lm} +2Y_{lm} \\ +2Y_{lm} +2Y_{lm} & -i(+2Y_{lm} -2Y_{lm}) \end{pmatrix}$$

$$C_l^{P^E P^E / P^B P^B} \text{ corresponds to } C_l^{EE/BB}. \quad (C_l^{AB} = \langle A_{lm} B_{lm} \rangle)$$

➔ We derive the formulae for $\Phi_{lm}^{E/B}$.

Derived formulae

After tedious calculation, we finally derive

$$\begin{aligned}\Phi_{lm}^{E,L} &= 4\pi A \int \frac{k^2 dk}{(2\pi)^3} \int_{\eta_{LSS}}^{\eta_0} d\eta (1+z)^4 (\bar{a}_{2,0}^E(k, \eta)) h_{lm}^{k,(L)} \epsilon_l^{(0)}(k(\eta - \eta_0)), \\ \Phi_{lm}^{E/B,VE/VB} &= 4\pi A \int \frac{k^2 dk}{(2\pi)^3} \int_{\eta_{LSS}}^{\eta_0} d\eta (1+z)^4 \sqrt{2} (\bar{a}_{2,1}^E(k, \eta)) h_{lm}^{k,(VE/VB)} \phi_l^{(1)}(k(\eta - \eta_0)), \\ \Phi_{lm}^{E/B,TE/TB} &= 4\pi A \int \frac{k^2 dk}{(2\pi)^3} \int_{\eta_{LSS}}^{\eta_0} d\eta (1+z)^4 \sqrt{2} (\bar{a}_{2,2}^E(k, \eta)) h_{lm}^{k,(TE/TB)} \phi_l^{(2)}(k(\eta - \eta_0)).\end{aligned}$$

Primordial perturbations and their evolutions

$$\begin{aligned}h_{(lm)}^{\lambda,k} &= \int d\hat{\mathbf{k}} (-1)^\lambda h^{-\lambda}(\mathbf{k})(-\lambda Y_{(lm)}(\hat{\mathbf{k}}))^* \\ \langle h_{(lm)}^{\alpha,k} [h_{(l'm')}^{\alpha',k'}]^* \rangle &= \begin{cases} \delta_{ll'} \delta_{mm'} \delta^{\alpha\alpha'} \frac{(2\pi)^3}{k^2} \delta(k-k') P_L(k) & (\alpha = L) \\ \delta_{ll'} \delta_{mm'} \delta^{\alpha\alpha'} \frac{(2\pi)^3}{k^2} \delta(k-k') P_V(k) & (\alpha = VE, VB) \\ \delta_{ll'} \delta_{mm'} \delta^{\alpha\alpha'} \frac{(2\pi)^3}{k^2} \delta(k-k') P_T(k) & (\alpha = TE, TB) \end{cases} \\ \bar{a}_{2,m}^E(k, \eta) &: \text{Transfer function}\end{aligned}$$

Photon-Photon scattering

$$A \equiv 96 \sqrt{\frac{\pi}{5}} A_e \mu_0 a_{\text{rad}} T_0^4 c^{-1} \omega_0 = 1.11 \times 10^{-38} \left(\frac{\nu_0}{100\text{GHz}} \right) \text{m}^{-1}$$

Radial functions

$$\begin{aligned}\phi_l^{(m)} &= \begin{cases} \epsilon_l^{(m)} & (\text{for E-mode}) \\ \beta_l^{(m)} & (\text{for B-mode}) \end{cases} \\ \epsilon_l^{(0)}(x) &= \sqrt{\frac{3(l+2)!}{8(l-2)!}} \frac{j_l(x)}{x^2}, \\ \epsilon_l^{(1)}(x) &= \frac{1}{2} \sqrt{(l-1)(l+2)} \left[\frac{j_l(x)}{x^2} + \frac{j_l'(x)}{x} \right], \\ \epsilon_l^{(2)}(x) &= \frac{1}{4} \left[-j_l(x) + j_l''(x) + 2 \frac{j_l(x)}{x^2} + 4 \frac{j_l'(x)}{x} \right], \\ \beta_l^{(0)}(x) &= 0, \\ \beta_l^{(1)}(x) &= \frac{1}{2} \sqrt{(l-1)(l+2)} \frac{j_l(x)}{x}, \\ \beta_l^{(2)}(x) &= \frac{1}{2} \left[j_l'(x) + 2 \frac{j_l(x)}{x} \right].\end{aligned}$$

Outline

- Introduction
- Calculation of Φ_{ab}
- Power spectra of circular polarization
- Summary

Calculation of circular polarization

Now, we calculate V using the formulae for P_{ab} , Φ_{ab} , and V

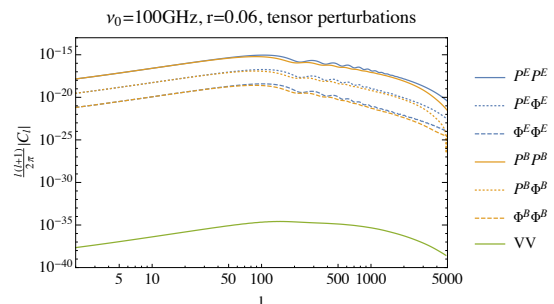
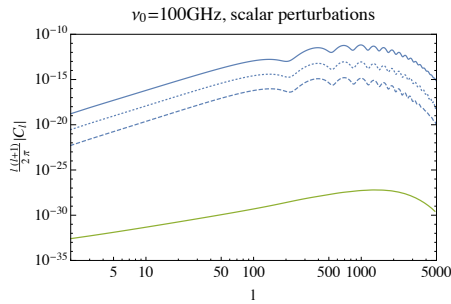
$$V(\hat{\mathbf{n}}) = \epsilon_{abc} P^{ab}(\hat{\mathbf{n}}) \Phi_b^c(\hat{\mathbf{n}}).$$

$$\begin{aligned}
 V_{lm} &= \int d\hat{\mathbf{n}} V(\hat{\mathbf{n}}) Y_{lm}^*(\hat{\mathbf{n}}) \\
 P_{ab}(\hat{\mathbf{n}}) &= \sum_{lm} (P_{lm}^E Y_{(lm)ab}^{TE}(\hat{\mathbf{n}}) + P_{lm}^B Y_{(lm)ab}^{TB}(\hat{\mathbf{n}})) \\
 \Phi_{ab}(\hat{\mathbf{n}}) &= \sum_{lm} (\Phi_{lm}^E Y_{(lm)ab}^{TE}(\hat{\mathbf{n}}) + \Phi_{lm}^B Y_{(lm)ab}^{TB}(\hat{\mathbf{n}}))
 \end{aligned}
 \quad \rightarrow \quad
 \begin{aligned}
 V^{lm} &= \sum_{l_1 m_1} \sum_{l_2 m_2} (P_{l_1 m_1}^E \Phi_{l_2 m_2}^E \int d\hat{\mathbf{n}} \epsilon^{ab} Y_{(l_1 m_1)ac}^E(\hat{\mathbf{n}}) Y_{(l_2 m_2)b}^E(\hat{\mathbf{n}}) Y_{lm}^*(\hat{\mathbf{n}}) \\
 &\quad + P_{l_1 m_1}^E \Phi_{l_2 m_2}^B \int d\hat{\mathbf{n}} \epsilon^{ab} Y_{(l_1 m_1)ac}^E(\hat{\mathbf{n}}) Y_{(l_2 m_2)b}^B(\hat{\mathbf{n}}) Y_{lm}^*(\hat{\mathbf{n}}) \\
 &\quad + P_{l_1 m_1}^B \Phi_{l_2 m_2}^E \int d\hat{\mathbf{n}} \epsilon^{ab} Y_{(l_1 m_1)ac}^B(\hat{\mathbf{n}}) Y_{(l_2 m_2)b}^E(\hat{\mathbf{n}}) Y_{lm}^*(\hat{\mathbf{n}}) \\
 &\quad + P_{l_1 m_1}^B \Phi_{l_2 m_2}^B \int d\hat{\mathbf{n}} \epsilon^{ab} Y_{(l_1 m_1)ac}^B(\hat{\mathbf{n}}) Y_{(l_2 m_2)b}^B(\hat{\mathbf{n}}) Y_{lm}^*(\hat{\mathbf{n}}))
 \end{aligned}$$

Power spectra of circular polarization

$$\begin{aligned}
 C_l^{VV} = \langle V_{lm} V_{lm} \rangle &= \sum_{l_1 m_1 l_2 m_2 (\text{odd})} \left((C_{l_1}^{PEPE} C_{l_2}^{\Phi^E \Phi^E} - C_{l_1}^{PE\Phi^E} C_{l_2}^{PE\Phi^E}) + (C_{l_1}^{PBPB} C_{l_2}^{\Phi^B \Phi^B} - C_{l_1}^{PB\Phi^B} C_{l_2}^{PB\Phi^B}) \right. \\
 &\quad \left. + 2C_{l_1}^{PEPB} C_{l_2}^{\Phi^E \Phi^B} - 2C_{l_1}^{PE\Phi^B} C_{l_2}^{PE\Phi^E} \right) |C_{l_1 m_1 l_2 m_2}^{l-m}|^2 \\
 &+ \sum_{l_1 m_1 l_2 m_2 (\text{even})} \left(C_{l_1}^{PEPE} C_{l_2}^{\Phi^B \Phi^B} + C_{l_1}^{PBPB} C_{l_2}^{\Phi^E \Phi^E} + 2C_{l_1}^{PE\Phi^E} C_{l_2}^{PB\Phi^B} \right. \\
 &\quad \left. - C_{l_1}^{PE\Phi^B} C_{l_2}^{PE\Phi^B} - C_{l_1}^{PB\Phi^E} C_{l_2}^{PB\Phi^E} - 2C_{l_1}^{PEPB} C_{l_2}^{\Phi^E \Phi^B} \right) |C_{l_1 m_1 l_2 m_2}^{l-m}|^2
 \end{aligned}$$

Pink terms are zero in parity conserved universe.



$$\sqrt{\langle V^2 \rangle} = \sqrt{\int \frac{d^2 l}{(2\pi)^2} C_l^{VV}} \simeq \begin{cases} 3 \times 10^{-14} & (\text{for scalar perturbations}) \\ 7 \times 10^{-17} \left(\frac{r}{0.06}\right) & (\text{for tensor perturbations}) \end{cases}$$

Uniform circular polarization

Uniform circular polarization can be produced by chiral GWs.

$$\langle V_{lm} \rangle = \sum_{l_1 m_1} (C_{l_1}^{P^E \Phi^B} - C_{l_1}^{P^B \Phi^E}) (-G_{l_1 - m_1 l_1 m_1}^{lm})$$

$$= \begin{cases} \sum_{l_1} (C_{l_1}^{P^E \Phi^B} - C_{l_1}^{P^B \Phi^E}) \frac{(2l_1+1)}{\sqrt{4\pi}} & (l = m = 0) \\ 0 & (\text{others}) \end{cases}$$

$$\langle V_{00} \rangle = 2.6 \times 10^{-17} \Delta\chi \left(\frac{r}{0.06} \right)$$

$$\begin{aligned} 2P_T(k) &= P_{T,R}(k) + P_{T,L}(k) \\ P_{T,L}(k) &\equiv (1 + \Delta\chi)P_T(k) \\ P_{T,R}(k) &\equiv (1 - \Delta\chi)P_T(k) \end{aligned}$$

In addition, there is the cosmic variance of V_{00} .

$$\langle \tilde{V}_{00} \tilde{V}_{00} \rangle = \sum_l \frac{(2l+1)^2}{4\pi} \left(C_l^{P^E P^E} C_l^{\Phi^B \Phi^B} + C_l^{P^B P^B} C_l^{\Phi^E \Phi^E} + 2C_l^{P^E \Phi^E} C_l^{P^B \Phi^B} \right. \\ \left. - C_l^{P^E \Phi^B} C_l^{P^E \Phi^B} - C_l^{P^B \Phi^E} C_l^{P^B \Phi^E} - 2C_l^{P^E P^B} C_l^{\Phi^E \Phi^B} \right) |H_l^0|^2$$

$$\tilde{V}_{00} = V_{00} - \langle V_{00} \rangle$$

$$\sqrt{\langle \tilde{V}_{00} \tilde{V}_{00} \rangle} = 1.5 \times 10^{-18} \left(\frac{r}{0.06} \right)^{1/2}$$

No dependence of $\Delta\chi$

Degeneracy for uniform V

Induced by chiral GW

$$\langle V_{00} \rangle = 2.6 \times 10^{-17} \Delta\chi \left(\frac{r}{0.06} \right)$$

$$\begin{aligned} 2P_T(k) &= P_{T,R}(k) + P_{T,L}(k) \\ P_{T,L}(k) &\equiv (1 + \Delta\chi)P_T(k) \\ P_{T,R}(k) &\equiv (1 - \Delta\chi)P_T(k) \end{aligned}$$

Cosmic variance

$$\sqrt{\langle \tilde{V}_{00} \tilde{V}_{00} \rangle} = 1.5 \times 10^{-18} \left(\frac{r}{0.06} \right)^{1/2}$$

$$\tilde{V}_{00} = V_{00} - \langle V_{00} \rangle$$

To establish that GW background is chiral with 2σ in V_{00} , the parameters should satisfy

$$\Delta\chi > 0.12 \left(r/0.06 \right)^{-1/2}$$

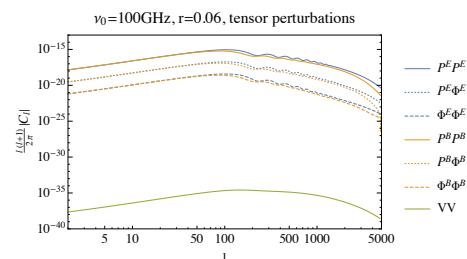
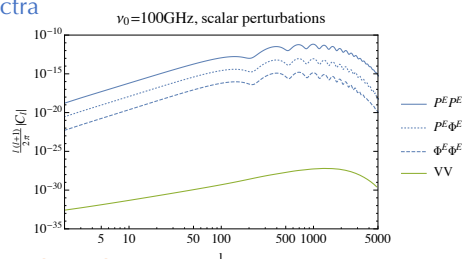
Outline

- Introduction
- Calculation of Φ_{ab}
- Power spectra of circular polarization
- Summary

What we did

- We made the formulations for circular polarization induced by primordial scalar, vector, tensor perturbations.
- Using the formulations, we calculated the power spectra and uniform circular polarizations.

Power spectra



Uniform circular polarization

$$\langle V_{00} \rangle = 2.6 \times 10^{-17} \Delta\chi \left(\frac{r}{0.06} \right)$$

$$\sqrt{\langle \tilde{V}_{00} \tilde{V}_{00} \rangle} = 1.5 \times 10^{-18} \left(\frac{r}{0.06} \right)^{1/2}$$

Hiroyuki Kitamoto

National Center for Theoretical Sciences

“Schwinger Effect in Inflaton-Driven Electric Field”

(10+5 min.)

[JGRG28 (2018) 110821]

Schwinger Effect in Inflaton-Driven Electric Field

Hiroyuki Kitamoto (NCTS)

Based on arXiv:1807.03753

Introduction (Statistical isotropy of inflation)

- Concerning the primordial universe, we find no significant evidence for violation of rotational symmetry from the current status of cosmic microwave background observations ['13 J. Kim, E. Komatsu, '18 Planck Collaboration](#)

$$\langle \zeta_{\mathbf{k}} \zeta_{\mathbf{k}'} \rangle = (2\pi)^3 \delta^{(3)}(\mathbf{k} + \mathbf{k}') P(\mathbf{k})$$

$$P(\mathbf{k}) = P_0(|\mathbf{k}|) \left\{ 1 + g_* (\hat{\mathbf{k}} \cdot \hat{\mathbf{n}})^2 \right\}, \quad |g_*| \lesssim 10^{-2} \quad \hat{\mathbf{n}}: \text{preferred direction}$$

- From a theoretical viewpoint, an anisotropic inflation can be obtained if an U(1) gauge field has a classical value like an inflaton

$$A_i \neq 0$$

- In fact, if the gauge field respects the conformal symmetry as its kinetic term is canonical, the electromagnetic field decays with the cosmic expansion and then there is no statistical anisotropy

Introduction (Model with a canonical kinetic term)

$$ds^2 = -dt^2 + a^2(t)d\mathbf{x}^2 \quad H \equiv \frac{1}{a} \frac{da}{dt} \simeq \text{const.}$$

$$= a^2(\tau)(-d\tau^2 + d\mathbf{x}^2)$$

$$S_{\text{gauge}} = \int \sqrt{-g} d^4x \left[-\frac{1}{4} g^{\mu\rho} g^{\nu\sigma} F_{\mu\nu} F_{\rho\sigma} \right] = \int d^4x \left[-\frac{1}{4} \eta^{\mu\rho} \eta^{\nu\sigma} F_{\mu\nu} F_{\rho\sigma} \right] \quad \text{conformal symmetry}$$

$$\Rightarrow \quad \frac{d^2}{d\tau^2} A = 0 \Leftrightarrow \frac{d}{d\tau} A = \text{const.} \quad \begin{array}{l} \text{temporal gauge: } A_0 = 0 \\ \text{homogeneity: } A_i = A(\tau)\delta_i^1 \end{array}$$

$$\Rightarrow \quad E_{\text{phys}} = -a^{-2} \frac{d}{d\tau} A \propto a^{-2}$$

The electric field decays with the cosmic expansion \Rightarrow Isotropic inflation

If the conformal symmetry is broken, this discussion does not hold true

Introduction (Model with a dilatonic coupling)

'09, '10 M. Watanabe,
S. Kanno, J. Soda

$$S_{\text{bg}} = \int \sqrt{-g} d^4x \left[\frac{M_{\text{pl}}^2}{2} R - \frac{1}{2} g^{\mu\nu} \partial_\mu \varphi \partial_\nu \varphi - V(\varphi) - \frac{1}{4} \underline{f^2(\varphi)} g^{\mu\rho} g^{\nu\sigma} F_{\mu\nu} F_{\rho\sigma} \right]$$

Solving the classical field eqs. by use of the ansatz: $f(\varphi) = \exp \left\{ \frac{2c}{M_{\text{pl}}^2} \int d\varphi \frac{V}{\partial_\varphi V} \right\}$,

$$f = (a^{-4} + qa^{-4c})^{\frac{1}{2}} \rightarrow a^{-2} \quad \text{for } c > 1 \quad q: \text{integration const.}$$

$$E_{\text{phys}} = -fa^{-1} \frac{d}{dt} A = \underline{f^{-1} a^{-2} E} \rightarrow E \quad E = \frac{\sqrt{3\epsilon_V(c-1)}}{c} M_{\text{pl}} H$$

$$\epsilon_V \equiv \frac{1}{2} \left(\frac{M_{\text{pl}} \partial_\varphi V}{V} \right)^2$$

we obtain a persistent electric field (inflaton-driven electric field)

$c - 1 \lesssim 10^{-7}$ to satisfy the observational bound $g_* = 24 \frac{c-1}{c} N^2 \lesssim 10^{-2}$

Motivation

- We consider the case that a charged test scalar field exists

$$S_{\text{test}} = \int \sqrt{-g} d^4x \left[-g^{\mu\nu} (\partial_\mu + ieA_\mu) \phi^* (\partial_\nu - ieA_\nu) \phi - m^2 \phi^* \phi \right]$$

- A strong electric field leads to the pair production of charged particles (Schwinger effect), and the pair production induces the U(1) current

$$\tilde{j} = 2e \int \frac{d^3k}{(2\pi)^3} v_{\mathbf{k}} n_{\mathbf{k}} \quad \begin{array}{l} n_{\mathbf{k}}: \text{particle number} \\ v_{\mathbf{k}}: \text{velocity of particle} \end{array}$$

- It is reasonable to conjecture that if we take into account the Schwinger effect, the induced current screens the inflaton-driven electric field
- Evaluating the induced current, and solving the field eqs. with it, we verify the no-anisotropic hair conjecture for inflation

Differences from other studies

The studies of Schwinger effect in inflation are divided into the two groups

- Our case ⊙ By introducing a dilatonic coupling, the classical field eqs. show that the electric field approaches to a constant value E

$$E_{\text{phys}} = -f a^{-1} \frac{d}{dt} A = E, \quad f = a^{-2} \quad \Rightarrow \quad A = -\frac{E}{3H} a^{1+2}$$

'17 J. J. Geng, B. F. Li, J. Soda, A. Wang, Q. Wu, T. Zhu, '18 H. Kitamoto

- Without mentioning the mechanism to generate a persistent electric field, the electric field is fixed at a constant value E

$$E_{\text{phys}} = -a^{-1} \frac{d}{dt} A = E \quad \Rightarrow \quad A = -\frac{E}{H} a^1$$

'14 T. Kobayashi, N. Afshordi, '16 T. Hayashinaka, T. Fujita, J. Yokoyama, '18 T. Hayashinaka, S. S. Xue, '18 M. Banyeres, G. Domenech, J. Garriga

Validity of WKB approximation

$$\text{Klein-Gordon eq.:} \quad \left\{ \frac{d^2}{d\tau^2} + \omega_{\mathbf{k}}^2(\tau) \right\} \tilde{\phi}_{\mathbf{k}}(x) = 0 \quad \tilde{\phi} = a\phi$$

$$\omega_{\mathbf{k}}^2 = (k_1 - eA)^2 + k_2^2 + k_3^2 + (m^2 - 2H^2)a^2$$

$$A = -\frac{E}{3H}a^{1+2}$$

At $a \rightarrow 0$, the WKB approximation is trivially valid

$$\omega_{\mathbf{k}} \simeq |\mathbf{k}| \quad \Rightarrow \quad \omega_{\mathbf{k}}^{-4} \left(\frac{d\omega_{\mathbf{k}}}{d\tau} \right)^2 \simeq 0, \quad \omega_{\mathbf{k}}^{-3} \frac{d^2\omega_{\mathbf{k}}}{d\tau^2} \simeq 0$$

At $a \rightarrow \infty$, the validity is ensured due to the presence of f

$$\omega_{\mathbf{k}} \simeq \frac{eE}{3H}a^{1+2} \quad \Rightarrow \quad \omega_{\mathbf{k}}^{-4} \left(\frac{d\omega_{\mathbf{k}}}{d\tau} \right)^2 \simeq 9 \left(\frac{eE}{3H^2}a^2 \right)^{-2}, \quad \omega_{\mathbf{k}}^{-3} \frac{d^2\omega_{\mathbf{k}}}{d\tau^2} \simeq 12 \left(\frac{eE}{3H^2}a^2 \right)^{-2}$$

Particle number and Induced current

In the semiclassical picture,

$$n_{\mathbf{k}} = \exp \left\{ 4 \operatorname{Im} \int^{\tau_*} d\tau' \omega_{\mathbf{k}}(\tau') \right\}, \quad \omega_{\mathbf{k}}(\tau_*) \equiv 0$$

'61 V. L. Pokrovskii,
I. M. Khalatnikov

$$\tilde{j} = 2e \int \frac{d^3k}{(2\pi)^3} v_{\mathbf{k}} n_{\mathbf{k}}, \quad v_{\mathbf{k}} = (k_1 - eA)/\omega_{\mathbf{k}}$$

$$\begin{aligned} \tilde{j}_0 &= 0, \\ \tilde{j}_i &= \tilde{j}(t)\delta_i^1 \end{aligned}$$

We evaluate the late time behavior at $\frac{eE}{H^2}a^2 \gg 1$:

$$\tilde{j} \simeq \frac{e^3 E^2}{4\pi^3} \frac{a^7}{7H} \exp \left\{ -\pi \frac{m^2 - 2H^2}{eEa^2} \right\}$$

At $\frac{|m^2 - 2H^2|}{eEa^2} \ll 1$, the contribution from the mass term becomes irrelevant

$$\tilde{j} \simeq \frac{e^3 E^2}{4\pi^3} \frac{a^7}{7H}$$

Field eqs. with Induced current

$$\left\{ \begin{array}{l} V = 3M_{\text{pl}}^2 H^2 \\ 3H \frac{d}{dt} \varphi + \partial_\varphi V - f^{-1} \partial_\varphi f \cdot E_{\text{phys}}^2 = 0 \\ \frac{d}{dt} (f a^2 E_{\text{phys}}) + \underline{a^{-1} \tilde{j}} = 0 \end{array} \right.$$

Solving them by use of the ansatz: $f(\varphi) = \exp \left\{ \frac{2c}{M_{\text{pl}}^2} \int d\varphi \frac{V}{\partial_\varphi V} \right\}$,

$$f = a^{-2} \left\{ 1 - \frac{1}{1 + \frac{3}{2} \frac{1}{c-1}} \cdot \frac{e^3 E}{4\pi^3} \frac{a^6}{42H^2} \right\}$$

for $c > 1$

$$E_{\text{phys}} = E \left\{ 1 - \frac{\frac{3}{2} \frac{1}{c-1}}{1 + \frac{3}{2} \frac{1}{c-1}} \cdot \frac{e^3 E}{4\pi^3} \frac{a^6}{42H^2} \right\}$$

Considering the first-order backreaction, the electric field decays with the cosmic expansion \Rightarrow The statistical isotropy of this model is indicated

Summary

- In the inflation theory with a dilatonic coupling between the inflaton and the U (1) gauge field, a persistent electric field (and then an anisotropic inflation) is obtained as a solution of the classical field eqs.
- We investigated the pair production of scalar particles in the inflaton-driven electric field. In particular, we evaluated the induced current due to the pair production
- Solving the field eqs. with the induced current, we found that the first-order backreaction screens the electric field with the cosmic expansion
- The result indicates that the statistical isotropy of inflation holds true regardless of whether the dilatonic coupling is present or not

Open problems

- In order to prove the no-anisotropic hair conjecture completely, the whole time evolution of the electric field should be investigated
- For the investigation, we need to evaluate the induced current on general backgrounds E_{phys}, f

e.g. if the WKB approximation is valid,

$$\tilde{j} \simeq \frac{e^3}{4\pi^3} \int_{t_0}^t dt' a^3(t') f^{-2}(t') E_{\text{phys}}^2(t') \exp \left\{ -\pi \frac{m^2 - 2H^2}{ef^{-1}(t') E_{\text{phys}}(t')} \right\}$$

- The investigation of the pair production of charged fermions in the inflaton-driven electric field is another future subject

Wednesday 9th November

Invited lecture 9:00–9:45

[Chair: Shinji Mukohyama]

Alexei A. Starobinsky

L.D. Landau Institute for Theoretical Physics

**“Looking for quantum-gravitational corrections to $R + R^2$
inflation”**

(40+10 min.)

[JGRG28 (2018) 110901]

Looking for quantum-gravitational corrections to $R + R^2$ inflation

Alexei A. Starobinsky

Landau Institute for Theoretical Physics RAS,
Moscow - Chernogolovka, Russia

The 28th Workshop on General Relativity and
Gravitation in Japan - JGRG28

Rikkyo University, Tokyo, Japan, 09.11.2018



Present status of inflation

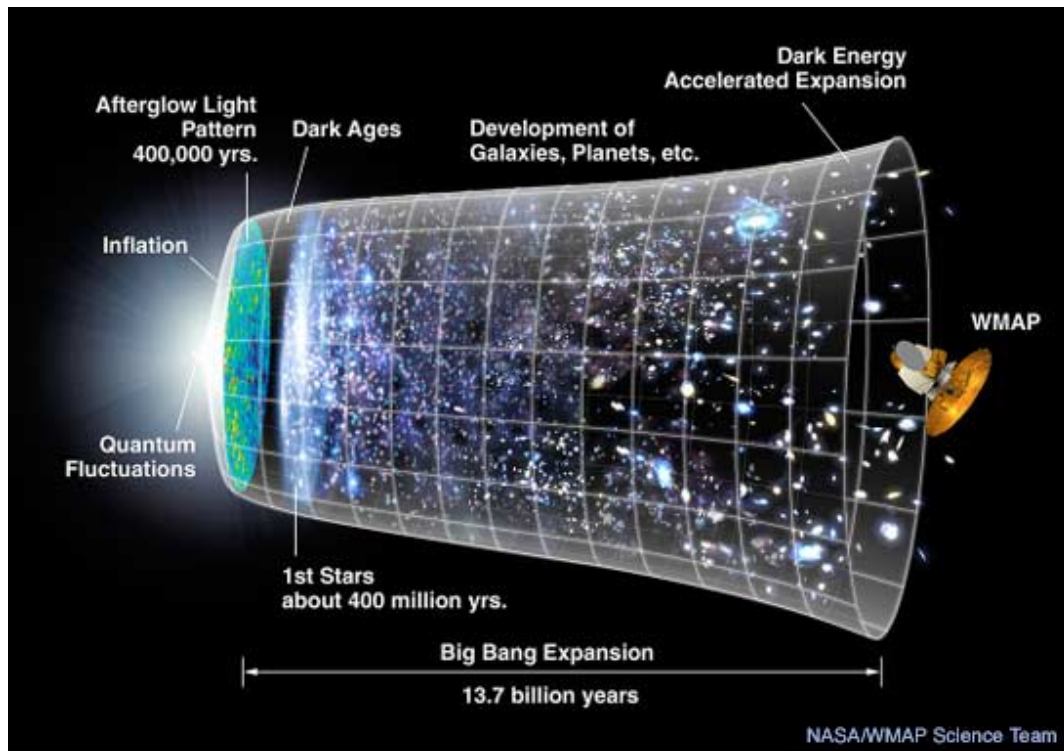
The simplest one-parametric inflationary models

Inflation in $f(R)$ gravity

Quantum corrections to the simplest model during inflation

Conclusions





Inflation

The inflationary scenario is based on the two cornerstone independent ideas (hypothesis):

1. Existence of **inflation** (or, quasi-de Sitter stage) – a stage of accelerated, close to exponential expansion of our Universe in the past preceding the hot Big Bang with decelerated, power-law expansion.
2. The origin of all inhomogeneities in the present Universe is the effect of **gravitational creation of particles and field fluctuations** during inflation from the adiabatic vacuum (no-particle) state for Fourier modes covering all observable range of scales (and possibly somewhat beyond).

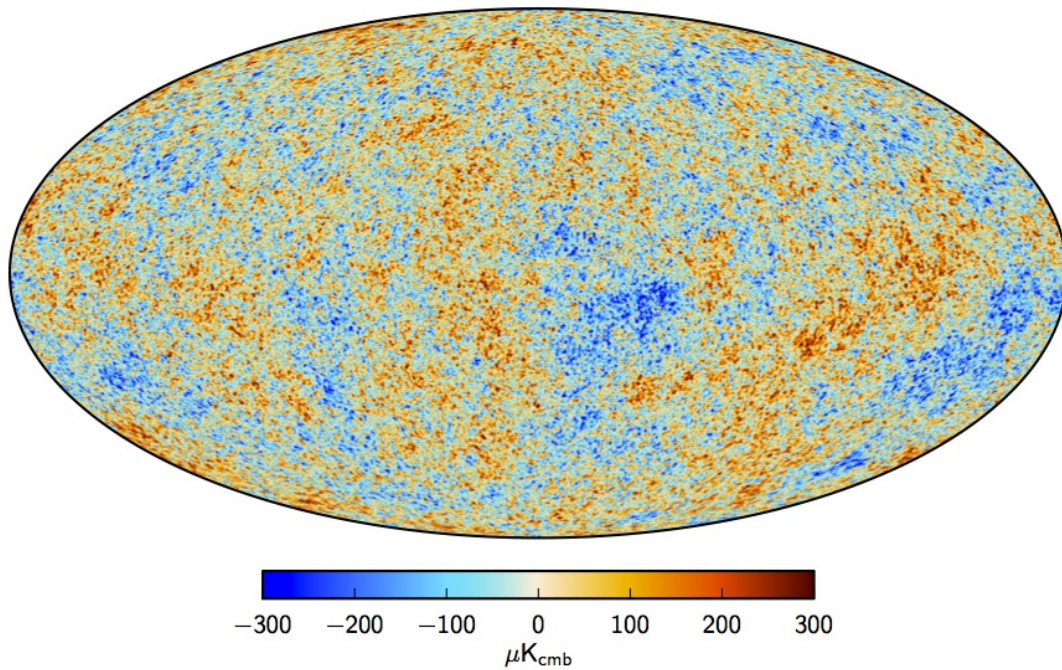
Existing analogies in other areas of physics.

1. The present dark energy.
2. Creation of electrons and positrons in an external electric field.



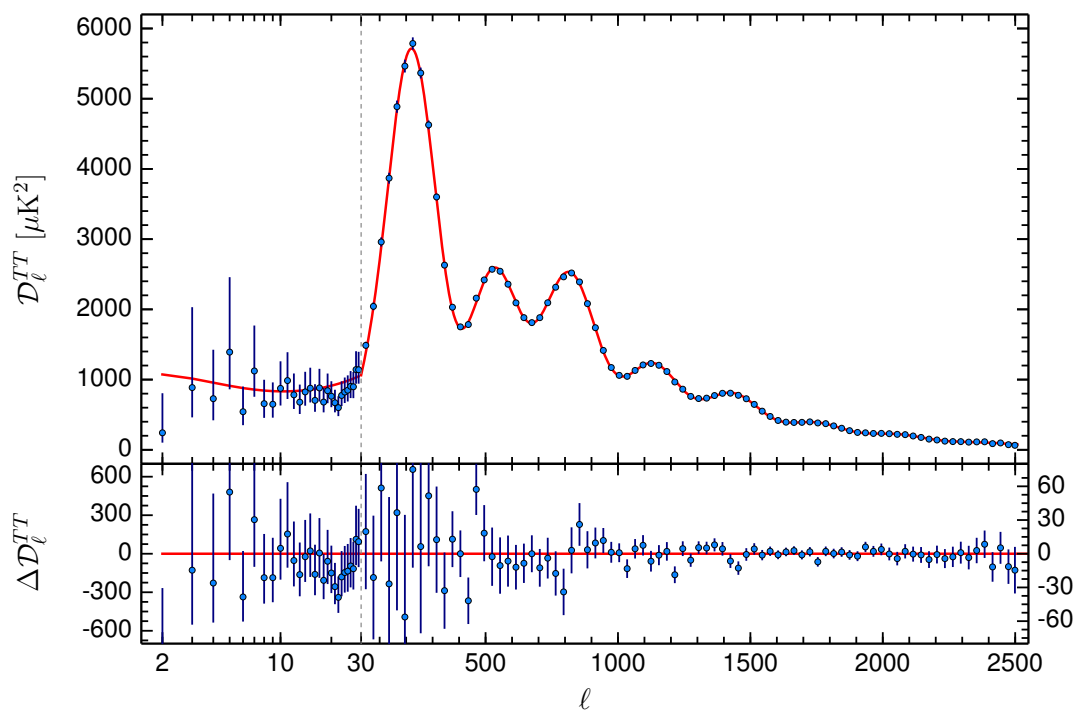
CMB temperature anisotropy

Planck-2015: P. A. R. Ade et al., arXiv:1502.01589



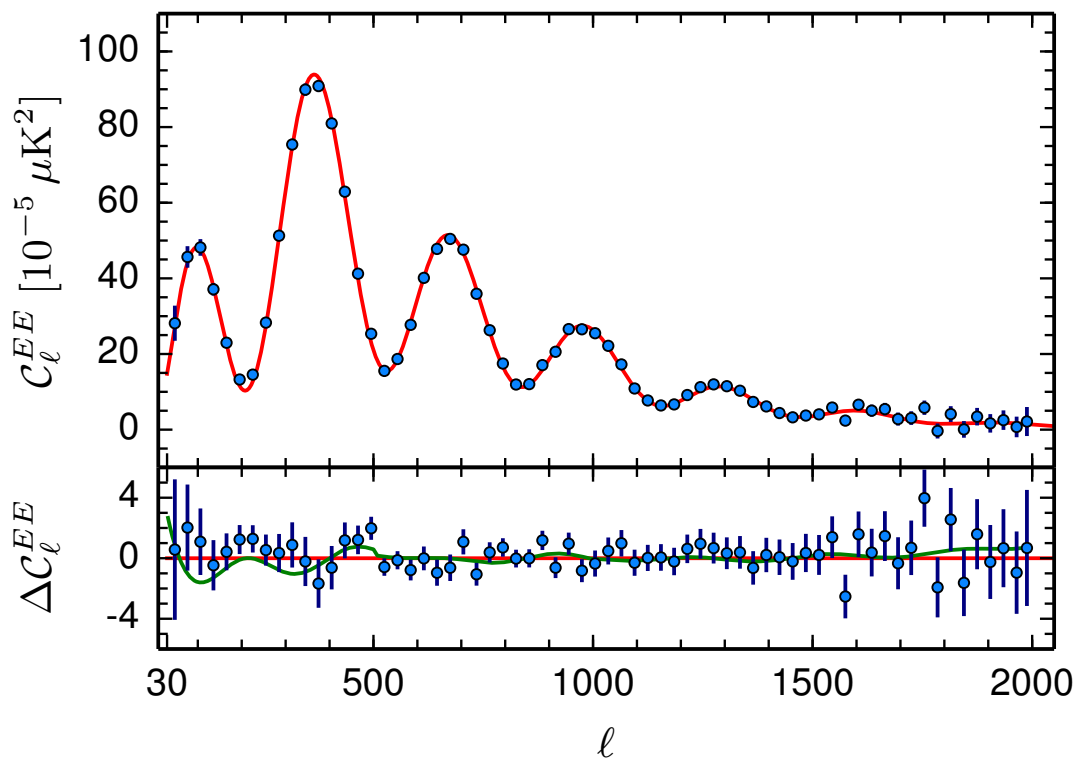
Navigation icons: back, forward, search, etc.

CMB temperature anisotropy multipoles



Navigation icons: back, forward, search, etc.

CMB E-mode polarization multipoles



Navigation icons: back, forward, search, etc.

Present status of inflation

Now we have numbers: [N. Agranim et al., arXiv:1807.06209](#)

The primordial spectrum of scalar perturbations has been measured and its deviation from the flat spectrum $n_s = 1$ in the first order in $|n_s - 1| \sim N_H^{-1}$ has been discovered (using the multipole range $l > 40$):

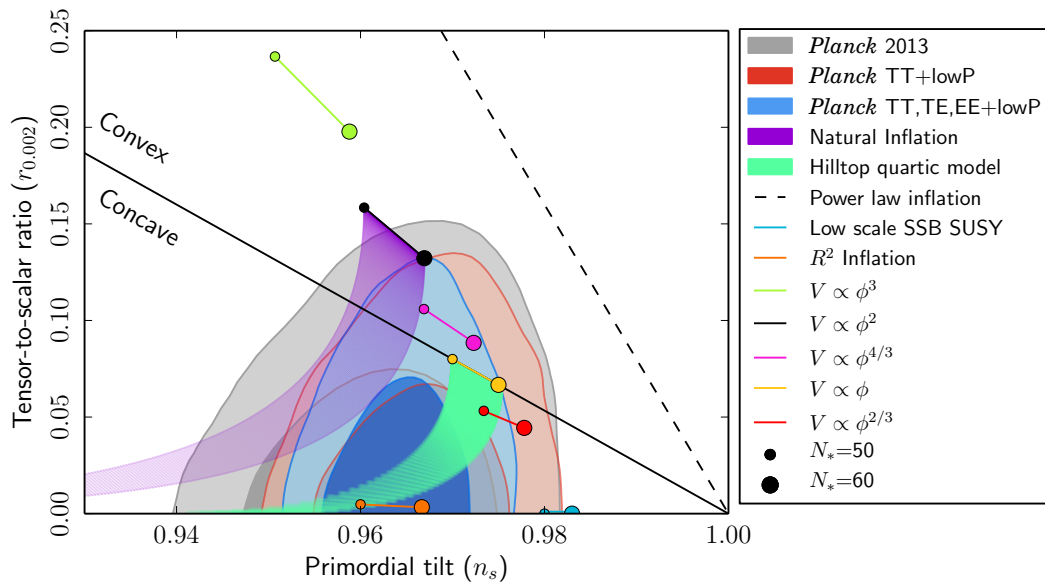
$$\langle \mathcal{R}^2(\mathbf{r}) \rangle = \int \frac{P_{\mathcal{R}}(k)}{k} dk, \quad P_{\mathcal{R}}(k) = (2.10 \pm 0.03) \cdot 10^{-9} \left(\frac{k}{k_0} \right)^{n_s - 1}$$

$$k_0 = 0.05 \text{ Mpc}^{-1}, \quad n_s - 1 = -0.035 \pm 0.004$$

Two fundamental observational constants of cosmology in addition to the three known ones (baryon-to-photon ratio, baryon-to-matter density and the cosmological constant). Existing inflationary models can predict (and predicted, in fact) one of them, namely $n_s - 1$, relating it finally to $N_H = \ln \frac{k_B T_\gamma}{\hbar H_0} \approx 67.2$. (note that $(1 - n_s)N_H \sim 2$).

Navigation icons: back, forward, search, etc.

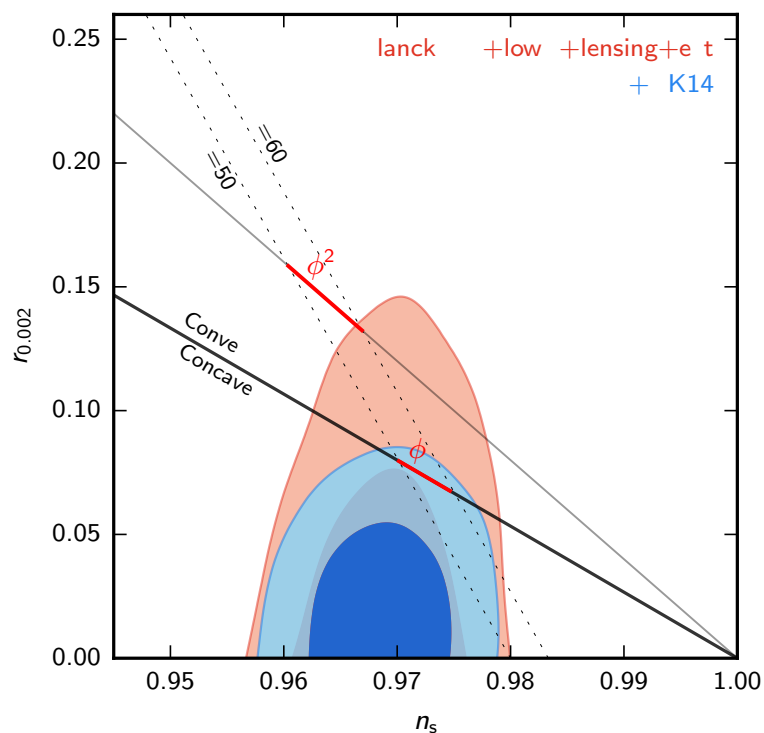
Direct approach: comparison with simple smooth models



Navigation icons: back, forward, search, etc.

Combined BICEP2/Keck Array/Planck results

P. A. R. Ade et al., Phys. Rev. Lett. 116, 031302 (2016)



Navigation icons: back, forward, search, etc.

The simplest models producing the observed scalar slope

$$\mathcal{L} = \frac{f(R)}{16\pi G}, \quad f(R) = R + \frac{R^2}{6M^2}$$

$$M = 2.6 \times 10^{-6} \left(\frac{55}{N} \right) M_{\text{Pl}} \approx 3.1 \times 10^{13} \text{ GeV}$$

$$n_s - 1 = -\frac{2}{N} \approx -0.036, \quad r = \frac{12}{N^2} \approx 0.004$$

$$N = \ln \frac{k_f}{k} = \ln \frac{a_0 T_\gamma}{k} - \mathcal{O}(10), \quad H_{dS}(N = 55) = 1.3 \times 10^{14} \text{ GeV}$$

The same prediction from a scalar field model with $V(\phi) = \frac{\lambda\phi^4}{4}$ at large ϕ and strong non-minimal coupling to gravity $\xi R\phi^2$ with $\xi < 0$, $|\xi| \gg 1$, including the Brout-Englert-Higgs inflationary model.

The simplest purely geometrical inflationary model

$$\begin{aligned} \mathcal{L} &= \frac{R}{16\pi G} + \frac{N^2}{288\pi^2 P_{\mathcal{R}}(k)} R^2 + (\text{small rad. corr.}) \\ &= \frac{R}{16\pi G} + 5.1 \times 10^8 R^2 + (\text{small rad. corr.}) \end{aligned}$$

The quantum effect of creation of particles and field fluctuations works **twice** in this model:

- at super-Hubble scales during inflation, to generate space-time metric fluctuations;
- at small scales after inflation, to provide scalaron decay into pairs of matter particles and antiparticles (AS, 1980, 1981).

Weak dependence of the time t_r when the radiation dominated stage begins:

$$N(k) \approx N_H + \ln \frac{a_0 H_0}{k} - \frac{1}{3} \ln \frac{M_{\text{Pl}}}{M} - \frac{1}{6} \ln(M_{\text{Pl}} t_r)$$

The most effective decay channel: into minimally coupled scalars with $m \ll M$. Then the formula

$$\frac{1}{\sqrt{-g}} \frac{d}{dt} (\sqrt{-g} n_s) = \frac{R^2}{576\pi}$$

(Ya. B. Zeldovich and A. A. Starobinsky, JETP Lett. 26, 252 (1977)) can be used for simplicity, but the full integral-differential system of equations for the Bogoliubov α_k, β_k coefficients and the average EMT was in fact solved in AS (1981). Scalaron decay into graviton pairs is suppressed (A. A. Starobinsky, JETP Lett. 34, 438 (1981)).

For this channel of the scalaron decay:

$$N(k) \approx N_H + \ln \frac{a_0 H_0}{k} - \frac{5}{6} \ln \frac{M_{\text{Pl}}}{M}$$

◀ ◻ ▶ ◀ ◻ ▶ ◀ ≡ ▶ ◀ ≡ ▶ ≡ 🔍 ↻

Possible microscopic origins of this phenomenological model.

1. Follow the purely geometrical approach and consider it as the specific case of the fourth order gravity in 4D

$$\mathcal{L} = \frac{R}{16\pi G} + AR^2 + BC_{\alpha\beta\gamma\delta} C^{\alpha\beta\gamma\delta} + (\text{small rad. corr.})$$

for which $A \gg 1$, $A \gg |B|$. Approximate scale (dilaton) invariance and absence of ghosts in the curvature regime $A^{-2} \ll (RR)/M_p^4 \ll B^{-2}$.

One-loop quantum-gravitational corrections are small (their imaginary parts are just the predicted spectra of scalar and tensor perturbations), non-local and qualitatively have the same structure modulo logarithmic dependence on curvature.

◀ ◻ ▶ ◀ ◻ ▶ ◀ ≡ ▶ ◀ ≡ ▶ ≡ 🔍 ↻

2. Another, completely different way:

consider the $R + R^2$ model as an **approximate** description of GR + a non-minimally coupled scalar field with a large negative coupling ξ ($\xi_{conf} = \frac{1}{6}$) in the gravity sector::

$$L = \frac{R}{16\pi G} - \frac{\xi R\phi^2}{2} + \frac{1}{2}\phi_{,\mu}\phi^{,\mu} - V(\phi), \quad \xi < 0, \quad |\xi| \gg 1 .$$

Geometrization of the scalar:

for a generic family of solutions during inflation and even for some period of non-linear scalar field oscillations after it, the scalar kinetic term can be neglected, so

$$\xi R\phi = -V'(\phi) + \mathcal{O}(|\xi|^{-1}) .$$

No conformal transformation, we remain in the the physical (Jordan) frame!



These solutions are the same as for $f(R)$ gravity with

$$L = \frac{f(R)}{16\pi G}, \quad f(R) = R - \frac{\xi R\phi^2(R)}{2} - V(\phi(R)).$$

For $V(\phi) = \frac{\lambda(\phi^2 - \phi_0^2)^2}{4}$, this just produces $f(R) = \frac{1}{16\pi G} \left(R + \frac{R^2}{6M^2} \right)$ with $M^2 = \lambda/24\pi\xi^2 G$ and $\phi^2 = |\xi|R/\lambda$.

The same theorem is valid for a multi-component scalar field, as well as for the mixed Higgs- R^2 model.



Inflation in the mixed Higgs- R^2 Model

M. He, A. A. Starobinsky and J. Yokoyama, JCAP **1805** (2018) 064; arXiv:1804.00409.

$$\mathcal{L} = \frac{1}{16\pi G} \left(R + \frac{R^2}{6M^2} \right) - \frac{\xi R \phi^2}{2} + \frac{1}{2} \phi_{,\mu} \phi^{,\mu} - \frac{\lambda \phi^4}{4}, \quad \xi < 0, \quad |\xi| \gg 1$$

In the attractor regime during inflation (and even for some period after it), we return to the $f(R) = R + \frac{R^2}{6M^2}$ model with the renormalized scalaron mass $M \rightarrow \tilde{M}$:

$$\frac{1}{\tilde{M}^2} = \frac{1}{M^2} + \frac{24\pi\xi^2 G}{\lambda}$$

More generally, R^2 inflation (with an arbitrary n_s, r) serves as an intermediate **dynamical** attractor for a large class of scalar-tensor gravity models.

◀ ◻ ▶ ◀ ◻ ▶ ◀ ≡ ▶ ◀ ≡ ▶ ≡ ◀ ≡ ▶ ◀ ≡ ▶ ◀ ≡ ▶

Inflation in $f(R)$ gravity

The simplest model of modified gravity (= geometrical dark energy) considered as a phenomenological macroscopic theory in the fully non-linear regime and non-perturbative regime.

$$S = \frac{1}{16\pi G} \int f(R) \sqrt{-g} d^4x + S_m$$

$$f(R) = R + F(R), \quad R \equiv R^\mu{}_\mu$$

Here $f''(R)$ is not identically zero. Usual matter described by the action S_m is minimally coupled to gravity.

Vacuum one-loop corrections depending on R only (not on its derivatives) are assumed to be included into $f(R)$. The normalization point: at laboratory values of R where the scalaron mass (see below) $m_s \approx \text{const}$.

Metric variation is assumed everywhere. Palatini variation leads to a different theory with a different number of degrees of freedom.

◀ ◻ ▶ ◀ ◻ ▶ ◀ ≡ ▶ ◀ ≡ ▶ ≡ ◀ ≡ ▶ ◀ ≡ ▶ ◀ ≡ ▶

Field equations

$$\frac{1}{8\pi G} \left(R^\nu_\mu - \frac{1}{2} \delta^\nu_\mu R \right) = - \left(T^\nu_{\mu(vis)} + T^\nu_{\mu(DM)} + T^\nu_{\mu(DE)} \right) ,$$

where $G = G_0 = \text{const}$ is the Newton gravitational constant measured in laboratory and the effective energy-momentum tensor of DE is

$$8\pi G T^\nu_{\mu(DE)} = F'(R) R^\nu_\mu - \frac{1}{2} F(R) \delta^\nu_\mu + (\nabla_\mu \nabla^\nu - \delta^\nu_\mu \nabla_\gamma \nabla^\gamma) F(R) .$$

Because of the need to describe DE, de Sitter solutions in the absence of matter are of special interest. They are given by the roots $R = R_{ds}$ of the algebraic equation

$$Rf'(R) = 2f(R) .$$

The special role of $f(R) \propto R^2$ gravity: admits de Sitter solutions with [any](#) curvature.



Reduction to the first order equation

In the absence of spatial curvature and $\rho_m = 0$, it is always possible to reduce these equations to a first order one using either the transformation to the Einstein frame and the Hamilton-Jacobi-like equation for a minimally coupled scalar field in a spatially flat FLRW metric, or by directly transforming the 0-0 equation to the equation for $R(H)$:

$$\frac{dR}{dH} = \frac{(R - 6H^2)f'(R) - f(R)}{H(R - 12H^2)f''(R)}$$

See, e.g. H. Motohashi and A. A. Starobinsky, *Eur. Phys. J C* **77**, 538 (2017), but in the special case of the $R + R^2$ gravity this was found and used already in the original AS (1980) paper.



Analogues of large-field (chaotic) inflation: $f(R) \approx R^2 A(R)$ for $R \rightarrow \infty$ with $A(R)$ being a slowly varying function of R , namely

$$|A'(R)| \ll \frac{A(R)}{R}, \quad |A''(R)| \ll \frac{A(R)}{R^2}.$$

Analogues of small-field (new) inflation, $R \approx R_1$:

$$f'(R_1) = \frac{2f(R_1)}{R_1}, \quad f''(R_1) \approx \frac{2f(R_1)}{R_1^2}.$$

Thus, all inflationary models in $f(R)$ gravity are close to the simplest one over some range of R .

◀ ◻ ▶ ◀ ◻ ▶ ◀ ≡ ▶ ◀ ≡ ▶ ≡ 🔍 ↻

Perturbation spectra in slow-roll $f(R)$ inflationary models

Let $f(R) = R^2 A(R)$. In the slow-roll approximation $|\ddot{R}| \ll H|\dot{R}|$:

$$P_{\mathcal{R}}(k) = \frac{\kappa^2 A_k}{64\pi^2 A_k'^2 R_k^2}, \quad P_g(k) = \frac{\kappa^2}{12A_k \pi^2}$$

$$N(k) = -\frac{3}{2} \int_{R_f}^{R_k} dR \frac{A}{A'R^2}, \quad \kappa^2 = 8\pi G$$

where the index k means that the quantity is taken at the moment $t = t_k$ of the Hubble radius crossing during inflation for each spatial Fourier mode $k = a(t_k)H(t_k)$.

◀ ◻ ▶ ◀ ◻ ▶ ◀ ≡ ▶ ◀ ≡ ▶ ≡ 🔍 ↻

Different types of quantum corrections to the simplest model

- ▶ Logarithmic running of the free model parameter M with curvature.
- ▶ Terms with higher derivatives of R considered perturbatively (to avoid the appearance of ghosts).
- ▶ Terms arising from the conformal anomaly.



First type: logarithmic running with curvature

Due to the scale-invariance of the $R + R^2$ model for $R \gg M^2$, one may expect logarithmic running of the dimensionless coefficient in front of the R^2 term for large energies and curvatures. This running should be also related to the imaginary part of the effective action describing the scalaron decay after the end of inflation.

The concrete 'asymptotically safe' model with

$$f(R) = R + \frac{R^2}{6M^2 \left[1 + b \ln \left(\frac{R}{\mu^2} \right) \right]}$$

was recently investigated in L.-H. Liu, T. Prokopec, A. A. Starobinsky, Phys. Rev. D **98**, 043505 (2018); arXiv:1806.05407.



However, comparison with CMB observational data on $n_s - 1$ shows that b is small by modulus: $|b|N_H \lesssim 1, |b| \lesssim 10^{-2}$. Thus, from the observational point of view this model can be simplified to

$$f(R) = R + \frac{R^2}{6M^2} \left[1 - b \ln \left(\frac{R}{\mu^2} \right) \right],$$

for which the analytic solution exists:

$$n_s - 1 = -\frac{4b}{3} \left(e^{\frac{2bN}{3}} - 1 \right)^{-1}$$

$$r = \frac{16b^2}{3} \frac{e^{\frac{4bN}{3}}}{\left(e^{\frac{2bN}{3}} - 1 \right)^2}$$

For $|b|N \ll 1$, these expressions reduce to those for the $R + R^2$ model.

◀ ◻ ▶ ◀ ◻ ▶ ◀ ≡ ▶ ◀ ≡ ▶ ≡ 🔍 ↻

Second type: terms with higher derivatives of R

$$S = \frac{1}{2\kappa^2} \int d^4x \sqrt{-g} \left[R + \alpha R^2 + \gamma R \square R \right], \quad \alpha = \frac{1}{6M^2}$$

An inflationary regime in this model was first considered in S. Gottlöber, H.-J. Schmidt and A. A. Starobinsky, *Class. Quant. Grav.* **7**, 803 (1990). But this model, if taken in full, has a scalar ghost in addition to a physical massive scalar and the massless graviton.

Its recent re-consideration avoiding ghosts:

A. R. R. Castellanos, F. Sobreira, I. L. Shapiro and A. A. Starobinsky, arXiv:1810.07787.

◀ ◻ ▶ ◀ ◻ ▶ ◀ ≡ ▶ ◀ ≡ ▶ ≡ 🔍 ↻

Invited lecture 9:45–10:30

[Chair: Shinji Mukohyama]

Jean-Philippe Uzan

CNRS / Institut d'Astrophysique de Paris

“Astrophysical Stochastic Gravitational Wave Background”

(40+10 min.)

[JGRG28 (2018) 110902]

Astrophysical Stochastic Gravitational Wave Background

Jean-Philippe UZAN

*Astro-models w. I. Dvorkin, K. Olive, J. Silk, E. Vangioni
GW background w. G. Cusin, I. Dvorkin, C. Pitrou*



Gravity waves

Since September 2015, we can detect GW with interferometers

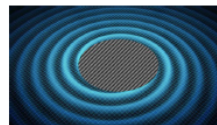
5 binary BH systems and 1 binary NS system

But there are many other types of sources

(1) binary inspiralling objects



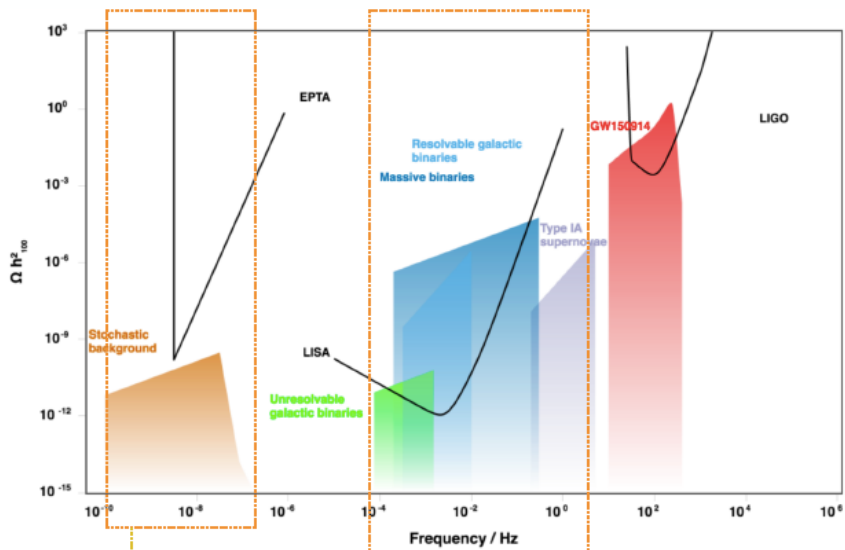
(2) binary merging objects



(3) exploding supernovae



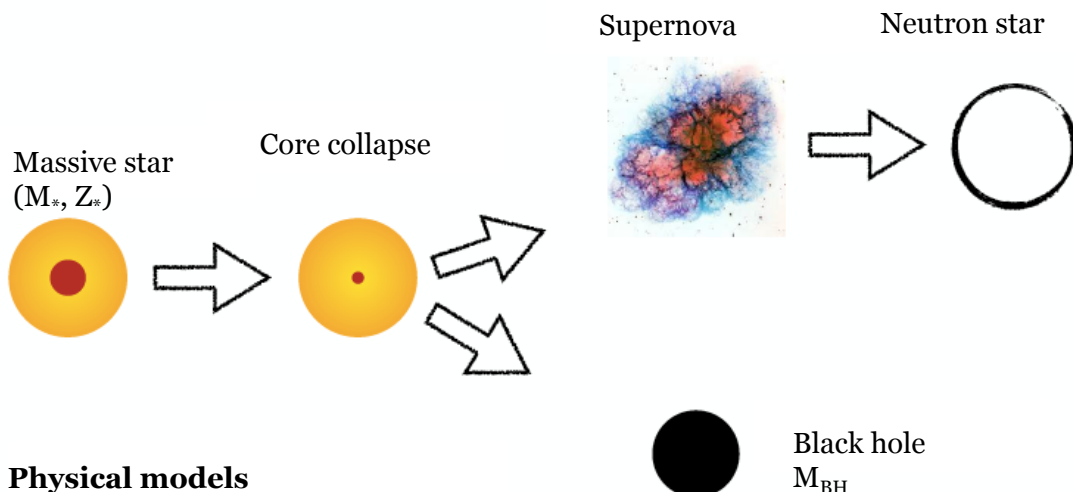
Sources: sensitivity curves and expected fluxes



cosmological background (inflation, cosmic strings...)

expected regime of frequencies and strain for astrophysical stochastic background

Origin of stellar mass black holes



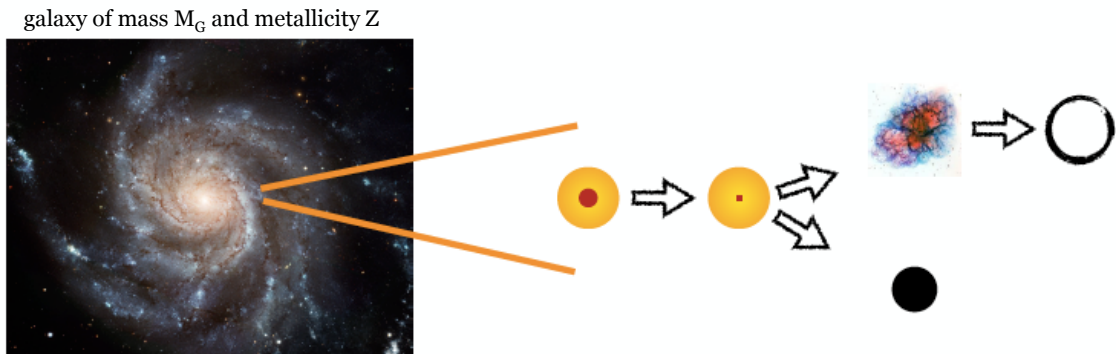
Physical models

Stellar evolution model
Initial mass of the star, binarity

Environmental properties

Chemical composition
Properties of the host galaxy

Galaxy stellar population evolution



Each galaxy has a stellar formation history that depends on its mass and metallicity.

A stellar evolution model gives the lifetime of the star and $m_{\text{BH}} = g_s(M_*, Z_*)$ so that one can predict

- the rate of SN
- the rate of BH formation
- the BH mass spectrum

as a function of time after the galaxy formation (and then redshift)

How to predict the BH binaries formation rate

For a galaxy of mass M_G and metallicity Z

- The star formation rate

$$\psi(z) \quad [\text{Springel-Hernqvist (2003)}]$$

- Initial mass function

$$\phi(M_*) = \frac{dN_*}{dM_*} \propto M_*^{-\alpha} \quad [\text{Salpeter } \alpha=2.35]$$

- Stellar evolution model

$$m_{\text{BH}} = g_s(M_*, Z_*) \quad [\text{Woosley-Weaver (1995)}]$$

$$\tau(M_*, Z_*) \quad [\text{Fryer et al. (2012)}]$$

$$\tau(M_*, Z_*) \quad [\text{Limongi et al. (2017)}]$$

BH formation rate

$$\mathcal{R}_1(m, t) = \psi[M_G, t - \tau(M_*)] \phi(M_*) \times dM_*/dm$$

black holes formed from given initial mass

Fraction of BH in binary systems

$$\beta(M_{\text{BH}})$$

Birth rate of binaries

$$\mathcal{R}_2(m, t) = \beta \mathcal{R}_1(m, t)$$

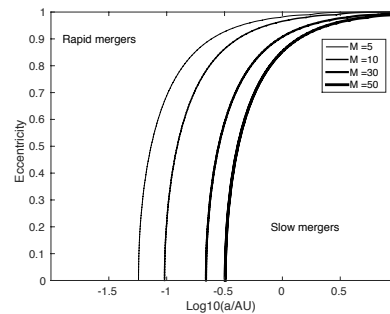
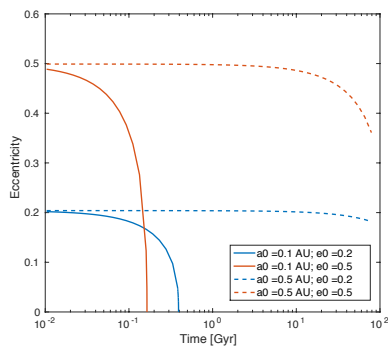
$$\mathcal{R}_{\text{bin}}(m, m') = \mathcal{R}_2(m) \mathcal{R}_2(m') P(m, m')$$

BH mergers rate

This depends on the lifetime of the binary BH systems, that is on their orbital parameters at formation (and eventually environment)

$$\mathcal{R}_f[m, m', a_f, t] = \mathcal{R}_{bin}(m, m') f(a_f)$$

$$\mathcal{R}_m[m, m', a_f, t] = \mathcal{R}_f[m, m', a_f, t - \tau_m(m, m', a_f)]$$



Stress-energy tensor of a GW

The GW stress-energy tensor is quadratic in $h_{\mu\nu}$ and obtained by expanding the Einstein tensor to second order.

Long but textbook computation gives

$$t_{\mu\nu} = \frac{c^4}{32\pi G} [\partial_\mu h_{\alpha\beta} \partial_\nu h^{\alpha\beta}]$$

where the [...] is defined as

$$[A(t)] \equiv \frac{1}{T_0} \int_0^{T_0} dt A(t)$$

The GW energy density is then defined as

$$t^{00} = \frac{c^2}{32\pi G} [\dot{h}_{ij}^{TT} \dot{h}_{ij}^{TT}]$$

Energy density

This leads to the definition of the

$$\rho_{\text{GW}}(\nu_0) = t^{00}$$

from which one defines the density parameter

$$\Omega_{\text{GW}}(\nu_0) = \frac{1}{\rho_c} \frac{d\rho_{\text{GW}}}{d \ln \nu_0}$$

In a FL universe, it gives (I shall come back on this later)

$$\Omega_{\text{GW}}(\nu_0) = \frac{1}{\rho_c} \int \frac{dz}{(1+z)^4 H(z)} \int d\theta_G n_G(z; \theta_G) \mathcal{L}_G(\nu_G; \theta_G)$$

$\nu_G = \nu_0(1+z)$

Elements to predict Ω_{GW}

It depends on

- the background cosmology;
- the distribution of galaxies $n(M_G, z)$;

- the subgalactic physics (SFR, IMF, stellar evolution, binarity);

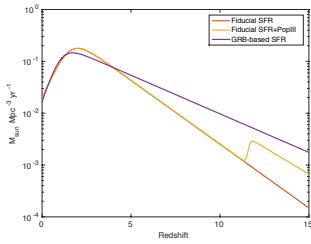
- the GW emission of each type of source

To integrate over the galaxy distribution one needs the Halo mass function (calibrated on numerical simulations [Tinker et al. (2008)])

$$\frac{dn}{dM_G}(M_G, z)$$

Evolution models

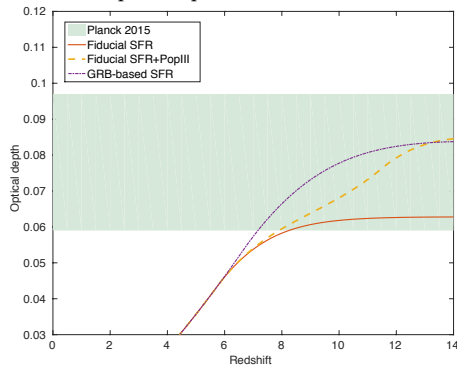
SFR as function of redshift



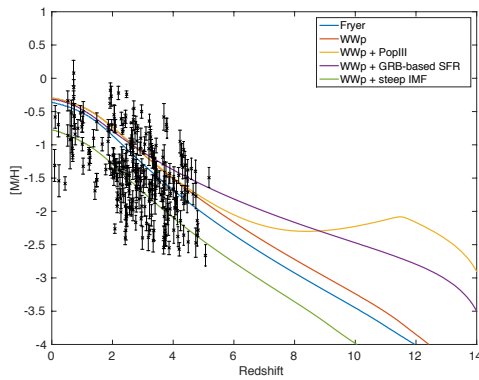
Parameters of the models

	Model name	Ref.	Parameters	Parameter values
BH masses	WWp	Woosley & Weaver (1995)	A, β, γ	0.3, 0.8, 0.2
	Fryer	Fryer et al. (2012)	-	-
	WWp+K	Kinugawa et al. (2014)	$Z_{\text{limit}}/Z_{\odot}$	0.001 or 0.01
SFR	Fiducial	Vangioni et al. (2015)	v, z_m, a, b	0.178, 2.00, 2.37, 1.8
	PopIII			0.002, 11.87, 13.8, 13.36
	GRB-based			0.146, 1.72, 2.8, 2.46
IMF	Fiducial	Salpeter (1955)	x	2.35
	Steep IMF	Chabrier et al. (2014)	x	2.7

Optical depth as function of redshift

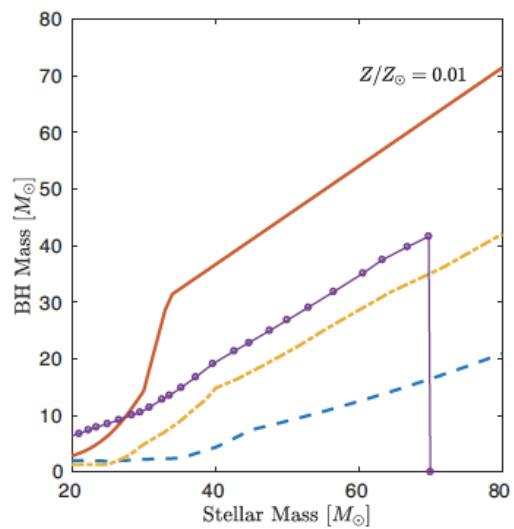
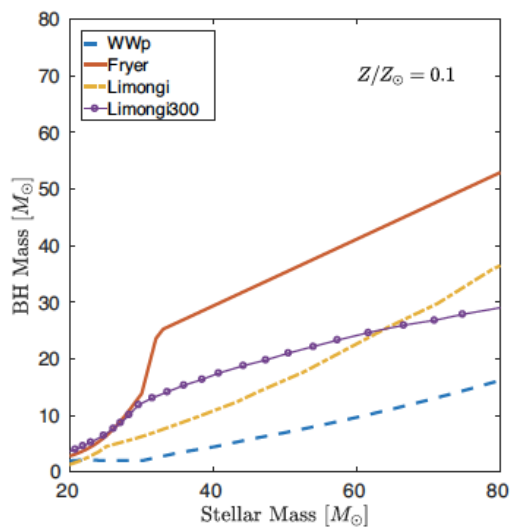


Metallicity as function of redshift



[Dvorkin, Vangioni, Silk, JPU, Olive, [1604.04288](#)].

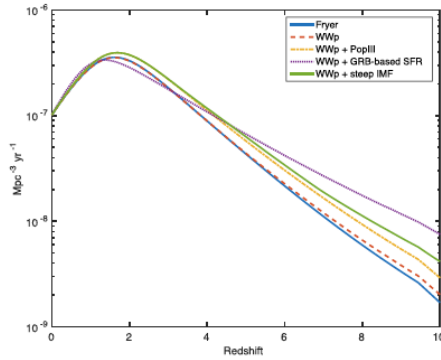
BH mass & influence of metallicity



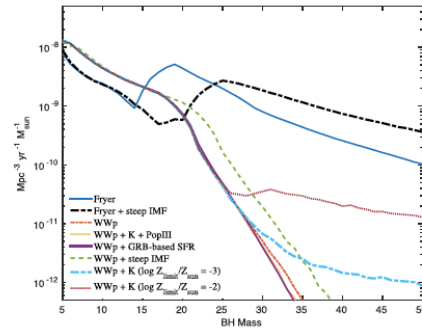
[Dvorkin, JPU, Vangioni, Silk, [1709.09197](#)].

BH merger rate

Total merger rate normalized to $10^{-7} \text{ Mpc}^{-3} \text{ yr}^{-1}$ at $z=0$.



Merger rate by unit BH mass at $z=0$



Merger rate by unit mass as function of z

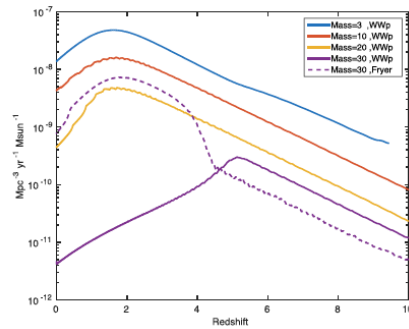


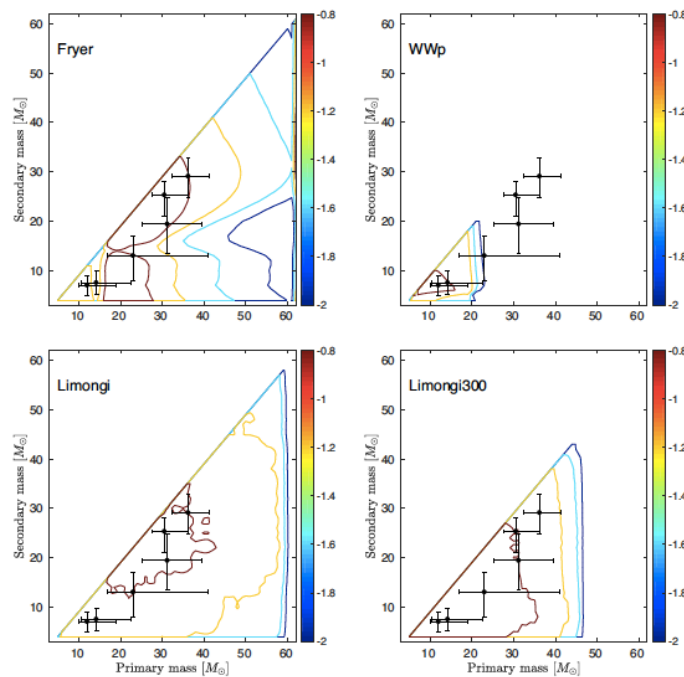
Table 1. Merger rates deduced from LIGO O1 observations assuming different astrophysical models (see text for discussion).

	Rate [$\text{Gpc}^{-3} \text{ yr}^{-1}$]
Fryer	18
WWp	59
Limongi	15
Limongi300	32

[Dvorkin, Vangioni, Silk, JPU, Olive, [1604.04288](#)].

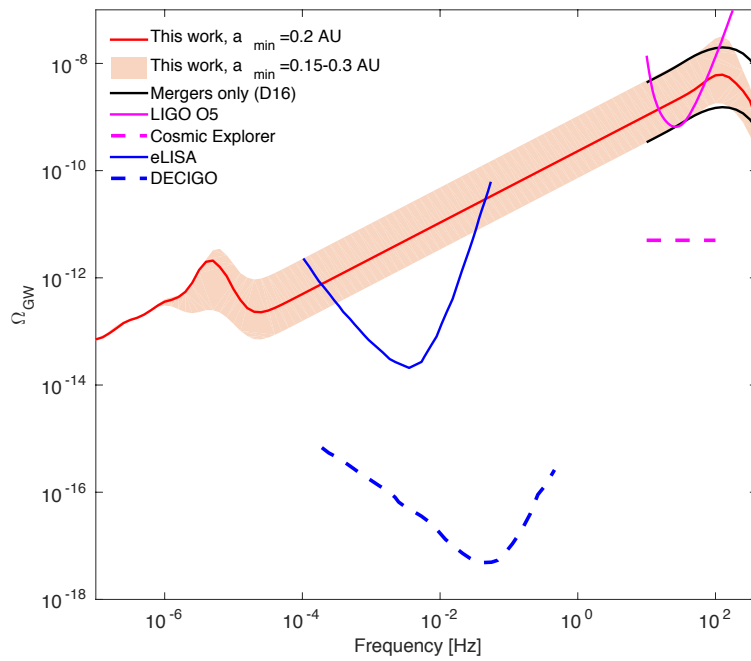
Comparing astrophysical models

Log_{10} of the detection rate in units of $M_{\odot}^{-2} \text{ yr}^{-1}$.



[Dvorkin, JPU, Vangioni, Silk, [1709.09197](#)]

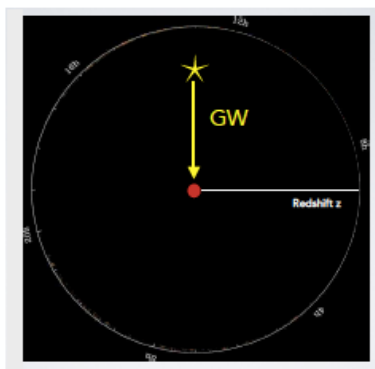
GW background



[Dvorkin, JPU, Vangioni, Silk, [1607.06818](#)]

Anisotropy of the AGWB

This assumes that the spacetime is spatially strictly homogeneous and isotropic (FL)

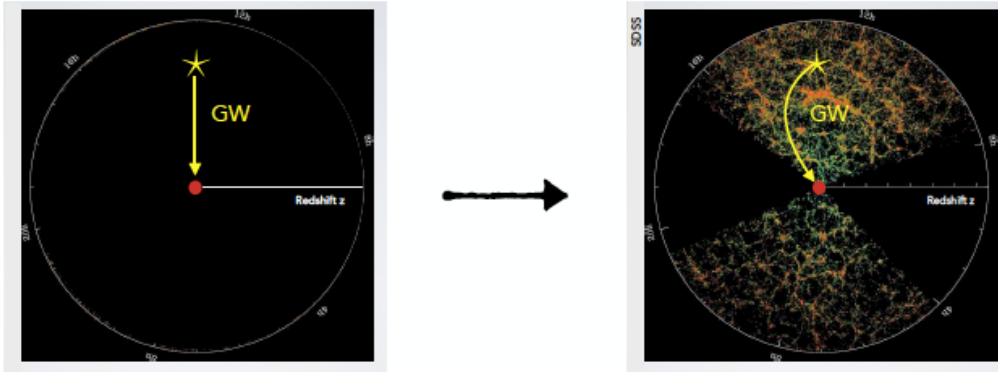


- Isotropic distribution of sources (**no structures**)
- Propagation of GW in **homogeneous** medium

This is indeed not realistic

Anisotropy of the AGWB

Univers has large scale structure:



Sources are not isotropically distributed + light propagates in a perturbed spacetime

$$\Omega_{\text{GW}}(\nu_0) = \int d^2\mathbf{e}_0 \Omega_{\text{GW}}(\nu_0, \mathbf{e}_0)$$

$$\Omega_{\text{GW}}(\nu_0, \mathbf{e}_0) = \frac{1}{\rho_c} \frac{d^3\rho_{\text{GW}}(\nu_0, \mathbf{e}_0)}{d \ln \nu_0 d^2\mathbf{e}_0}$$

Strain and density

At the observer the GW is the superposity of many individual strains produced by different astrophysical systems

$$h_0(\mathbf{x}_0, t_0, \mathbf{e}_0; t) \propto \sum_i^{N(\mathbf{e}_0)} h_i[P_{\text{em}}(\mathbf{x}_0, t_0, \mathbf{e}_0), t] e^{i\varphi_i}$$

Its energy density from direction \mathbf{e}_0 is

$$\frac{d^2\rho_{\text{GW}}}{d^2\mathbf{e}_0}(\mathbf{x}_0, t_0, \mathbf{e}_0) \propto [\dot{h}_0(t_0, \mathbf{x}_0, \mathbf{e}_0; t) \dot{h}_0(t_0, \mathbf{x}_0, \mathbf{e}_0; t)]$$

$$\propto \sum_i^{N(\mathbf{e}_0)} \sum_j^{N(\mathbf{e}_0)} [\dot{h}_i[P_{\text{em}}, t] \dot{h}_j^*[P_{\text{em}}, t]] e^{i(\varphi_i - \varphi_j)}$$

$$\propto \sum_i^{N(\mathbf{e}_0)} [\dot{h}_i[P_{\text{em}}, t] \dot{h}_i^*[P_{\text{em}}, t]] ,$$

Since sources are incoherent

Strain and density

So the energy density,

[Cusin, Pitrou, JPU, 1711.11345]

$$\frac{d^2 \rho_{GW}}{d^2 e_o}(\mathbf{x}_o, t_o, e_o) \propto \sum_i^{N(e_o)} \frac{d^2 \rho_{GW,i}}{d^2 e_o}[P_{em}(\mathbf{x}_o, t_o, e_o)]$$

is a stochastic quantity. So it has a non-vanishing correlation function

$$C(e_o \cdot e'_o) = \left\langle \frac{d^2 \rho_{GW}}{d^2 e_o}(e_o) \frac{d^2 \rho_{GW}}{d^2 e'_o}(e'_o) \right\rangle$$

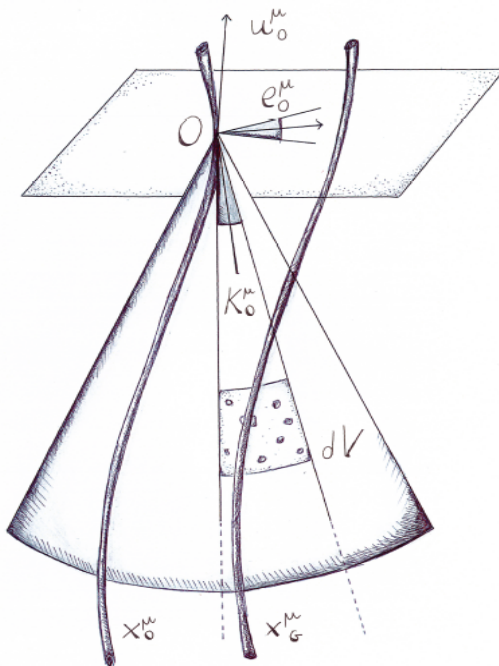
The strain is also a stochastic variable, but uncorrelated on the sky because sources are incoherent

$$\begin{aligned} & \langle h_{obs}(\mathbf{x}_o, t_o, e_o; t) h_{obs}(\mathbf{x}_o, t_o, e'_o; t) \rangle \\ & \propto \delta^2(e_o - e'_o) \left\langle \sum_i^{N(e_o)} |h_i[P_{em}(t_o, \mathbf{x}_o, e_o), t]|^2 \right\rangle \end{aligned}$$

The strain is not correlated while its energy density is.

The good quantity to describe the AGWB is NOT the strain but its energy density.

Anisotropy of the AGWB



u_0^μ Observer 4-velocity

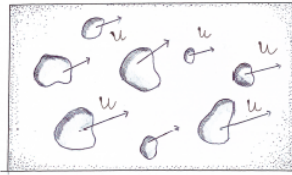
e_0^μ Direction of observation

dV 3D-physical volume

It is given by the intersection of the 4-volume and the observer past-light cone.

[Cusin, Pitrou, JPU, 1704.06184]

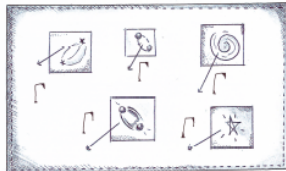
Anisotropy of the AGWB



(1) Cosmological scale

(1) **cosmological scale.** The observer receives flux of GW in a solid angle around the direction of observation. Galaxies: point-like sources moving with the cosmic flow

cosmological approach



(2) Galactic scale

(2) **galactic scale.** A source -i inside a galaxy is characterized by parameters $\theta^{(i)}$ and is moving with velocity Γ . Effective luminosity and frequency of a galaxy defined taking into account contributions sources

statistical approach



(3) Astrophysical scale

(3) **local scale.** Scale of single sources emitting GW inside a galaxy

astrophysical approach

Anisotropy of the AGWB: GW propagation

As in electromagnetism, it can be shown that in the eikonal limit GW follows null geodesics.

$$k^\mu = \frac{dx^\mu}{d\lambda} \quad k^\mu k_\mu = 0 \quad \frac{Dk^\mu}{D\lambda} \equiv k^\nu \nabla_\nu k^\mu = 0$$

The observer 4-velocity defines a preferred notion of spatial sections. The GW 4-vector can then be decomposed as:

$$k^\mu = E (u^\mu - e^\mu)$$

Direction of observation $e^\mu u_\mu = 0, \quad e^\mu e_\mu = 1$

Energy/Cyclic frequency $E = 2\pi\nu \equiv -u_\mu k^\mu$

Spatial projection of the GW 4-vector: $p^\mu \equiv (g^{\mu\nu} + u^\mu u^\nu) k_\nu = -E e^\mu$

Anisotropy of the AGWB: redshift

The general definition of the redshift is then

$$1 + z_G \equiv \frac{\nu_G}{\nu_0} = \frac{u_G^\mu k_\mu(\lambda_G)}{u_0^\mu k_\mu(\lambda_0)}$$

Given initial conditions at the observer

$$x^\mu(\lambda_0) = x_0^\mu, \quad \left. \frac{dx^\mu(\lambda)}{d\lambda} \right|_{\lambda=\lambda_0} = E_0(u_0^\mu - e_0^\mu).$$

One gets

$$x^\mu(\lambda, x_0^\mu, e_0^\mu) \quad z(\lambda, x_0^\mu, e_0^\mu) \quad e^\mu(\lambda, x_0^\mu, e_0^\mu)$$

AGWB: general derivation

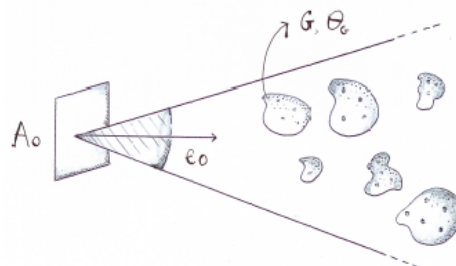
Galaxy G, at z_G and observed in e_0 . Associated flux:

$$\Phi(e_0, z_G, \theta_G) \equiv \frac{\text{Energy}}{A_0 \Delta t_0}$$

θ_G parameters describing G (mass, metallicity...)

$$\int d\nu_0 \Phi(e_0, \nu_0, z_G, \theta_G) \equiv \Phi(e_0, z_G, \theta_G)$$

specific flux



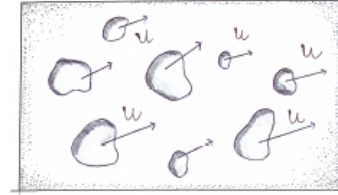
To find the total flux received, we need to **sum the contributions** from all the galaxies in the solid angle $d\Omega_0$

AGWB: (1) cosmological scales

For each galaxy, characterized by θ_G we define

$$\int_0^\infty \mathcal{L}_G(\nu_G, \theta_G) d\nu_G = L_G(\theta_G) \quad \text{effective luminosity}$$

$$\nu_G = (1 + z_G)\nu_O \quad \text{effective frequency}$$



The flux measured by the observer in the frequency band $[\nu_O, \nu_O + d\nu_O]$

$$\Phi(z_G, e_O, \theta_G) \equiv \frac{1}{4\pi D_L^2(z_G, e_O)} L_G(\theta_G)$$

$$\Phi_\nu(z_G, e_O, \nu_O, \theta_G) d\nu_O \equiv \frac{(1 + z_G)}{4\pi D_L^2(z_G, e_O)} \mathcal{L}_G(\nu_G, \theta_G) d\nu_O \quad d\nu_G(1 + z_G) = d\nu_O$$

AGWB: (2) galactic scales

The effective luminosity (per unit frequency) can be split as

$$\mathcal{L}_G(\theta_G, \nu_G) = \mathcal{L}_G^I(\theta_G, \nu_G) + \boxed{\mathcal{L}_G^M(\theta_G, \nu_G) + \mathcal{L}_G^{SN}(\theta_G, \nu_G)}$$

There are 2 types of contributions.

Inspiraling binaries

$$\mathcal{L}_G^I(\theta_G, \nu_G) = \sum_{(i)}^I \int d\theta^{(i)} \mathcal{N}^{(i)}(\theta^{(i)}, \theta_G) \int d^3\Gamma f(\Gamma, \theta_G) \frac{dE_G^{(i)}}{dt_G d\nu_G}(\nu_G, \Gamma, \theta_G)$$

Mergers and supernovae

$$\boxed{\mathcal{L}_G^{M,SN}(\theta_G, \nu_G)} = \sum_{(i)}^{M,SN} \int d\theta^{(i)} \frac{d\mathcal{N}^{(i)}}{dt_G}(\theta^{(i)}, \theta_G) \int d^3\Gamma f(\Gamma, \theta_G) \frac{dE_G^{(i)}}{d\nu_G}(\nu_G, \Gamma, \theta_G)$$

AGWB: General expression

$$\frac{d^3 \rho_{\text{GW}}}{d\nu_0 d^2 \Omega_0}(\nu_0, e_0) = \int d\lambda \int d\theta_G \Phi[x^\mu(\lambda), \nu_0, \theta_G] \frac{d^3 \mathcal{N}_G}{d\lambda d^2 \Omega_0}[x^\mu(\lambda), \theta_G]$$

$$\Phi = \frac{1 + z_G}{D_L^2} \mathcal{L}_G \quad \frac{d^3 \mathcal{N}_G[x^\mu(\lambda), \theta_G]}{d^3 V[x^\mu(\lambda)]} = n_G[x^\mu(\lambda), \theta_G] \frac{d^3 V[x^\mu(\lambda)]}{d^3 V[x^\mu(\lambda)]} = n_G[x^\mu(\lambda), \theta_G] \frac{1}{D_A^2(\lambda) d^2 e_0 \sqrt{p_\mu(\lambda) p^\mu(\lambda)} d\lambda}$$

$$\frac{d^3 \rho_{\text{GW}}}{d\nu_0 d^2 \Omega_0}(\nu_0, e_0) = \frac{1}{4\pi} \int d\lambda \int d\theta_G \frac{\sqrt{p_\mu(\lambda) p^\mu(\lambda)}}{[1 + z_G(\lambda)]^3} n_G[x^\mu(\lambda), \theta_G] \mathcal{L}_G(\nu_G, \theta_G)$$

Spatial displacement (points to $\frac{\sqrt{p_\mu(\lambda) p^\mu(\lambda)}}{[1 + z_G(\lambda)]^3}$)
Effective luminosity (points to $\mathcal{L}_G(\nu_G, \theta_G)$)
redshift (points to $[1 + z_G(\lambda)]^3$)
Galaxy number density (points to $n_G[x^\mu(\lambda), \theta_G]$)

[Cusin, Pitrou, JPU, 1704.06184]

AGWB: General expression

This expression is covariant, valid in **any** spacetime geometry.

- It requires
- the determination of the past lightcone structure
[geodesis of the spacetime]
 - a cosmological model
[galaxy distribution, ...]
 - an astrophysical model
[type of sources / emissivity / effective luminosity]

At background level (FL), it recovers the standard formula used in the literature

$$\frac{d^3 \rho_{\text{GW}}}{d\nu_0 d^2 \Omega_0}(\nu_0) = \frac{1}{4\pi H_0} \int d\bar{z} \frac{1}{E(\bar{z})} \frac{1}{(1 + \bar{z})^4} \int d\theta_G \bar{n}_G(\bar{z}, \theta_G) \mathcal{L}_G(\nu_G, \theta_G)$$

Perturbed FL

Spacetime metric at linear order in (scalar) perturbation

$$ds^2 = a^2 \left[-(1 + 2\psi)d\eta^2 + (1 - 2\phi)\delta_{ij}dx^i dx^j \right]$$

Bardeen potentials

$$\psi = \Psi + \Pi, \quad \phi = \Psi - \Pi.$$

Velocity field

$$u^\mu \equiv \frac{1}{a}(1 - \psi, v^i) \equiv \bar{u}^\mu + \delta u^\mu$$

Perturbed FL: general expression

Gathering these 3 elements and plugging in the general formula, one gets

$$\Omega_{\text{GW}} = \frac{1}{4\pi} \bar{\Omega}_{\text{GW}} + \delta\Omega_{\text{GW}}(\mathbf{e}, \nu_0)$$

$$\delta\Omega_{\text{GW}}(\mathbf{e}, \nu_0) = \frac{\nu_0}{\rho_c} \mathcal{E}(\eta_0, \mathbf{x}_0, \mathbf{e}, \nu_0)$$

$$\mathcal{E} = \frac{1}{4\pi} \int d\eta a^4 \int d\theta_G \bar{n}_G \mathcal{L}_G(\nu_G, \theta_G) \left[\delta_G + 4\Psi + 4\Pi - 2\mathbf{e} \cdot \nabla v - 6 \int_{\eta_0}^{\eta} d\eta' \dot{\Psi} \right]$$

Local physics

Local overdensity

Einstein effect

Doppler

Integrated « SW »

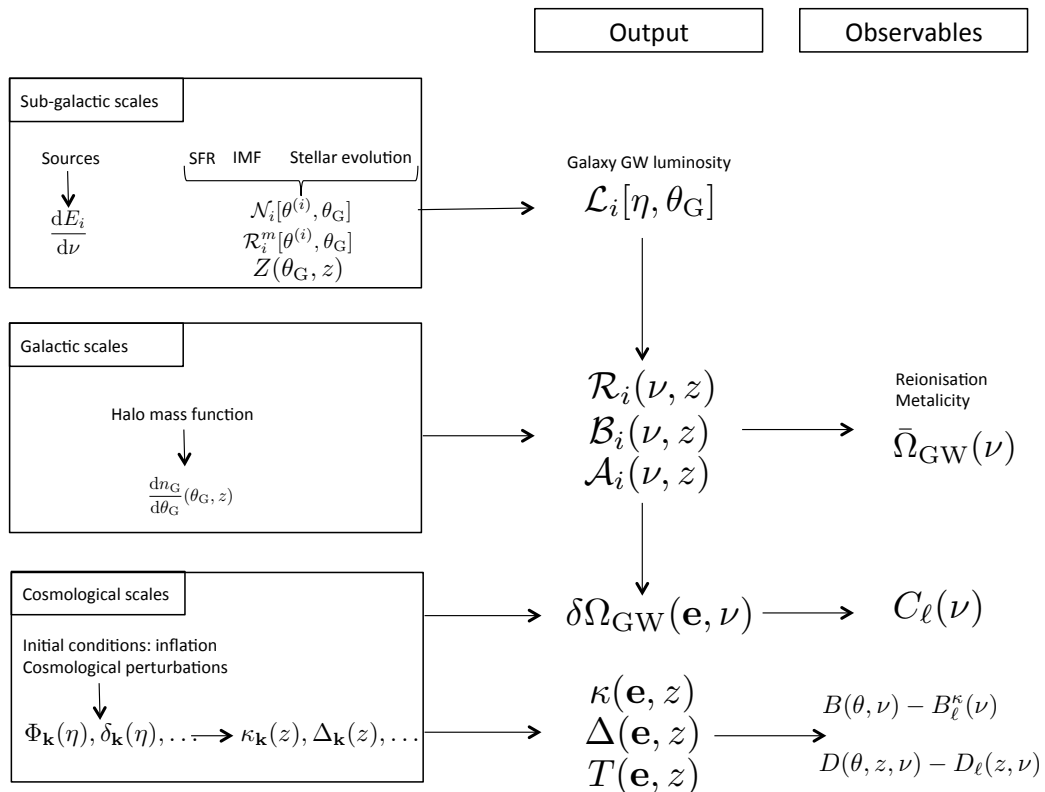
Perturbed FL: general expression

$$\delta\Omega_{GW}(\mathbf{e}, \nu_o) = \frac{\nu_o}{4\pi\rho_c} \int_{\eta_*}^{\eta_o} d\eta \mathcal{A}(\eta, \nu_o) \left[\delta_G + 4\Psi - 2\mathbf{e} \cdot \nabla v + 6 \int_{\eta}^{\eta_o} d\eta' \dot{\Psi} \right] \\ + \frac{\nu_o}{4\pi\rho_c} \int_{\eta_*}^{\eta_o} d\eta \mathcal{B}(\eta, \nu_o) \left[\mathbf{e} \cdot \nabla v - \Psi - 2 \int_{\eta}^{\eta_o} d\eta' \dot{\Psi} \right]$$

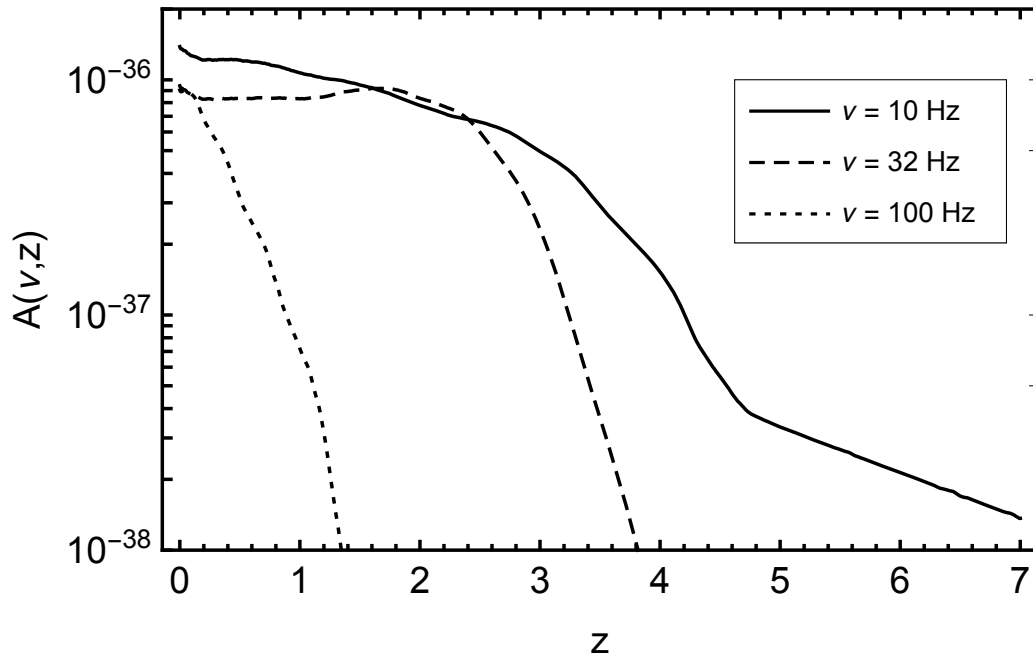
$$\mathcal{A}(\eta, \nu_o) \equiv a^4 \bar{n}_G(\eta) \int d\theta_G \mathcal{L}_G(\eta, \bar{\nu}_G, \theta_G)$$

$$\mathcal{B}(\eta, \nu_o) \equiv a^3 \nu_o \bar{n}_G(\eta) \int d\theta_G \left. \frac{\partial \mathcal{L}_G}{\partial \nu_G} \right|_{\bar{\nu}_G}(\eta, \bar{\nu}_G, \theta_G)$$

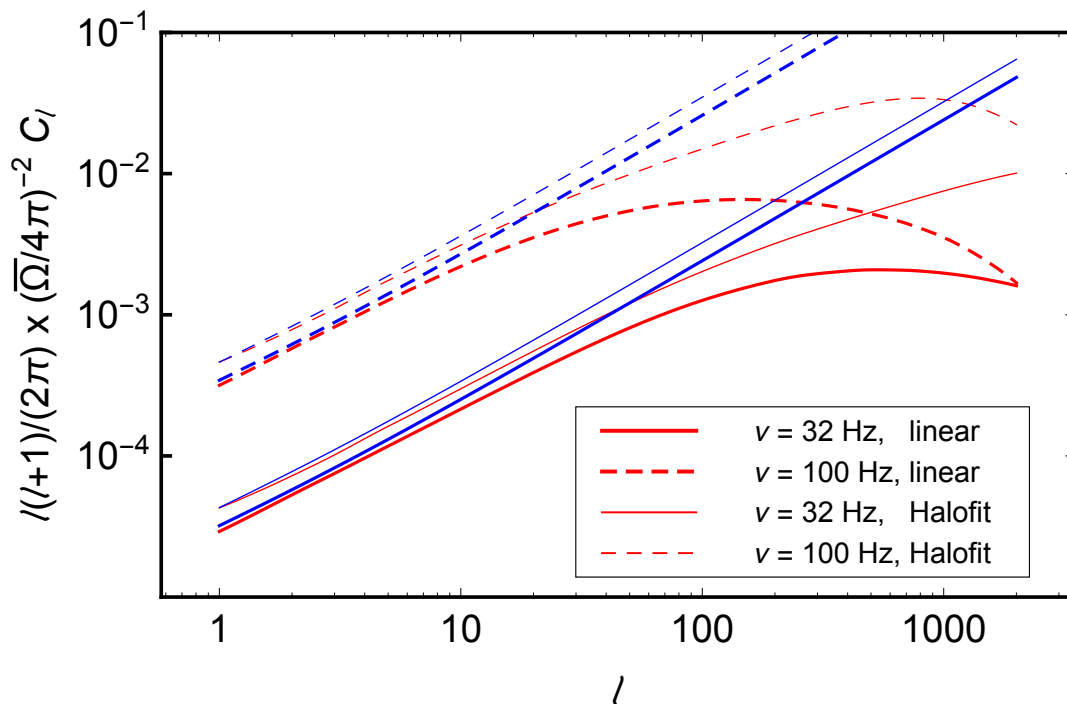
Now one needs the angular power spectrum of this thing.



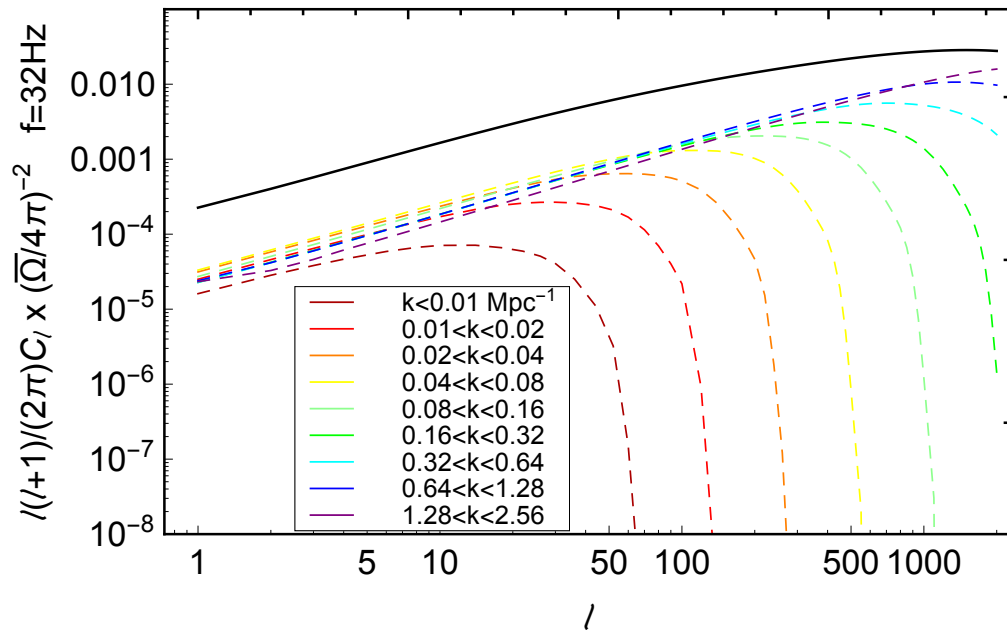
BH-mergers source function



Cl: first prediction – BH mergers



Cl: first prediction – BH mergers



[Cusin, Dvorkin, Pitrou, JPU, (in prep.)]

Cl: analytic estimation

On large scales, the dominant contribution arises from the density contrast and from the contribution at late time.

Assuming bias scales at $(1+z)^{1/2}$ and matter dominated

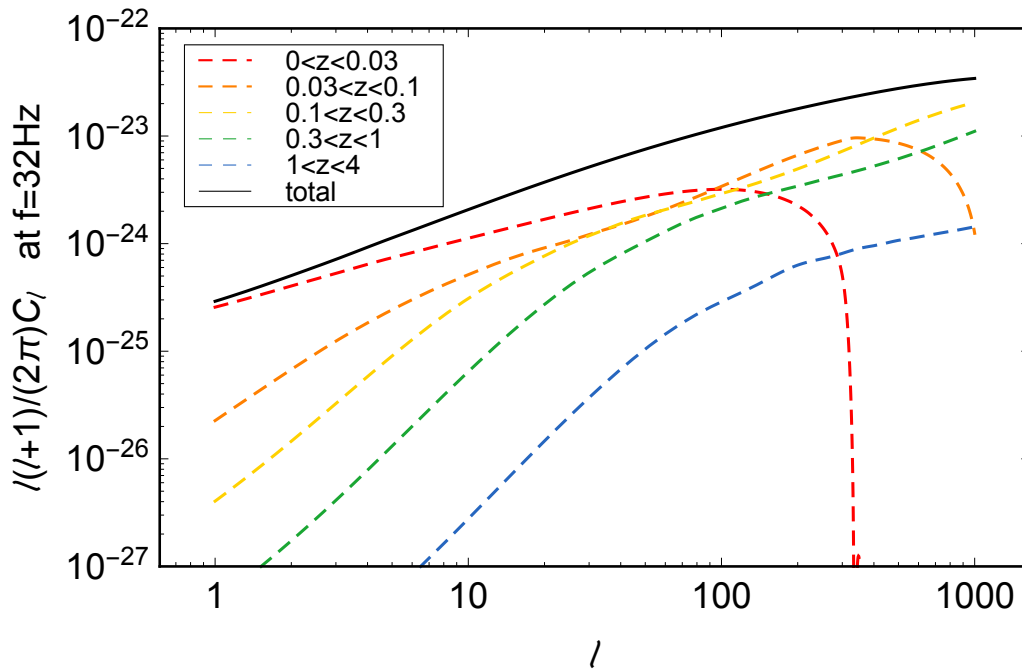
$$\left(\ell + \frac{1}{2}\right)C_\ell(\nu_0) \simeq \left[\frac{\nu_0 \mathcal{A}(\eta_0, \nu_0) b(\eta_0)}{4\pi \rho_c} \right]^2 \int_{k_{\min}} P_\delta(k) dk$$

Variance due to the large scale structure can be estimated to be

$$\sigma_{\text{GW}}^2(\nu_0) \equiv \sum_{\ell} \frac{(2\ell + 1)}{4\pi} C_\ell(\nu_0)$$

	32 Hz	100 Hz
NL	14%	32%
L	8%	16%

Cl: z-dependence

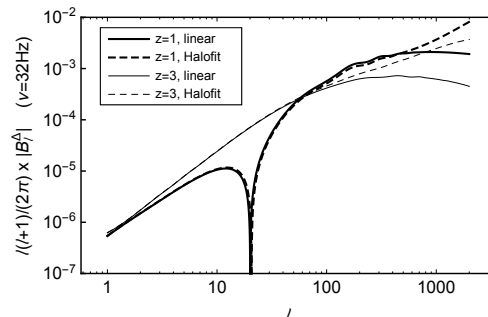
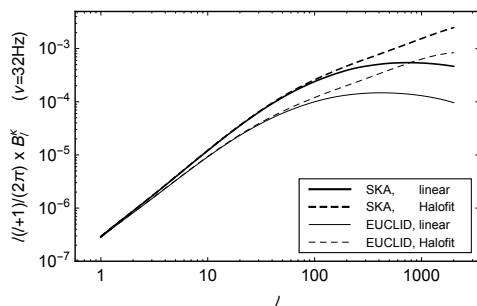
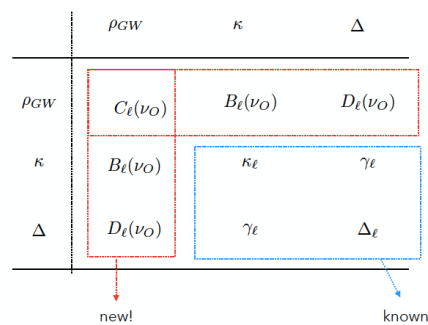


Cross-correlations

General expression has a cosmological and a local astrophysical components

New observables correlated with all other cosmological probe

Long way to detection but still a lot of thing to dig



Conclusions

First expression of the astrophysical GW background

First shape of the angular power spectrum for BH-merger sources

Stellar evolution models lead to significantly different predictions for binary-BH systems distribution.

Lots need to be done:

- explore dependence on astrophysical models
- most of the astrophysical parameters are badly known
- explore effects of the cosmology
- include other sources

It opens a potential new window bridging astrophysics and cosmology

- understand the population of stellar BH
- test correlation between BH and dark matter distribution.

- Upper bounds obtained by LIGO up to $l=7$

- and indeed, you can even put PBH....

References and sources

Astrophysical models

- *Metallicity-constrained merger rates of binary black holes and the stochastic gravitational wave background* [[1604.04288](#)], I. Dvorkin, E. Vangioni, J. Silk, J.-P. Uzan, and K. Olive, *Month. Not. R. Astron. Soc.* **461**, 3877 (2016).
- *A synthetic model of the gravitational wave background from evolving compact objects* [[1607.06818](#)], I. Dvorkin, J.-P. Uzan, E. Vangioni, and J. Silk, *Phys. Rev. D* **94**, 103011 (2016)
- *Exploring stellar evolution with gravitational-wave observations* [[1709.09197](#)], I. Dvorkin, J.-P. Uzan, E. Vangioni, and J. Silk, *Month. Not. Astron. Soc.* **479**, 121 (2018)

AGWB formalism

- *Anisotropy of the astrophysical gravitational wave background I: analytic expression of the angular power spectrum and correlation with cosmological observations*, G. Cusin, C. Pitrou, and J.-P. Uzan, *Phys. Rev. D* **96**, 103019 (2017)
- *The signal of the stochastic gravitational wave background and the angular correlation of its energy density* [[arXiv:1711.11345](#)], G. Cusin, C. Pitrou, and J.-P. Uzan, *Phys. Rev. D* **97**, 123527 (2018)

Numerical computation

- *First predictions of the angular power spectrum of the astrophysical gravitational wave background* [[1803.03236](#)] G. Cusin, I. Dvorkin, C. Pitrou, and J.-P. Uzan, *Phys. Rev. Lett.* **120**, 231101 (2018)

Nov. 16th

26th CGPM

The International System of Units (SI)

Palais des Congrès, Versailles | Friday 16th November 2018 | 11 a.m. Paris time (10:00 UTC)

Witness a historic moment; join an open session of the General Conference on Weights and Measures (CGPM) considering the revision of the SI – including redefinition of four of the base units



Connect to the BIPM's YouTube channel on 16 November 2018 at 11 a.m. Paris time (10:00 UTC), to watch the live open session of the 26th General Conference on Weights and Measures:

<https://www.youtube.com/thebipm>



ON THE MOON AGAIN!

GET YOUR TELESCOPE OUT TO SHARE THE MOON ON JULY 12 AND 13 2019

SUPPORT COMMITTEE

- Nabila Aghanim (IAS, Orsay, France)
- Djounai Baba Aissa (CRAAG, Algeria)
- Steven Balbus (Oxford University, England, UK)
- Damdin Batmunkh (Mongolian Academy of Sciences, Mongolia)
- Zouhair Benkhaldoun (Cadi Ayyad University, Morocco)
- Sevar Helgi Björnsson (Iceland)
- Hasnaa Chenmaoui (Hassan II Casablanca University, Morocco)
- Jean-François Cleroy (Astronaut, France)
- Françoise Combes (Observatoire de Paris, Collège de France)
- Robert A. Craddock (Smithsonian Institution, Washington, USA)
- Peter Dunsby (University of Cape Town, South Africa)
- Dirk Frimout (Astronaut, Belgium)
- Claudie Haigneré (European Space Agency, Astronaut, France)
- Kamil Hornoch (Ondrejov, Czech Republic)
- Maram Kaire (ASPA, Senegal)
- Kevin Gøvender (IAU, South Africa)
- James W. Head III (Brown University, USA)
- Gulchera Kokhirova (Institute of Astrophysics, Dushanbe, Tajikistan)
- Michel Mayor (Observatoire de Genève, Suisse)
- John Mather (Nobel Prize Physics 2006, USA)
- Claire Moutou (CFHT, Hawaii & IRAP, Toulouse, France)
- Chingis Omarov (Fesenkov Astrophysical Institute, Kazakhstan)
- Arno Penzias (Astrophysicist, Nobel Laureate Physics, 1978)
- Saul Perlmutter (Berkeley University, Nobel Laureate in Physics, 2011, USA)
- Martin Rees (Cambridge, England)
- Hubert Reeves (France)
- Adam Riess, (Nobel Laureate in Physics, 2011, USA)
- Pranav Sharma (Birla Science Centre, Hyderabad, India)
- B.G.Sidharth (Birla Science Centre, Hyderabad, India)
- George Smoot (Nobel Laureate, 2006, USA)
- Naoshi Sugiyama (Nagoya University, Japan)
- Joseph Taylor (Nobel Laureate in Physics, 1993, USA)
- Solomon Tessema Belay (Ethiopia)
- Caroline Terquem (Oxford University, England)
- Michel Tognini (European Space Agency, Astronaut, France)
- Amanda Weltman (University of Cape Town, South Africa)
- Simon White (MPI for Astrophysics, Munich, Germany)
- Alexander Wolszczan (Penn State University, USA)

JOIN ON
<https://www.onthemoonagain.org>

Session S5A 10:45–12:00

[Chair: Hideki Asada]

Atsushi Nishizawa

KMI, Nagoya University

**“Test of the equivalence principle at cosmological distance with
gravitational waves”**

(10+5 min.)

[JGRG28 (2018) 110903]

Test of the equivalence principle at cosmological distance with gravitational waves

Atsushi Nishizawa (KMI, Nagoya U.)

Nov. 5-9, 2018 @ Rikkyo U.
28th JGRG

Test of gravity with GWs

- GWs from 5 BBH and 1 BNS have been detected so far.

LIGO Scientific Collaboration 2016-2017

- GW propagation

$$h''_{ij} + (2 + \nu)\mathcal{H}h'_{ij} + (c_T^2 k^2 + a^2 \mu^2)h_{ij} = 0$$

- graviton mass $\mu \leq 7.7 \times 10^{-23}$ eV

LIGO Scientific
Collaboration 2017

- From GW170817/GRB170817A, GW speed has been measured so precisely

LSC + Fermi + INTEGRAL, ApJL 848, L13

$$-3 \times 10^{-15} < \frac{c_T - c}{c} < 7 \times 10^{-16}$$

- Constraint on amplitude damping rate

$$-75.3 \leq \nu \leq 78.4$$

Arai & Nishizawa 2018

GW amplitude damping

Set $c_T = 1$, $\mu = 0$, $h''_{ij} + (2 + \nu)\mathcal{H}h'_{ij} + k^2 h_{ij} = 0$

↓

$$h = e^{-\mathcal{D}} h_{\text{GR}} \quad \mathcal{D} = \frac{1}{2} \int_0^z \frac{\nu}{1+z'} dz'$$

Nishizawa 2018

↓

in Horndeski theory

$$e^{-\mathcal{D}} = \frac{M_*(z)}{M_*(0)} = \sqrt{\frac{G_{\text{gw}}(0)}{G_{\text{gw}}(z)}} \quad G_{\text{gw}} : \text{gravitational constant for GWs}$$

effective distance to a source $d_{\text{L,eff}}(z) = \sqrt{\frac{G_{\text{gw}}(z)}{G_{\text{gw}}(0)}} d_{\text{L}}(z)$

Source redshift is necessary to compare with true distance.

Equivalence principle in modified gravity

GWs $G_{\text{gw}} \quad \mathcal{L}_{\text{gw}} = \frac{1}{64\pi G_{\text{gw}}} \left\{ \dot{h}_{ij}^2 - a^{-2} (\nabla h_{ij})^2 \right\}$

galaxy clustering G_{matter}
 $k^2 \Psi = -4\pi G_{\text{matter}}(k, \tau) \delta \rho_m$

All are G_{N}
in GR

gravitational lensing G_{light}
 $k^2 (\Psi + \Phi) = -8\pi G_{\text{light}}(k, \tau) \delta \rho_m$

Well constrained at small scale, but not at cosmological distance yet.

In modified gravity that explains the cosmic accelerating expansion, the equivalence principle is likely to be broken.

Horndeski theory

$$S = \int dx^4 \sqrt{-g} \left(\sum_{i=2}^5 \mathcal{L}_i + \mathcal{L}_m \right)$$

Horndeski 1974
Deffayet, Gao, Steer, and Zahariade 2011
Kobayashi, Yamaguchi, Yokoyama 2011

$$\mathcal{L}_2 = G_2(\phi, X),$$

$$\mathcal{L}_3 = -G_3(\phi, X)\square\phi,$$

$$\mathcal{L}_4 = G_4(\phi, X)R + G_{4,X}(\phi, X) [(\square\phi)^2 - (\nabla_\mu\nabla_\nu\phi)(\nabla^\mu\nabla^\nu\phi)],$$

$$\mathcal{L}_5 = G_5(\phi, X)G_{\mu\nu}(\nabla^\mu\nabla^\nu\phi)$$

$$- \frac{1}{6}G_{5,X}(\phi, X) [(\square\phi)^3 - 3(\square\phi)(\nabla_\mu\nabla_\nu\phi)(\nabla^\mu\nabla^\nu\phi) + 2(\nabla^\mu\nabla_\alpha\phi)(\nabla^\alpha\nabla_\beta\phi)(\nabla^\beta\nabla_\mu\phi)]$$

- Most general scalar-tensor theory containing up to 2nd order spacetime derivatives.
- A single scalar field, but with four arbitrary functions of ϕ and $X = -\nabla_\mu\phi\nabla^\mu\phi/2 \longrightarrow G_2, G_3, G_4, G_5$

Gravitational constants in Horndeski theory

In the limit of quasi-static approximation,

De Felice, Kobayashi, Tsujikawa 2011
Pogosian & Silvestri 2016

Poisson eq.

$$G_{\text{matter}} = G_N \frac{M_{\text{pl}}^2}{M_*^2} (1 + \alpha_T + \beta_\xi^2) \quad \alpha_T = c_T^2 - 1$$

lensing eq.

$$G_{\text{light}} = G_N \frac{M_{\text{pl}}^2}{M_*^2} \left(1 + \frac{\alpha_T}{2} + \frac{\beta_\xi^2 + \beta_B\beta_\xi}{2} \right)$$

from scalar field fluctuations

Model parameter estimation

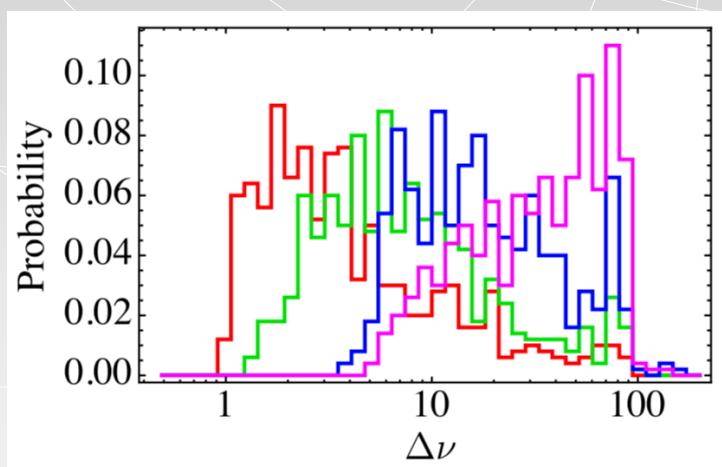
We estimate parameter errors with the Fisher information matrix.

- generate 500 sources with $\text{SNR} > 8$ for each case.
- source direction & inclination angles: uniformly random
- GW waveform:
 - phenomenological IMR waveform (PhenomD) for BBH
Khan et al. 2016
 - post-Newtonian inspiral waveform for BH-NS and BNS

Sensitivity with 2nd gen. detectors

Nishizawa 2018

HLV network, redshift prior $\Delta z = 10^{-3}$



constant ν, μ

- $30M_{\odot} - 30M_{\odot}$
- $10M_{\odot} - 10M_{\odot}$
- $10M_{\odot} - 1.4M_{\odot}$
- $1.4M_{\odot} - 1.4M_{\odot}$

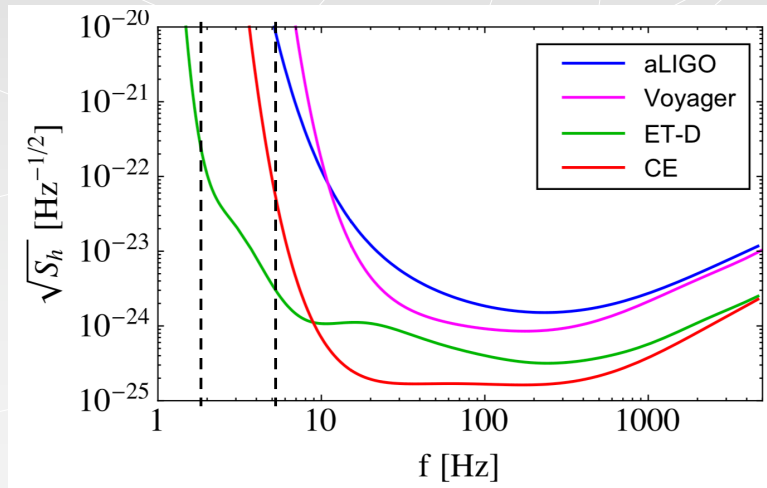
ν is measured with the error of $O(1)$

$$\left[h''_{ij} + (2 + \nu)\mathcal{H}h'_{ij} + c^2k^2h_{ij} = 0 \right]$$

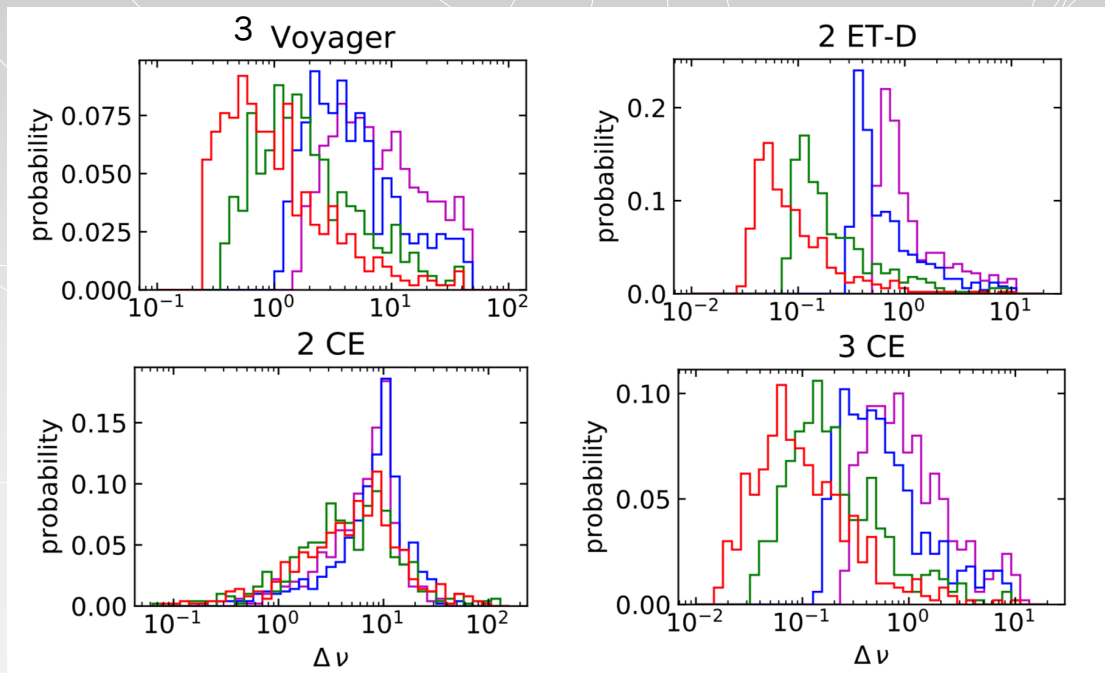
3rd gen. detectors

BNS can be observed for long time because of good sensitivity at low frequencies (1-10Hz).

Using time-dependent (Earth rotation) antenna pattern functions for BNS. (1 day at 2 Hz, 2 hours at 5 Hz before merger)



Sensitivity with 3rd gen. detectors



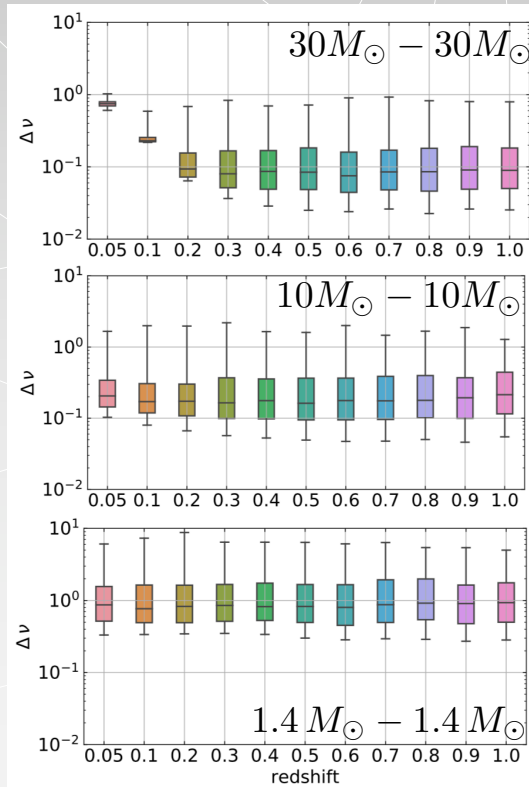
\mathcal{M} is measured with the error of O(0.01). Nishizawa & Arai, in prep.

Redshift dependence

$$\Delta\nu \sim 0.03$$

$$\Delta\nu \sim 0.07$$

$$\Delta\nu \sim 0.3$$



detector network
3 CE @ H, L, V

thick bars (25-75%)
thin bars (5-95%)

ν errors are independent
of source redshifts

$$\Delta\nu \sim \frac{2}{\log(1+z) \times \text{SNR}}$$

smaller errors for
heavier binaries
(due to larger SNR)

Summary

- The equivalence principle at cosmological distance has not been tested precisely yet and can be a key test for modified gravity theories that explain the cosmic accelerating expansion.
- Gravitational constant for GWs is probed by measuring the amplitude damping rate ν during GW propagation.
- current constraint from GW170817

$$-75.3 \leq \nu \leq 78.4$$
Arai & Nishizawa 2018

current detector network (aLIGO, KAGRA, etc.)

$$\Delta\nu \sim \mathcal{O}(1)$$

future detector network (ET-D, CE, etc.)

$$\Delta\nu \sim \mathcal{O}(0.01) \quad \longleftrightarrow \quad \dot{G}_N/G_N \lesssim 0.02 H_0$$

Yuki Watanabe

NIT, Gunma College

**“Probing the Starobinsky R² inflation with CMB precision
cosmology”**
(10+5 min.)

[JGRG28 (2018) 110904]

Probing the Starobinsky R^2 inflation with CMB precision cosmology

Yuki Watanabe
NIT, Gunma College

Based on JHEP 02(2018)118 [arXiv:1801.05736] with I. Dalianis;
JHEP 02(2015)105 [arXiv: 1411.6746] with T. Terada, Y. Yamada, J. Yokoyama

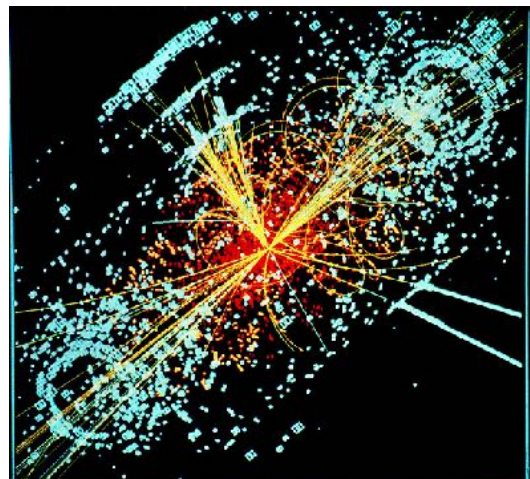
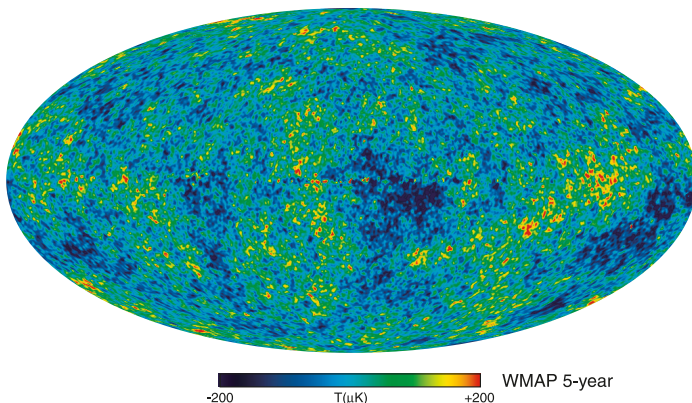


The 28th Workshop on General Relativity
and Gravitation in Japan
JGRG28

Tachikawa Memorial Hall, Rikkyo University
November 9, 2018

CMB observations and BSM physics

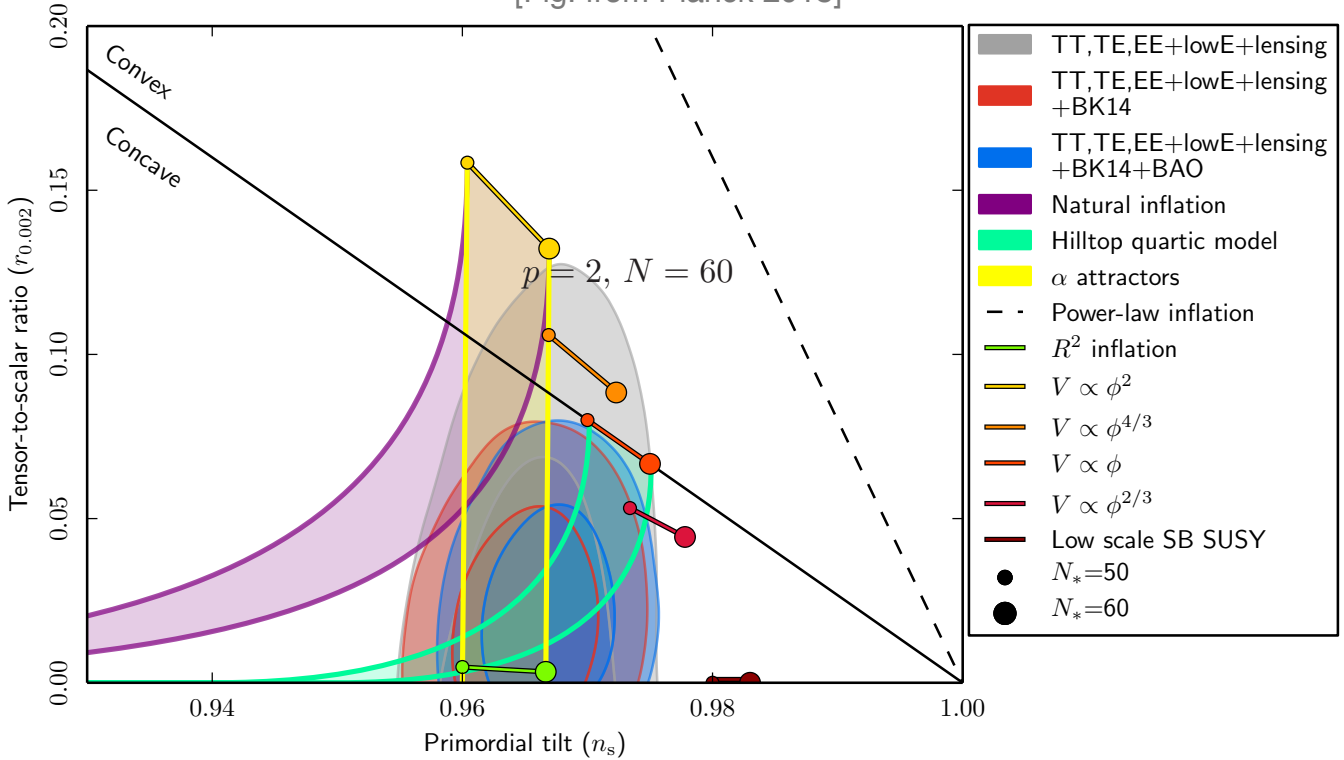
- (n_s, r) precision measurements from CMB
- No signal of physics beyond the Standard Model (BSM) at the LHC



credit: NASA

CMB constraint on inflation models

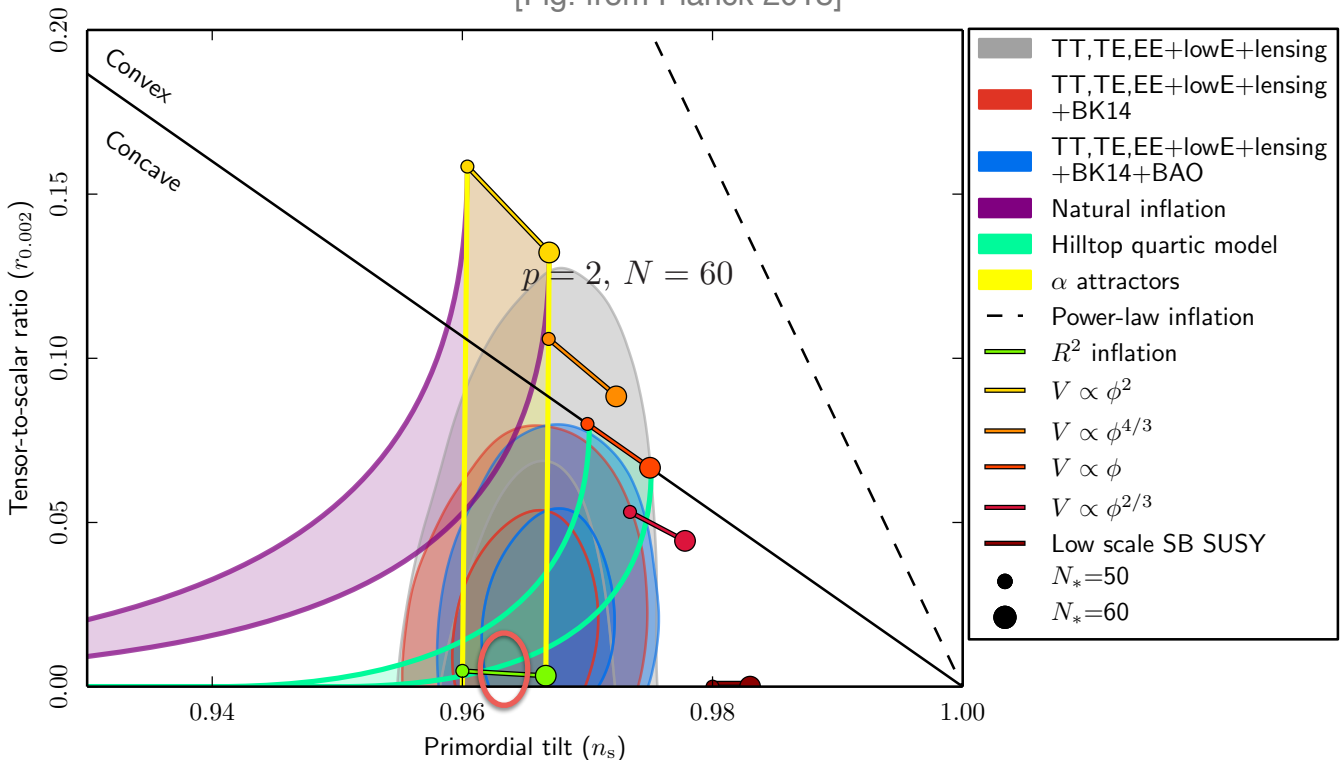
[Fig. from Planck 2018]



- Monomial potentials ($p \geq 2$) in GR are disfavored.

CMB constraint on inflation models

[Fig. from Planck 2018]



- Monomial potentials ($p \geq 2$) in GR are disfavored.
- What if we could nail down to further precision?

Starobinsky R² Inflation

[Starobinsky 1980; Mukhanov & Chibisov 1981]

$$S = \frac{1}{2\kappa^2} \int d^4x \sqrt{-g} \left(R + \frac{R^2}{6M^2} \right) + S_m$$

$$S_m = \int d^4x \sqrt{-g} \left[-\frac{1}{2} (\nabla\sigma)^2 - V(\sigma) \right] \quad \leftarrow \text{Higgs}$$

+ minimally coupled SM, RHN
+ “desert” or BSM

- One of the oldest models of Inflation, before models of Sato and Guth
- A single parameter **M** characterizes the model.

R² Inflation as scalar-tensor theory

[Whitt 1984; Maeda 1988]

$$S_J = \frac{1}{2\kappa^2} \int d^4x \sqrt{-\hat{g}} \left(\hat{R} + \frac{\hat{R}^2}{6M^2} \right) + S_m$$

$$S_m = \int d^4x \sqrt{-\hat{g}} \left[-\frac{1}{2} (\hat{\nabla}\hat{\sigma})^2 - V(\hat{\sigma}) \right]$$

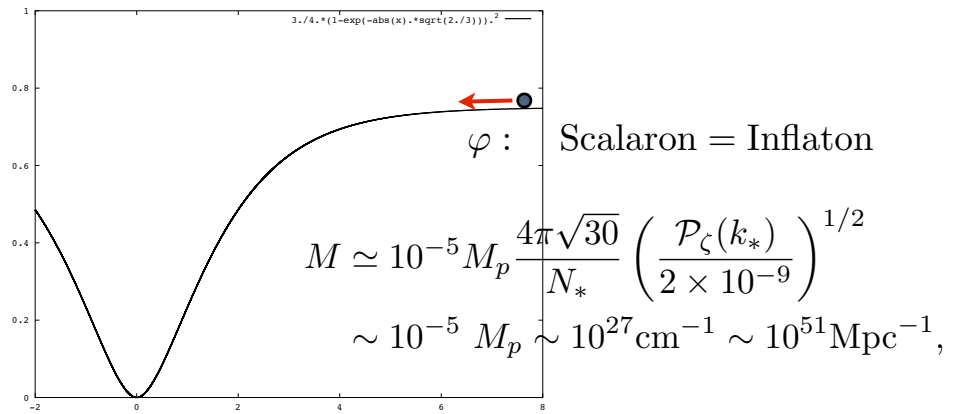
Jordan frame $\hat{g}_{\mu\nu}$ $\hat{g}_{\mu\nu} = g_{\mu\nu} \Omega^2$ $\Omega^2 = 2\kappa^2 \left| \frac{\partial \mathcal{L}_J}{\partial \hat{R}} \right| = 1 + \frac{\hat{R}}{3M^2} \equiv e^{\sqrt{\frac{2}{3}}\kappa\varphi}$
 Einstein frame $g_{\mu\nu}$ $\hat{R} = \Omega^2 [R + 3\Box(\ln \Omega^2) - \frac{3}{2}g^{\mu\nu}\partial_\mu(\ln \Omega^2)\partial_\nu(\ln \Omega^2)]$

$$S_E = \int d^4x \sqrt{-g} \left[\frac{1}{2\kappa^2} R - \frac{1}{2} (\nabla\varphi)^2 - U(\varphi) - \frac{1}{2} e^{-\sqrt{\frac{2}{3}}\kappa\varphi} (\nabla\hat{\sigma})^2 - e^{-\sqrt{\frac{8}{3}}\kappa\varphi} V(\hat{\sigma}) \right]$$

$$U(\varphi) = \frac{3}{4} M^2 M_p^2 \left(1 - e^{-\sqrt{\frac{2}{3}}\kappa\varphi} \right)^2 = \begin{cases} \frac{3}{4} M^2 M_p^2 & \text{for } \varphi \gg \varphi_f \\ \frac{1}{2} M^2 \varphi^2 & \text{for } \varphi \ll \varphi_f \end{cases}$$

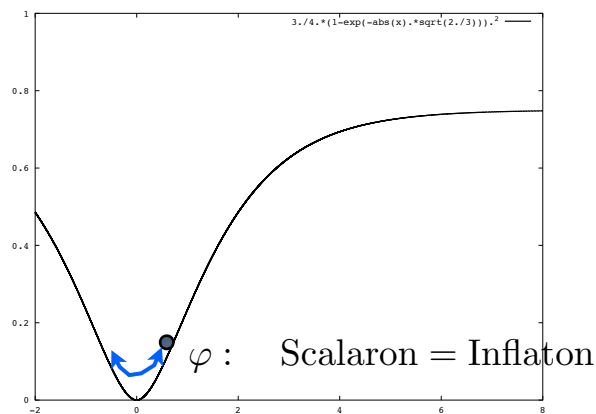
φ : Scalon = Inflaton

R² Inflation [Starobinsky 1980]



$$U(\varphi) = \frac{3}{4} M^2 M_p^2 \left(1 - e^{-\sqrt{\frac{2}{3}} \kappa \varphi} \right)^2 = \begin{cases} \frac{3}{4} M^2 M_p^2 & \text{for } \varphi \gg \varphi_f \\ \frac{1}{2} M^2 \varphi^2 & \text{for } \varphi \ll \varphi_f \end{cases}$$

R² Inflation [Starobinsky 1980]



$$U(\varphi) = \frac{3}{4} M^2 M_p^2 \left(1 - e^{-\sqrt{\frac{2}{3}} \kappa \varphi} \right)^2 = \begin{cases} \frac{3}{4} M^2 M_p^2 & \text{for } \varphi \gg \varphi_f \\ \frac{1}{2} M^2 \varphi^2 & \text{for } \varphi \ll \varphi_f \end{cases}$$

Gravitational reheating by scalaron decay

[YW & Komatsu gr-qc/0612120; YW 1011.3348; YW & White 1503.08430]

$$\sigma \equiv e^{-\frac{\kappa}{\sqrt{6}}\varphi} \hat{\sigma}$$

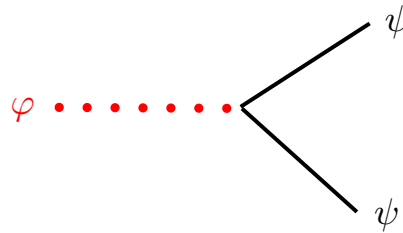
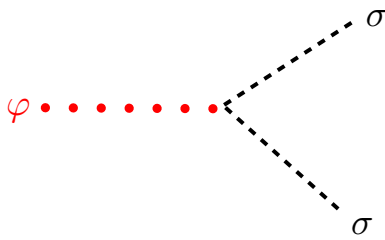
$$\mathcal{L}_{\text{scalar}} = -\frac{1}{2}\partial_\mu\sigma\partial^\mu\sigma - \frac{\kappa\sigma}{\sqrt{6}}\partial_\mu\sigma\partial^\mu\varphi - \frac{\kappa^2\sigma^2}{12}\partial_\mu\varphi\partial^\mu\varphi - \frac{m_\sigma^2}{2}e^{-\frac{2}{\sqrt{6}}\kappa\varphi}\sigma^2$$

$$\psi \equiv e^{-\frac{3\kappa}{2\sqrt{6}}\varphi} \hat{\psi}$$

$$\mathcal{L}_{\text{fermion}} = -\bar{\psi}\not{D}\psi - e^{-\frac{1}{\sqrt{6}}\kappa\varphi}m_\psi\bar{\psi}\psi$$



$$\mathcal{L}_{3\text{leg}} = \frac{1}{\sqrt{6}M_{\text{Pl}}}\varphi\partial^\mu\sigma\partial_\mu\sigma + \frac{2m_\sigma^2}{\sqrt{6}M_{\text{Pl}}}\varphi\sigma^2 + \frac{m_\psi^2}{\sqrt{6}M_{\text{Pl}}}\varphi\bar{\psi}\psi$$



Gravitational reheating by scalaron decay

[YW & Komatsu gr-qc/0612120; YW 1011.3348; YW & White 1503.08430]

$$\Gamma(\varphi \rightarrow \sigma\sigma) = \frac{\mathcal{N}_\sigma(M^2 + 2m_\sigma^2)^2}{192\pi M_{\text{Pl}}^2 M}$$

$$\simeq \frac{\mathcal{N}_\sigma M^3}{192\pi M_{\text{Pl}}^2} + \frac{\mathcal{N}_\sigma m_\sigma^2 M}{48\pi M_{\text{Pl}}^2}$$

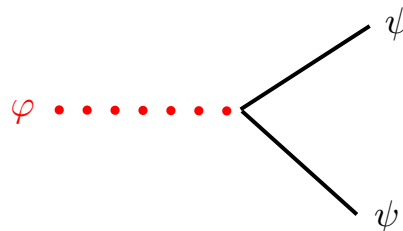
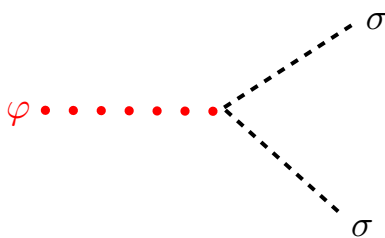
$$\Gamma(\varphi \rightarrow \bar{\psi}\psi) = \frac{\mathcal{N}_\psi m_\psi^2 M}{48\pi M_{\text{Pl}}^2}$$

Leading term



$$H_{\text{rh}} = \Gamma$$

$$T_{\text{rh}} \simeq 0.1\sqrt{\Gamma_{\text{tot}}M_p} \left(\frac{\mathcal{N}_{\text{tot}}}{100}\right)^{-1/4}$$



Gravitational reheating by scalaron decay

[YW & Komatsu gr-qc/0612120; YW 1011.3348; YW & White 1503.08430]

$$\Gamma(\varphi \rightarrow \sigma\sigma) = \frac{\mathcal{N}_\sigma(M^2 + 2m_\sigma^2)^2}{192\pi M_{\text{Pl}}^2 M}$$

$$\simeq \frac{\mathcal{N}_\sigma M^3}{192\pi M_{\text{Pl}}^2} + \frac{\mathcal{N}_\sigma m_\sigma^2 M}{48\pi M_{\text{Pl}}^2} \quad \Gamma(\varphi \rightarrow \bar{\psi}\psi) = \frac{\mathcal{N}_\psi m_\psi^2 M}{48\pi M_{\text{Pl}}^2}$$

Leading term
↓

$$T_{\text{rh}} \simeq 0.1 \sqrt{\Gamma_{\text{tot}} M_p} \left(\frac{\mathcal{N}_{\text{tot}}}{100} \right)^{-1/4} \sim 10^{-9} M_p,$$

$$N_* \simeq 54 + \frac{1}{3} \ln \left(\frac{T_{\text{rh}}}{10^9 \text{ GeV}} \right),$$

If we know the matter sector (e.g. SM minimally coupled to gravity),
inflationary predictions can be made without uncertainty.

Predictions depend on reheating temperature

scalaron mass

$$M \simeq 10^{-5} M_p \frac{4\pi\sqrt{30}}{N_*} \left(\frac{\mathcal{P}_\zeta(k_*)}{2 \times 10^{-9}} \right)^{1/2}$$

$$\sim 10^{-5} M_p \sim 10^{27} \text{ cm}^{-1} \sim 10^{51} \text{ Mpc}^{-1},$$

$$\sim 10^{13} \text{ GeV}$$

e-folds of inflation

$$N_* \simeq 54 + \frac{1}{3} \ln \left(\frac{T_{\text{rh}}}{10^9 \text{ GeV}} \right),$$

grav. waves

$$r = \frac{\mathcal{P}_\gamma(k)}{\mathcal{P}_\zeta(k)} \simeq 16\epsilon \simeq \frac{12}{N_*^2}.$$

tilt and running of spectra

$$n_s - 1 = \frac{d \ln \mathcal{P}_\zeta(k)}{d \ln k} \simeq -6\epsilon_V + 2\eta_V \simeq -\frac{2}{N_*},$$

$$n_t = \frac{d \ln \mathcal{P}_\gamma(k)}{d \ln k} \simeq -2\epsilon_V \simeq -\frac{3}{2N_*^2},$$

$$\frac{dn_s}{d \ln k} \simeq 16\epsilon_V \eta_V - 24\epsilon_V^2 - 2\xi_V^2 \simeq -\frac{2}{N_*^2},$$

$$\frac{dn_t}{d \ln k} \simeq 4\epsilon_V \eta_V - 8\epsilon_V^2 \simeq -\frac{3}{N_*^3},$$

Preheating in R² inflation (Minkowski) [Takeda & YW 1405.3830]

$$\phi(x, t) = \phi_0(t) + \delta\phi(x, t)$$

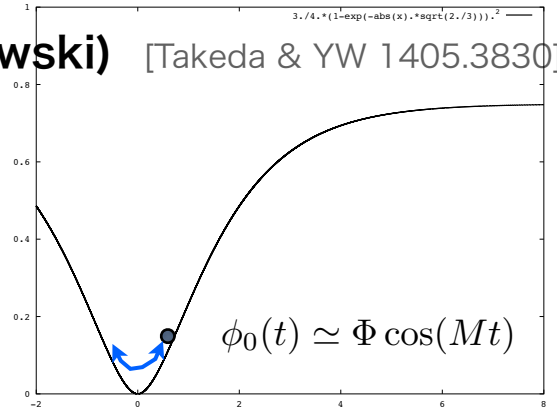
$$\delta\ddot{\phi}_k + \omega_k^2 \delta\phi_k = 0$$

$$\omega_k^2 = k^2 + M^2 \left[1 + \frac{7}{6} \left(\frac{\Phi}{M_p} \right)^2 \right] - \sqrt{6} M^2 \frac{\Phi}{M_p} \cos(Mt) + \frac{7}{6} M^2 \left(\frac{\Phi}{M_p} \right)^2 \cos(2Mt)$$

$$\delta\phi_k'' + \left[A_{1k} - 2q_1 \cos(2\hat{T}) \right] \delta\phi_k = 0$$

$$q_1 \equiv 2\sqrt{6} \frac{\Phi}{M_p},$$

$$A_{1k} \equiv 4 + 4 \left(\frac{k}{M} \right)^2 + \frac{7}{36} q_1^2$$



2nd narrow resonance:

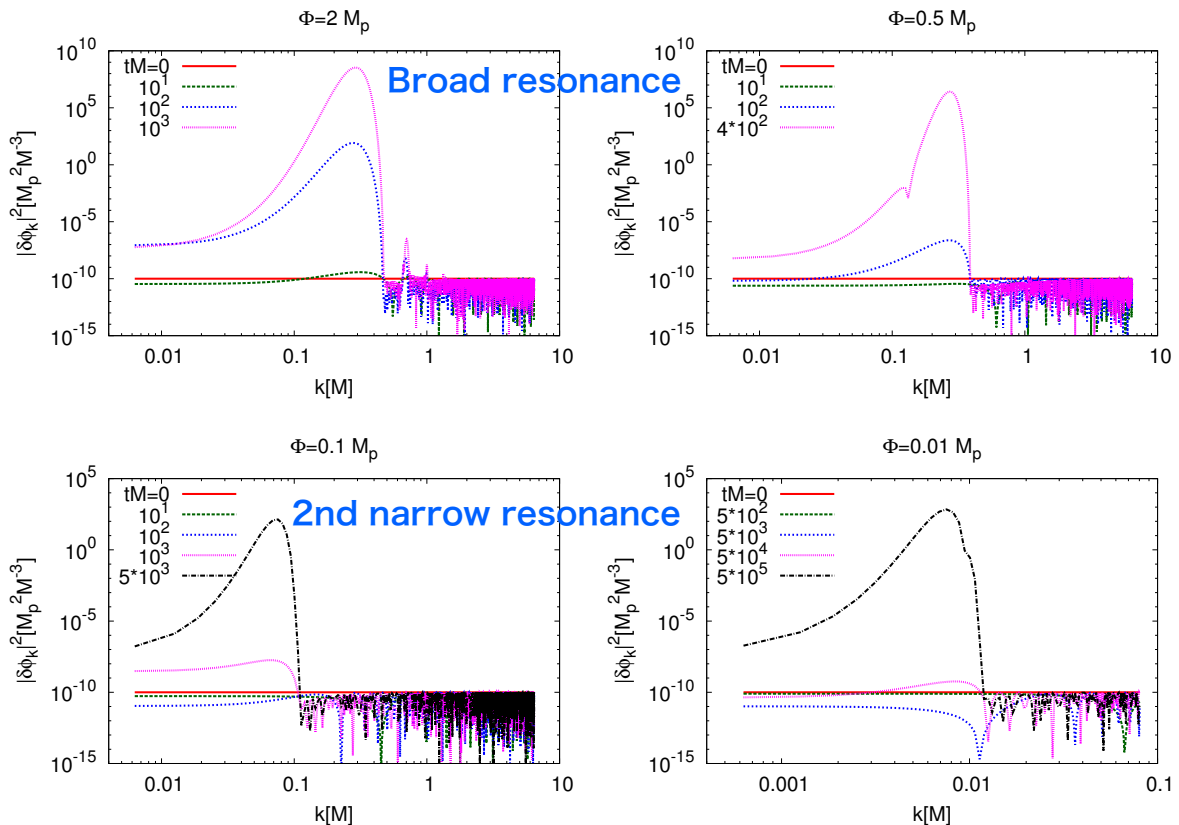
$$0 \leq \frac{k}{M} < \frac{q_1}{3\sqrt{2}} \quad -\frac{q^2}{12} < A_k - 4 < \frac{5q^2}{12}, \quad \Phi < 0.2M_p$$

Broad resonance: $|d\omega/dt|/\omega^2 > 1$ $0.2M_p \lesssim \Phi \lesssim 2M_p$

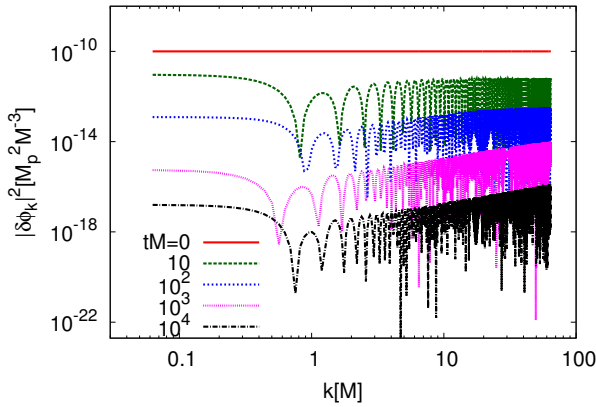
$$\left(\frac{k}{M} \right)^2 < -1 - \frac{7}{6} \left(\frac{\Phi}{M_p} \right)^2 + \sqrt{6} \frac{\Phi}{M_p} \cos(Mt) + \left(\frac{3}{2} \right)^{\frac{1}{3}} \left(\frac{\Phi}{M_p} \right)^{\frac{2}{3}} |\sin(Mt)|^{\frac{2}{3}},$$

Parametric resonant spectrum

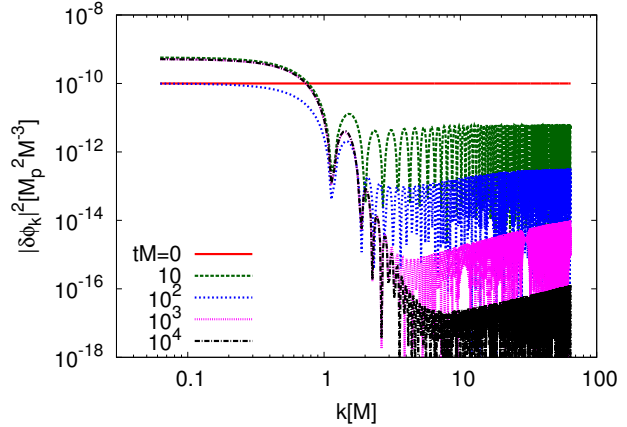
[Takeda & YW 1405.3830]



Preheating in R² inflation (Friedmann) [Takeda & YW 1405.3830]



Without back-reaction from metric, Hubble damping wins over instabilities.



With back-reaction from metric, preheating is balanced with Hubble damping.

MS eqn:

$$\delta\ddot{\phi}_k + 3H\delta\dot{\phi}_k + \underbrace{\left[\frac{k^2}{a^2} + V''(\phi_0) + \Delta F \right]}_{\omega_k^2} \delta\phi_k = 0,$$

Back-reaction
from metric:

$$\Delta F \equiv \frac{2\dot{\phi}_0}{M_p^2 H} V'(\phi_0) + \frac{\dot{\phi}_0^2}{M_p^4 H^2} V(\phi_0).$$

Metric preheating in R² inflation [Takeda & YW 1405.3830]

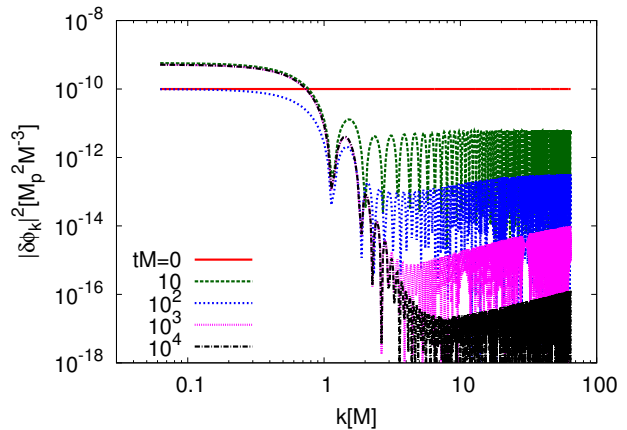
$$\phi_0(t) \simeq \phi_0(t_{\text{ini}}) \left(\frac{a_{\text{ini}}}{a} \right)^{\frac{3}{2}} \sin(Mt)$$

$$\omega_k^2 \simeq \frac{k^2}{a^2} + M^2 \left(1 - \sqrt{6} \frac{\phi_0}{M_p} + \frac{2\dot{\phi}_0 \phi_0}{H M_p^2} \right)$$

$$\widetilde{\delta\phi}_k'' + \left[A_{3k} - 2q_3 \cos(2\hat{T}) \right] \widetilde{\delta\phi}_k = 0$$

$$q_3 \equiv \frac{a_{\text{ini}}^3 \phi_0^2(t_{\text{ini}}) M}{2a^3 H M_p^2}, \quad A_{3k} \equiv 1 + \frac{k^2}{a^2 M^2}.$$

$$\widetilde{\delta\phi}_k \equiv a^{3/2} \delta\phi_k$$



1st narrow resonance: $-q^2 < A_k - 1 < q^2$,

$$0 \leq \frac{k}{M} \lesssim a_{\text{ini}} H_{\text{ini}} \sqrt{\frac{3a_{\text{ini}}}{a H M}} \propto a^{1/2}$$

The resonance is not strong enough to form quasi-stable objects!

Higher derivative SUGRA [Cecotti 1987; Ferrara & Porrati 2014]

R is the supercurvature

$$S = \int d^4x d^4\theta E (N(\mathcal{R}, \bar{\mathcal{R}}) + J(\phi, \bar{\phi} e^{gV})) \quad \phi, \mathbf{V} \text{ are the matter sector}$$

$$+ \left[\int d^4x d^2\Theta 2\mathcal{E} \left(F(\mathcal{R}) + P(\phi) + \frac{1}{4} h_{AB}(\phi) W^A W^B \right) + \text{H.c.} \right]$$

↓ **duality trans. by T, S (T is the Lagrange multiplier)**

$$S = \int d^4x d^2\Theta 2\mathcal{E} \frac{3}{8} (\bar{\mathcal{D}}\bar{\mathcal{D}} - 8\mathcal{R}) e^{-K/3} + W + \frac{1}{4} h_{AB} W^A W^B + \text{H.c.}$$

Kahler pot: $K = -3 \ln \left(\frac{T + \bar{T} - N(S, \bar{S}) - J(\phi, \bar{\phi} e^{gV})}{3} \right),$

Superpot: $W = 2TS + F(S) + P(\phi).$

Starobinsky SUGRA R2 inflation

[Terada, YW, Yamada, Yokoyama 1411.6746; Dalianis & YW 1801.05736]

$$\mathcal{L} = -3M_P^2 \int d^4\theta E \left[1 - \frac{4}{m_\Phi^2} \mathcal{R}\bar{\mathcal{R}} + \frac{\zeta}{3m_\Phi^4} \mathcal{R}^2 \bar{\mathcal{R}}^2 \right]$$

$$N(S, \bar{S}) = -3 + \frac{12}{m_\Phi^2} S\bar{S} - \frac{\zeta}{m_\Phi^4} (S\bar{S})^2$$

↓
S, ImT are stabilized.

$$F(S) = 0,$$

Real part of T becomes the inflaton:

$$V = \frac{3m_\Phi^2}{4} \left(1 - e^{-\sqrt{2/3} \widehat{\text{Re}} T} \right)^2$$

$$S = \int d^4x d^2\Theta 2\mathcal{E} \frac{3}{8} (\bar{\mathcal{D}}\bar{\mathcal{D}} - 8\mathcal{R}) e^{-K/3} + W + \frac{1}{4} h_{AB} W^A W^B + \text{H.c.}$$

$$K = -3 \ln \left(\frac{T + \bar{T} - N(S, \bar{S}) - J(\phi, \bar{\phi} e^{gV})}{3} \right),$$

$$W = 2TS + F(S) + P(\phi).$$

↓
Grav. coupling to matter

Starobinsky SUGRA R2 inflation

[Terada, YW, Yamada, Yokoyama 1411.6746; Dalianis & YW 1801.05736]

$$\mathcal{L} = -3M_P^2 \int d^4\theta E \left[1 - \frac{4}{m_\Phi^2} \mathcal{R}\bar{\mathcal{R}} + \frac{\zeta}{3m_\Phi^4} \mathcal{R}^2\bar{\mathcal{R}}^2 \right]$$

$$N(S, \bar{S}) = -3 + \frac{12}{m_\Phi^2} S\bar{S} - \frac{\zeta}{m_\Phi^4} (S\bar{S})^2$$

$$F(S) = 0,$$

Real part of T becomes the inflaton:

$$V = \frac{3m_\Phi^2}{4} \left(1 - e^{-\sqrt{2/3}\widehat{\text{Re}}T} \right)^2$$

SUSY breaking field:

$$J(z, \bar{z}) = |z|^2 - \frac{|z|^4}{\Lambda^2},$$

Z may dominate after inflation.

$$P(z) = \mu^2 z + W_0,$$

Constraints from gravitino abundance

[Terada, YW, Yamada, Yokoyama 1411.6746]

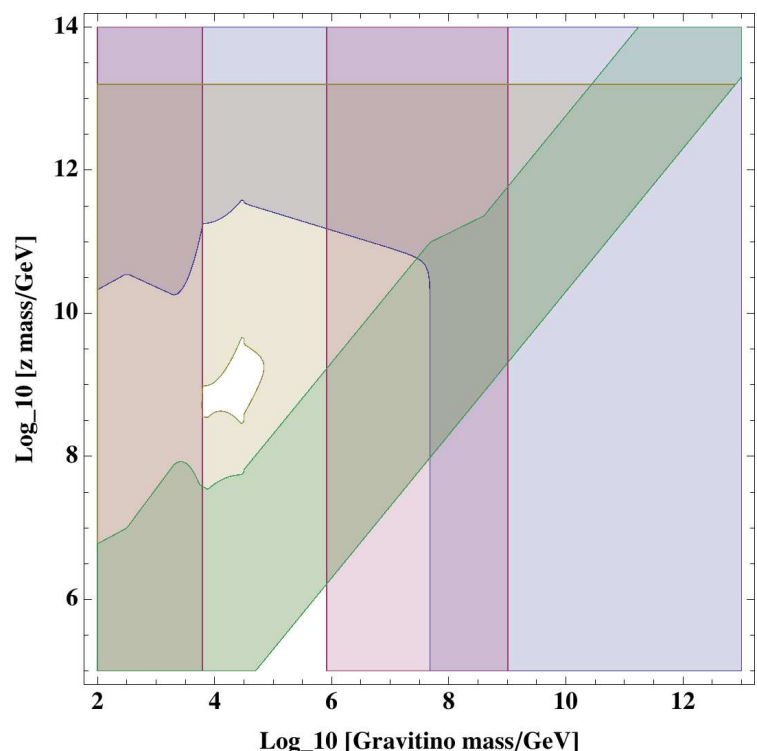
Gravitinos generated from:

- 1) inflaton decay
- 2) thermal scatterings
- 3) decay of particles
- 4) decay of oscillating Z

Wino LSP is assumed for:

gravitino mass $> 10^{4.5}$ GeV
 \rightarrow anomaly mediation

gravitino mass $< 10^{4.5}$ GeV
 \rightarrow gravity mediation

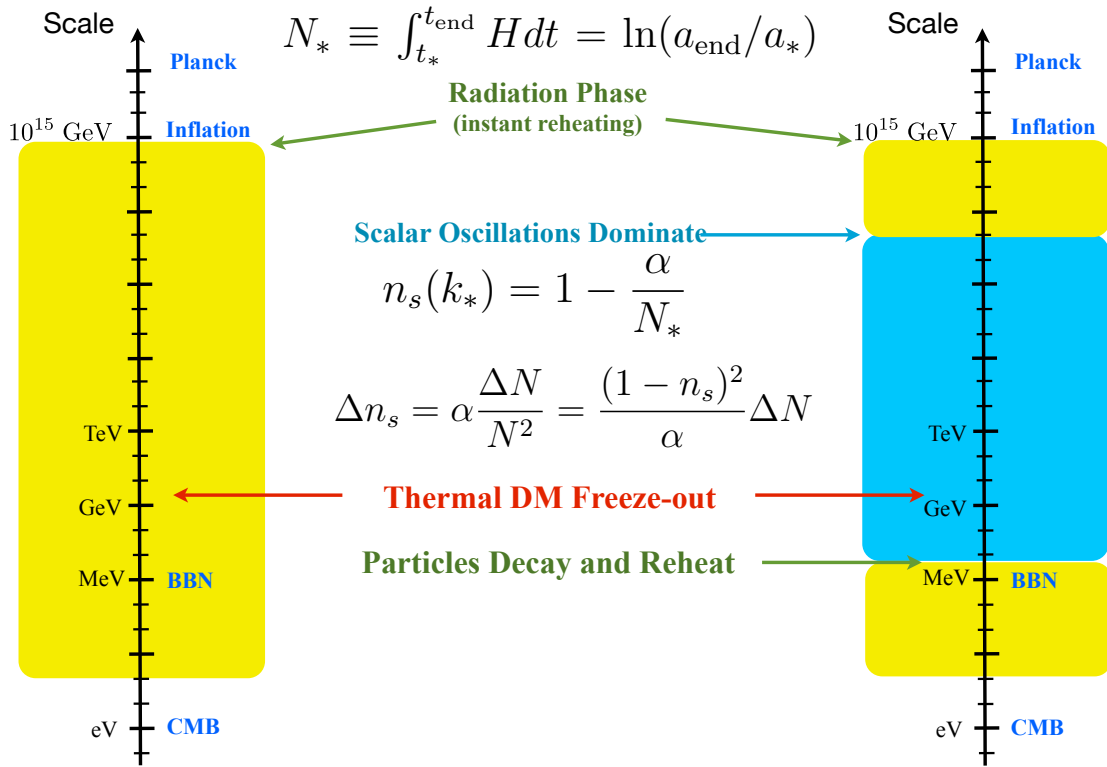


CMB uncertainties from the post-inflationary evolution

[Easter, Galvez, Ozsoy, Watson 2013]

Thermal History

Alternative History



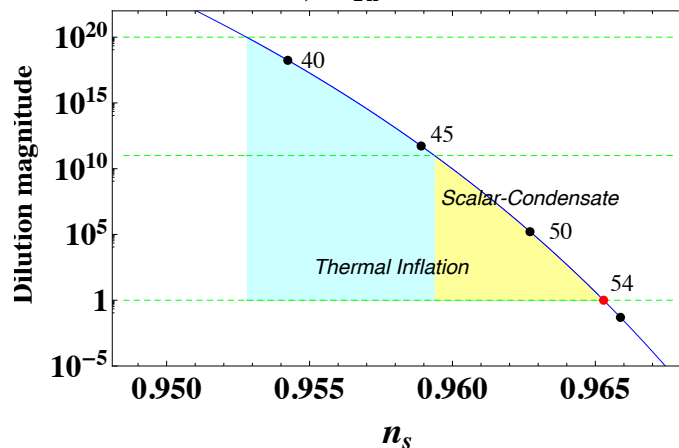
Shift in (n_s, r) due to late entropy production

- After inflaton decay, a diluter field X (modulus, flaton) may dominate the universe until BBN. Decays of X produce **entropy**:

$$\Delta N_X = \frac{1}{3} \ln \left[\left(\frac{g_*(T_X^{\text{dom}})}{g_*(T_X^{\text{dec}})} \right)^{1/4} D_X \right] \equiv \frac{1}{3} \ln \tilde{D}_X$$

$$D_X \equiv 1 + \frac{S_{\text{after}}}{S_{\text{before}}} = 1 + \frac{g_s(T_X^{\text{dec}}) g_*(T_X^{\text{dom}}) T_X^{\text{dom}}}{g_*(T_X^{\text{dec}}) g_s(T_X^{\text{dom}}) T_X^{\text{dec}}} \simeq \frac{T_X^{\text{dom}}}{T_X^{\text{dec}}} \geq 1$$

$$R^2, T_{\text{rh}} = 10^9 \text{ GeV}$$



Supersymmetric dark matter cosmology

Merits: Gauge coupling unification, stable dark matter, baryogenesis, stringy UV completion, ...

1. Gravitino LSP

2. Neutralino LSP (WIMP)

- Thermal DM (freeze out): thermal scatterings with the MSSM, messenger fields
- Non-thermal DM (freeze in): decays, thermal scatterings

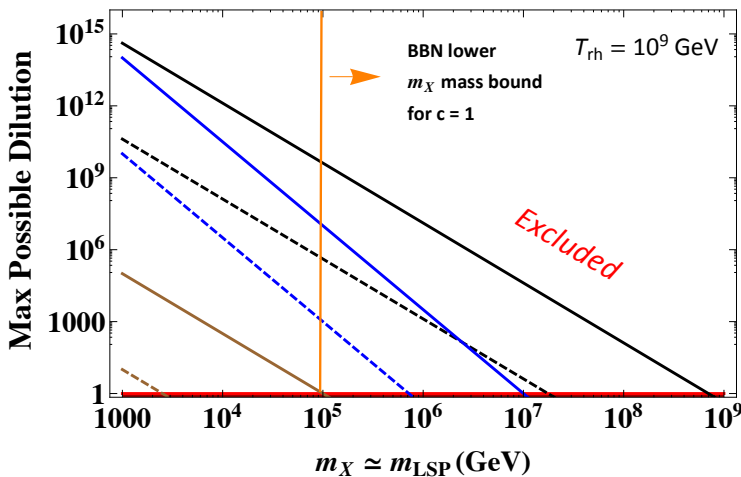
Light WIMP mass is disfavored by the LHC.

$\Omega_{\text{DM}h^2}$ is severely constrained when **sparticle masses increase**:

$$\Omega_{3/2} \propto m_{3/2}^\alpha \left(\frac{m_{\tilde{g}}}{m_{3/2}} \right)^\beta \left(\frac{m_{\tilde{f}}}{m_{3/2}} \right)^\gamma T_{\text{rh}}^\delta, \quad m_{3/2} < m_{\tilde{g}}, m_{\tilde{f}},$$

$$\Omega_{\tilde{\chi}^0} \propto m_{\tilde{\chi}^0}^{\tilde{\alpha}} m_{3/2}^{\tilde{\beta}} \left(\frac{m_{\tilde{f}}}{m_{3/2}} \right)^{\tilde{\gamma}} T_{\text{rh}}^{\tilde{\delta}}, \quad m_{\tilde{\chi}^0} < m_{3/2}, m_{\tilde{f}}$$

Alternative cosmic histories and SUSY



—	Dilution Bound
—	c=1, Gravitino LSP
- -	c=10 ⁸ , >> >>
—	c=1, Thermal Neutralino LSP
- -	c=10 ⁸ , >> >>
—	c=1, Thermal Gravitino LSP
- -	c=10 ⁸ , >> >>

$$\Gamma_X = \frac{c}{4\pi} \frac{m_X^3}{M_{\text{Pl}}^2}$$

★ High reheating temp. generally overproduce light LSP

→ Dilution of DM abundance is necessary: **diluter field X**

• If $D_X = 1$ then $T_{\text{rh}} \lesssim \tilde{m}$ or $\tilde{m} \sim \text{TeV}$

• If $\mathcal{O}(\text{TeV}) < (m_{\text{LSP}}, \tilde{m}) < T_{\text{rh}}$ then $D_X \geq D_X^{\text{min}} \equiv \frac{\Omega_{\text{LSP}}^{\leq}}{0.12 h^{-2}}$

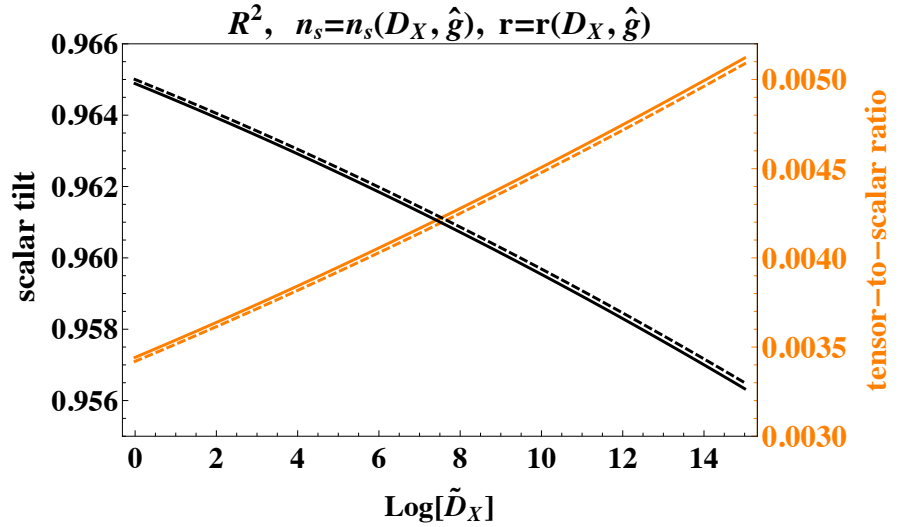
where \tilde{m} the sparticle mass scale.

CMB observables: Starobinsky R2 inflation

$$n_s^{(\text{th})} \Big|_{R^2} = 0.965,$$

$$r^{(\text{th})} \Big|_{R^2} = 0.0034$$

$$N^{(\text{th})} = 54$$



$$N_* \Big|_{R^2} = 55.9 + \frac{1}{4} \ln \epsilon_* + \frac{1}{4} \ln \frac{V_*}{\rho_{\text{end}}} + \frac{1}{12} \ln \left(\frac{g_{* \text{rh}}}{100} \right) + \frac{1}{3} \ln \left(\frac{T_{\text{rh}}}{10^9 \text{ GeV}} \right) - \Delta N_X$$

CMB observables: Starobinsky R2 inflation

[Dalianis & YW 1801.05736]

$$\mathcal{L} = -3M_P^2 \int d^4\theta E \left[1 - \frac{4}{m^2} \mathcal{R} \bar{\mathcal{R}} + \frac{\zeta}{3m^4} \mathcal{R}^2 \bar{\mathcal{R}}^2 \right] \quad + \text{MSSM, Z, X, (messengers)}$$

Gravitino DM (in GeV units)

#	m_Z	$m_{\tilde{g}}$	$m_{\tilde{f}}$	$m_{3/2}$ (LSP)	D_X	N_*	n_s	r	Origin
4	10^3	10^3	10^4	10	1	54	0.965	0.0034	Th

Neutralino DM

#	m_Z	$m_{3/2}$	$m_{\tilde{f}}$	$m_{\tilde{\chi}^0}$ (LSP)	$D_{(X)}$	N_*	n_s	r	Origin
4	10^5	10^5	10^5	10^3	1	54	0.965	0.0034	Th

CMB observables: Starobinsky R2 inflation

[Dalianis & YW 1801.05736]

$$\mathcal{L} = -3M_P^2 \int d^4\theta E \left[1 - \frac{4}{m^2} \mathcal{R}\bar{\mathcal{R}} + \frac{\zeta}{3m^4} \mathcal{R}^2\bar{\mathcal{R}}^2 \right] + \text{MSSM, Z, X, (messengers)}$$

Gravitino DM (in GeV units)

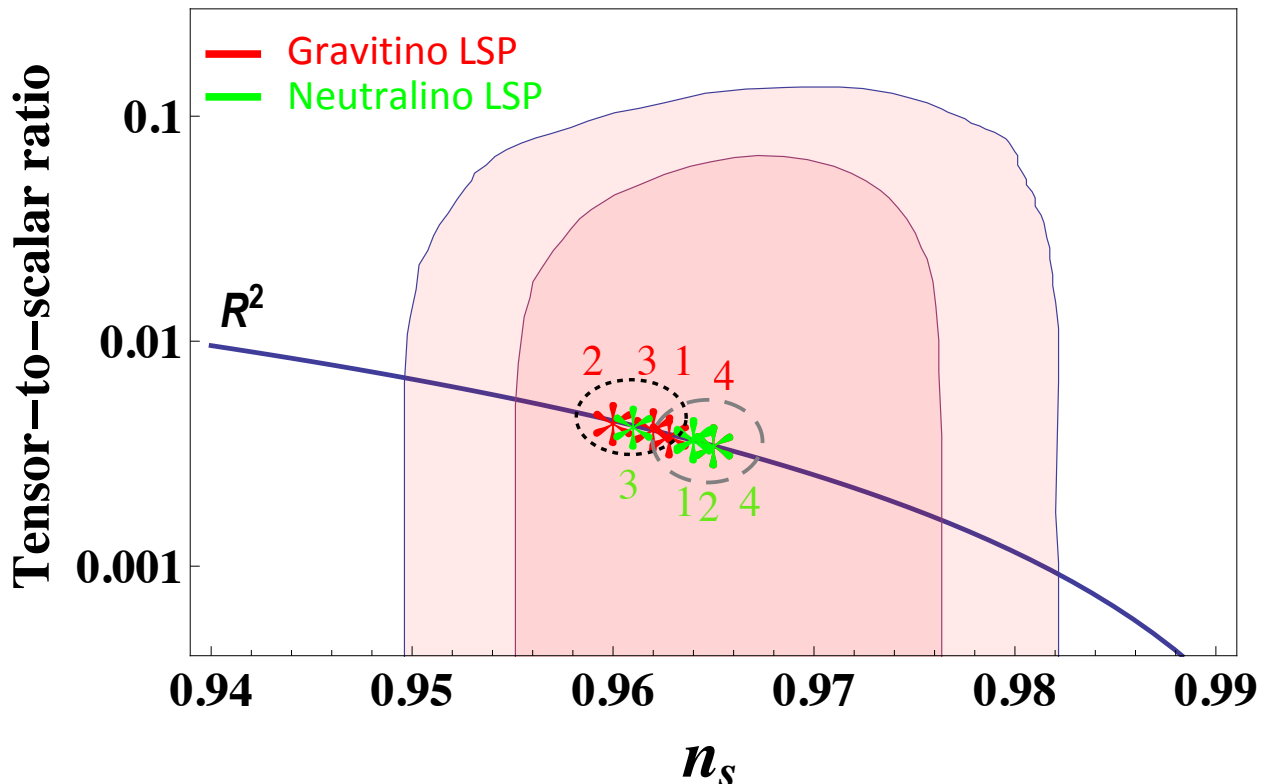
#	m_Z	$m_{\tilde{g}}$	$m_{\tilde{f}}$	$m_{3/2}$ (LSP)	D_X	N_*	n_s	r	Origin
1	10^4	10^4	10^4	10^2	$10^4 _{\min}$	$51 _{\max}$	$0.963 _{\max}$	$0.0038 _{\min}$	Th
2	10^4	10^4	10^5	10^3	$10^{10} _{\min}$	$46 _{\max}$	$0.960 _{\max}$	$0.0044 _{\min}$	Th
3	10^6	10^5	10^6	10^4	$10^6 _{\min}$	$49 _{\max}$	$0.962 _{\max}$	$0.0041 _{\min}$	Non-th
4	10^3	10^3	10^4	10	1	54	0.965	0.0034	Th

Neutralino DM

#	m_Z	$m_{3/2}$	$m_{\tilde{f}}$	$m_{\tilde{\chi}^0}$ (LSP)	$D_{(X)}$	N_*	n_s	r	Origin
1	10^7	10^6	10^6	10^3	$10^2 _{\min}$	$52 _{\max}$	$0.964 _{\max}$	$0.0036 _{\min}$	Non-th
2	10^9	10^8	10^8	10^3	$10^2 _{\min}$	$52 _{\max}$	$0.964 _{\max}$	$0.0036 _{\min}$	Th
3	10^8	10^7	10^7	10^5	$10^8 _{\min}$	$48 _{\max}$	$0.961 _{\max}$	$0.0042 _{\min}$	Non-th
4	10^5	10^5	10^5	10^3	1	54	0.965	0.0034	Th

CMB observables: Starobinsky R2 inflation

[Dalianis & YW 1801.05736]



Conclusion

- We cannot exclude or verify SUSY by (n_s, r) precision measurements even if R2 inflation is verified.
- Nevertheless we can support the presence of BSM physics by ruling out the “BSM-desert” hypothesis for a particular inflation model.
- Hence precision cosmology can offer us complementary constraints to the parameter space of SUSY.

Chulmoon Yoo

Nagoya University

**“PBH abundance from random Gaussian curvature
perturbations and a local density threshold”**

(10+5 min.)

[JGRG28 (2018) 110905]

PBH Abundance from random Gaussian curvature perturbations and a local density threshold

arXiv:1805.03946

Chulmoon Yoo(Nagoya Univ.)

with Tomohiro Harada
Jaume Garriga
Kazunori Kohri

Main message 1

2

arXiv:1805.03946

Significantly improved from the 1st version

Submission history

From: Chul-Moon Yoo [[view email](#)]

[v1] Thu, 10 May 2018 12:56:03 UTC (541 KB)

[v2] Wed, 1 Aug 2018 05:26:04 UTC (667 KB)

[v3] Mon, 10 Sep 2018 01:20:48 UTC (667 KB)

[v4] Fri, 26 Oct 2018 00:37:26 UTC (750 KB)

Large modification



PTEP

accepted version



Please check it (again)!!

Main message 2

A new procedure to estimate PBH abundance

- ◎ Better motivated than Press-Schechter
- ◎ Non-linearity is taken into account
- ◎ Optimized criterion proposed in Shibata-Sasaki(1999)
- ◎ No window function dependence for a narrow spectrum

Please use our procedure!!!

(Although it is a bit(?) more complicated than PS...)

Introduction

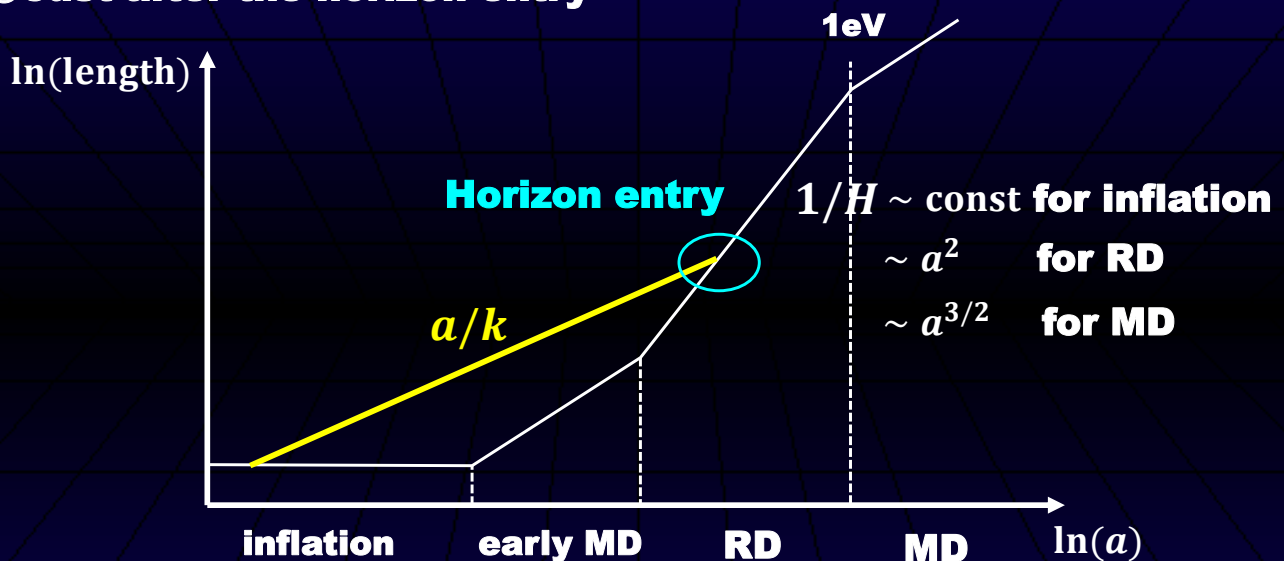
Primordial BHs

[Zeldovich and Novikov(1967),Hawking(1971)]

- ◎ Remnant of primordial non-linear inhomogeneity
- ◎ Trace the inhomogeneity in the early universe
- ◎ May provide a fraction of dark matter and BH binaries
- ◎ Several aspects
 - Inflationary models which provide a large number of PBHs
 - Threshold of PBH formation
 - Observational constraints on PBH abundance
 - Spin distribution of PBHs

PBH formation epoch

- ◎ Just after the horizon entry



- ◎ Mass of PBH in RD era

$$M \sim 1/H \propto a^2 \propto 1/T^2 \propto 1/E^2 \Rightarrow M \sim M_{\text{pl}} \left(\frac{E_{\text{pl}}}{E} \right)^2 \sim 1M_{\odot} \left(\frac{1\text{GeV}}{E} \right)^2$$

Press-Schechter formalism and the point at issue

Perturbation Variables

©Spatial metric

$$dl^2 = a^2 e^{-2\zeta} \tilde{\gamma}_{ij} dx^i dx^j$$

©Relation between ζ and density perturbation δ

$$\delta = -\frac{4(1+w)}{3w+5} \frac{1}{a^2 H^2} e^{5/2\zeta} \Delta e^{-\zeta/2}$$

with long wave-length approx. comoving slicing, $p = w\rho$

©Newtonian counterpart

$\zeta \sim \phi$: Newton potential, $\delta \sim \rho$: density

Press-Schechter

◎ Simplest conventional estimation (Press-Schechter)

- **Assumption 1: threshold is given by the amplitude of ζ or δ**
- **Assumption 2: Gaussian distribution for ζ or δ**
- **Production probability (PBH fraction to the total density) β_0**

$$\beta_0 = 2(2\pi\sigma^2)^{1/2} \int_{|\delta_{\text{th}}|}^{\infty} \exp\left[-\frac{\delta^2}{2\sigma^2}\right] d\delta = \text{erfc}\left(\frac{|\delta_{\text{th}}|}{\sqrt{2}\sigma}\right)$$

◎ Points at issue

- δ has an upper bound $\sim \mathcal{O}(1) \Rightarrow$ cannot be a Gaussian variable
- $\zeta \sim$ potential \Rightarrow depends on environments

δ_{th} and Statistics of ζ

◎ Threshold should be set based on δ

◎ Statistical properties are well known for ζ

◎ What we have to do

- **Statistics of $\zeta \Rightarrow$ probability of $\delta \Rightarrow$ PBH formation prob.**
- **w/ long-wavelength approx. and w/o linear approx.**

◎ Relation between ζ and δ w/ long-wavelength approx.

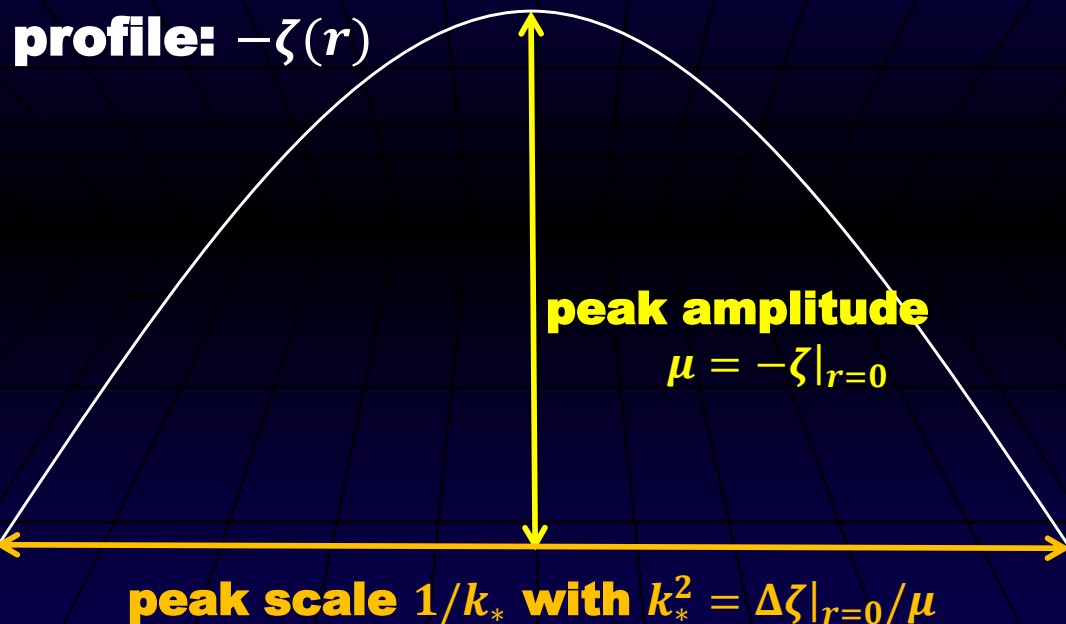
$$\delta = -\frac{4(1+w)}{3w+5} \frac{1}{a^2 H^2} e^{5/2\zeta} \Delta e^{-\zeta/2}$$

comoving slicing, $p = w\rho$

Our Procedure

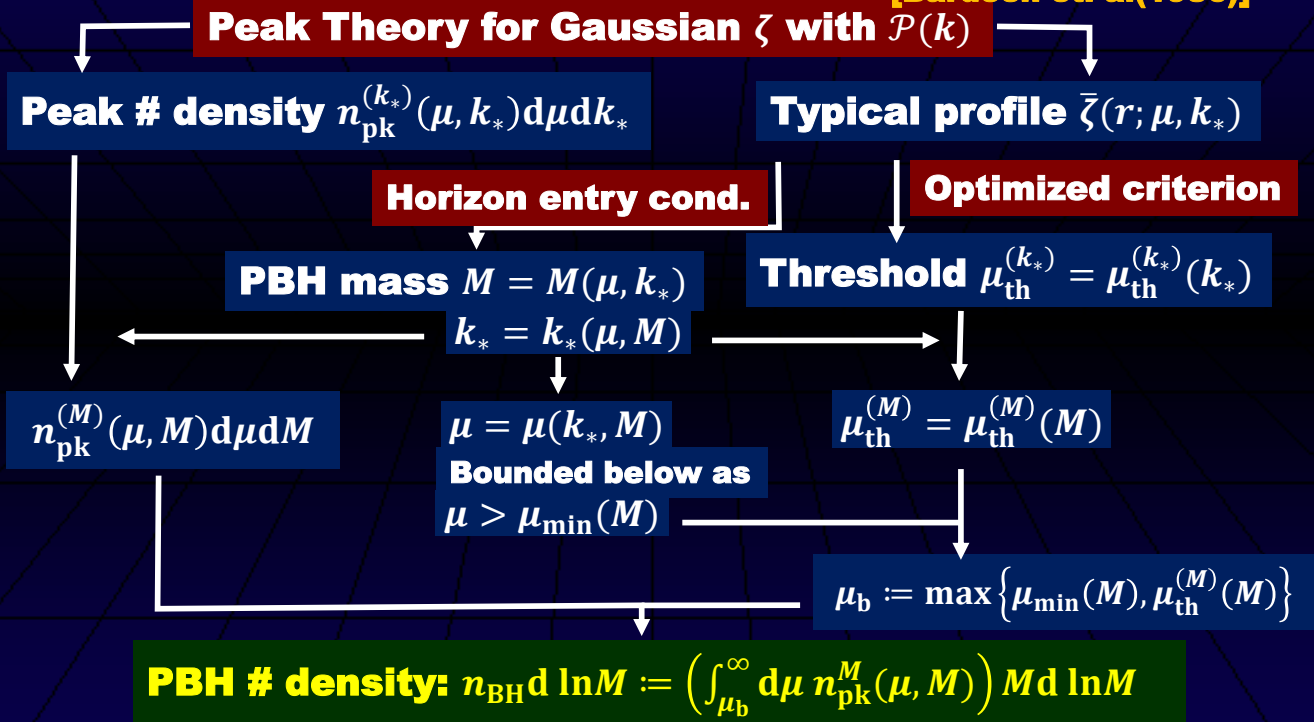
Variables for Profile of ζ

©Variables: $\mu = -\zeta|_{r=0}$, $k_*^2 = \Delta\zeta|_{r=0}/\mu$



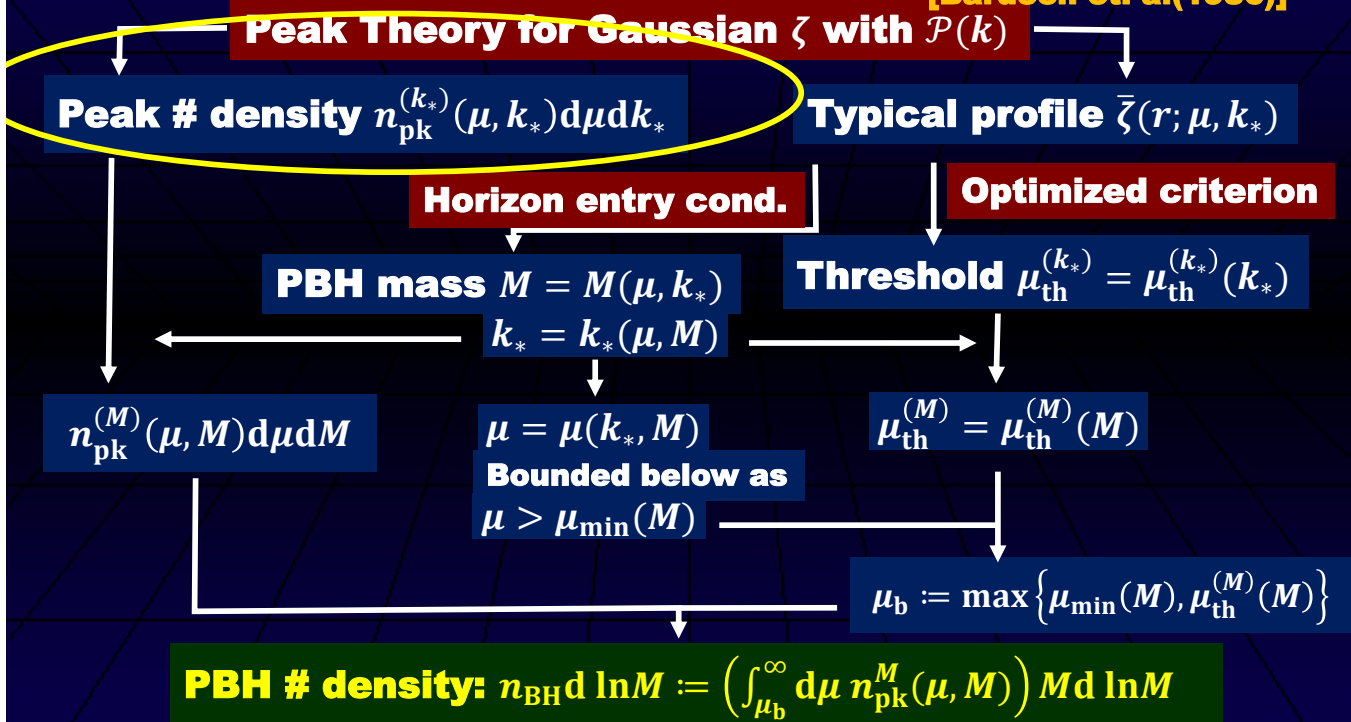
Flow Chart

[Bardeen et. al(1986)]



Flow Chart

[Bardeen et. al(1986)]



Expansion around Extremum

©Probability distribution of linear combinations of $\zeta(x^i)$

$$\mathcal{P}(V_I)d^nV = (2\pi)^{-n/2}|\det\mathcal{M}|^{-1/2}\exp\left[-\frac{1}{2}V_I(\mathcal{M}^{-1})^{IJ}V_J\right]d^nV$$

correlation matrix: $\mathcal{M}_{IJ} = \langle V_I V_J \rangle = \int \frac{d\vec{k}}{(2\pi)^3} \frac{d\vec{k}'}{(2\pi)^3} \langle \tilde{V}_I^*(\vec{k}) \tilde{V}_J(\vec{k}') \rangle$

©Taylor expansion of ζ

$$\zeta = \zeta_0 + \zeta_1^i x_i + \frac{1}{2} \zeta_2^{ij} x_i x_j + O(x^3)$$

©Non-zero correlations in pairs of $\zeta_0, \zeta_1^i, \zeta_2^{ij}$

$$\sigma_0^2 := \int \frac{dk}{k} \mathcal{P}(k) = \langle \zeta_0 \zeta_0 \rangle \quad \sigma_1^2 := \int \frac{dk}{k} k^2 \mathcal{P}(k) = -3 \langle \zeta_0 \zeta_2^{ii} \rangle = 3 \langle \zeta_1^i \zeta_1^i \rangle$$

$$\sigma_2^2 := \int \frac{dk}{k} k^4 \mathcal{P}(k) = 5 \langle \zeta_2^{ii} \zeta_2^{ii} \rangle = 15 \langle \zeta_2^{ii} \zeta_2^{jj} \rangle = 15 \langle \zeta_2^{ij} \zeta_2^{ij} \rangle \text{ with } i \neq j$$

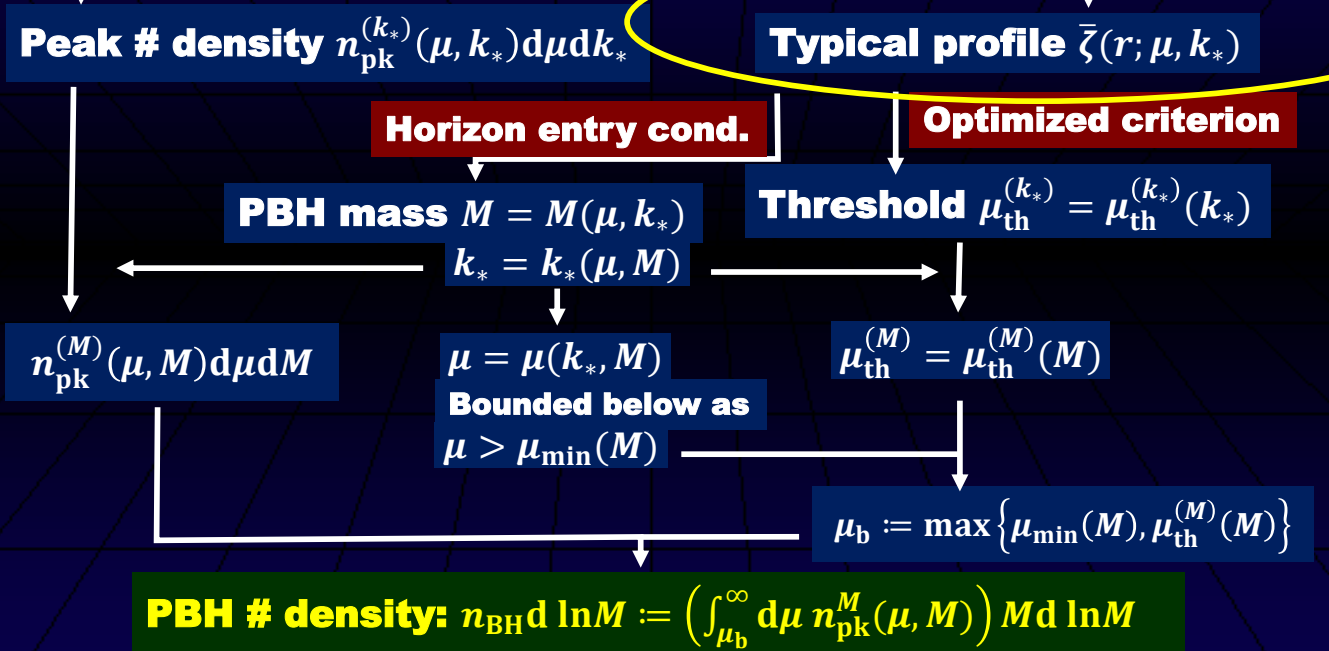
©Peak number density(skip details...) [Bardeen et. al(1986)]

$$\rightarrow n_{\text{pk}}^{(k_*)}(\mu, k_*) d\mu dk_* = \frac{2 \cdot 3^{3/2}}{(2\pi)^{3/2}} \mu k_* \frac{\sigma_2}{\sigma_0 \sigma_1^3} f\left(\frac{\mu k_*^2}{\sigma_2}\right) P_1\left(\frac{\mu}{\sigma_0}, \frac{\mu k_*^2}{\sigma_2}\right) d\mu dk_*$$

Flow Chart

[Bardeen et. al(1986)]

Peak Theory for Gaussian ζ with $\mathcal{P}(k)$



Typical Peak Profile

◎ Typical peak profile for a given set of (μ, k_*)

◎ Mean value of $\zeta(r)$ with the conditional probability $P(\zeta(r)|\mu, k_*)$
[Bardeen et. al(1986)]

$$\bar{\zeta}(r; \mu, k_*) = \mu \left(-\frac{1}{1-\gamma^2} \left(\psi + \frac{\sigma_1^2}{\sigma_2^2} \Delta\psi \right) + \frac{k_*^2}{\gamma(1-\gamma^2)} \frac{\sigma_0}{\sigma_2} \left(\gamma^2 \psi + \frac{\sigma_1^2}{\sigma_2^2} \Delta\psi \right) \right)$$

where $\psi(r) = \frac{1}{\sigma_0^2} \langle \zeta(r)\zeta_0 \rangle = \frac{1}{\sigma_0^2} \int \frac{dk}{k} \frac{\sin(kr)}{kr} \mathcal{P}(k)$

◎ Variance

$$\frac{\langle \Delta\zeta(r)^2 | \mu, k_* \rangle}{\sigma_0^2} = 1 - \frac{\psi^2}{1-\gamma^2} - \frac{1}{\gamma^2(1-\gamma^2)} \left(2\gamma^2 \psi + \frac{\sigma_1^2}{\sigma_2^2} \Delta\psi \right) \frac{\sigma_1^2}{\sigma_2^2} \Delta\psi$$

$$- \frac{5}{\gamma^2} \left(\frac{\psi'}{r} - \frac{\Delta\psi}{3} \right)^2 - \frac{1}{\gamma^2} \psi'^2 \sim \mathcal{O}(1) \Rightarrow \Delta\zeta(r)^2 \sim \sigma_0^2 \ll 1$$

Flow Chart

[Bardeen et. al(1986)]

Peak Theory for Gaussian ζ with $\mathcal{P}(k)$

Peak # density $n_{\text{pk}}^{(k_*)}(\mu, k_*) d\mu dk_*$

Typical profile $\bar{\zeta}(r; \mu, k_*)$

Horizon entry cond.

Optimized criterion

PBH mass $M = M(\mu, k_*)$

Threshold $\mu_{\text{th}}^{(k_*)} = \mu_{\text{th}}^{(k_*)}(k_*)$

$k_* = k_*(\mu, M)$

$n_{\text{pk}}^{(M)}(\mu, M) d\mu dM$

$\mu = \mu(k_*, M)$

$\mu_{\text{th}}^{(M)} = \mu_{\text{th}}^{(M)}(M)$

Bounded below as
 $\mu > \mu_{\text{min}}(M)$

$\mu_b := \max \{ \mu_{\text{min}}(M), \mu_{\text{th}}^{(M)}(M) \}$

PBH # density: $n_{\text{BH}} d \ln M := \left(\int_{\mu_b}^{\infty} d\mu n_{\text{pk}}^M(\mu, M) \right) M d \ln M$

Compaction Function

◎ Definition of the compaction function \mathcal{C}

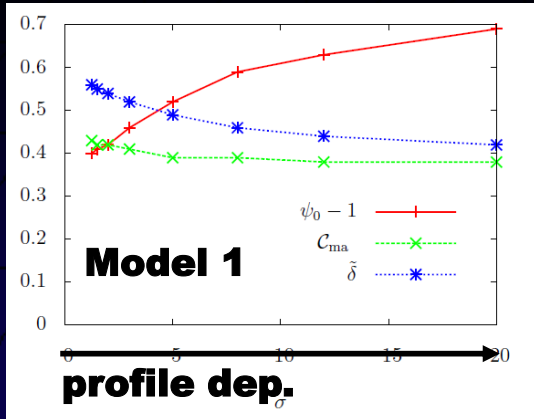
$$\mathcal{C} := \frac{\delta M}{R} \quad \delta M = M_{\text{MS}}(r) - M_{\text{F}}(re^{-\zeta})$$

◎ Compaction function \mathcal{C} and averaged density perturbation $\bar{\delta}$

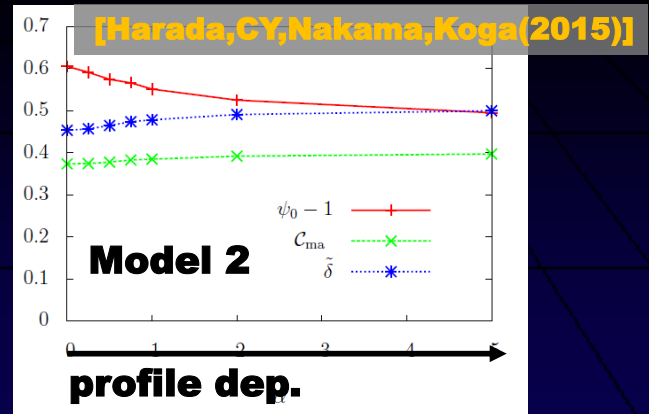
$$\mathcal{C} = \frac{1}{2} \bar{\delta} (HR)^2$$

◎ Criterion for \mathcal{C}^{max} at $r = r_m$

$$\mathcal{C}^{\text{max}} > \frac{1}{2} \delta_{\text{th}} = 0.267 \text{ in comoving slice (0.4 for CMC slice)}$$



JGRG28@Rikkyo



[Harada, CY, Nakama, Koga (2015)]

Chulmoon Yoo

Threshold for $\bar{\zeta}$

◎ Shape of the profile

$$g(r; k_*) := \frac{\bar{\zeta}(r)}{\mu} = -\frac{1}{1-\gamma^2} \left(\psi + \frac{\sigma_1^2}{\sigma_2^2} \Delta\psi \right) + \frac{k_*^2}{\gamma(1-\gamma^2)} \frac{\sigma_0}{\sigma_2} \left(\gamma^2 \psi + \frac{\sigma_1^2}{\sigma_2^2} \Delta\psi \right)$$

$$\psi(r) = \frac{1}{\sigma_0^2} \int \frac{dk \sin(kr)}{k} \frac{\mathcal{P}(k)}{kr}$$

◎ Compaction function

$$\mathcal{C} = \frac{1}{3} [1 - (1 - r\zeta')^2] \Rightarrow \mu = \frac{1 - \sqrt{1 - 3\mathcal{C}}}{r g'}$$

◎ Threshold $\mathcal{C}_{\text{th}} \Rightarrow$ Threshold $\mu_{\text{th}}^{(k_*)}(k_*)$

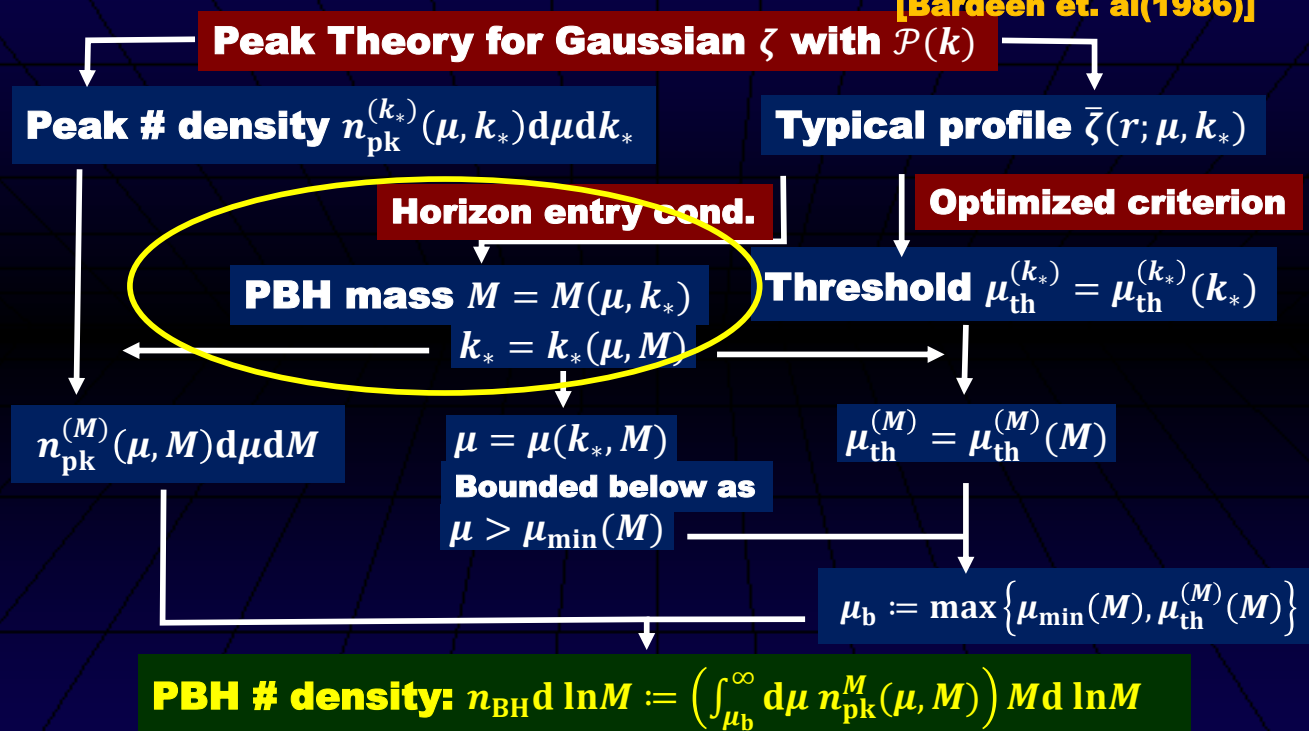
$$\mu_{\text{th}}^{(k_*)}(k_*) = \frac{1 - \sqrt{1 - 3\mathcal{C}_{\text{th}}}}{\bar{r}_m(k_*) g'_m(k_*)} = \frac{2 - \sqrt{4 - 6\delta_{\text{th}}}}{2\bar{r}_m(k_*) g'_m(k_*)}$$

NRF-JSPS workshop@Shikotsuko

Chulmoon Yoo

Flow Chart

[Bardeen et. al(1986)]



Horizon Entry and Threshold

© Estimation of the PBH mass for the typical profile

$$M(\mu, k_*) = \frac{1}{2} \alpha H^{-1} = \frac{1}{2} \alpha R \Big|_{r=\bar{r}_m} = \frac{1}{2} \alpha a \bar{r}_m e^{-\bar{\zeta}} = M_{\text{eq}} k_{\text{eq}}^2 \bar{r}_m^2(k_*) e^{-2\bar{\zeta}(\mu, k_*)}$$

horizon entry

where we have assumed $\alpha \sim \mathcal{O}(1)$ factor

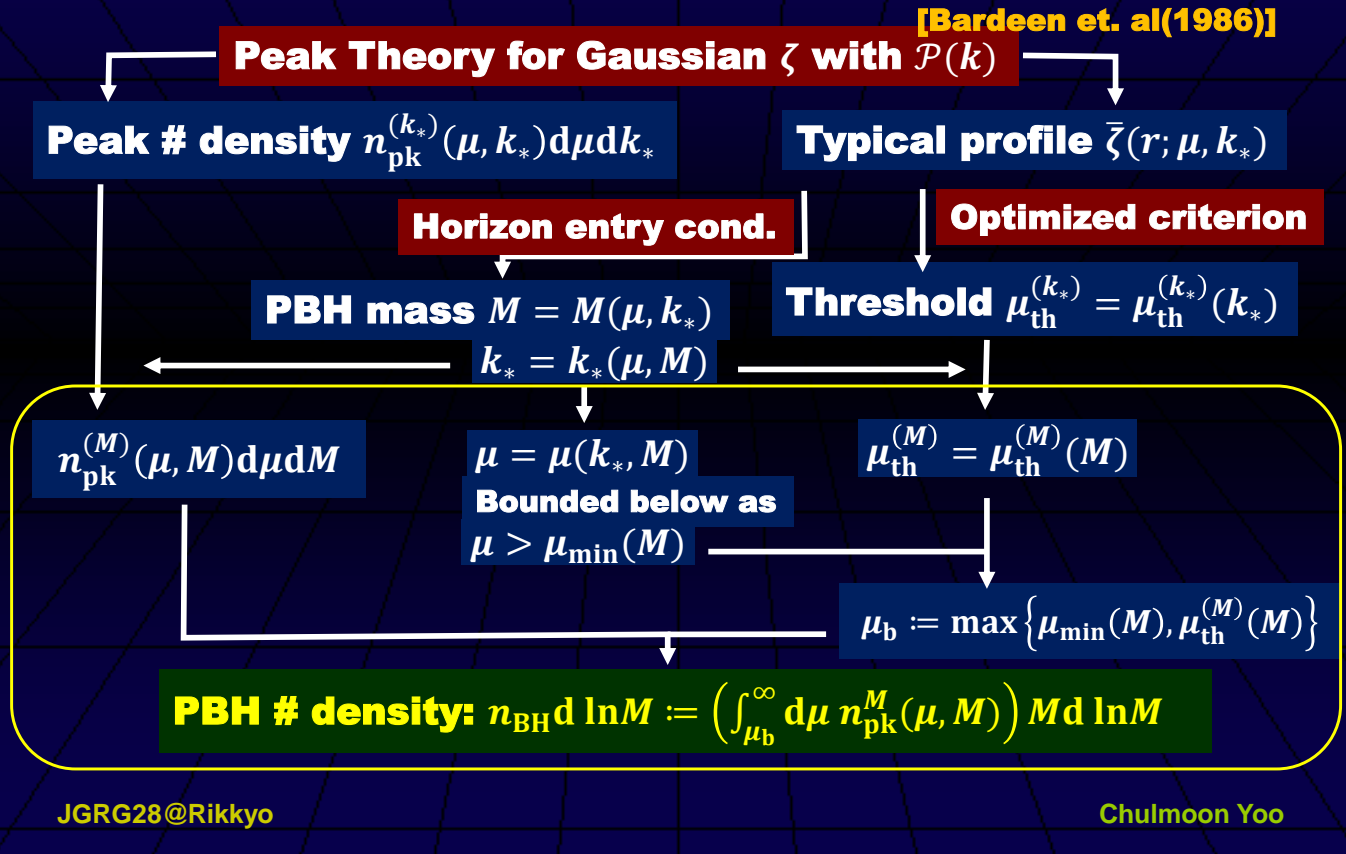
note $\alpha = K(k_)(\mu - \mu_{\text{th}}(k_*))^\gamma$ with $\gamma \simeq 0.36$
if we take into account the critical behavior

© We obtain the relation of M, k_*, μ

$$M = M(\mu, k_*) \longleftrightarrow k_* = k_*(\mu, M) \longleftrightarrow \mu = \mu(M, k_*)$$

Flow Chart

[Bardeen et. al(1986)]



An Extended Spectrum

An Extended $\mathcal{P}(k)$

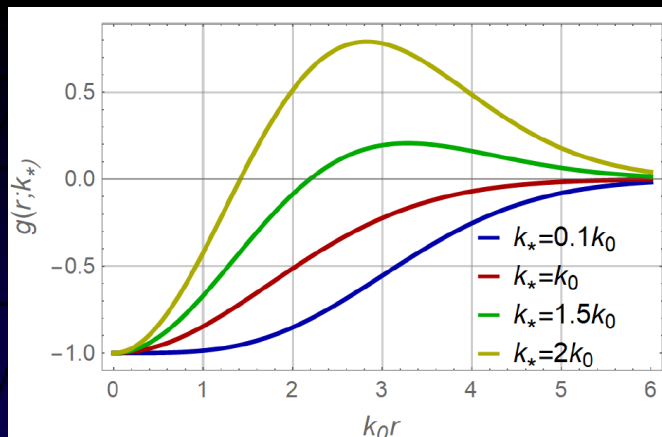
$$\odot \mathcal{P}(k) = 3 \sqrt{\frac{6}{\pi}} \sigma^2 \left(\frac{k}{k_0}\right)^3 \exp\left(-\frac{3k^2}{2k_0^2}\right)$$

© Moments

© 2 point correlation

$$\sigma_n^2 = \frac{2^{n+1}}{3^n \sqrt{\pi}} \Gamma\left(\frac{3}{2} + n\right) \sigma^2 k_0^{2n} \quad \psi(r) = \exp\left(-\frac{k_0^2 r^2}{6}\right)$$

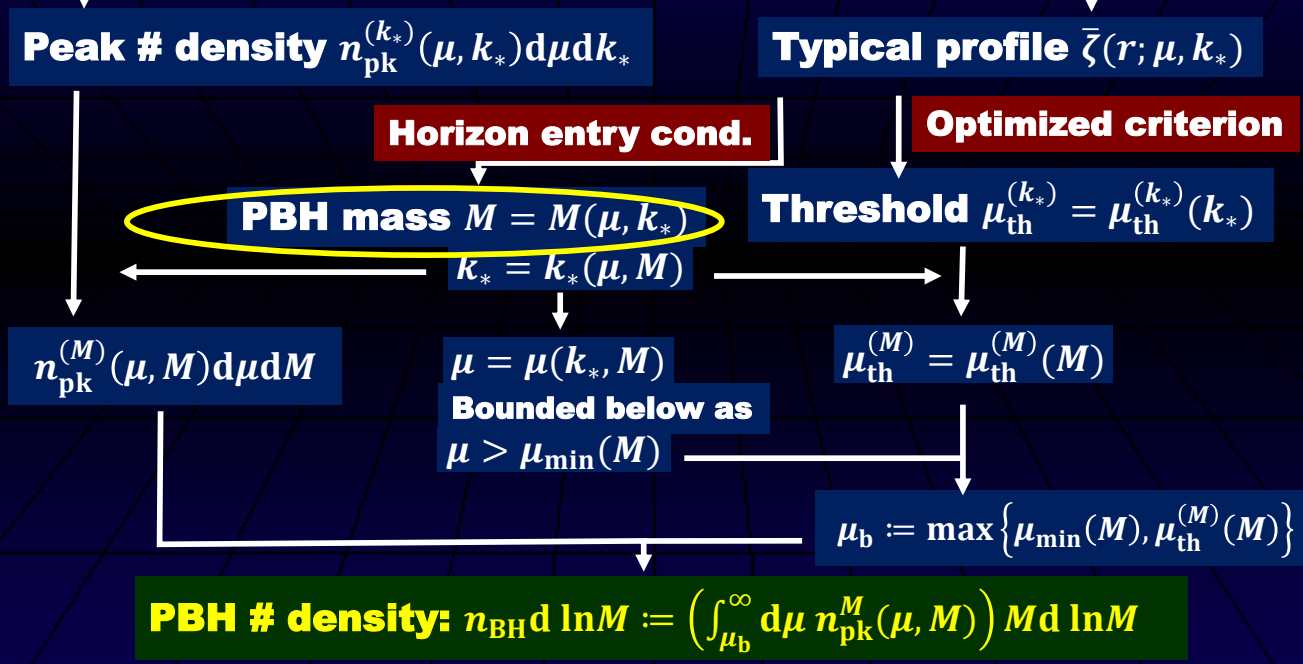
© Profile $g(r; k_*)$



Flow Chart

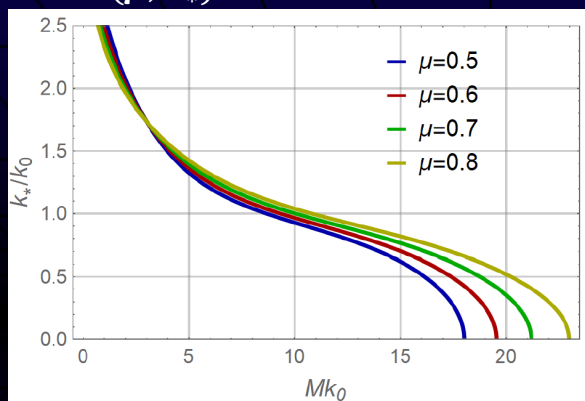
[Bardeen et. al(1986)]

Peak Theory for Gaussian ζ with $\mathcal{P}(k)$

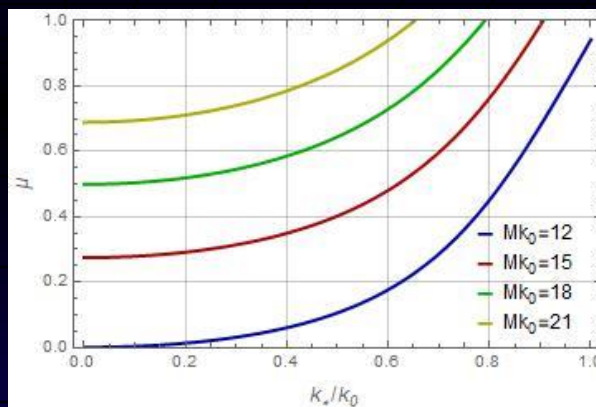


$M(\mu, k_*)$

© $M = M(\mu, k_*)$



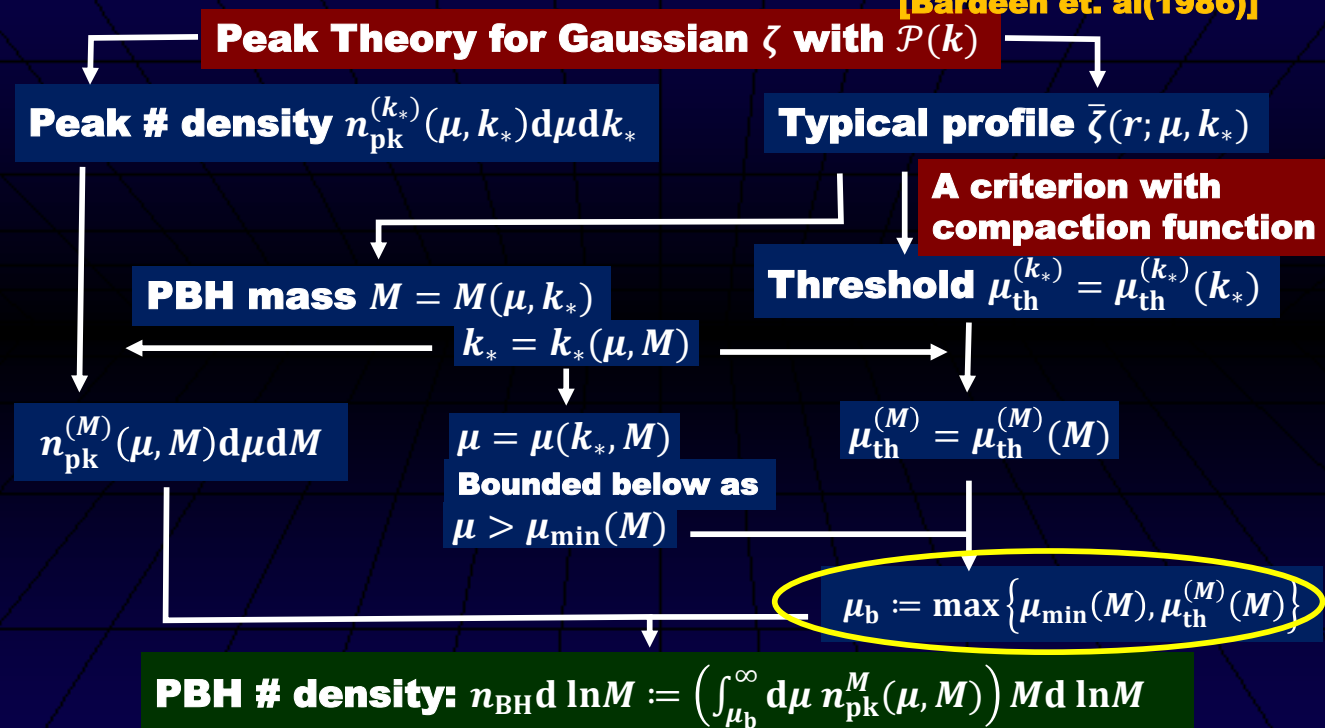
© $\mu(k_*, M)$



$$\mu_{\min}(M) = \mu(0, M)$$

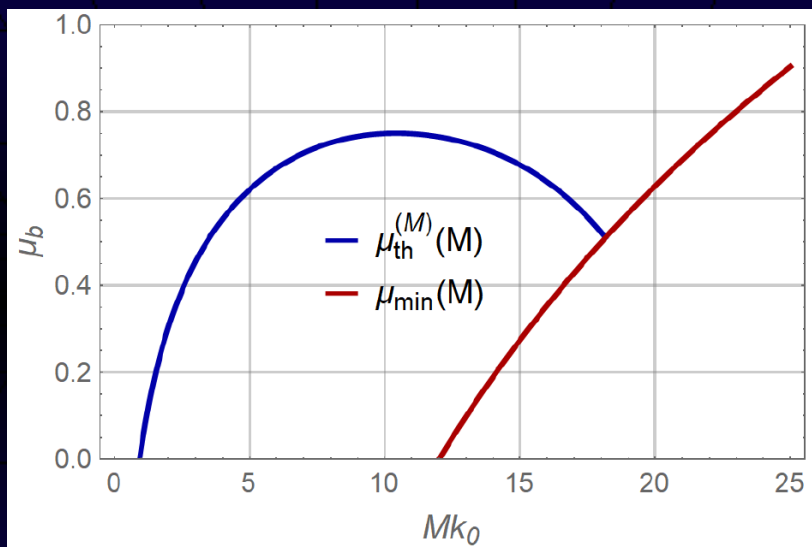
Flow Chart

[Bardeen et. al(1986)]



$\mu_{th}^{(M)}(M)$

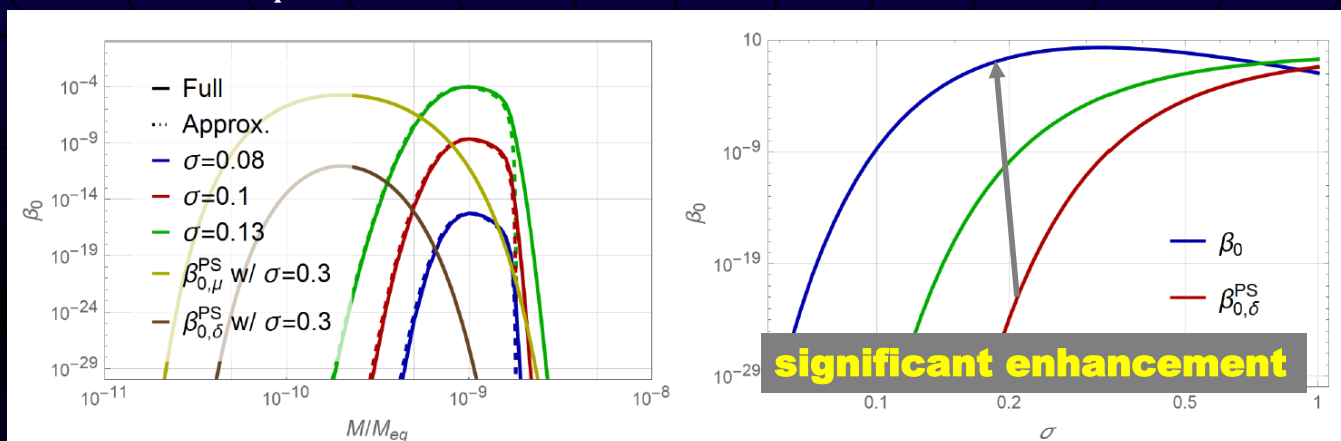
© $\mu_{th}^{(M)}$



© Steeper suppression in larger mass

$\beta_0(M)$

© $k_0 = 10^5 k_{eq}$



© Spectrum shift by one order of mag.

$$\frac{M}{M_{eq}} \approx \frac{k_{eq}^2}{k_0^2} \bar{r}_m^2 k_0^2 e^{-2\mu\zeta_m} \sim \frac{k_{eq}^2}{k_0^2} \times 10$$

© Significantly larger abundance

- Optimized criterion
- No suppression from a window function

Note on Window Function

◎ Don't we need a Window function any more?

◎ Two roles in the PS formalism

1. Smooth out the smaller scale inhomogeneity

2. Introduce the scale dependence of the mass spectrum

◎ For our specific power spectrum

· No smaller scale inhomogeneity (single scale)

· The scale dependence is automatically induced by the random variable k_* , which characterizes the profile

◎ We need a window function for a broad spectrum

Main message

A new procedure to estimate PBH abundance

◎ Better motivated than PS

◎ Non-linearity is taken into account

◎ Optimized criterion is implemented

◎ No window function dependence for a narrow spectrum

Please use our procedure!!!

◎ A bit(?) complicated, but see 1805.03946
for the analytic expression for the monochromatic case
for a simpler approximate formula

Thank you for your attention

Marcus Christian Werner

Yukawa Institute for Theoretical Physics, Kyoto University

“New developments in optical geometry”

(10+5 min.)

[JGRG28 (2018) 110908]

New Developments in Optical Geometry

Marcus C. Werner, Kyoto University



9 November 2018
JGRG28, Rikkyo University, Tokyo



Introduction

Gravitational lensing theory can be approached in three ways:

- ① null geodesics in 4-dimensional spacetime;
- ② standard approximation used in astronomy: quasi-Newtonian impulse approximation in Euclidean 3-space;



Gravitational lensing theory can be approached in three ways:

- ① null geodesics in 4-dimensional spacetime;
- ② standard approximation used in astronomy: quasi-Newtonian impulse approximation in Euclidean 3-space;
- ③ **optical geometry**: 3-dimensional manifold whose geodesics are spatial projections of null geodesics, by Fermat's principle:

Static spacetime: Riemannian optical geometry.

E.g., for $ds^2 = g_{tt}dt^2 + g_{ij}dx^i dx^j$,
 null curves obey $dt^2 = h_{ij}dx^i dx^j$
 with **optical metric** $h_{ij} = -\frac{g_{ij}}{g_{tt}}$.

Stationary spacetime: Finslerian optical geometry.



The Mathematics of Gravity and Light

AMS MRC Conference at Whispering Pines, Rhode Island, USA,
 coorganized with Arlie Petters (Duke) and Chuck Keeton (Rutgers)



Bookstore MathSciNet® Journals Member Directory Employment Services



The American Mathematical Society presents
Mathematics Research Communities

Introduction	MRC Week 1a, June 3 - 9, 2018
Call for 2020 Proposals	<i>The Mathematics of Gravity and Light</i>
2019 Program	Organizers: Charles Keeton , Rutgers University Arlie Petters , Duke University Marcus Werner , Kyoto University



The isoperimetric problem

In **Euclidean** geometry, an area A bounded by perimeter L satisfies

$$L^2 \geq 4\pi A,$$

the **isoperimetric inequality**. The limiting case is the **circle**.



The isoperimetric problem

The theorem of Dido, queen of Carthage!
814BC?

カルタゴの女王デイードー

*Devenere locos, ubi nunc ingentia cernis
moenia surgentemque novae Karthaginis arcem
mercatique solum, facti de nomine Byrsam
taurino quantum possent circumdare tergo.*

Aeneis I 365-368

古代ローマの「アエネーイス」



The isoperimetric problem

In **Euclidean** geometry, an area A bounded by perimeter L satisfies

$$L^2 \geq 4\pi A,$$

the **isoperimetric inequality**. The limiting case is the **circle**.

Question: what does the isoperimetric problem imply for optical geometry? Constraints on **time delays**/angles for lensed images?



The isoperimetric problem

In **Euclidean** geometry, an area A bounded by perimeter L satisfies

$$L^2 \geq 4\pi A,$$

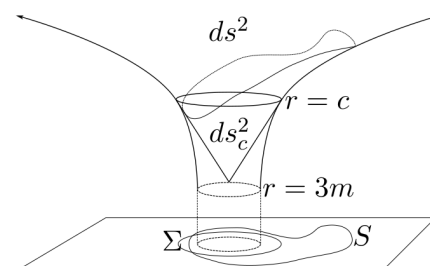
the **isoperimetric inequality**. The limiting case is the **circle**.

Question: what does the isoperimetric problem imply for optical geometry? Constraints on **time delays**/angles for lensed images?

Theorem

In Schwarzschild equatorial optical geometry, assume sets S and $\Sigma := \{r \leq c\} \supseteq \{r = 3m\}$ satisfy $|S| \geq |\Sigma|$. Then, $|\partial S| \geq |\{r = c\}|$.

[Roesch & Werner (2018), forthcoming]



The Gauss-Bonnet method

A closed area $A \subset M$ in metric surface (M, h) with piecewise-smooth boundary $\partial A = \cup_i \gamma_i$ obeys the Gauss-Bonnet theorem,

$$\chi(A) = \int_A \frac{K}{2\pi} dA + \sum_i \left(\int_{\gamma_i} \frac{k}{2\pi} dt + \frac{\theta(N_i^-, N_i^+)}{2\pi} \right),$$

with Euler characteristic χ , Gaussian curvature K , exterior jump angle $\theta(N_i^+, N_i^-)$ at vertex i , geodesic curvature $k : \nabla_{\dot{\gamma}} \dot{\gamma} = kN$.



The Gauss-Bonnet method

A closed area $A \subset M$ in metric surface (M, h) with piecewise-smooth boundary $\partial A = \cup_i \gamma_i$ obeys the Gauss-Bonnet theorem,

$$\chi(A) = \int_A \frac{K}{2\pi} dA + \sum_i \left(\int_{\gamma_i} \frac{k}{2\pi} dt + \frac{\theta(N_i^-, N_i^+)}{2\pi} \right),$$

with Euler characteristic χ , Gaussian curvature K , exterior jump angle $\theta(N_i^+, N_i^-)$ at vertex i , geodesic curvature $k : \nabla_{\dot{\gamma}} \dot{\gamma} = kN$.

Note for later: by definition, $k = 0$ iff γ is geodesic.



A closed area $A \subset M$ in metric surface (M, h) with piecewise-smooth boundary $\partial A = \cup_i \gamma_i$ obeys the Gauss-Bonnet theorem,

$$\chi(A) = \int_A \frac{K}{2\pi} dA + \sum_i \left(\int_{\gamma_i} \frac{k}{2\pi} dt + \frac{\theta(N_i^-, N_i^+)}{2\pi} \right),$$

with Euler characteristic χ , Gaussian curvature K , exterior jump angle $\theta(N_i^+, N_i^-)$ at vertex i , geodesic curvature $k : \nabla_{\dot{\gamma}} \dot{\gamma} = kN$.

Note for later: by definition, $k = 0$ iff γ is geodesic.

This can be applied to gravitational lensing, e.g. on a domain

- including the lens, for topological image multiplicity;
- excluding the lens, for the asymptotic deflection angle,

$$\hat{\alpha} = - \int_{A_\infty} K dA.$$

[Gibbons & Werner, *Class. Quantum Grav.* (2008)]



But stationary spacetimes?

Given the Kerr solution in Boyer-Lindquist coordinates,

$$ds^2 = \frac{\Delta}{\rho^2} (dt - a \sin^2 \theta d\phi)^2 - \frac{\sin^2 \theta}{\rho^2} ((r^2 + a^2)d\phi - a dt)^2 - \frac{\rho^2}{\Delta} dr^2 - \rho^2 d\theta^2,$$

solving for the optical geometry, one finds

$$dt = \sqrt{h_{ij}(x) dx^i dx^j} + \beta_i(x) dx^i,$$

where h is a Riemannian metric, and $\beta \propto a$ is a one-form.



Given the Kerr solution in Boyer-Lindquist coordinates,

$$ds^2 = \frac{\Delta}{\rho^2} (dt - a \sin^2 \theta d\phi)^2 - \frac{\sin^2 \theta}{\rho^2} ((r^2 + a^2)d\phi - a dt)^2 - \frac{\rho^2}{\Delta} dr^2 - \rho^2 d\theta^2,$$

solving for the optical geometry, one finds

$$dt = \sqrt{h_{ij}(x) dx^i dx^j} + \beta_i(x) dx^i,$$

where h is a Riemannian metric, and $\beta \propto a$ is a one-form.

This is **not** Riemannian but a special case of **Finsler geometry** called **Kerr-Randers optical geometry** (away from the ergoregion boundary).



Finsler geometry

A Finsler manifold (M, F) , with $x \in M$, $V \in T_x M$, has a smooth function $F : TM \setminus 0 \rightarrow \mathbb{R}_0^+$ with is **homogeneous** such that $F(x, \lambda V) = \lambda F(x, V)$, $\lambda > 0$, and **convex** such that the Hessian

$$g_{ij}(x, V) = \frac{1}{2} \frac{\partial^2 F^2(x, V)}{\partial V^i \partial V^j}$$

is positive definite.



A Finsler manifold (M, F) , with $x \in M$, $V \in T_x M$, has a smooth function $F : TM \setminus 0 \rightarrow \mathbb{R}_0^+$ with is **homogeneous** such that $F(x, \lambda V) = \lambda F(x, V)$, $\lambda > 0$, and **convex** such that the Hessian

$$g_{ij}(x, V) = \frac{1}{2} \frac{\partial^2 F^2(x, V)}{\partial V^i \partial V^j}$$

is positive definite. Note, using Euler's theorem of homogeneity,

$$F^2(x, V) = g_{ij}(x, V) V^i V^j.$$



A Finsler manifold (M, F) , with $x \in M$, $V \in T_x M$, has a smooth function $F : TM \setminus 0 \rightarrow \mathbb{R}_0^+$ with is **homogeneous** such that $F(x, \lambda V) = \lambda F(x, V)$, $\lambda > 0$, and **convex** such that the Hessian

$$g_{ij}(x, V) = \frac{1}{2} \frac{\partial^2 F^2(x, V)}{\partial V^i \partial V^j}$$

is positive definite. Note, using Euler's theorem of homogeneity,

$$F^2(x, V) = g_{ij}(x, V) V^i V^j.$$

There is also a unique torsion-free and almost metrically compatible connection called the **Chern connection** $\Gamma^i_{jk}(x, V)$.

$$\text{viz., } \Gamma^i_{jk}(x, V) = \frac{1}{2} g^{is} \left(\frac{\delta g_{sj}}{\delta x^k} + \frac{\delta g_{sk}}{\delta x^j} - \frac{\delta g_{jk}}{\delta x^s} \right),$$

$$\text{where } \frac{\delta}{\delta x^i} = \frac{\partial}{\partial x^i} - (\{^j_{ik}\} V^k - C^j_{ik} \{^k_{mn}\} V^m V^n) \frac{\partial}{\partial V^j}, \text{ with Cartan tensor } C_{ijk} = \frac{1}{2} \frac{\partial g_{ij}(x, V)}{\partial V^k}.$$



How to apply the Gauss-Bonnet method to gravitational lensing in stationary spacetimes like Kerr, with Finslerian optical geometry?



How to apply the Gauss-Bonnet method to gravitational lensing in stationary spacetimes like Kerr, with Finslerian optical geometry?

- 1 **Osculating Riemannian geometry:** find a suitable vector field \bar{V} yielding a fiducial optical geometry $\bar{g}_{ij}(x) = g_{ij}(x, \bar{V}(x))$;

[Werner, *Gen. Rel. Grav.* (2012); Jusufi, Werner et al., *Phys. Rev. D* (2017); Jusufi & Övgün, (2018)]



How to apply the Gauss-Bonnet method to gravitational lensing in stationary spacetimes like Kerr, with Finslerian optical geometry?

- ① **Osculating Riemannian geometry**: find a suitable vector field \bar{V} yielding a fiducial optical geometry $\bar{g}_{ij}(x) = g_{ij}(x, \bar{V}(x))$;

[Werner, *Gen. Rel. Grav.* (2012); Jusufi, Werner et al., *Phys. Rev. D* (2017); Jusufi & Övgün, (2018)]

- ② **Riemannian Gauss-Bonnet** in spatial, **not** optical, geometry where light rays are **non-geodesic** curves $\Rightarrow k \neq 0$.

[Ono, Ishihara & Asada, *Phys. Rev. D* (2017; 2018)]



How to apply the Gauss-Bonnet method to gravitational lensing in stationary spacetimes like Kerr, with Finslerian optical geometry?

- ① **Osculating Riemannian geometry**: find a suitable vector field \bar{V} yielding a fiducial optical geometry $\bar{g}_{ij}(x) = g_{ij}(x, \bar{V}(x))$;

[Werner, *Gen. Rel. Grav.* (2012); Jusufi, Werner et al., *Phys. Rev. D* (2017); Jusufi & Övgün, (2018)]

- ② **Riemannian Gauss-Bonnet** in spatial, **not** optical, geometry where light rays are **non-geodesic** curves $\Rightarrow k \neq 0$.

[Ono, Ishihara & Asada, *Phys. Rev. D* (2017; 2018)]

- ③ **Finslerian Gauss-Bonnet** applied directly to Kerr-Randers. Basic steps to be discussed in the following.

[Gudapati & Werner, in preparation]



For Finsler surfaces, this yields [Itoh, Sabau & Shimada, *Kyoto J. Math.* (2010)]

$$\begin{aligned} \chi(A) &= \int_A \frac{1}{L} (N^*(K\omega^1 \wedge \omega^2 - J\omega^1 \wedge \omega^3) - dL \wedge N^*(\omega^3)) \\ &+ \sum_i \left(\int_{\gamma_i} \frac{k^{(N)}}{L\sigma} dt + \frac{\lambda(N_i^-, N_i^+)}{L} \right), \end{aligned}$$

with coframe fields ω^j over $TM \setminus 0$, normal vector fields N , Gaussian curvature K , indicatrix length L , Landsberg scalar J , the Landsberg angle λ , and length parameter $\sigma^2 = g(\gamma, N)_{ij} \dot{\gamma}^i \dot{\gamma}^j$.

Note, in particular, the following property of the so-called N -parallel curvature $k^{(N)}$:



Note on geodesics and curvature

In Finsler geometry, a covariant derivative is defined **with respect to** a vector field V , that is $(\nabla_Y^{(V)} X)^i = \frac{dX^i}{dt} + \Gamma^i_{jk}(x, V) X^j Y^k$.

Now Finsler **geodesics**, minimizing Finslerian curve length, satisfy

$$\nabla_{\dot{\gamma}}^{(\dot{\gamma})} \dot{\gamma} = 0.$$



Note on geodesics and curvature

In Finsler geometry, a covariant derivative is defined **with respect to** a vector field V , that is $(\nabla_{\dot{Y}}^{(V)} X)^i = \frac{dX^i}{dt} + \Gamma^i_{jk}(x, V)X^j Y^k$.

Now Finsler **geodesics**, minimizing Finslerian curve length, satisfy

$$\nabla_{\dot{\gamma}}^{(\dot{\gamma})} \dot{\gamma} = 0.$$

However, unlike in Riemannian geometry, there exist also **different autoparallels**, called N -parallels,

$$\nabla_{\dot{\gamma}}^{(N)} N = 0.$$

N -parallel curvature, defined by the relation $\nabla_{\dot{\gamma}}^{(N)} N = -\frac{k^{(N)}}{\sigma^2} \dot{\gamma}$, vanishes for those N -parallels, **not** for the geodesics.



Concluding remarks

- The Gauss-Bonnet method **can** be extended to the Finslerian optical geometry of stationary spacetimes;
- However, the Riemannian simplification with $k = 0$ for geodesic light rays does **not** carry over to Finsler geometry;



- The Gauss-Bonnet method **can** be extended to the Finslerian optical geometry of stationary spacetimes;
- However, the Riemannian simplification with $k = 0$ for geodesic light rays does **not** carry over to Finsler geometry;
- A technical similarity with the Asada group's Riemannian approach emerges thus even in the Finslerian treatment;

- The Gauss-Bonnet method **can** be extended to the Finslerian optical geometry of stationary spacetimes;
- However, the Riemannian simplification with $k = 0$ for geodesic light rays does **not** carry over to Finsler geometry;
- A technical similarity with the Asada group's Riemannian approach emerges thus even in the Finslerian treatment;
- We are currently exploiting this Gauss-Bonnet theorem for the concrete case of Kerr-Randers optical geometry.